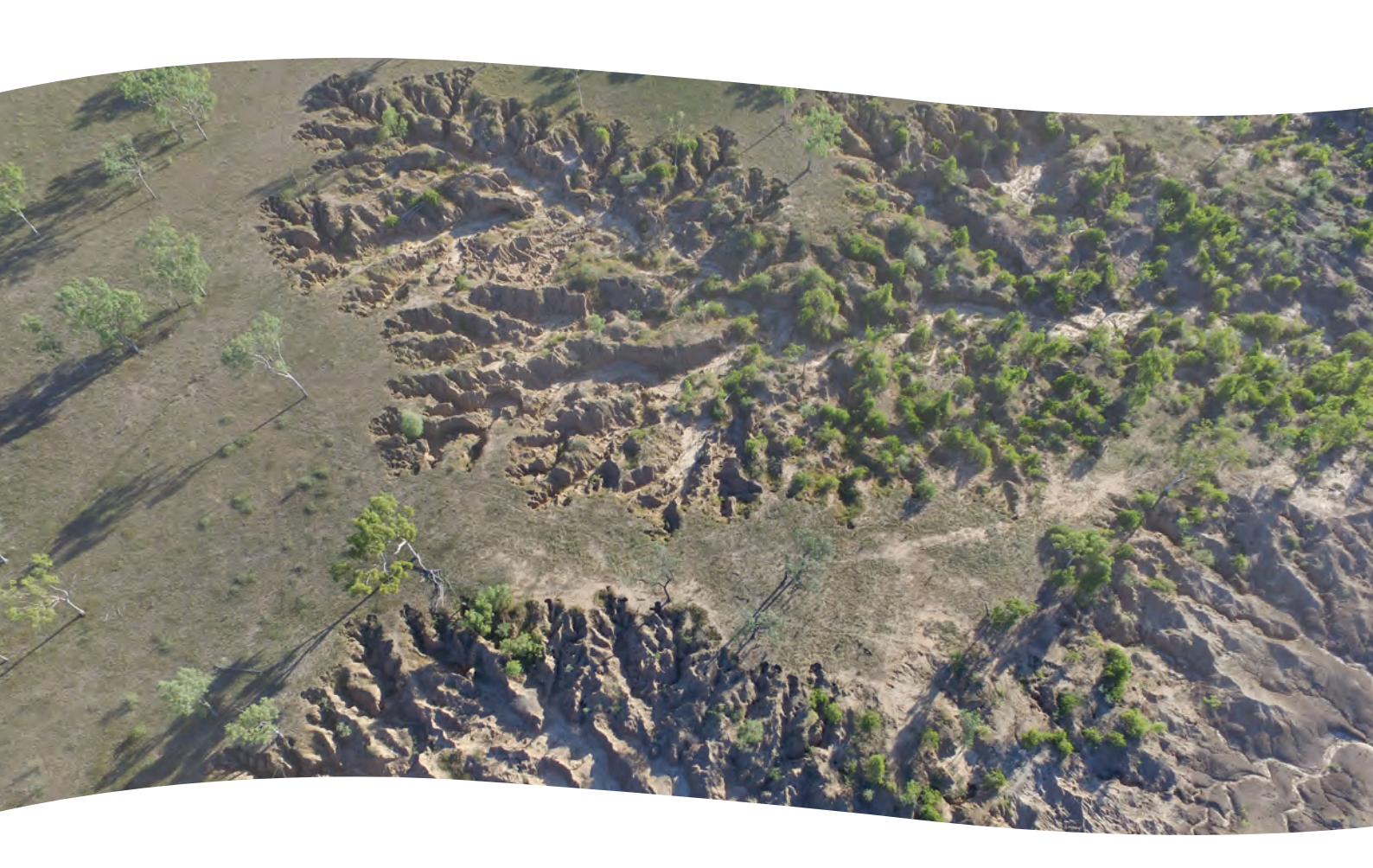


National **Environmental Science** Programme

# Reducing sediment sources to the Reef: Managing alluvial gully erosion

Andrew Brooks, Graeme Curwen, John Spencer, Jeff Shellberg, Alexandra Garzon-Garcia, Jo Burton and Fabio Iwashita in collaboration with Trish Butler





# Reducing sediment sources to the Reef: Managing alluvial gully erosion

Andrew Brooks<sup>1</sup>, Graeme Curwen<sup>2</sup>, John Spencer<sup>2</sup>, Jeff Shellberg<sup>2</sup>, Alexandra Garzon-Garcia<sup>3</sup>, Jo Burton<sup>3</sup> and Fabio Iwashita<sup>2</sup>

<sup>1</sup> Griffith Centre for Coastal Management, Griffith University

<sup>2</sup> Australian Rivers Institute, Griffith University

<sup>3</sup> DSITI

In Collaboration with Trish Butler<sup>4</sup>
<sup>4</sup>Cape York Sustainable Futures





Supported by the Australian Government's National Environmental Science Programme



Reducing sediment sources to the Reef: managing alluvial gully erosion is licensed by Griffith University for use under a Creative Commons Attribution 4.0 Australia licence. For licence conditions see: https://creativecommons.org/licenses/by/4.0/

National Library of Australia Cataloguing-in-Publication entry: 978-1-925088-97-7

Brooks, A., Spencer, J., Curwen, G, Shellberg, J., Garzon-Garcia, A, Burton, J. & Iwashita, F. (2016) *Reducing sediment sources to the Reef: Managing alluvial gully erosion*. Report to the National Environmental Science Programme. Reef and Rainforest Research Centre Limited, Cairns (375pp.).

Published by the Reef and Rainforest Research Centre on behalf of the Australian Government's National Environmental Science Programme (NESP) Tropical Water Quality (TWQ) Hub.

The Tropical Water Quality Hub is part of the Australian Government's National Environmental Science Programme and is administered by the Reef and Rainforest Research Centre Limited (RRRC). The NESP TWQ Hub addresses water quality and coastal management in the World Heritage listed Great Barrier Reef, its catchments and other tropical waters, through the generation and transfer of world-class research and shared knowledge.

This publication is copyright. The Copyright Act 1968 permits fair dealing for study, research, information or educational purposes subject to inclusion of a sufficient acknowledgement of the source.

The views and opinions expressed in this publication are those of the authors and do not necessarily reflect those of the Australian Government.

While reasonable effort has been made to ensure that the contents of this publication are factually correct, the Commonwealth does not accept responsibility for the accuracy or completeness of the contents, and shall not be liable for any loss or damage that may be occasioned directly or indirectly through the use of, or reliance on, the contents of this publication.

Cover photographs: Andrew Brooks

This report is available for download from the NESP Tropical Water Quality Hub website: <a href="http://www.nesptropical.edu.au">http://www.nesptropical.edu.au</a>

### **CONTENTS**

List of Tables	i
List of Figures	iii
Acronyms	vii
Acknowledgements	ix
Executive Summary	1
1. Summary report	13
1.1 Background	13
1.2 Research Objectives of this Study	13
2. Key Findings	16
2.1 Recent trends in erosion sources within the upper Normanby and Laura R (Brooks, Curwen & Spencer)	<b>16</b> ime 2
(2011/15)	
2.2 Gully Exclusion Experiment: Vegetation Data (Shellberg, Brooks, Curwen)  2.2.1 Overview	23 24 er .29 32
2.3 Gully Cattle Exclusion Experiment: LiDAR Data (Brooks, Curwen, Shell	
Spencer, Iwashita)	38 42
2.4 Bioavailable nutrients and organics in alluvial gully sediment (Garzon-Ga	
Burton, Brooks)	45
2.5 Gully Slope Stabilisation Treatment Trials – updated survey (Spencer, Bro	50
2.5.1 Study Overview	
2.5.3 Results	60
2.5.4 Summary	
2.6 Alluvial Gullies along the Bowen River Floodplain	
References	
Annandicas	72

### **LIST OF TABLES**

Table 1:	Comparison between sediment and nutrient contributions from alluvial gullies vs other intensive land uses in the GBR Wet Tropics catchments5
Table 2:	Summary statistics of the LiDAR blocks resurveyed in 201516
Table 3:	Summary of annual water year rainfall totals over the study period18
Table 4:	Ratio of change on rainfall normalised erosion rates for each LiDAR block expressed as time 2 (2011-15)/time 1(2009-11)
Table 5:	Comparison of water flow statistics in the Laura and Normanby Rivers for the two study period intervals
Table 6:	Summary of erosion results from the grazing exclosure plots at the three sites for which sufficient data is available to make valid comparisons regarding the erosion rates from the experimental plots (i.e. excluding CRGC)42
Table 7:	Two tailed t test results for Normanby grazing exclosure trials43
Table 8:	Description of the plot treatments at the Crocodile rehabilitation site56
Table 9:	Average annual sediment contributions from the Burdekin catchment based on monitoring data from 2005-2009 broken down by particle size classes65

## **LIST OF FIGURES**

Figure 1:	Annual sediment contributions from primary sources in 7 common Normanby
Fig 0.	LiDAR blocks normalised per 100mm incident rainfall (RF)
Figure 2:	Net erosion across the three monitoring periods (4 years)
Figure 3:	Percentage change in mean annual sediment yield compared to (cf) external
<b>-</b> :	untreated controls for the four years surveyed9
Figure 4:	Large alluvial gully complex along Parrot Ck, a tributary entering the Bowen River just downstream of the Bowen Development Rd
Figure 5:	Satellite image of the alluvial gully sites shown above along Parrot Ck11
Figure 6:	An extremely active alluvial gully system in the vicinity of the Bowen/Burdekin junction (note farm track in bottom right of picture for scale)12
Figure 7:	Map of the Normanby catchment showing the LiDAR blocks reflown in October 2015. The orange blocks were flown in 2015 and the area in yellow represents the sections common to all three time slices which forms the basis for the current analysis
Figure 8:	Annualised erosion rates summarised across the 7 common LiDAR blocks from 2009-11 (WY 2010-11) and 20011-15 (WY 2012-15). Error bars represent the standard error between the 7 blocks at the total block scale. The low erosion rates from colluvial gullies are likely an artefact that the reflown LiDAR blocks concentrated on floodplain areas with predominantly alluvia gully and channel erosion, as well as the fact that there are many small colluvial gullies that may be below the limit of detection of the method17
Figure 9:	Annual Sediment contributions from different sources normalised per 100mm of incident rainfall18
Figure 10:	East Normanby River in the immediate aftermath of the flood generated by Cyclone Ita (photo Tim Hughes)19
Figure 11:	Close up of channel bank in the east Normanby River in the immediate aftermath of Cyclone Ita showing how little bank erosion occurred during this large event due to the dense riparian vegetation (photo Tim Hughes)20
Figure 12:	Mean daily discharge for the study period, Laura R at Coalseam Ck gauge20
Figure 13:	Mean daily discharge for the study period Normanby River at Battle Camp gauge21
Figure 14:	West Normanby River below the Cooktown Highway (-15.762320°S 144.976602°E) showing a) the location of the fenced cattle exclusion area and vegetation plots with a LiDAR background and b) the location of the fenced area and vegetation plots with an aerial photo background. Note that recareas in <b>Figure 14</b> a are zones of active gully erosion between 2009 and 2011 repeat LiDAR.
Figure 15:	Changes in ground cover inside and outside the West Normanby cattle exclusion site from 2011 to 2015 showing a) total % organic cover (grass, weeds, leaves, sticks, mulch) and b) % perennial grass cover, c) perennial grass tussock count, and d) pasture biomass yield
Figure 16:	Annual rainfall by water year (Oct-Sept) from 2011 to 2015 at Lakeland, Kings Plains, Crocodile, and Springvale27
Figure 17:	Changes in ground cover at different geomorphic units (terrace, gully, hillslope) inside and outside the West Normanby cattle exclusion site from

	2011 to 2015 showing a) total % organic cover (grass, weeds, leaves, sticks,
	mulch) and b) % perennial grass cover28
Figure 18:	Differences in pasture yield and grass biomass inside (right) and outside (left)
	the West Normanby cattle exclusion fence on a) the high terrace (left picture)
	and b) inactive gully slopes (right picture)28
Figure 19:	Measurement distributions of scour (negative) or fill (positive) at permanent
	vegetation plot reference stakes, accurate to 5mm, for fenced and grazed
	areas of the West Normanby gullies between 2011 and 201529
Figure 20:	Maps of the cattle exclusion fence in the 'Old Hay Paddock' at Crocodile
	Station (-15.710042° S; 144.679232° E) with a) LiDAR hillshade background
	and b) aerial photograph background showing locations of vegetation
	monitoring points inside and outside the exclusion area30
Figure 21:	Changes in ground cover in cover inside and outside the Crocodile Station
	'Old Hay Paddock' cattle exclusion site from 2011 to 2015 showing a) total %
	organic cover (grass, weeds, leaves, sticks, mulch) and b) % grass cover
	(standing perennial or annual grass)31
Figure 22:	Changes in vegetation cover and biomass a) before fencing at Plot 508 gully
	bottom in Nov-2011, b) after fencing at Plot 508 gully bottom in Nov-2012, c)
	grazed control at Plot 515 hillslope in Nov-2011, d) grazed control Plot 515
	hillslope in Nov-201231
Figure 23:	Grass and weed cover inside the cattle exclusion fence (left) and outside
	(right) in June 201532
Figure 24:	Hillshade LiDAR map of the cattle exclusion fence at GNGC6 (-15.896374°S)
	144.994678°E) and neighbouring spelled GNGC9 on the Granite Normanby
	on Springvale Station. Note that red areas are zones of active gully erosion
	between 2009 and 2011 repeat LiDAR32
Figure 25:	Changes in ground cover inside and outside the Granite Normanby cattle
	exclusion site from 2012 to 2015 showing a) total % organic cover (grass,
	weeds, leaves, sticks, mulch), b) % cover of perennial grass, c) perennial
	tussock count, and d) pasture yield (kg/ha)34
Figure 26:	Changes in ground cover at different geomorphic units (terrace, gully,
	hillslope) inside and outside the Granite Normanby cattle exclusion site from
	2012 to 2015 showing a) % cover of perennial grass and b) perennial grass
	tussock counts
Figure 27:	Differences in grass cover and biomass between the fenced gully (Left,
	GNGC6) and the grazed area (Right, GNGC9) on the high terrace of the
<b>F</b> :	Granite Normanby in a) April 2013 and b) November 201535
Figure 28:	Measurement distributions of scour (negative) or fill (positive) at permanent
	vegetation plot reference stakes, accurate to 5mm, for fenced and grazed
	areas of the Granite Normanby gullies between 2012 and 2015
Figure 29:	Map of the upper Normanby/Laura catchment showing the locations of the 4
<b>-</b>	grazing exclusion trial sites
Figure 30:	Exclusion plot layout at the West Normanby Bridge site in block N4 on
	Springvale Station. Also shown are the locations of the polygons within which
	erosion was detected by aerial LiDAR in the first period in green (LHS), and
	the second period in red (RHS)40

Figure 31:	Exclusion plot layout at the Granite Normanby River site in block N7 on
	Springvale Station. Also shown are the locations of the polygons within which
	erosion was detected by aerial LiDAR in the first period in green (LHS), and
Figure 22:	the second period in red (RHS)40 Exclusion plot layout at the Mosquito Yard site on Kings Plains Station in block
Figure 32:	·
	N10. Also shown are the locations of the polygons within which erosion was
	detected by aerial LiDAR in the first period in green (LHS), and the second
Fig 22.	period in red (RHS)
Figure 33:	Exclusion plots on Crocodile Station at block N17. Also shown are the
	locations of the polygons within which erosion was detected by aerial LiDAR in
=: 0.4	the first period in green (LHS), and the second period in red (RHS)41
Figure 34:	Example of primary gully erosion into an alluvial terrace on Springvale Station
	Normanby catchment
Figure 35:	Example of secondary incision into a >50 yr old primary gully floor -
	Springvale Station – Normanby catchment
Figure 36:	Aerial LiDAR DEMs of the Crocodile Station gully rehabilitation trial site with
	the rehabilitation trials plots overlaid on the 2009 DEM (LHS) (before
	treatment) and the 2015 DEM (RHS) 4 years post-treatment
Figure 37:	Example of a regraded alluvial gully in the Bowen catchment of unknown age
	with a constructed berm to exclude overland flow from the gully and with no
	soil treatment. This is the equivalent of the plot 1 control site - in which the
	gully is regraded with only direct rainfall driving high levels of ongoing erosion.54
Figure 38:	Photos of the treatment 7 x 25m 12% slope plots at the time of implementation
	in December 2011 and after the first wet season in 2012, and after 4 wet
	seasons in 201554
Figure 39:	Oblique aerial photograph of the Crocodile trial plots with the control area
	(CRGC1-28) to the right (note the actual areas used for control erosion
	measurements are smaller plots within the area indicated. Note
<b>-</b>	people/vehicles for scale (photo: John Brisbin)
Figure 40:	Remnant gully pedestal immediately downslope from plot 3 in June 2015,
	which is potentially buffering base level lowering downslope from plots 2-4 to a
Figure 44.	greater extent than the other plots
Figure 41:	DEM of Difference from 2012 (top) and 2013 (bottom); i.e. after one and two
	wet seasons respectively from Shellberg and Brooks (2013). Note that the
	images are presented in mirror to their actual orientation on the ground for
Eiguro 42:	ease of visualisation
Figure 42:	DEM of difference from 2013 to 2015. Note that range of fill and scour in this
	survey is much greater than that used for the previous survey, given that some
Ciaura 42.	of the deep rills are now up to ¾ of a metre deep
Figure 43:	Net annual erosion data for the 3 surveys completed since the inception of the
Figure 44.	gully regrade trials
Figure 44:	Daily rainfall at the DNRM gauging station on the Laura River at Coalseam Ck,
	which is the closest available daily rainfall record that covers the full trial
	period (additional data from the Crocodile Station homestead are
Eiguro 45.	forthcoming)
Figure 45:	Annual rainfall at the Coalseam Ck gauge which is around 23km from the site.
	The annual average for the 2014 and 2015 water years is around 740 mm60

Figure 46:	The relative change in sediment yield for the 7 treatment plots compared to (cf) the external untreated sections of gully adjacent to the study plots. Annual yields for Plots 1, 5, 6 & 7 were adjusted down by 30% for the last survey period to account for possible over estimation due to base level influence at these plots. The external control was the average of all sub-plots
Figure 47:	April 2013: Average percent (%) ground cover of live standing grass, live weeds, and dead organic matter (mulch) at CRGC1-29 at the end of the 2013 wet season (from Shellberg & Brooks, 2013)
Figure 48:	April 2013: CRGC1-29 plots and vertical and oblique photographs of upper (top) and lower (bottom) plots. Vegetation grid (4 m <sup>2</sup> ) is included for reference in the photographs season (from Shellberg & Brooks, 2013)
Figure 49:	Map showing the area along the lower Bowen River within which there is a major concentration of largely highly active alluvial gully complexes. The areas mapped in blue are hillslope gullies in the Oakey Ck sub-catchment64
Figure 50:	Turbid waters in the lower Bowen River (above) following a local storm 24 hrs earlier, while the river several km upstream, which was unaffected by the storm, remains clear (below). The area impacted by the storms has numerous highly connected alluvial gullies which deliver high suspended sediment loads directly to the Bowen main stem channel almost instantaneously upon receiving rainfall
Figure 51:	Large alluvial gully complex along Parrot Ck, a tributary entering the Bowen River just downstream of the Bowen Development Rd
Figure 52: Figure 53:	Satellite image of the alluvial gully sites shown above along Parrot Ck68 An extremely active alluvial gully system in the vicinity of the Bowen/Burdekin junction (note farm track in bottom right of picture for scale)

### **ACRONYMS**

BACI ..... Before-After Control-Impact

C ..... Carbon

**DOE** ..... Department of the Environment

**DRP** ..... Dissolved reactive phosphorous

GBR..... Great Barrier Reef

N ..... Nitrogen

**NESP** ...... National Environmental Science Programme

P ..... Phosphorous

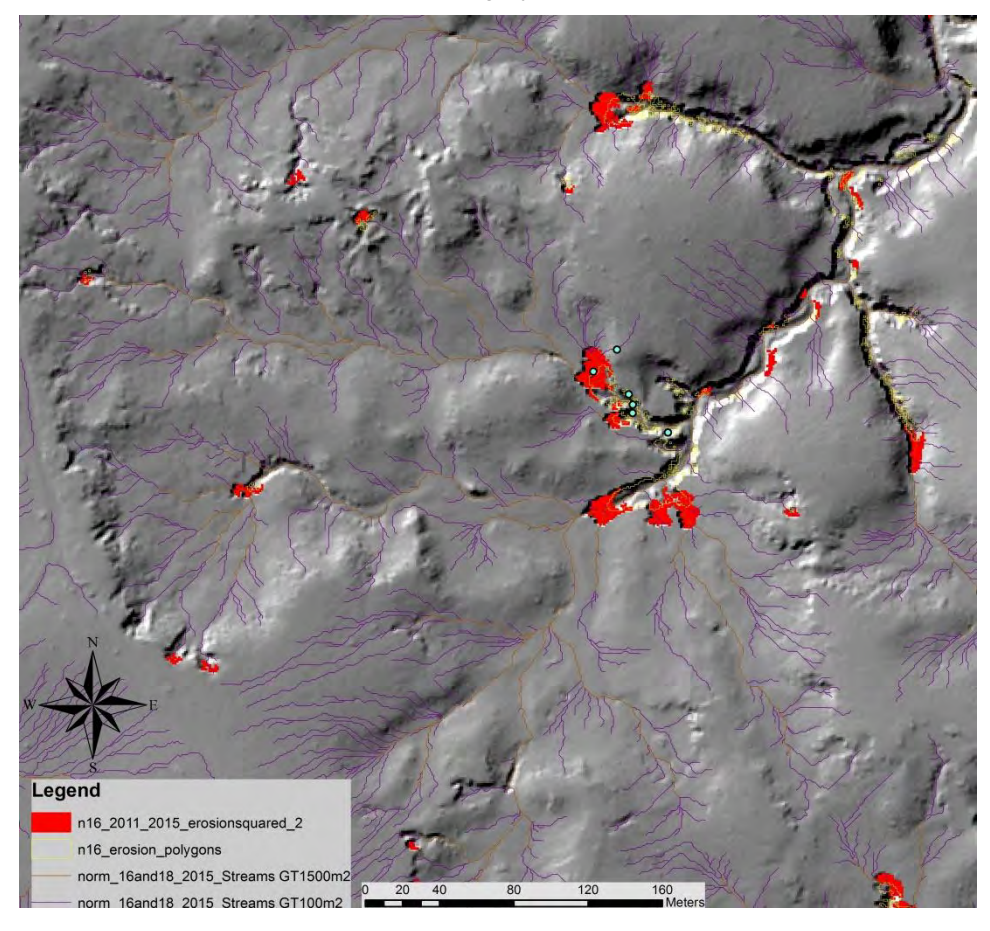
TN ..... Total Nitrogen

TOC ..... Total Organic Carbon

TWQ..... Tropical Water Quality



Oblique aerial of an alluvial gully in the Bowen Catchment.



Examples of LiDAR change detection between 2009-11 & 11-15 showing up to 10m of extension per year in alluvial gullies.

### **ACKNOWLEDGEMENTS**

We thank the traditional owners of all the country we have traversed to make this project happen including: Balngarawarra, Guguwarra, Western Yalanji, Bulgunwarra, Djugunwarra, Kuku Thaypan, Lama Lama, Olkola, and the Kalpowar Land Trust. We thank Daryl and Lynda Paradise from Kings Plains, Roy and Carlene Shepard from Crocodile Station, Damian Curr and Bridget Adams from Springvale Station, the Harrigan family from Normanby Station for their support of the project and for facilitating access to their land to enable us to collect the data that is central to this project. Many thanks to Lucas Armstrong, Brad Guy, Emma-Lee Harper, and Georgina Friend who conducted extremely hard field work for the cattle exclusion site monitoring. Tom Bezant and John Ross provided excellent fencing work at exclusion sites.



An example of attempted gully stabilisation in the Bowen catchment by gully regrading and the construction of a BERM – but with no soil treatment. Such an approach has in all likelihood increased sediment production from this gully.

### **EXECUTIVE SUMMARY**

### **Short-Term Erosion Rates in the Normanby Catchment**

Extensive LiDAR surveys in the Normanby catchment in 2009 and 2011 provided a large dataset of short term erosion rates from gullies, secondary ephemeral channels and large channels, which was the baseline for the new sediment budget produced for that catchment in 2013. In this study, we resampled 5536 ha of the previous surveyed LiDAR data in seven blocks focused on areas with the highest concentration of gullies and channels to test whether a consistent pattern of erosion has persisted amongst all process zones since the last survey.

### **Key Results**

1) Short term erosion rates from 2011 – 2015 vary considerably between different source process zones compared to the previous rates from 2009-11.

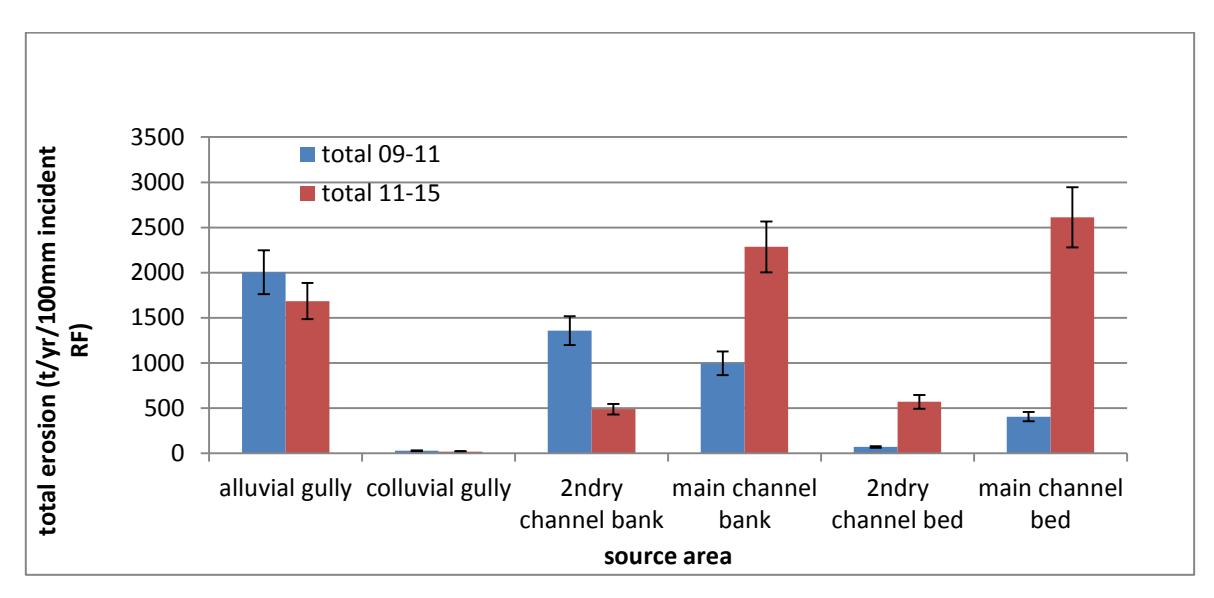


**Figure 1:** Annual sediment contributions from primary sources in 7 common Normanby LiDAR blocks normalised per 100mm incident rainfall (RF).

- a) Net gully erosion rates vary in a fairly predictable manner across large areas as a function of annual rainfall (which was lower and more variable over the latter period), but are highly variable at the scale of individual gullies. Based on these data, a more detailed understanding of factors controlling the variation in sitespecific gully erosion rates is required to help improve and prioritise gully rehabilitation efforts.
- b) Channel erosion rates do not respond to annual rainfall variability per se, rather they vary according to the magnitude and frequency of local flood events, which may or may not be correlated with annual rainfall totals. Channel erosion is much more difficult to predict without a much greater understanding of the variability of flood discharge at a range of scales throughout the drainage network (i.e. a distributed network of flow and rain gauges).

c) Relative changes at the LiDAR block scale (i.e. 300 – 1500 ha in area) indicate that current land use is not a strong control of net short-term change in the most active cohort of gullies detectable by aerial LiDAR, (which likely dominate sediment supplied from gullies) rather rainfall variability and other factors at the site scale are more dominant controls (such as stage of gully evolution and variation in soil erodibility).

### Implications:

These data indicate that if rehabilitation efforts were, for example, solely targeting gully erosion sources that apparent reductions in sediment yield at sources associated with gully management efforts could very easily be overwhelmed by channel erosion downstream. Given these findings the following considerations should be taken into account.

- A holistic catchment scale approach to tackling sediment sources is needed (e.g. implementing catchment scale riparian management programmes within the channel network; erosion reduction programmes in gully source areas; ensuring new land use disturbance sources are minimised). That is, whole of catchment resilience needs to be increased.
- 2) A hierarchical distributed monitoring programme throughout catchments is needed to detect changes in all erosion processes simultaneously. This should include fine resolution sediment tracing, detailed aerial and terrestrial LiDAR at nested scales, and traditional gauging of sediment yields at various catchment scales. These results demonstrate that if total sediment load at a downstream station was the only monitoring being undertaken (e.g. at an end-of-catchment super-gauge), and a major investment had been made in gully remediation during the monitoring period it is likely that no change would have been detected in this monitoring period due to the activation of a different set of sediment sources other than those being targeted by gully remediation. In such a scenario it is probable that false conclusions could have been reached about the success or otherwise of upper-catchment rehabilitation works due to a misunderstanding of the internal system dynamics.
- 3) The fact that grazing pressure was not a strong predictor of short-term large-scale gully erosion detectable by aerial LiDAR does not suggest that land use is and was not a key driver in initiating gullies and driving gully condition toward the state they are in today. Chronic land use disturbance still needs to be managed. However, these data indicate that there is large temporal hysteresis and time lags between initiation and recovery of alluvial gullies with exposed sodic sub-soils. Therefore, more proactive intervention to stabilize alluvial will also be needed to reduce erosion rates and sediment yields to achieve management goals in the next few decades.
- 4) Due to the coarse nature of aerial LIDAR that is only able to detect largescale erosion processes, additional finer resolution erosion monitoring will be needed in the future detect finer resolution responses to land management, such as soil surface erosion and nutrient loss above and within gullies.

### See Section 2 and Appendix A

### **Grazing Exclusion Trials**

Grazing exclusion sites in small alluvial gully catchments were established at 4 locations in the Normanby catchment in 2011/12 (total area 11.7 ha) as part of a Before-After Control-Impact (BACI) experimental design with dozens of plot-scale measurements sites inside and outside of fenced areas. In this report we present the preliminary results on vegetation response over the 2011-2015 period (as part of a 10-20 year study), as well as erosion rates from aerial LiDAR on large-scale change within exclusion and grazed areas.

- 1) Vegetation Changes at Exclusion Sites
  - a) Vegetation responded to varying degrees depending on the geomorphic units the sites were situated on within the gully complexes (e.g. high terrace surface, inactive gully hillslope, active gully slope) as well as the gully depth and stage of evolution.
  - b) Un-eroded high terrace surfaces had some positive changes to pasture condition (cover, tussock counts, biomass) following grazing exclusion. No major vegetation improvements were detected inside deep mature alluvial gullies with exposed sodic sub-soils. In shallow alluvial gullies, vegetation response was improved on inactive gully slopes and gully bottoms, but was still minimal at the most eroded plots with exposed sub-soils, which are likely to be the parts of the gully contributing the majority of the surface erosion.
  - c) Seasonal and inter-annual rainfall variability was a far more significant control on vegetation conditions than whether they were grazed or not over this period, but with greater vegetation cover and resilience during dry years in ungrazed areas.

### Implications:

- d) These results suggest that one to two decades will be required before we see any significant improvements in perennial grass cover in the internal eroded areas of gullies where cattle have been excluded, in order to overcome the signal of annual rainfall variability and the potential lag response of passive vegetation colonization.
- e) In some cases, passive vegetation recovery onto sodic sub-soils might not ever occur, or at least take many decades until the full cycle of gully evolution is reached.
- f) Since vegetation colonization onto very active gully surfaces of deep well developed gully complexes appears to be minimal in the short-term, it is unlikely that significant reductions in gully surface erosion and slumping from direct rainfall will result from cattle exclusion and vegetation response (see below). However, vegetation improvements in the un-eroded upslope catchments of alluvial gullies (here < 25% of totally gully catchment area) could promote infiltration, reduce runoff, and slow head scarp retreat rates in the long-term. The extent to which this contributes to significant reductions in gully sediment yields will need more investigation over the coming decade.</p>
- g) To reduce gully erosion sediment yields for short-term management goals to the GBR (i.e. next 10 years), it will be necessary to conduct additional management interventions beyond just cattle exclusion to hasten the recovery, such as supplementary grass seeding from the air or ground, organic mulching of sodic soils, fire and weed management, and slope stabilization through bioengineering.

h) Managing chronic grazing disturbance of sodic soils along river frontage is essential to preventing the new initiation of alluvial gullies and promoting passive hydrogeomorphic recovery where possible. Fencing cattle out of these sensitive areas remains a critical first step in any gully management scenario that seeks to manage this erosion in the long-term, regardless of whether exclusion leads to major short-term sediment and nutrient reductions in its own right.

### 2) Erosion Rates from Aerial LiDAR Data at Exclusion Sites

- a) Aerial LiDAR surveys only detect large-scale erosion features in alluvial gullies, such as scarp retreat and slumping over the short term (i.e. few years), but not rilling or soil surface stripping that is < 0.2m deep. Plot scale measurements of surface erosion and deposition (i.e. at posts within the centre of each 4m² survey plot) showed no major trends from grazing exclusion over 4 years, but did highlight the variability and magnitude of surface erosion and deposition within gullies that are common over large areas. Surface erosion and rilling can contribute up to 70% of total sediment and nutrient yield from gullies at the event or annual scale, and so the sediment yield represented by the LiDAR data is an absolute minimum.</p>
- b) BACI comparisons with aerial LiDAR howed there were significant reductions in large-scale erosion as a result of 3 4 years of excluding cattle from three exclusion sites with major active gully erosion (combined area of 11.7 ha), although the statistical effect was contributed from just one of the sites that was the site that was least constrained in terms of grazing pressure inside and outside the exclosure (i.e. the grazed area was inside a set of large yards that were periodically grazed, and the ungrazed area was outside the yards, and still had low level grazing).
- c) Specifically the LiDAR measurements show:
  - i) That there was a significant difference in erosion detectable by aerial LiDAR between the fenced and grazed areas prior to the exclosures being established, with there being more erosion in the fenced areas than the unfenced at the start of the study (p=0.0026)
  - ii) That there was a significant decline in erosion rates in the second period compared to the first period in both the fenced and grazed plots (p=0.0001)
  - iii) That there was a significant difference in gully erosion detectable by aerial LiDAR between the pooled fenced and grazed areas 3-4 years after the establishment of the exclosures (p=0.007)
  - iv) Small plot size and the relatively small erosion dataset (n=35 grazed; n=29 fenced erosion cells) and high standard deviations (26 to 36% of mean) affects the statistical power of these tests. More robust statistical analysis following BACI design utilizing higher resolution data from larger exclusion plots will be needed in the future.

### Implications:

d) The coarse nature of aerial LiDAR and ability to only detect large-scale erosion features over short time periods highlights the need to monitor surface and gully

- erosion and yield at a finer resolution, using more sensitive techniques such as 1) ground-based terrestrial LiDAR, and 2) via sediment and nutrient yield gauging at gully outlets. Grazing exclusion areas could also be much larger to increase the sample size of gullies across larger areas, and reduce the potential confounding effect of wallaby grazing.
- e) Regardless of the intensity of monitoring, in areas of deep active gully erosion with exposed sodic sub-soils, it is highly unlikely that grazing exclusion alone will reduce soil erosion in these active features or make a large reduction in overall sediment yields on timescales of one to two decades. More intensive rehabilitation of these active features will be needed following bioengineering and slope stabilization approaches that are matched to the stage of gully evolution.
- f) Cattle exclusion and vegetation recovery may be more effective at reducing sediment and nutrient loss in shallower gullies or younger gullies earlier in the stage of evolution. More detailed measurements will be needed in these types.
- g) Future studies should test the effect of cattle exclusion and vegetation recovery on nutrient budgets as well as sediment budgets, especially the fine-scale processes of nutrient losses from soil surfaces.

### Alluvial Gullies as Major Sources of Bioavailable Nutrients

In a first of its kind, a pilot study was conducted at four sites in the Normanby catchment that looked at the levels of bioavailable nutrients found in soils that were actively eroding via alluvial gully erosion.

### **Main findings**

 While it has been documented that gullies are an important source of fine sediment to the GBR, it is also apparent the gully sources are a much under-appreciated source of nutrients as well. When compared to typical values of anthropogenic nitrogen (TN) and phosphorous (TP) from other major land uses in GBR catchments, it is apparent that gullies could be even more significant sources than intensive agricultural land per unit area.

**Table 1:** Comparison between sediment and nutrient contributions from alluvial gullies vs other intensive land uses in the GBR Wet Tropics catchments. Note the sediment yields from gullies are absolute minima, given that they only represent erosion detectable from aerial LiDAR.

Gully/land use	sediment (t/ha/y)	TN (kg/ha/y)	TP (kg/ha/y)
Granite Normanby	114.0	54.0	23.7
Laura - Crocodile station	29.2	10.5	0.3
Laura - Crocodile Gap	28.8	12.6	1.6
Sugar cane	1.2	22.2	2.7
Banana	1.8	25.3	3.1
Nature conservation	0.2	3.6	0.3

- The data highlight that the surface soils on the terraces into which the alluvial gullies are migrating have total organic carbon (TOC) concentrations that are 54 to 77 times larger (depending on particle size fraction) than the sub-surface soil, while TN is enhanced 5 to 10 times in surface soils compared to sub-surface.
- The data indicate little difference between bioavailable nutrient indicators in sampled hillslope (n=1) and alluvial gullies (n=3) for all particle size fractions sampled. Much more sampling would be required to confirm this trend.
- There are significant differences in C, N, and P content among soils/sediments in the
  different geomorphic units measured, with the general pattern being terrace > bank
  surface > gully floor > bank subsurface. This result indicates that accurate estimation
  of nutrient and organic losses from gullies must rely on sampling and measurement of
  the different units.
- The upper 10-20cm of alluvial terrace soil profiles appear to be an important long term store of bioavailable nutrients and organics, whilst gully floors may act as a temporary store depending on gully evolution stage.
- Primary gully erosion into terrace alluvium is ubiquitous in catchments like the Normanby and Burdekin (**Figure 34**).
- Particle size significantly influences nutrient and organic content and would influence bioavailability - hence particle size fractionation should be a major consideration in future study designs.
- The <10um fraction is generally enriched in bioavailable nutrients compared to the <63um fraction (1.4 to 3.3 times on average for carbon and nitrogen fractions), which is generally enriched compared to whole soil irrespective of gully geomorphic unit (with some exceptions e.g., DRP) (1.4 to 9.5 times on average for carbon and nitrogen fractions). These results from gullies in the Normanby catchment are consistent with results from key soil types in the Burdekin and Johnstone catchments (Burton et al., 2015).</p>
- Although terrace soil had the highest concentration of most nutrients and organics, sub-soil was generally the main source of sediment in these alluvial gullies, due to the sheer volume of sub-soil delivered from active gully erosion detectable by aerial LiDAR. Given that much of the undetected erosion from aerial LiDAR is likely to be from surface erosion of exposed sub-soil surfaces within the gully, the relative contributions from the sub-surface component could be even higher than that reported in this study.
- The sources of organics and nutrient export from alluvial gullies would vary depending on the type of erosional process occurring in the alluvial gully (i.e. headscarp retreat vs. secondary incision vs. soil surface stripping) and their stage of evolution (e.g., gully depth and age). However these findings should be confirmed with larger sample replication. Hence, it is critical that we have a good understanding of the different forms and age of gully erosion around catchments
- The contribution of terrace soil to nutrient export varied with the stage of gully evolution. In the initial stages of gully evolution [very shallow gullies (<1.0 m) growing fast into the terrace deposits], terrace soil is the main source of nutrient export. As a result it should be a priority to protect terrace deposits from fast headscarp retreat as these deposits contain large pools of carbon and nutrients that, when lost, would be very difficult to restore. These terrace soil organic and nutrient pools may also be the most bioavailable and have a larger relative impact once in the aquatic environment.</p>

- As gully incision occurs, the main source of most nutrient fractions was clearly gully bank subsurface sediment (from headscarp retreat, sidewall slumping, surface erosion). Although this sediment has lower nutrient concentration than terrace surface soil or gully floors, the sheer quantity of exported sediment from this source (detectible by LiDAR) makes it the largest contributor of nutrients. Therefore, despite the nutrient enrichment of the surface soils (which are a component of both gully headscarp and sidewall retreat) gully sub-soils would tend to be the main source of nutrients by volume. Hence, there is no one component of a gully system that can be prioritised over another; the whole gully should be stabilised as all components are significant nutrient sources.
- When secondary incision erodes organic and nutrient rich sediment deposited on gully floors, this sediment may become a very important source of organics and nutrient export; even more so than bank subsurface soil. The protection of gully floor organics and nutrient deposits should be part of gully rehabilitation designs and should be prioritized when these deposits are rich in organics and nutrients.
- The majority of the nitrogen in alluvial gully soils/sediments is in organic form (more than 96% in all particle sizes and geomorphic units). The exported organic N from alluvial gullies is potentially bioavailable and thus may be mineralized into dissolved inorganic nitrogen during stream transport, once it gets to the estuarine or marine environment, or be used directly by algae in dissolved organic form.

### Gully Regrading and Bioengineering Treatment Plots – 4 years on

A series of experimental erosion plots established in 2011 have been resurveyed in 2015 to test the ongoing response of gully headwall regrading and soil surface treatments since the last terrestrial LiDAR survey in 2013. The results from the first 2 years are reported in detail by Shellberg and Brooks (2013), while results from the last two years and whole period are reviewed here. The Crocodile Station gully rehabilitation trial site was established to trial different bioengineering approaches for stabilizing active gully headwalls in highly sodic alluvial soils. Primary active gully headscarp and sidewall retreat represent a major source of fine suspended sediment and nutrients contributed to the stream network in the Laura and Normanby River catchments, as measured by large-scale gully erosion rates across >5000 ha (Appendix A). Developing optimal approaches for stabilizing such gully headscarps and associated gully side walls is critical if the sediment and nutrient inputs from gullies are to be reduced in any meaningful way within appropriate management timeframes (i.e. one to two decades).

The Crocodile Station site includes a set of un-battered control sites and regraded control and treatment plots established to test which set of soil amendments would provide the greatest degree of sediment reduction over the short term, in addition to the influence of machine regrading on sediment erosion.

#### The trials showed that:

Largest aggregate reduction in sediment yield across the first 2 – 4 years
was the site treated with hydromulch (seed, mulch, gypsum, fertilizer),
although this was mainly due to the lower erosion than all other treatments in
the first year due to instant soil surface protection and binding. After 4 years,
aggregate erosion is 10% of the untreated un-battered control.

- Plots treated with compost and gypsum, and either native or exotic grasses, performed in a very similar manner and provided the most sustainable results. After the first year, these plots were performing better than the hydromulch treated plot. They have established a self-sustaining vegetation community, albeit not with the original planted grass species but rather invading exotic grasses and weeds. After 4 years aggregate erosion is just over 20% of the untreated un-battered control.
- Grass biomass yield and ground cover was significantly greater in both the sites treated with compost and gypsum than the hydromulch treated plot – which despite having the lowest aggregate erosion rates, didn't perform as well in year two in terms of biomass.
- The treatments without gypsum and fertilizer did not perform well enough to warrant them be used as ongoing treatments. The gypsum did however neutralize the soil sodicity and significantly improved infiltration, but this alone was not sufficient to significantly reduce surface erosion rates.
- The battered control plot without any soil treatment increased erosion rates above the untreated control and background rates, as did the gypsum only treatment and the straw/exotic grass seed treatment. Therefore, regrading gully slopes without a full suite of soil amendments will only increase erosion, not decrease it.

### Other lessons from these trials:

- Over time the erosion results became more influenced by the antecedent base-level conditions of each plot despite being shaped equally at the start. Coincidentally, the most successful plots were buffered from base level control by a remnant pedestal, while the least successful were partially influenced by gully channel bank erosion in the larger gully complex. Ongoing analysis of these plots is not recommended after this 4 year period due to this confounding factor.
- Great care must be taken to ensure gully base level is adequately controlled during gully slope stabilization, otherwise treatments can be undermined by downstream base level controls.
- When scaling these treatments up to the whole of gully scale, a range of additional controls on gully floor incision will need to be applied in concert to ensure secondary incision doesn't occur.

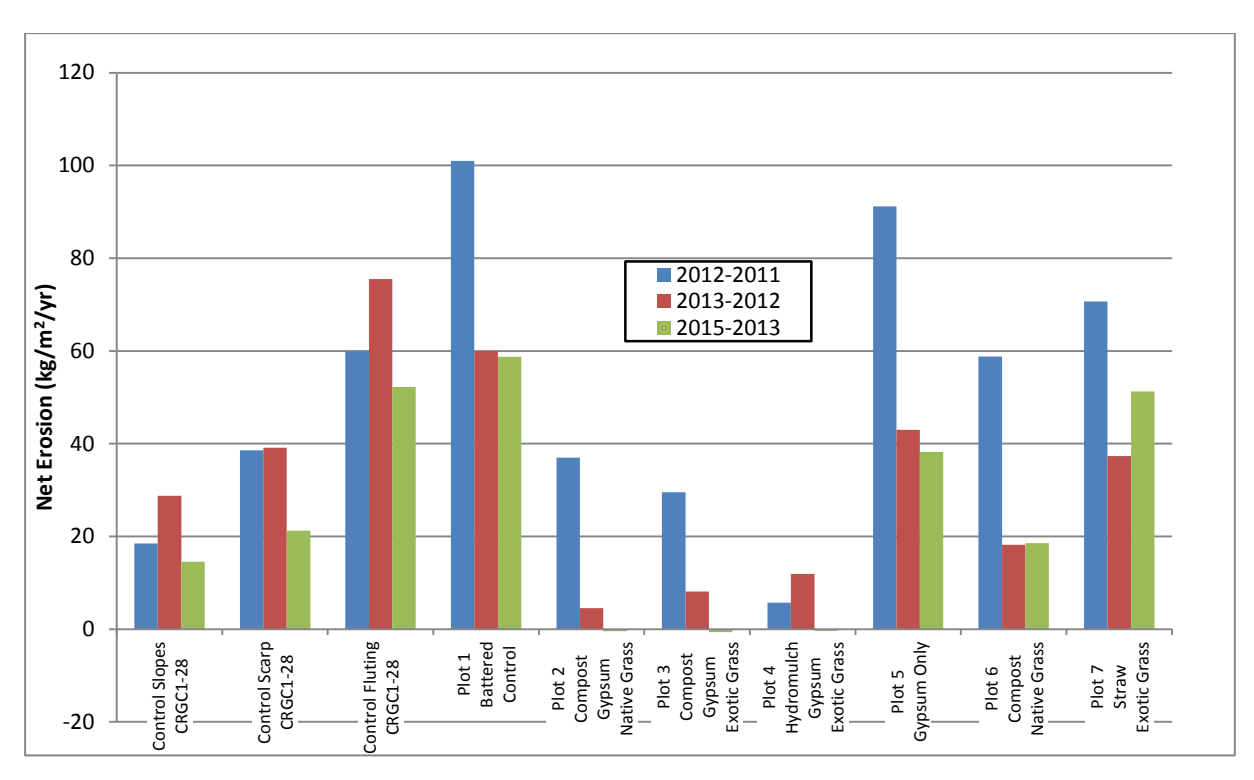
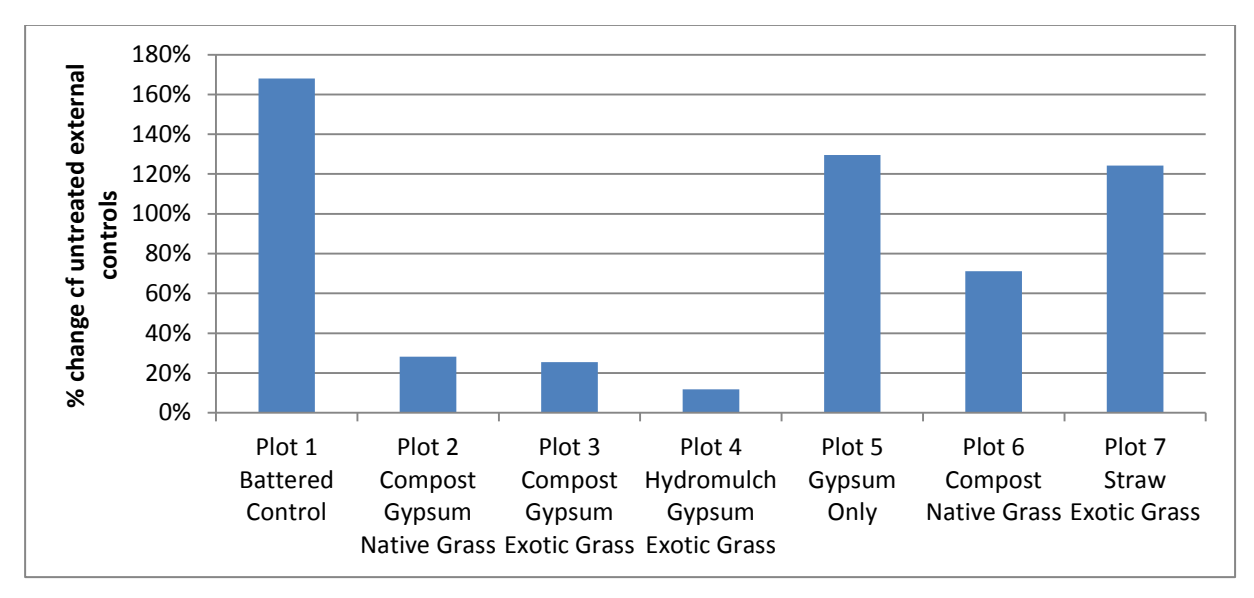


Figure 2: Net erosion across the three monitoring periods (4 years)



**Figure 3:** Percentage change in mean annual sediment yield compared to (*cf*) external untreated controls for the four years surveyed

## Alluvial Gullies in the Bowen Catchment, and implications for managing sediment and nutrient sources to the GBR

Having identified the significant role that alluvial gullies play in the Normanby catchment, it is an open question as to what extent such gullies play a role as sediment and nutrient sources in other GBR catchments. In this project we began the process of assessing the likely role of alluvial gullies in the Bowen catchment. However, much more data is required to fully understand the role of these gullies in this catchment. Preliminary mapping was undertaken

along the lower 100km of the Bowen River to assess the potential that alluvial gullies are playing as a dominant source of suspended sediment to this, the highest sediment producing sub-catchment in the entire GBR.

The Burdekin catchment is estimated to produce 47% of the suspended sediment input to the GBR lagoon, and of this, 65% of the Burdekin load is sourced from the Bowen/Bogie subcatchments, and more than 50% of this is from the Bowen sub-catchment, which represents 9% of the total catchment area of the Burdekin catchment.

Along the lower 100km of Bowen River floodplain, we mapped around 330 large alluvial and colluvial gully complexes, having an average area of 7.8 ha (stdev – 19ha).

The alluvial gullies in this area are some of the largest and most active gullies we have witnessed anywhere in northern Australia, and based on rates observed for similar types of gullies elsewhere, several hundred of these gullies could on their own be contributing a large proportion of the suspended sediment load from the Bowen River. Hence, it is a high priority to begin the collection of LiDAR data in this area, along with field measurements of sediment yield, so that we can begin to measure the rates of sediment production from these gullies and hence be able to prioritise management effort in this area.

#### **Recommendations:**

- 1. Immediately acquire aerial LiDAR data over the entire lower 100km of the Bowen floodplain as a basis for more accurately mapping the distribution of alluvial gullies and as a baseline for measuring ongoing large-scale erosion rates.
- 2. Undertake historic aerial photo analysis to determine rates of activity of a representative selection of the mapped alluvial gullies.
- 3. Begin the process of sampling gullies with terrestrial LiDAR to measure erosion rates at high resolution to understand both surficial and deep-seated erosion.
- 4. Undertake detailed mapping of gully types to help in ranking management priority of the gullies and to best match the appropriate treatment to gully type.
- 5. Undertake detailed soil analysis to better understand the role of soil chemistry and particle size on rates of gully activity and gully form and hence aiding the process of identifying the optimal treatments for stabilising the wide range of gullies that are found in the Bowen area.



**Figure 4:** Large alluvial gully complex along Parrot Ck, a tributary entering the Bowen River just downstream of the Bowen Development Rd



Figure 5: Satellite image of the alluvial gully sites shown above along Parrot Ck.



**Figure 6:** An extremely active alluvial gully system in the vicinity of the Bowen/Burdekin junction (note farm track in bottom right of picture for scale).

### 1. SUMMARY REPORT

### 1.1 Background

Following extensive research effort under the previous Reef Rescue programme (Brooks et al., 2013), a new empirical sediment budget was derived for the Normanby Basin that completely recast what were previously thought to be the dominant sediment sources in this catchment, and by extension the entire northern part of the Great Barrier Reef (GBR). With a catchment area of around  $24,353 \, \mathrm{km^2}$ , the Normanby basin is estimated to deliver about 50% of the sediment contributed to the northern section of the GBR, although few empirical data are available from any of the other basins to confirm this figure. From the data presented in Brooks et al. (2013), we now know that the vast majority (85-90%) of fine sediment (i.e. both < 10 $\mu$ m and < 63 $\mu$ m fractions) is sourced from sub-surface erosion processes, including main channel erosion (8%), small ephemeral tributary channel erosion (52%), and from both alluvial (24%) and colluvial gully (13%) erosion. These data are our best current source estimates, but will be continued to be refined as more empirical data become available at finer scales to continue refine the sediment budget.

Of these sources alluvial gully erosion in particular probably represents the dominant source of erosion that has been accelerated by land-use pressure, but myriad small colluvial gullies are also a significant source of sediment albeit typically not as well connected to the main stream network as alluvial gullies. Cattle grazing, fire regime changes, weed invasion, tree thickening, fenceline disturbance, and road erosion can all accelerated alluvial and colluvial gully erosion directly or indirectly. It is also likely that a significant proportion of the erosion in secondary channels is accelerated by land-use, given that these channels are more directly impacted by grazing pressure right to the bank tops and into the channels themselves, but also due to elevated sand bedload delivered from gully erosion in the catchments of these small tributary systems. In a comprehensive study of the drivers of channel erosion in this and other catchments (Brooks et al., 2014), it was found that bed material accumulation was strongly correlated with channel erosion. It is difficult to put a precise figure on the extent to which channel erosion is accelerated above long-term "background rates" (i.e. last 5000 years prior to the arrival of Europeans), but given that the available evidence indicates alluvial gully erosion rates have increased up to 10 fold above "background rates" since European settlement (Brooks et al. 2013; Shellberg et al. 2016), it would not be unreasonable to expect that channel erosion rates may have doubled in that period due to the combined effect of direct disturbance by cattle and other feral animals, and increased bedload sediment supply.

### 1.2 Research Objectives of this Study

### Extension of short term erosion rate dataset

One of the key limitations of the dataset upon which the 2013 Normanby sediment budget was based, was that much of the data was based on short term erosion rates derived from aerial LiDAR data collected during the study period 2009 – 2011. Hence, one of the key objectives of this new research was to extend the period of record for the erosion through the acquisition of new LiDAR data enabling us to assess erosion rates and the relative

contributions from different source areas over the period 2011-2015. Of the original 41 blocks (or 78,250 ha) of LiDAR data captured across the Normanby in 2009, around 22% (or 16,310 ha) was reflown in 2011, representing 0.7% of the total catchment area. Sufficient resources were not available to refly all of this again in 2015, so the refly focused on 7 of the LiDAR blocks in the upper Normanby and Laura Rivers, with a total area of 5536 ha, or 0.23% of the total catchment and 7% of the original 2009 data.

The analyses of these data provide the basis for addressing the following research questions:

- 1. Have annual erosion rates between 2011-2015 remained consistent with the trend observed in the period 2009-11?
- 2. Have the relative contributions from different source processes remained consistent through time?
- 3. If the rates and the relative contributions from different sources have not remained consistent, can this be explained by changes in:
  - a. Rainfall
  - b. Flood regime
  - c. Land use
- 4. What are the implications of these findings for catchment-based strategies for targeting sediment sources?

### **Gully Rehabilitation Trials**

Having determined in the 2013 sediment budget that gully erosion, and notably alluvial gully erosion in highly dispersive sodic soils, was a major source of the anthropogenic sediment load to the Normanby catchment and the northern GBR, a series of initial gully rehabilitation trials were established in 2011 to begin the process of determining the most effective means of reducing erosion from catchment sediment sources in the most timely fashion. Details of these trials and 20011-2013 results have been previously published in Shellberg and Brooks (2013). In this study we have the opportunity to report on a further two years of monitoring of erosion rates following rehabilitation at the experimental plot scale on Crocodile Station. We also provide some preliminary results from of a series of grazing exclusion trials established in 2011/12 and monitored through 2015, as part of a longer-term 10-20 year monitoring program.

At the grazing exclusion sites the following questions are addressed:

- 1. Is there any evidence for a response after 3 4 years of grazing exclusion in vegetation biomass, community composition, or ground cover on different geomorphic units?
- 2. Is there any evidence suggesting that significant reductions in sediment yield might be achieved on decadal timescales (i.e. to make significant in-roads into Reef Plan targets) from grazing exclusion alone in areas\_dominated by active alluvial gully erosion?
- 3. Do the initial trends support the notion that grazing exclusion alone from gully erosion hotspot areas will make significant inroads into Reef Plan sediment and nutrient reduction targets over the next decade?

At the Crocodile experimental plot sites we address the following research questions:

- 1. Are the rehabilitation and erosion reduction trends that were apparent after 2 years of monitoring still on the same trajectory after 4 years?
- 2. Is there any evidence that cyclones impacted these sites and if so did they have a disproportionate impact on the sites?
- 3. How resilient do these treatments appear to be after 4 years, and can we learn anything yet about the likely longer term behaviour of these treatments?
- 4. What can we learn from these plots in terms of erosion processes that is relevant for up-scaling these plot-scale treatments to whole of gully treatments?

### Gullies as Key Sources of Anthropogenic Bioavailable Nutrients

Gullies are now well documented as being major sources of fine sediment to the GBR. One of the important knowledge gaps regarding these gullies, is to what extent do these also represent important sources of particulate nutrients? To date, GBR water quality models have assumed gullies, and grazing land more generally, are not dominant contributors of elevated nutrient loads to the GBR, with most of the elevated loads attributed to intensive agriculture in the wetter coastal areas where most intensive agriculture is focused. So in this research we undertook a pilot study in some gullies within the Normanby catchment, for which we have reasonably accurate estimates of their sediment contribution, and posed the question as to how much nutrients these gullies were also supplying to the stream network and into the GBR lagoon?

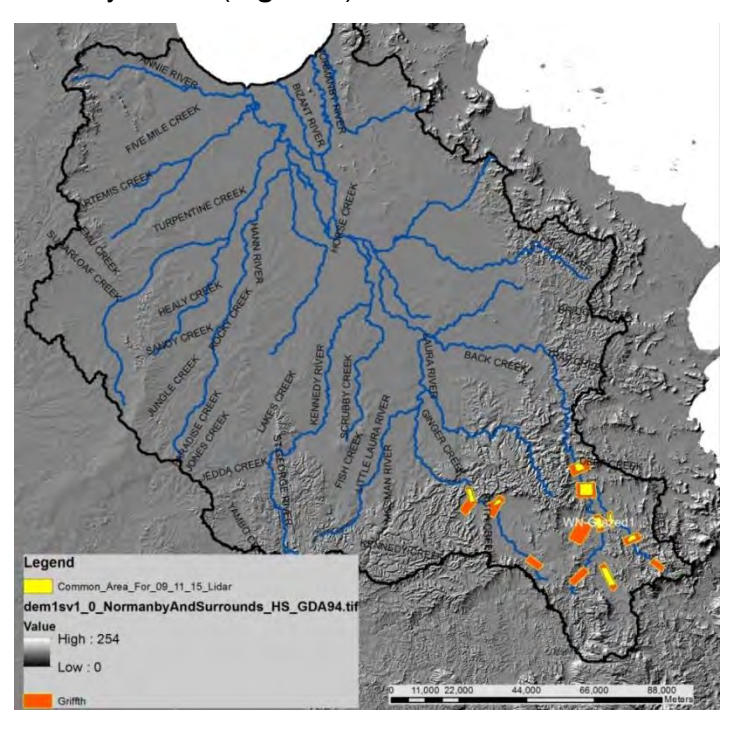
### Alluvial Gully erosion in other GBR catchments

We now have a very clear picture of the extent of alluvial gully erosion in the Normanby catchment. These gullies pose a clear threat to GBR water quality not only in terms of fine suspended sediment but also in terms of particulate nutrients. To what extent are similar processes also occurring in other GBR catchments? In this part of the project we present preliminary mapping data from the lower Bowen River and explore the extent to which such sources may be dominating the sediment load from the Burdekin River.

### 2. KEY FINDINGS

# 2.1 Recent trends in erosion sources within the upper Normanby and Laura Rivers (Brooks, Curwen & Spencer)

In this study we resampled 5536 ha of LiDAR data for which we have corresponding data from 2009 and 2011, focused in the previously defined gully erosion hotspots within the upper Laura and Normanby Rivers (**Figure 7**).



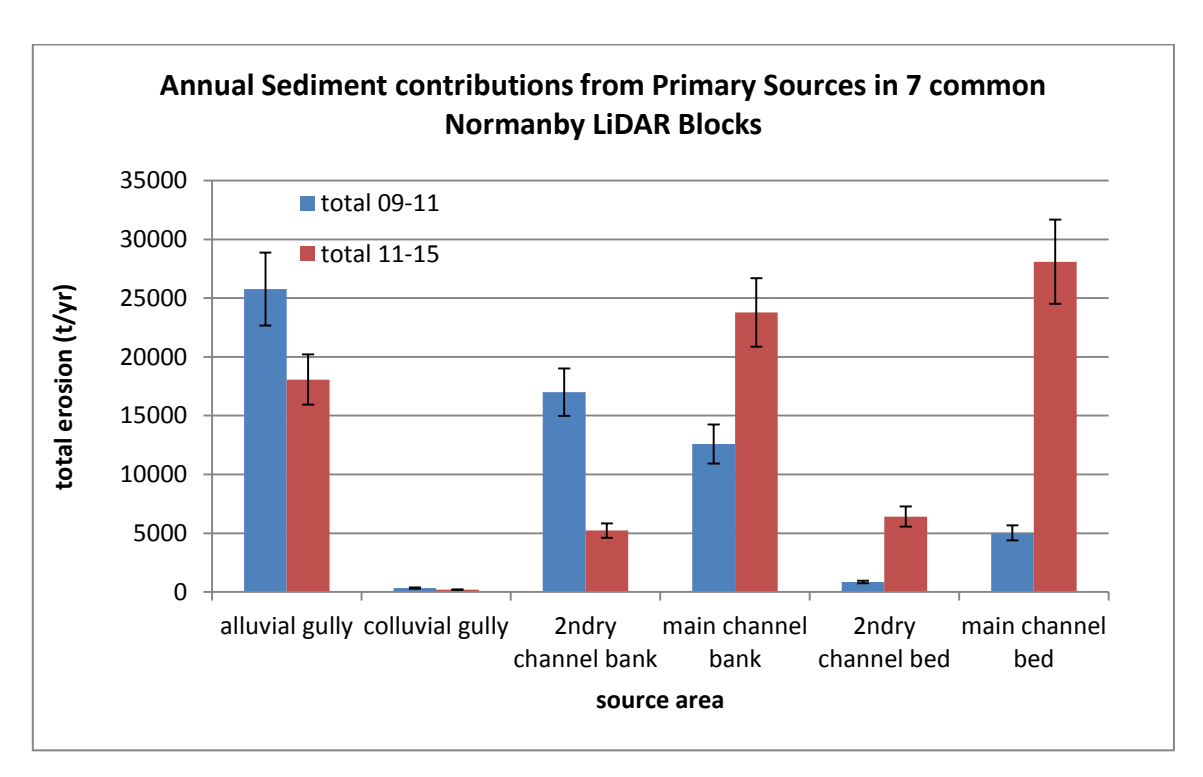
**Figure 7:** Map of the Normanby catchment showing the LiDAR blocks reflown in October 2015. The orange blocks were flown in 2015 and the area in yellow represents the sections common to all three time slices which forms the basis for the current analysis

Table 2: Summary statistics of the LiDAR blocks resurveyed in 2015

Block	Common area 09-11-15 (ha)	total area Google Gullies (ha)	total area Lidar Mapped Gullies (ha)
4	1021.7	27.4	200.4
5	1491.5	33.7	304.1
7	1113.1	84.5	239.5
9	397.9	5.3	75.9
10	616.1	7.1	126.2
16	613.3	27.5	148.1
17	283.3	1.9	36.6
total	5536.8	187.3	1130.7
	-	% of bare ground alluvial gullies in blocks	% of block area alluvial gullies
		17%	20%
Total a	area of GE gullies across Normanby	catchment =	2431 ha

# 2.1.1 Changes in Short term Erosion Contributions Between Time 1 (2009/11) to Time 2 (2011/15)

From the 5536 ha sampled in the most recent study, relative contributions from the key sources to the overall sediment budget over the year period from 2011-15, differ significantly to the previous period 2009-11 (**Figure 8**). It must be stressed that these results have not been up-scaled to the whole catchment sediment budget in this study. Indeed it would be questionable to do so from this relatively confined sample, so we cannot directly compare the overall contributions from the previous sediment budget, but it is fairly evident that they differ significantly. It also should be stressed that aerial LiDAR can only detect large-scale erosion processes, such as major scarp retreat, slumping, bank erosion, and channel aggradation/degradation. Aerial LiDAR over short time periods cannot detect surface erosion, scalding and soil surface stripping, and rilling, and so the detected yields represent an absolute minimum.



**Figure 8:** Annualised erosion rates summarised across the 7 common LiDAR blocks from 2009-11 (WY 2010-11) and 20011-15 (WY 2012-15). Error bars represent the standard error between the 7 blocks at the total block scale. The low erosion rates from colluvial gullies are likely an artefact that the reflown LiDAR blocks concentrated on floodplain areas with predominantly alluvial gully and channel erosion, as well as the fact that there are many small colluvial gullies that may be below the limit of detection of the method.

### 2.1.2 Drivers of change between time 1 and time 2

Normalising for annual rainfall (i.e. per 100mm annual rainfall **Table 3**, **Figure 9**) helps to explain some of the variability in annual sediment yield from gullies (explaining 84% of the net inter annual variability). Not surprisingly this has little bearing on the channel erosion rates, which are more flood event and threshold driven phenomenon.

		Kings Plains Stn.	East Normanby	Laura PO	Coalseam Ck	all yrs av
period 1	WY 2010	1157	1003	598	765	
	WY 2011	1982	1564	1595	1617	1285
	WY 2012	1469	1264	1204	1201	
period 2	WY 2013	1006	922	1057	1156	
	WY 2014	1406	1380	1116	1093	
	WY 2015	987	735	538	391	1058
ratio period 2 to period 1 =						0.82

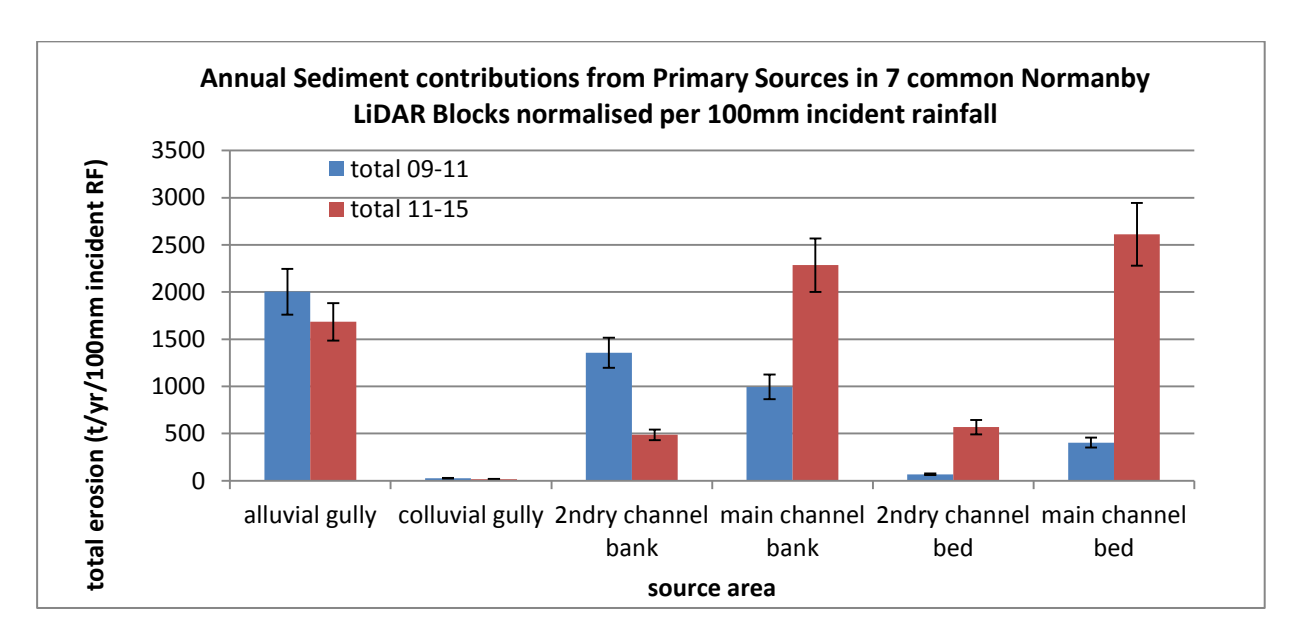


Figure 9: Annual Sediment contributions from different sources normalised per 100mm of incident rainfall.

Insights into why the channel erosion processes differ so markedly between the two periods are more apparent from the flow data from the Laura and Normanby Rivers, given that channel processes are influenced more by the magnitude and duration of individual flood events than total annual rainfall. Interestingly, secondary channel bank erosion rates are significantly lower than the earlier period (36% on average compared to the previous period), while bed erosion rates for the same secondary channels have increased 8 fold on average (**Table 4**), albeit with one extreme outlier in Block 10 on Kings Plains station. Main channel bank erosion has also increased significantly in the second period by a factor of 2.3 on average, while main channel bed erosion increased on average by a factor of 6.5. The changes in the extent of erosion in the main channels likely reflect the impacts of larger floods generated by Cyclones Oswald and Ita in particular (**Figure 10**). It is interesting to note, however, that whilst the cyclone Ita flood was the second largest flood on record in the East Normanby River, and significant mobilisation of the bed was evident, due to the extent of riparian vegetation within the channel it is remarkable how little erosion resulted from this flood.

**Table 4:** Ratio of change on rainfall normalised erosion rates for each LiDAR block expressed as time 2 (2011-15)/time 1(2009-11)

	sed c	ontributior	n per					
change ratio	block (t/	100mm R	F/yr)					
sed source	N4	N5	N7	N9	N10	N16	N17	total
alluvial gully	1.56	1.07	0.54	1.12	1.09	0.71	0.29	0.84
colluvial gully	0.72	0.76	1.65	0.00				0.70
2ndry channel	0.55	0.50	0.22	0.77	0.54	0.20	0.20	0.36
main channel bank	14.5	3.62	1.70	0.79	28.9	4.73	0.00	2.30
2ndry channel bed	3.05	26.18	0.50		657	1.33	0.30	8.24
main channel bed	55.2	9.43	4.86	2.93	4.93	1.51		6.46
total	4.18	2.51	0.72	0.89	2.31	1.42	0.23	1.58



**Figure 10:** East Normanby River in the immediate aftermath of the flood generated by Cyclone Ita (photo Tim Hughes)

Table 5: Comparison of water flow statistics in the Laura and Normanby Rivers for the two study period intervals

	Normanby River at Battlecamp		Laura River a Ck	
	2009-11	2009-11 2011-15		2011-15
Total Q (GI)	2500	2140	996	990
# days > 100 cumecs	100	49	31	15
# days > 500 cumecs	4	7	2	3
# days > 1000 cumecs	0	3	0	2



**Figure 11:** Close up of channel bank in the east Normanby River in the immediate aftermath of Cyclone Ita showing how little bank erosion occurred during this large event due to the dense riparian vegetation (photo Tim Hughes).

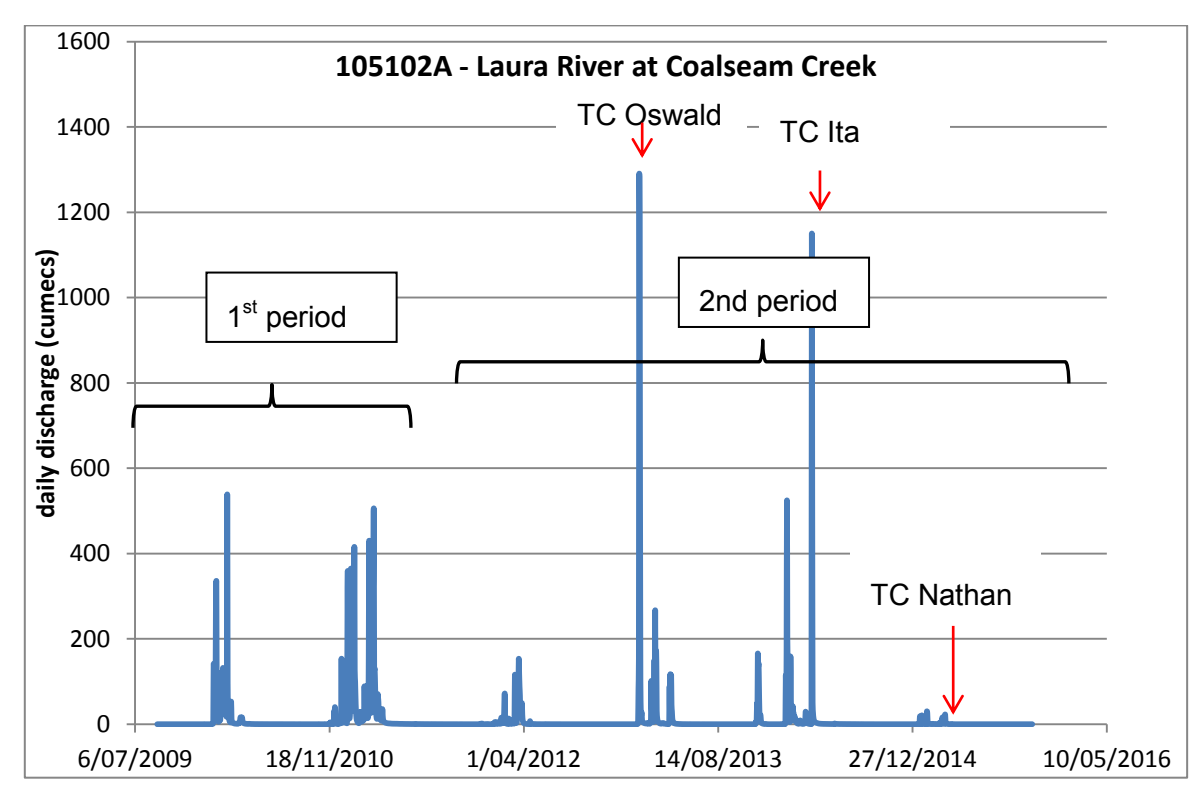


Figure 12: Mean daily discharge for the study period, Laura R at Coalseam Ck gauge.

From the water flow data presented in **Figure 12** and **Figure 13** and the summary statistics in **Table 5**, it is apparent that the flow regimes differ markedly for the two periods, with total

discharge being almost the same, despite the latter period being twice as long as the former. There were double the number of moderate sized events (i.e. 100-500 cumecs) in the earlier period compared to the latter, while there were a number of very large events in the latter period, and none in the former period. These patterns would appear to explain why channel erosion in secondary channels was much greater in the earlier period, given that it can be assumed that many of the smaller tributaries had extended high flows to generate the moderate flows in the main channels. The absence of very large flood events in the former period would also explain why main channel erosion was lower in this period than in the latter period, which experienced several very large cyclone events. Threshold driven mass bank failures in the main channels are more likely to have been driven by these larger events than the earlier moderate events.

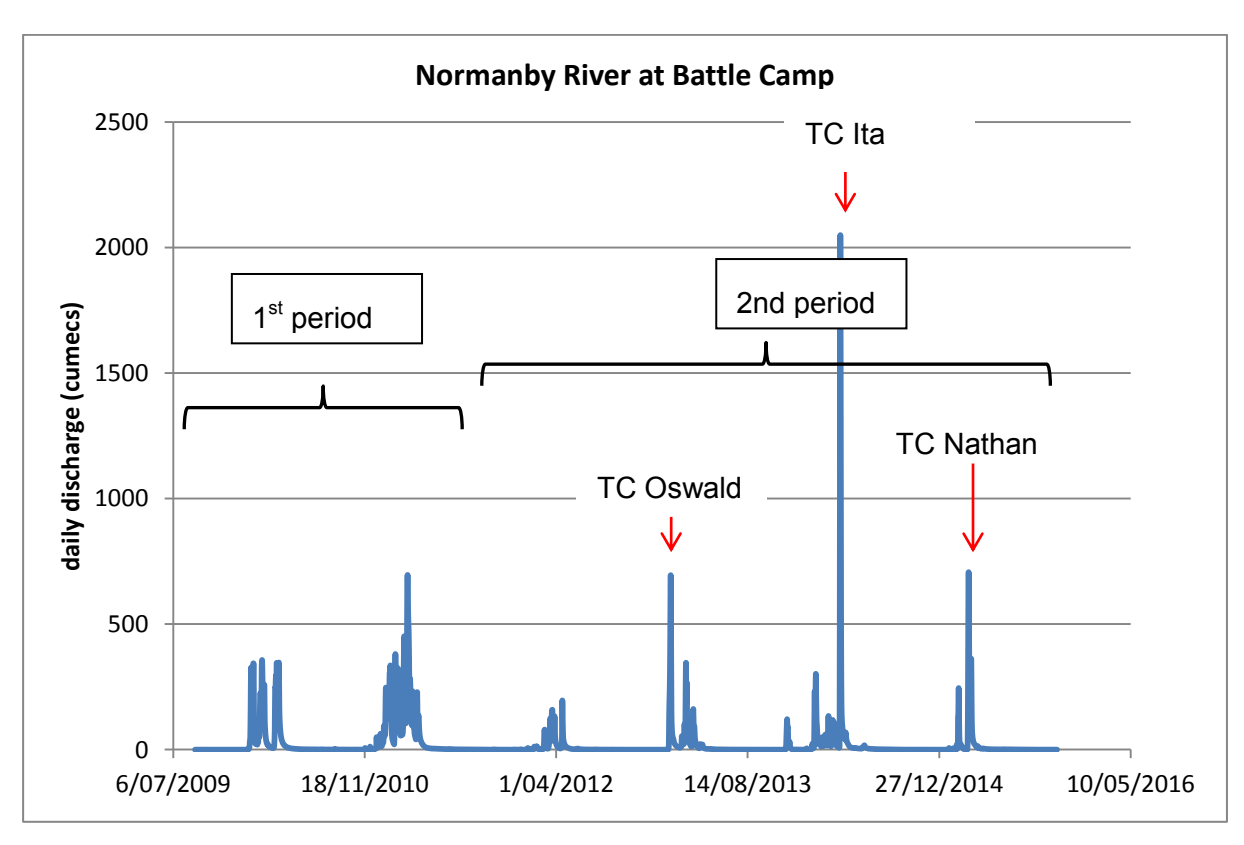


Figure 13: Mean daily discharge for the study period Normanby River at Battle Camp gauge

### Spatial Variability in Erosion Response at the Block Scale

The data presented in **Table 4** shows the ratio of change in rainfall normalised erosion rates for the two time periods for the individual blocks, enabling us to analyse the data in comparative detail. Whilst the overall trends as described above are clear, it is apparent that there is considerable spatial variability from block to block. Looking firstly at the alluvial gully data, it is evident that Block N4 just to the north of the highway bridge crossing over the East and West Normanby Rivers has had a 56% annual increase in alluvial gully activity rates in the second period, while block 9 on the East Normanby River has had a 12% increase. Blocks 5 and 10 further down the Normanby River have had 7% and 12% increases respectively in the second period, over and above that explained by annual rainfall.

Obviously, some of this variability would be explained by the fact that the available monthly and annual rainfall data does not reflect local scale variability in rainfall magnitude, intensity and duration. More detailed rainfall gauging data at the local scale might help to explain some of this variability. Interestingly, Block 7 on the Granite Normanby, which is a major hotspot of alluvial gully erosion at the catchment scale, experienced a significant reduction in annual average alluvial gully erosion rates. Blocks N16 and N17, which are both on the Laura River, also experienced significant reductions in alluvial gully erosion rates. Explaining this variability should be the subject of further research, but likely includes variation in local rainfall magnitude, duration and intensity, as well as variations in the stage of gully evolution, soil geochemistry and erodibility. Understanding such spatial variability in erosion rates is important for rehabilitation prioritisation and for tailoring rehabilitation measures to the local conditions.

### Land use as a control on spatial variability in erosion response

From the change ratio data presented in **Table 4**, it is interesting to consider what these results mean in terms of their relationship to local-scale land-use intensity. Blocks N4, N7 & N9 on the Normanby River are within a large cattle station that has been very intensively grazed over the period of the study, as have blocks 16 and 17 on the Laura River. At block N7, with reduced erosion rates over the second period, the landowner was paid by Reef Rescue to spell (reduce) cattle numbers on the east side of the Granite Normanby (Abbey Lea Paddock). However, this spelling effort was marginal at best, and cattle continued to graze the area, suggesting that cattle grazing alone was not sufficient to cause this reduced erosion.

By contrast blocks N5 and N10 are on a grazing property that was purchased for conservation purposes at around the start of the second time interval, at which time it was significantly destocked. The results would tend to suggest that reducing grazing pressure over this relatively short time scale (4 years) has not had a measurable effect on large-scale erosion rates at this broad scale. In the absence of any other controls on gully erosion rates (such as direct management intervention), it is likely that incident rainfall will continue to control sediment production from gullies for the foreseeable future. The effect of complete cattle exclusion on gully erosion rates is explored in more detailed in section 2.2 and 2.3 and Appendix B.

Despite the considerable variability in gully activity rates in the different blocks, secondary channel erosion (i.e. smaller ephemeral channels) all experienced substantially lower rates of erosion in this period, even when the gully erosion rates in the same vicinity showed increased rates of activity. It is also unusual that there seems to be a distinct disconnect between secondary channel bed erosion rates (which have increased dramatically in places) and the associated bank erosion. Main channel erosion (bed and banks) have typically both increased in most blocks, which is more in line with previous findings (Brooks et al., 2014) where it was demonstrated that channel bank erosion is strongly correlated with bed erosion and deposition. The more consistent trend in main channel erosion is likely explained by a whole-of-system response to a larger event operating at a larger scale than represented by the LiDAR blocks.

Full details of the LiDAR analysis methods and the detailed block summaries can be found in Appendix A

# 2.2 Gully Exclusion Experiment: Vegetation Data (Shellberg, Brooks, Curwen)

### 2.2.1 Overview

A full description of the gully exclusion trials and the vegetation survey approach is outlined in Shellberg and Brooks (2013) and Appendix B. Multiple exclusion sites were established across the upper Normanby catchment so as to capture the spatial and morphological diversity of alluvial gullies. The goal of these trials was to begin to demonstrate and quantify over the long term (20+ years) the potential for vegetation recovery and reduction in sediment erosion and yield in existing alluvial gullies after cattle exclusion and removal of chronic disturbance. Thus, the influence of removing cattle was tested in the absence of any other gully stabilization measures. Short-term results (4 years) can be used as indicative of the future potential for recovery from grazing exclusion, if any, but these short-term results are not intended to be conclusive, and are reported on here as preliminary data.

Study designs followed a before-after, control impact (BACI) design (Underwood 1994a; 1994b; Smith 2002) that monitored vegetation, soil conditions, and vertical erosion at the plot scale (4 m²) distributed across gullies (2011, 2012, 2013, 2015) and sediment erosion via repeat aerial LiDAR topographic surveys at the gully-complex scale (2-5 ha) (2009, 2011, 2015). Initial cattle exclusion fencing and "before" vegetation monitoring were installed and conducted in 2011/2012. Repeat aerial LiDAR topographic surveys were flown in 2009 and 2011 for "before" erosion conditions) (above). Initial "after" vegetation monitoring was conducted in 2012/2013 and again in 2015. Repeat aerial LiDAR topographic surveys again were flown in 2015 for "after" erosion monitoring by comparison to 2009 and 2011 data. Rainfall data were collected daily at the following cattle stations: Kings Plain, Lakeland, Crocodile (see Appendix 4).

Assessment of vegetation and soil conditions at the plot scale followed protocols modified from Wilke (1997), Rolfe et al. (2004) and Karfs et al. (2009) (see data sheets and survey instructions in Appendix B). At dozens of plot locations inside and outside the exclosure, a permanent vegetation marker was established at each plot using a star picket. Each plot was  $2m \times 2m \ (4m^2)$  and identified by using a PVC grid centred on the star picket. Initial pasture conditions were assessed just before the break-of-season (November), when vegetation conditions are at their annual low before the next wet season. In some years pasture conditions were assessed after the wet season (April) for comparison. Within each plot area  $(4 \ m^2)$ , a suite of semi-quantitative measurements and photographs were made of the pasture ground vegetation conditions, as well as soil and erosion conditions. These conditions included:

- Aerial projected % cover of all organic material (excluding cow dung)
- Aerial projected % cover of individual cover components (leaves/sticks, dead matted grass, standing vegetation, standing weeds)
- % cover of just perennial grass
- # of species and species identification
- # of perennial tussocks
- Visual pasture yield estimate (standing biomass) from QDPIF picture templates
- Grass and weed species dominance

- Soil condition (erosion, deposition, crust integrity)
- Vertical erosion or deposition at a reference stake (upslope/downslope)(±3mm)
- Overall land condition rating (A,B,C,D)
- Detailed photographs of vegetation plot condition and species from multiple standard angles for future comparisons.

At all plots in March 2012 when the floristic characteristics of grass were best for proper identification, grass and other weed species were collected and pressed at each plot for later identification. The Queensland Herbarium professionally identified the pressed plants. These data will be used for 10-20 year comparisons of vegetation community change.

The experimental monitoring program is intended to continue for at least a 10 to 20 year period for a full assessment of changes over the long-term. Additional LiDAR surveys and vegetation monitoring will be needed. Where data on "before" conditions are limited due to initial 2011/2013 efforts and lack of funding, more detailed data on vegetation, gully erosion, sediment yield, soil heterogeneity, and hydrological conditions should be collected at control and treatment sites to better quantify inherent conditions and potential changes, which will value add to initial efforts (e.g., terrestrial LiDAR, differences in soil infiltration rates, vegetation colonization by species, etc.).

Some key questions this research poses and might be able to answer include:

- How does vegetation cover change over time in existing gullies, surrounding catchments, and specific geomorphic units with and without cattle exclusion?
- Does cattle exclusion and vegetation recovery have any influence on soil erosion?
- How do cattle and animal track density change over time inside/outside exclosures?
- What are the complicating influences of weeds, fire, and wallaby grazing?
- Are experimental methods robust enough for quantification of long-term change?
   What additional information could be collected now or in the future (control/treatment) to value add to these existing data?

### 2.2.2 Results - Case Study 1: West Normanby River

A full description of the methods can be found in Appendix B and Shellberg and Brooks (2013). The layout of the vegetation plots sampled can be seen in **Figure 14**.

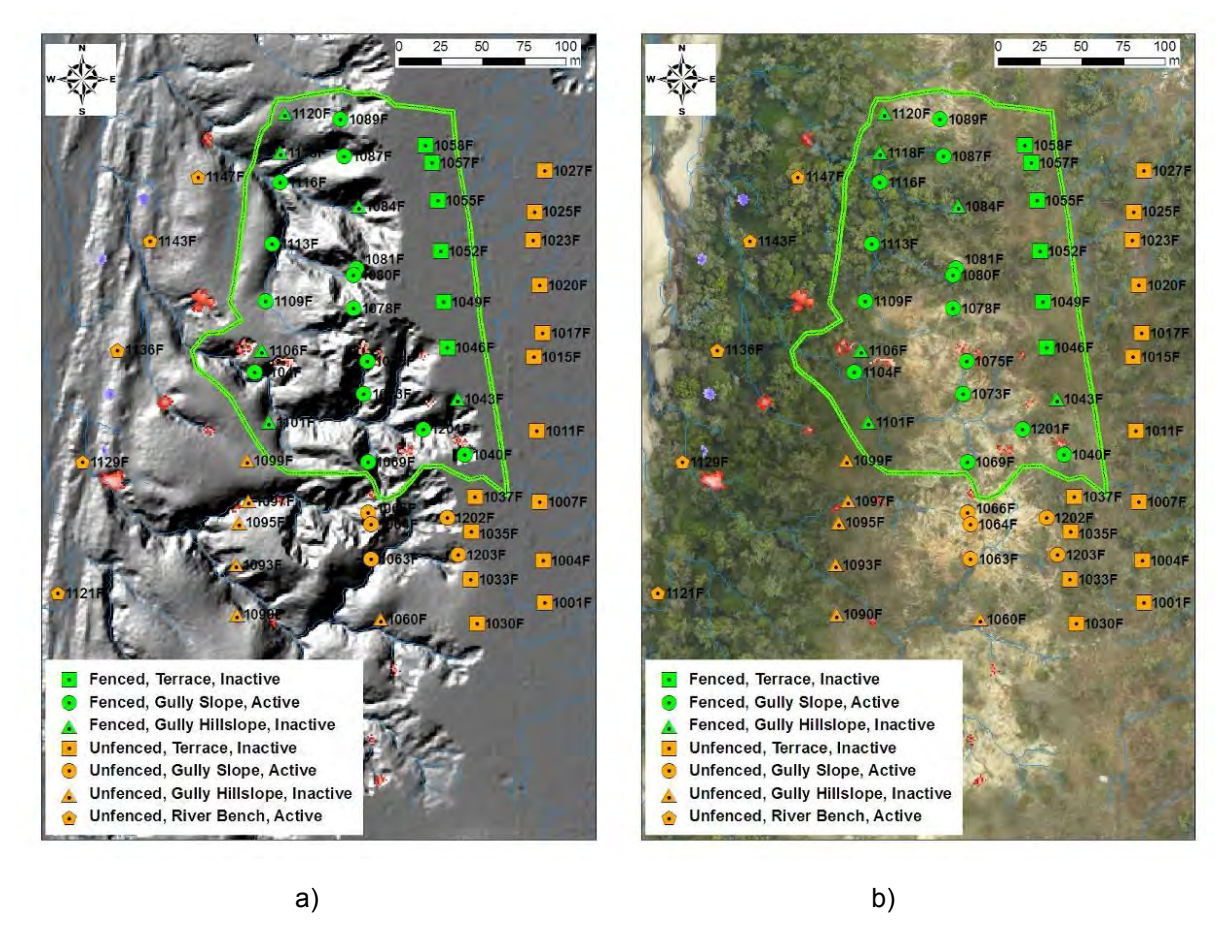


**Figure 14:** West Normanby River below the Cooktown Highway (-15.762320°S, 144.976602°E) showing a) the location of the fenced cattle exclusion area and vegetation plots with a LiDAR background and b) the location of the fenced area and vegetation plots with an aerial photo background. Note that red areas in **Figure 14**a are zones of active gully erosion between 2009 and 2011 repeat LiDAR.

Preliminary results between 2011 and 2015 indicated that both % total organic cover and % cover of perennial grass changed seasonally, as expected, with greater cover after the wet season (**Figure 15**). At both fenced and grazed sites, variability in % total organic cover between Nov-11 and May-13 did not display major trends (Figure 15a). However, total cover was much reduced at both fenced and grazed sites by Nov-15 due to a regional drought and below average wet season rainfall (**Figure 16**). The % cover of perennial grass increased in both fenced and grazed sites between Nov-11 and May-13 (Figure 15b), but also was reduced by Nov-15 due to below average rainfall (**Figure 16**). Both tussock counts and pasture yield were also lower by Nov-15 (**Figure 15**cd). From these data it appears that rainfall variability and dry years can have major influences on ground cover, both inside and outside of cattle exclusion areas.

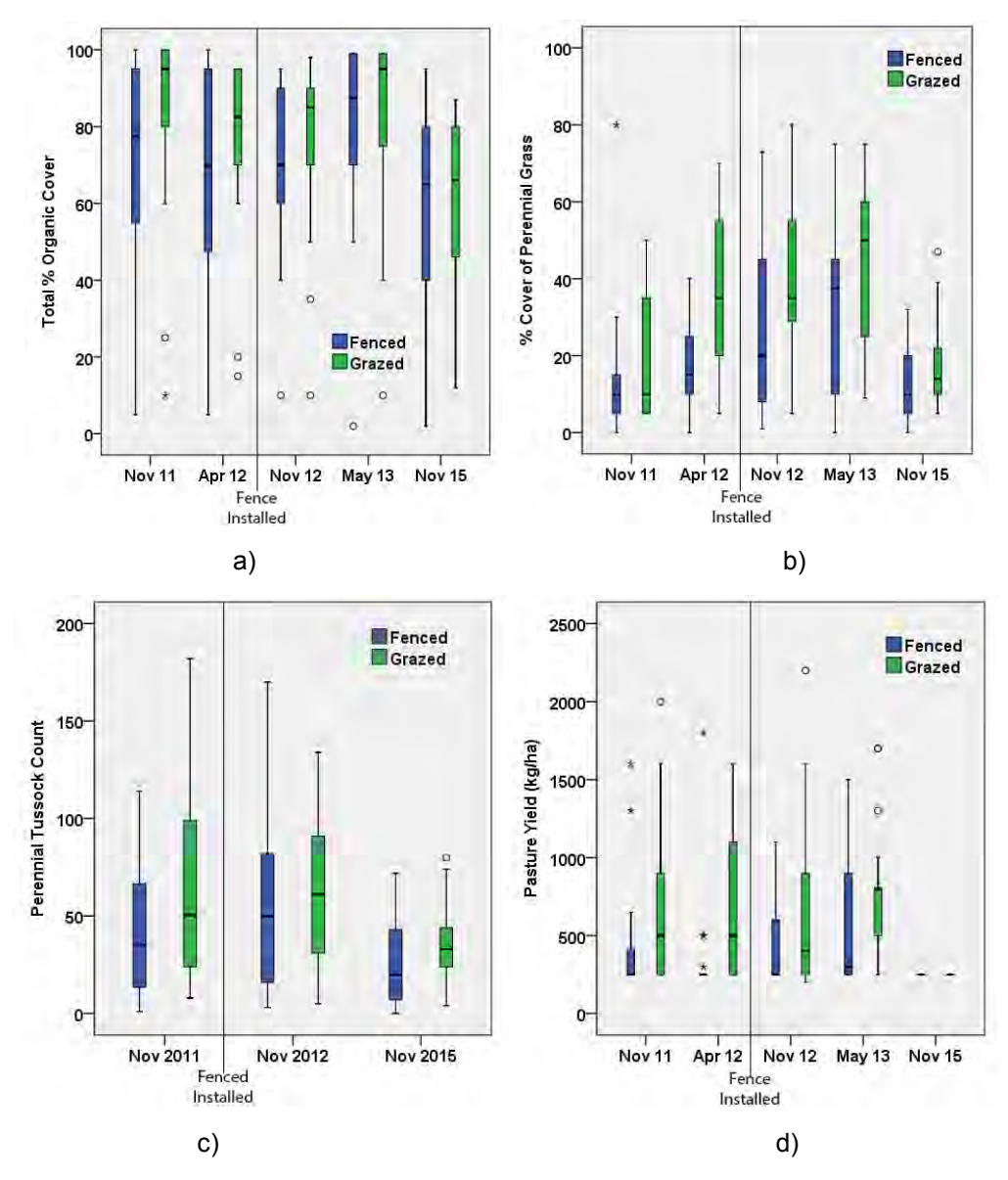


**Figure 15:** Changes in ground cover inside and outside the West Normanby cattle exclusion site from 2011 to 2015 showing a) total % organic cover (grass, weeds, leaves, sticks, mulch) and b) % perennial grass cover, c) perennial grass tussock count, and d) pasture biomass yield.

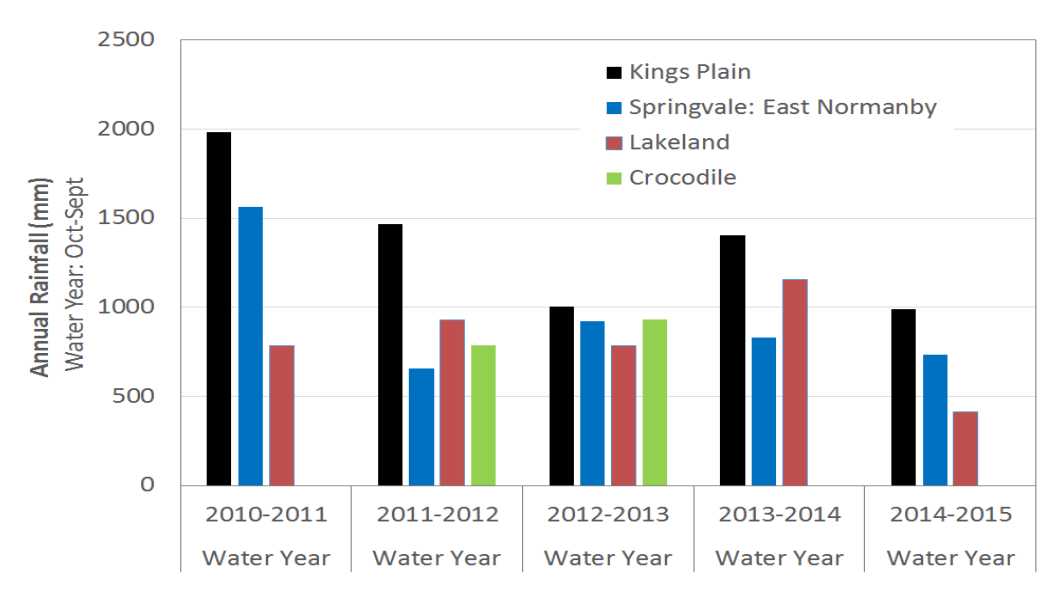


**Figure 16:** Annual rainfall by water year (Oct-Sept) from 2011 to 2015 at Lakeland, Kings Plains, Crocodile, and Springvale.

When vegetation cover is examined by different geomorphic units (high terrace, active gully slope, inactive gully hillslope) both inside and outside the fence, the general trends were similar. Total % organic cover varied between seasons and years between Nov-11 and Apr-13 with no major trends (**Figure 17**a). However, Nov-15 total cover was much reduced at all geomorphic units due to dry years (**Figure 16**). The % cover of perennial grass increased in both fenced and grazed geomorphic units between Nov-11 and May-13 (**Figure 17**b), but also was reduced by Nov-15 due to below average rainfall (**Figure 16**).

Cover on intact high terrace flats improved the most for % perennial grass cover in fenced areas, with the largest increase in % grass cover occurring on fenced high terrace flats after fence installation (**Figure 17**b, Fenced, High Terrace, April 2013). Pasture yield also increased on these terrace flats compared to outside areas, and less so on inactive gully slopes (**Figure 18**). Removal of cattle grazing on these high terrace flats contributed to this increase. However, % perennial grass cover also increased at grazed (unfenced) high terrace flats, but not as dramatically between Apr-12 and Apr-13. The % perennial grass cover also increased between Nov-11 and Apr-13 at other geomorphic sites, both fenced and unfenced, until the major drop in cover by Nov-15 after below average rainfall.

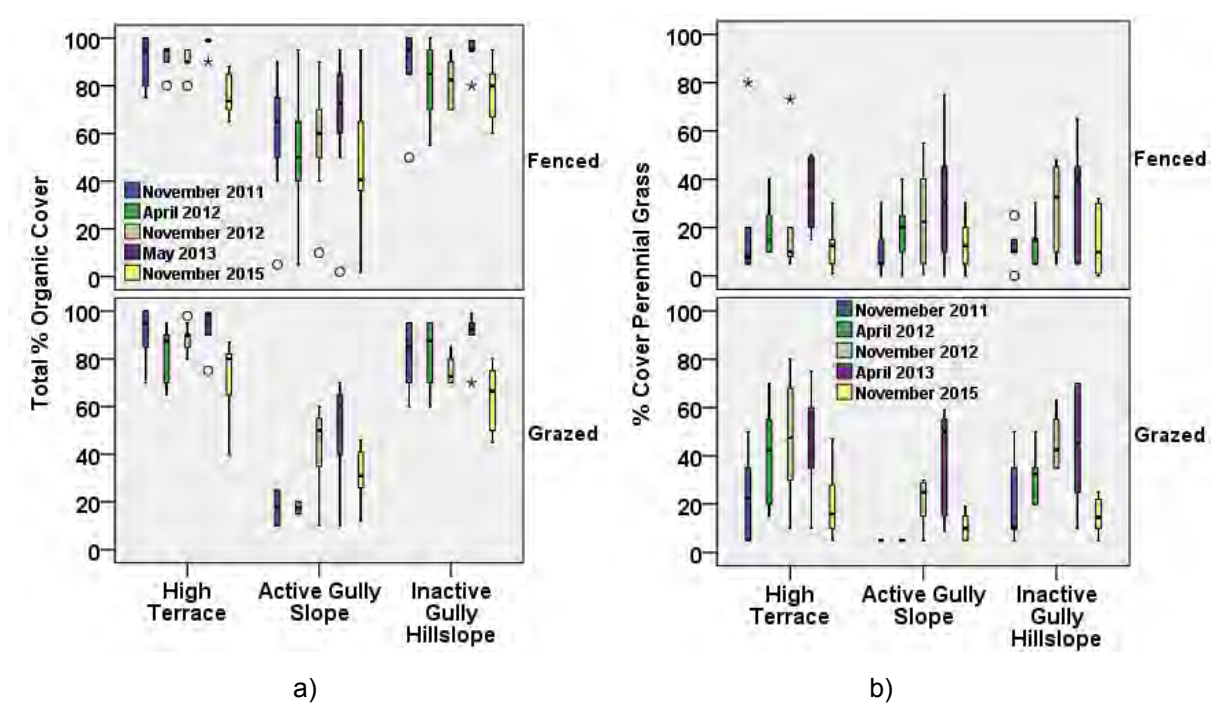


**Figure 17:** Changes in ground cover at different geomorphic units (terrace, gully, hillslope) inside and outside the West Normanby cattle exclusion site from 2011 to 2015 showing a) total % organic cover (grass, weeds, leaves, sticks, mulch) and b) % perennial grass cover.



**Figure 18**: Differences in pasture yield and grass biomass inside (right) and outside (left) the West Normanby cattle exclusion fence on a) the high terrace (left picture) and b) inactive gully slopes (right picture).

Point measurements of scour and fill (± 5mm) at permanent vegetation plot reference stakes between 2011 and 2015 indicated much variability, but no clear trends (**Figure 18**). The spread of the data increased over time due to ongoing erosion and deposition at the most active gully sites. Longer-term data will be needed to understand trends from rainfall and runoff variability, and gully evolution at the site scale.

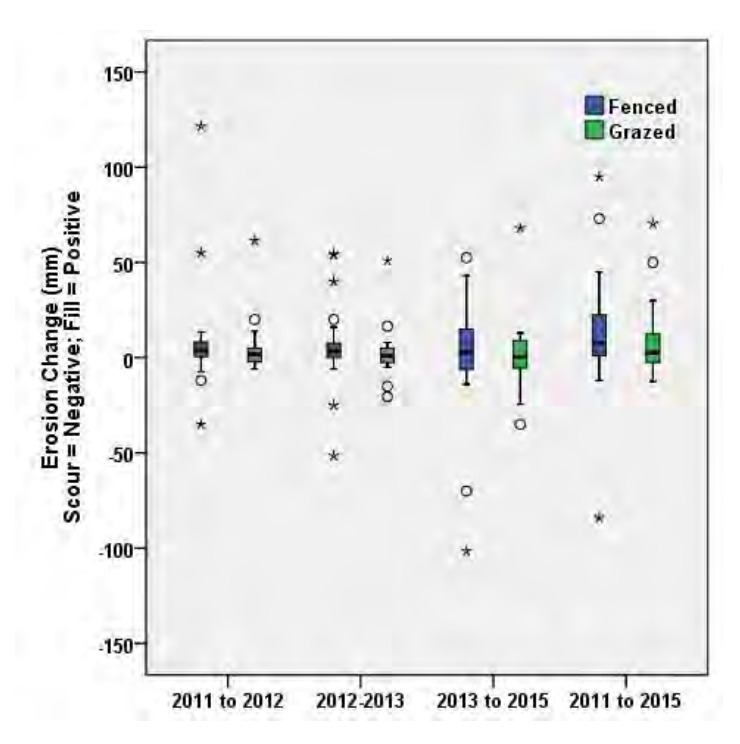


**Figure 19:** Measurement distributions of scour (negative) or fill (positive) at permanent vegetation plot reference stakes, accurate to 5mm, for fenced and grazed areas of the West Normanby gullies between 2011 and 2015.

These preliminary data display the usefulness of a before-after, control-impact (BACI) study design to begin understanding potential changes over time from land management actions (e.g., cattle fencing). The chosen metrics appear to be picking some changes in pasture condition with management of cattle over short-time periods (2011-2015), especially on high terrace catchments above gullies, but less so inside gullies. However, the year to year and seasonal variability in rainfall appears to be overriding any influences of grazing, especially during dry years with below normal rainfall (e.g., O'Reagain and Bushell 2011). Longer term datasets (+10 years) will allow for the robust statistical analysis of these datasets, in order to fully assess changes and the potential for cattle exclusion, natural resilience and recovery potential to have any influence on vegetation cover above or within gullies and gully erosion yields.

## 2.2.3 Results - Case Study 2: Crocodile Station Paddock Tributary to the Laura River

A full description of the methods for this site can be found in Appendix B and Shellberg and Brooks (2013).

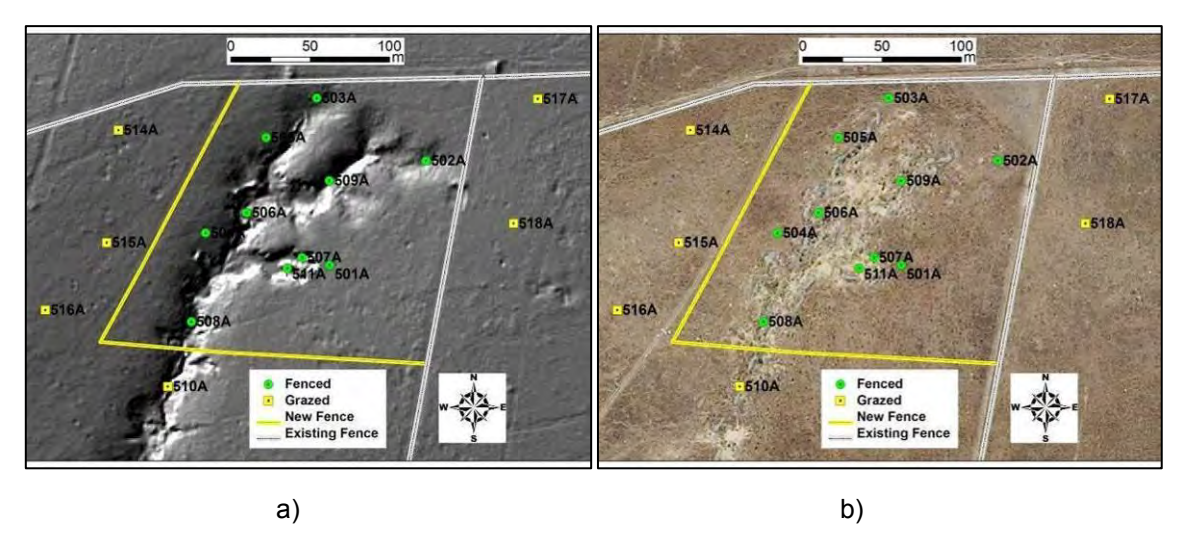


**Figure 20:** Maps of the cattle exclusion fence in the 'Old Hay Paddock' at Crocodile Station (-15.710042° S; 144.679232° E) with a) LiDAR hillshade background and b) aerial photograph background showing locations of vegetation monitoring points inside and outside the exclusion area.

Preliminary results indicated that both % total organic cover and % cover of perennial grass changed seasonally, as expected, with greater cover after the wet season (**Figure 21**). Total % cover at fenced sites within the gully area increased over time between Nov-11 and Apr-13, while % total cover at grazed sites remained relatively constant (**Figure 21**a). Total cover was reduced at both fenced and grazed sites by Nov-15 due to dry years and below average rainfall (**Figure 16**), but total cover inside the fenced area was generally greater than outside (**Figure 21**a).

Before the fence was installed, the % perennial grass cover was greater outside the proposed fence area than inside. Over time and after the fence was installed, this pattern shifted, with the median % perennial grass cover greater inside the fence than outside between Apr-12 and Nov-15 (Figure 21b). Increases in both grass and weed cover were quickly observed inside the fenced area between Nov-11 and Nov-12 (Figure 22ab), with less detectable changes outside (Figure 22cd). The below average rainfall in 2015 dramatically reduced the perennial grass cover both inside and outside the fence (Figure 21). However, the grass cover inside the fenced area remained elevated compared to outside even in dry conditions (Figure 21b; Figure 23).

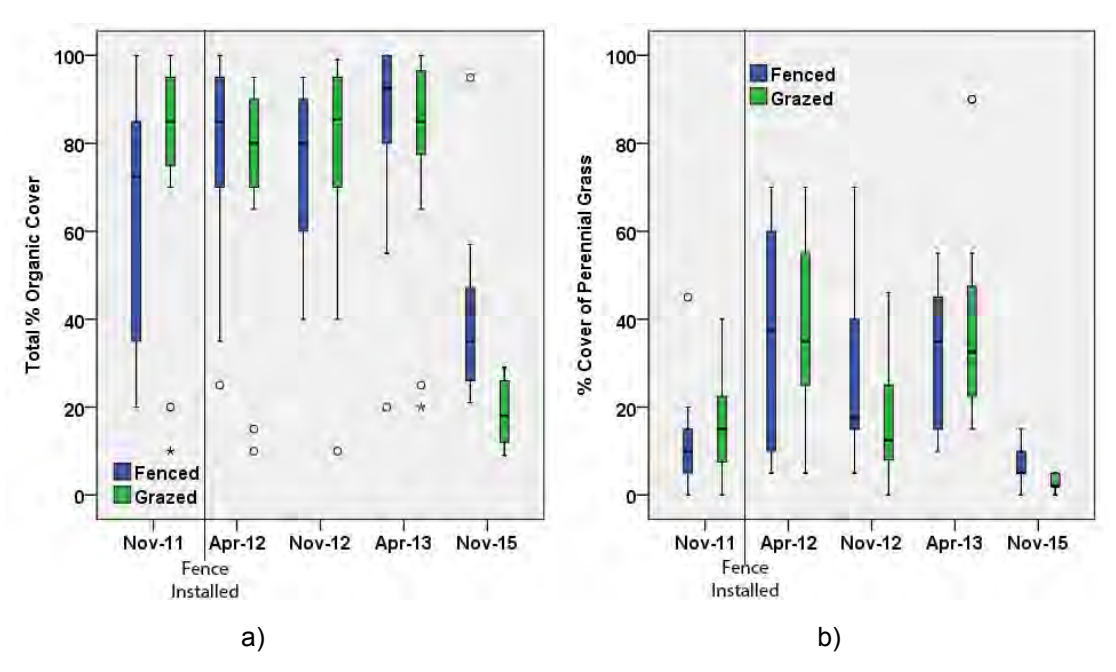


**Figure 21:** Changes in ground cover in cover inside and outside the Crocodile Station 'Old Hay Paddock' cattle exclusion site from 2011 to 2015 showing a) total % organic cover (grass, weeds, leaves, sticks, mulch) and b) % grass cover (standing perennial or annual grass).

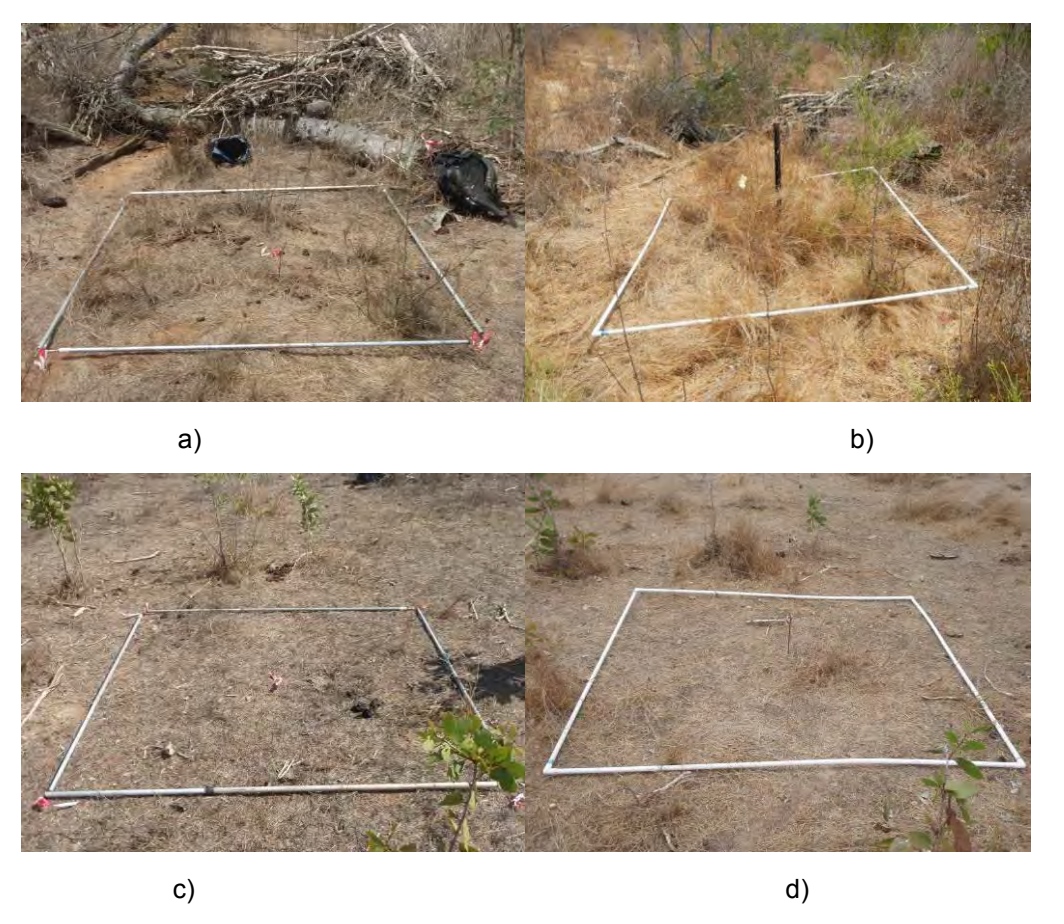


**Figure 22:** Changes in vegetation cover and biomass a) before fencing at Plot 508 gully bottom in Nov-2011, b) after fencing at Plot 508 gully bottom in Nov-2012, c) grazed control at Plot 515 hillslope in Nov-2011, d) grazed control Plot 515 hillslope in Nov-2012.

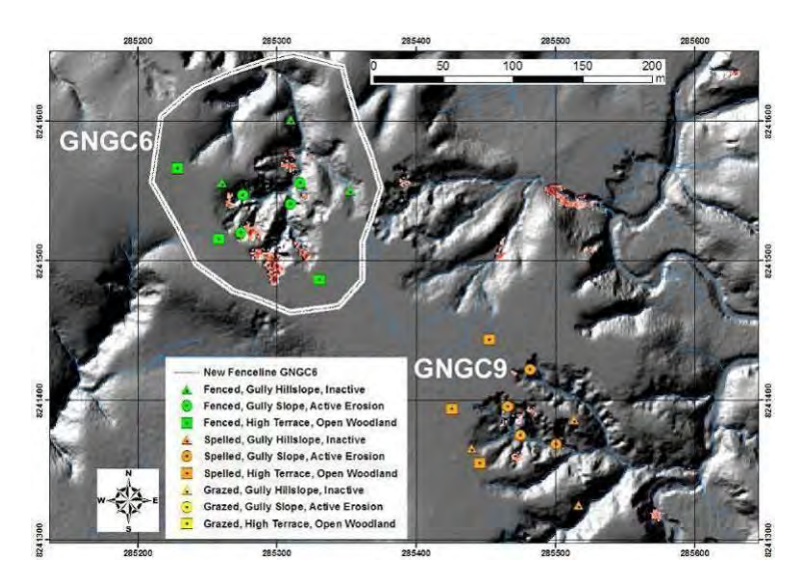


Figure 23: Grass and weed cover inside the cattle exclusion fence (left) and outside (right) in June 2015.

From these data it is evident that both grazing pressure and rainfall variability can have detectable influences on ground cover. However, major drought conditions can lead to a reduction in vegetation cover regardless of grazing pressure, but with greater vegetation cover and resilience during dry years in ungrazed areas. Longer term datasets (+10 years) on pasture condition will allow for the robust statistical analysis of the influence of management treatments (e.g., cattle fencing) on vegetation and erosion, from natural variability due to rainfall or other factors.

### 2.2.4 Results - Case Study 3: Granite Normanby River (2012-2015)

For a full description of the methods refer to Appendix B and Shellberg and Brooks (2013).



**Figure 24:** Hillshade LiDAR map of the cattle exclusion fence at GNGC6 (-15.896374°S; 144.994678°E) and neighbouring spelled GNGC9 on the Granite Normanby on Springvale Station. Note that red areas are zones of active gully erosion between 2009 and 2011 repeat LiDAR.

Preliminary results indicated that both % total organic cover and % cover of perennial grass changed seasonally, as expected, with greater cover after the wet season (**Figure 25**). Total % cover within the fenced cattle exclusion gully remained relative stable over time between Nov-12 and Nov-15, while % total cover at grazed sites declined over time (**Figure 25**a). Total cover was reduced at both fenced and grazed sites by Nov-15 due to below average rainfall (**Figure 16**), but total cover inside the fenced area was generally greater than outside (**Figure 21**a).

Before the fence was installed, the % perennial grass cover was greater outside the proposed fence area than inside (**Figure 25**b). Over time and after the fence was installed, this pattern shifted, with the median % perennial grass cover greater inside the fence than outside in Apr-13 and Nov-15 (**Figure 25**b). Increases in grass cover were quickly observed inside the fenced area on high terrace flats between Nov-12 and Apr-13 (**Figure 25**b; **Figure 27**), whereas perennial grass cover actually decreased in the grazed area by Apr-13. By 2015, a very dry year and below average rainfall reduced the perennial grass cover and tussock counts overall, but the decline was greater in the grazed area than the fenced area (**Figure 25**bc).

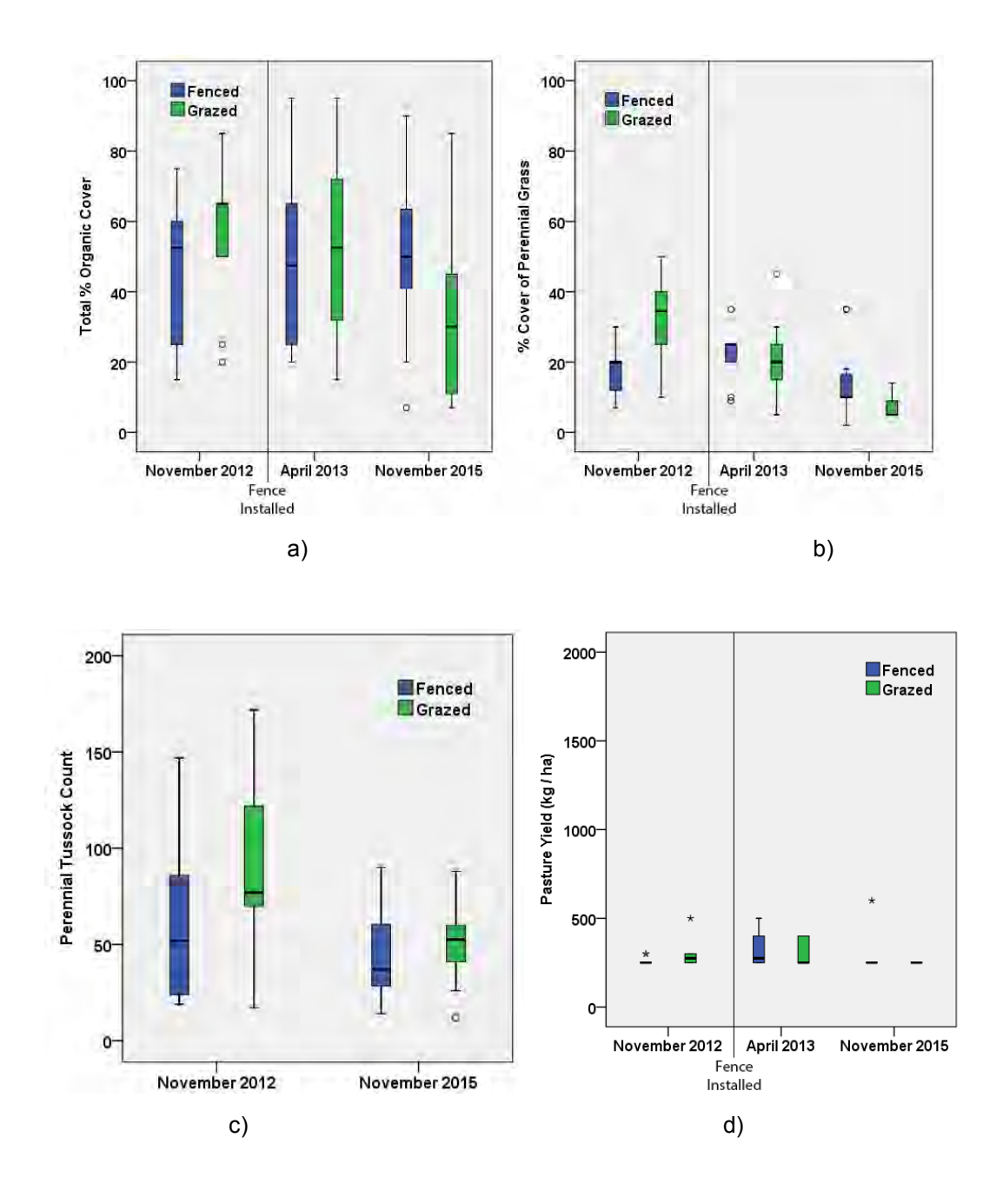


**Figure 25:** Changes in ground cover inside and outside the Granite Normanby cattle exclusion site from 2012 to 2015 showing a) total % organic cover (grass, weeds, leaves, sticks, mulch), b) % cover of perennial grass, c) perennial tussock count, and d) pasture yield (kg/ha).

When per cent cover of perennial grass is examined by different geomorphic units (high terrace, active gully slope, inactive gully hillslope), perennial grass cover in fenced geomorphic units increased from Nov-12 to Apr-13, and then slightly decreased in Nov-15 after a below average rainfall year (**Figure 26**a; **Figure 16**). In comparison, grazed geomorphic units saw more consistent declines in grass cover, especially for active and inactive gully slopes (**Figure 26**a). Tussock counts decreased for most geomorphic units from Nov-12 to Nov-15, except for fenced active gully slopes that has a slight increase (**Figure 26**b).

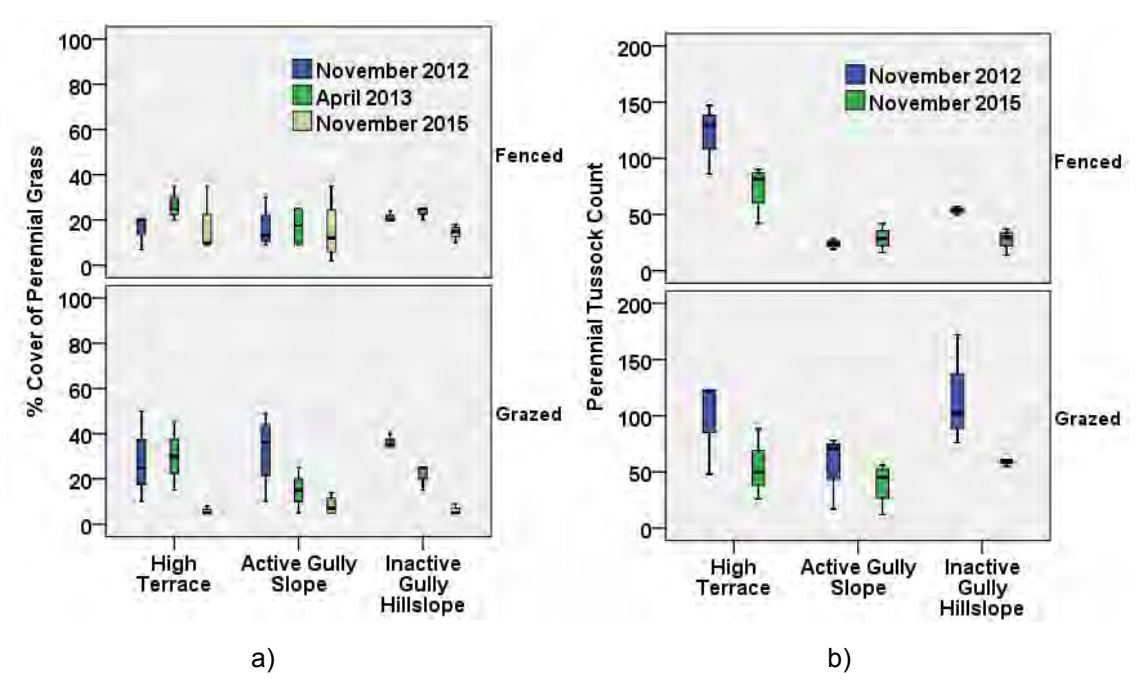


**Figure 26:** Changes in ground cover at different geomorphic units (terrace, gully, hillslope) inside and outside the Granite Normanby cattle exclusion site from 2012 to 2015 showing a) % cover of perennial grass and b) perennial grass tussock counts.



**Figure 27:** Differences in grass cover and biomass between the fenced gully (Left, GNGC6) and the grazed area (Right, GNGC9) on the high terrace of the Granite Normanby in a) April 2013 and b) November 2015.

From these data it is evident that both grazing pressure and rainfall variability can have major influences on ground and grass cover. In this case, grazing reduced total and grass cover on most geomorphic units, while cover within the fenced area remained more resilience to climate variability.

Point measurements of scour and fill (± 5mm) at permanent vegetation plot reference stakes between 2012 and 2015 indicated relatively consistent erosion/deposition distributions at fenced sites, and increased erosion at grazed sites (**Figure 28**). The increased erosion at

grazed sites was the result of active surface erosion at two internal gully plots, with questionable influence from ongoing grazing activity on the terrace flat or internal gully.

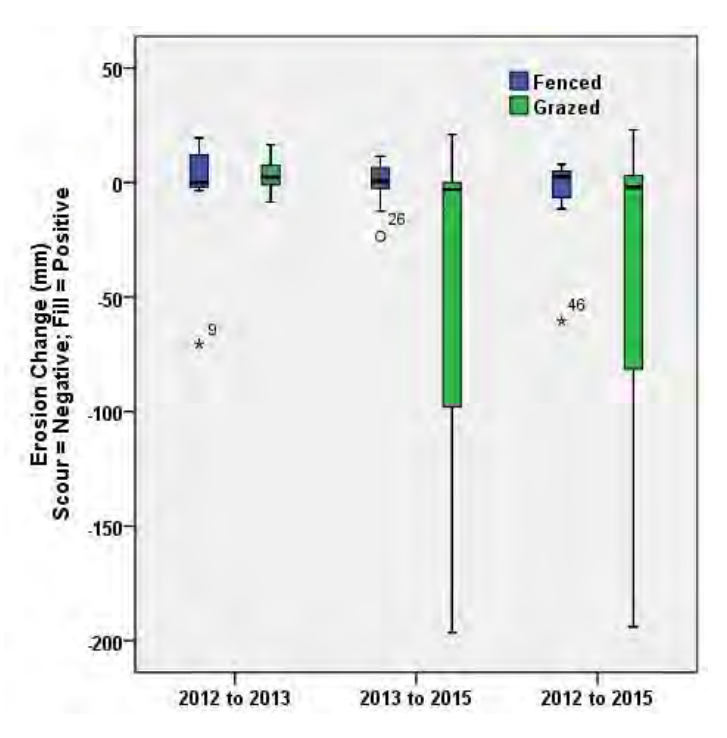


**Figure 28:** Measurement distributions of scour (negative) or fill (positive) at permanent vegetation plot reference stakes, accurate to 5mm, for fenced and grazed areas of the Granite Normanby gullies between 2012 and 2015.

### 2.2.5 Summary of findings from Vegetation Surveys

A full discussion of the results from the vegetation plot surveys is provided in Appendix B, as well earlier summaries in Shellberg and Brooks (2013). Given that the exclusions have only been in place for 3 to 4 years, it was deemed that there was insufficient data to undertake a robust statistical analysis at this point, and therefore the following is a summary of the preliminary take home messages.

- Vegetation responded to cattle exclusion to varying degrees depending on the geomorphic units the sites were situated on within the gully complexes (e.g. high terrace surface, inactive gully hillslope, active gully slope) as well as the gully depth and stage of evolution.
- Un-eroded high terrace surfaces had some positive changes to pasture condition (cover, tussock counts, biomass) following grazing exclusion. No major vegetation improvements were detected inside deep mature alluvial gullies with exposed sodic sub-soils (i.e. West Normanby, Granite Normanby, Kings Plains). In shallow alluvial gullies, vegetation response was improved on inactive gully slopes and gully bottoms, but was still minimal at the eroded plots with exposed sub-soils (i.e. Crocodile Paddock).
- Seasonal and inter-annual rainfall variability was a far more significant control on vegetation conditions than whether they were grazed or not over this period, but with greater vegetation cover and resilience during dry years in ungrazed areas.

- Plot scale measurements of surface erosion and deposition showed no major trends from grazing exclusion over 4 years, but did highlight the variability and magnitude of surface erosion and deposition within gullies that are common over large areas and can contribute significantly to the total sediment and nutrient yield from gullies at the event or annual scale.
- A final complicating factor on the results presented here is the potential impact of
  marsupial grazing (wallabies) on perennial grass recovery inside gullies. These
  internal gully areas were preferential grazing areas for wallabies due to cover
  and remnant native perennial grasses (e.g., Kangaroo grass) on many inactive
  gully slopes. Dingos and pigs are actively poisoned on these properties with
  1080 bait, which could increase wallaby populations. Reduced 1080 baiting of
  dingos on some conservation minded properties could help keep wallabies on
  the move and under control. This wallaby influence problem would be minimized
  if much larger exclusion areas were trialled.

#### **Management Implications:**

- These results suggest that least one to two decades will be required before we see any significant improvements in perennial grass cover in the internal eroded areas of gullies where cattle have been excluded, in order to overcome the signal of annual rainfall variability and potential lag response of passive vegetation colonization.
- In some cases, passive vegetation recovery onto sodic sub-soils might not ever occur, or at least take many decades until the full cycle of gully evolution is reached.
- Since vegetation colonization onto very active gully surfaces of deep mature gully complexes appears to be minimal in the short-term, it is unlikely that reductions in gully surface erosion and slumping from direct rainfall will result from cattle exclusion and vegetation response. However, vegetation improvements in the un-eroded upslope catchments of alluvial gullies (here < 25% of total gully catchment area; the other 75% being the gully itself) could promote infiltration, reduce runoff, and slow head scarp retreat rates in the longterm. This will need more investigation over the coming decade.
- To reduce gully erosion sediment yields for short-term management goals to the GBR, it will be necessary to conduct additional management interventions beyond just cattle exclusion to hasten the recovery, such as supplementary grass seeding from the air or ground, organic mulching of sodic soils, fire and weed management, and slope stabilization through bioengineering (see Shellberg and Brooks 2013, and Appendix B).
- Managing chronic grazing disturbance of sodic soils along river frontage is still
  essential to preventing the new initiation of alluvial gullies and promoting passive
  hydrogeomorphic recovery where possible. Fencing cattle out of these sensitive
  areas remains a critical first step in any gully management scenario that seeks to
  manage this erosion in the long-term, regardless of whether exclusion leads to
  major short-term sediment and nutrient reductions in its own right.

# 2.3 Gully Cattle Exclusion Experiment: LiDAR Data (Brooks, Curwen, Shellberg, Spencer, Iwashita)

### 2.3.1 Overview of Aerial LiDAR Analysis of Cattle Exclusion Trial Sites

As part of the Normanby Reef Rescue project undertaken between 2009 and 2013 (see Brooks et al., 2013; Shellberg and Brooks, 2013), a series of grazing exclusion trials were established at four sites within the Normanby catchment (**Figure 29**). The primary purpose was to detect any changes in vegetation cover in gully catchments from cattle exclusion, and measure any erosion response from large-scale aerial LiDAR surveys. A detailed description of the exclusion area setup and vegetation data is included in a separate technical report in Appendix B (Shellberg et al.), as well as the section above.

The exclusion areas are all located within existing LiDAR blocks (N4, N7, N10 and N17) and were established around the same time that the second LiDAR monitoring period began in 2011 prior to the 2012 wet season. Hence for each of the trials sites we have a full Before-After Control-Impact (BACI) study design, with 2 years of before monitoring data and control sites delineated outside the fenced ungrazed sites, with 4 years of aerial LiDAR data forming the basis for assessing large-scale erosion rates post cattle exclusion.

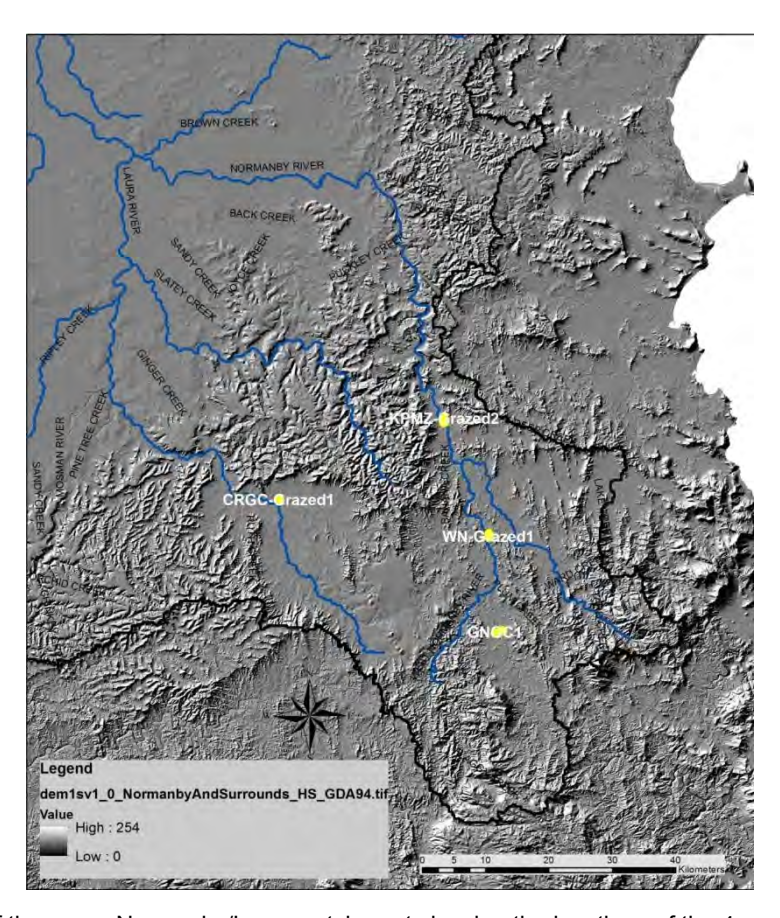


Figure 29: Map of the upper Normanby/Laura catchment showing the locations of the 4 grazing exclusion trial sites

The spatial layout of the exclusion areas and the associated control areas are shown for each of the sites in Figure 30 to Figure 33. The control and treatment areas at each gully

site were selected as much as possible to minimise differences in controlling variables. However, with experimental treatment areas it is extremely difficult to find identical gullies. For example soil particle size, geochemistry and sedimentary architecture can vary considerably over short distances, which have not been quantified in this or other studies on equivalent landscapes. Factors such as gully base level elevation can also be important controls on gully activity (Brooks et al., 2009), something which is a factor in the opportunistic gully comparisons at the Kings Plains sites. Thus in these situations, the reliance on beforeafter data is important to define the internal trajectories and behaviour of each gully. Ideally a BACI catchment experiment would be set up with sediment gauges at gully outlets to accurately measure the sediment yield (e.g., Shellberg et al., 2013a), along with finer scale erosion data internal to gullies (e.g., terrestrial LiDAR). Unfortunately the funds for detailed monitoring like this were not available for this study. Rather, this study relies upon two aerial LiDAR surveys that define the "before" conditions, and a new set of aerial LiDAR was acquired as part of the current project enabling us to assess broad change after 3-4 years of cattle exclusion.

It is essential to note that aerial LiDAR analysis is a fairly crude tool for measuring fine scale erosion detail over relatively short time periods (especially in the vertical dimension < 0.2m). Thus these data can only detect erosion deeper than 0.2m and greater than 2 m² in area, which over this timescale tends to be large-scale scarp retreat and slumping in gullies, as well as secondary incision into the gully floor. Aerial LiDAR cannot detect small-scale soil surface erosion or rilling from direct rainfall or overland flow, which is widespread inside or above the gullies and can represent up to 70% of measured sediment yield outputs at the event to annual scales (e.g., Shellberg et al., 2013a). It is hypothesized that there is a positive correlation between the detectable and undetectable erosion, and in this case we are testing for large-scale changes from short-term management response.

Due to the limited extent of measurable large-scale erosion data from the Crocodile Paddock gully site (see **Figure 33**) this site has been excluded from the erosion analysis. Longer-term monitoring and more detailed datasets of surficial erosion (i.e. terrestrial LiDAR) will be needed to better quantify potential changes to grazing exclusion at this site.

To test the statistical significance of the average (mean) erosion response to cattle exclusion, we have pooled the LiDAR erosion data from three exclusion sites (West, Granite, Kings) to increase the sample size (n=3 plots; incorporating 35 erosion polygons > 10m² in grazed areas and 29 in fenced areas). This may have the effect of dampening (averaging) the analysis of any individual site response, but is useful to assess the overall regional response, and makes statistical analysis possible. We filtered any erosion polygons less then 10m² so that the data is not negatively skewed by a profusion of erosion in single/few cell polygons, given that erosion data at this scale is also less reliable than the larger areas and scale. These data are however, still included in the total erosion data for each of the plots. Erosion polygon data were then normalised for area and then two tailed t-test and Mann-Whitney test used to test the following hypotheses:

- 1. That there is no difference in large-scale gully erosion between the grazed and fenced areas between 2009 and 2011 (i.e. before data)
- 2. That there is no difference in large-scale gully erosion between the grazed and fenced areas between 2011 and 2015 (i.e. post treatment data)
- 3. That there was no difference in large-scale gully erosion between erosion rates in the fenced area for the two periods (i.e. 2009-2011 vs. 2011-2015)

4. That there was no difference in large-scale gully erosion between erosion rates in the grazed area for the two periods (i.e. 2009-2011 vs. 2011-2015)

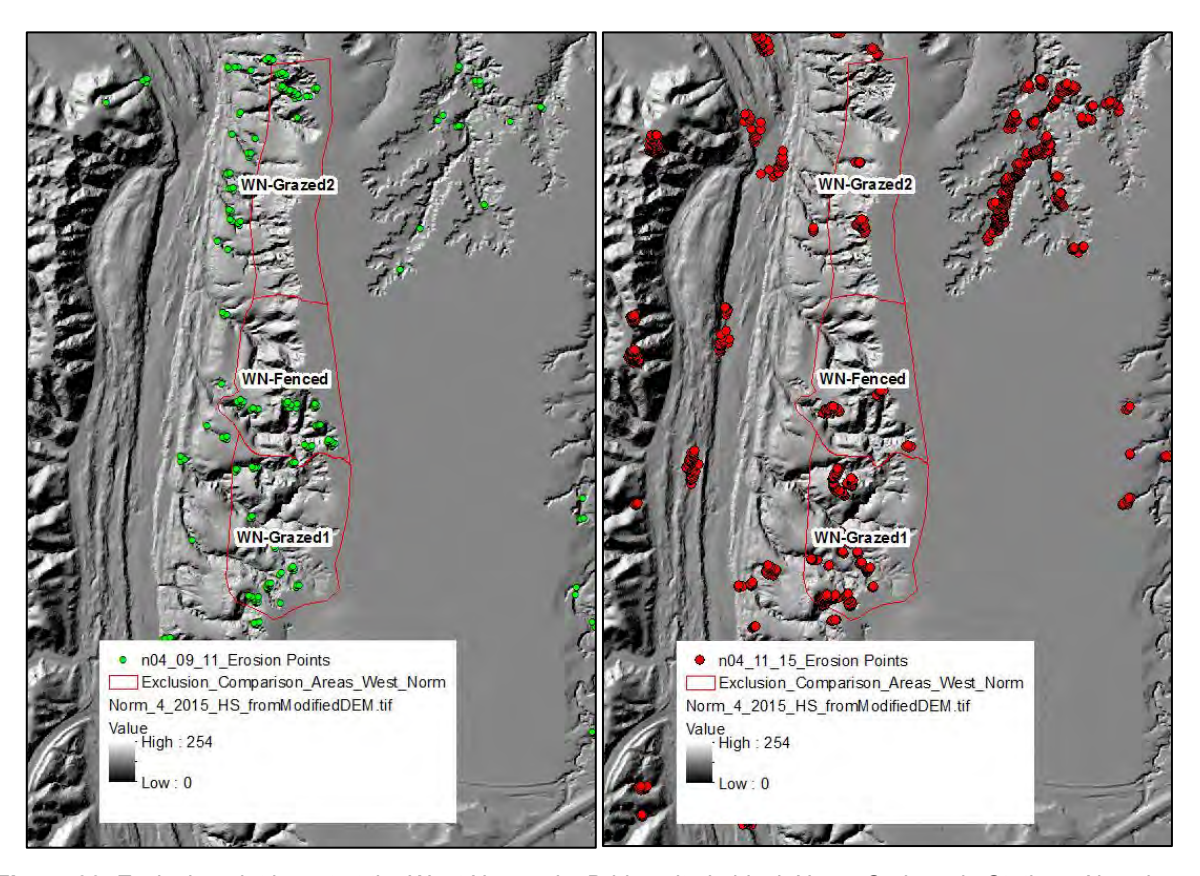


**Figure 30:** Exclusion plot layout at the West Normanby Bridge site in block N4 on Springvale Station. Also shown are the locations of the polygons within which erosion was detected by aerial LiDAR in the first period in green (LHS), and the second period in red (RHS).

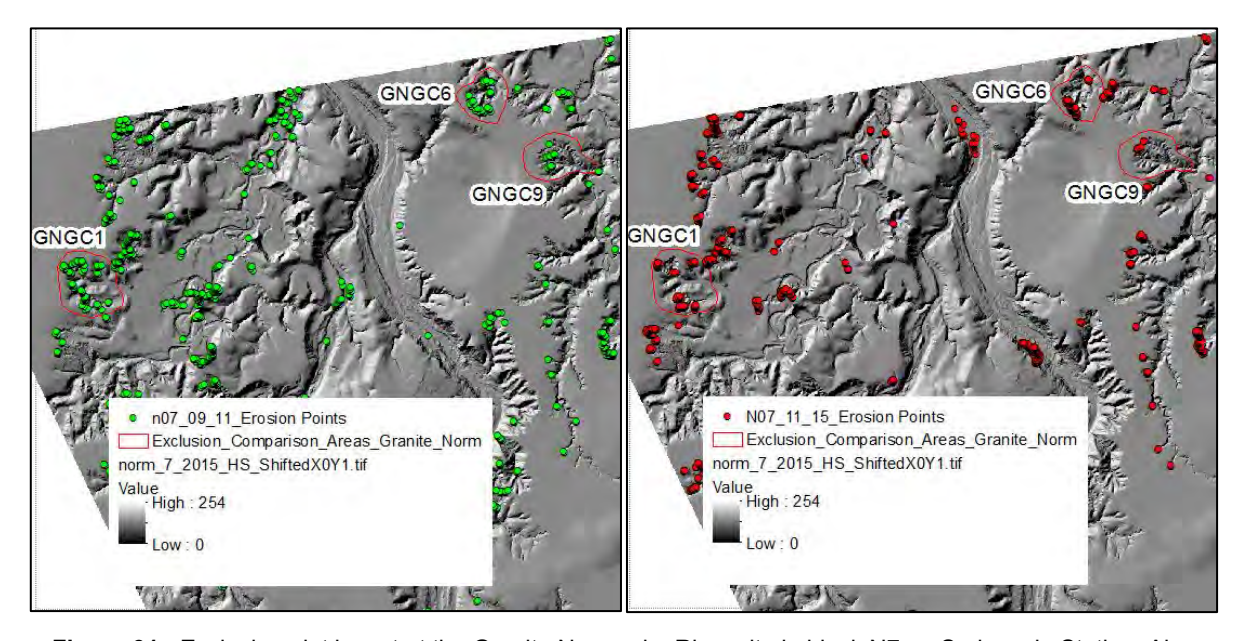


**Figure 31:** Exclusion plot layout at the Granite Normanby River site in block N7 on Springvale Station. Also shown are the locations of the polygons within which erosion was detected by aerial LiDAR in the first period in green (LHS), and the second period in red (RHS).

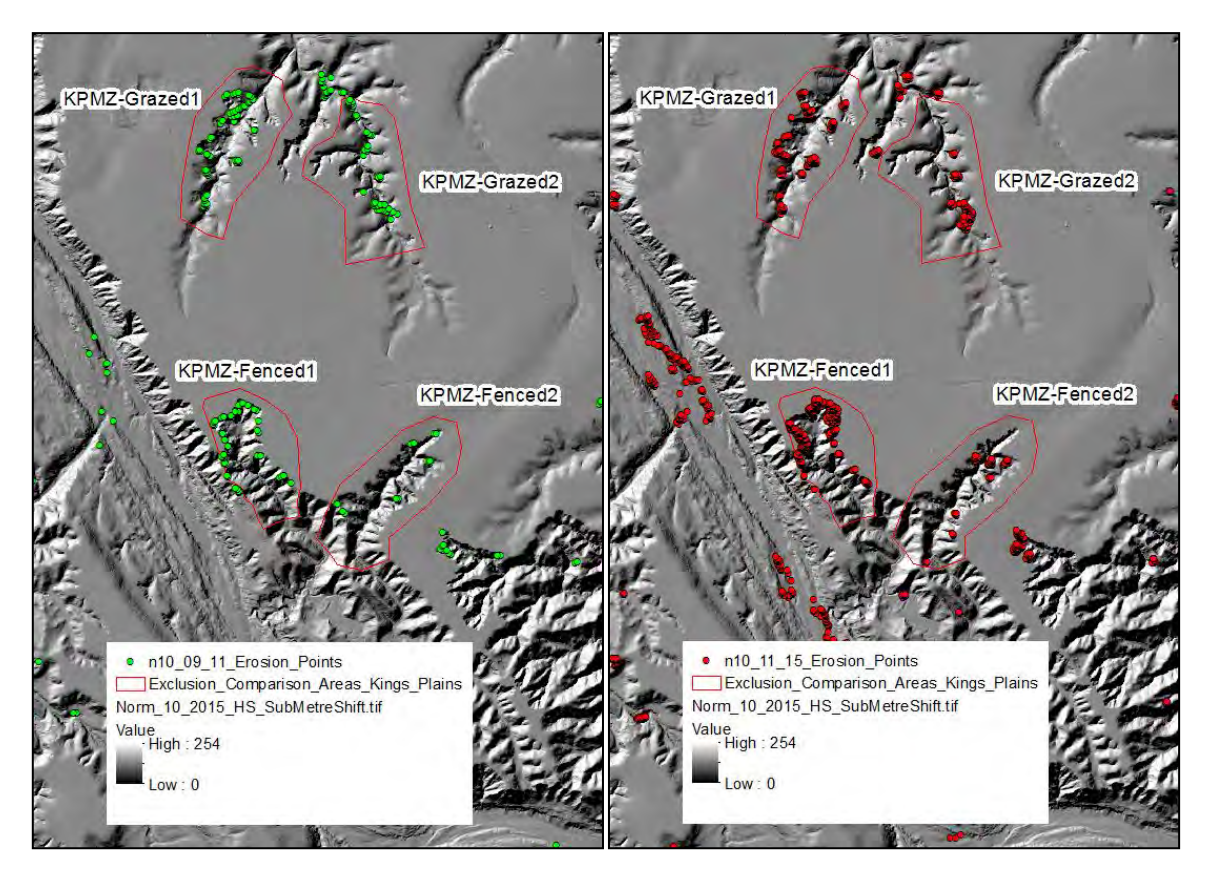


**Figure 32:** Cattle exclusion area and aerial LiDAR analysis areas (control-impact) at the Mosquito Yard site on Kings Plains Station in block N10. Also shown are the locations of the polygons within which erosion was detected by aerial LiDAR in the first period in green (2009-2011, LHS), and the second period in red (2011-2015, RHS). Note that the "Fenced" sites in this case are outside of the Mosquito yards.

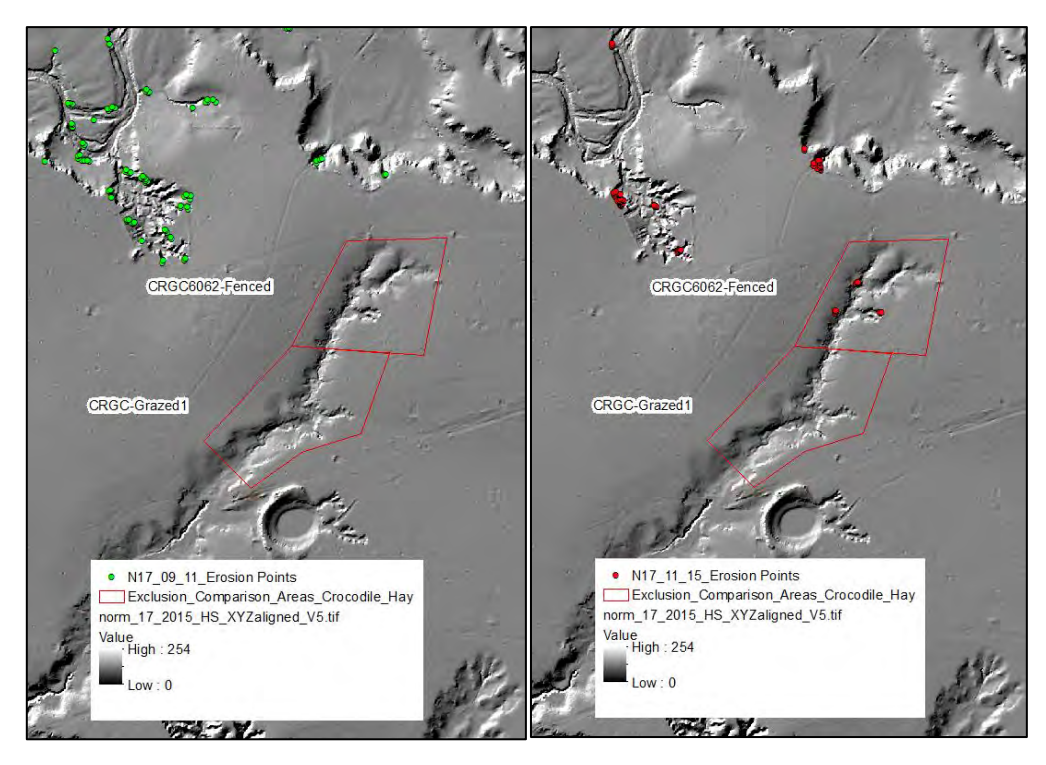


**Figure 33:** Exclusion plots on Crocodile Station at block N17. Also shown are the locations of the polygons within which erosion was detected by aerial LiDAR in the first period in green (LHS), and the second period in red (RHS).

### 2.3.2 Results of Aerial LiDAR Analysis of Cattle Exclusion Trial Sites

The plot area and sediment yield data for the respective plots are summarised in **Table 6**. The LiDAR change detection undertaken in these plots was the same approach taken in the broader analysis across the 7 common LiDAR blocks (See Appendix A).

The results of these tests on pooled data are shown in **Table 6** and they indicate the following:

- i) That there was a significant difference in erosion detectable by aerial LiDAR between the fenced and grazed areas prior to the exclosures being established, with there being more erosion in the fenced areas than the unfenced at the start of the study (p=0.0026)
- That there was a significant decline in erosion rates in the second period compared to the first period in both the fenced and grazed plots (p=0.0001)
- iii) That there was a significant difference in gully erosion detectable by aerial LiDAR between the pooled fenced and grazed areas 3-4 years after the establishment of the exclosures. I.e. the sediment yield declined more in the fenced areas than the grazed areas (p=0.007)
- iv) Small plot size and the relatively small erosion dataset (n=35 grazed; n=29 fenced erosion cells) and high standard deviations (26 to 36% of mean) affects the statistical power of these tests. More robust statistical analysis following BACI design utilizing higher resolution data from larger exclusion plots will be needed in the future.

**Table 6:** Summary of erosion results from the grazing exclosure plots at the three sites for which sufficient data is available to make valid comparisons regarding the erosion rates from the experimental plots (i.e. excluding CRGC).

		total yield m <sup>3</sup>		specific yield t/ha/yr			
Summary	area m²	2009-11	2011-15	2009-11	2011-15	plot change ratio	block change ratio
WN4 grazed 1	35127	169.2	264.5	38.5	30.1	0.78	1.56
WN4 grazed 2	30836	135.9	200.5	35.3	26.0	0.74	1.56
GN7 grazed 1	21694	363.9	356.8	134.2	65.8	0.49	0.54
GN7 grazed 2	15545	61.5	32.8	31.6	8.4	0.27	0.54
KPMZ grazed 1	27728	496.9	1265.5	143.4	182.6	1.27	1.09
KPMZ grazed 2	37030	85.6	106.3	18.5	11.5	0.62	1.09
WN4 Fenced	32040	238.7	138.2	59.6	17.3	0.29	1.56
GN7 Fenced	12487	521.7	345.6	334.2	110.7	0.33	0.54
KPMZ Fenced 1	35829	332.2	542.9	74.2	60.6	0.82	1.09
KPMZ Fenced 2	37030	602.4	499.0	130.1	53.9	0.41	1.09

	Mean					Standard Dev		
							F-test p-	
		Grazed	Fenced	p-value	Grazed	Fenced	value	
	2011	6,519.9	8,362.1	0.0026	1,490.7	2,895.5	0.0006	
	2015	3,815.7	4,257.7	0.166	1,270.2	1,205.9	0.798	
p-value		0.0001	0.0001		0.084	0.0001		

Table 7: Two tailed t test results for Normanby grazing exclosure trials

#### 2.3.3 Discussion of Aerial LiDAR Data at Cattle Exclusion Trial Sites

These preliminary LiDAR results indicate there was a detectable response of large-scale deep gully erosion to cattle exclusion over the short-term at three exclusion sites (West, Granite, Kings Plains), although the erosion rates were more influenced by rainfall totals and inherent gully evolution, than the cattle exclusion. The results appear to be particularly influenced by the results from the Kings Plains site, which was the least well constrained of the three sites, in that grazing pressure was intermittent, and the exclusion not complete. The results provide some suggestion that exclusion is an important part of the solution to reducing sediment yields from these gullies, but when combined with other evidence from the broader analysis at the block scale and the finer resolution plot scale data, it suggests that on its own it will not be nearly enough to achieve the ambitious targets of a 50% reduction in sediment yields within a decade. No major changes to vegetation or surface erosion measured in the field at the plot scale were observed in the field inside these mature alluvial gullies after 4 years of cattle exclusion (see section above). However, these results might not be transferable to shallower alluvial gullies, gullies with larger uneroded catchment areas (>25% of total) where grazing is excluded, or gullies earlier in their evolutionary cycle. For example, at the shallow gullies at the Crocodile Old Hay Paddock, vegetation response to cattle exclusion appeared to be more successful, although the erosion response was largely below the LiDAR limit of detection.

Overall, aerial LiDAR is not sufficient in detail to detect soil surface erosion and rilling at the scale of the treatments and vegetation plots measurement points. The soil surface erosion response, currently below the aerial LiDAR detection limit, showed no major trends at the plot scale from grazing exclusion over 4 years, but did highlight the variability and magnitude of surface erosion and deposition within gullies that are common over large areas. Non-headcut surface erosion in alluvial gullies can represent from 1 to 70% of measured sediment yield outputs at the event to annual scales (e.g., Shellberg et al., 2013a), and hence the sediment yields from these gullies could be significantly higher than reported here. The ratio of sediment load output from gully catchments derived from 1) deep gully erosion vs. 2) surface erosion, stripping, and rilling inside these large gully complexes is unknown.

Longer-term monitoring, sediment yield gauging at gully outlets, and more detailed datasets of surficial erosion (i.e. terrestrial LiDAR) inside alluvial gullies and in catchment areas above scarps, will be needed to better quantify potential sediment yield changes to grazing exclusion or other management intervention. Quantifying the detailed soil surface erosion

response at a much finer resolution would require terrestrial LiDAR scanning at 5mm pixel resolution to detect changes over short periods. Furthermore it is likely to take a lot longer than the 4 years of this preliminary trial for the effects of grazing exclusion to show a measureable change in aerial LiDAR data. Hence in this case in the short-term, aerial LiDAR is probably not the right tool to be picking up detailed erosion change.

Recent management strategies proposed by government have placed significant hope in the role of grazing exclusion from gullied areas as a front line strategy for reducing sediment and nutrient yields from gullied areas. Grazing exclusion is a critical first step in any gully management strategy, by removing the chronic disturbance pressure and preventing new gullies from forming as a result of cattle pads, low ground cover, and increased water runoff. However, these initial results would tend to suggest that significant reductions in erosion rates from active alluvial gullies on timescales of 1-2 decades are going to require more intensive stabilization measures if we are to come close to meeting the ambitious 50% sediment yield reduction targets over a decade set by government.

As demonstrated elsewhere in this report (Appendix C), we now know that alluvial gullies are also significant sources of bioavailable nutrients. Hence, any future studies looking at the effect of grazing exclosures on catchment water quality, should also monitor the potential benefits of cattle exclusion on nutrient contributions from gullies. This is especially the case for surface erosion not detected by aerial LiDAR. It may be that the benefits to water quality from fairly subtle increases in vegetation cover and resistance that do not have a measurable impact on large-scale gully sediment production (i.e., scarps and slumps), do have an effect on nutrient retention on soil surfaces and deposits within the gully complex.

# 2.4 Bioavailable nutrients and organics in alluvial gully sediment (Garzon-Garcia, Burton, Brooks)

### 2.4.1 Background

Gully erosion is a major source of fine sediment pollution to the Great Barrier Reef (GBR). This can be inferred from the knowledge that the large, dry, grazing-dominated catchments in the Tropics (e.g. Fitzroy, Burdekin) deliver the largest sediment loads to the GBR (Garzon-Garcia et al., 2015; Joo et al., 2012; Kroon et al., 2012). Sediment source tracing studies that have indicated that subsurface soil is the predominant sediment source in these catchments, particularly in areas with active gully erosion (Hughes et al., 2009; Olley et al., 2013; Wilkinson et al., 2015). Alluvial gully erosion has been shown to be the dominant form of gully erosion in the Normanby Catchment (Brooks et al., 2013), and while data doesn't exist as to the relative contribution of the different gully forms for other catchments, it is likely that in catchments such as the Bowen River, alluvial gullies are a significant, if not the dominant source.

Fine sediment and nutrient delivery to the GBR has detrimental chemical/biological effects on the reef (Bainbridge et al., 2012; Brodie et al., 2010; Brodie et al., 2012; Wolanski et al., 2008). Recent work undertaken in the Burdekin and Johnstone River catchments has demonstrated that there are significant quantities of bioavailable nutrients (nitrogen and phosphorus) associated with fine sediments derived from eroded soils (Burton et al., 2015). This work also indicated that sediments have the ability to produce dissolved inorganic nitrogen (DIN) from their organic N sources as they move through the waterways, thereby contributing to the DIN pool. Hence, given that we know alluvial gully erosion constitutes a significant component of the anthropogenically accelerated sediment load in the Normanby and Mitchell catchments where it has been studied in detail (Shellberg et al., 2010; Brooks et al., 2013; Shellberg et al., 2016), by extension they are also contributing substantially to the anthropogenic DIN pool. Consequently, effective management practices should aim at reducing not only sediment yields from alluvial gullies, but also organics and nutrient yields. Research has been carried out in a number of key catchments within the GBR to identify the key sources of fine sediment (Bainbridge et al., 2016; Bainbridge et al., 2014; Hughes et al., 2009; Olley et al., 2013; Wilkinson et al., 2015), however very little is currently known about sources of organics and nutrients, particularly within the catchments of the dry tropics dominated by grazing. An understanding of the key sources of organics and nutrients and their bioavailability and quantity associated with alluvial gully erosion is fundamental to inform management decisions.

In this report, results for various key indicators of bioavailable nutrients and organics (the term carbon is used interchangeably with organics in this report) are presented and analysed for three alluvial and one hillslope gully in the Normanby River catchment. The key indicators were selected based on previous and ongoing research conducted by Burton et al. (2015). The nutrient fractions and organic pools associated with different particle size fractions (total soil, <63 um, and 10 um) were determined for different gully geomorphic units including terrace surface soil, gully bank surface soil, gully bank sub-surface soil, and gully floor deposits. The total sediment, organic and nutrient export from the three alluvial gullies and their geomorphic units, was estimated using detailed annual sediment budgets coupled with nutrient and organic composition data from this study. A sensitivity analysis was also

carried out to understand the effect of changes in gully depth, sediment yield and geomorphic unit on relative contributions to organics and nutrient export from alluvial gullies.

Note that this report presents nutrient export budget results and interpretation of data from a limited number of gullies. Considering the low level of replication, results are to be considered as an indication only of the nutrient and organic pools within different components of gully complexes and of the range of organic and nutrient yields from gullies in the Normanby catchment, and should not be extrapolated.

### 2.4.2 Main findings

- Alluvial gullies are important sources of organics and potentially bioavailable nutrients to the aquatic environment.
- The data indicate little difference between bioavailable nutrient indicators in sampled hillslope (n=1) and alluvial gullies (n=3) for all particle size fractions sampled.
- There are significant differences in C, N, and P content among soils/sediments in the geomorphological units measured with the general pattern being terrace > bank surface > gully floor > bank subsurface. This result indicates that accurate estimation of nutrient and organic losses from gullies must rely on sampling and measurement of the different units.
- The upper 10-20cm of alluvial terrace soil profiles appear to be an important long term store of bioavailable nutrients and organics, whilst gully floors may act as a temporary store depending on gully evolution stage.
- Total organic carbon (TOC) soil content in the terrace surface soils was from 54 to 77 times larger (depending on particle size fraction) and total nitrogen (TN) from 5 to 10 times larger than in bank subsurface soil in alluvial gullies.
- Primary gully erosion into terrace alluvium is ubiquitous in catchments like the Normanby and Burdekin (**Figure 34**).
- Particle size significantly influences nutrient and organic content and would influence bioavailability - hence particle size fractionation should be a major consideration in future study designs.
- The <10um fraction is generally enriched in bioavailable nutrients compared to the <63um fraction (1.4 to 3.3 times on average for carbon and nitrogen fractions), which is generally enriched compared to whole soil irrespective of gully geomorphic unit (with some exceptions e.g., DRP) (1.4 to 9.5 times on average for carbon and nitrogen fractions). These results from gullies in the Normanby catchment are consistent with results from key soil types in the Burdekin and Johnstone catchments (Burton et al., 2015).</li>
- Although terrace soil had the highest concentration of most nutrients and organics, gully bank sub-soil was generally the main source of sediment in these alluvial gullies, due to the sheer volume of sub-soil delivered from active gully erosion detectable by aerial LiDAR.
- The sources of organics and nutrient export from alluvial gullies would vary depending on the type of erosional process occurring in the alluvial gully (i.e. headscarp retreat vs. secondary incision vs. surface erosion from exposed subsurface side walls) and their stage of evolution (e.g., gully depth and age) – however these findings should be confirmed with larger sample replication.

- In general, terrace soil was found to be the main source of total organic carbon export when headscarp retreat contributes the majority of sediment.
- The contribution of terrace soil to nutrient export varied with the stage of gully evolution. In the initial stages of gully evolution [very shallow gullies (<1.0 m) growing fast into the terrace deposits], terrace soil is the main source of nutrient export. As a result it should be a priority to protect terrace deposits from fast headscarp retreat as these deposits contain large pools of carbon and nutrients that, when lost, would be very difficult to restore. These terrace soil organic and nutrient pools may also be the most bioavailable and have a larger relative impact once in the aquatic environment.</p>
- As gully incision occurs, the main source of most nutrient fractions was clearly bank subsurface sediment. Although this sediment has lower nutrient concentration than terrace surface soil or gully floors, the sheer quantity of exported sediment from this source (detectible by LiDAR) makes it the largest estimated contributor. It is also likely that most surface erosion (not detected by aerial LiDAR) is sourced from exposed sub-surface material in the gully scarps and sidewalls, and hence the proportion contributed from the sub-surface material is likely to be even higher than reported here. Therefore, despite the nutrient enrichment of the surface soils (which are a component of both gully headscarp and sidewall retreat) gully sub-soils would tend tobe the main source of nutrients by volume. Hence, there is no one component of a gully system that can be prioritised over another; the whole gully should be stabilised as all components are significant nutrient sources.
- When secondary incision erodes organic and nutrient rich sediment deposited on gully floors, this sediment may become a very important source of organics and nutrient export; even more so than bank subsurface soil. The protection of gully floor organics and nutrient deposits should be part of gully rehabilitation designs and should be prioritized when these deposits are rich in organics and nutrients.
- The majority of the nitrogen in alluvial gully soils/sediments is in organic form (more than 96% in all particle sizes and geomorphic units). The exported organic N from alluvial gullies is potentially bioavailable and thus may be mineralized into dissolved inorganic nitrogen during stream transport, once it gets to the estuarine or marine environment, or be used directly by algae in dissolved organic form.
- While it has long been recognised that gullies are an important source of fine sediment to the GBR, it is also apparent the gully sources are a much underappreciated source of nutrients as well. When compared to typical values of anthropogenic nitrogen and phosphorous from other major land uses in GBR catchment, it is apparent that gullies could be even more significant sources than intensive agricultural land per unit area.

Gully/land use	sediment (t/ha/y)	TN (kg/ha/y)	TP (kg/ha/y)	
Granite Normanby	114.0	54.0	23.7	
Laura - Crocodile station	29.2	10.5	0.3	
Laura - Crocodile Gap	28.8	12.6	1.6	
Sugar cane	1.2	22.2	2.7	
Banana	1.8	25.3	3.1	
Nature conservation	0.2	3.6	0.3	

(see table 7 in Appendix C)

One of the most important implications of our findings is that alluvial gully erosion cannot continue to be overlooked as an important source of nutrients and potentially bioavailable nutrients to the aquatic environment. There is a fundamental need to increase our understanding of the links between organics and nutrient sources, alluvial gully erosional processes and instream processing. For example, it is crucial to understand differences in the bioavailability of exported sediment from different geomorphic unit sources once in the aquatic environment. Although various indicators of the bioavailability of these sediments were quantified in this study, on-going research is still necessary to define which of these indicators would be the best to predict the impact of organics and nutrients on primary production in the freshwater and marine environment (Burton et al., 2015) and what controls this bioavailability (Garzon-Garcia et al. in prep). The role of vegetation and litter has been proposed as crucial, not only to the rehabilitation of carbon and nitrogen pools in gullied landscapes, but to reduce the impacts of eroded sediment during its transport in the aquatic environment by promoting mineral nitrogen use by microbes during mineralization of vegetation litter carbon (Garzon-Garcia, 2014). Further research is necessary to better understand the role of vegetation in mediating these relationships.

This study gives some indication of management priorities to reduce organics and nutrient export from alluvial gullies and identifies the importance of (i) sampling and analysing key gully features separately, and (ii) understanding the stage of evolution of the gully / combination of erosion processes occurring (i.e. head scarp retreat vs. secondary incision vs. surface erosion within the gully; **Figure 34**, **Figure 35**). The findings of this study should be further tested by sampling a larger number of alluvial gullies (replicated by gully type), including sampling of exported sediment and empirical gauging yield, examining the effects of changes in sediment particle size, determining the relative bioavailability of nutrient derived from different sources, and using sediment source tracing to determine the relative contribution of each geomorphic unit. It is recommended that sampling design targets main geomorphic units from gully categories based on erosional process (e.g., soil surface stripping, rilling, scalding, fast headscarp retreat, primary incision, secondary incision, widening, etc.)



Figure 34: Example of primary gully erosion into an alluvial terrace on Springvale Station Normanby catchment



**Figure 35:** Example of secondary incision into a >50 yr old primary gully floor — Springvale Station — Normanby catchment

# 2.5 Gully Slope Stabilisation Treatment Trials – updated survey (Spencer, Brooks, Shellberg)

In this section we present some updated results from gully stabilization trials carried out at a site on Crocodile Station on the Laura River, in the Normanby catchment. A full description of the demonstration trial site is contained in Shellberg and Brooks (2013), but a brief summary of the study design and the results from the first two years is provided here.

### 2.5.1 Study Overview

The Crocodile Station gully rehabilitation trial site was established to trial approaches for stabilizing active gully headwalls in duplex sodic soils on alluvial terraces. As detailed in the broader analysis of gully erosion rates across >5000 ha of the Laura and Normanby River catchments (Appendix A), primary active gully headscarp retreat represents a major source of fine suspended sediment and nutrients contributed to the stream network. Therefore developing optimal approaches for stabilizing such gully headscarps and associated gully side walls is critical if the sediment and nutrient inputs from gullies are to be reduced within appropriate management timeframes (i.e. one to two decades).

The Crocodile Station trial site includes trials of a number of different strategies for demonstration purposes (e.g. use of rock and wood grade control structures etc.), but a set of controlled plots were established to test which set of soil amendments would provide the greatest degree of sediment reduction over the short term. In this report we will focus on the gully regrading soil amendment trials, given that the other treatments were more qualitative demonstrations and we don't have quantitative data on their performance.

Results from an example of a full gully treatment at CRGC1-40 (**Figure 36**) were reported on in Shellberg and Brooks (2013) but no further data on this site is presented here. The results from the first two years show significant reductions in sediment yield at this full gully scale as well, although there was evidence that secondary incision was occurring and continues at this site from the first year post-treatment. Anecdotally it would appear, that this has not progressed significantly over the last two years, but this is partly a function of the lower rainfall over the last two wet seasons. This does highlight, however, the importance of incorporating well designed mechanisms to prevent secondary incision into regraded gullies.

All sites were selected on the basis that they represent an example of an alluvial gully complex where the gully is incising into alluvial terrace material that is no longer over topped by floodwaters. While we have not dated this site specifically, from equivalent sites that have been dated in the Normanby catchment (see Pietsch et al., 2014) we can surmise that these deposits are of late Pliestocene age (20-30Ka). Hence, overbank flooding and backwater inundation (sensu Shellberg et al., 2013b) does not occur at this site under the current hydrologic regime. Overland flow into the gully from up-slope catchment contributions were fairly minimal on the western side-wall with a small catchment area, but significant on the eastern sidewall and head scarps (Figure 1). For plot treatments on the western side-wall, diversion berms were built around the experimental site at the outset to ensure that the hydrological driver being tested was just the rain falling directly on the plots. There is a great deal of focus in much of the gully management literature derived from hillslope gullies about the importance of the contributing catchment area as a key driver of gully location and

activity (e.g. Wilkinson et al 2015), and hence the importance of reducing overland flow into gully heads and thereby slowing down gully activity rates. This is an important consideration in hillslope gullies, as well as many alluvial gullies, however, alluvial gullies that are situated in areas with highly sodic sub-soil do not necessarily require any upslope catchment area to erode at relatively high rates. All they require is direct rainfall on the active gully area itself to progress, but erosion can be enhanced by both upslope catchment runoff and river backwater (Shellberg et al., 2013b). In this experiment, we exclude any additional overland flow from the gully and any erosion that is measured is a function of direct rainfall onto the plots themselves.

Aerial LiDAR DEMs of the experimental plots before treatment and after 4 years post-treatment are shown in **Figure 36**, while a summary of the treatments is shown in **Figure 37** and a more detailed description of the plot treatments is shown in **Table 8**. Also shown in **Figure 37** are the treatment plots as they looked immediately post-construction, after the first wet season and then after 4 wet seasons.

The objective of these trials was to show what the most effective soil remediation approaches are in situations where gully head scarp grading is required to halt gully migration into highly sodic alluvial terrace soils. The trials were NOT suggesting that this is a one size fits all solution that should be applied to all alluvial gullies, rather that anything done with highly sodic soils will require soil remediation strategies along the lines of the most effective strategies applied in these trials.

Whilst there are a large array of treatment combinations that could have been trialed in experimentation, we tested the influence of gypsum application, fertilizer application, compost application, exotic and native grass sowing, and slope lengths. The various treatments that were applied were selected on the basis that they are the sort of things that either have been trialed in the past (e.g. **Figure 37** which is equivalent to Plot 1), or most importantly are locally practical measures for stabilization that might be applied by soil conservation experts to stabilize a gully headwall. Thus the treatments trialed were such that they optimized the chances of the respective treatment working.

The key results from the first two years of these trials have been presented in Shellberg and Brooks (2013). In this study we report on an additional two years of monitoring using terrestrial laser scanning to measure the ongoing erosion rates since the last survey in 2013. One additional question from this period was whether the two tropical cyclones that passed through this area over this period had any measurable impact on these sites. At a policy level, concerns have been raised as to the likely resilience of gully rehabilitation sites that are subject to cyclone impacts, so it was thought this may represent an opportunity to evaluate the effect of cyclones on gully rehabilitation sites. As it turned out, Cyclone Ita and Cyclone Nathan had fairly benign rainfall rates in this area, generating rainfall that was not out of the



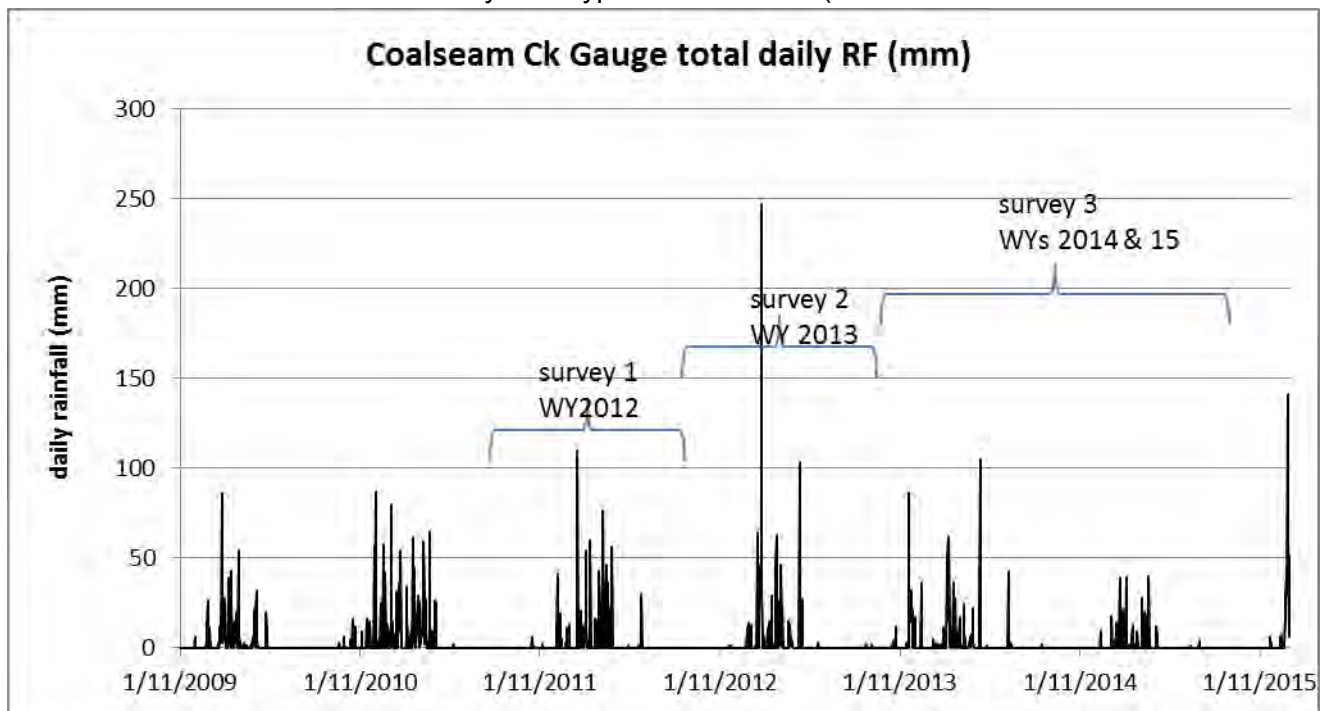


**Figure 44**). The best indication we have as to how a major cyclonic event might affect these gully rehabilitation sites comes from the cyclone Oswald event early 2013, already reported in Shellberg and Brooks (2013) for erosion at these plots, and incorporated into the date presented here.

The key additional component presented here that builds on these results enables us to 1) see how persistent the trends are that were established in the first two years, 2) whether this might provide some insight into the level of ongoing maintenance that will be required if such strategies were implanted over large areas, and 3) what factors need to be considered if scaling these trial plots up to a full gully treatment programme.

### 2.5.2 Plot Contingency Lessons with Hindsight

One of the potential confounding issues that has become apparent with these plots as time has progressed is the effect of the interaction between the plots themselves the broader set of erosion process occurring with the gully complex. When the various treatment plots were original setup from mechanical reshaping and mixing, the plot slopes and conditions were fairly equal. The first few years of comparison of response to rainfall-runoff erosion were valid for understanding the isolated effects of different soil treatments. However, over time the effect of antecedent geomorphic conditions became more pronounced. That is, future gully erosion is contingent on past rill erosion and inherited base level conditions (Phillips 2013; Bennett et al. 2015). Some of the deeper rilling that has occurred on some of the treatments plots is partly a function of differential amounts of base level control associated with the incision and lateral movement of the main channel within the gully complex. This is best seen in the oblique aerial image shown in **Figure 39**. The developing channel with the main gully complex (indicated by the dashed white line) impinges more closely to plots 5-7 than it does the other plots, while plots 2-4, and to a lesser extent plot 1, are somewhat buffered from the effect of this base level control by the remnant gully pedestal immediately

downslope from plots 2 and 3. Further discussion around this potential interaction is discussed below. However, the worst case scenario here is that some of the observed erosion rates at plots 5-7 and 1 might be somewhat higher than might have been the case had base level control been consistent across all plots, with lower relative erosion rates at plots 2-4. Thus continued analysis of this site beyond the first 1-2 to 4 years is not recommended for quantitative comparison purposes.

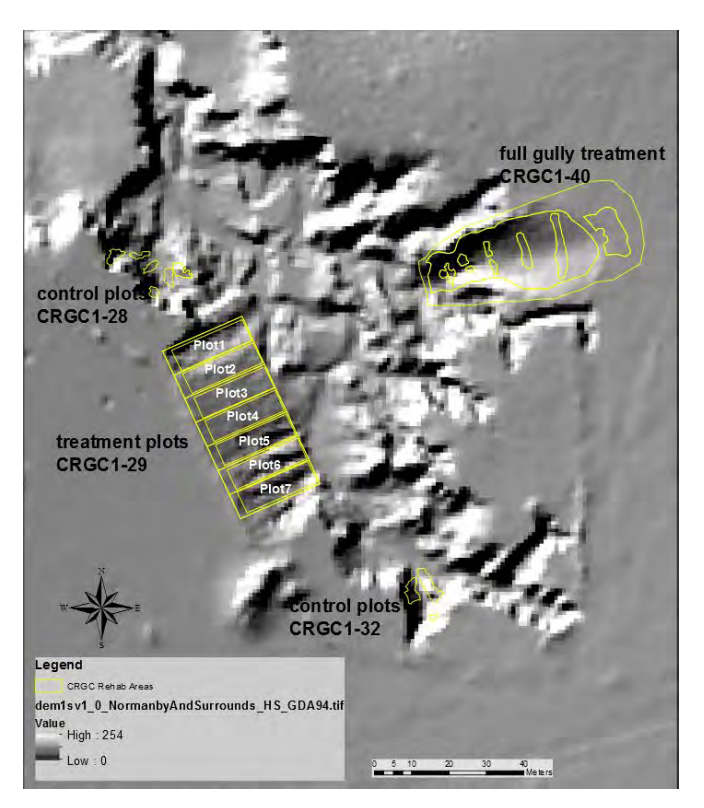


**Figure 36:** Aerial LiDAR DEMs of the Crocodile Station gully rehabilitation trial site with the rehabilitation trials plots overlaid on the 2009 DEM (LHS) (before treatment) and the 2015 DEM (RHS) 4 years post-treatment.



**Figure 37:** Example of a regraded alluvial gully in the Bowen catchment of unknown age with a constructed berm to exclude overland flow from the gully and with no soil treatment. This is the equivalent of the plot 1 control site in which the gully is regraded with only direct rainfall driving high levels of ongoing erosion.

- 1. No Treatment
- 2. Gypsum, Compost, Native Grass
- 3. Gypsum, Compost, Exotic Grass
- 4. Gypsum, Hydromulch, Exotic Grass
- 5. Gypsum Only
- 6. Compost, Native Grass
- 7. Straw, Exotic Grass





**Figure 38:** Photos of the treatment 7 x 25m 12% slope plots at the time of implementation in December 2011 and after the first wet season in 2012, and after 4 wet seasons in 2015.



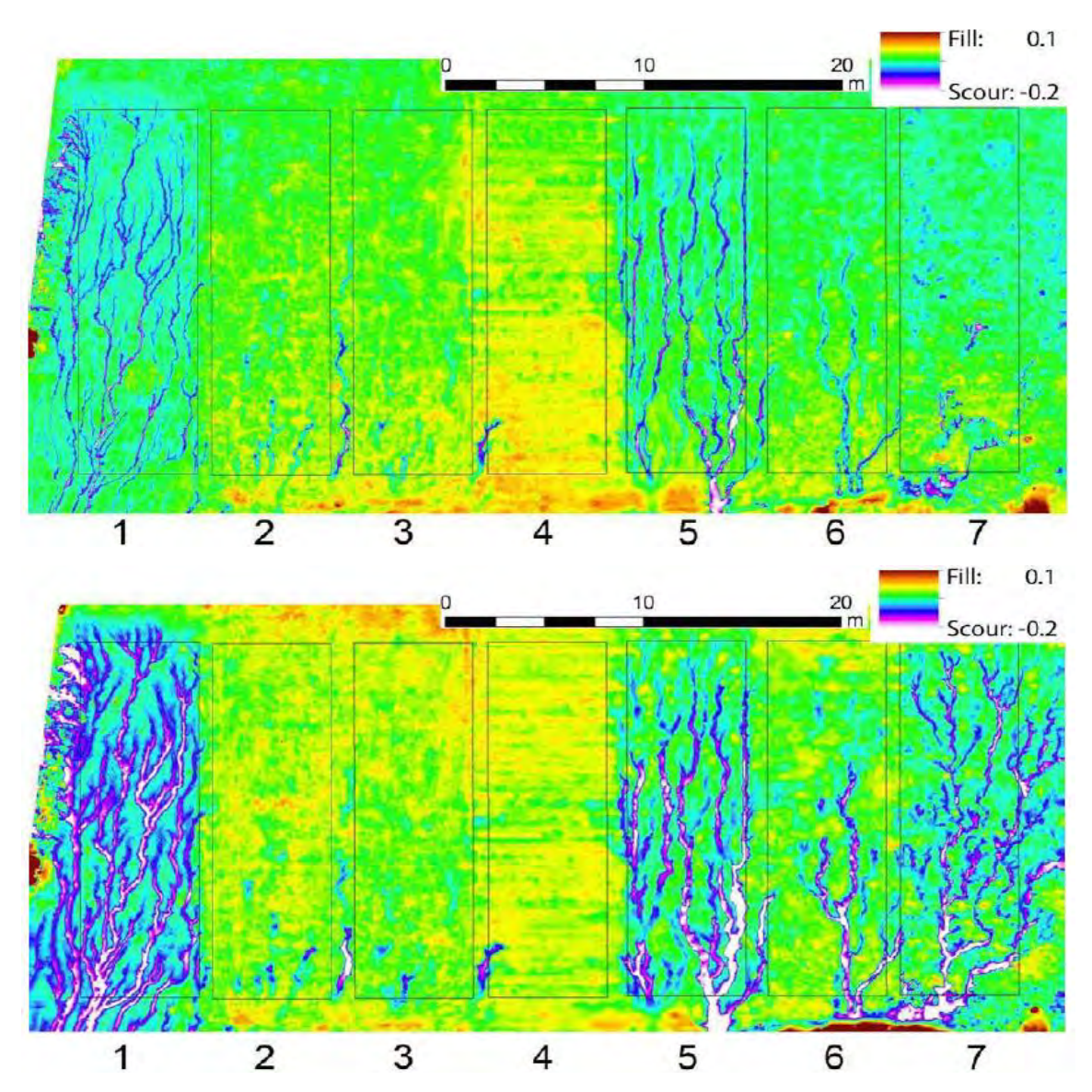
**Figure 39:** Oblique aerial photograph of the Crocodile trial plots with the control area (CRGC1-28) to the right (note the actual areas used for control erosion measurements are smaller plots within the area indicated. Note people/vehicles for scale (photo: John Brisbin).



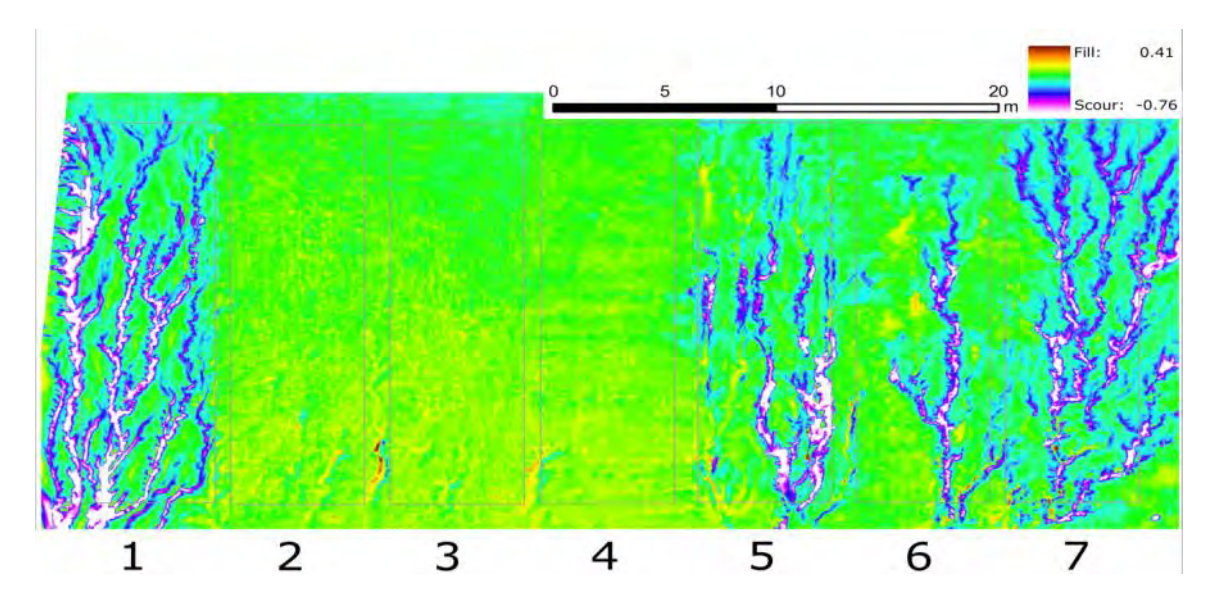
**Figure 40:** Remnant gully pedestal immediately downslope from plot 3 in June 2015, which is potentially buffering base level lowering downslope from plots 2-4 to a greater extent than the other plots.

 Table 8: Description of the plot treatments at the Crocodile rehabilitation site

Gully	Plot #	Treatment	Gypsum	Mulch	Grass
CRGC1-29	1	Regrade Only	None	None	None
CRGC1-29	2	Regrade, Gypsum, Compost, Native Grass	80t/ha	25mm surface compost	Native grass: Kangaroo (Themeda triandra), Black spear (Heteropogon contortus), Queensland bluegrass (Dichanthium sericeum) (180 kg/ha or 3.8 kg/210 m²)
CRGC1-29	3	Regrade, Gypsum, Compost, Exotic Grass	80t/ha	25mm surface compost	Exotic grass: Indian bluegrass (Bothriochloa pertusa), Saraji Sabi grass (Urochloa mosambicensis), Jap millet (Echinochloa esculenta) (180 kg/ha or 3.8 kg/210 m²)
CRGC1-29	4	Regrade, Gypsum, Hydromulch, Exotic Grass	90t/ha	10mm surface hydromulch	Exotic grass: Indian bluegrass (Bothriochloa pertusa), Saraji Sabi grass (Urochloa mosambicensis), Jap millet (Echinochloa esculenta), verano stylo (Stylosanthes hamata) (100 kg/ha or 2.1 kg/210 m²)
CRGC1-29	5	Regrade, Gypsum	80t/ha	None	None
CRGC1-29	6	Regrade, Compost, Native Grass	None	25mm surface compost	Native grass: Kangaroo (Themeda triandra), Black spear (Heteropogon contortus), Queensland bluegrass (Dichanthium sericeum) (180 kg/ha or 3.8 kg/210 m²)
CRGC1-29	7	Regrade, Straw, Exotic Grass	None	25mm surface straw	Exotic grass: Indian bluegrass (Bothriochloa pertusa), Saraji Sabi grass (Urochloa mosambicensis), Jap millet (Echinochloa esculenta) (180 kg/ha or 3.8 kg/210 m²)
CRGC1-28	CRGC1- 28	No Treatment Control Side-Wall	None	None	None



**Figure 41:** DEM of Difference from 2012 (top) and 2013 (bottom); i.e. after one and two wet seasons respectively from Shellberg and Brooks (2013). Note that the images are presented in mirror to their actual orientation on the ground for ease of visualisation.



**Figure 42:** DEM of difference from 2013 to 2015. Note that range of fill and scour in this survey is much greater than that used for the previous survey, given that some of the deep rills are now up to  $\frac{3}{4}$  of a metre deep.

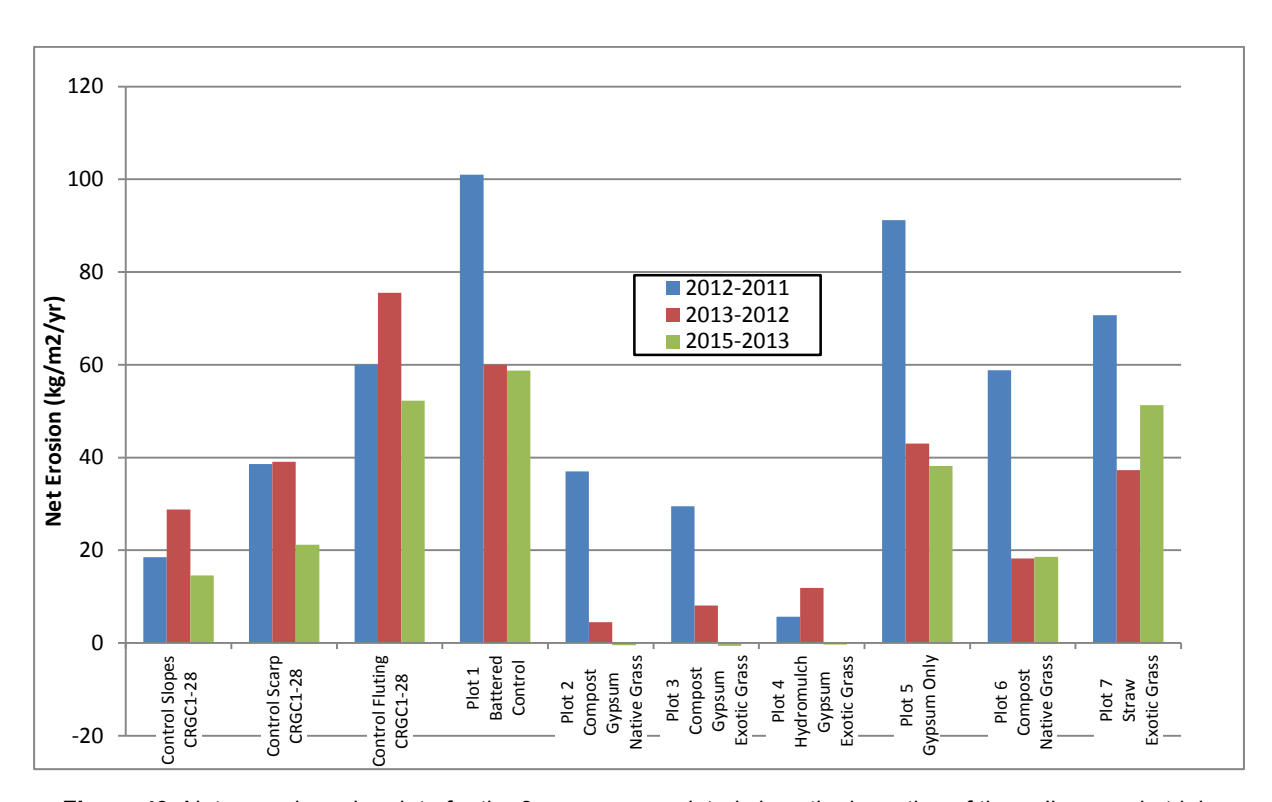


Figure 43: Net annual erosion data for the 3 surveys completed since the inception of the gully regrade trials

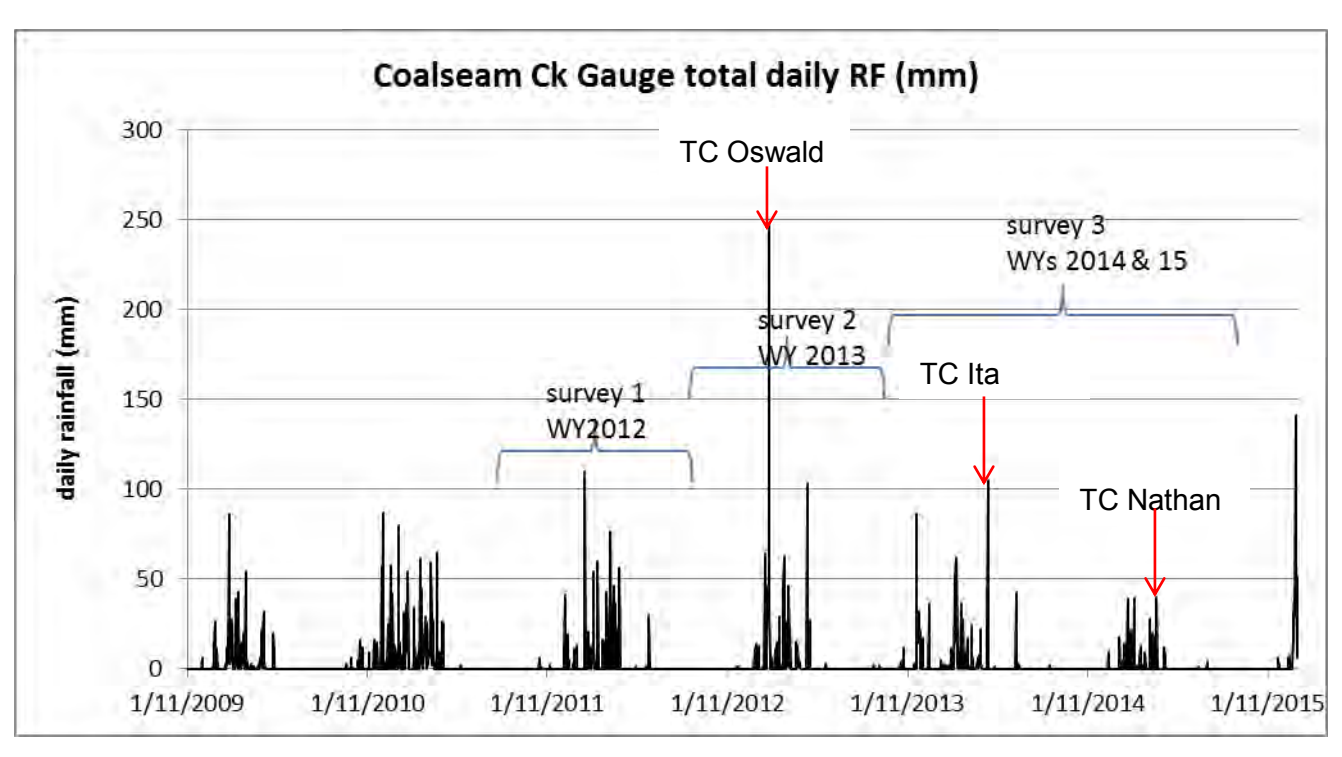
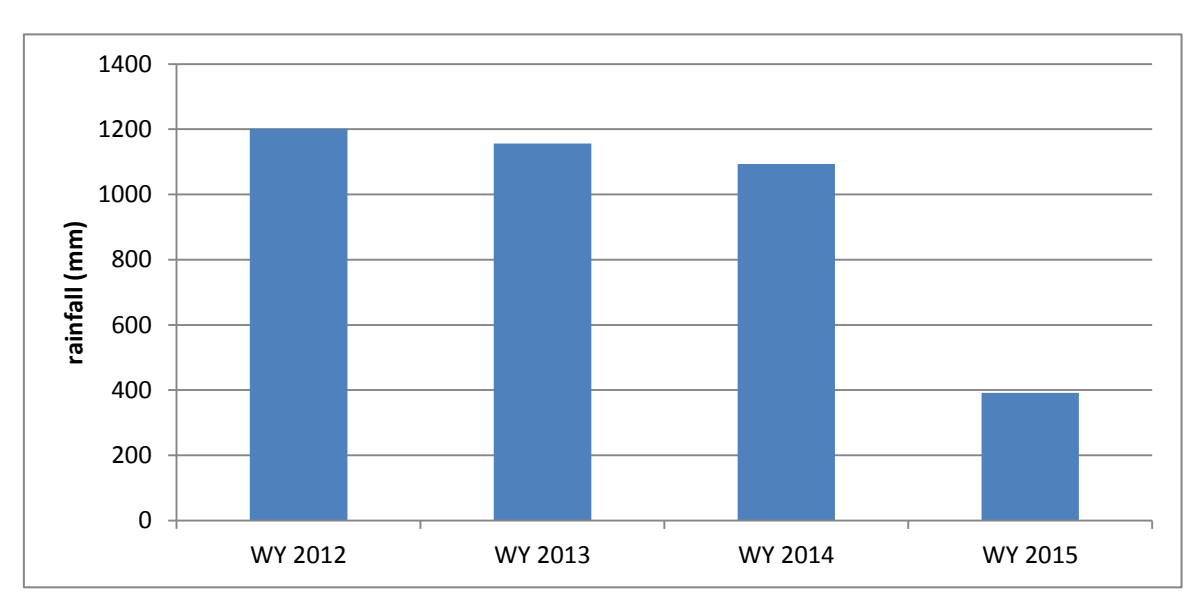


Figure 44: Daily rainfall at the DNRM gauging station on the Laura River at Coalseam Ck, which is the closest available daily rainfall record that covers the full trial period (additional data from the Crocodile Station homestead are forthcoming).



**Figure 45:** Annual rainfall at the Coalseam Ck gauge which is around 23km from the site. The annual average for the 2014 and 2015 water years is around 740 mm.

#### 2.5.3 Results

A detailed description of the results for the first two wet seasons post trial initiation is presented in Shellberg and Brooks (2013) and the reader is strongly advised to refer to this in addition to this update. In this update we focus on the erosion rate data that has resulted since the last survey in 2013. The previous report includes detailed results on the response of a range of variables to the various treatments, including vegetation biomass, root biomass, soil infiltration rates, exchangeable sodium percent, and bulk density.

Net erosion data for all plots (**Figure 43**) shows a consistent pattern of relative yield between the plots with plots 1, 5 and 6 showing similar annual rates for the last two years compared to the earlier surveys, with plot 7 showing a relative increase. Plots 2-4 have all declined to a point which is below the level of detection for the terrestrial LiDAR technique, given that these three plots were the ones with the most vegetation and some stubble still remained after the plots were mown prior to survey. While it appears that there has been net sediment accretion on each of these plots (i.e. negative net erosion), this is highly unlikely given that there is no source from upslope that could be causing deposition on these slopes. It is more likely that there has been a small amount of additional erosion, but we cannot detect this amongst the noise that is the low levels of vegetation stubble remaining on the plots.

The annual rainfall for the 2015 water year was significantly below average for this area and the previous 3 years of the study (**Figure 16**) notwithstanding the passage of Cyclone Nathan further to the north in this period, and substantially less than the rainfall over the previous 3 years of the study. This has the effect of bringing the annual average over the two water years comprising this survey to around 740mm, which is around 70% of the previous two years. Hence given the lower rainfall over this period, we would expect the net erosion rates to be lower for all of the plots, all other things being equal. The fact that plots 1, 5, 6 and 7 are all either about the same or slightly more in the case of plot 7, may suggest that, as outlined above, the role of differential base level control has had some bearing on

these results. From **Figure 39** it is evident the plot most influenced by the base level controlled rill erosion is plot 7, with plots 6 and 5 also potentially influenced, as well as plot 1. However, the fact that these sites have maintained similar trajectories to those established in the earlier two surveys, would tend to suggest that the effect of any base level influence is not alone sufficient to have dominated the most recent erosion patterns and rates at the plots. The initial patterns and degree of erosion in 2012 were dominated by the treatment measures and the initial rilling that recent erosion was contingent on. At most, base level influence will have altered the relative degree of difference between the most effective treatments (plots 2-4) compared to the control site with no soil treatment (plot 1) and the other external controls.

Accounting for the possibility of some over-estimation of yields in plots 1, 5, 6 & 7, and underestimation in plots 2-4, we compared the plot erosion over the 4 water years surveyed to the pooled external control data. This allowed for the assessment of the relative improvements to sediment yields achieved by the various treatments. From these data it is clear that only treatments that include gypsum, compost and/or hydromulch are worth seriously considering. Regrading slopes without any soil treatment has the effect of actually increasing erosion rates by around 60%, and even the treatments with only gypsum or straw mulch and seed have resulted in net erosion above background gully erosion rates. The gypsum + hydromulch performed slightly better overall in terms of net 4 year sediment yield (11% to 25% for plots 2 & 3), due to the initial protection against the first wet season rains afforded by the bonded fiber matrix in the hydromulch. However, in the longer-term grass cover response with the hydromulch was significantly less than that with the two plots that incorporated gypsum, compost and grass seed. Thus compost blankets with grass seed and gypsum provide the most self-sustaining solution. Exotic grass and weed invasion into compost blankets from surrounding areas remains a problem however for trying to establish specific vegetation communities. As flagged in Shellberg and Brooks (2013), it would be interesting to trial a combination of compost and hydromulch.

#### 2.5.4 Summary

The results from this study suggest that significant reductions to sediment yields from headscarps and sidewalls of alluvial gullies can be achieved in a few years through the combination of regrading, neutralization of soil sodicity by the addition of gypsum to the near surface soil, and the recreation of an organic soil horizon through the addition of compost and/or hydromulch. The results suggest that reductions of the background sediment yield in the order of 90% are achievable over the short term for gully side walls, providing base level erosion of the main gully is appropriately controlled. Such gains are inevitably a function of the rainfall regime experienced immediately after the treatment is established (both extreme events and sufficient wet season rainfall to support seeding survival). This may be an argument for using hydromulch in the first instance and then subsequently augmenting the soil profile with additional compost once the slope has been stabilized and survived the first wet season. This would, however, only be possible in some locations and would have to be weighed up against the potential for destabilizing the site simply by accessing it to reapply the compost/mulch. Alternative combinations of a deeper compost layer coupled with hydromulch should be further investigated.

The results of the surveys following an additional two wet seasons suggest that in those treatments where there is no base level lowering, that erosion rates are decreasing, even taking into account the lower rainfall over this latter period. This is the case even though grass cover had to be completely removed (mown down to almost nothing) to enable each LiDAR survey to be completed. Hence, these results would indicate that the sediment reductions shown in Figure 46 could be maintained over multi-decadal time frames, providing new incisional processes can be halted through base level control. If strategies such as those trialed here are to be scaled up and implemented within appropriate sections of gully side walls and head scarps across GBR catchments, the major challenge henceforth will be developing complementary strategies for dealing with 1) slope drainage features on longer slopes than trialed here, 2) steeper slopes where large-scale earth moving is prohibitive. 3) catchment runoff control with diversion banks and contour berms in remote bushland, 4) grade control structures to prevent secondary incision into the primary gully floor, and 5) grade control structures to ensure a stable interface is maintained between the treated gully sidewalls and the main part of the gully. Given the dominance of alluvial gullies as fine sediment and nutrient sources to the GBR, the future health of the GBR rests on our overcoming such challenges.

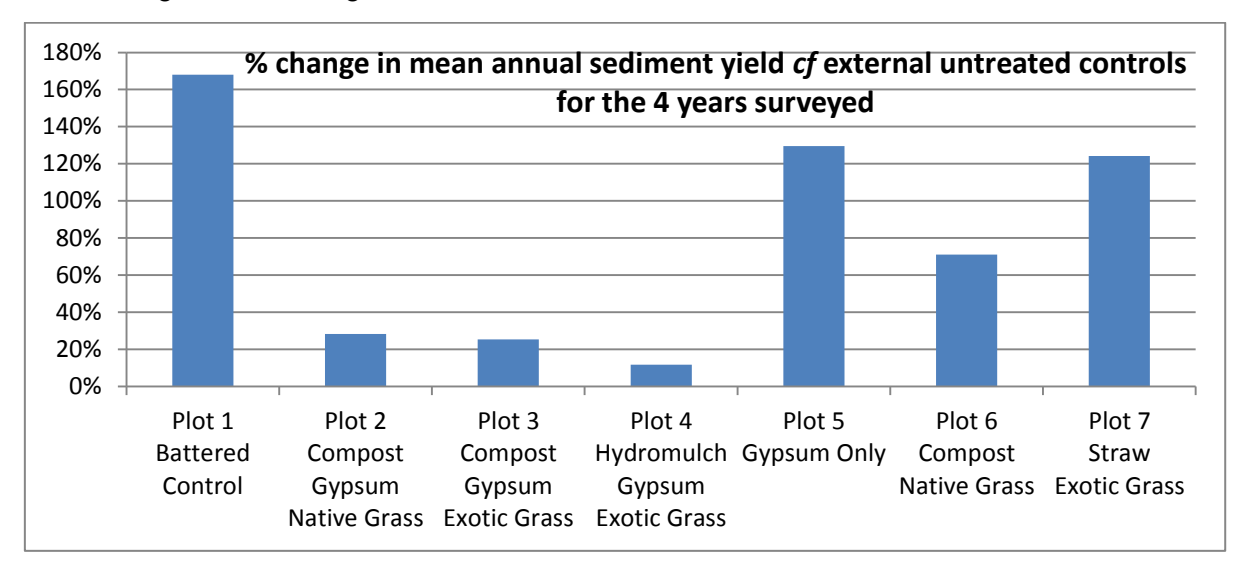


**Figure 46:** The relative change in sediment yield for the 7 treatment plots compared to (cf) the external untreated sections of gully adjacent to the study plots. Annual yields for Plots 1, 5, 6 & 7 were adjusted down by 30% for the last survey period to account for possible over estimation due to base level influence at these plots. The external control was the average of all sub-plots.

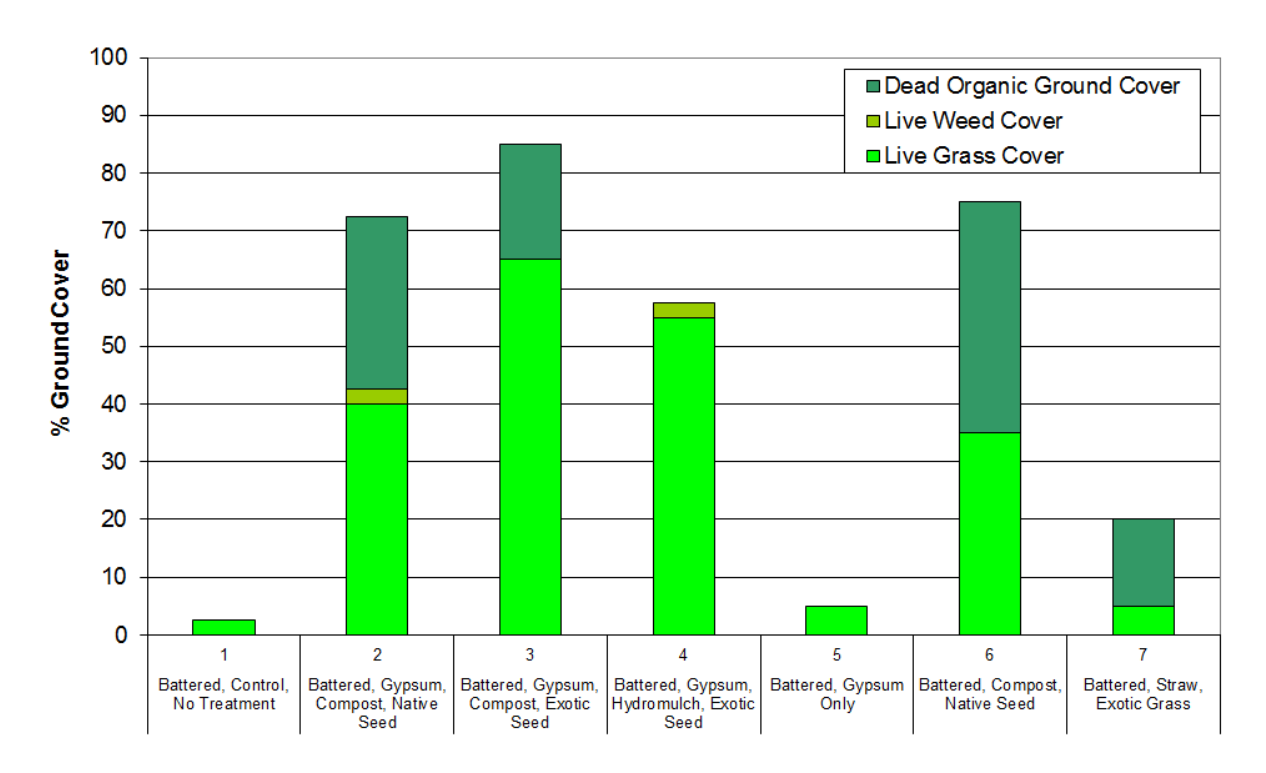


**Figure 47:** April 2013: Average percent (%) ground cover of live standing grass, live weeds, and dead organic matter (mulch) at CRGC1-29 at the end of the 2013 wet season (from Shellberg & Brooks, 2013).

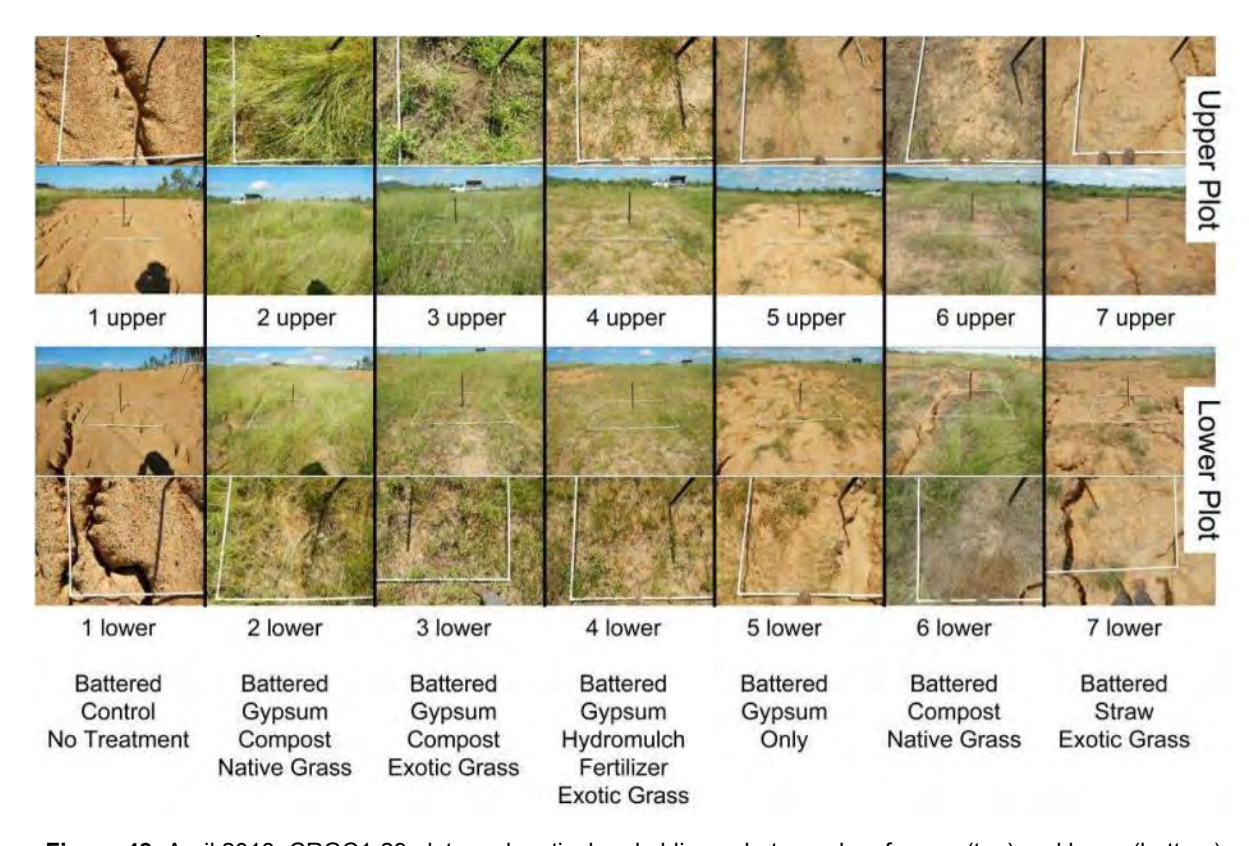


**Figure 48:** April 2013: CRGC1-29 plots and vertical and oblique photographs of upper (top) and lower (bottom) plots. Vegetation grid (4 m<sup>2</sup>) is included for reference in the photographs season (from Shellberg & Brooks, 2013).

### 2.6 Alluvial Gullies along the Bowen River Floodplain

Preliminary mapping of alluvial and hillslope gullies was undertaken along the lower 100km of the Bowen River floodplain using the highest resolution imagery available in Google Earth (**Figure 49**). Whilst this is only preliminary mapping, which should be repeated using LiDAR survey data, the initial mapping shows that there are around 330 large active gully complexes with a total area of around 2500 ha. The average gully complex area is 7.8ha (stdev 19 ha). Included within this is a major area of hillslope gullies in the Oakey Creek sub-catchment.

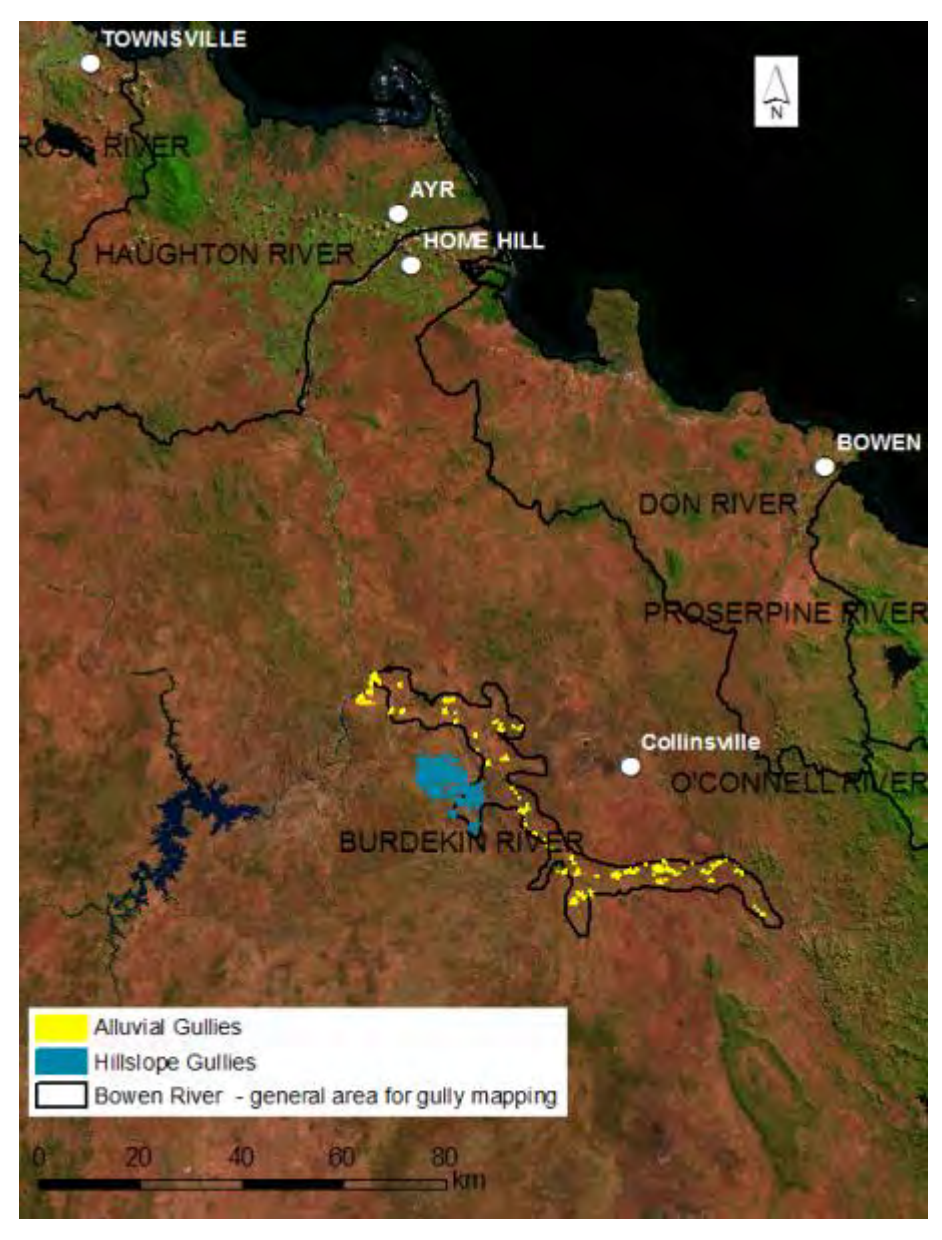


**Figure 49:** Map showing the area along the lower Bowen River within which there is a major concentration of largely highly active alluvial gully complexes. The areas mapped in blue are hillslope gullies in the Oakey Ck subcatchment.

The Burdekin River (catchment area  $\sim 130,000~\text{km}^2$ ) is estimated to deliver about 47% of the total suspended sediment load to the GBR (Waters et al., 2013). Monitoring data indicates that the Bowen/Bogie catchment contributes  $\sim 65\%$  of the silt/clay load at the Burdekin River mouth from just 9 % of the total Burdekin catchment area (Bainbridge et al., 2014). This equates to around 30% of the total input to the GBR lagoon, making it by far the single most significant source hotspot contributing sediment to the entire GBR (**Table 9**).

**Table 9:** Average annual sediment contributions from the Burdekin catchment based on monitoring data from 2005-2009 broken down by particle size classes.

Burdekin Sediment	load 9	6 break	down	by					
Budget 2005-2009	partic	le size		ā	av loads (M	t/yr: 200	5-2009)		
	clay	silt	sand	total	clay	silt	sand	total	% of total at outlet
Burdekin R (below dam)	52%	41%	6%	100%	1.32	1.05	0.15	2.52	30%
Bowen R (@ Myuna) Lower Bowen/Burdekin ungauged tribs include: Oaky Ck, Pelican Ck, Lower	27%	49%	24%	100%	1.02	1.84	0.90	3.76	45%
Bowen R; Bogie R) Lower Burdekin @ Inkerman (catchment	36%	38%	25%	100%	0.79	0.83	0.55	2.16	26%
outlet)	37%	44%	19%	100%	3.12	3.71	1.60	8.44	100%
Bowen + Lwr Bowen &	2004	450/	250			444	214		700
tribs +BogieR	30%	45%	25%	100%	1.80	2.67	1.45	5.92	70%
% of total at outlet					58%	72%	91%	70%	

Data source: Bainbridge et al., (2014) Water Resources Research

What is it about the Bowen catchment that makes it such a dominant source of sediment to the GBR? A key factor is that the Bowen catchment enters the Burdekin mainstream channel downstream of the Burdekin Falls Dam – which traps a significant proportion of the sediment sourced from its upstream tributaries (Bainbridge et al., 2014). However, this is only part of the explanation. The other key characteristic of the Bowen River, particularly along the lower 100km of the river, is that the alluvial floodplains and terraces in this section of the catchment have all of the characteristics of the Pleistocene age terraces that have been shown elsewhere to be littered with large alluvial gully complexes (Brooks et al., 2009; Brooks et al., 2013; Shellberg et al., 2016). These gully complexes are delivering vast quantities of fine sediment directly into the main channels of the Bowen and Burdekin (downstream of the Bowen confluence), which is then transported directly out of the Burdekin catchment to the reef lagoon. Sediment contributed to the channel at this point in the drainage network has few opportunities for deposition before it reaches the catchment outlet. Hence, not only are these sediment sources akin to a series of intensive point sources, they are also highly connected to the reef lagoon.

The alluvial gullies along this section of the Bowen River are some of the largest and most active alluvial gullies the authors have come across northern Australia, and it is hypothesised that they are disproportionately contributing to the huge sediment loads that are regularly delivered from the Bowen River to the Burdekin. It is conceivable that some of the more

active gullies are contributing up to 1000 t/ha/yr of sediment, and at this rate, several hundred of these large gully complexes could be contributing 50% or more of the total suspended sediment load from the Bowen catchment.

The connectivity of the alluvial gully sediment sources was graphically demonstrated when an early wet season storm hit the area in November 2015 causing the river to become highly turbid almost instantaneously (**Figure 50**). By comparison, sections of the river immediately upstream, which were unaffected by the storm cells, were running clear. Clear water flow is the typical scenario for the dry season base flows in this part of the Bowen River.



**Figure 50:** Turbid waters in the lower Bowen River (above) following a local storm 24 hrs earlier, while the river several km upstream, which was unaffected by the storm, remains clear (below). The area impacted by the storms has numerous highly connected alluvial gullies which deliver high suspended sediment loads directly to the Bowen main stem channel almost instantaneously upon receiving rainfall.

Given the concentration of these large alluvial gullies along the lower Bowen catchment, and the disproportionate contribution of sediment from these sources, developing appropriate methods to rehabilitate these gullies is arguably the single highest priority sediment management task across all GBR catchments. This is especially so if serious inroads are to be made into improving GBR water quality over the next decade.



**Figure 51:** Large alluvial gully complex along Parrot Ck, a tributary entering the Bowen River just downstream of the Bowen Development Rd

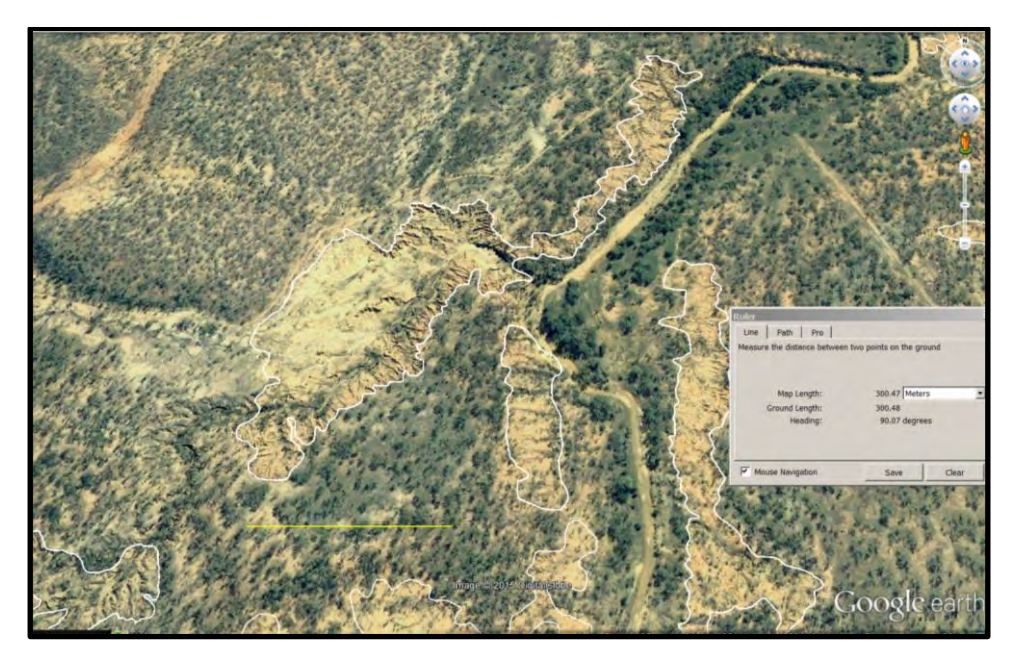


Figure 52: Satellite image of the alluvial gully sites shown above along Parrot Ck.



**Figure 53:** An extremely active alluvial gully system in the vicinity of the Bowen/Burdekin junction (note farm track in bottom right of picture for scale).

### REFERENCES

- Bainbridge Z, Lewis S, Smithers S, Wilkinson S, Douglas G, Hillier S, et al. (2016). Clay mineral source tracing and characterisation of Burdekin River (NE Australia) and flood plume fine sediment. Journal of Soils and Sediments; 16: 687-706.
- Bainbridge ZT, Lewis SE, Smithers SG, Kuhnert PM, Henderson BL, Brodie JE. (2014). Fine-suspended sediment and water budgets for a large, seasonally dry tropical catchment: Burdekin River catchment, Queensland, Australia. Water Resources Research; 50: 9067-9087.
- Bainbridge ZT, Wolanski E, Alvarez-Romero JG, Lewis SE, Brodie JE. (2012). Fine sediment and nutrient dynamics related to particle size and floc formation in a Burdekin River flood plume, Australia. Marine Pollution Bulletin 2012; 65: 236-248.
- Brodie J, Schroeder T, Rohde K, Faithful J, Masters B, Dekker A, et al. (2010). Dispersal of suspended sediments and nutrients in the Great Barrier Reef lagoon during river-discharge events: conclusions from satellite remote sensing and concurrent flood-plume sampling. Marine and Freshwater Research; 61: 651-664.
- Brodie JE, Kroon FJ, Schaffelke B, Wolanski EC, Lewis SE, Devlin MJ, et al. (2012) Terrestrial pollutant runoff to the Great Barrier Reef: An update of issues, priorities and management responses. Marine Pollution Bulletin; 65: 81-100.
- Brooks, A.P., Shellberg, J.G., Knight, J., Spencer, J. (2009) Alluvial gully erosion across the Mitchell fluvial megafan, Queensland Australia. *Earth Surface Processes and Landforms*, 34, pp. 1951 1969
- Brooks, A.P., Olley, J., Iwashita, F., Spencer, J., McMahon, J., Curwen, G., Saxton., N. and S. Gibson. (2014a) Reducing Sediment Pollution in Queensland Rivers: Towards the Development of a method to Quantify and Prioritise Bank Erosion in Queensland Rivers based on field evidence from the Upper Brisbane, O'Connell and Normanby Rivers. Final Summary Report to Qld State Government, Department of Science Information Technology Innovation and the Arts, Griffith University, pp 76. https://www.researchgate.net/publication/275584562
- Brooks, A.P., Spencer, J., Olley, J., Pietsch, T., Borombovits, D., Curwen, G., Shellberg, J., Howley, C., Gleeson, A., Simon, A., Bankhead, N., Klimetz, D., Eslami-Endargoli, L., Bourgeault, A., (2013) An Empirically-based Sediment Budget for the Normanby Basin: Sediment Sources, Sinks, and Drivers on the Cape York Savannah. Griffith University, 506pp.

#### https://www.researchgate.net/publication/258337838

- Burton J, Moody P, DeHayr R, Chen C, Lewis S, Olley J. Sources of bioavailable particulate nutrients: Phase 1 (RP128G). Department of Science, Information Technology and Innovation, Brisbane, Australia, 2015.
- Garzon-Garcia A, Wallace R, Huggins R, Turner RDR, Smith RA, Orr D, et al. (2015). Total suspended solids, nutrient and pesticide loads (2013–2014) for rivers that discharge to the Great Barrier Reef. Great Barrier Reef Catchment Loads Monitoring Program Department of Science, Information Technology and Innovation, Brisbane, Australia.

- Hughes AO, Olley JM, Croke JC, McKergow LA. (2009). Sediment source changes over the last 250 years in a dry-tropical catchment, central Queensland, Australia. Geomorphology 2009; 104: 262-275.
- Joo M, Raymond MAA, McNeil VH, Huggins R, Turner RDR, Choy S. Estimates of sediment and nutrient loads in 10 major catchments draining to the Great Barrier Reef during 2006-2009. Marine Pollution Bulletin 2012; 65: 150-166.
- Kroon FJ, Kuhnert PM, Henderson BL, Wilkinson SN, Kinsey-Henderson A, Abbott B, et al. River loads of suspended solids, nitrogen, phosphorus and herbicides delivered to the Great Barrier Reef lagoon. Marine Pollution Bulletin 2012; 65: 167-181.
- Olley, J. Brooks, A. Spencer, J. Pietsch, T. Borombovits, D. (2013) Subsoil erosion dominates the supply of fine sediment to rivers draining into Princess Charlotte Bay, Australia. *Journal of Environmental Radioactivity* v 124 pp 121-129.
- O'Reagain, P.J. and Bushell, J.J., 2011. *The Wambiana Grazing Trial: Key Learnings for Sustainable and Profitable Management in a Variable Environment.* The State of Queensland, Department of Employment, Economic Development and Innovation with funding from Meat and Livestock Australia, 51 pp.
- Pietsch, T.J., Brooks, A.P., Spencer, J., Olley, J.M., Borombovits, D. (2015). Age, distribution and significance within a sediment budget of in-channel benches in the Normanby River, Queensland, Australia. Geomorphology *Volume 239, 15 June 2015, Pages 17-40*
- Shellberg, J.G., Brooks, A.P. (2013) *Alluvial Gully Prevention and Rehabilitation Options for Reducing Sediment* Loads in the Normanby Catchment and Northern Australia. Prepared by Griffith University, Australian Rivers Institute for the Australian Government Caring for Our Country Reef Rescue Program, Cooktown, Qld.
- Shellberg, J., Brooks, A., Spencer, J., 2010. Land-use change from indigenous management to cattle grazing initiates the gullying of alluvial soils in northern Australia, 19th World Congress of Soil Science, Soil Solutions for a Changing World. 1 6 August 2010. Published on CDROM., Brisbane, Australia, pp. 59-62.
- Shellberg, J.G., Brooks, A.P., Rose, C.W., 2013a. Sediment production and yield from an alluvial gully in northern Queensland, Australia. Earth Surface Processes and Landforms, 38, 1765-1778. DOI: 1710.1002/esp.3414.
- Shellberg, J.G., Brooks, A.P., Spencer, J., Ward, D., 2013b. The hydrogeomorphic influences on alluvial gully erosion along the Mitchell River fluvial megafan, northern Australia. Hydrological Processes, 27(7), 1086-1104.
- Shellberg, J.G., Spencer, J., Brooks, A.P., Pietsch, T., 2016. Degradation of the Mitchell River Fluvial Megafan by Alluvial Gully Erosion Increased by Post-European Land Use Change, Queensland, Australia. Geomorphology, http://dx.doi.org/10.1016/j.geomorph.2016.04.021.
- Waters, D. K., Carroll, C., Ellis, R., Hateley, L., McCloskey, J., Packett, R., ... & Fentie, B. (2013). Modelling reductions of pollutant loads due to improved management practices in the Great Barrier Reef Catchments-Whole of GBR, Volume 1 Department of Natural Resources and Mines. Technical Report (ISBN: 978-1-7423-0999)

- Wilkinson SN, Olley JM, Furuichi T, Burton J, Kinsey-Henderson AE. (2015). Sediment source tracing with stratified sampling and weightings based on spatial gradients in soil erosion. Journal of Soils and Sediments 2015; 15: 2038-2051.
- Wolanski E, Fabricius KE, Cooper TF, Humphrey C. (2008). Wet season fine sediment dynamics on the inner shelf of the Great Barrier Reef. Estuarine Coastal and Shelf Science 2008; 77: 755-762.

## **APPENDICES**

**Appendix A:** Normanby Aerial LiDAR

**Appendix B:** Vegetation Recovery and Large-Scale Erosion Response from Cattle Exclusion from Gully Catchments, Full Report - (Shellberg, Brooks, Curwen,

Spencer, Iwashita)

Appendix C: Bioavailable Nutrients from Gullies, Full Report - (Garzon-Garcia, Burton &

Brooks)

# **APPENDIX A: NORMANBY AERIAL LIDAR**

Andrew Brooks<sup>1</sup>, Graeme Curwen<sup>2</sup>, and John Spencer<sup>1</sup>

<sup>1</sup> Griffith Centre for Coastal Management, Griffith University <sup>2</sup>Australian Rivers Institute, Griffith University

# **TABLE OF CONTENTS**

List of Tables	77
List of Figures	80
1. Normanby Aerial LiDAR 2015 refly – and summary of erosion analysis	88
1.1 Background	
1.2 New LiDAR Capture in 2015	89
1.2.1 Summary of erosion from all LiDAR Blocks for the three common per	riods91
1.2.2 Trends in total erosion by source	
1.2.3 Annual trends in erosion by source and normalized for rainfall	93
2. LiDAR Block Processing	
2.1 Data Processing Modifications	100
2.2 Improved Process for aligning consecutive LiDAR Blocks	100
2.2.1 LiDAR Block 7 Alignment Processing	101
2.2.2 A new approach to checking Lidar alignment	115
2.2.3 DEM Alignment Procedure	
2.3 Improved Delineation of Colluvial Boundary	
2.4 Updated Land unit classification	128
2.4.1 Processing Sequence to Consolidate Old and New Classification Sci	nemes146
3. LiDAR Block Results	151
3.1 Normanby LiDAR Block 4	151
3.1.1 Alluvial and Colluvial geology	152
3.1.2 Google Earth gullies	153
3.1.3 Comparison of alluvial gullies to colluvial gullies	155
3.1.4 Comparison of Google Earth gullies to LiDAR gullies in the alluvial zo	one155
3.1.5 Gully Expansion 2009 – 2011	155
3.1.6 Landscape Classification	
3.1.7 Historical air photos	156
3.1.8 Historical gully extent	
3.1.9 Observations from Erosion processing of 2011 to 2015 timestep	
3.1.10 Observations from Deposition processing of the 2011 to 2015 times	-
3.2 Normanby LiDAR Block 5	
3.2.1 Google Earth mapped gullies	
3.2.2 Comparison of alluvial gullies to colluvial gullies	
3.2.3 Comparison of Google Earth gullies to LiDAR gullies in the alluvial zo	
3.2.4 Gully Expansion 2009 – 2011	
3.2.5 Landscape Classification	
3.2.6 Historical air photos	
3.2.7 Summary results 2011 – 2015 and reprocessed 2009-11 data	
3.2.8 Observations from Erosion processing	
3.2.9 Observations from Deposition processing	
3.3 Normanby LiDAR Block 7	
3.3.1 Alluvial and Colluvial geology	
3.3.2 Google Earth mapped gullies	
3.3.3 Comparison of alluvial gullies to colluvial gullies	185

,	3.3.4 Comparison of Google Earth gullies to LiDAR gullies in the alluvial zone	185
;	3.3.5 Gully Expansion 2009 – 2011	185
,	3.3.6 Landscape Classification	186
;	3.3.7 Historical air photos	187
,	3.3.8 LiDAR 2015 Erosion Summary Data & Reprocessed 2009-11 data	188
3.	4 Normanby LiDAR Block 9	188
;	3.4.1 Alluvial and Colluvial geology	190
,	3.4.2 LiDAR derived data	191
,	3.4.3 Observations	193
;	3.4.4 Comparison of Google Earth gullies to LiDAR gullies in the alluvial zone	195
,	3.4.5 Gully Expansion 2009 – 2011	195
,	3.4.6 Landscape Classification	196
,	3.4.7 Historical air photos	197
	3.4.8 Historical gully extent	
	3.4.9 LiDAR 2015 data analysis	
	3.4.10 Erosion/Deposition processing	
,	3.4.11 Observations from Deposition processing	206
,	3.4.12 Summary Erosion 2015 Data & reprocessed 2009-11 data	208
3.	5 Normanby LiDAR Block 10	209
;	3.5.1 Alluvial and Colluvial geology	209
,	3.5.2 Google Earth mapped gullies	210
;	3.5.3 LiDAR derived data	211
	3.5.4 Observations from erosion and deposition analysis	
;	3.5.5 Comparison of alluvial gullies to colluvial gullies	214
	3.5.6 Comparison of Google Earth gullies to LiDAR gullies in the alluvial zone	
;	3.5.7 Gully Expansion 2009 – 2011	215
	3.5.8 Landscape Classification	
	3.5.9 Historical air photos	
	3.5.10 LiDAR 2015 Data Processing	
	3.5.11 Erosion/Deposition processing	
	3.5.12 Observations from Deposition processing	
	3.5.13 Summary 2015 Erosion Data + reprocessed 2009-11 data	
	6 Normanby LiDAR Block 16	
	3.6.1 Alluvial and Colluvial zones	
;	3.6.2 LiDAR derived data	229
	3.6.3 Statistics	
	3.6.4 Aggressive filtering of erosion and deposition data	
	3.6.5 Observations	
	3.6.6 Erosion and deposition	
	3.6.7 Comparison of alluvial gullies to colluvial gullies	
;	3.6.8 Comparison of Google Earth gullies to LiDAR gullies in the alluvial zone	233
	3.6.9 Gully Expansion 2009 – 2011	
,	3.6.10 Landscape Classification	234
;	3.6.11 Historical air photos	236
;	3.6.12 Historical gully extent	236
;	3.6.13 Comparison of gully volume and erosion calculations using reprocessed	2009
	LiDAR and original 2009 LiDAR	237

3.6.14 LiDAR 2015 data processing	238
3.6.15 Erosion/Deposition processing	240
3.6.16 Observations from Erosion processing:	241
3.6.17 Observations from Deposition processing	245
3.6.18 Summary Erosion 2015 data + reprocessed 2009-11 data	246
3.7 Normanby LiDAR Block 17	247
3.7.1 Alluvial and Colluvial zones	248
3.7.2 LiDAR derived data	248
3.7.3 Statistics	250
3.7.4 Aggressive filtering of erosion and deposition data	250
3.7.5 Observations	251
3.7.6 Erosion and deposition	251
3.7.7 Comparison of Google Earth gullies to LiDAR gullies in the alluvial zone	252
3.7.8 Gully Expansion 2009 – 2011	253
3.7.9 Landscape Classification	253
3.7.10 Historical air photos	
3.7.11 Historical gully extent	254
3.7.12 Comparison of gully volume and erosion calculations using reprocessed	d 2009
LiDAR and original 2009 LiDAR.	
3.7.13 LiDAR 2015 Data Processing	
3.7.14 Summary Erosion 2015 data & reprocessed 2009-11 data	258
4. Normanby Rainfall and Flow data	259
4.1 Rainfall data for study period (2009-2015)	
4.2 Cyclones & Tropical lows during the monitoring period	
4.2.1 Cyclone Oswald Jan 22 – 23, 2013 (Tropical Low over Normanby)	
4.2.2 Severe Tropical Cyclone Ita - April 11-12, 2014	
4.2.3 Severe Tropical Cyclone Nathan – March 20, 2015	

# **LIST OF TABLES**

Table A1:	Area of the common LiDAR blocks from 2009, 2011 and 2015 for which erosion change detection was undertaken90
Table A2:	Ratio of change on rainfall normalised erosion rates for each LiDAR block expressed as time 2 (2011-15)/ time 1 (2009-11)
Table A3:	Comparison of flow statistics in the Laura and Normanby Rivers for the two study period intervals
Table A4:	Differences in mean elevation in 10 sample polygons between timesteps 2009-2011 and 2011-2015. Only 2 of 20 samples had differences greater that 10 cm. Vertical alignments of 3 Lidar time slices seem satisfactory101
Table A5:	Changes in colluvial and alluvial land unit area between 2011 LiDAR data and the 2015 data
Table A6:	Changes in % of colluvial and alluvial land in each LiDAR block between 2011 and 2015
Table A7:	Areas of Alluvial and Colluvial in common areas - from original 1:1mill soils dataset and areas after modification of boundaries
Table A8:	Changes in areas as % of original area
Table A9:	Areas of gullies classified as Alluvial or Colluvial before and after boundary modification
Table A10:	Percent change in area of gully classification127
Table A11:	Erosion Classes
Table A12:	Deposition Classes
Table A13:	General statistics for Norm 4
Table A14:	Quantifying LiDAR and GE gullies in alluvial and colluvial geology154
Table A15:	Alluvial and colluvial gullies had a similar rate of erosion when expressed as yield per hectare per year, but colluvial gullies were an order of magnitude less in area and volume of erosion than alluvial gullies155
Table A16:	The area of bare ground gullies captured from GE mapping was approximately 10% of the gully area seen in LiDAR, but the volume of erosion from bare ground (GE) gullies was 20% of the volume measured from alluvial gullies from LiDAR imagery. This supports field observations of erosion advancing under vegetation.
Table A17:	Area of expansion of gullies between 2009 and 2011155
Table A18:	Meta data for historical air photos covering Norm 4
Table A19:	A remarkably consistent rate of erosion was calculated over 5 decade and 2 decade intervals from air photos, with a small spike in rate over the shortest interval, from 1994 to 2009. The gully did not expand in area between 2009 and 2011, but erosion from incisions along drainage lines produced 19

	driving gully expansion have reduced, but the gully floor has not yet reached stable equilibrium15	
Table A20:	General statistics for Norm 516	5
Table A21:	Quantifying LiDAR and GE gullies in alluvial and colluvial geology16	7
Table A22:	Values for erosion and deposition on land units in Norm 516	7
Table A23:	Comparison of erosion and deposition between alluvial and colluvial geology.	
Table A24:	Comparison of erosion activity in LiDAR and Google Earth gullies16	8
Table A25:	Area of expansion of gullies between 2009 and 201116	9
Table A26:	Area of each landscape classification in block16	9
Table A27:	Meta data of air photos used to identify gullies in Norm 517	0
Table A28:	Erosion rates for 4 gullies over 5 decades, 2 decades (from air photos) and years (from LiDAR)	
Table A29:	General statistics for Normanby 7 LiDAR block	2
Table A30:	Gully area digitised from LiDAR and Google Earth in alluvial and colluviations geology	
Table A31:	Comparison of erosion activity in alluvial and colluvial gullies18	5
Table A32:	Comparison of erosion activity in LiDAR and Google Earth gullies18	5
Table A33:	Area of expansion of gullies between 2009 and 201118	6
Table A34:	General statistics for Block 919	0
Table A35:	Just under half the area of alluvial surfaces was eroded by gullies or channe at different stages of development. 15% of alluvial surfaces were eroded by gullies, but GE gullies captured under half of this extent. Few gullies extended into colluvial areas	y ed
Table A36:	Statistics from adjusting difference raster for bias19	2
Table A37:	Values of adjusted change raster filtered to remove noise from terraces19	3
Table A38:	Comparison of erosion from LiDAR alluvial gullies and Google Earth mappe gullies	
Table A39:	Gully expansion between 2009 and 201119	6
Table A40:	Details of air photos covering a broad expanse of gully to the east of the machannel in Norm 9	
Table A41:	Variability of erosion rates from different gullies over different time scales highlighted by comparing N09g1 and N09g2. Yield calculated from gully between 2009 and 2011 was 43% of 5 decade average, but 23% of 2 decade average. Erosion from gully 2 between 2009 and 2011 was 90% of 5 decade average, but 180% of 2 decade average. These values oscillated above an below the average yield of 13 air photo gullies over the same time scales19	1 le le

Table A42:	The reduction in data volume to determine real and defensible erosion a deposition	
Table A43:	General statistics for Normanby 10 LiDAR block.	209
Table A44:	Gully area digitised from LiDAR and Google Earth in alluvial and collugeology	
Table A45:	Statistics of raw difference raster, and corrections applied to reduce bias non-eroding surfaces.	
Table A46:	Values of change raster filtered to remove noise.	212
Table A47:	Comparison of erosion activity in alluvial and colluvial gullies	214
Table A48:	Comparison of erosion activity in LiDAR and Google Earth gullies	215
Table A49:	Area of expansion of gullies between 2009 and 2011	215
Table A50:	Meta data for air photos in Norm 10	217
Table A51:	Erosion rates calculated from air photo records and repeat LiDAR analysis N10 g1. Yield between 2009 and 2011 was 128% of 5 decade rate, but 61% 2 decade rate. Rate of erosion over 5 decades in N10 g1 was below average rate of 13 air photo gullies, but rate over 2 decades was greater that average. Yield calculated from Repeat LiDAR was slightly below average rate.	6 of the nan ate.
Table A52:	The reduction in data volume to determine real and defensible erosion a deposition.	
Table A53:	The reduction in data volume to determine real and defensible erosion a deposition.	
Table A54:	Summary of daily rainfall events over threshold for the two observation periods	
Table A55:	Summary of annual water year rainfall totals over the study period	261
Table A56:	Summary flow statistics for the Normanby and Laura Rivers over the survey periods.	

# **LIST OF FIGURES**

Figure A1:	LiDAR blocks in the Normanby and adjacent catchments in 2009 and 201189
Figure A2:	Map of the Normanby catchment showing the LiDAR blocks reflown in October 2015. The area in yellow represents the sections common to all three time slices which forms the basis for the current analysis90
Figure A3:	LiDAR flight lines from 2015 (red) showing the original 2009 blocks (yellow outline) and the 2011 refly blocks (orange outline)91
Figure A4:	Summary data of total erosion from the two periods for which minimum erosion rates have been determined from aerial LiDAR data. Error bars represent the standard error between the 7 blocks at the total block scale92
Figure A5:	Annualised erosion rates summarised across the 7 common LiDAR blocks from 2009-11 (WY 2010-11) and 20011-15 (WY 2012-15). Error bars represent the standard error between the 7 blocks at the total block scale93
Figure A6:	Annual Sediment contributions from different sources normalised per 100mm of incident rainfall. Anualised rainfall is the average of the 4 monthly rainfal records shown in Section 4.1
Figure A7:	East Normanby River in the immediate aftermath of the flood generated by Cyclone Ita (photo Tim Hughes)
Figure A8:	Close up of the lower bank of the East Normanby River in the immediate aftermath of Cyclone Ita, indicating how little bank erosion there was in general as a result of this large flood
Figure A9:	Daily rainfall at the DNRM gauging station on the Laura River at Coalseam Ck.
Figure A10:	Mean daily discharge for the study period Laura R at Coalseam Ck gauge 98
Figure A11:	Mean daily discharge for the study period Normanby R at Battlecamp gauge99
Figure A12:	Mean elevations in ten 100m by 100m polygons to sample for vertical alignment and distribution of 10 polygons of 100m by 100m to sample vertical alignment
Figure A13:	No consistent offset was found by comparing contour lines at northern southern, Eastern or western aspects of slopes
Figure A14:	Alluvial and Colluvial at 1:1 million, plus common area for 09, 11 and 15 with Lidar as overlay
Figure A15:	Redraw of boundary to reclassify this obvious hill124
Figure A16:	Block 7 - hill area on west of block contracted, extra hill added in south west corner
Figure A17:	Block 16 - area of hills increased for both patches125
Figure A18:	Block 10 had increase in area of colluvial in south west corner - no gullies were in the colluvial area.

Figure A19:	Alluvial and Colluvial at 1:1 million, plus common area for 09 11 and 15 Lidar put on the map146
Figure A20:	Redraw of boundary to reclassify this obvious hill146
Figure A21:	Alluvial and Colluvial gullies merged to 1 layer. Note the gullies on the hill bottom left will still be classified alluvial because that was the original low resolution 1:1mill classification
Figure A22:	Digitised features from 2009 Lidar have been dropped into the 1:1million layer to completely classify the area, and clipped to the common area for 2009 - 2011 - 2015 Lidar
Figure A23:	Model builder routine for dropping the digitised features into the 1:1mill alluvial/colluvial layer. Cookie cutter out the area of digitised features, then drop in the digitised features.
Figure A24:	Problem with intersecting erosion polygons with the classified surface was that small sections of polygon would be split off from the main patch, and each segment would turn up in the attribute table with the same value of erosion, thus double or triple counting the volume of erosion
Figure A25:	Polygons of erosion were converted to points, which would give one precise location to intersect with the classified surface
Figure A26:	The centroid of the erosion polygon falls onto one part of the classified surface. The points have all the information of the highly specific classification, including the area and volume of erosion, and now also the details of the classified surface it sits on.
Figure A27:	Norm 4 location (left); Digitising on 2009 LiDAR (right)
Figure A28:	2009 DEM152
Figure A29:	Alluvial and colluvial geology in Norm 4153
Figure A30:	Location of Google Earth gullies in Norm 4 and surrounding area153
Figure A31:	Large volumes of erosion came from gullies and secondary channels. The contribution from road drainage, 415 m³ was on a par with the second largest producing unit in Norm 4, a 700m section of secondary channel with active bank erosion
Figure A32:	All 9 landscape classes are represented in Norm 4. Approximately half of the block was alluvial gullies. Main channel banks and secondary channels had similar areas of 12 to 13% of total area. Inset flood plains along main channels and secondary channels also had a similar area, being 7 to 8% of total area.
Figure A33:	Area of each landscape classification in block 4156
Figure A34:	Incision of gully floor is the main erosion activity in the gully identified from air photos

Figure A35:	Incision of gully floor was not seen in the 1952 image, but between 1957 and 2009 the advance of the longest incision was 218 m, an average of 4 m per year. In comparison, head wall advance at different locations was between 20 and 40 m, an average annual advance of less than 1m
Figure A36:	Erosion stats for Block 4 by geomorphic unit; 2009-11 (top); 2011-15 (bottom).
Figure A37:	Largest volume of erosion in one patch on left (3923m³) was on the West Normanby, second largest on right (1219m³) on the East Normanby160
Figure A38:	The largest patch of erosion that was not bedload was from this 11m tall bank on the East Normanby main channel, with a volume of 23,754m <sup>3</sup> 160
Figure A39:	This erosion patch was the largest volume classified as "gully extension into ancient flood plain", though technically it would be a direct result of the road runoff. Erosion volume was measured as 532m³ in total, made up of 468m³ from deep erosion and 63m³ from shallow erosion
Figure A40:	A 12m tall bank on a secondary channel produced 400m³ material from the collapsing upper edge of the bank. Imagery shows this to be an active erosion zone. 380m³ of the total was from erosion deeper than 0.5m. This area was the second largest patch by volume coming from erosion of ancient flood plain
Figure A41:	Third largest patch of erosion into ancient flood plain was also a collapsing bank, shown by black arrow. White arrow shows location of 2 <sup>nd</sup> largest erosion patch
Figure A42:	Fourth largest patch of erosion into ancient flood plain is associated with a road crossing the East Normanby, volume of erosion was 355m <sup>3</sup> in total162
Figure A43:	The largest erosion patch with-in a gully is seen as an incision into a gully floor here in this gully spanning the main road near the West Normanby. 328m³ of material in total was exported between the Lidar imaging163
Figure A44:	The largest volume produced by bonafide head wall extension was 145m <sup>3</sup> from this gully163
Figure A45:	Development of this gully was mapped with historical air photo imagery. The main activity has been an advance of the incision in the gully floor. Total erosion from within the gully was 989m³. Of this, 924m³ was from incisions.
Figure A46:	a) N5 location; b) Digitising on 2009 LiDAR; c) 2009 DEM165
Figure A47:	Alluvial and colluvial geology in Norm 5. Note that some low hills near the south east corner of the repeat LiDAR footprint are not mapped as colluvial but possible should be, but overall the mapped boundary nicely delineates flat alluvial surfaces from slopes of colluvial surfaces
Figure A48:	Location of Google Earth gullies in Norm 5166
Figure A49:	Distribution of landscape classes in Norm 5
Figure A50:	Detail of gully head wall location in 1952 and 1987 for N5 wg1 in Norm 5171

Figure A51:	Erosion stats for Block 5 by geomorphic unit; 2009-11 (top); 2011-15 (bottom).
Figure A52:	Plot of 4000 points sampled to calculate correction factor. On right is statistics around the noise
Figure A53:	On left, difference layer after horizontal correction of $X = 0$ , $Y=1$ . On right difference layer after furthur horisontal correction of $X=0.5$ and $Y=0.25174$
Figure A54:	Statistics supporting the XY shift to minimise variance in 25,000 points sampled
Figure A55:	Differences between erosion 2009-11; 2011-15175
Figure A56:	Arrowed gully advanced 20m between 2011 and 2015 Lidar176
Figure A57:	Detail of secondary channel; note inset flood plain getting eroded at hairpin bend near top left of picture
Figure A58:	Overview of erosion in main channel and secondary stream177
Figure A59:	Erosion in main channel and secondary stream with orthophoto from 2009.177
Figure A60:	Gully with advance of around 20m178
Figure A61:	An example of slump erosion, which is unusual in this region178
Figure A62:	Headwall advance across a broad front179
Figure A63:	Advancing gully headwalls with orthophoto from 2009 for context179
Figure A64:	Detail of gully extension and incisions into gully floor. Headwalls have advanced 5-10m180
Figure A65:	Detail of massive gully head wall advances180
Figure A66:	Patterns of deposition in N5 between 2011 and 2015181
Figure A67:	a) Norm 7 location; b) Digitising on LiDAR; c) DEM from 2009 LiDAR182
Figure A68:	Alluvial and colluvial geology in Norm 7183
Figure A69:	Distribution of gullies mapped from Google Earth
Figure A70:	Quantifying erosion and deposition in alluvial and colluvial zones184
Figure A71:	Landscape classification in Norm 7186
Figure A72:	Area of each landscape unit in alluvial and colluvial zones
Figure A73:	Example of a gully that looked so clear in LiDAR (left), but was frustratingly difficult to define from visual imagery (right)
Figure A74:	Erosion stats for Block 7 by geomorphic unit 2009-11 (top); 2011-15 (bottom).
Figure A75:	Location of Norm 9 (left); Features in Norm 9 (right)189
Figure A76:	Elevation ranges in and around Norm 9189
Figure A77:	Norm 9 sits at the head of a broad alluvial plain. Narrower bands of alluvium follow water courses between rising slopes of colluvial geology to the east and south of the block. 93% of the repeat LiDAR footprint was alluvial geology. 190

Figure A78:	Distribution of Google Earth (GE) mapped gullies in and around Norm 9190
Figure A79:	Distribution of sample polygons to test bias in the difference raster; and statistics table
Figure A80:	Location diagram and erosion and deposition hot spots in Norm 9194
Figure A81:	Sum of erosion and deposition for landscape classes in the alluvial zone. In a significant deviation from the pattern in other LiDAR blocks, erosion from main channel banks dominated losses from other sources. Deposition on open and vegetated river main channel bed in Norm 9 was the largest volumes measured of all LiDAR blocks except Norm 40, which covered a section of Morehead River that had many anabranching channels with significant movement of sandbanks and bars. These data suggests the upper East Normanby River to be actively reforming main channel dimensions195
Figure A82:	Landscape classification in Norm 9196
Figure A83:	Gullies were 38% of the block area, combined area of main and secondary channel flood plains was 42%197
Figure A84:	Development of gully one and 2 between 1951 and 2009198
Figure A85:	Statistics supporting the XY shift to minimise variance in 40,000 points sampled. 4 shifts are presented here; 1) do nothing, 2) X0 Y1 based on values from the 90 <sup>th</sup> and 95 <sup>th</sup> percentile, 3) X1 Y1 based on analysis of a count of the number of erosion cells with values less than or equal to -0.5 i.e. how many cells exceeded the threshold for real erosion, 4) nudging the 2015 DEM by X0.5m Y1m – which produced best statistics for Std dev, 90 <sup>th</sup> and 95 <sup>th</sup> percentiles and had by far the lowest count of noisy cells, nearly half the amount of the next best fit
Figure A86:	Panel A adjustment was X0 Y1, panel B adjustment was X1 Y1, panel C adjustment was X 0.5 Y 1. The area of "deep erosion" in the gully extending towards the top left of the picture, before editing, for A 1944m2; B 1650m2 and C 1300m2. The half metre shift in X direction resulted in 34% less erroneous erosion polygons to sift through to find the real signal, thus proving the worth of pursuing sub metre nudges to correct for mis-alignment in horizontal plane.
Figure A87:	Overview of erosion across Norm 9
Figure A88:	Multiple gully head walls advancing202
Figure A89:	Reworking of the shallow gully floor202
Figure A90:	Overlay of erosion between 2009-2011 and 2011-2015. Erosion of the west side of the channel between 2009 and 2011, the blue outline, has continued between 2011 and 2015, the orange patch. The large patch of deposition on the east side of the bend between 2009 and 2011 was added to between 2011 and 2015, though not by such a large extent. The lower end of the 09-11 deposition has eroded between 2011 and 2015. It looks as though the channel is migrating towards the inside of the bend

Figure A91:	A smallish erosion patch, seen as blue outline, between 09-11 expand between 11-15. The bar in mid channel has received deposits in both tir steps	
Figure A92:	On the east side of the East Normanby two sites continued eroding during the 11-15 time step. Erosion on the high bank on the outside of the bend was less between 11-15 than 09-11	ss
Figure A93:	Deposition on the bar and bench, erosion on the outside of the bend20	6
Figure A94:	Deposition at junction of secondary channel and main channel20	7
Figure A95:	Erosion stats for Block 9 by geomorphic unit; 2009-11 (top); 2011-15 (bottom)	•
Figure A96:	a) Norm 10 location; b) Digitising on LiDAR; c) DEM from 2009 LiDAR20	9
Figure A97:	Alluvial and colluvial geology in Norm 1021	0
Figure A98:	Distribution of gullies mapped from Google Earth21	0
Figure A99:	Locations of polygons for checking bias in the difference raster, and statistic table	
Figure A100:	Location diagram and detail of erosion and deposition hotspots in Norm 10	
Figure A101:	Quantifying erosion and deposition in alluvial and colluvial zones21	4
Figure A102:	Landscape classification in Norm 1021	6
Figure A103:	Area of each landscape unit in alluvial and colluvial zones21	6
Figure A104:	Gully perimeter in 1952, 1987 and 2009. Variability in rates of erosion over different time scales was found, with the rate over 5 decades from 1950s to 2009 being 81 m²/ha/yr; over 2 decades from 1890's being 170 m³/ha/yr, and over 2 years from 2009 to 2011 being 104 m³/ha/yr21	to id
Figure A105:	On left is un-modified difference layer. On right is difference layer wit intervals masked until the flat areas are revealed21	
Figure A106:	Plot of 25000 points sampled to calculate correction factor. On right statistics around the noise	
Figure A107:	On left, difference layer after X0 Y1 correction. On right difference layer after furthur correction of X 0.5, Y -0.75. The improved alignment of DEM value resulted in about 30,000 polygons for editing being reduced to around 3,300 That is substantial!	es O.
Figure A108:	Statistics supporting the sub-metre XY shift to minimise variance in 40,00 points sampled.	
Figure A109:	Overview of erosion in N1022	2
Figure A110:	The volume of erosion of 1106m <sup>3</sup> from incision into this gully floor an widening of the walls was second only to a patch of erosion bedload erosion in the main channel. See fig 7.	in

Figure A111:	: The largest patch of erosion by volume; 1190m³ of bedload erosion in th main channel. Other patches of lesser volume are nearby22		
Figure A112:	The deepest vertical distance of erosion was a collapsed bank at the mouth of a gully – arrowed. There was also plenty of bedload erosion in the secondar channel downstream of the gully outlet		
Figure A113:	Rapidly expanding gully headscarp migrating into terrace alluvium224		
Figure A114:	Example of a bank mass failure – which are a fairly rare phenomenon in the Normanby		
Figure A115:	Plenty of examples of reworking of an existing gully floor		
Figure A116:	Distribution of deposition in N10, 2011 to 2015226		
Figure A117:	Erosion stats for Block 10 by geomorphic unit 2009-11 (top); 2011-19 (bottom)		
Figure A118:	Plot of 25,000 points sampled to calculate correction factor. On right is statistics around the noise.		
Figure A119:	On left, difference layer after initial XYZ correction. A definite bias of erosion on North and East facing slopes can be seen. On right difference layer after sub-metre XY correction.		
Figure A120:	Statistics supporting the XY shift to minimise variance in 40,000 points sampled		
Figure A121:	Overview of erosion locations in N16		
Figure A122:	(L) The largest volume patch of erosion 1613m³ – main channel bedload242		
Figure A123:	(R) Second largest by volume, 1496m³, from a bench along the main channel 242		
Figure A124:	(L) Third largest by volume, 1471m³, from main channel bench242		
Figure A125:	(R) This corner of a secondary stream eroded heavily between 2009 and 2011. More recent erosion was less, though we can say a bank face los material up to 5.6m in depth		
Figure A126:	(L) Gully arrowed had headwall extension of 32m between 2011 and 2015 Headwall extension between 09 and 11 was 37m243		
Figure A127:	(R) Extensive gully headwall activity as part of a secondary incision243		
Figure A128:	Plenty of reworking of old gully floor, with less activity at headwall zone24		
Figure A129:	Patterns of deposition in N16.		
Figure A131:	On left is un-modified difference layer. On right is difference layer with intervals masked until the flat areas are revealed		
Figure A132:	Plot of 25000 points sampled to calculate correction factor. On right is statistics around the noise.		
Figure A133:	Erosion stats for Block 17 by geomorphic unit (2009-11 (top); 2011-19 (bottom)		

Figure A134:	Daily rainfall at the DNRM gauging station on the Laura River at Coalseam Ck.
Figure A135:	Map of the upper Normanby River showing the locations of the 4 sites for which monthly or daily rainfall records are derived261
Figure A136:	Monthly rainfall totals (gap-filled in red) for the study period at the 4 sites shown above
Figure A137:	Correlations between monthly rainfall totals at the Coalseam Ck gauge and the Laura Post Office and the East Normanby gauge site and Kings Plains Station. These relationships were used to fill missing data in the gauge records.
Figure A138:	Correlation between daily rainfall at Coalseam Ck with Laura Post Office over the last 10 years (missing data days removed)263

# 1. NORMANBY AERIAL LIDAR 2015 REFLY – AND SUMMARY OF EROSION ANALYSIS

Prepared by: Andrew Brooks & Graeme Curwen

### 1.1 Background

The broad distribution of the most active gullies at the catchment scale in the Normanby was determined from detailed mapping of individual gullies in Google Earth (GE). To complement this, as outlined in detail within Brooks et al (2013a), a substantial amount of LiDAR was captured in 2009 across the Normanby and some surrounding basins, and the full extent of visible gullies mapped. This enabled an estimate to be made of the extent to which the GE mapping under estimated the full extent of gullies. Typically the full extent of gullies was around 5-7 times more than the extent determined in GE – although the GE gullies are the bare ground parts of the gullies and will tend to represent the more active portion.

A total of 50 blocks of LiDAR were flown between May and August 2009 by Terranean (now RPS); covering a total area of 1065.4 km<sup>2</sup> (Figure A1). This includes 41 blocks in the Normanby (782.5 km<sup>2</sup>), 5 blocks in the Stewart (88.9 km<sup>2</sup>), 3 blocks in the Jeannie (107.1 km<sup>2</sup>) and 1 block in the Annan (86.7 km<sup>2</sup>). The Normanby catchment has an area of 24,353 km<sup>2</sup> and the 2009 LiDAR covered 3.2% of the catchment.

In 2011 around 22% of the original data capture was reflown as a basis for measuring short term erosion rates from gullies and channels. The areas with both 2009 and 2011 LiDAR data comprised 14 blocks covering 163.1 km², which is 0.7% of the catchment. The Airborne LiDAR data is the key dataset that underpins the gully sediment yield data across the Normanby. By extension this now provides an unprecedented basis for the prioritisation of gully management in what is arguably one of the highest priority catchments draining to the Great Barrier Reef.

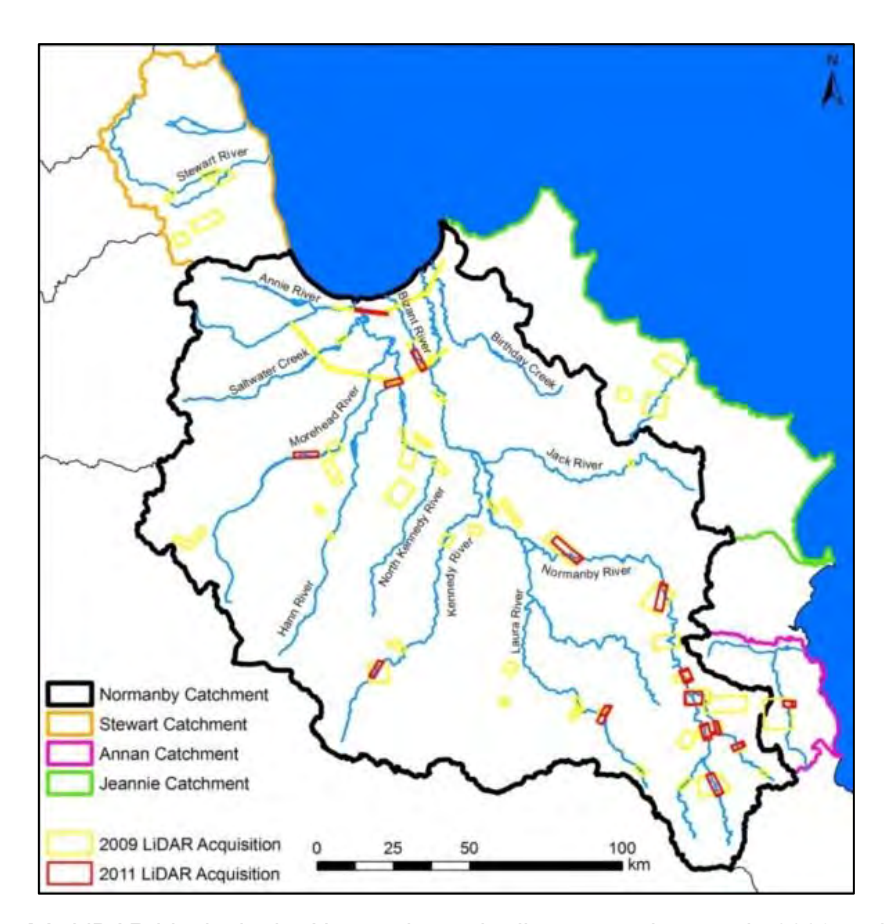
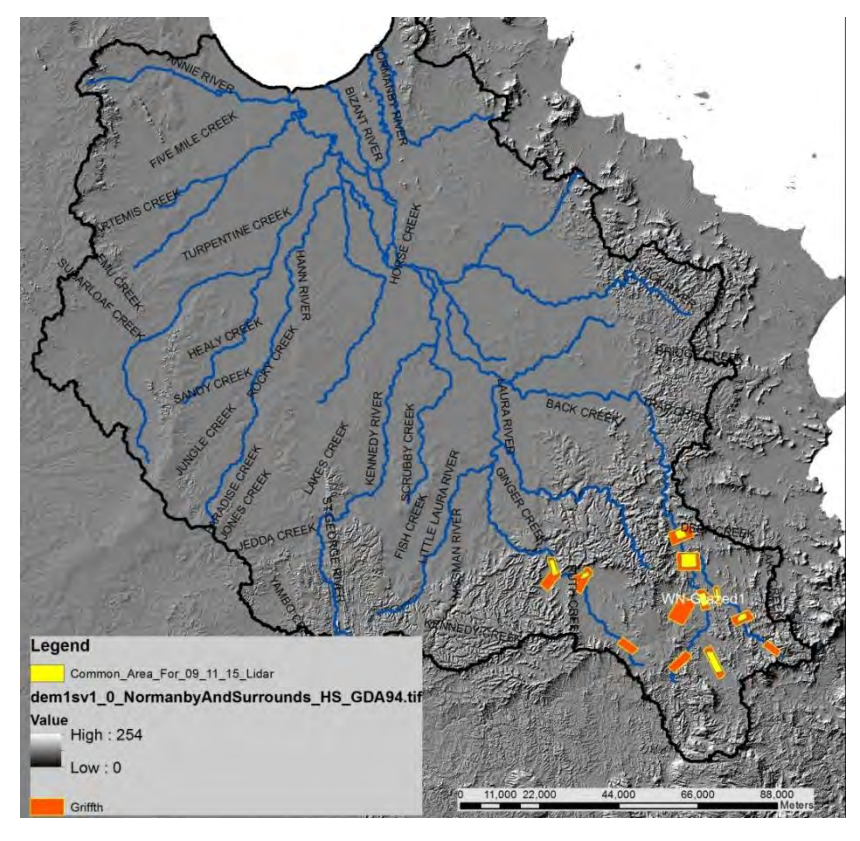


Figure A1: LiDAR blocks in the Normanby and adjacent catchments in 2009 and 2011.

### 1.2 New LiDAR Capture in 2015

In late October 2015 a further LiDAR data capture was completed prior to the onset of the 2015/16 wet season. Due to limited resources the extent of the recapture was significantly less than the previous two time slices, however, it was concentrated in the areas with the highest concentrations of active gullies. As shown in Figure A2 eleven blocks were reflown, and detailed analysis carried out on seven of the blocks which had common data between the 2009 and 2011 data captures (Figure A3). Geomorphic change detection to determine erosion rates was completed for a total area of 5,538 ha of the most heavily gullied areas in the catchment. This was the area that was common to all three LiDAR data captures, giving us two distinct time periods to compare gully erosion rates. The data capture areas included 4 sites where cattle exclusion plots had been established in 2011/12, as well as the gully treatment demonstration site at Crocodile Station (see Shellberg and Brooks, 2013). Whilst the total area recaptured in 2015 only represents 0.23% of the total catchment (5536 ha), it captures 7.7% of all mapped active gullies from Google Earth (Table A1) in the Normanby. The LiDAR data also shows that 20% of the land area sampled consists of alluvial gullies in various stages of development, 17% (187 ha) of which could be classified as highly active.



**Figure A2:** Map of the Normanby catchment showing the LiDAR blocks reflown in October 2015. The area in yellow represents the sections common to all three time slices which forms the basis for the current analysis.

**Table A1:** Area of the common LiDAR blocks from 2009, 2011 and 2015 for which erosion change detection was undertaken.

	total area Google				
Block	Common area 09-11-15 (ha)	Gullies	total area LiDAR		
		(ha)	Mapped Gullies (ha)		
4	1021.7	27.4	200.4		
5	1491.5	33.7	304.1		
7	1113.1	84.5	239.5		
9	397.9	5.3	75.9		
10	616.1	7.1	126.2		
16	613.3	27.5	148.1		
17	283.3	1.9	36.6		
	5536.8	187.3	1130.7		
		% of highly active			
		gullies	% of blocks comprised of		
	% of all Normanby GE gullies sampled	in blocks	alluvial gullies		
	7.7%	17%	20%		

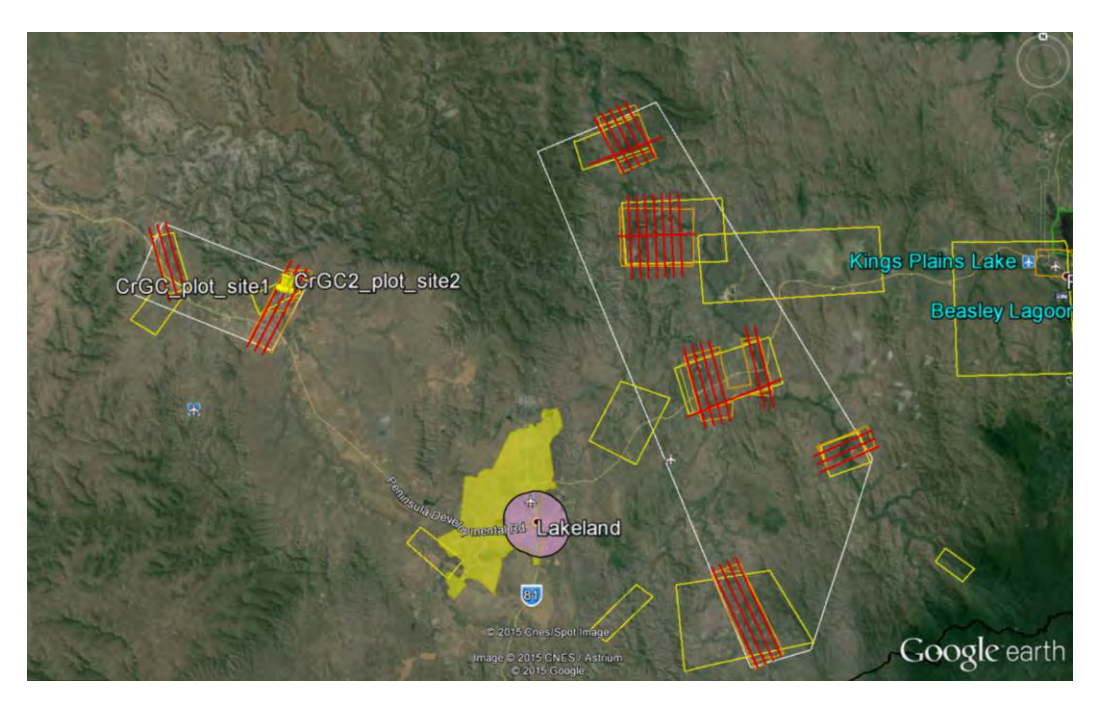


**Figure A3:** LiDAR flight lines from 2015 (red) showing the original 2009 blocks (yellow outline) and the 2011 refly blocks (orange outline).

#### 1.2.1 Summary of erosion from all LiDAR Blocks for the three common periods

A full description of the LiDAR processing methods is provided in Appendix 2 and the detailed results from the analysis within each of the LiDAR blocks is presented in Appendix 3. In the following sections we present the summary of the results for all of the common blocks for the three time slices. The results presented in Figure A4 have grouped some of the land unit classes defined in each block for clarity. The full breakdown into the various sub-components of the main units presented here (e.g. 3 sub-components for each of alluvial gullies, secondary channels and main channels) can be found in the block data in Appendix As explained in the block summaries, it is important to recognise that the erosion represented by repeat airborne LiDAR surveys should be considered to be the absolute minimum extent of erosion occurring in each of the surveyed blocks. The data resolution necessitates that the limit of detection for change between the timeslices is 0.5m at the first pass in both the horizontal and vertical planes. Once erosion has been detected at this level, we then reincorporate erosion in the range 0.2-0.5m in the polygons immediately adjacent to the eroding polygons at the 0.5m level. This technique is good for detecting rapidly advancing headscarps or bank erosion, but less so for detecting more subtle surface erosion processes which may make up a significant proportion of the total erosion. So for the vast majority of the land surface - including most of the internal surfaces of the gullies, a limit of detection (LoD) of 0.5m applies, and by definition this means that it is highly likely that we have significantly underestimated total sediment supply in the short term, particularly from within gullies. It is not uncommon to see gully sidewall lowering of 10-50cm within gullies over period of a few years. Obviously longer term monitoring will pick up such changes eventually once they become large enough to exceed the LoD of the method. Nevertheless, these short term data should be regarded as the minimum contributions from these sources in these locations.

It is also important to remember that these LiDAR blocks are a sample of the erosion processes that are occurring across the entire catchment. In the broader sediment budget study (Brooks et al., 2013) these changes were placed in their broader catchment context as part of the empirically based sediment budget. However, it was beyond the scope of this study to update the catchment model to reflect changes evident from these data. Rather these data serve to highlight the non-linear relationships that exist in these landscapes between rainfall floods and sediment and nutrient contributions from different sources, as well as highlighting the need for continuing to monitor erosion processes within these catchments, so that we can build our understanding of the complex dynamics of these systems. Any attempts to model these catchments over multiple decades will need to take into account these non-linear dynamics and the thresholds inherent in some of the key geomorphic processes in these catchments.

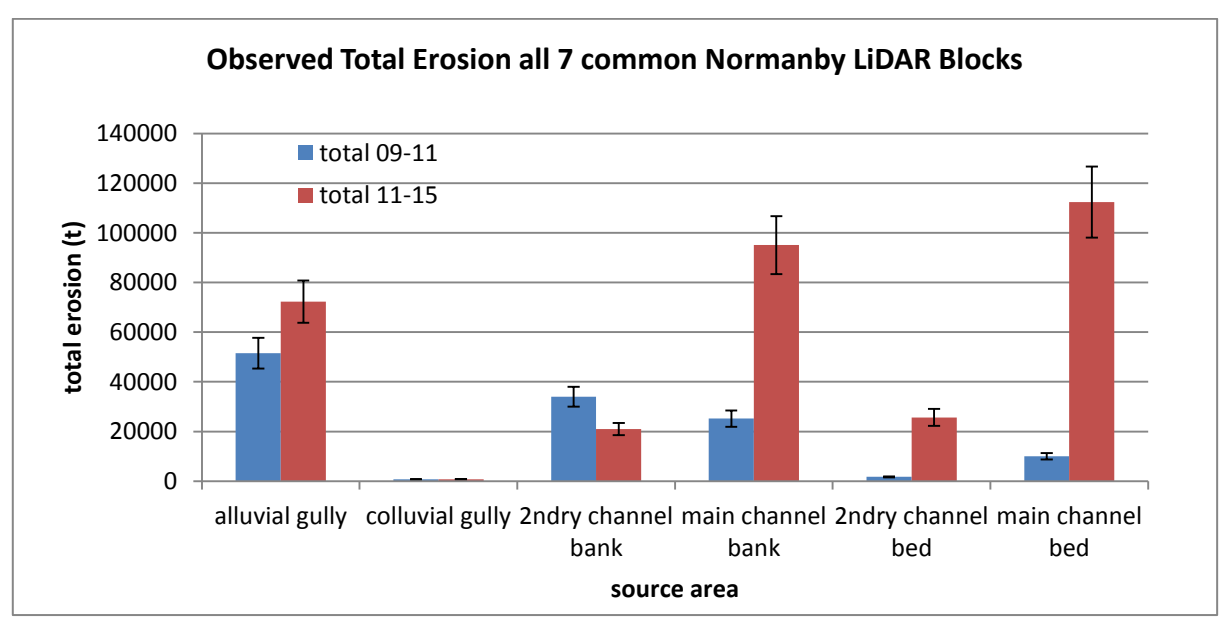


**Figure A4:** Summary data of total erosion from the two periods for which minimum erosion rates have been determined from aerial LiDAR data. Error bars represent the standard error between the 7 blocks at the total block scale.

#### 1.2.2 Trends in total erosion by source

Several trends are immediately obvious from the total erosion data presented at this scale, and it must be remembered that the first interval is erosion over a two year period (i.e. two wet seasons), while the second interval covers 4 wet seasons. Alluvial gully erosion is only marginally higher in the second period in absolute terms, while secondary channel erosion (small ephemeral channels) has actually declined. Main channel erosion however has increased dramatically. Note also that the vast bulk of gully erosion is from alluvial sources, which can partly be explained by the fact that there was a higher proportion of alluvium within the targeted LiDAR blocks. However, as outlined in Brooks et al. (2013) Google Earth gully mapping across the whole catchment indicates that alluvial gullies are significantly more prevalent and many of the colluvial gullies are functionally related to alluvial gullies (i.e. alluvial gullies that have extended right across a floodplain into colluvium at the valley margins).

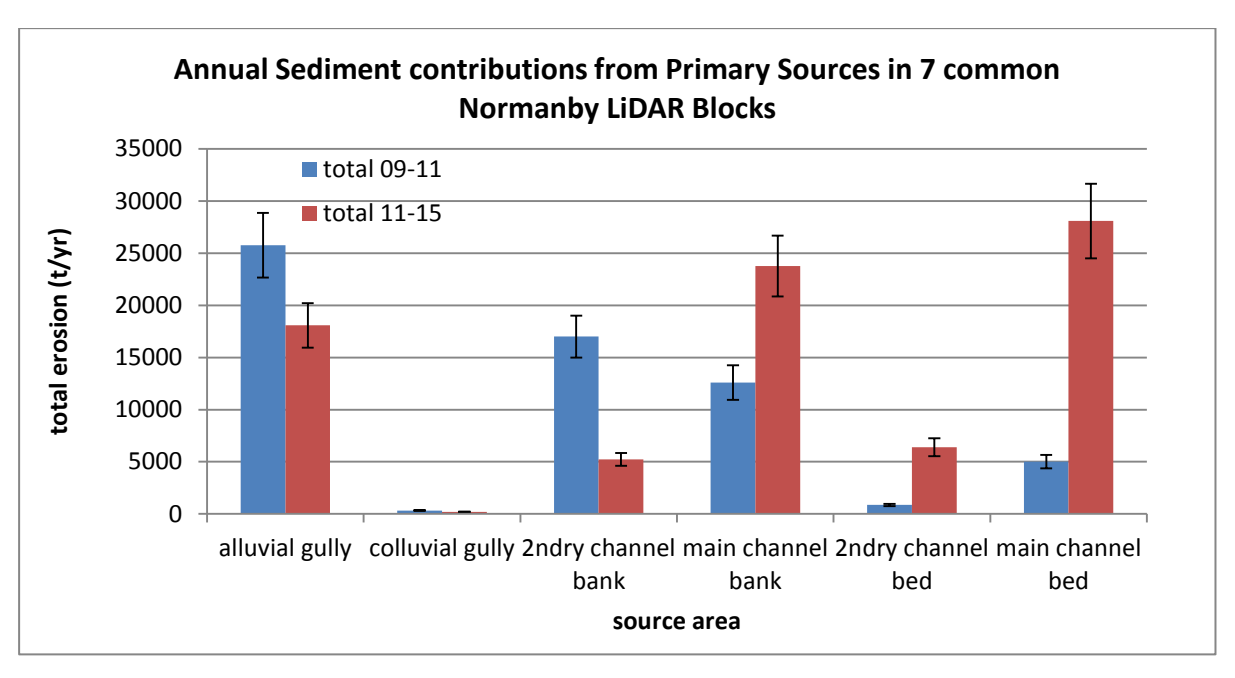


**Figure A5:** Annualised erosion rates summarised across the 7 common LiDAR blocks from 2009-11 (WY 2010-11) and 20011-15 (WY 2012-15). Error bars represent the standard error between the 7 blocks at the total block scale.

### 1.2.3 Annual trends in erosion by source and normalized for rainfall

The overall trends in erosion from the different process zones become more apparent once the data is represented as annualised erosion rates (Figure A5). From these data it can be seen that annual sediment production from both alluvial and colluvial gullies has declined over this period, as have erosion rates from secondary channels. Main channel bank and bed erosion have increased significantly. However, the more appropriate comparison to make is how the different process zones have responded as a function of incident rainfall. We would expect inter-annual variability in gully erosion rates to be fairly closely related to rainfall, although which particular rainfall metric is the most appropriate requires more research. At the scale of an individual gully we know that 24 hr rainfall is a good predictor of sediment yield from an individual gully (Shellberg et al., 2013). However, when looking at amalgamated trends in numerous gullies over a large area, in the absence of a network of continuous rain gauges distributed across the landscape, monthly or annual rainfall is likely to be a better predictor of broader trends in erosion rate. For this reason erosion data has been normalised to the annual rainfall data from the closest gauge to the respective LiDAR blocks. So blocks N4, N7, N9 - which are all located on Springvale Station, are normalised against the gap-filled East Normanby Gauge Rainfall data. Block N5 and N10 (Kings Plains) used the Kings Plains homestead data, while Blocks 16 & 17, which are located on Crocodile Station, used the gap filled rainfall data from Coalseam Ck Gauge, located on Crocodile. The correlations between the records used for gap filling are presented in Appendix The data presented in Figure A6 have been normalised to each 100mm of incident annual rainfall.

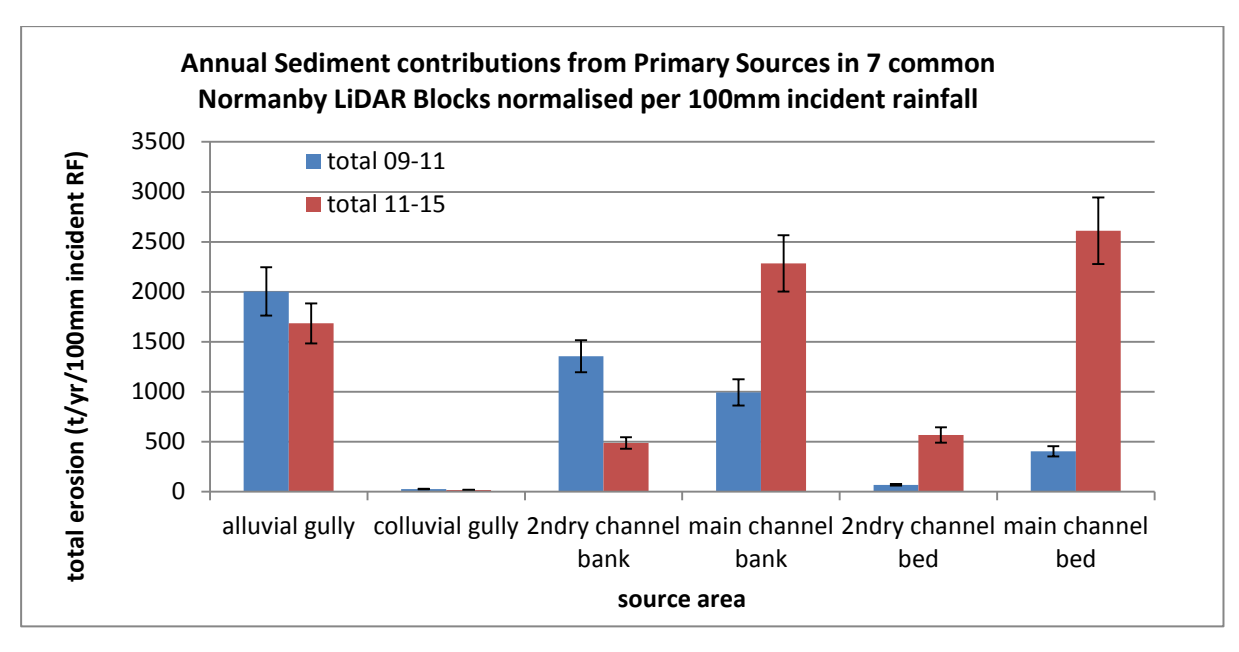


**Figure A6:** Annual Sediment contributions from different sources normalised per 100mm of incident rainfall. Anualised rainfall is the average of the 4 monthly rainfall records shown in Section 4.1.

If measured annual rainfall was a perfect predictor of inter-annual variability in gully erosion rates, we would expect to see no difference in the normalised sediment yields over the two periods. What the data show, however, is that normalised yield in the second period is 84% of that from period 1. This might also be expressed in terms of annual rainfall explaining 84% of the regional variability in sediment yields from alluvial gullies. Presumably if we had a better network of rain gauges and we delved further into the duration of rainfall events above a certain magnitude, amongst other things, we could improve the explanatory power. Nevertheless, accounting for this much of the inter-annual variability with a single simple metric would seem to provide considerable cause for optimism that we can develop generalised predictive models of alluvial gully sediment yields based on incident rainfall. The interesting feature of the two time periods represented in these data, is that during the second period three tropical cyclones passed through the Normanby catchment, which might have been expected to activate significant gully erosion. Whilst there is considerable spatial variability in the rate data from individual blocks (see Table A2) - which may be a function of local rainfall variability that has not been picked up in the available rainfall data – on average the cyclones did not seem to have an undue influence on gully activity rates.

The situation for channel erosion is quite different to that with gullies, for which we would not expect to find a direct relationship between annual incident rainfall and channel erosion, given that channel erosion is a threshold driven process, which is influenced more by the magnitude and duration of flow events, rather than total annual rainfall. Interestingly, secondary channel bank erosion rates are significantly down on the previous period (0.36 on average), while bed erosion rates for the same secondary channels have increased 8 fold on average (Table A2) albeit with one extreme outlier in Block 10 on Kings Plains station. Main channel bank erosion has also increased significantly in the second period by a factor of 2.3 on average, while main channel bed erosion increased on average by a factor of 6.5. The changes in the extent of erosion in the main channels likely reflects the impacts of larger flows generated by Cyclones Oswald and Ita in particular (Figure A7, Figure A9, Section 4). It

is interesting to note, however, that whilst the cyclone Ita flood was the second largest flood on record in the East Normanby River, and significant mobilisation of the bed was evident, due to the extent of vegetation within the channel it is remarkable how little erosion resulted from this flood (Figure A8).



**Figure A7:** East Normanby River in the immediate aftermath of the flood generated by Cyclone Ita (photo Tim Hughes).



**Figure A8:** Close up of the lower bank of the East Normanby River in the immediate aftermath of Cyclone Ita, indicating how little bank erosion there was in general as a result of this large flood.

From the flow data presented in Figure A10 and the summary statistics in Table A3, it is very apparent that the flow regimes differ markedly for the two periods, with total discharge being almost the same, despite the latter period being twice as long as the former. There were

double the number of moderate sized events in the earlier period compared to the latter, while there were a number of very large events in the latter period, and none in the former period. These patterns would appear to explain why channel erosion in secondary channels was much greater in the earlier period, given that it can be assumed that many of the smaller tributaries had high flows to generate these moderate flows in the main channels. The absence of very large events in the former period would also explain why main channel erosion was lower in this period than in the latter period, which experienced several very large events. Threshold driven mass bank failures in the main channels are more likely to have been driven by these larger events than the moderate events.

The data presented in Table A2 shows the ratio of change in rainfall normalised erosion rates for the two time periods for the individual blocks, enabling us to drill more deeply into the data. Whilst the overall trends as described above are clear, it is apparent that there is considerable spatial variability from block to block. Looking firstly at the alluvial gully data it is evident that Block N4 just to the north of the highway bridge crossing over the East and West Normanby Rivers has had a 56% annual increase in alluvial gully activity rates in the second period, while block 9 on the East Normanby River has had a 12% increase. Blocks 5 and 10 further down the Normanby River have had 7% and 12% increases respectively in the second period, over and above that explained by annual rainfall. Obviously, some of this variability would be explained by the fact that the available annual monthly and annual rainfall data does not reflect local scale variability in rainfall intensity and duration. More detailed rainfall gauging data at the local scale might help to explain some of this variability. Interestingly, Block 7 on the Granite Normanby, which is a major hotspot of alluvial gully erosion at the catchment scale experienced a significant reduction in annual average alluvial Blocks N16 and N17, which are both on the Laura River, also experienced significant reductions in alluvial gully erosion rates. Explaining this variability should be subject of further research, but likely includes variation in local rainfall magnitude, duration and intensity, as well as variations in soil geochemistry and erodibility.

It is interesting to consider what these results mean in terms of their relationship to local scale land-use intensity. Blocks N4, N7 & N9 on the Normanby River are within a large cattle station that has been very intensively grazed over the period of the study, as have blocks 16 and 17 on the Laura River. By contrast blocks N5 and N10 are on a grazing property that was purchased for conservation purposes at around the start of the second time interval, at which time it was significantly destocked. The results would tend to suggest that reducing grazing pressure over this relatively short time scale (4 years) has not had a measurable effect on erosion rates at this broad scale. In the absence of any other controls on gully erosion rates (such as direct management intervention), it is likely that incident rainfall will continue to control sediment production from gullies for the foreseeable future. The effect of complete cattle exclusion on gully erosion rates is explored in more detailed in Appendix 5 and 6.

Despite the considerable variability in gully activity rates in the different blocks, secondary channel erosion (i.e. smaller ephemeral channels) all experienced substantially lower rates of erosion in this period, even when the gully erosion rates in the same vicinity showed increased rates of activity. It is also unusual that there seems to be a distinct disconnect between secondary channel bed erosion rates (which have increased dramatically in places) and the associated bank erosion. Main channel erosion (bed and banks) have typically both increased in most blocks, which is more in line with previous findings (Brooks et al., 2014)

where it was demonstrated that channel bank erosion is strongly related to bed erosion and deposition. The more consistent trend in main channel erosion is likely explained by a whole of system response to a larger event operating at a large scale than represented by the LiDAR blocks.

**Table A2:** Ratio of change on rainfall normalised erosion rates for each LiDAR block expressed as time 2 (2011-15)/ time 1 (2009-11).

		ontribution	1					
change ratio	block (t/	100mm R	F/yr)					
sed source	N4	N5	N7	N9	N10	N16	N17	total
alluvial gully	1.56	1.07	0.54	1.12	1.09	0.71	0.29	0.84
colluvial gully	0.72	0.76	1.65	0.00				0.70
2ndry channel	0.55	0.50	0.22	0.77	0.54	0.20	0.20	0.36
main channel bank	14.5	3.62	1.70	0.79	28.9	4.73	0.00	2.30
2ndry channel bed	3.05	26.18	0.50		657	1.33	0.30	8.24
main channel bed	55.2	9.43	4.86	2.93	4.93	1.51		6.46
Total	4.18	2.51	0.72	0.89	2.31	1.42	0.23	1.58

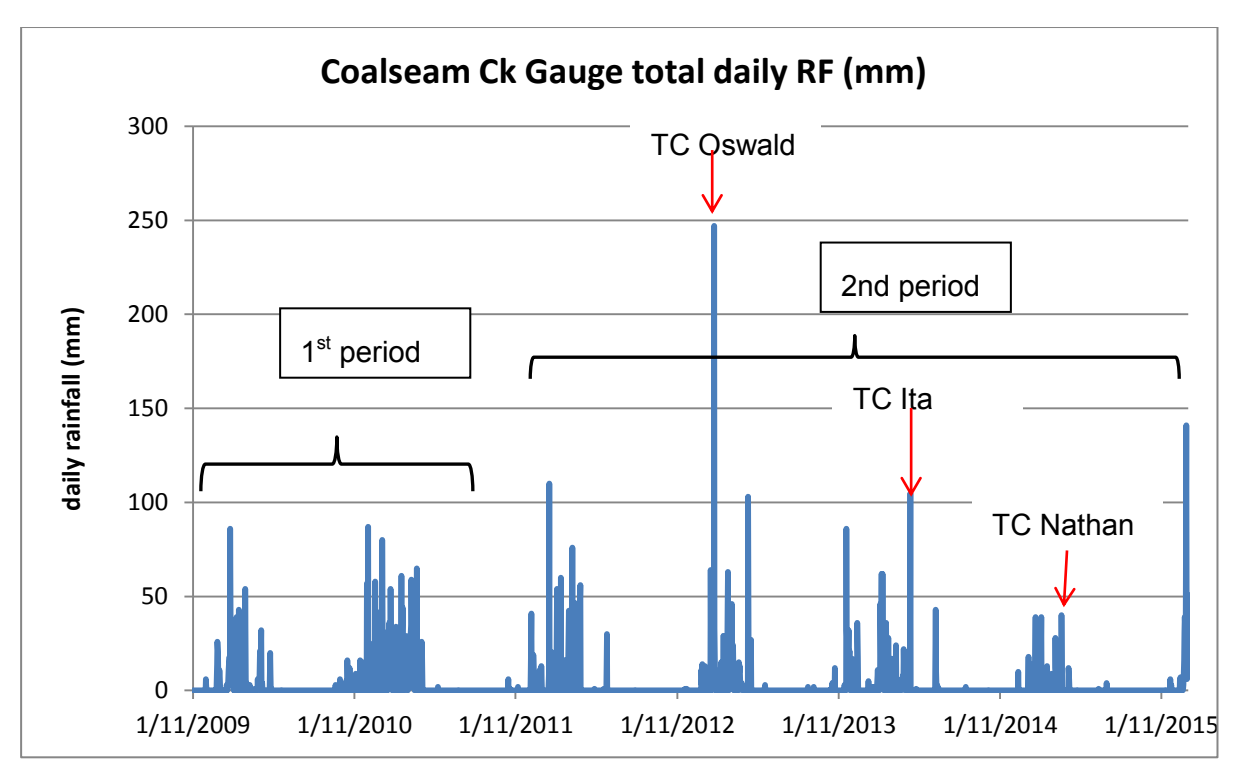


Figure A9: Daily rainfall at the DNRM gauging station on the Laura River at Coalseam Ck.

**Table A3:** Comparison of flow statistics in the Laura and Normanby Rivers for the two study period intervals

		y River at camp	Laura River at Coalseam Ck		
	2009-11	2011-15	2009-11	2011-15	
Total Q (GI) # days > 100	2500	2140	996	990	
cumecs # days > 500	100	49	31	15	
cumecs # days > 1000	4	7	2	3	
cumecs	0	3	0	2	

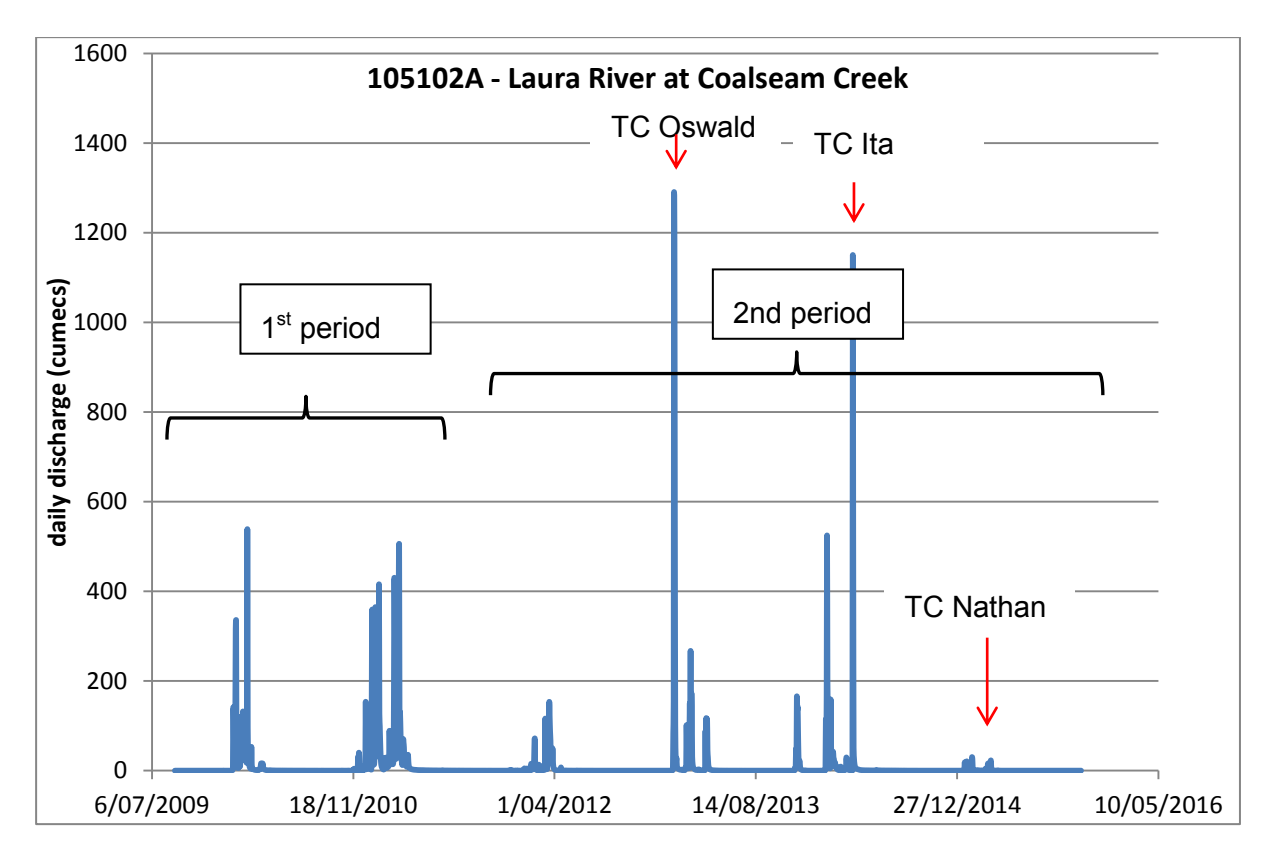


Figure A10: Mean daily discharge for the study period Laura R at Coalseam Ck gauge

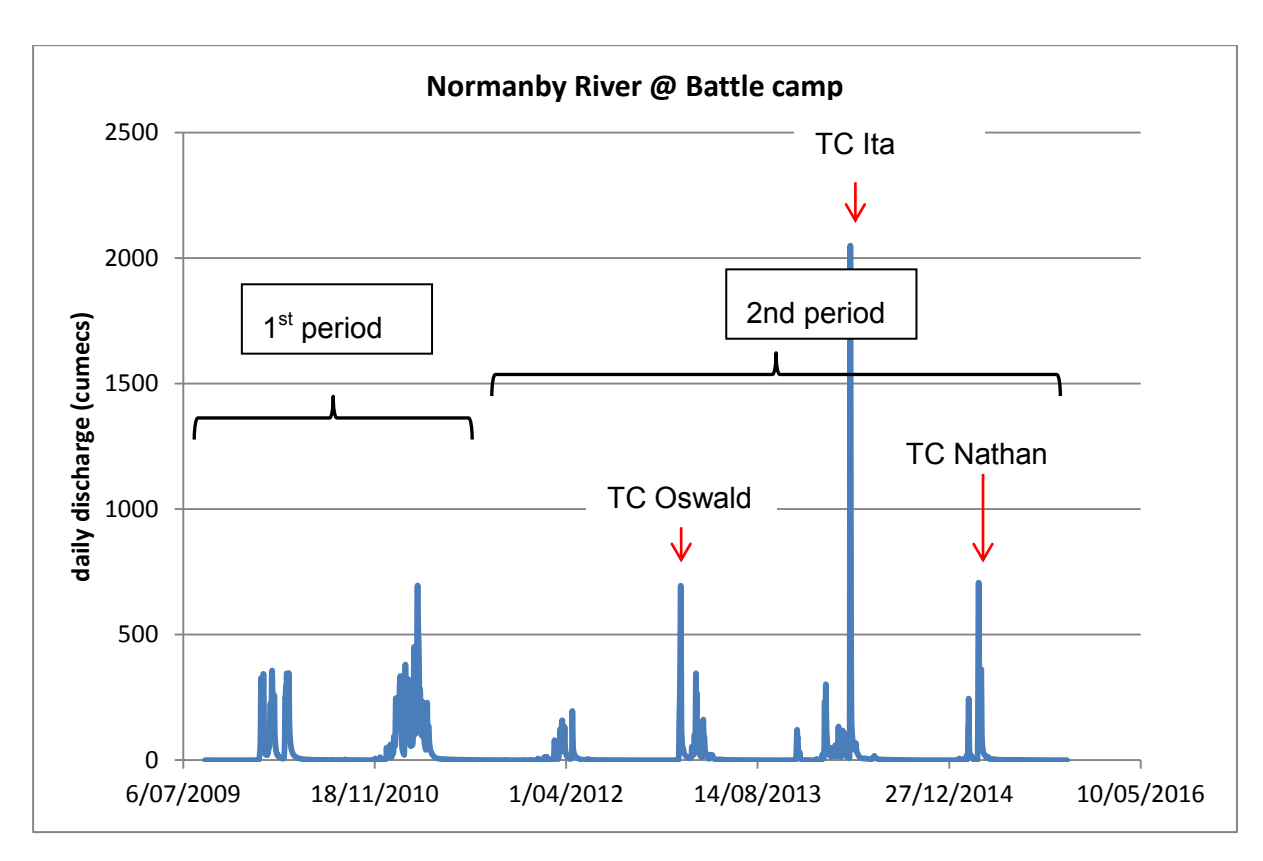


Figure A11: Mean daily discharge for the study period Normanby R at Battlecamp gauge

## 2. LIDAR BLOCK PROCESSING

Prepared by: Graeme Curwen and Andrew Brooks

## 2.1 Data Processing Modifications

A number of refinements have been made to the procedures for processing the LiDAR data since the last set of change detection analyses produced in Brooks et al., (2013). To ensure consistency between the new and old data, all of the old data has been reprocessed according to the updated procedures. The key improvements to the procedures used for processing the LiDAR data to ensure accurate change detection include the following:

- 1. An improved process for aligning LiDAR data at different time steps
- 2. An improved approach for noise filtering which recovers real erosion data that would otherwise have been lost in the filtering process
- Higher Resolution Definition of Alluvial and Colluvial areas based on new digitization of hillslope margins rather than the geology layer used previously which is somewhat coarse
- 4. New land unit classes which differentiates between primary gully head scarp retreat and secondary gully floor incision

Detailed descriptions of the modifications are outlined in the following sections, before the presentation of the detailed results from each LiDAR block.

# 2.2 Improved Process for aligning consecutive LiDAR Blocks

One of the most important processing steps to ensure data of the highest quality is used for the LiDAR change detection processing is to ensure that the respective DEMs are accurately aligned in X,Y and Z directions to minimize the degree of noise introduced to the procedure. Poor DEM alignment results in a low signal to noise ratio, which reduces your ability to detect real geomorphic change between the respective time slices. To this end we have developed procedures to minimize unnecessary noise by testing alignment increments in all directions, and then selecting the particular alignment that minimizes noise. The following is a worked example of the process used.

### 2.2.1 LiDAR Block 7 Alignment Processing

## Step 1 - Testing Vertical alignment on flat ground

**Table A4:** Differences in mean elevation in 10 sample polygons between timesteps 2009-2011 and 2011-2015. Only 2 of 20 samples had differences greater that 10 cm. Vertical alignments of 3 Lidar time slices seem satisfactory.

Sample location	Mean Difference 2009-2011	Mean Difference 2011-2015
1	0.0477	-0.0642
2	0.0626	-0.0398
3	0.0352	-0.0671
4	0.0195	0.0247
5	0.1077	-0.0693
6	0.0528	0.0035
7	0.1155	0.029
8	0.0575	0.0173
9	0.0886	-0.0695
10	0.0793	0.0093

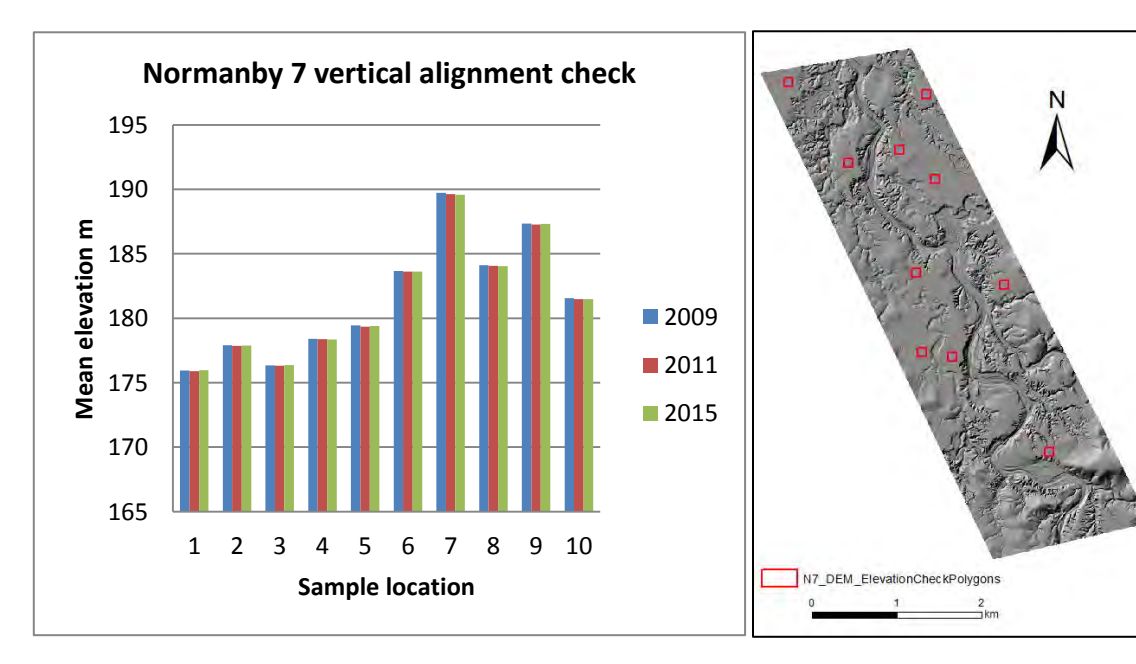


**Figure A12:** Mean elevations in ten 100m by 100m polygons to sample for vertical alignment and distribution of 10 polygons of 100m by 100m to sample vertical alignment

#### Step 2 - Horizontal offset checks

- 1 Toggle HS rasters. Observations something is going on for the 2015 Lidar.
- 2 Create contours at defined intervals and assess for offset.

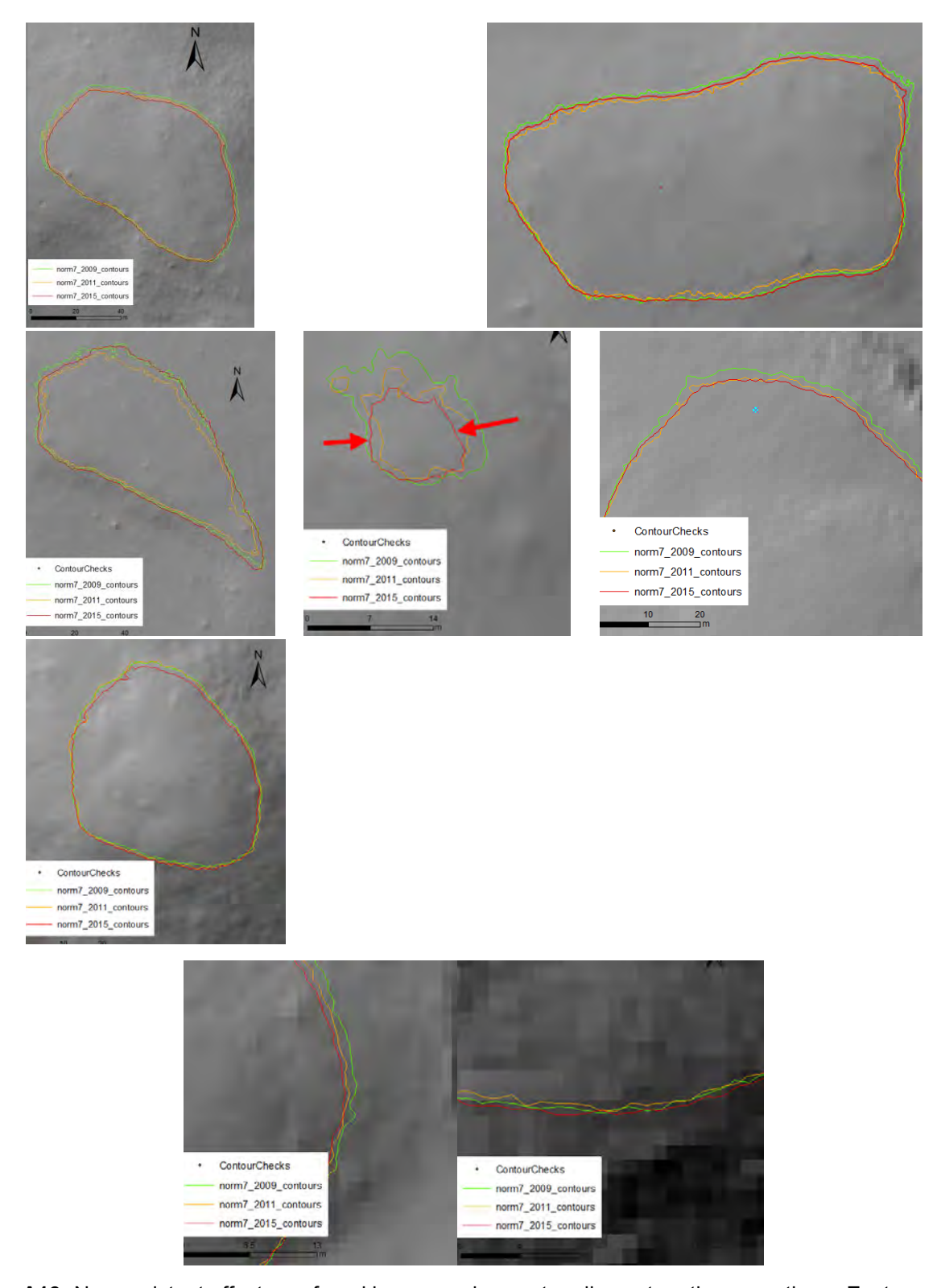


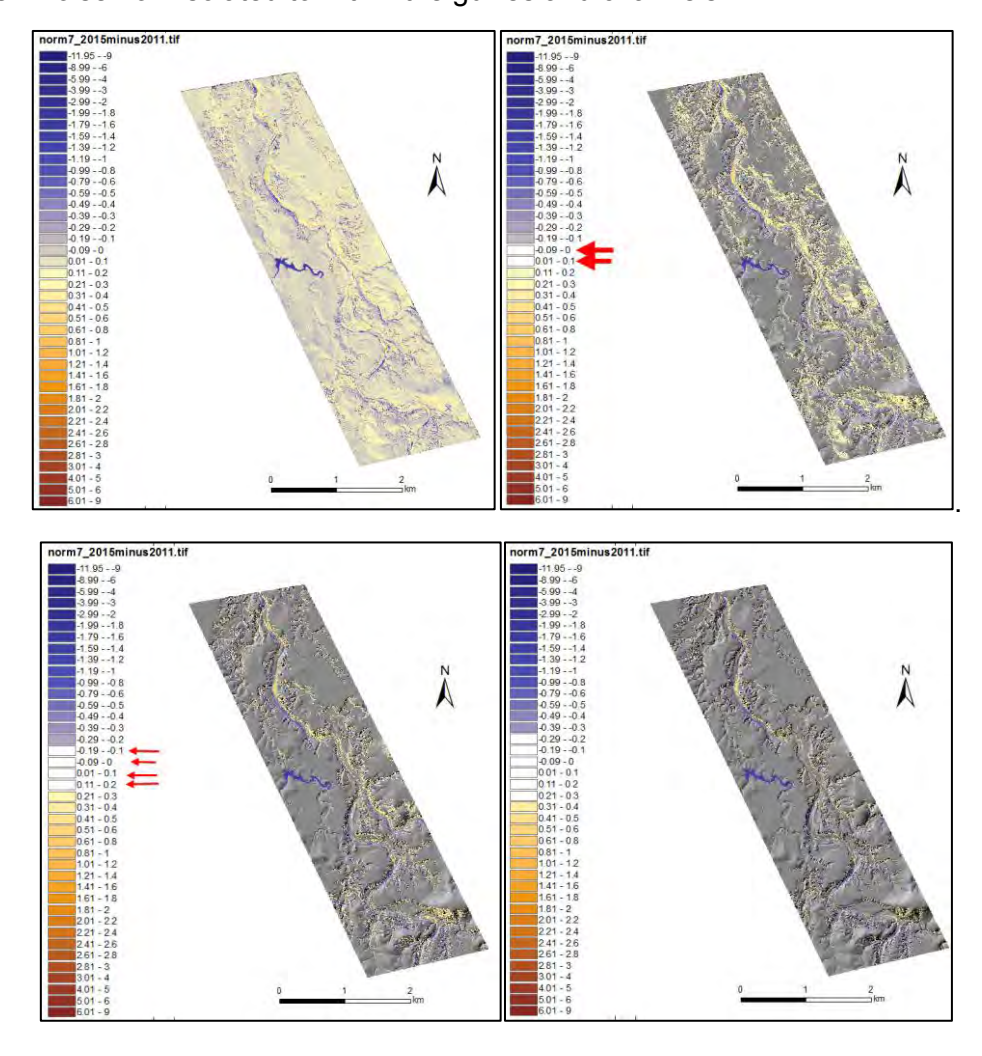
**Figure A13:** No consistent offset was found by comparing contour lines at northern, southern, Eastern or western aspects of slopes.

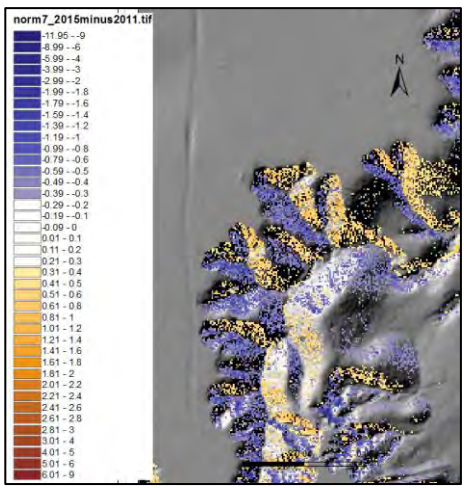
Step 3 - Difference layer inspection 2015 minus 2011

1)

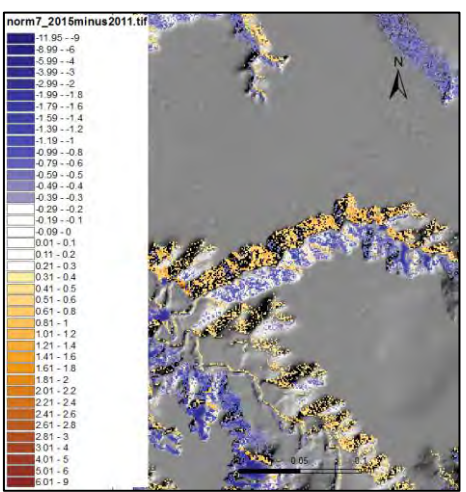
Difference layer	N7 2015-2011
Min	-11.94999695
Max	13.54000
Mean	0.00015151

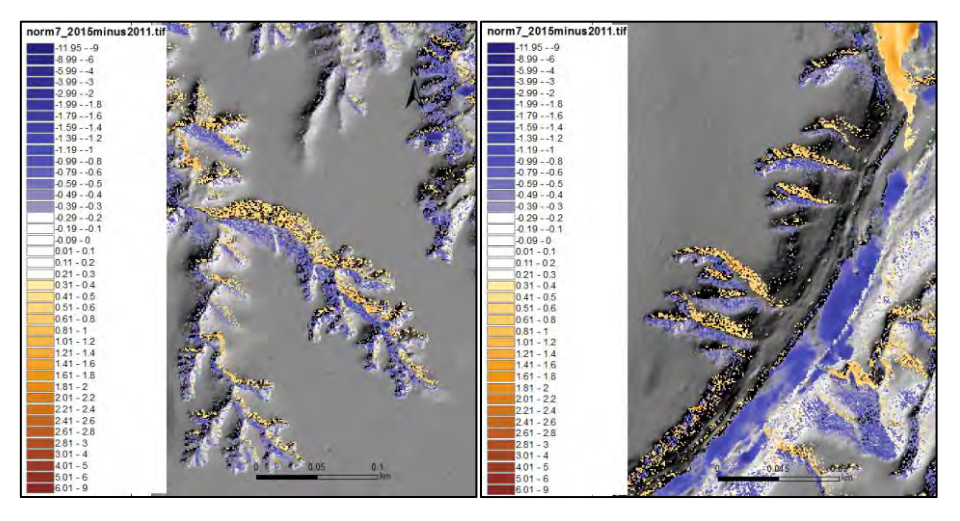
Evidence for clearing of noise from floodplain: 20cm above and below zero clears noise. Noise now isolated to within the gullies and channels



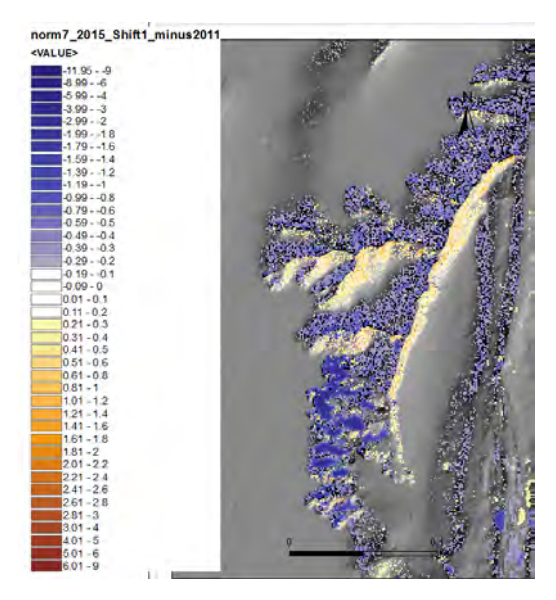


Evidence of horizontal offset l

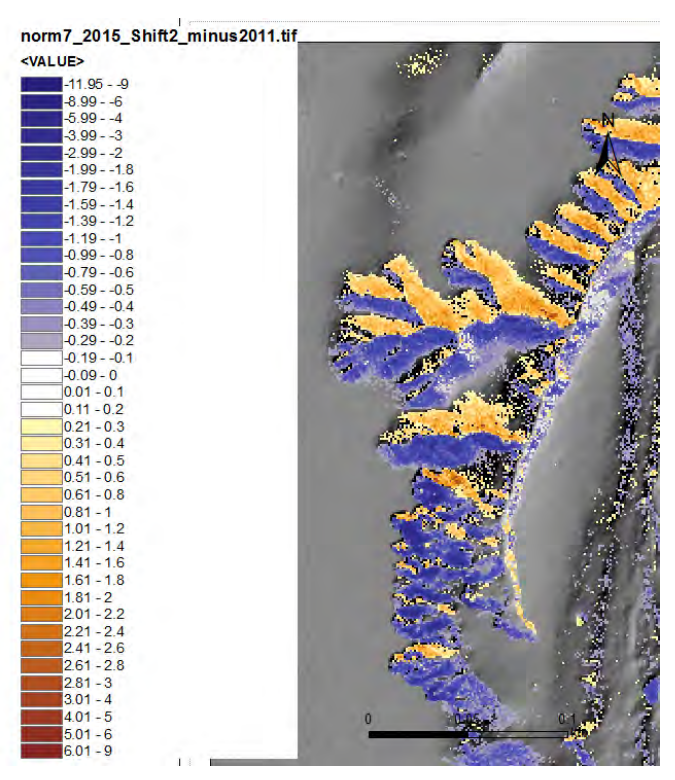




Shift 1: X shift = 0 Y shift +1m No immediate benefit

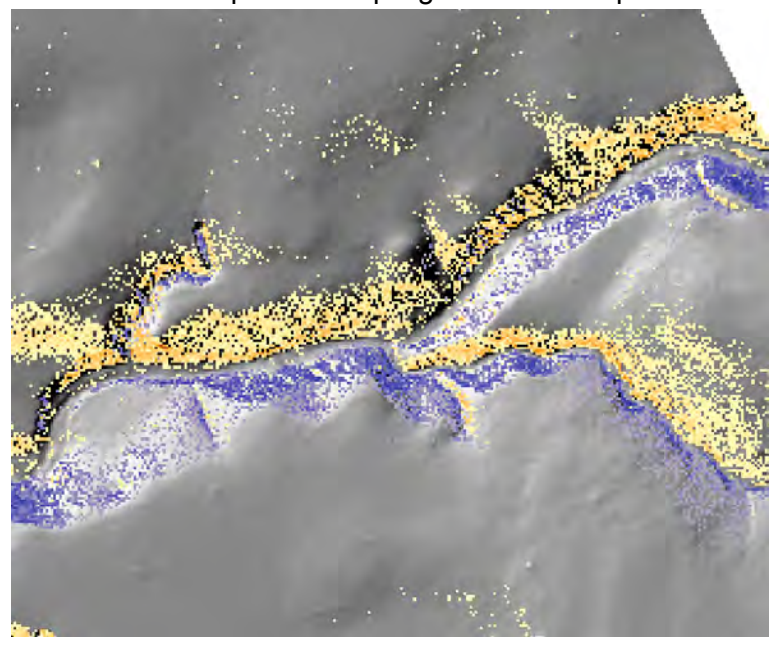


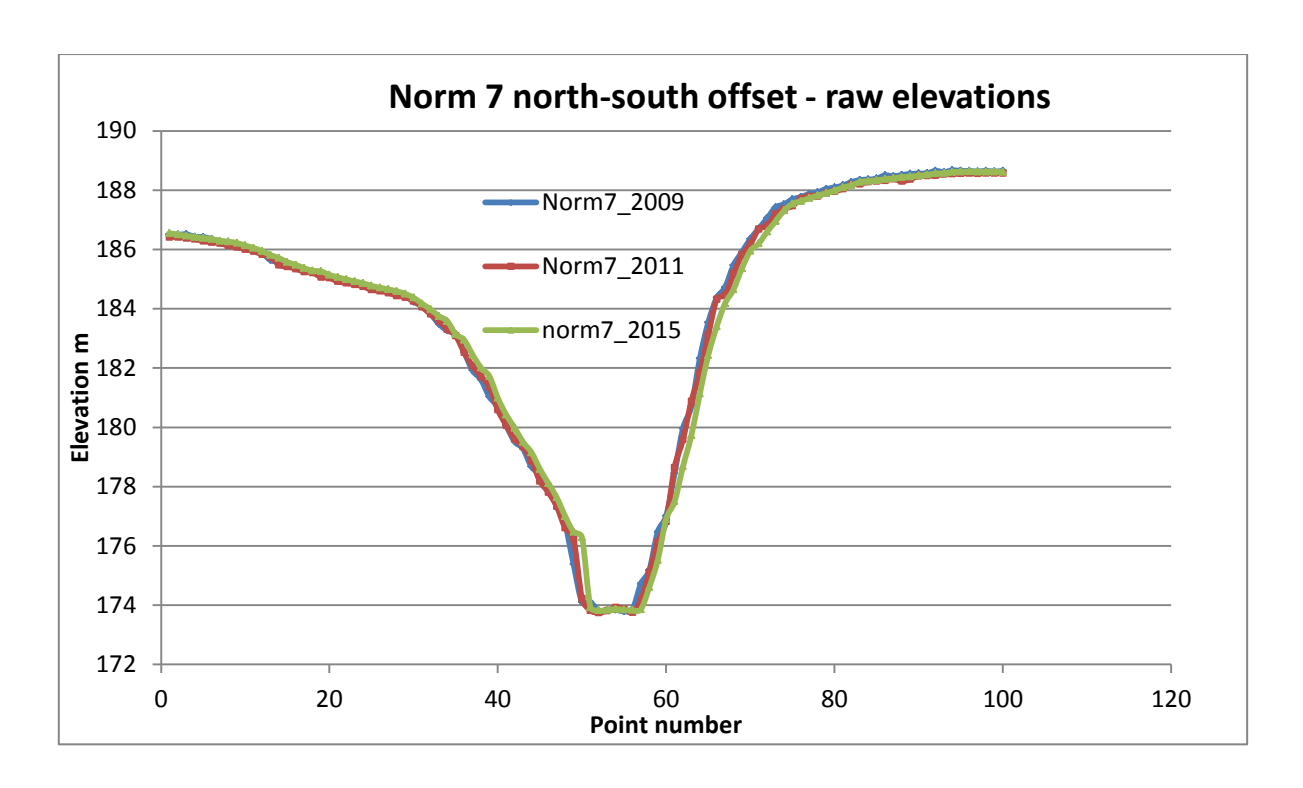
Shift 2: X shift = 0 Y shift -1m Worse effect with y = -1 shift

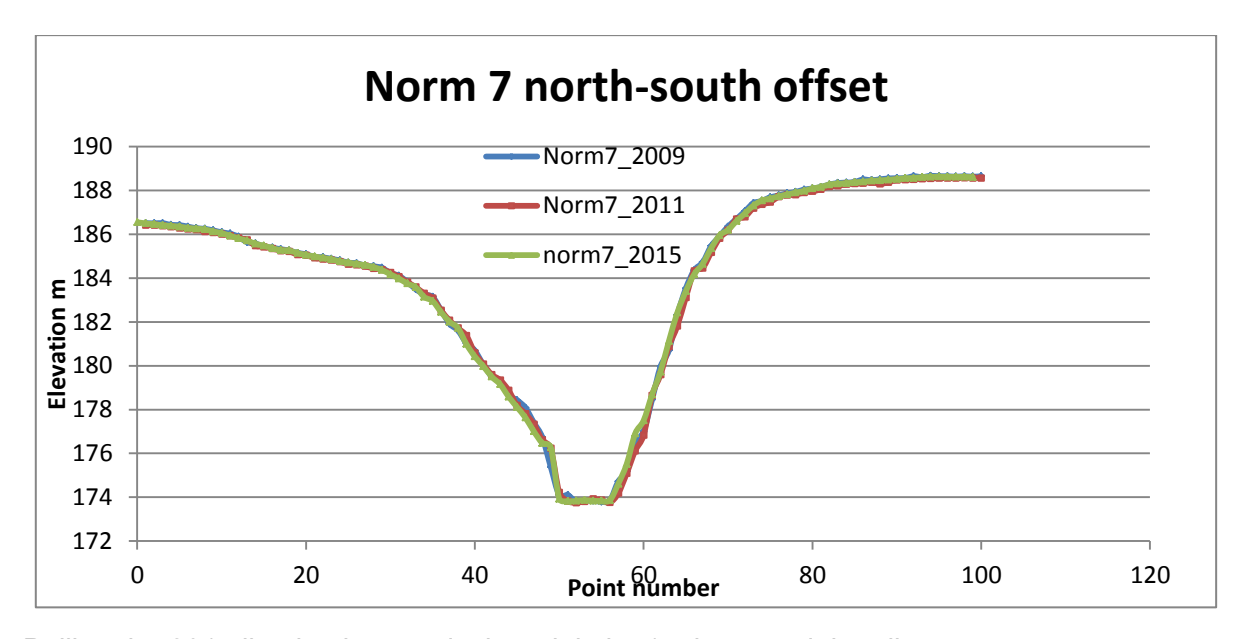


Shift 3: X shift = 0 Y shift 2m still not improved

Now to check with points sampling values – sample site below

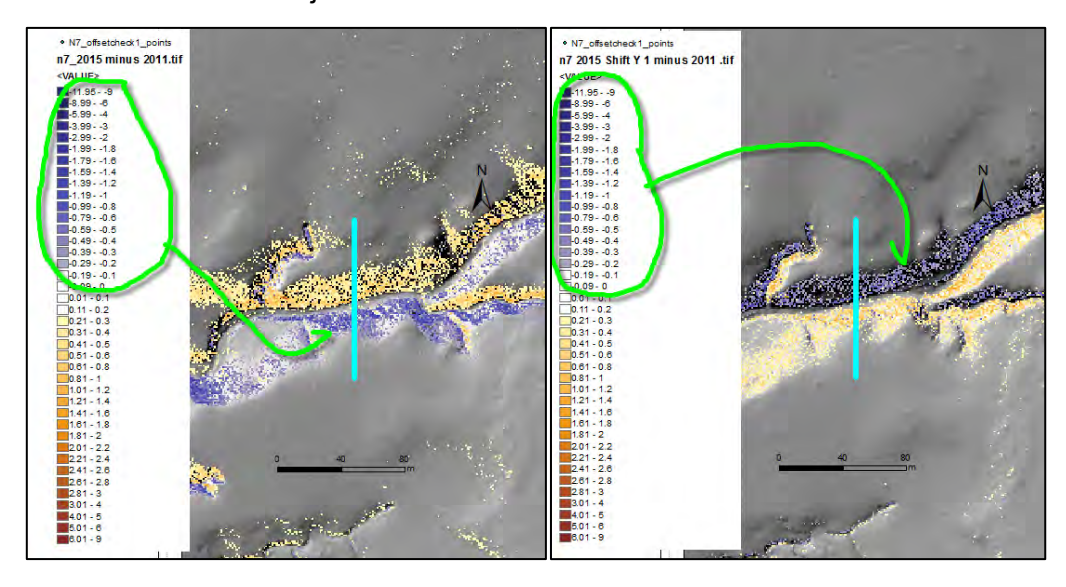






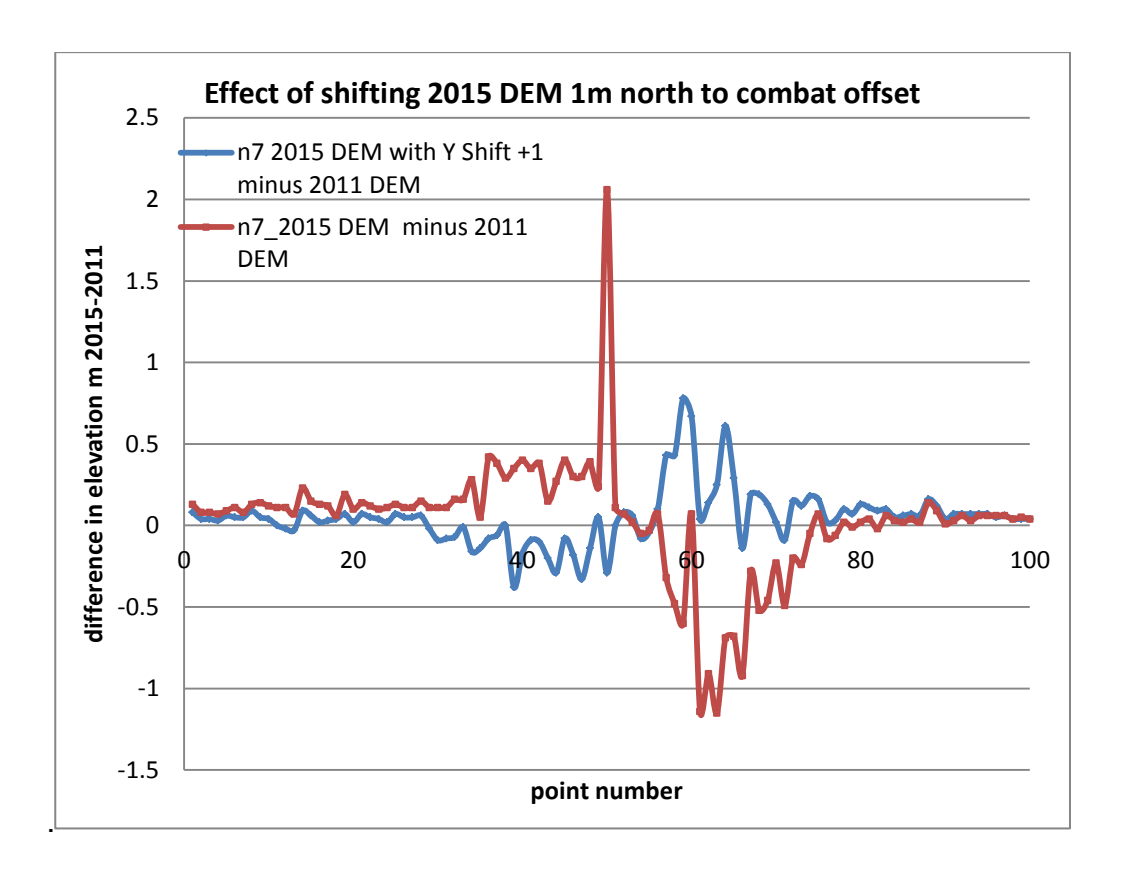
Pulling the 2015 line back towards the origin by 1m improved the alignment.

#### Alignment based on linear adjustment



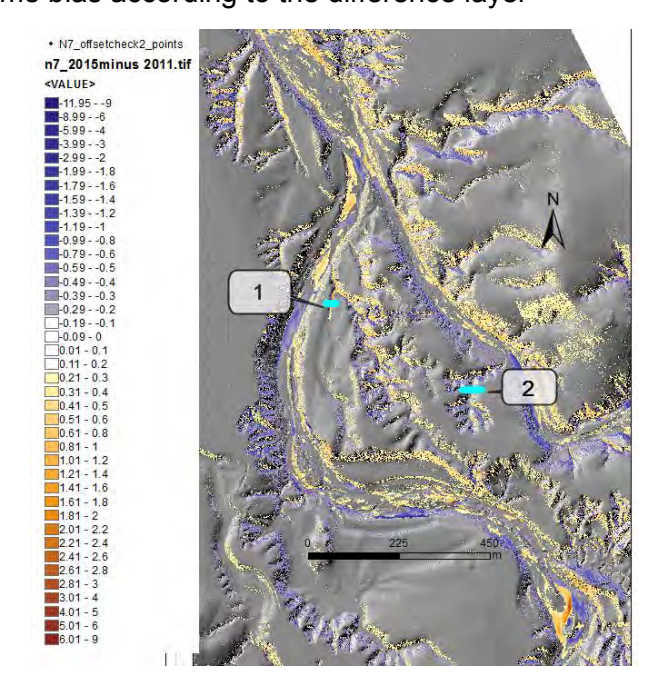
Compare difference layer 2015-2011 with the difference layer for the nudged 2015 DEM. The effect has been to shift the negative difference values from the south side of the gully to the north side.

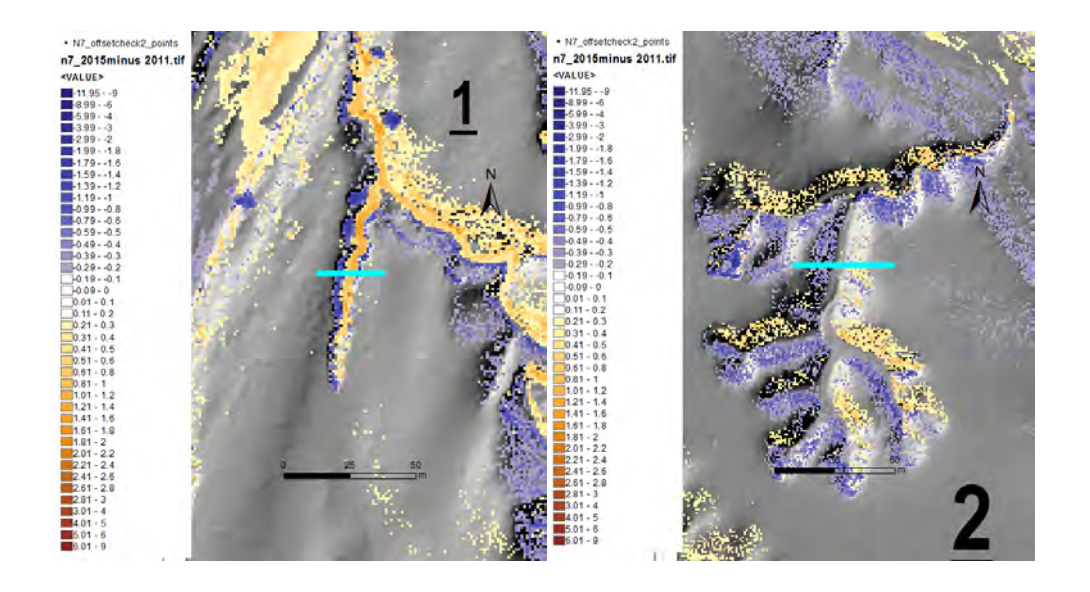
The graph below shows values from the raw difference layer and the nudged difference layer, with the bottom of the gully being where the lines cross over. Basically, the offset is below 1m, and the resolution of the raster – so cannot be corrected with whole metre increments, and therefore requires sub-metre increment adjustment

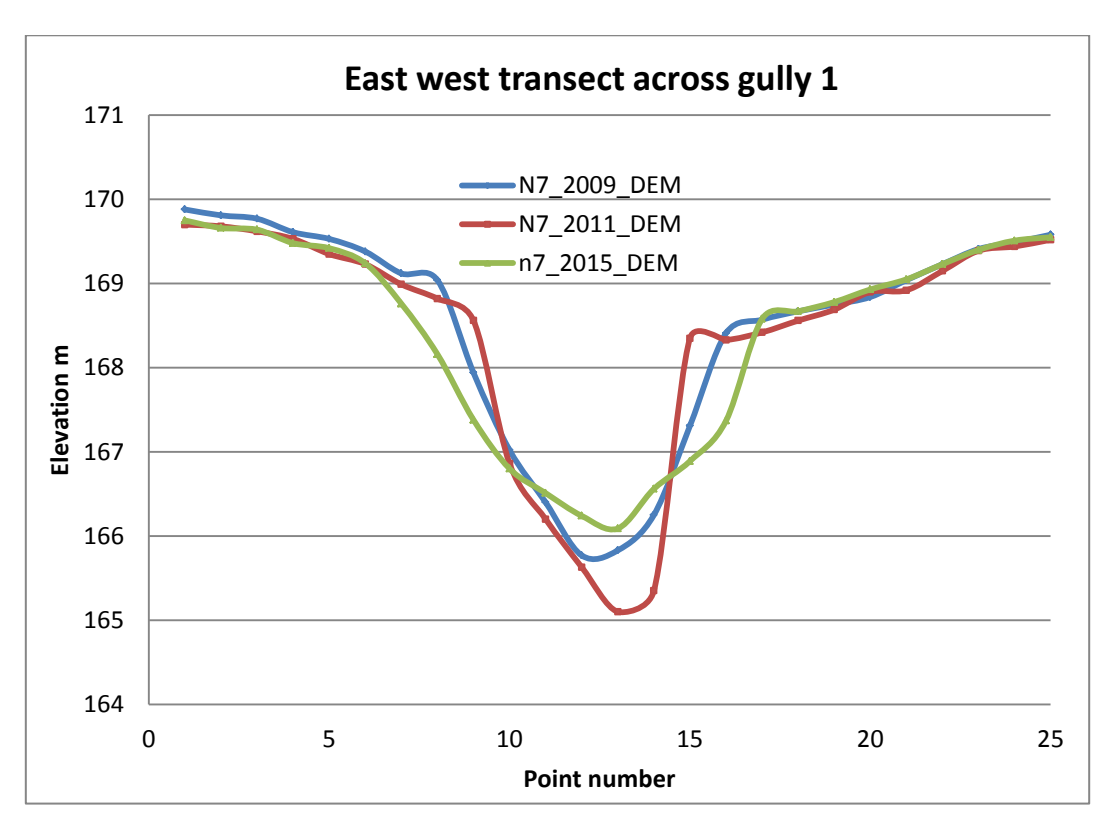


### East -West offset check

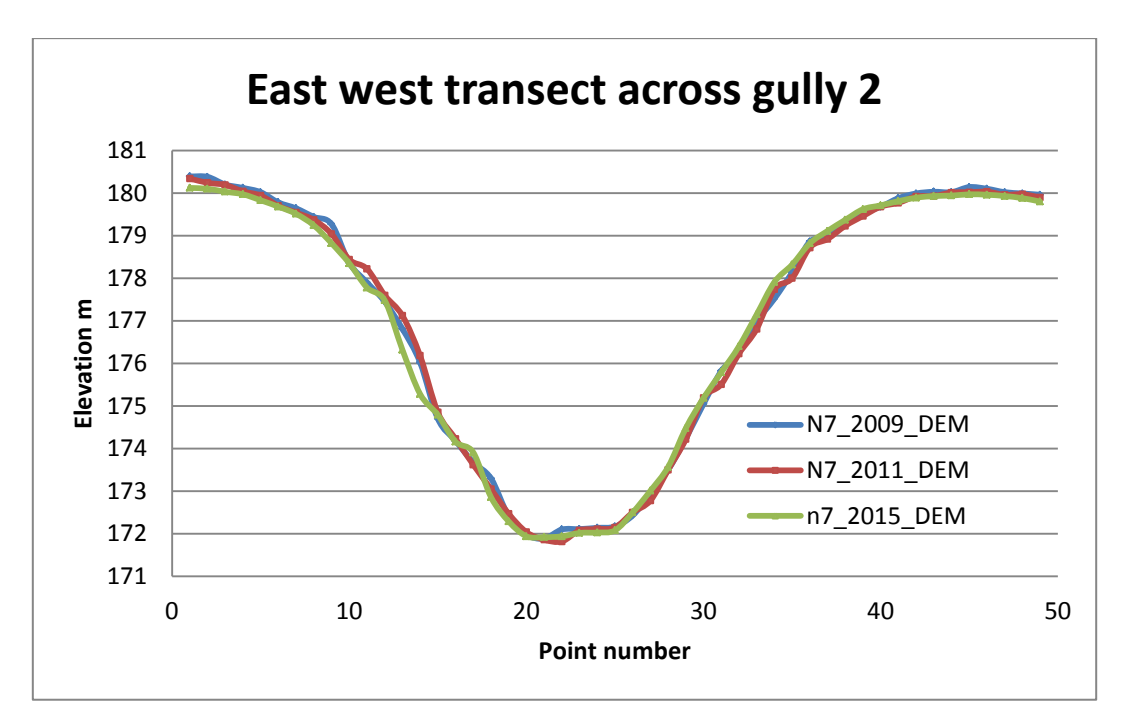
There is definitely some bias according to the difference layer



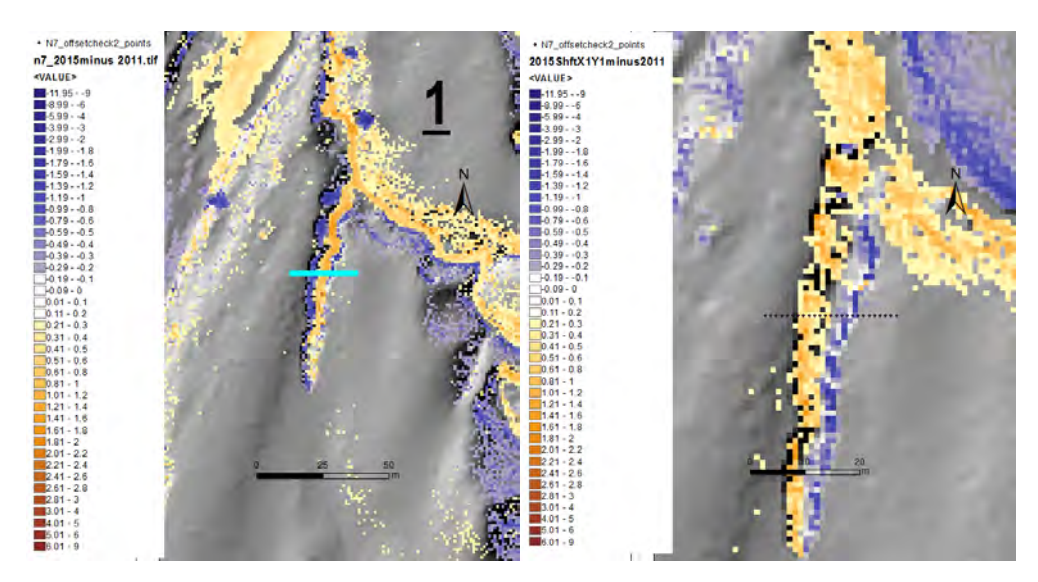




Gully 1 - The graph is consistent with the screen grab – the upper gully wall has widened, and there is filling of the gully floor on the lower right side.

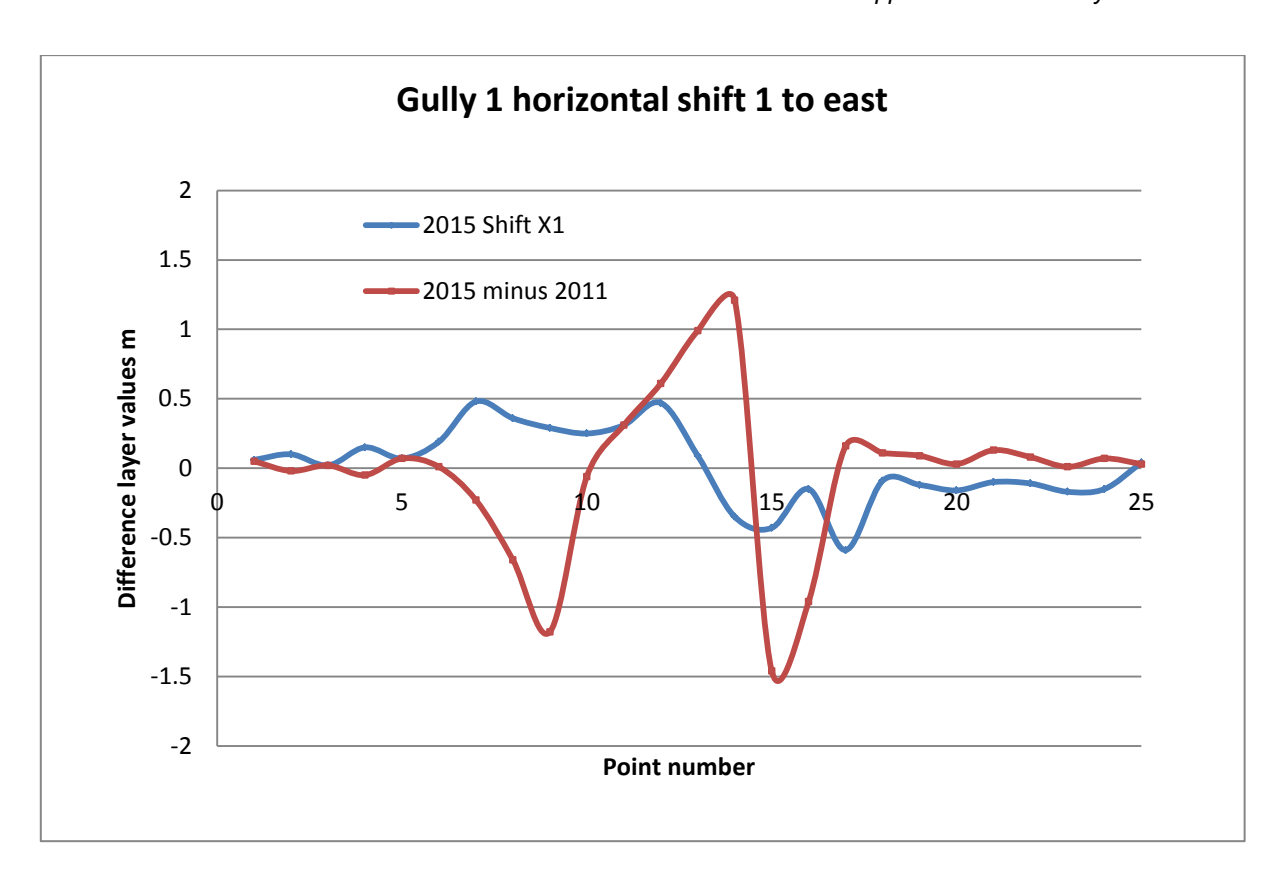


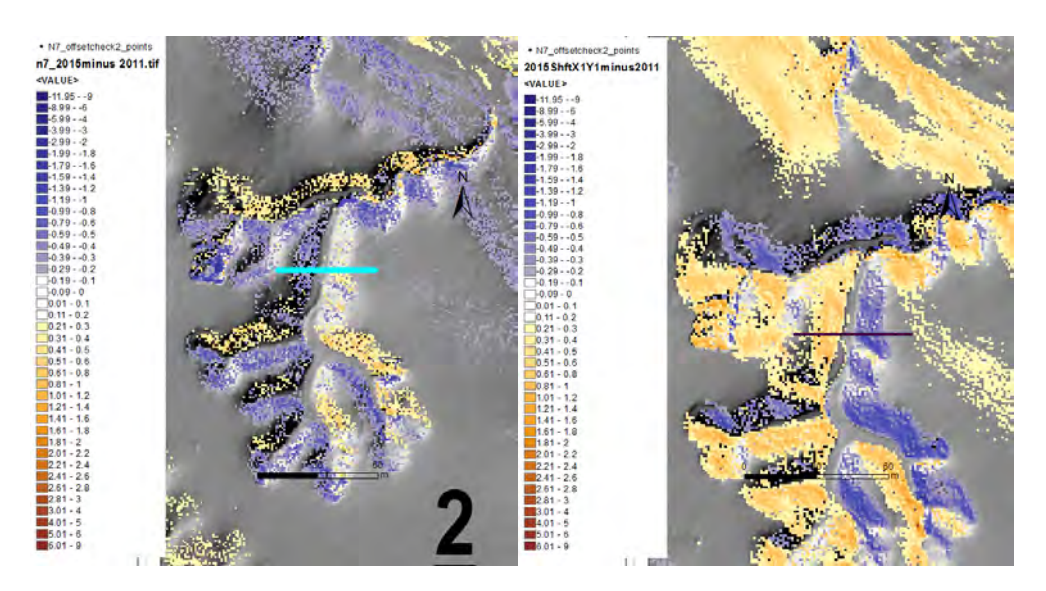
In Gully 2 it is hard to see any obvious problems in the curves. Efforts to correct the "offset" as seen in the difference layer cause the positive and negative values to flip to opposite sides of the gully.



Shifting 2015 DEM 1m to the right flipped the side of gully with erosion values from left to right. Panel on right has raster shifted 1m to the east.

This result is born out from sampling the original difference layer and the nudged difference later.



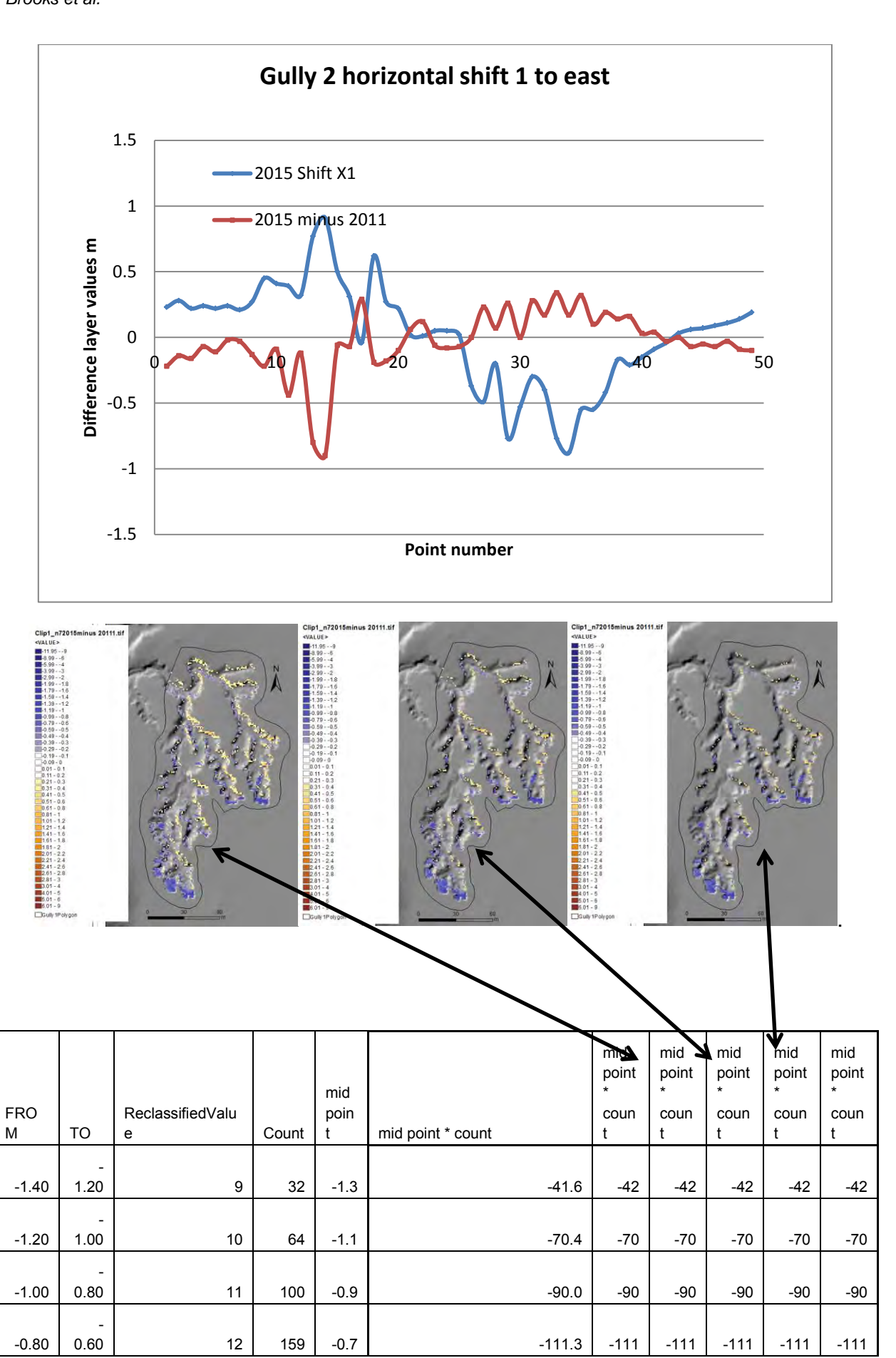


Same pattern seen in second gully.

Conclusion – the original position of 2015 DEM is not ideal, but shifting it 1m north or east by whole metre increments to adjust for the bias actually makes the problem worse – as seen in the more intense colouration of the shifted DEM; panel on the right.

The graph below shows the magnitude of difference is larger for the shifted DEM, seem by the blue line tracking further above and below the x axis that the red line.

Conclusion – Use the original 2015 DEM or adjust in sub-metre increments.



	_									
-0.60	0.50	13	137	-0.5	-68.5	-69	-69	-69	-69	-69
	-									
-0.50	0.40	14	201	-0.4	-81.2	-81	-81	-81	-81	-81
-0.40	0.30	15	352	-0.3	-105.6	-106	-106	-106	-106	-106
-0.40	0.30	15	352	-0.3	-105.0	-106	-100	-106	-106	-106
-0.30	0.20	16	545	-0.2	-109.0	-109	-109	-109	-109	-109
	_									
-0.20	0.10	17	1172	-0.1	-117.2	-117	-117	-117	-117	-117
			1323							
-0.10	0.00	18	9	0.0	-28.8	-29	-29	-29	-29	-29
0.00	0.10	19	3478	0.1	347.8	348	348	348	348	348
0.10	0.20	20	801	0.2	160.2	160	160	160	160	160
0.20	0.30	21	414	0.3	124.2	124	124	124	124	124
0.30	0.40	22	205	0.4	82.2	82	82	82	82	82
0.40	0.50	23	101	0.5	50.5	51	51	51	51	51
0.50	0.60	24	81	0.6	48.6	49	49	49	49	49
0.60	0.80	25	40	0.7	28.0	28	28	28	28	28
0.80	1.00	26	20	0.9	18.0	18	18	18	18	18
1.00	1.20	27	3	1.1	3.3	3	3	3	3	3
					Sum erosion					
					-823.6	-795	-678	-569	-463	-382

sum deposition						
	862.7	515	355	231	148	98
% of total	deposition					
remaining		60	41	27	17	11

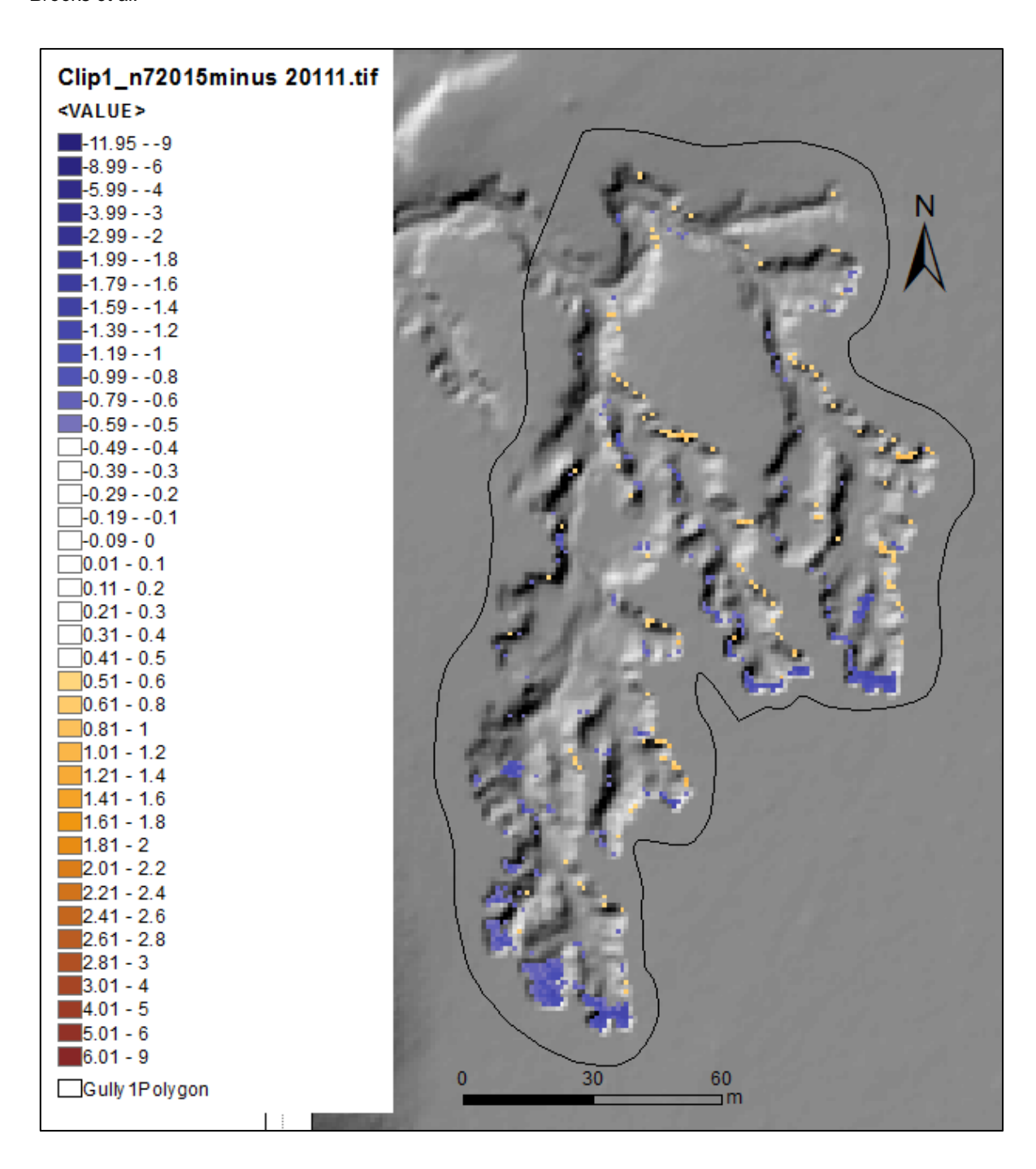
69

56

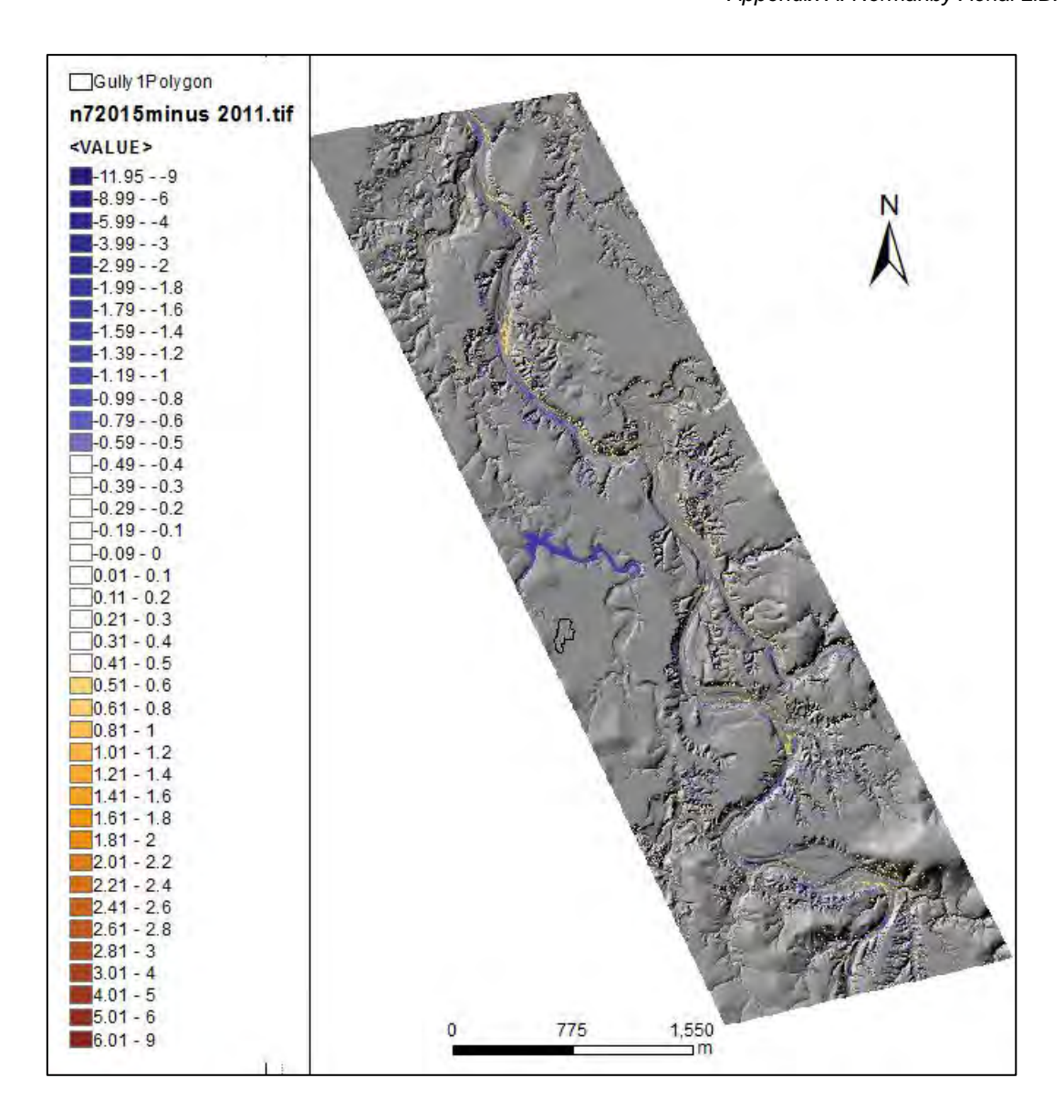
46

Below is pattern of erosion and deposition in gully 1 with values masked between 0.5 and - 0.5 m.

% of total erosion remaining



All of Normanby 7 with difference layer 2015-2011 with values between 0.5 and -0.5m masked, i.e. same noise filter as previously.



#### 2.2.2 A new approach to checking Lidar alignment

The method outlined above to check alignment of LiDAR at different timesteps relied on sampling DEMs with transects in isolated locations across slopes that showed patterns of bias. It proved frustrating to determine what the offset was in some cases. On the basis of this relatively time consuming analysis the DEM from the latter time step might be nudged 1 or 2 metres in any direction, and an analysis done to see if any real improvement in alignment had occurred.

A new approach is now outlined to automatically nudge the latter DEM with incremental X and Y values up to 3m from the original position, eg XY shifts of

0,1; 0,2; 0,3

1,1; 1,2; 1,3

2,1; 2,2; 2,3 and so on to generate 49 new rasters with offsets up to 3,3, -3,3; -3,-3; 3,-3. It can also be done with sub-metre increments.

This is run through Arc GIS model builder, but could be scripted in Python to add flexibility.

The 49 nudged rasters are all used to create difference layers by subtracting the earlier time step from the nudged raster, eg 2015X-1Y-3 minus 2011,

The objective is to find the difference layer with the least amount of noise, the assumption being that this will minimise the offset inherently built into capturing Lidar in remote locations with different foliage regimes in different years, no decent reference objects, no registered survey points, potentially using different aeroplanes, different Lidar units, being processed by different technicians using different software.

The method used in trials so far is to create a point shapefile with up to 100,000 points draping over slopes showing bias in the original difference layer.

The points drill down through the 49 new nudged difference layers, extracting cell values, which are then exported to excel for analysis.

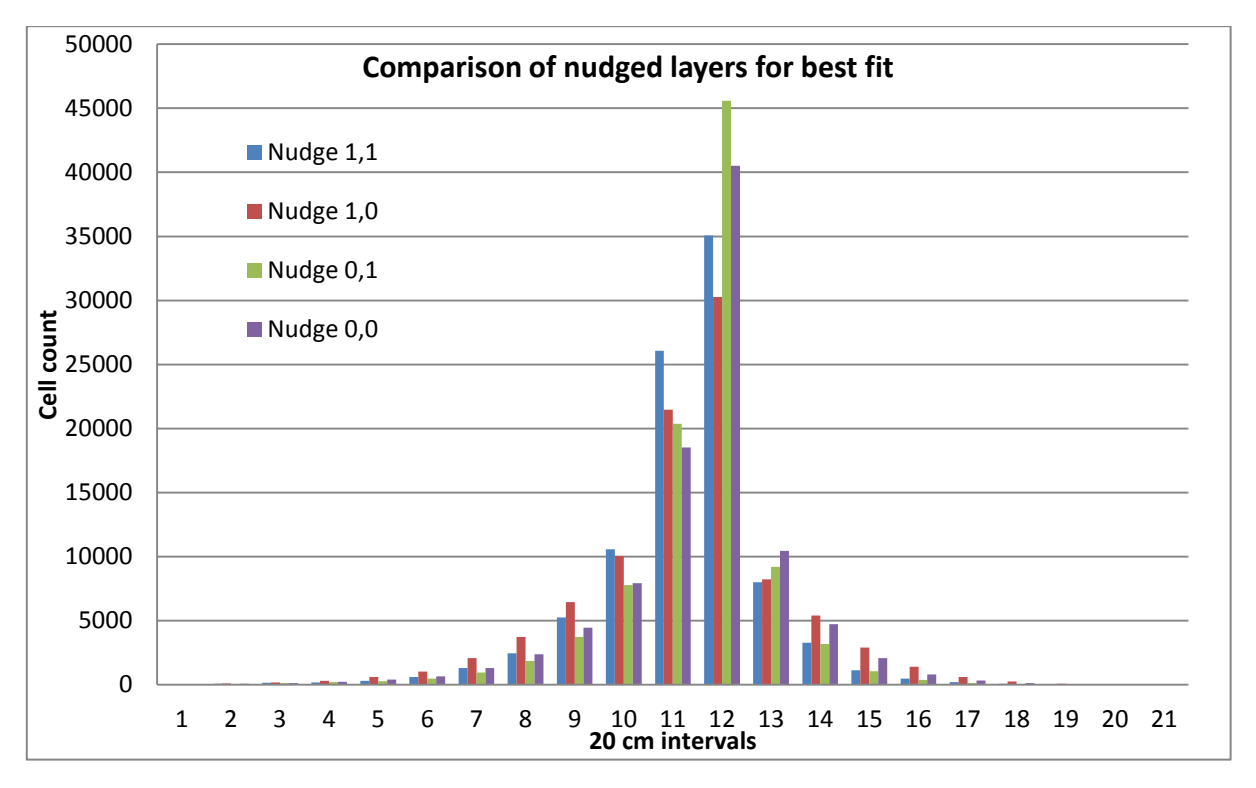
Statistics for Mean, max, min, std dev, 50<sup>th</sup> percentile, 90<sup>th</sup> percentile was calculated, and histograms generated.

Normanby Lidar from 2015, with selected coordinate shifts presented for comparison.

The mean is relatively meaningless and has not been considered.

The 0,1 shift has the lowest standard deviation value, lowest equal 90<sup>th</sup> percentile and lowest value at the 95 percentile.

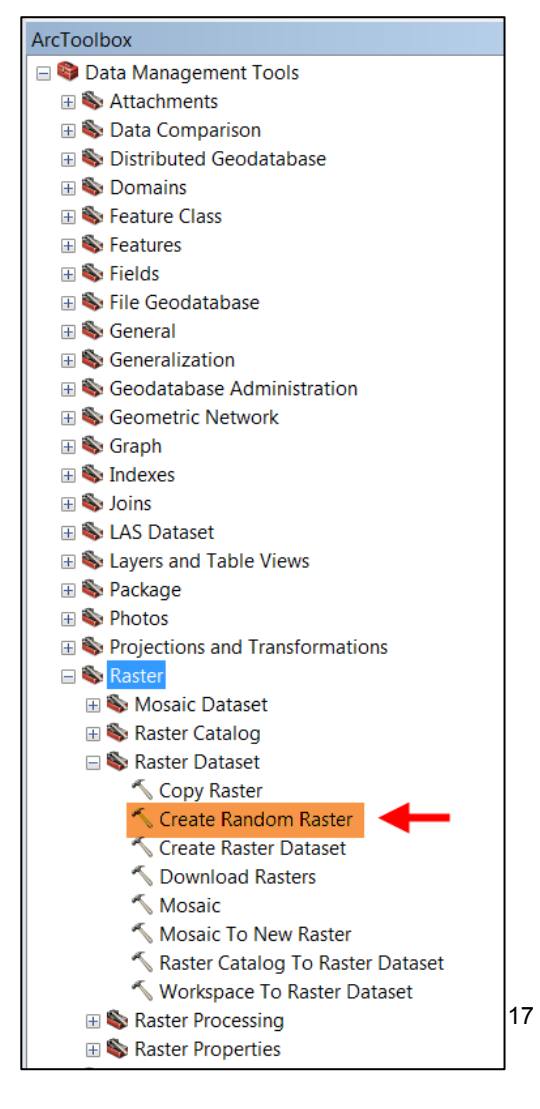
Nudge	1,1	1,0	0,1	0,0
mean	-0.05764	-0.05018	-0.01519	-0.00768
Std Dev	0.366593	0.460673	0.329014	0.396259
50 percentile	0	0	0.020004	0.029999
90 percentile	0.270004	0.440002	0.270004	0.360001
95 percentile	0.419998	0.630005	0.400009	0.529999
max	3.24001	3.07999	3.53	4.83
min	-7.39999	-9.39	-5.69	-8.28



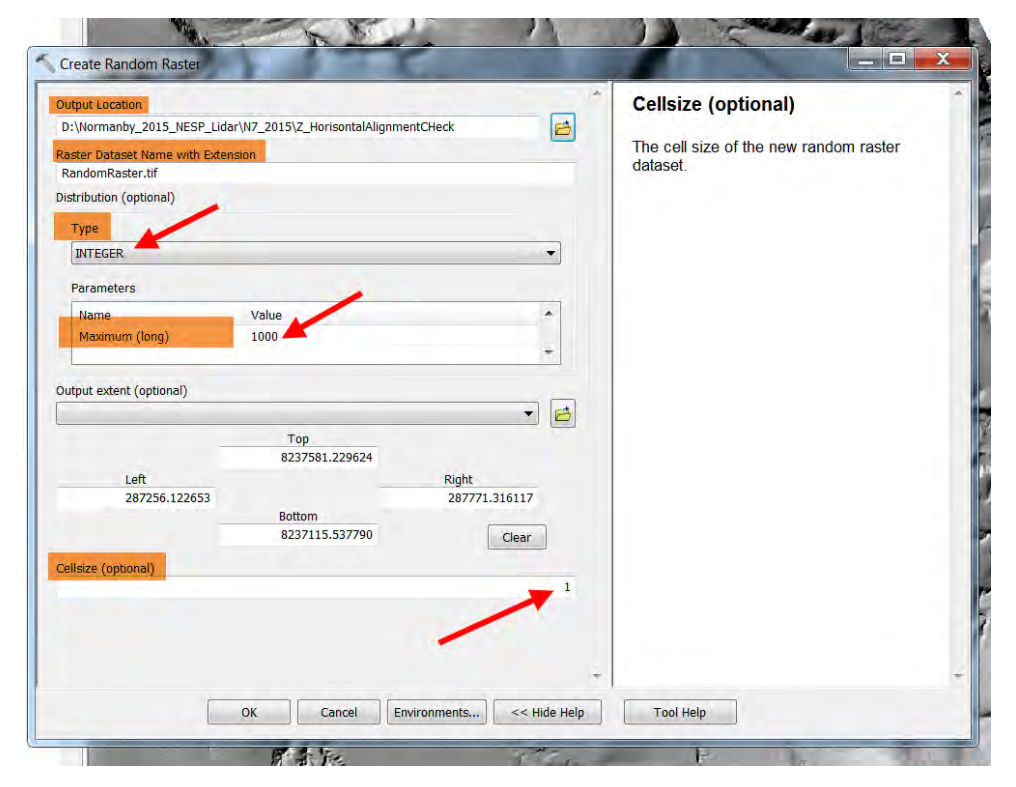
Bars for the 0,1 shift show the highest cell count in the range of lowest difference (bar 12).

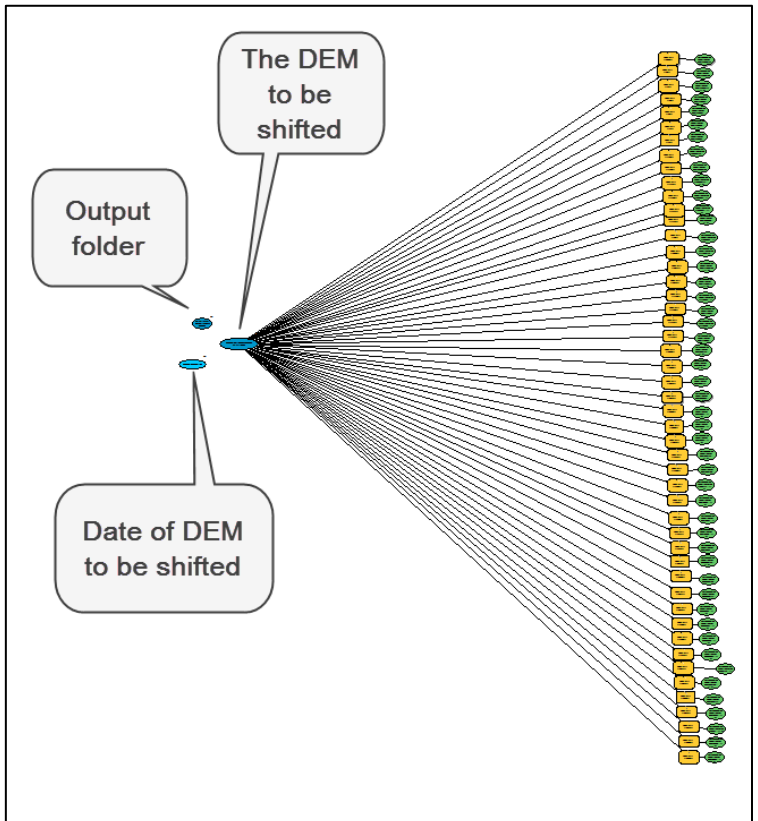
## 2.2.3 DEM Alignment Procedure

- Pick an area with terrain that includes opposing aspects of North, South, East and West, define this with an polygon that will be used as the extent of processing.
- 2. Create a random raster within the bounds of the polygon use integer setting, and around 1000 values
- 3. Set parameters

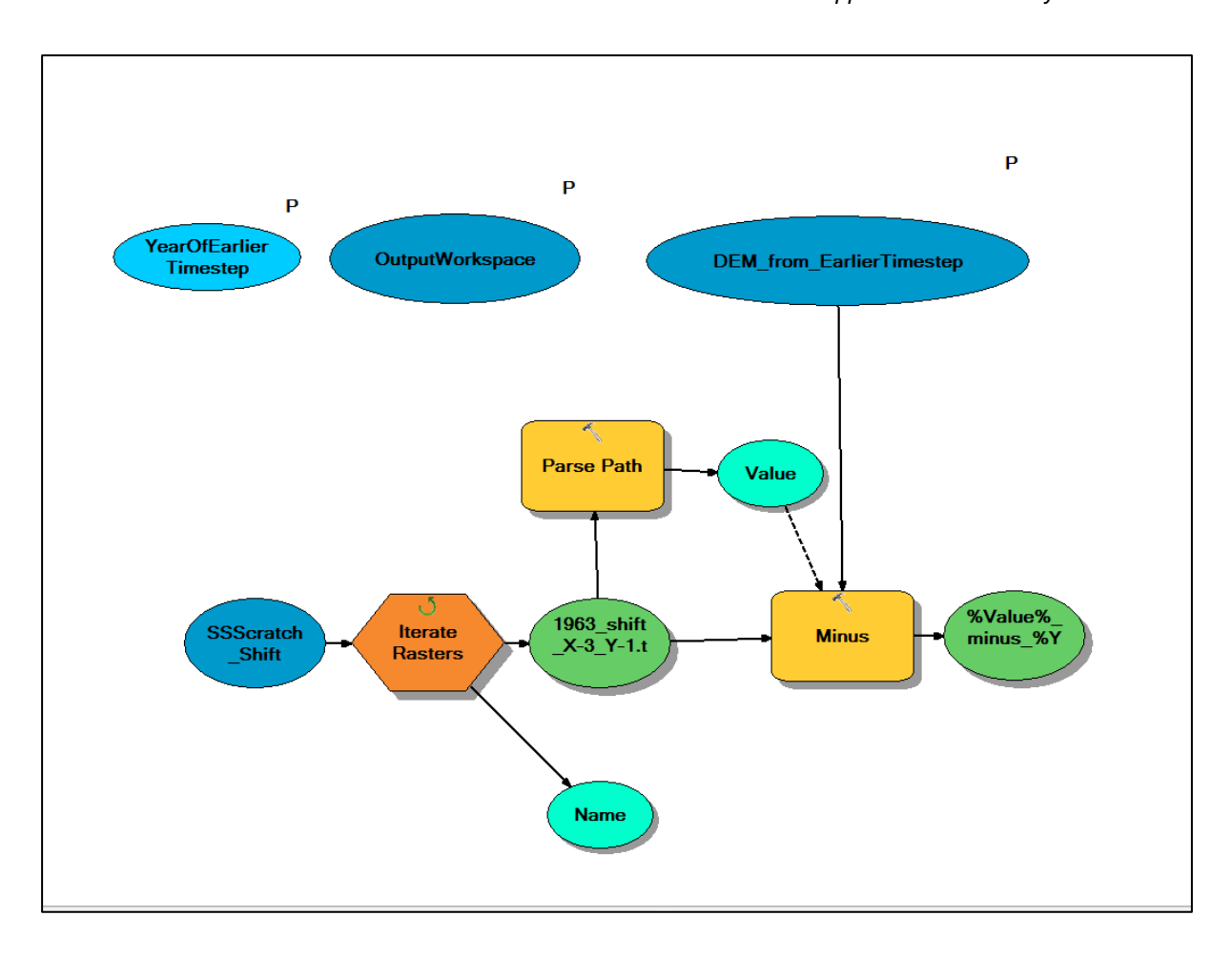


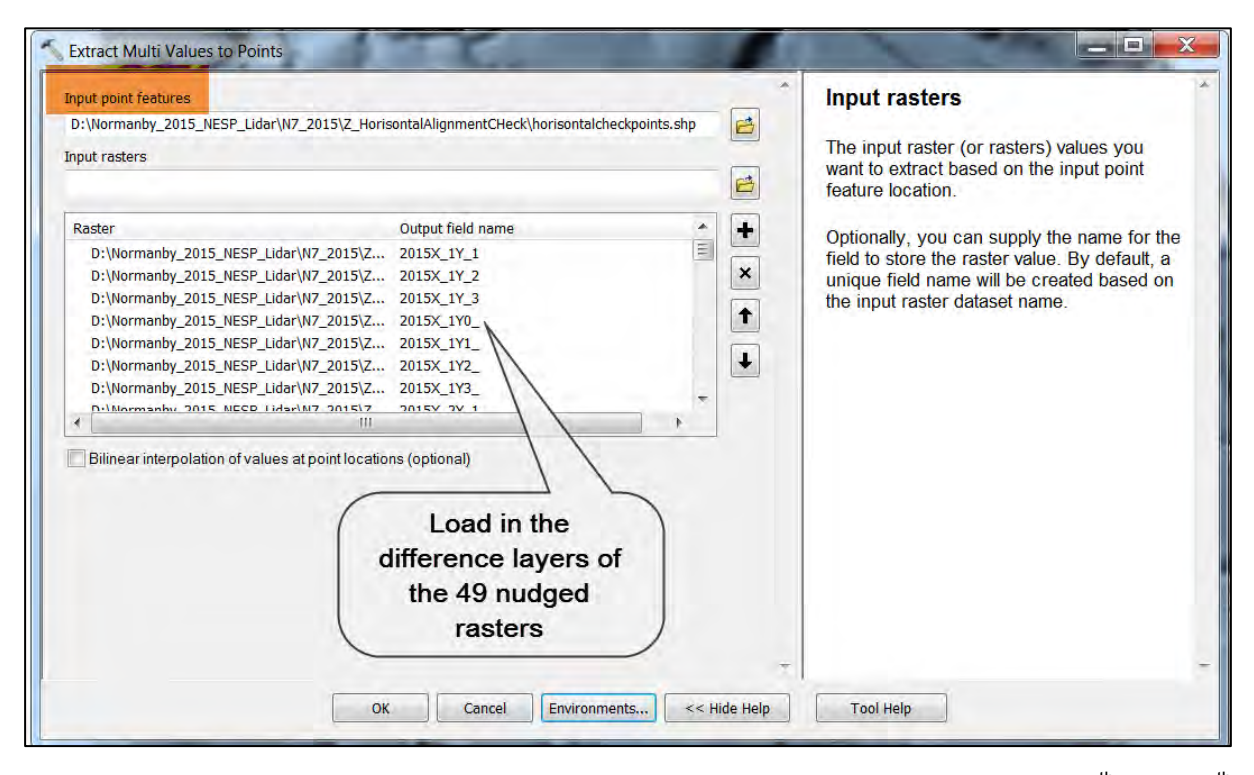
This is the Arc GIS model builder setup to generate 49 new versions of the latter DEM.





Make a difference layer for each of the 49 nudged rasters, again model builder automates this.





The shift X=0 and Y=1 had the lowest standard deviation, lowest value for the 90<sup>th</sup> and 95<sup>th</sup> percentile.

#### Brooks et al.

Conclusion is that shifting the 2015 DEM 1m in the Y coordinate will give the best alignment with the 2011 DEM, and thus reduce the amount of noise to be filtered.

						0.1 .11	001 11	05 ."
GRID_CODE	mean	max	min			Oth pctile		95 pctile
2015X0Y1_m	-0.022		-5.560		0.330	0.040		0.340
Z013V111 <sup>-</sup> III	-0.045		-7.050		0.340	0.020		2.380
2015X0_Y0_	-0.016	4.610	-5.060	0.050	0.382	0.040	0.290	0.470
2015X1Y0_m	-0.039	3.240	-4.760	0.030	0.392	0.020	0.260	0.480
2015X0Y2_m	-0.028	3.440	-6.300	0.060	0.515	0.040	0.450	0.730
2015X1Y2_m	-0.051	4.160	-7.520	0.030	0.529	0.020	0.470	0.740
2015X2Y1_m	-0.068	4.190	-8.240	0.030	0.546	0.010	0.470	0.760
2015X_1Y1_	0.001	4.590	-5.150	0.060	0.515	0.050	0.510	0.760
2015X_1Y0_	0.007	7.950	-4.940	0.060	0.551	0.050	0.570	0.820
2015X2Y0_m	-0.062	4.020	-7.770	0.030	0.568	0.010	0.490	0.830
2015X1Y_1_	-0.033	4.440	-4.690	0.030	0.605	0.030	0.570	0.930
2015X0Y_1_	-0.009	7.530	-4.890	0.050	0.603	0.040	0.630	0.930
2015X_1Y2_	-0.006	4.530	-5.920	0.060	0.637	0.050	0.650	0.990
2015X2Y2_m	-0.074	4.070	-8.290	0.030	0.669	0.010	0.640	0.990
2015X2Y 1	-0.057	5.080	-4.850	0.030	0.718	0.020	0.680	1.140
2015X_1Y_1	0.014	8.520	-5.050	0.060	0.715	0.050	0.810	1.150
2015X3Y1 m	-0.092	5.190	-8.570	0.000	0.775	0.000	0.740	1.160
2015X1Y3 m	-0.057	5.330	-7.800	0.030	0.770	0.020	0.780	1.180
2015X0Y3 m	-0.035	4.400	-7.130	0.030	0.759	0.040	0.780	1.190
2015X3Y0 m	-0.086	5.740	-8.100	0.030	0.787	0.000	0.750	1.210
2015X 2Y1	0.023	7.930	-5.380	0.060	0.746	0.060	0.850	1.210
2015X 2Y0	0.030		-5.120		0.771	0.060		1.260
2015X3Y2 m	-0.098		-8.660		0.859	0.000		1.320
2015X2Y3 m	-0.080		-8.490		0.863	0.010		1.330

Even greater improvements can be achieved with sub-metre adjustments.

Shifting the 2015 DEM by X,Y 0.5,-0.75m reduced the number of cells above the noise threshold from 3511 to 613. Isolating real erosion is far more viable with an 82% reduction in noise.

Shift name	Coordinate shift	mean	max	min	mode	std dev	50th pctile	90th pctile	95 pctile	Coord.	Count < -0.5	Coordinate shift
18	.5,75	0.022	1.405	1.880	0.015	0.207	0.017	0.262	0.357	.5,75	<mark>613</mark>	.5,75
13	.5,5	0.014	1.435	2.045	0.015	0.197	0.015	0.240	0.325	.5,5	623	.5,5
12	.25,5	- 0.001	1.392	- 1.745	0.038	0.203	-0.003	0.235	0.322	.25,5	692	.25,5
14	.75,5	0.029	1.485	2.213	0.022	0.215	0.030	0.272	0.362	.75,5	694	.75,5
19	.75,75	0.037	1.460	2.038	0.007	0.235	0.032	0.312	0.415	.75,- .75	789	.75,75
17	.25,75	0.007	1.350	1.878	0.015	0.225	0.000	0.270	0.382	.25,- .75	872	.25,75
08	.5,25	0.006	1.532	2.088	0.007	0.224	0.007	0.265	0.360	.5,25	927	.5,25
07	.25,25	0.009	1.482	1.788	0.023	0.240	-0.013	0.280	0.385	.25,- .25	1140	.25,25
09	.75,25	0.021	1.587	2.388	0.007	0.252	0.022	0.307	0.420	.75,- .25	1142	.75,25
23	.5,-1	0.030	1.530	2.125	0.015	0.270	0.015	0.365	0.480	.5,-1	1152	.5,-1
11	0,5	0.016	1.470	1.670	0.030	0.252	-0.020	0.295	0.410	0,5	1261	0,5
15	1,5	0.044	1.540	2.380	0.040	0.272	0.045	0.360	0.470	1,5	1270	1,5
22	.25,-1	0.015	1.465	2.123	0.023	0.275	0.000	0.355	0.482	.25,-1	1308	.25,-1
16	0,75	0.013	1.405	1.870	0.023	0.273	-0.018	0.333	0.430	0,75	1353	

				_								
24	.75,-1	0.045	1.645	2.128	0.007	0.301	0.035	0.412	0.537	.75,-1	1463	.75,-1
				_								
20	1,75	0.052	1.515	2.205	0.000	0.297	0.050	0.405	0.525	1,75	1505	1,75
				-								
10	1,25	0.036	1.620	2.555	0.040	0.293	0.042	0.372	0.497	1,25	1671	1,25
		-		-	-							
06	0,25	0.024	1.650	1.630	0.008	0.292	-0.030	0.340	0.475	0,25	1911	0,25
		-		-								
03	.5,0	0.002	1.630	2.130	0.015	0.296	0.000	0.360	0.480	.5,0	1919	.5,0
				-	-							
21	0,-1	0.000	1.720	2.120	0.070	0.314	-0.010	0.390	0.540	0,-1	2001	0,-1
				-								
04	.75,0	0.013	1.685	2.430	0.040	0.309	0.017	0.377	0.507	.75,0	2061	.75,0
		-		-	-							
02	.25,0	0.017	1.770	1.830	0.008	0.317	-0.020	0.377	0.512	.25,0	2305	.25,0
				-								
25	1,-1	0.060	1.820	2.210	0.000	0.359	0.060	0.500	0.640	1,-1	2430	1,-1
				-								
05	1,0	0.029	1.850	2.730	0.000	0.352	0.030	0.440	0.590	1,0	2722	1,0
		-		-								
01	0,0	0.032	2.030	1.870	0.000	0.365	-0.040	0.430	0.590	0,0	3511	0,0

# 2.3 Improved Delineation of Colluvial Boundary

Given the inherent inaccuracies of the original alluvial/colluvial boundary used in the 2013 classification of alluvial and colluvial gullies derived from the 1:1M geology boundary (Brooks et al., 2013), in this round of processing we improved the resolution of the definition by manually digitizing the colluvial boundaries from the LiDAR data. The tables below (Table A5, Table A6) show the extent of the change in area of each block in terms of area and percentage variation. In most blocks the colluvial area was increased, however, this does not necessarily translate to an increase in the gully erosion rates in the colluvial class. In a number of the blocks while the total colluvial area increased, the alluvial areas on valley bottoms were defined at a higher resolution, which in some cases resulted in lower sediment yields from colluvial gullies due to the fact that the active gullies were more accurately classified. An example of how a block has been redefined is shown in Figure A14 and Figure A15.

**Table A5:** Changes in colluvial and alluvial land unit area between 2011 LiDAR data and the 2015 data

	Origina	l dataset	Modified boundaries			
Block	Area Alluvial m <sup>2</sup>	Area Colluvial m <sup>2</sup>	Area Alluvial m <sup>2</sup>	Area Colluvial m <sup>2</sup>		
N4	8714180	1502535	8173168	2043546		
N5	12710000	2204754	12710029	2204757		
N7	9651940	1478883	9765956	1364863		
N9	3874010	105045	3723565	255489		
N10	5778780	384482	5740303	422956		
N16	5981540	151837	5849435	283944		
N17	2832870	0	2832875	0		

Table A6: Changes in % of colluvial and alluvial land in each LiDAR block between 2011 and 2015

	Area within Modified boundaries as % of 2011 dataset					
	Area Alluvial	Area Colluvial				
Block	% change	% change				
N4	94	136				
N5	100	100				
N7	101	92				
N9	96	243				
N10	99	110				
N16	98	187				
N17	100	0				

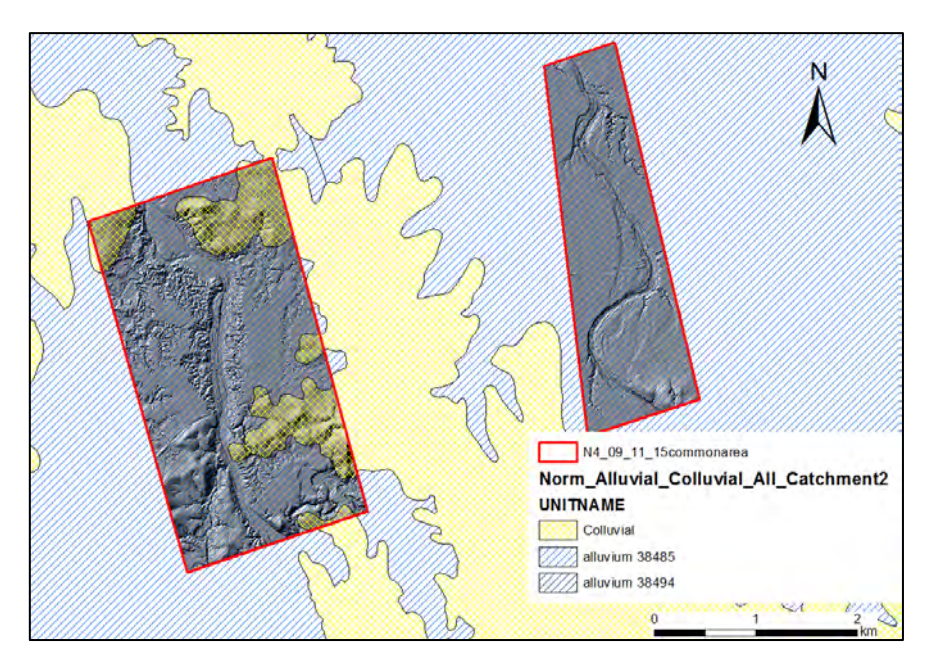


**Figure A14:** Alluvial and Colluvial at 1:1 million, plus common area for 09, 11 and 15 with Lidar as overlay

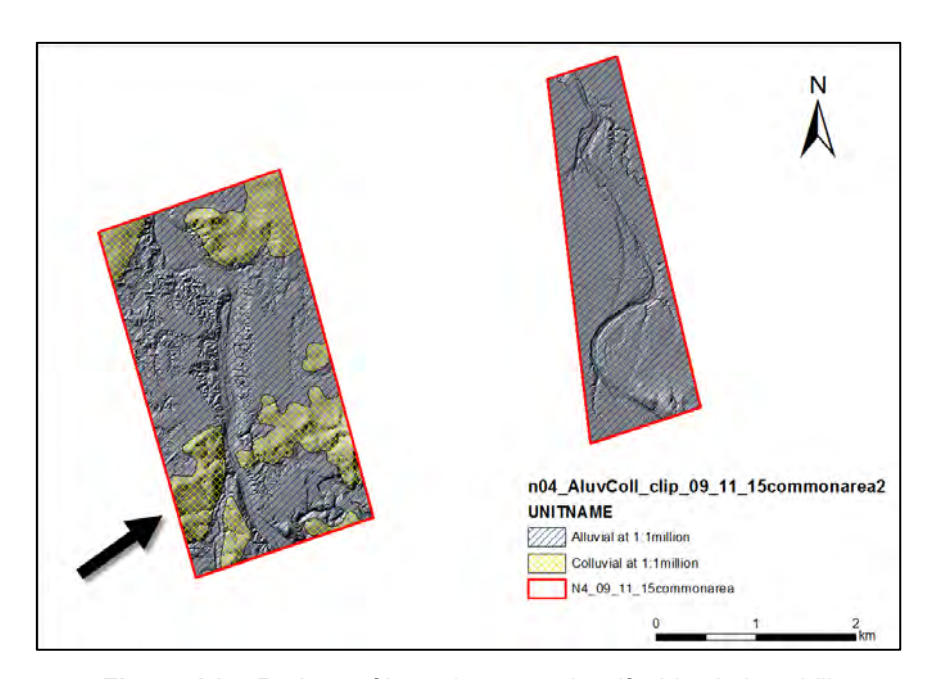


Figure A15: Redraw of boundary to reclassify this obvious hill

Examples of modifications to boundary of alluvium and colluvium and effect of gully classification

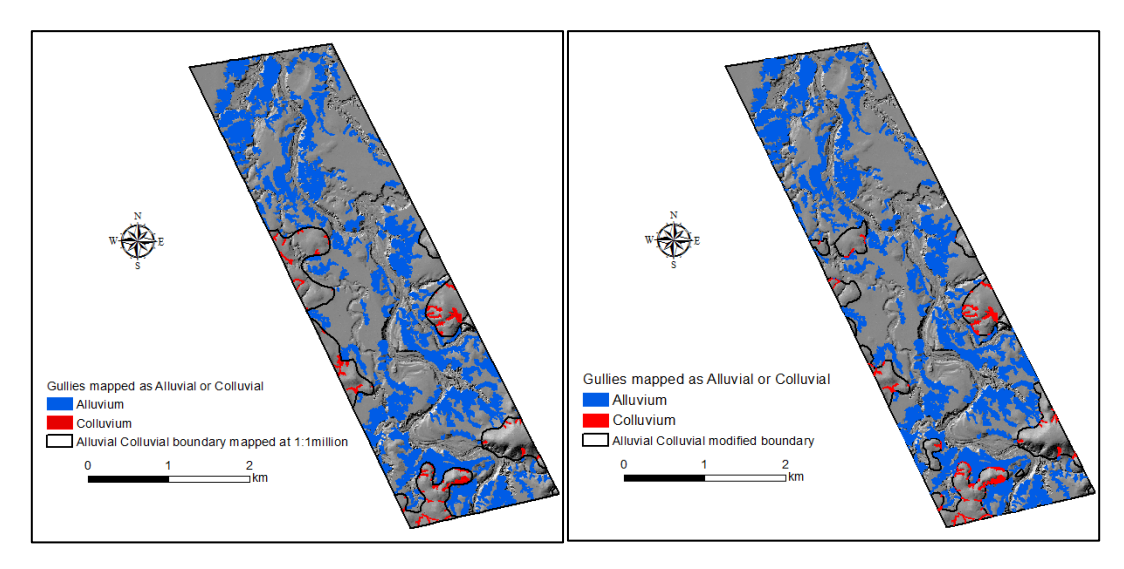


Figure A16: Block 7 - hill area on west of block contracted, extra hill added in south west corner.

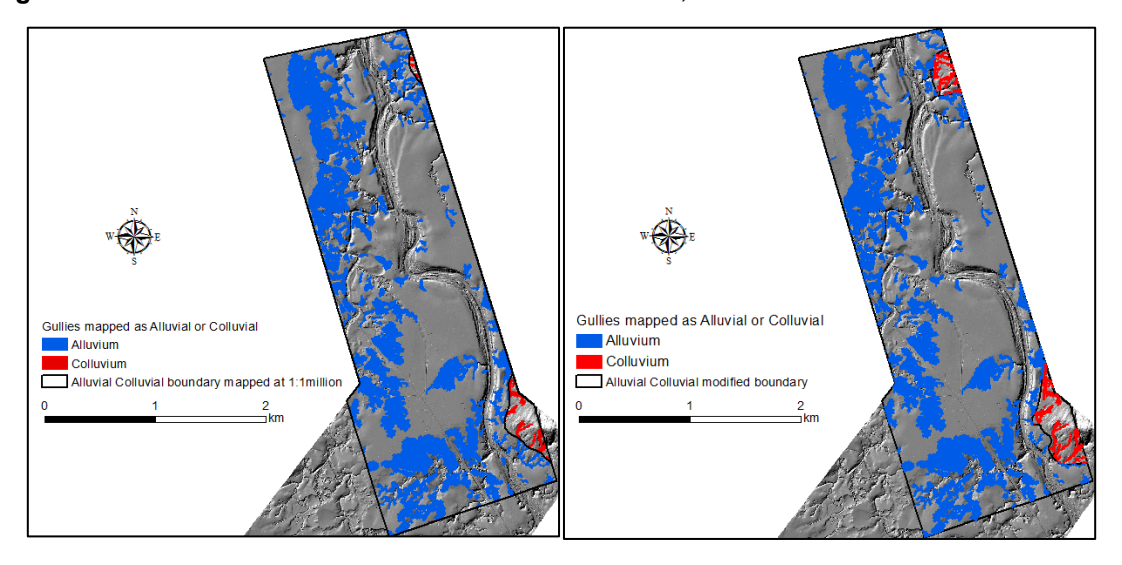
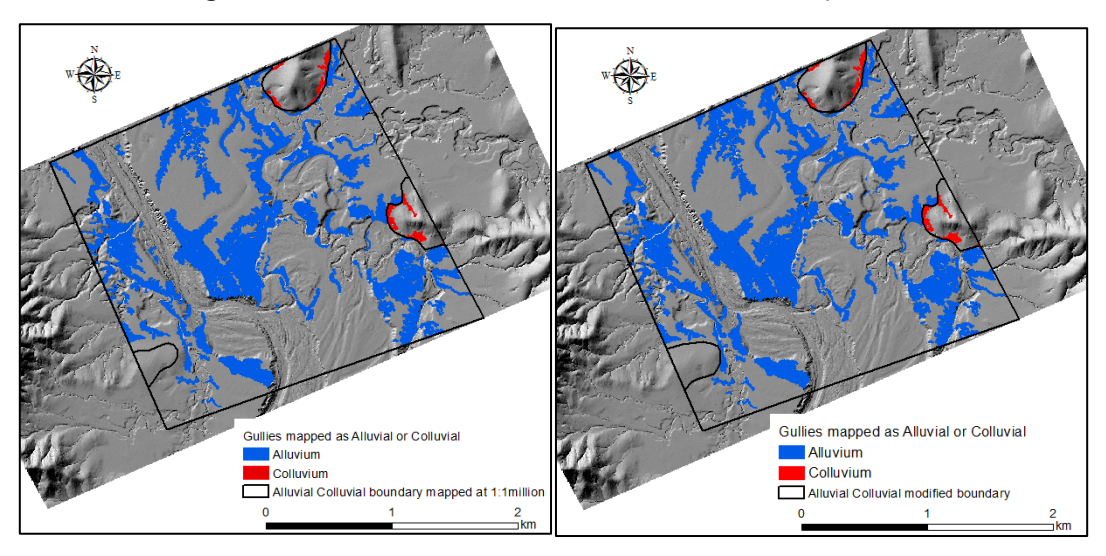


Figure A17: Block 16 - area of hills increased for both patches.



**Figure A18:** Block 10 had increase in area of colluvial in south west corner - no gullies were in the colluvial area.

Changes in areas of Alluvial/Colluvial soil type due to modifying boundaries.

**Table A7:** Areas of Alluvial and Colluvial in common areas - from original 1:1mill soils dataset and areas after modification of boundaries.

	Original boundaries		Modified boundaries	
	Area of	Area of		Area of
	alluvial	Colluvial	Area of	Colluvial
	m2	m2	alluvial m2	m2
N4	8714179	1502535	8173168	2043548
N5	12710029	2204757	12710029	2204757
N7	9651937	1478882	9765956	1364863
N9	3874009	105046	3723565	255489
N10	5778777	384482	5740303	422955
N16	5981541	151836	5849435	283943
N17	2832875	0	2832875	0
Sum	49543347	5827538	48795331	6575555

**Table A8:** Changes in areas as % of original area.

	Original boundaries		Modified boundaries	
	Area of	Area of	Area of	Area of
	alluvial as	Colluvial	alluvial as	Colluvial
	% of	as % of	% of	as % of
	original	original	original	original
N4	100	100	94	136
N5	100	100	100	100
N7	100	100	101	92
N9	100	100	96	243
N10	100	100	99	110
N16	100	100	98	187
N17	100		100	

Changes in areas of **gullies** classified as Alluvial or Colluvial due to changes in boundaries of Alluvial / Colluvial soil type

Table A9: Areas of gullies classified as Alluvial or Colluvial before and after boundary modification.

	Original boundaries		Modified boundaries	
	Gully		Gully	
	area in	Gully area	area in	Gully area
	alluvial	in colluvial	alluvial	in colluvial
	m2	m2	m2	m2
N4	1865503	156165	1769853	251815
N5	2840779	200206	2840779	200206
N7	2290664	103998	2305486	89176
N9	745318	13404	735133	23589
N10	1227876	32070	1227876	32070
N16	1447712	33287	1406228	74771
N17	366016	0	366016	0
Sum	10783868	539130	10651371	671627

 Table A10: Percent change in area of gully classification.

	Original boundaries		Modified boundaries	
	Area of Area of		Area of	Area of
	Alluvial	Colluvial	Alluvial	Colluvial
	as % of	as % of	as % of	as % of
	original	original	original	original
N4	100	100	94.9	161.2
N5	100	100	100.0	100.0
N7	100	100	100.6	85.7
N9	100	100	98.6	176.0
N10	100	100	100.0	100.0
N16	100	100	97.1	224.6
N17	100		100	

# 2.4 Updated Land unit classification

The following table outlines the classes of erosion and deposition from different geomorphic units that have been defined in this study. The breakdown of sediment sources from different process zones, summarised in the study are an amalgamation of some of these classes. For example, gully erosion is the compilation of classes 11 - 13. The examples shown here are derived from Normanby block N04. In broad terms the classes can be amalgamated as follows:

- Classes 11, 12, 13 deals with gullies at different scales
- Classes 21, 22, 23 deals with secondary channels.
- Classes 31, 32, 33, 34 deals with main channel
- Classes in the 40s deal with colluvial processes.

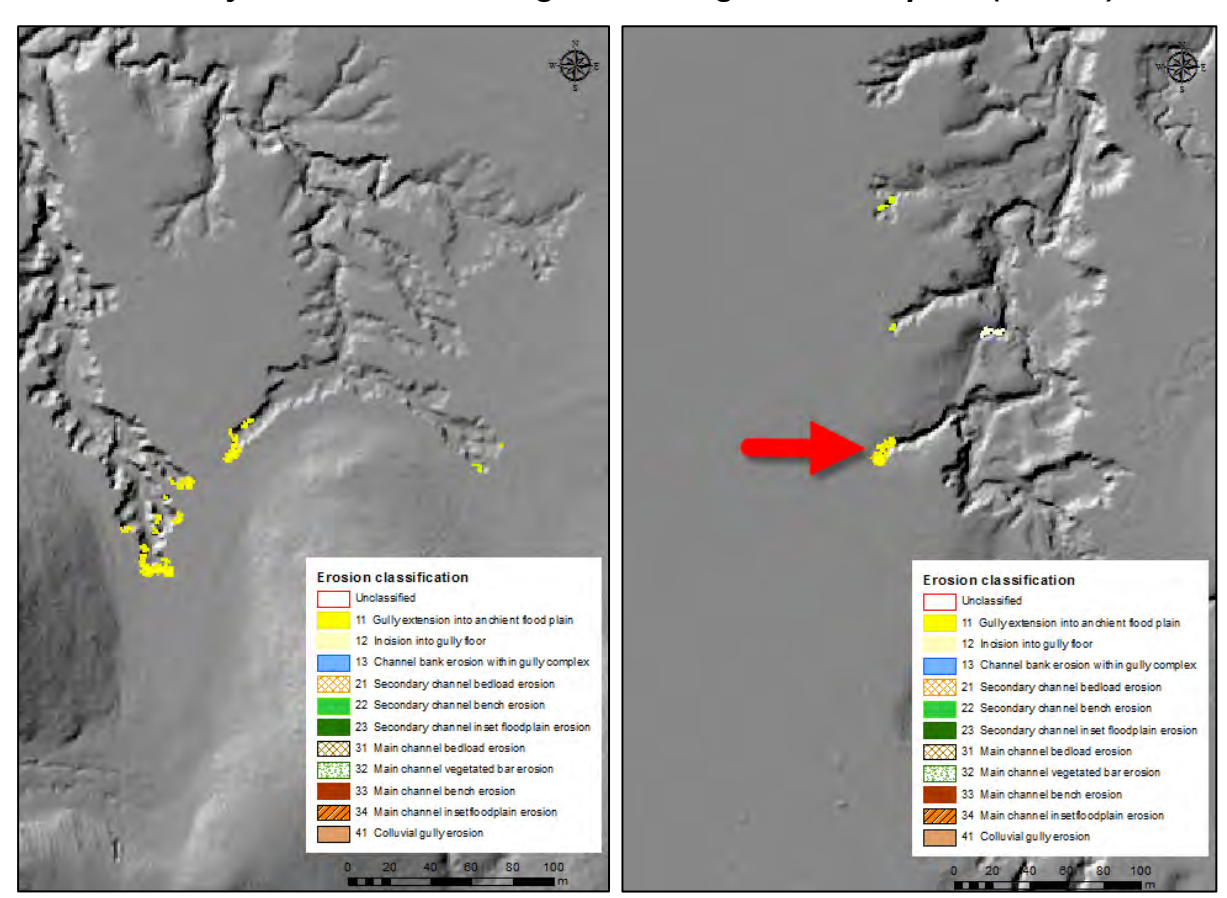
Table A11: Erosion Classes

Classification system for landscape for 2009 and 2011 Lidar. This overlay was used to classify erosion.		Classification system for 2011-2015 erosion. Each erosion polygon was manually classified according to where it was in the landscape, rather than using an overlay.			
Classification	Name	Description	Classification	Erosion description	Criteria
1	Water bodies	Water present as seen in orthophoto or discernible in HS raster	No erosion in water bodies.		
5	Gullies  Discrete units of erosion from water, cutting into banks, flood plain or hillside, resemble small ditches or valleys.		11	Gully extension into ancient flood plain	Gully headwall advancing across virgin old floodplain
			12	Incision into gully floor	Reworking of an existing gully floor, seen as a slot eating its way across a gully floor

			13	Channel bank erosion within gully complex	Erosion along the banks of a developing sinuous channel within a massive gully complex.
6	Secondary Channels	Larger flow features of the landscape that contain meandering flow paths, have several feeder gullies and permanent vegetation	21	Secondary channel bedload erosion	Erosion on the bottom of intermediate scale channels, or tributaries, mostly with a catchment that extends beyond the Lidar block.
0	Secondary channel inset flood plain Vegetated or open valley floor adjacent to secondary channels, below level of extensive ancient flood plain, signs of sculpting by flows may be visible in Lidar, likely to be inundated by flood flows.		22	Secondary channel bench erosion	Erosion on benches of intermediate scale channels, or tributaries, mostly with a catchment that extends beyond the Lidar block.
9			23	Secondary channel inset floodplain erosion	Erosion on inset floodplains of intermediate scale channels, or tributaries, mostly with a catchment that extends beyond the Lidar block.
2	Open River bed	Main channel bed of predominantly sand, stones or rock. Sparse vegetation may be present	31	Main channel bedload erosion	Scouring of lateral bars, point bars, and chute channels in the main channel.
4	Vegetated River Bed	Adjacent to main channel, covered with low or tall vegetation, characteristic sculpting by flow visible in Lidar, likely to be covered by average flood flows.	32	Main channel vegetated bar erosion	Erosion of vegetated bars within the main channel
3	Main Channel Banks	Obvious changes in land height between different levels within the main channel system	33	Main channel bench erosion	

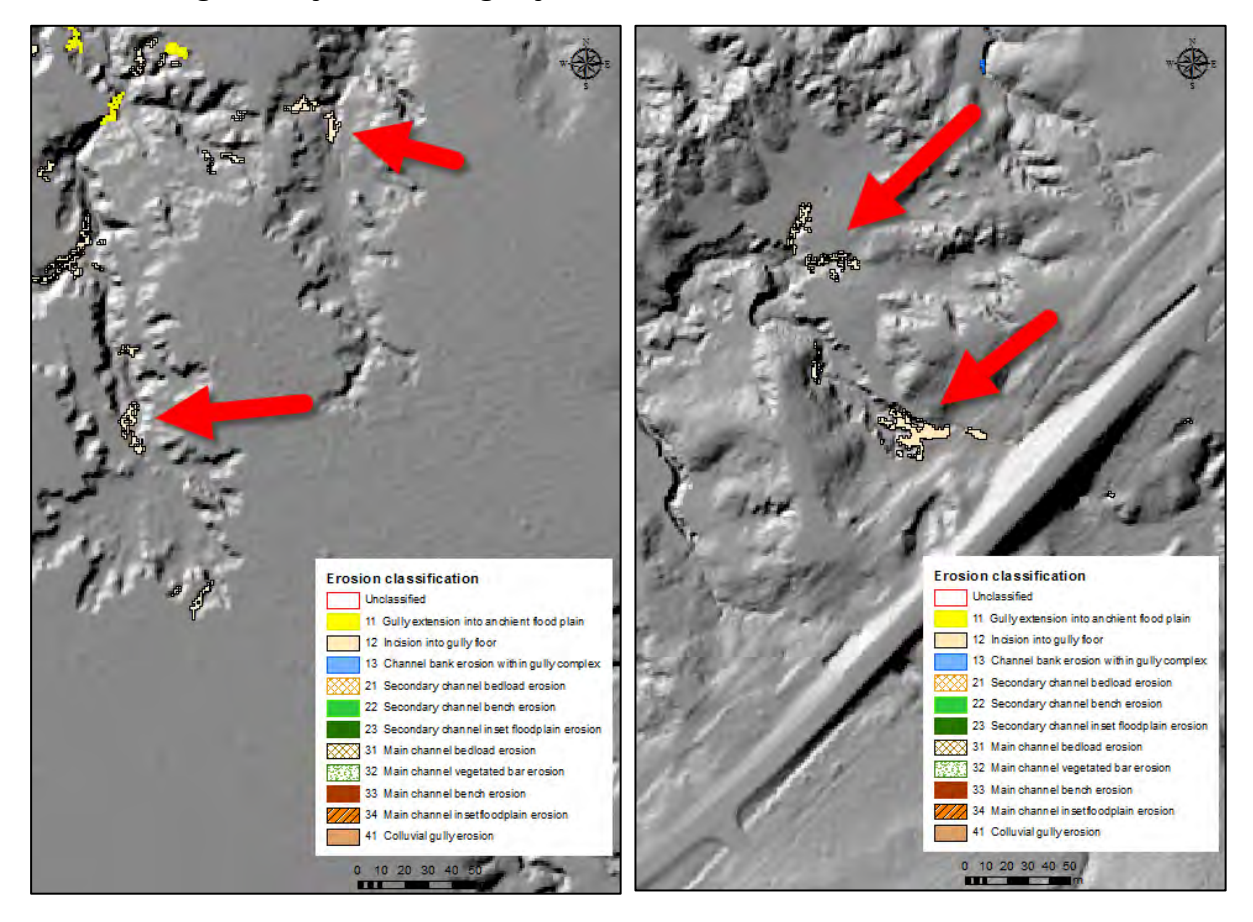
### Brooks et al.

	7	Road reserve	Roads, drains from roads and areas associated with roads	34	Main channel inset floodplain erosion	
	8	Main channel inset flood plain	Flat or nearly flat surfaces adjacent to main channel, vegetated, elevated above main channel but below the surface of extensive ancient flood plain.			
The	The above was intersected with Alluvial/Colluvial layer after gullies had been digitised to give alluvial or colluvial gully classification.			41.	Colluvial gully erosion	Erosion in gullies extending uphill on slopes above the flat levels of the old floodplain.

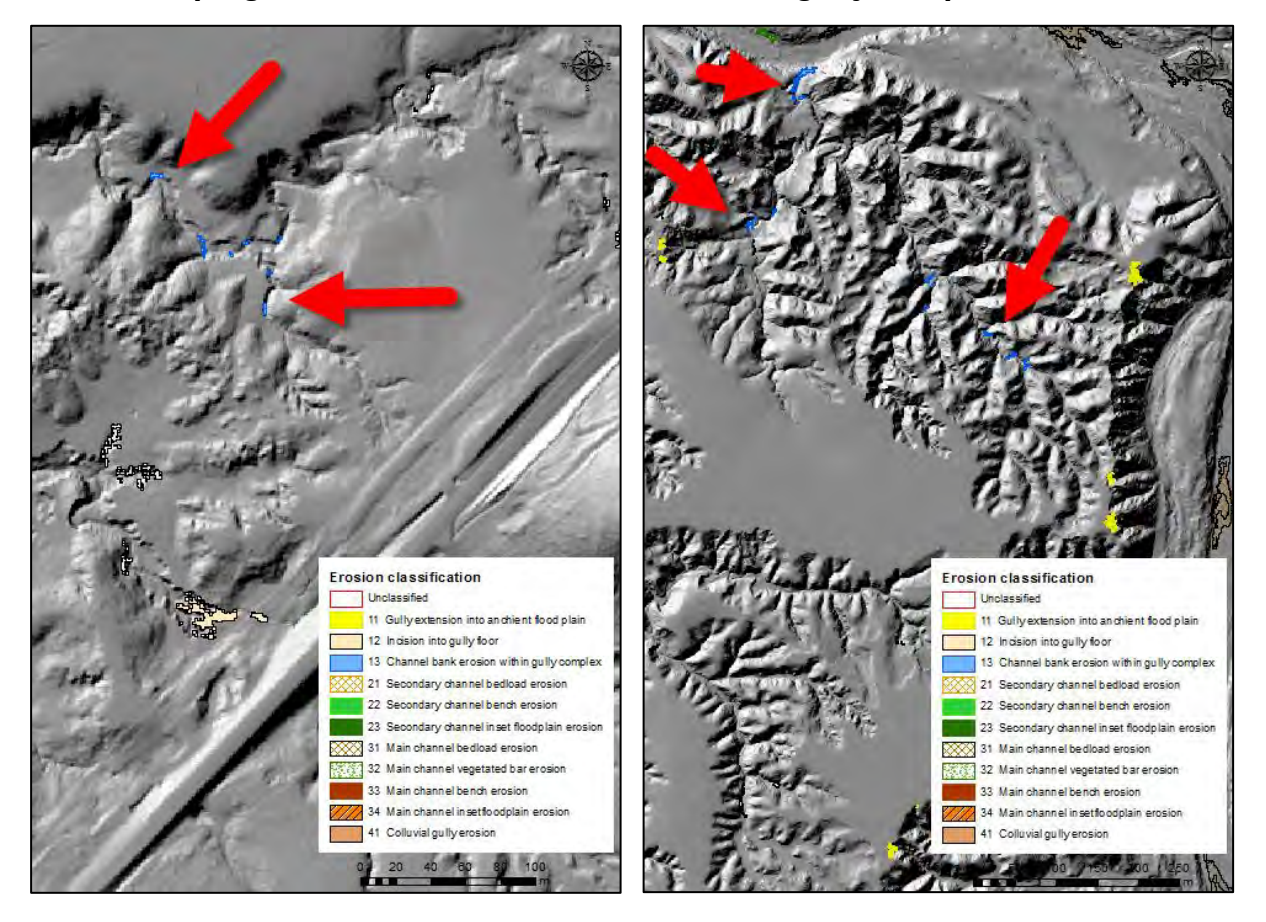


Class 11: Gully headwall advancing across virgin old floodplain (terrace)

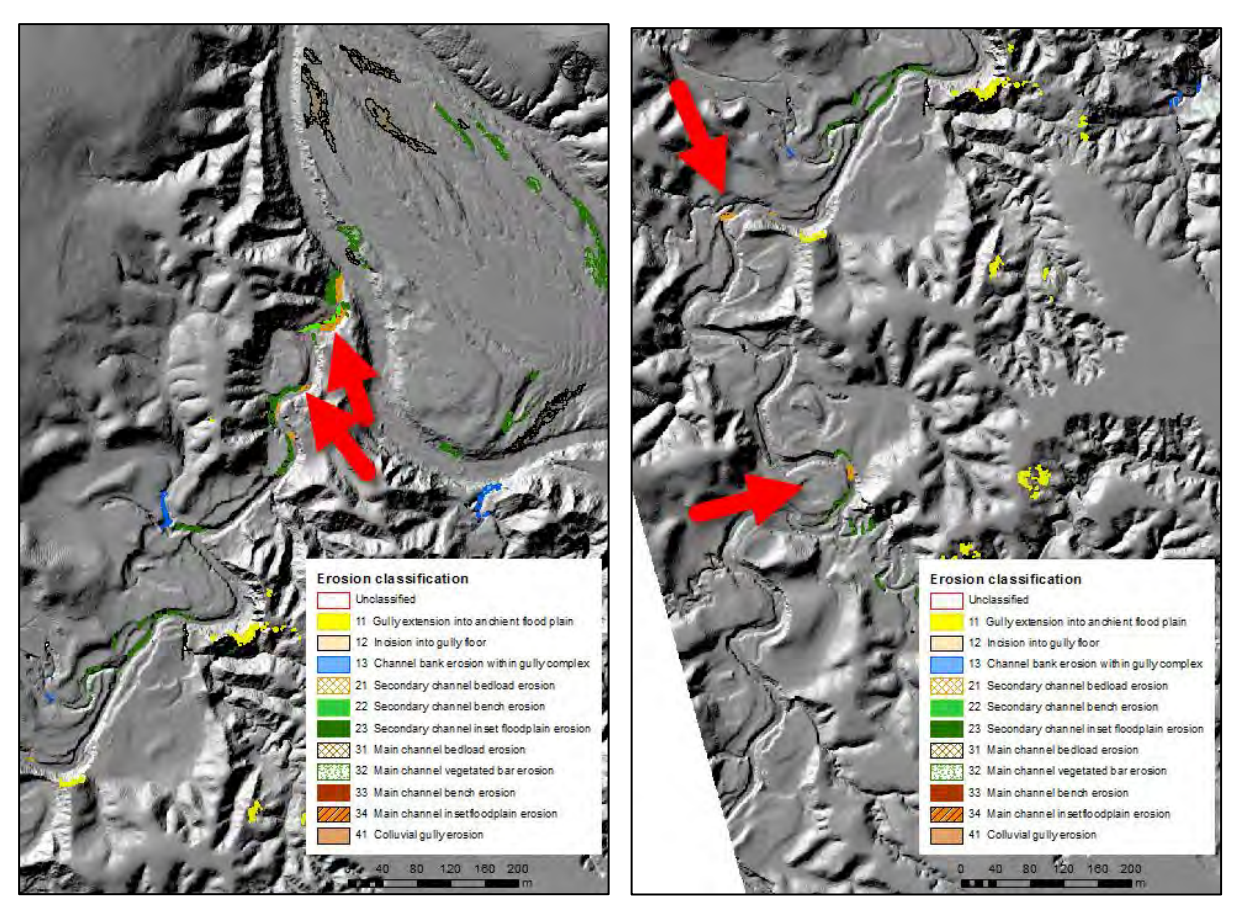
Class 12: Incision into gully floor. Reworking of an existing gully floor, seen as a slot eating its way across a gully floor



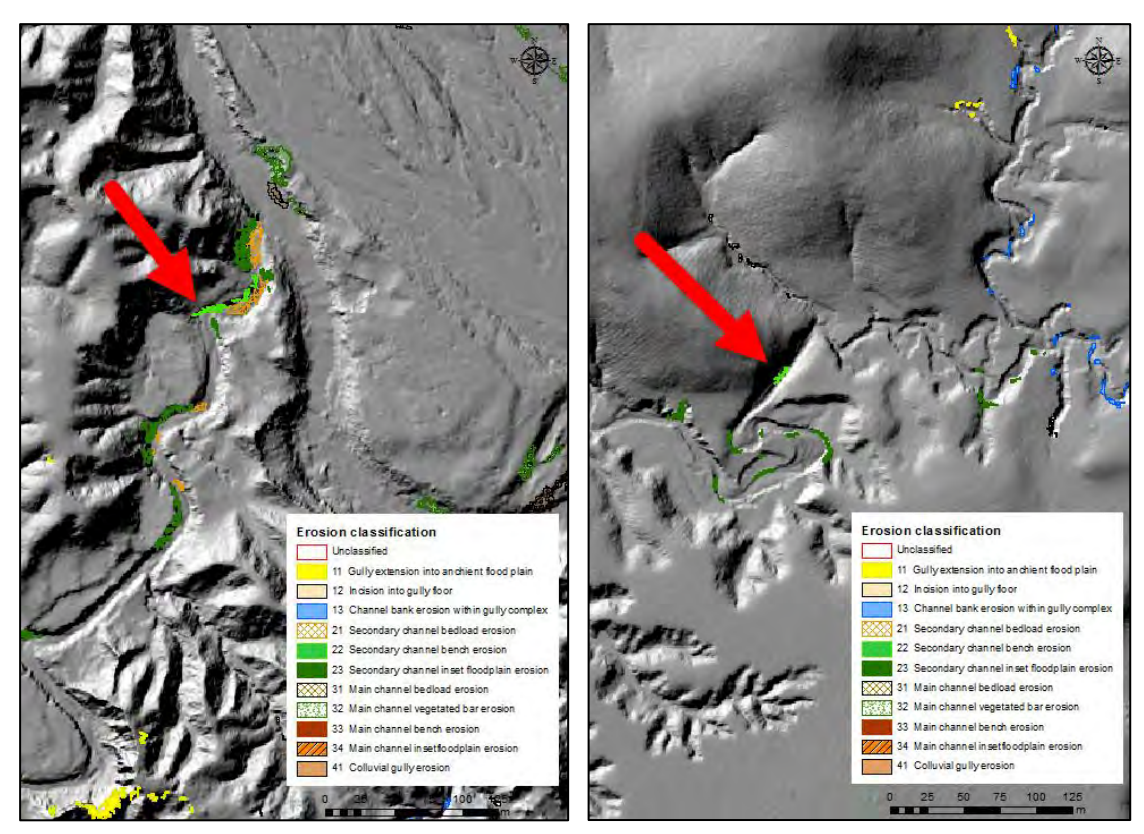
Class 13: Channel bank erosion within gully complex. Erosion along the banks of a developing sinuous channel within a massive gully complex.



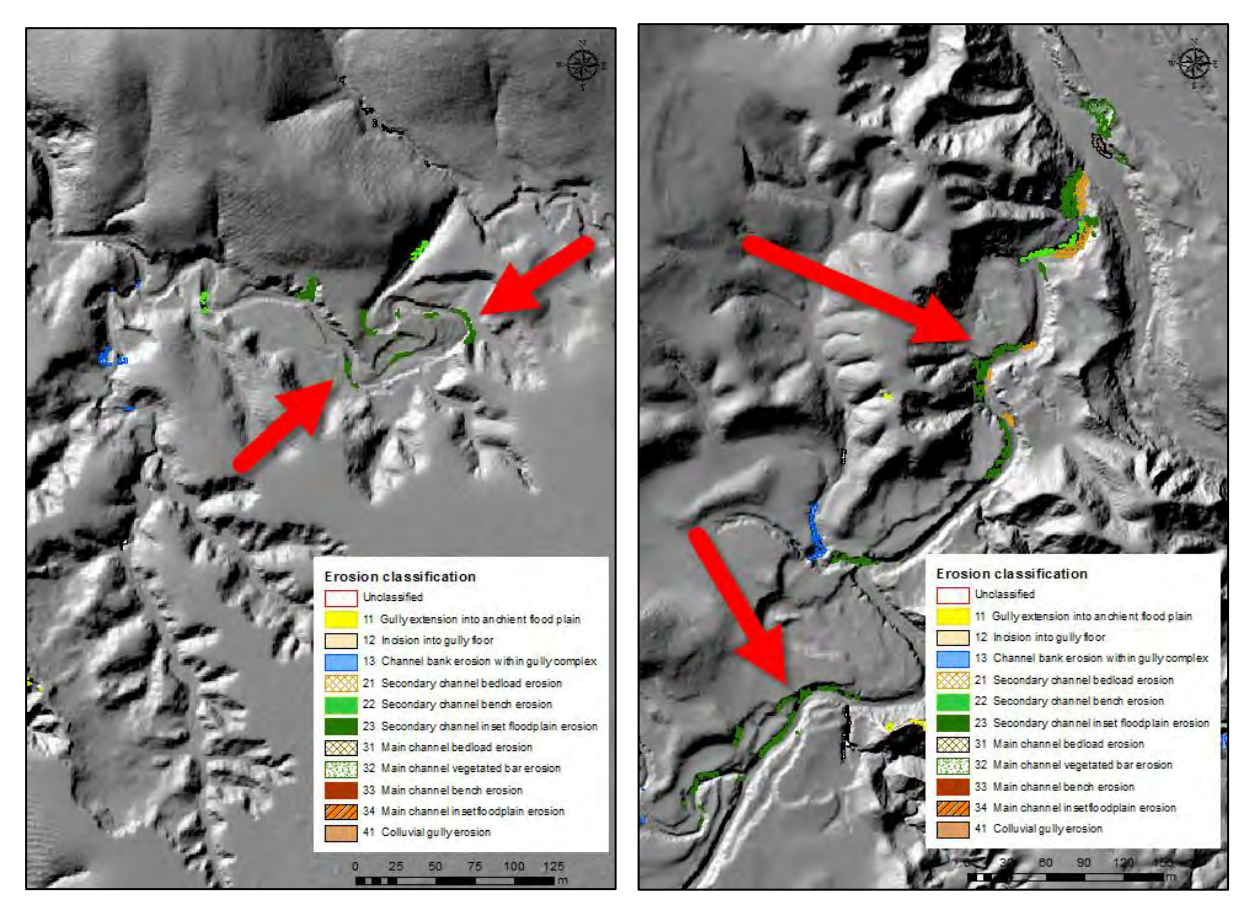
Class 21: Secondary channel bedload erosion. Erosion on the bottom of intermediate scale channels, or tributaries, mostly with a catchment that extends beyond the Lidar block.



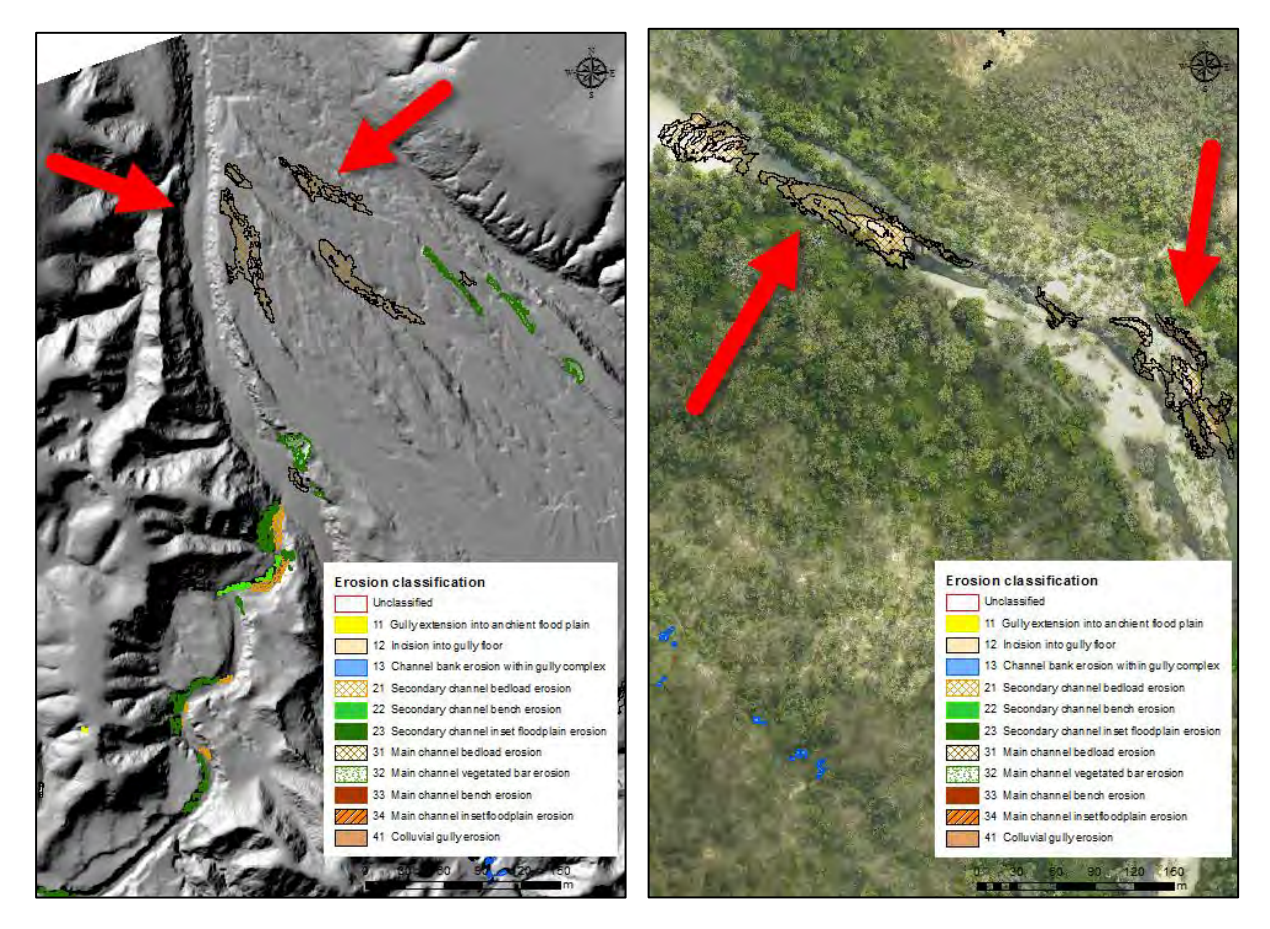
Class 22: Secondary channel bench erosion. Erosion on benches of intermediate scale channels, or tributaries, mostly with a catchment that extends beyond the Lidar block.



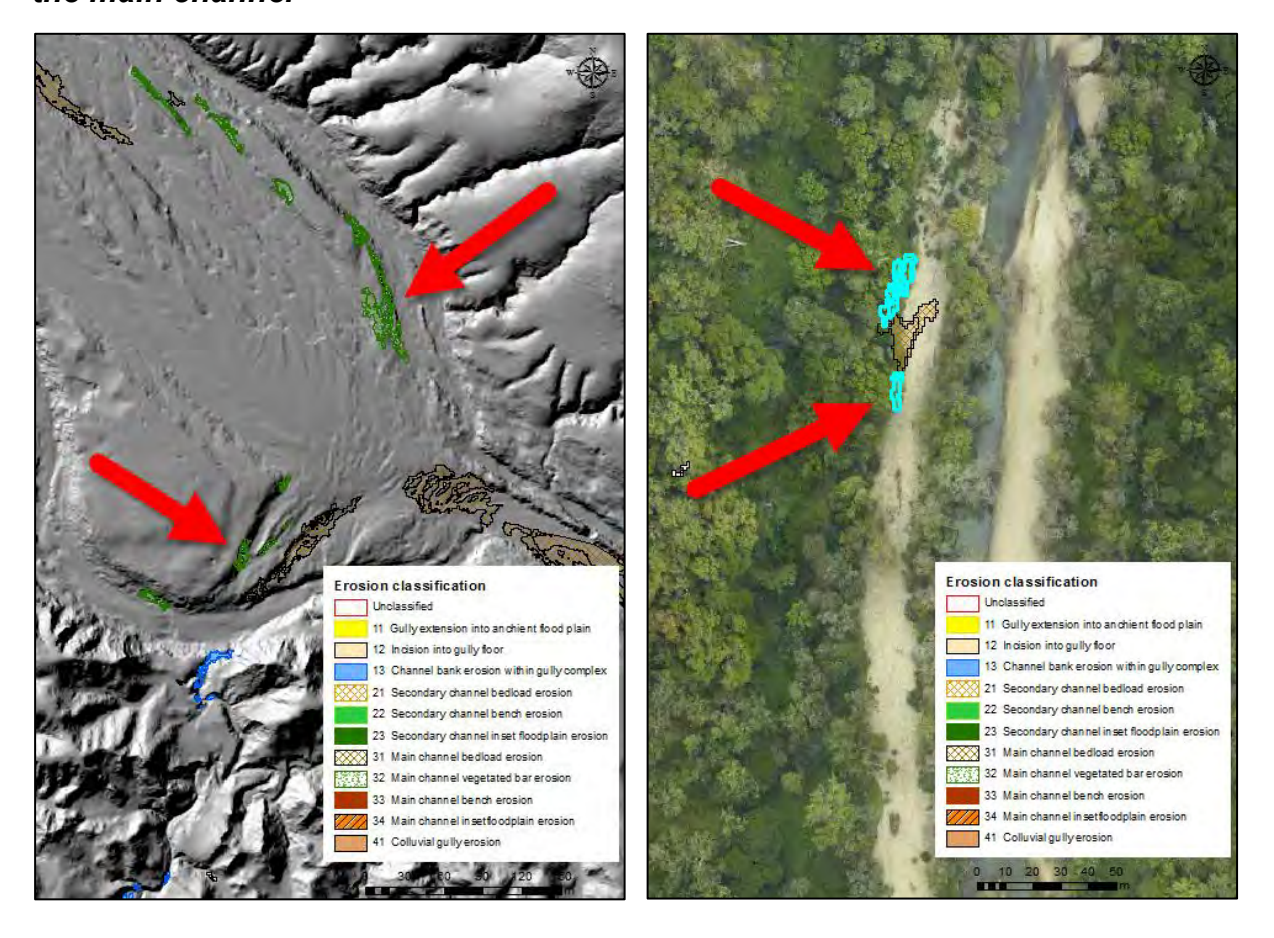
Class 23: Secondary channel inset floodplain erosion. Erosion on inset floodplains of intermediate scale channels, or tributaries, mostly with a catchment that extends beyond the Lidar block.



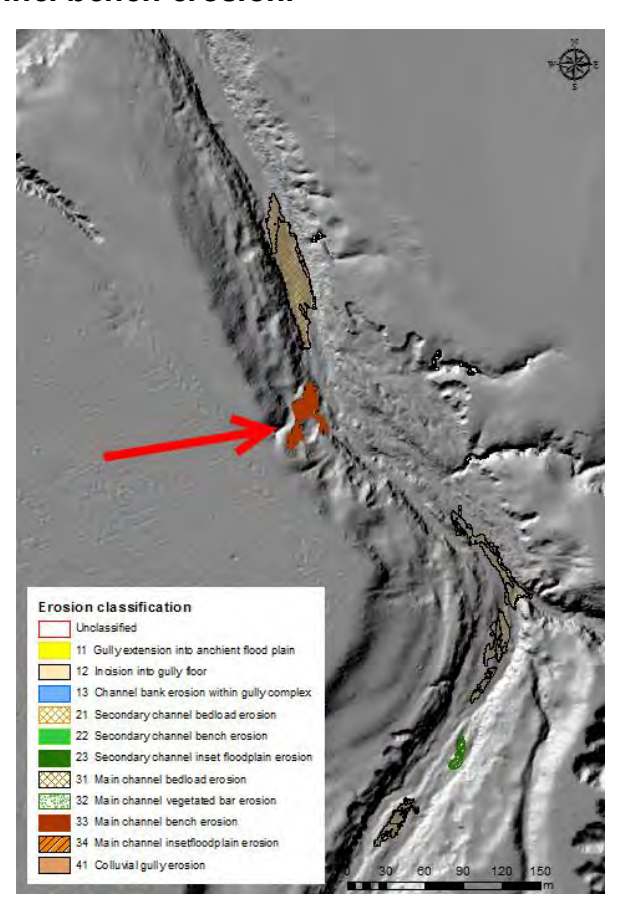
Class 31: Main channel bedload erosion. Scouring of lateral bars, point bars, chute channels in the main channel.



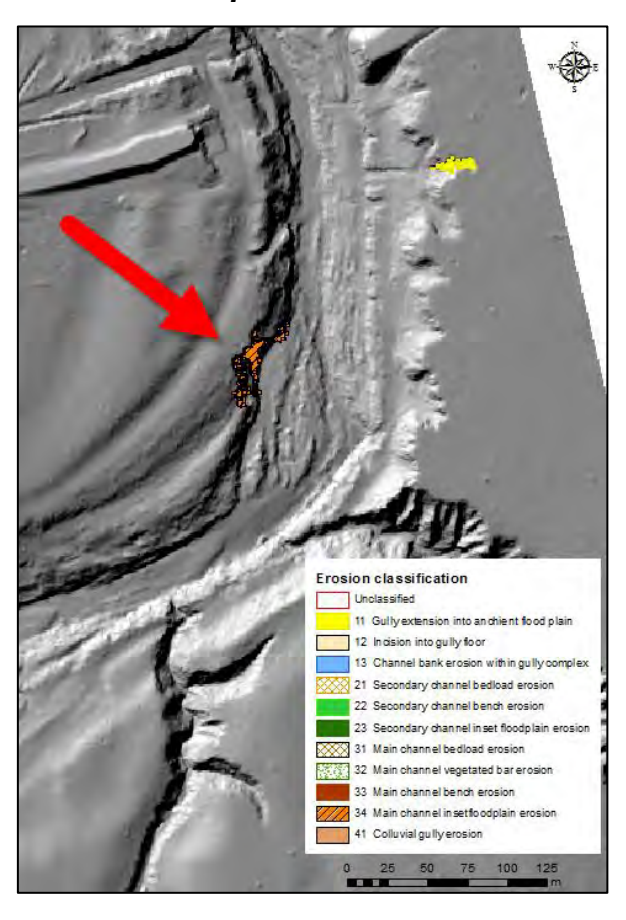
Class 32: Main channel vegetated bar erosion. Erosion of vegetated bars within the main channel



Class 33: Main channel bench erosion.



Class 34: Main channel inset floodplain erosion.



Class 41: Colluvial gully erosion. Erosion in gullies extending uphill on slopes above the flat levels of the old floodplain.

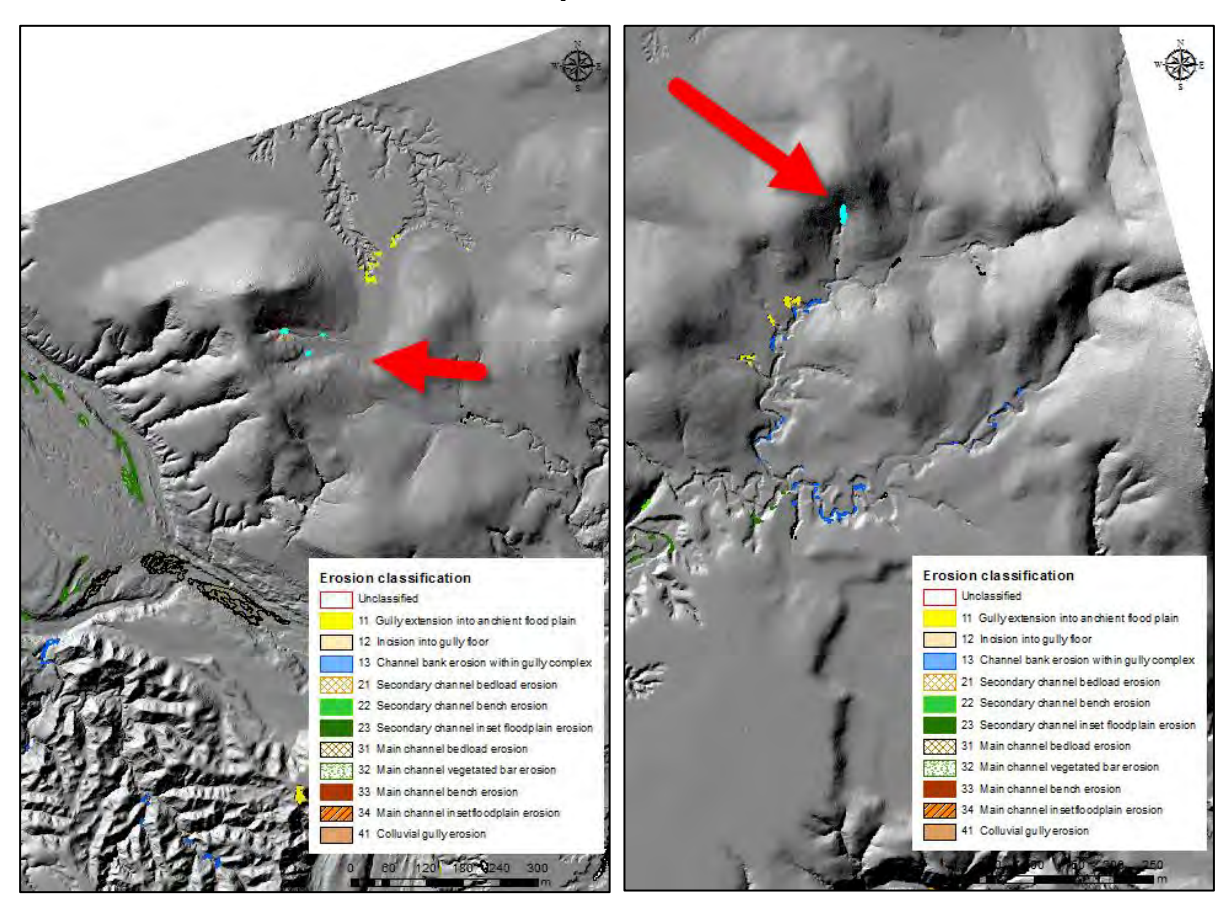
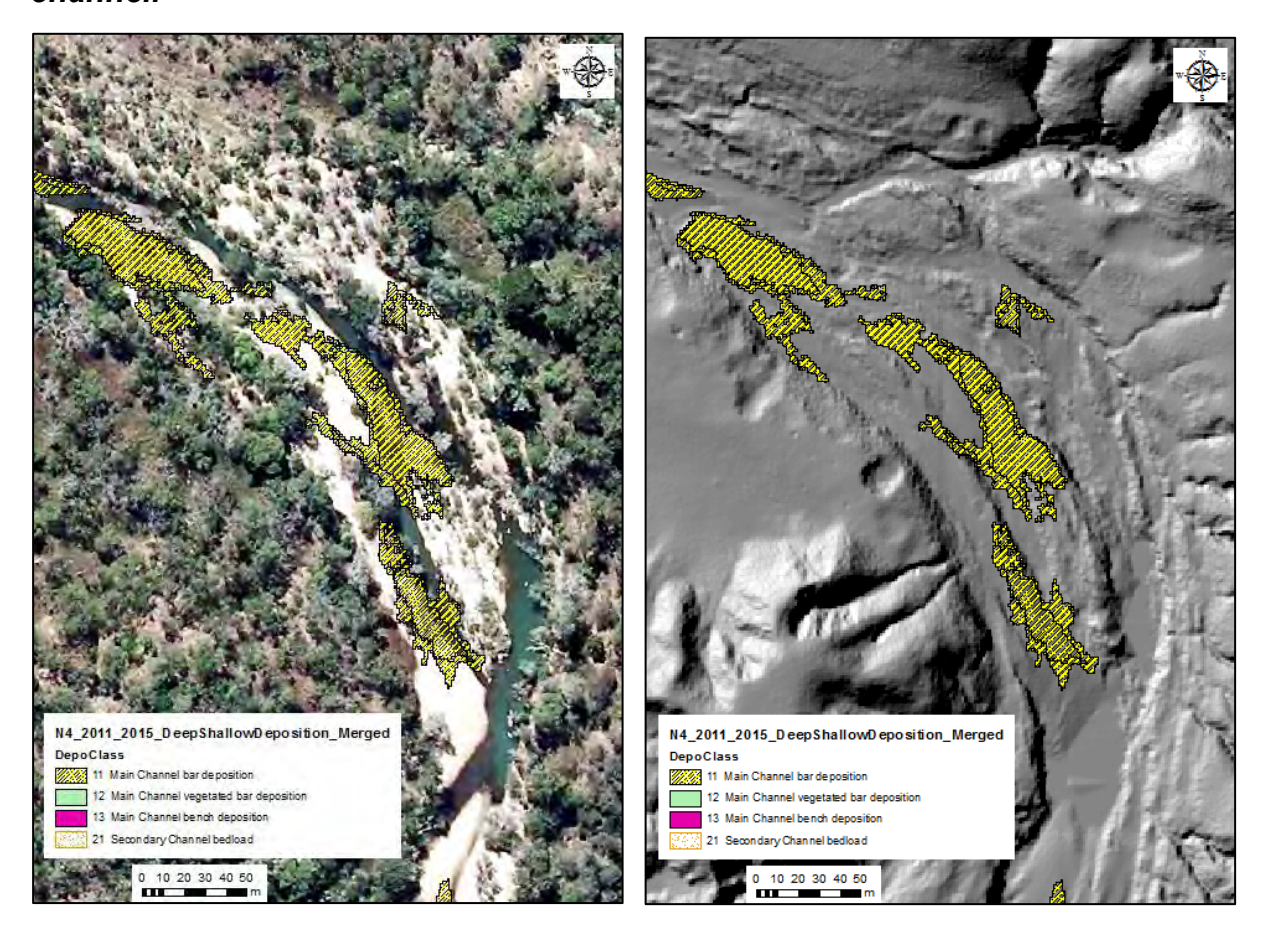
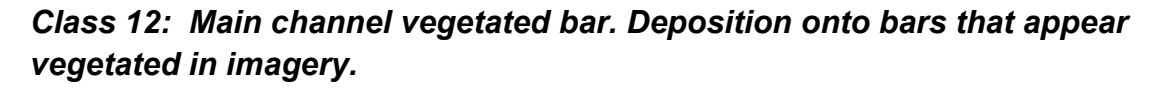


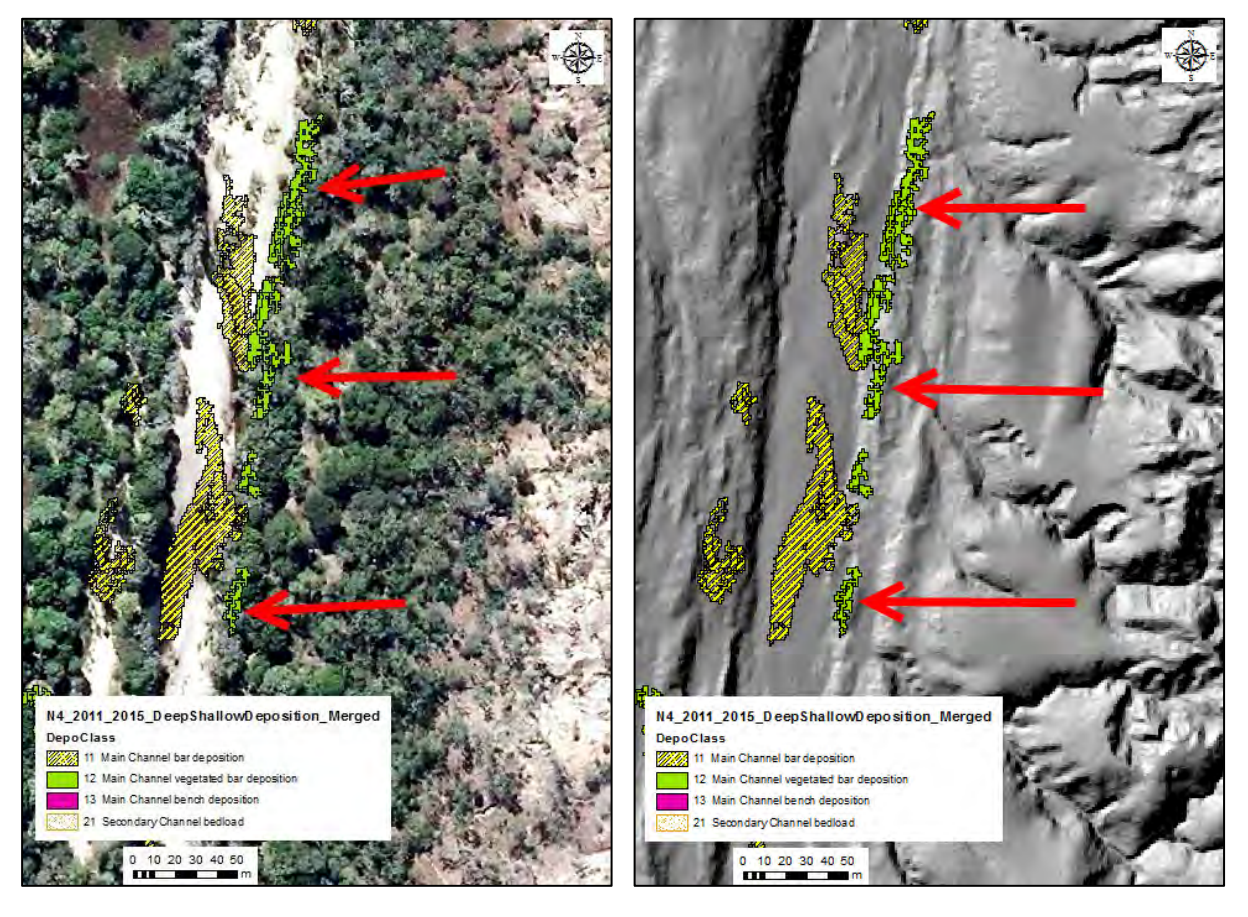
Table A12: Deposition Classes

Class	Deposition description	Criteria
11	Main channel bedload	Deposition onto open bars in the main channel.
12	Main channel vegetated bar	Deposition onto bars that appear vegetated in imagery.
13	Main channel bench	Deposition onto raised, linear features in the main channel.
21	Secondary channel bedload	Deposition onto the bed of secondary channels.

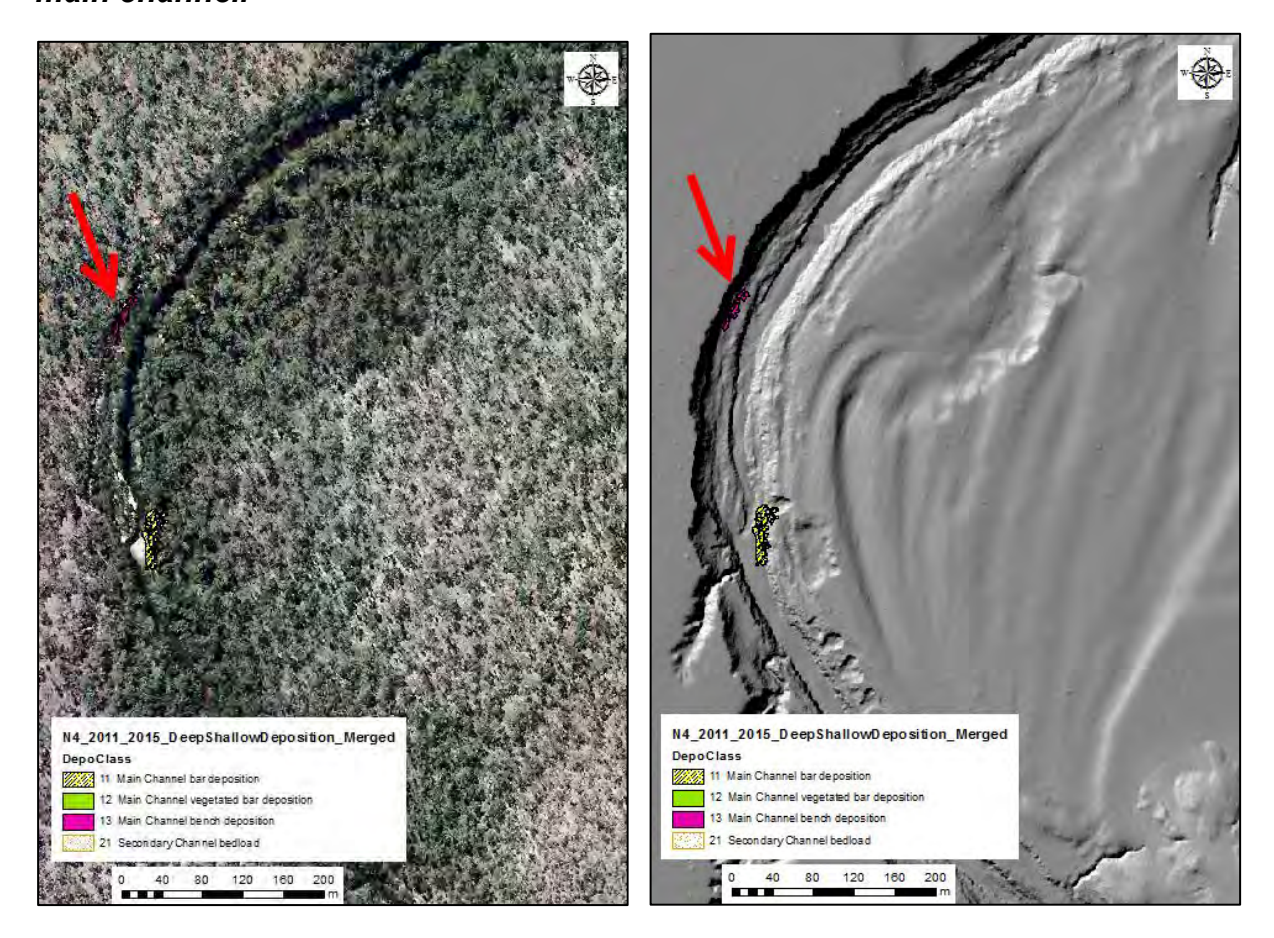
Class 11: Main channel bedload. Deposition onto open bars in the main channel.



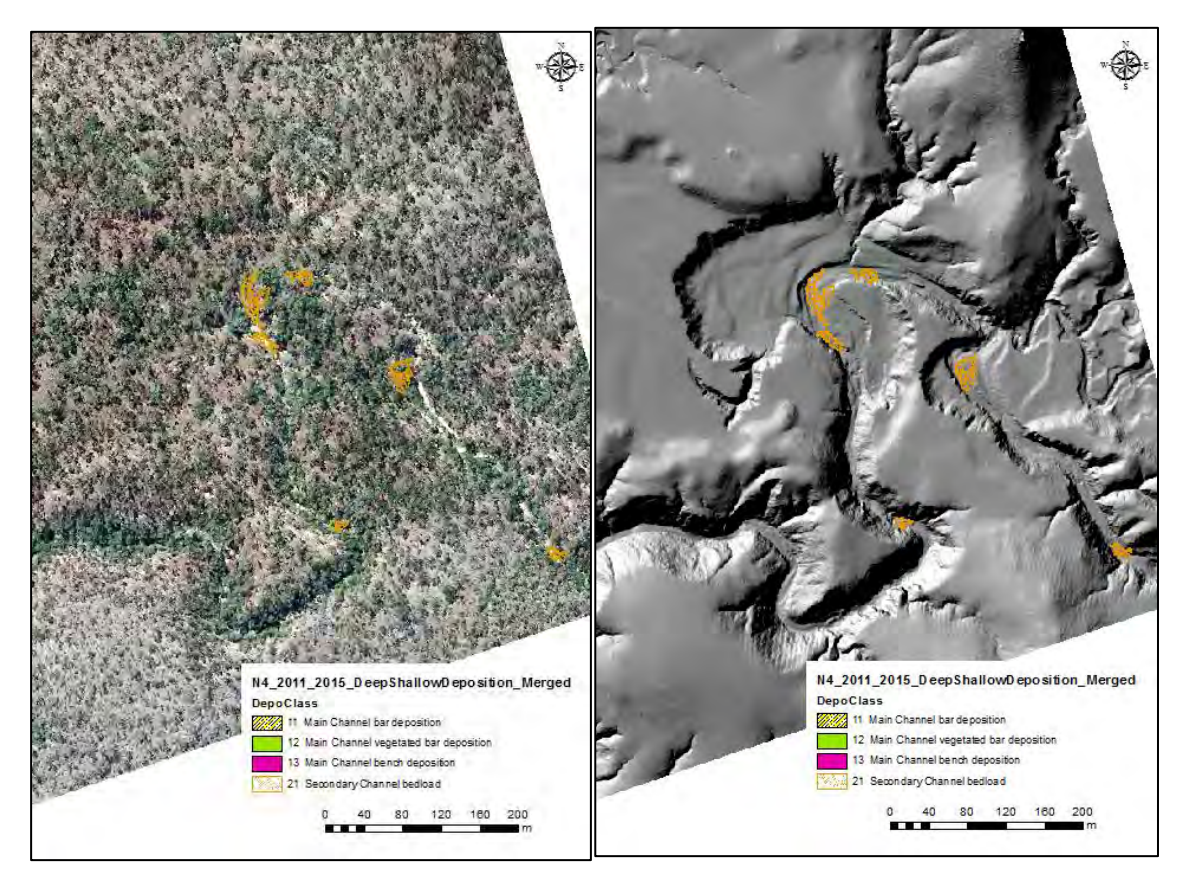




Class 13: Main channel bench. Deposition onto raised, linear features in the main channel.



Class 21: Secondary channel bedload. Deposition onto the bed of secondary channels.



# 2.4.1 Processing Sequence to Consolidate Old and New Classification Schemes

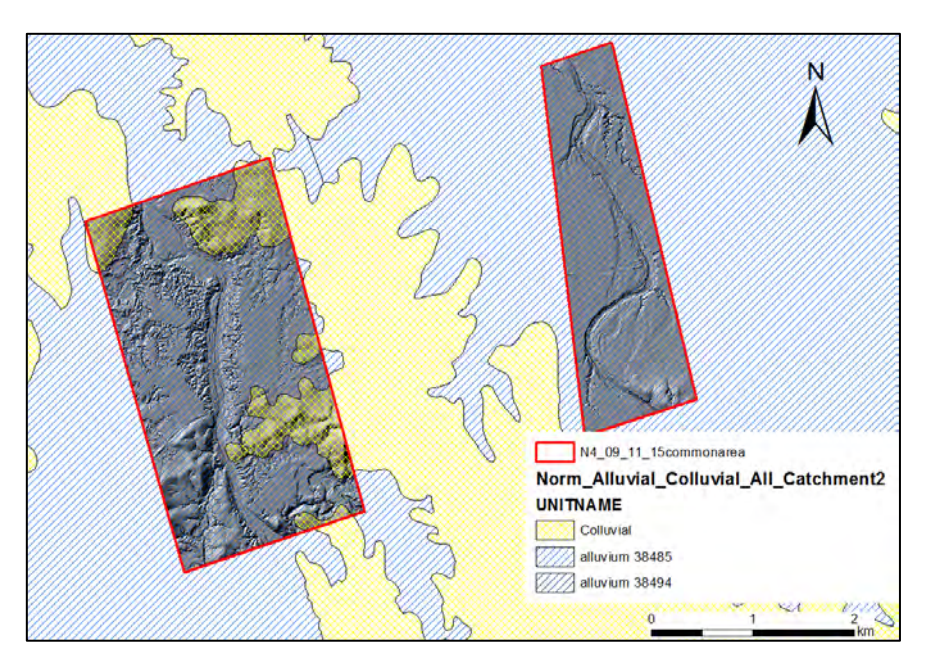


**Figure A19:** Alluvial and Colluvial at 1:1 million, plus common area for 09 11 and 15 Lidar put on the map.

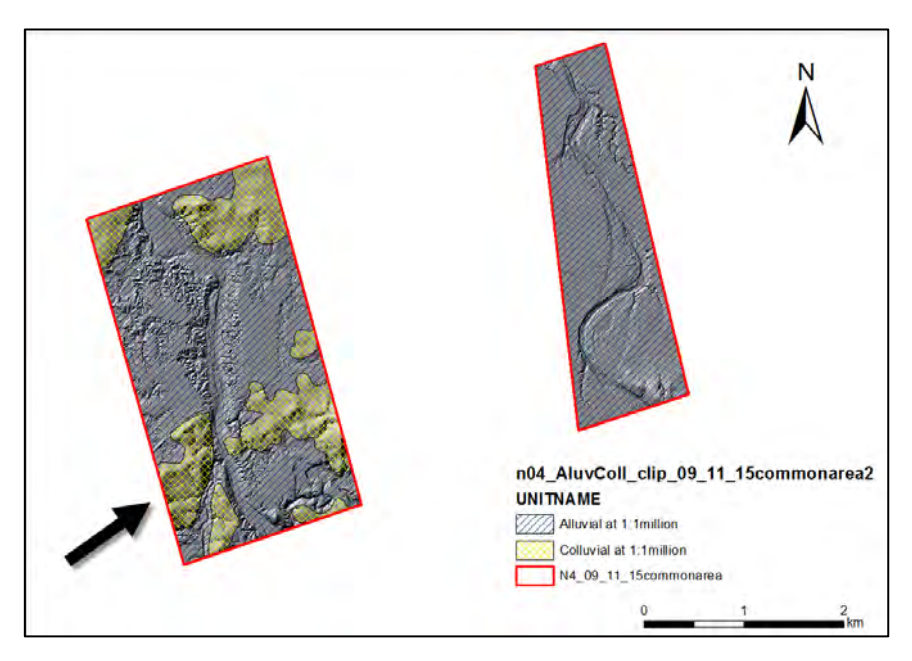
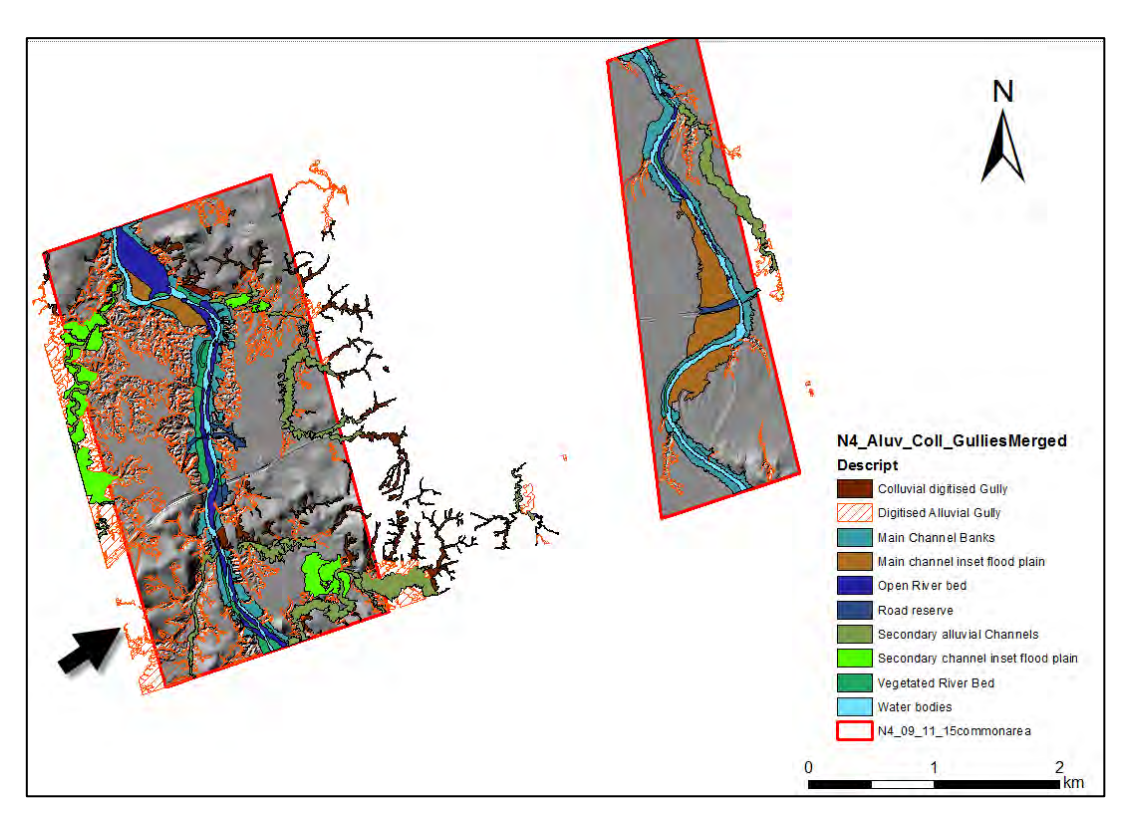
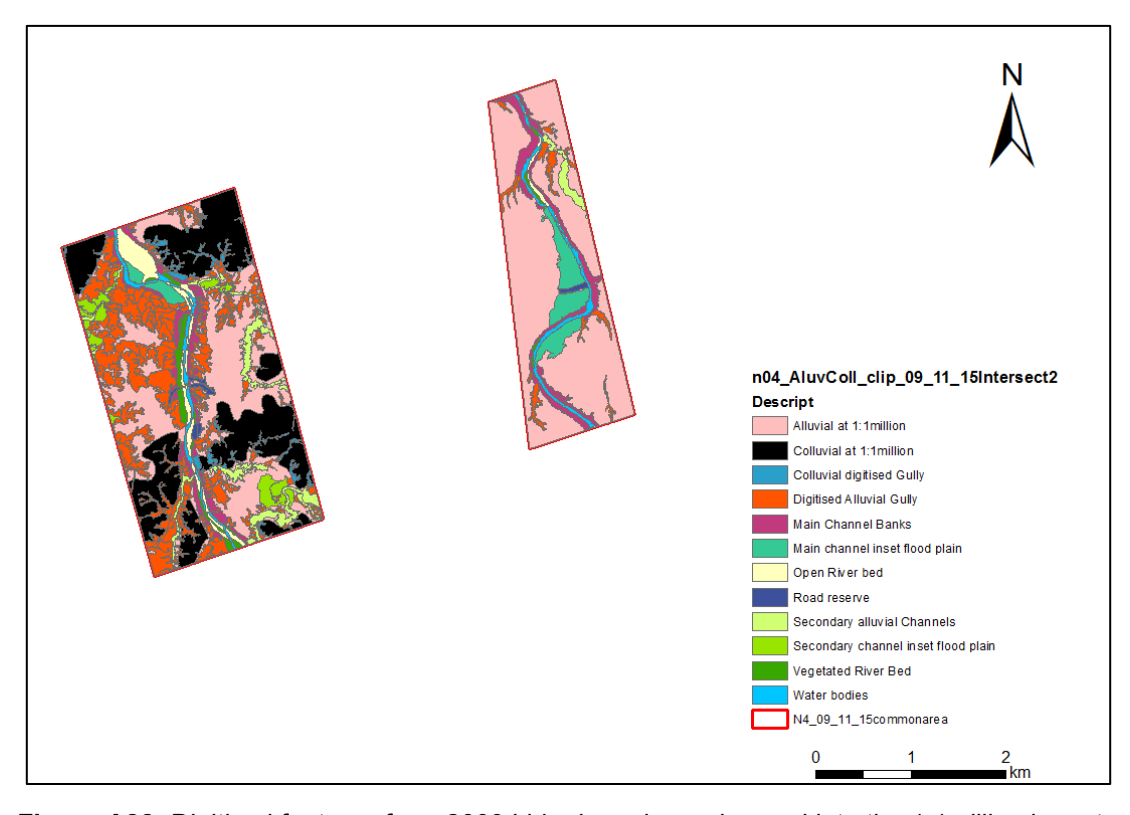


Figure A20: Redraw of boundary to reclassify this obvious hill.



**Figure A21:** Alluvial and Colluvial gullies merged to 1 layer. Note the gullies on the hill bottom left will still be classified alluvial because that was the original low resolution 1:1mill classification.



**Figure A22:** Digitised features from 2009 Lidar have been dropped into the 1:1million layer to completely classify the area, and clipped to the common area for 2009 - 2011 - 2015 Lidar

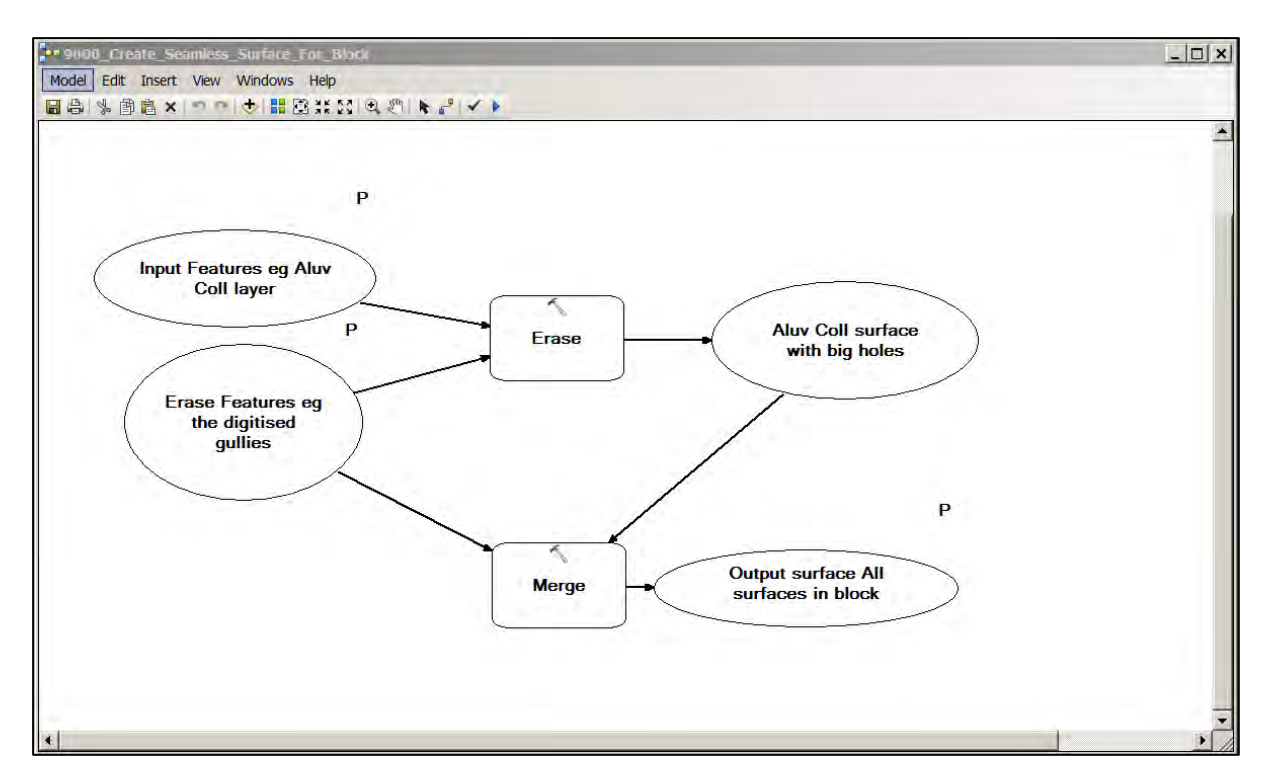


**Figure A23:** Model builder routine for dropping the digitised features into the 1:1mill alluvial/colluvial layer. Cookie cutter out the area of digitised features, then drop in the digitised features.

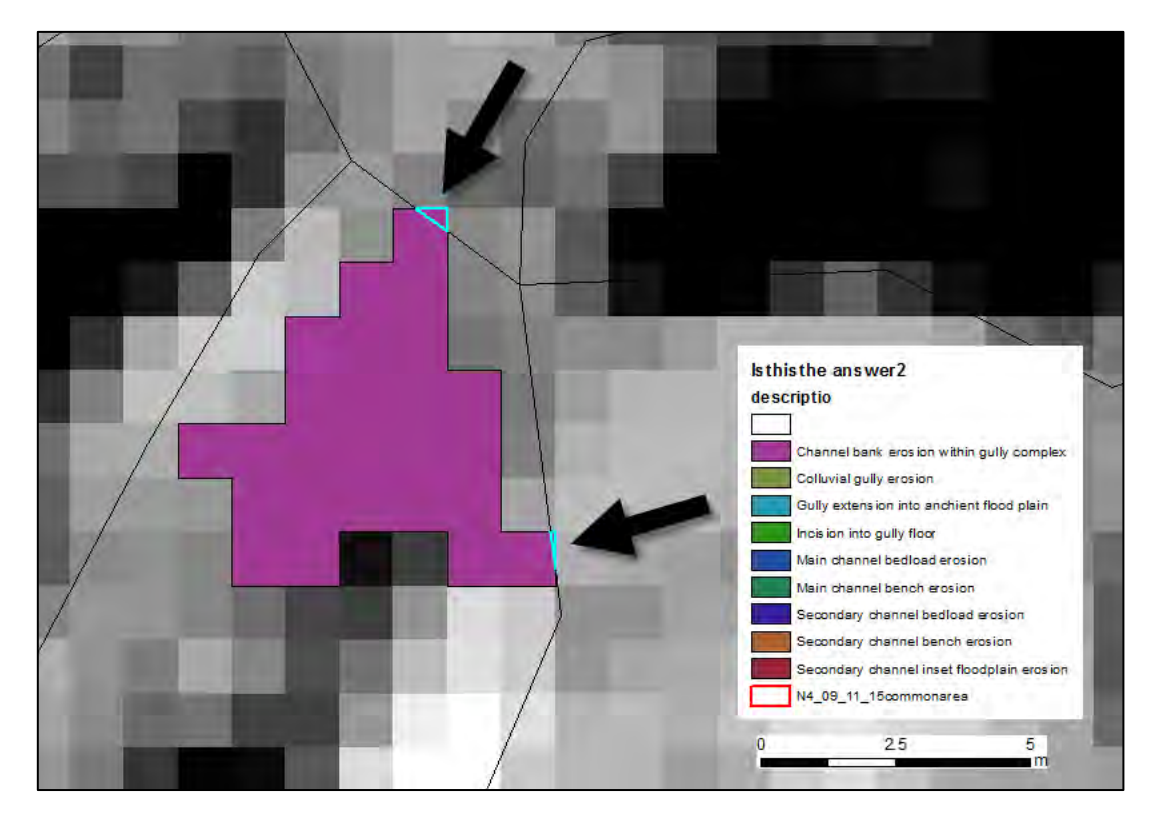


**Figure A24:** Problem with intersecting erosion polygons with the classified surface was that small sections of polygon would be split off from the main patch, and each segment would turn up in the attribute table with the same value of erosion, thus double or triple counting the volume of erosion.

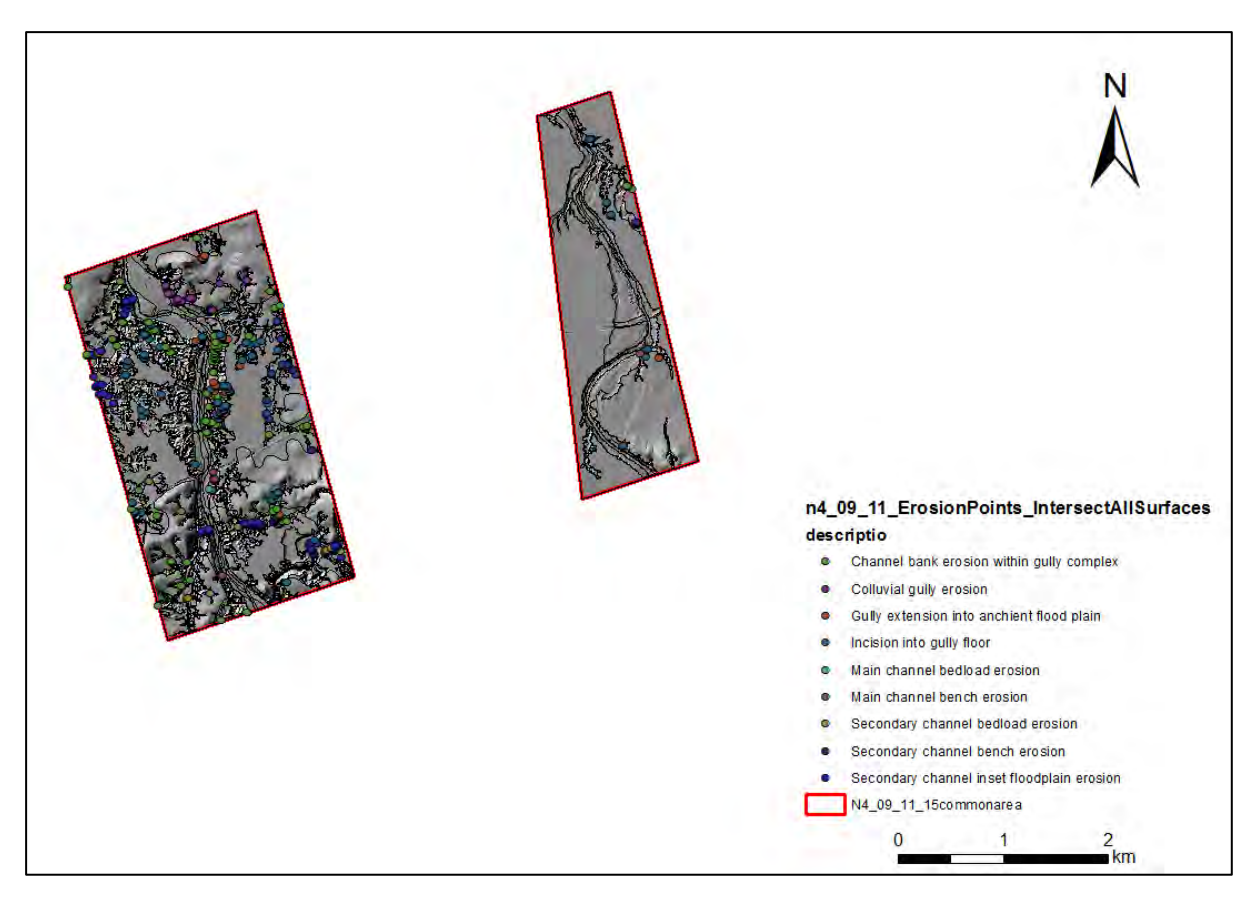


**Figure A25:** Polygons of erosion were converted to points, which would give one precise location to intersect with the classified surface.

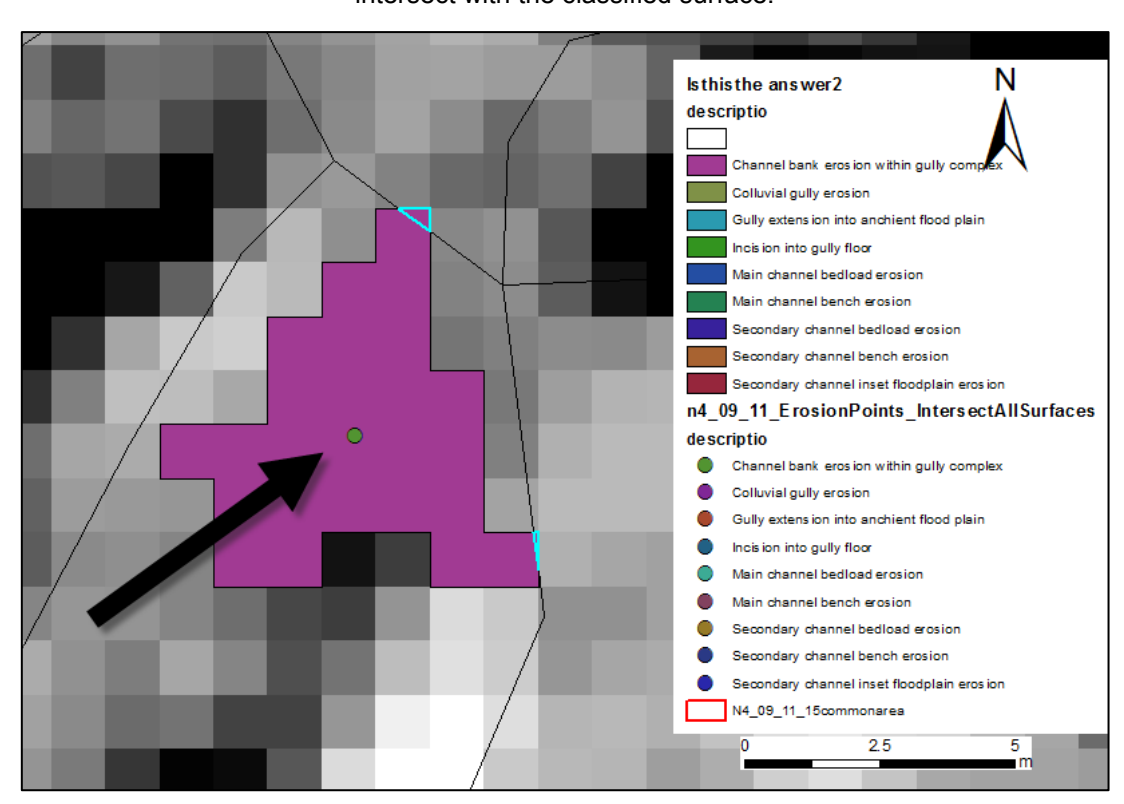


**Figure A26:** The centroid of the erosion polygon falls onto one part of the classified surface. The points have all the information of the highly specific classification, including the area and volume of erosion, and now also the details of the classified surface it sits on.

## Data was exported as 2 csv files:

- 1. A csv with areas and classification of the entire common area for 09 11 15 Lidar
  - a. Classification is at 2 levels
    - i. 1:1million
    - ii. Digitised features with remaining areas filled from 1:1mill layer
- 2. A csv with individual patches of erosion classified according to their location within a gully/secondary stream/main channel, with areas and volumes, tagged with the surface they sit on.

## 3. LIDAR BLOCK RESULTS

#### Prepared by: Andrew Brooks and Graeme Curwen

This section provides a detailed description of LiDAR change detection by Block.

# 3.1 Normanby LiDAR Block 4

Normanby LiDAR block (Norm 4) lies approximately 15km upstream of the junction of the East and West Normanby Rivers, with an elevation range of 118 to 264 m. LiDAR from 2009 was a rectangular footprint, but LiDAR flown in 2011 had an H shaped footprint to focus on alluvial areas. Features digitised on the original rectangular footprint have been clipped to the H shaped difference raster.

Active erosion was seen as linear gullies extending across alluvial surfaces towards colluvial slopes, incision of existing gully floors, and secondary channel widening. The 3<sup>rd</sup> highest source of measured erosion came from road drainage. Minimal erosion was detected in the East and West Normanby main channels.

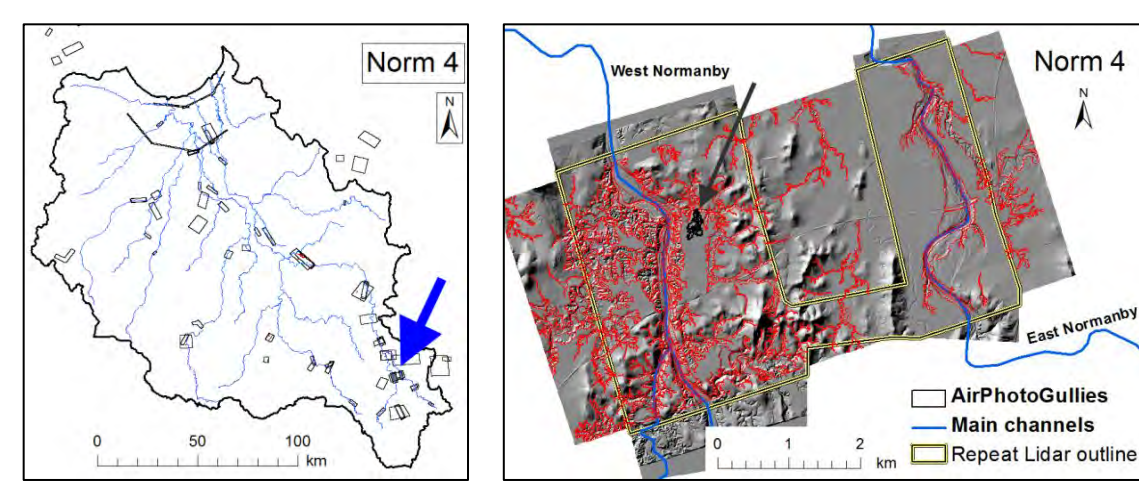


Figure A27: Norm 4 location (left); Digitising on 2009 LiDAR (right).

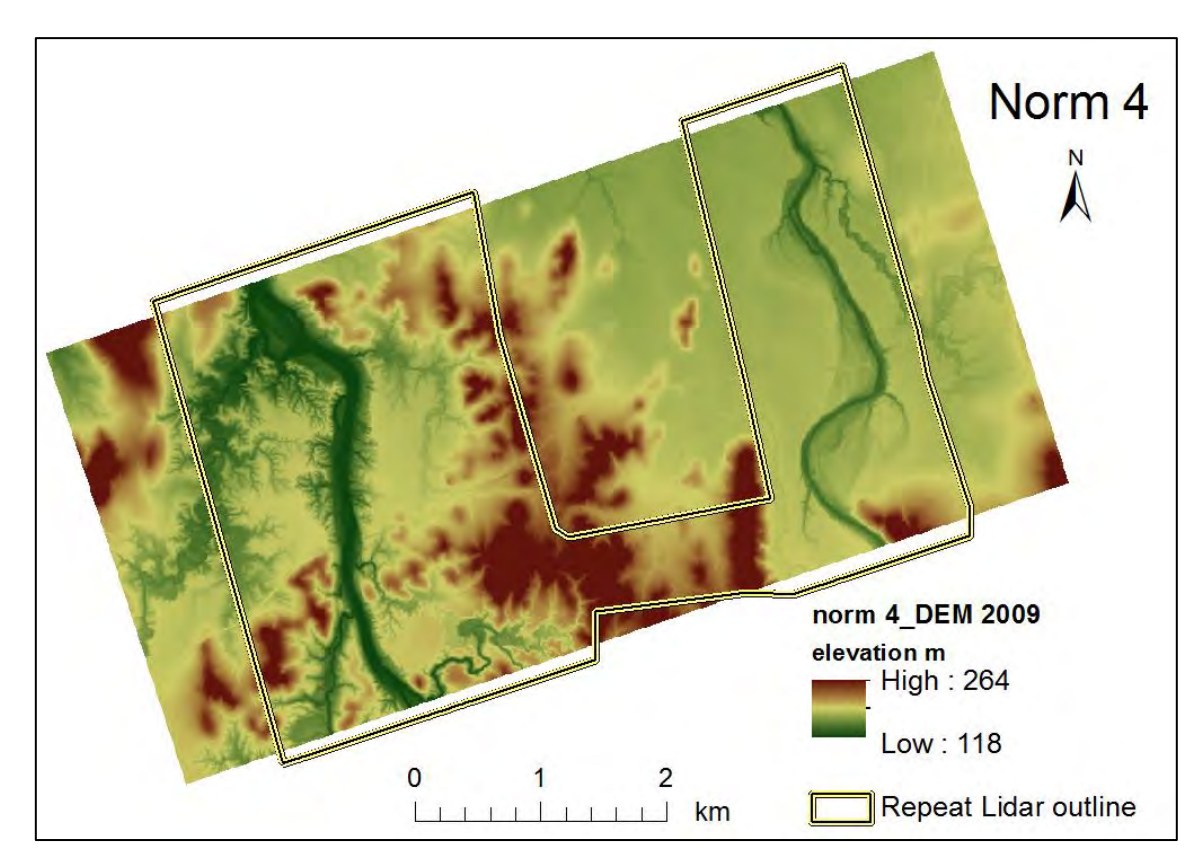


Figure A28: 2009 DEM.

Table A13: General statistics for Norm 4.

2009 LiDAR area	ha	4311
Reprocessed change raster area	ha	1662
Block elevation range	m	116 -263
Number of LiDAR digitised features		556
Number of Google Earth mapped gullies		114

## 3.1.1 Alluvial and Colluvial geology

Alluvial geology occupied 64% of Norm 4, with a range of hilly colluvial country rising to 120m above the valley floor separating the flood plains of the East and West Normanby rivers. The accuracy of the alluvial/colluvial boundary was checked against a 3° slope raster derived from the 30m DEM. It would appear the colluvial boundary should include additional land in the south western corner of the block, seen as elevated country in the DEM (Fig 4.3).

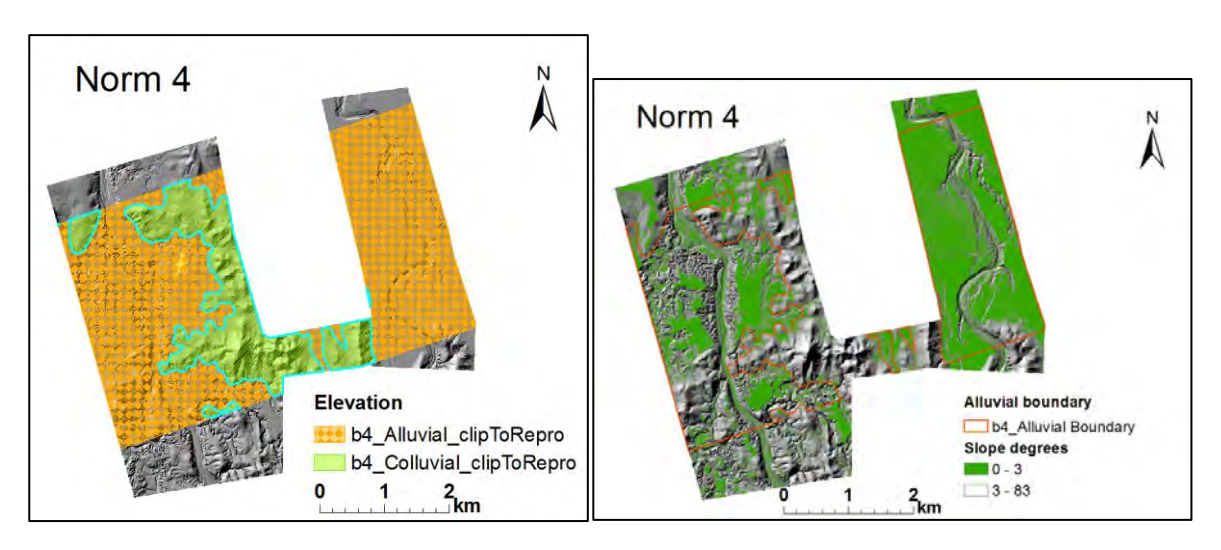


Figure A29: Alluvial and colluvial geology in Norm 4.

## 3.1.2 Google Earth gullies

Location of gullies mapped from Google Earth is shown in Figure A30. Density of GE gullies in NORM 4 was 0.019ha/km², which was the 10<sup>th</sup> ranked block of 13, with only 3 other blocks having a higher density of GE gullies. As can be seen in Figure A30, the location of GE gullies is mainly on alluvial geology, and predominantly in the West Normanby valley.

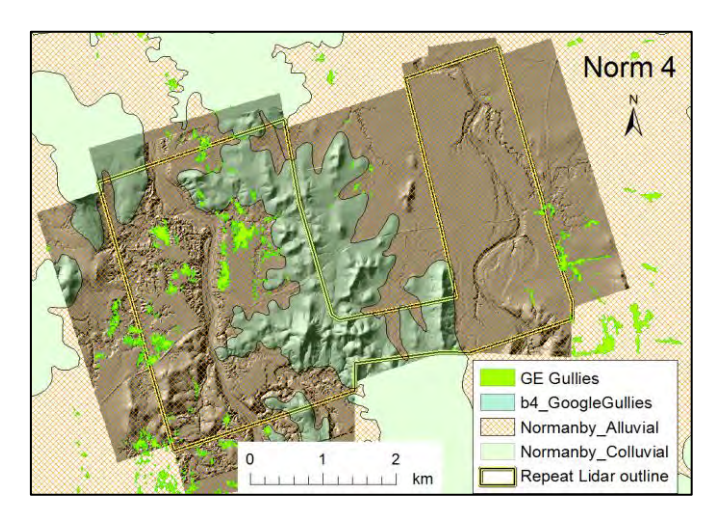


Figure A30: Location of Google Earth gullies in Norm 4 and surrounding area.

Colluvial

zone

392.8

37.3

Norm 4	Area ha	Area of all features digitised from LiDAR ha	Features as % of zone	Area of gullies digitised from LiDAR ha	Area of gullies as % of zone	Area of Google Earth digitised gullies ha	GE gullies as % of zone
Alluvial zone	1169.3	475.0	40.6	239.0	20.4	27.5	2.4

35.5

9.0

1.9

0.5

9.5

Table A14: Quantifying LiDAR and GE gullies in alluvial and colluvial geology.

It was found in Norm 4 that the area of gullies visible from vegetation penetrating LiDAR, 274ha, was approximately 10 times greater than that mapped from Google Earth, approximately 30ha. Not only was GE mapped gullies under representing the real area, but a problem highlighted in Norm 4 was that most erosion was occurring under vegetation, beyond the perimeter of GE mapped gullies.

It was found that 41% of the alluvial zone in Norm 4 was eroded by channels or gullies, and that alluvial gullies accounted for half of this area. Compared with this, the colluvial area had 9.5% of its area eroded, and the majority of this figure, 9%, was gully erosion.

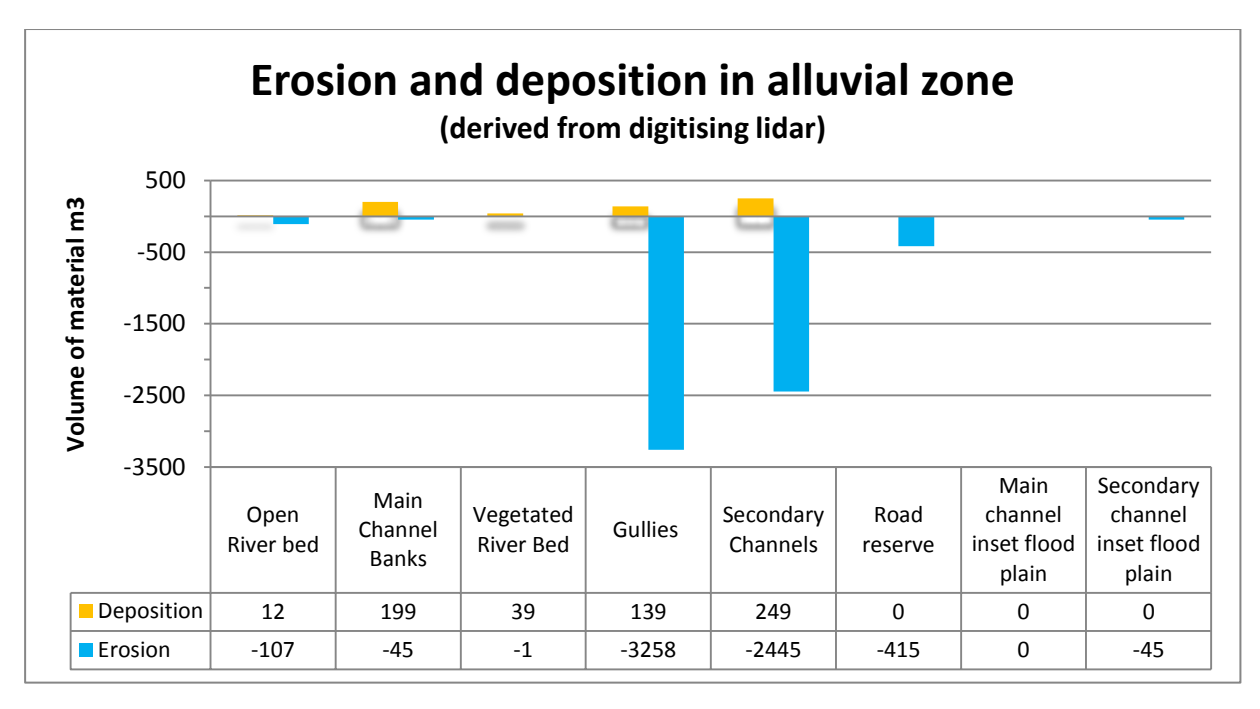


**Figure A31:** Large volumes of erosion came from gullies and secondary channels. The contribution from road drainage, 415 m<sup>3</sup> was on a par with the second largest producing unit in Norm 4, a 700m section of secondary channel with active bank erosion.

## 3.1.3 Comparison of alluvial gullies to colluvial gullies

**Table A15:** Alluvial and colluvial gullies had a similar rate of erosion when expressed as yield per hectare per year, but colluvial gullies were an order of magnitude less in area and volume of erosion than alluvial gullies.

Alluvial gullies				Colluvia	l gullies		
area ha	deposition m3	erosion m3	yield m3/ha/yr	area ha	deposition m3	erosion m3	yield m3/ha/yr
223.2	138	-3257	-14	31.3	0	-427	-14

## 3.1.4 Comparison of Google Earth gullies to LiDAR gullies in the alluvial zone

**Table A16:** The area of bare ground gullies captured from GE mapping was approximately 10% of the gully area seen in LiDAR, but the volume of erosion from bare ground (GE) gullies was 20% of the volume measured from alluvial gullies from LiDAR imagery. This supports field observations of erosion advancing under vegetation.

	Area ha	Erosion m <sup>3</sup>	Yield m³/ha/yr
LiDAR alluvial gullies	223.20	-3257.54	-13.97
GE alluvial gullies	27.98	-680.49	-11.61

## 3.1.5 Gully Expansion 2009 - 2011

Table A17: Area of expansion of gullies between 2009 and 2011.

Gully Expansion 2009 - 2011	
Number of gully expansion locations	69
Sum area of gully expansions ha	113.6
Mean area of expansion m2	1.7

#### 3.1.6 Landscape Classification

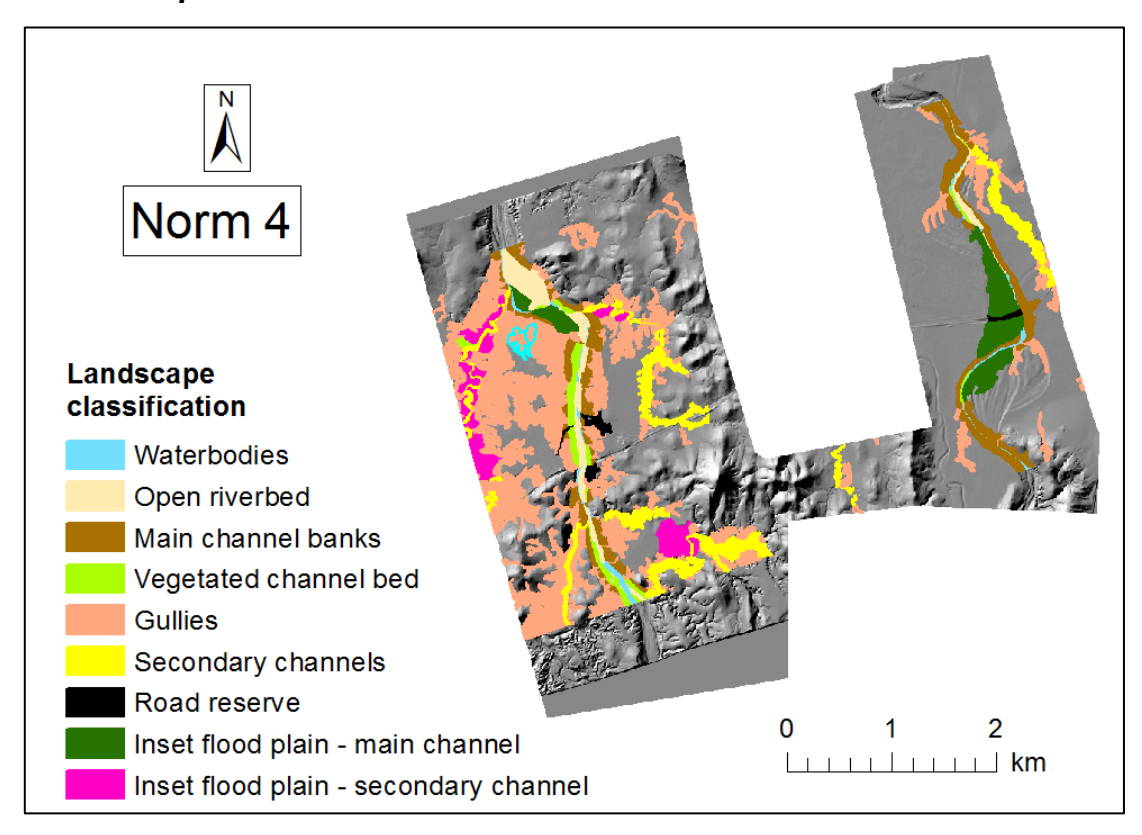


**Figure A32:** All 9 landscape classes are represented in Norm 4. Approximately half of the block was alluvial gullies. Main channel banks and secondary channels had similar areas of 12 to 13% of total area. Inset flood plains along main channels and secondary channels also had a similar area, being 7 to 8% of total area.

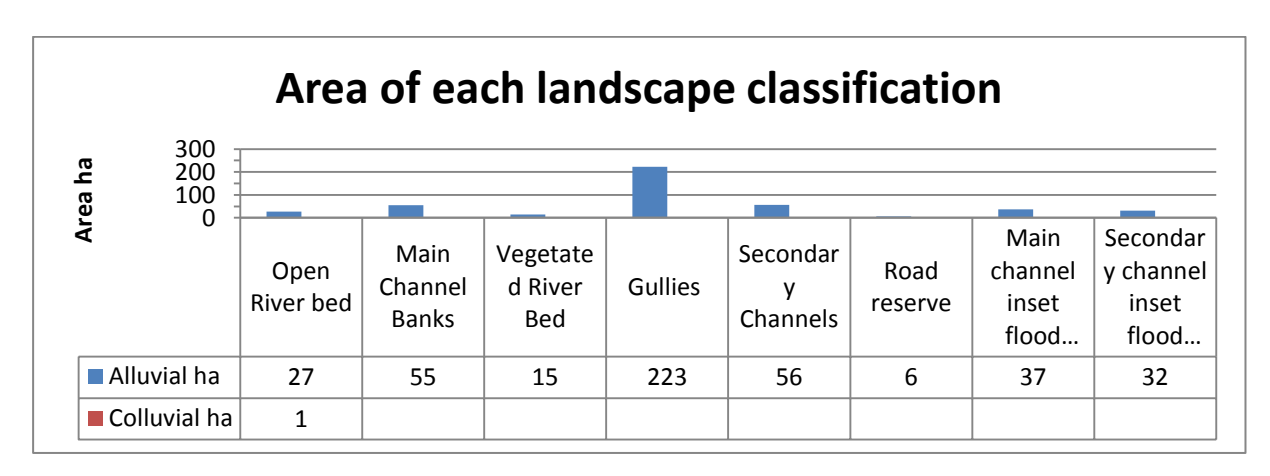


Figure A33: Area of each landscape classification in block 4.

#### 3.1.7 Historical air photos

One gully on Norm 4 was readily identified in air photos from 1952, 1957, 1982, 1987 and 1994; which was a record for time slices for this section of the Normanby project.

**Table A18:** Meta data for historical air photos covering Norm 4.

Image date	Photo ID	Scale	Flying height	RMS error	Air photo relative to 2009 LiDAR block
1/01/1952	QAP0150_146.tif	23900	12750ft	5.25352	
1/01/1957	QAP0730_015.tif	39600	20000ft	0.000	
1/01/1982	QAP4071_105.tif	24900	4600m	2.45737	
1/01/1987	qap_4111_182.tif	25000	4310m	0.00002	
19/10/1994	QAP5321_196.tif	25000	4630m	6.44978	

The gully to the east of the West Normanby was approximately 450m in length and 230m at its widest. The head scarp was 1.5- 2m below the surrounding flood plain, with a multi lobed incision about 2m deep advancing along several drainage lines.

Minimal erosion was measures at head walls, but the incisions advanced at up to 12m between 2009 and 2012.

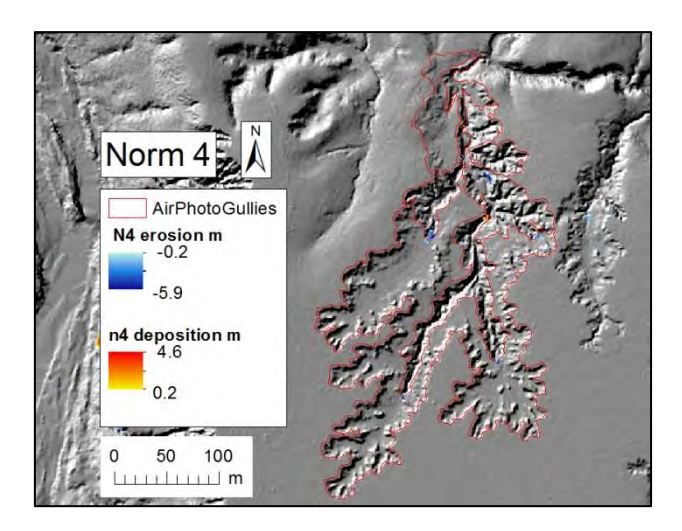
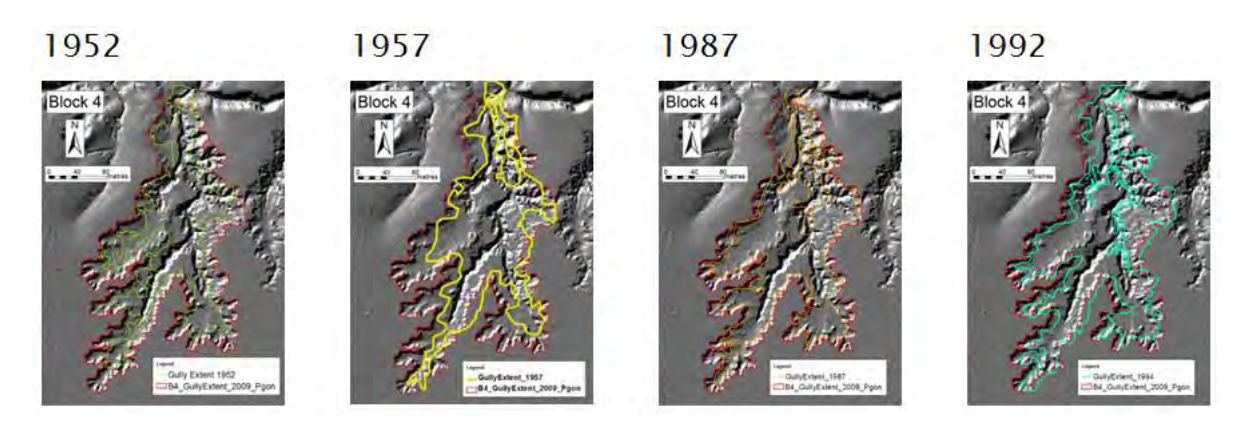


Figure A34: Incision of gully floor is the main erosion activity in the gully identified from air photos.

## 3.1.8 Historical gully extent

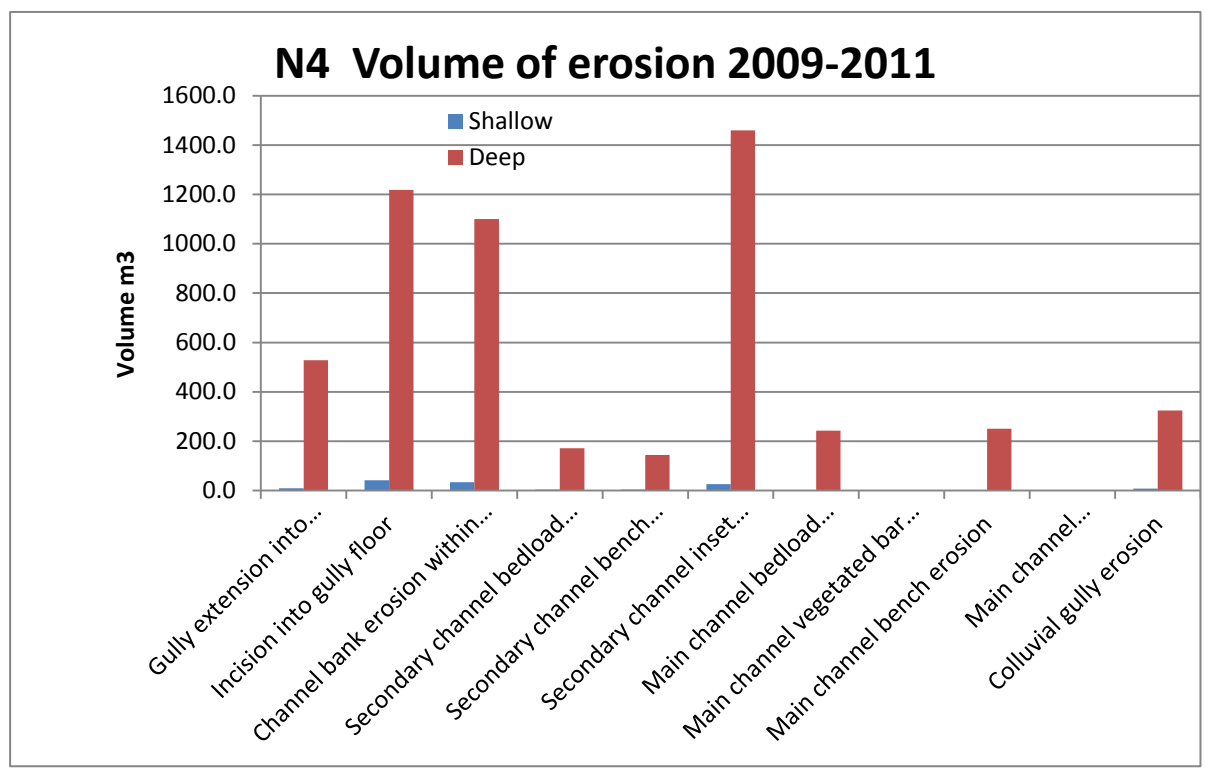


**Figure A35:** Incision of gully floor was not seen in the 1952 image, but between 1957 and 2009 the advance of the longest incision was 218 m, an average of 4 m per year. In comparison, head wall advance at different locations was between 20 and 40 m, an average annual advance of less than 1m.

**Table A19:** A remarkably consistent rate of erosion was calculated over 5 decade and 2 decade intervals from air photos, with a small spike in rate over the shortest interval, from 1994 to 2009. The gully did not expand in area between 2009 and 2011, but erosion from incisions along drainage lines produced 19 m³/ha/yr, approximately one fifth of the historical rate. It is possible the forces driving gully expansion have reduced, but the gully floor has not yet reached a stable equilibrium.

Interval	Gully area at start of period ha	Rate of loss m³/yr	Yield m3/ha/yr Based on 2009 gully
	or portou nu	<b>y</b> .	area
1952 - 2009	2.18	615	131
1957 - 2009	2.63	445	95
1987 - 2009	3.19	634	135
1994 - 2009	3.50	787	168
2009	4.70		
2009 - 2011	4.70	2205	470

#### 2015 data and reprocessed 2009-11 data



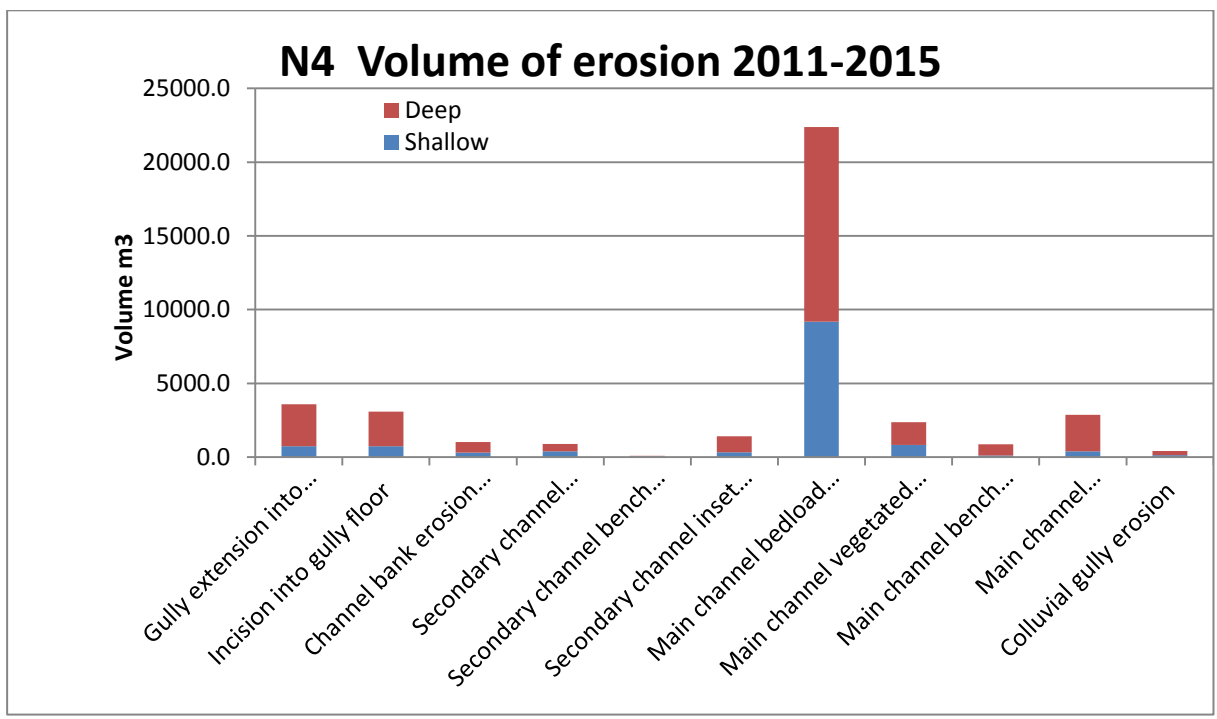
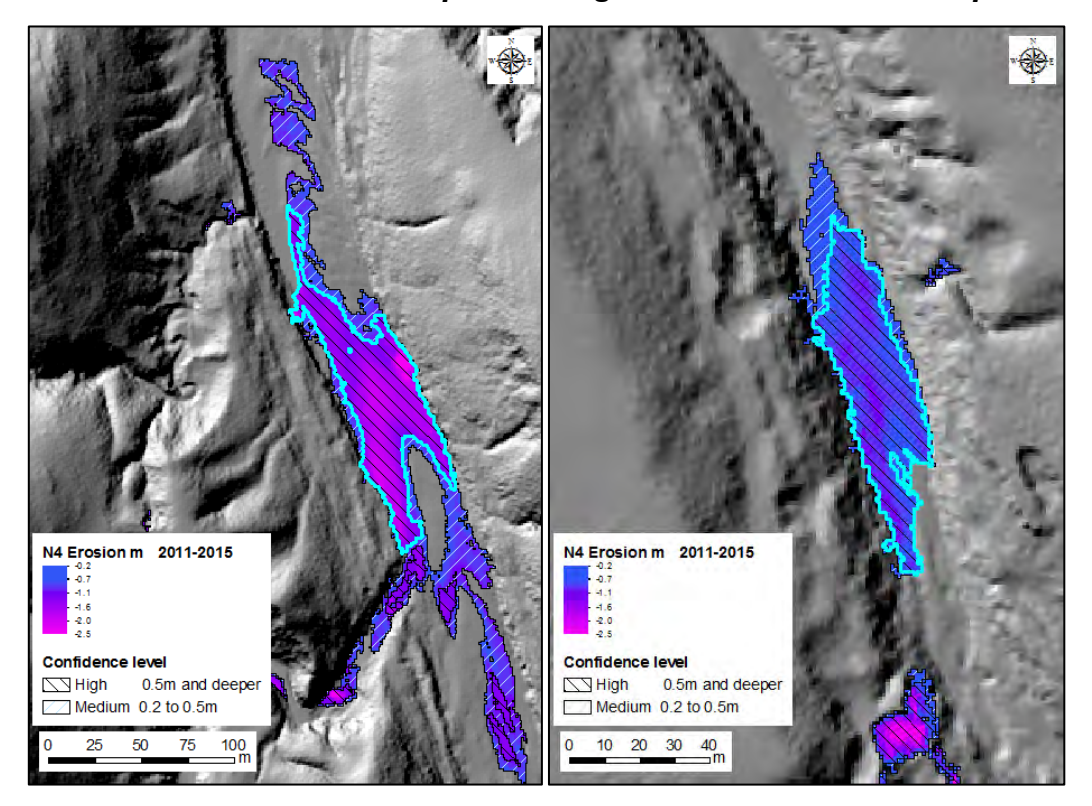


Figure A36: Erosion stats for Block 4 by geomorphic unit; 2009-11 (top); 2011-15 (bottom).

# 3.1.9 Observations from Erosion processing of 2011 to 2015 timestep



**Figure A37:** Largest volume of erosion in one patch on left (3923m<sup>3</sup>) was on the West Normanby, second largest on right (1219m<sup>3</sup>) on the East Normanby.



**Figure A38:** The largest patch of erosion that was not bedload was from this 11m tall bank on the East Normanby main channel, with a volume of 23,754m<sup>3</sup>.

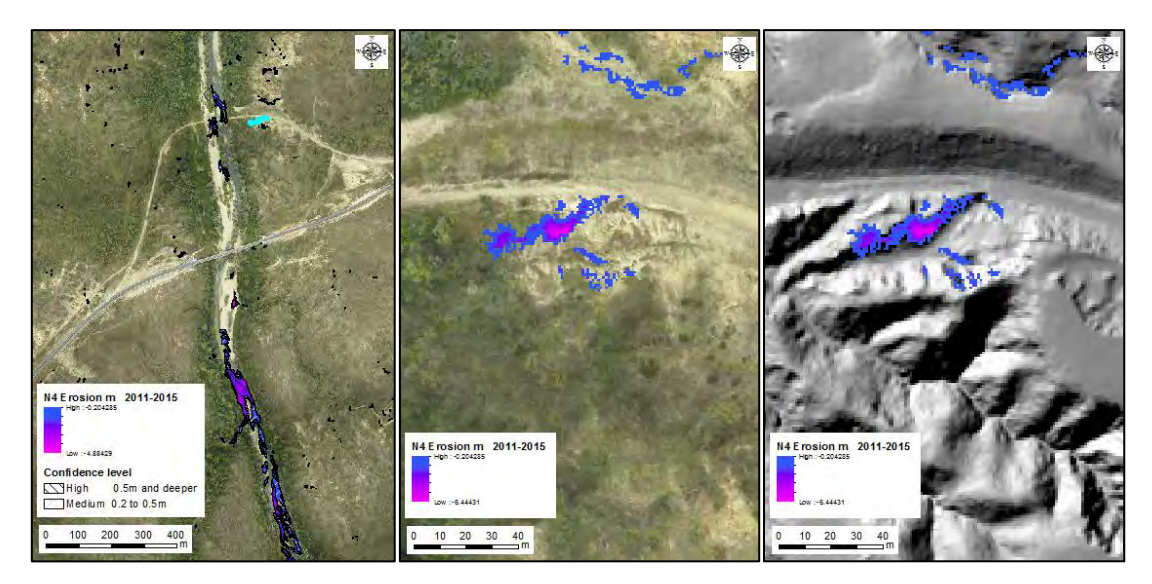


**Figure A39:** This erosion patch was the largest volume classified as "gully extension into ancient flood plain", though technically it would be a direct result of the road runoff. Erosion volume was measured as 532m³ in total, made up of 468m³ from deep erosion and 63m³ from shallow erosion.

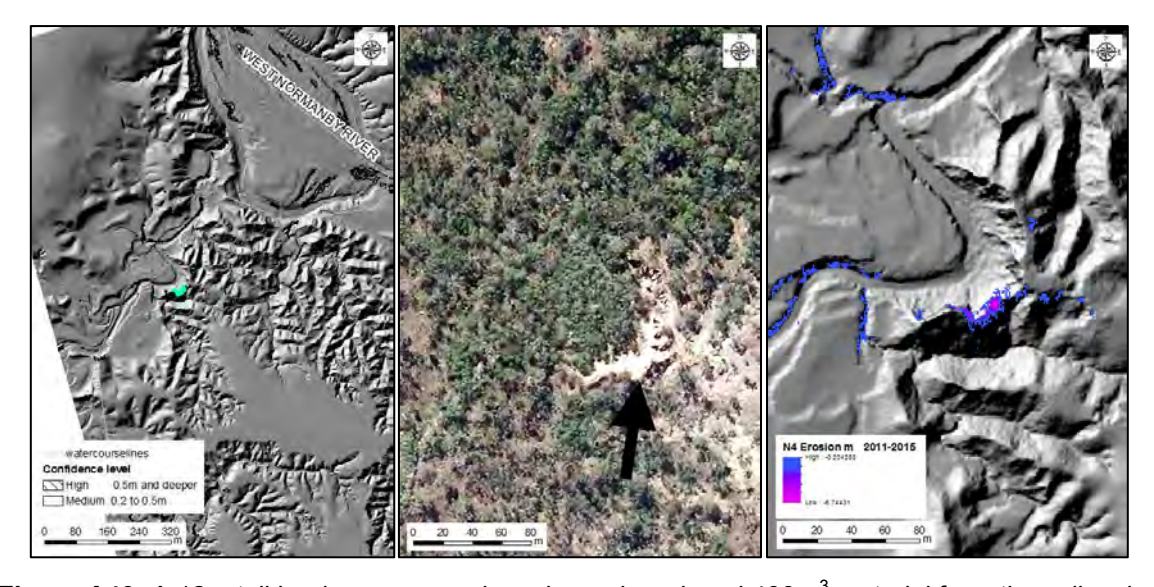


**Figure A40:** A 12m tall bank on a secondary channel produced 400m³ material from the collapsing upper edge of the bank. Imagery shows this to be an active erosion zone. 380m³ of the total was from erosion deeper than 0.5m. This area was the second largest patch by volume coming from erosion of ancient flood plain.

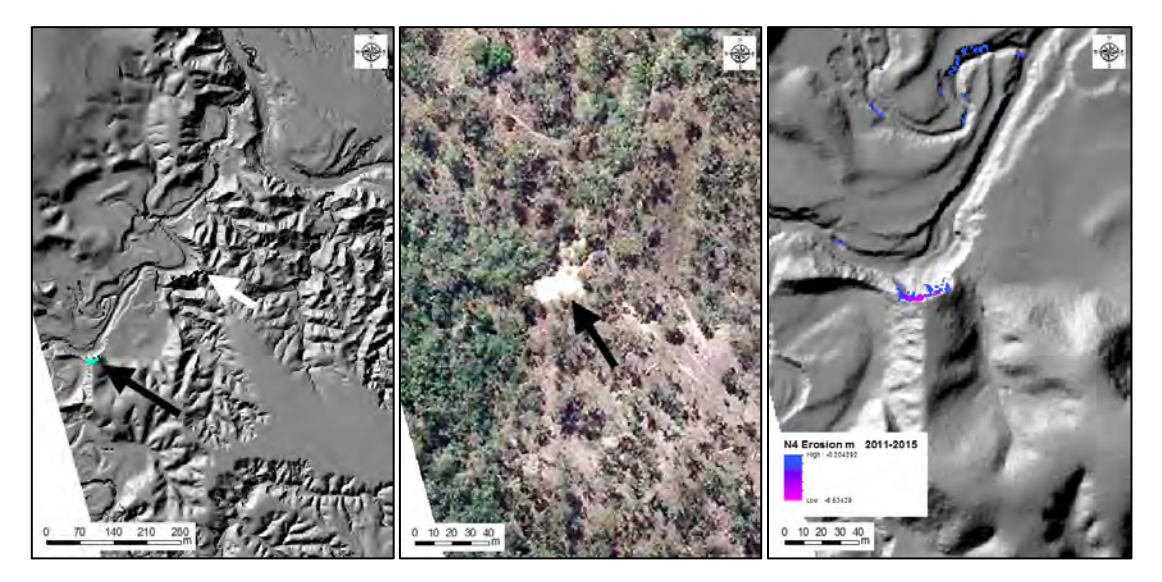


**Figure A41:** Third largest patch of erosion into ancient flood plain was also a collapsing bank, shown by black arrow. White arrow shows location of 2<sup>nd</sup> largest erosion patch.



**Figure A42:** Fourth largest patch of erosion into ancient flood plain is associated with a road crossing the East Normanby, volume of erosion was 355m<sup>3</sup> in total.

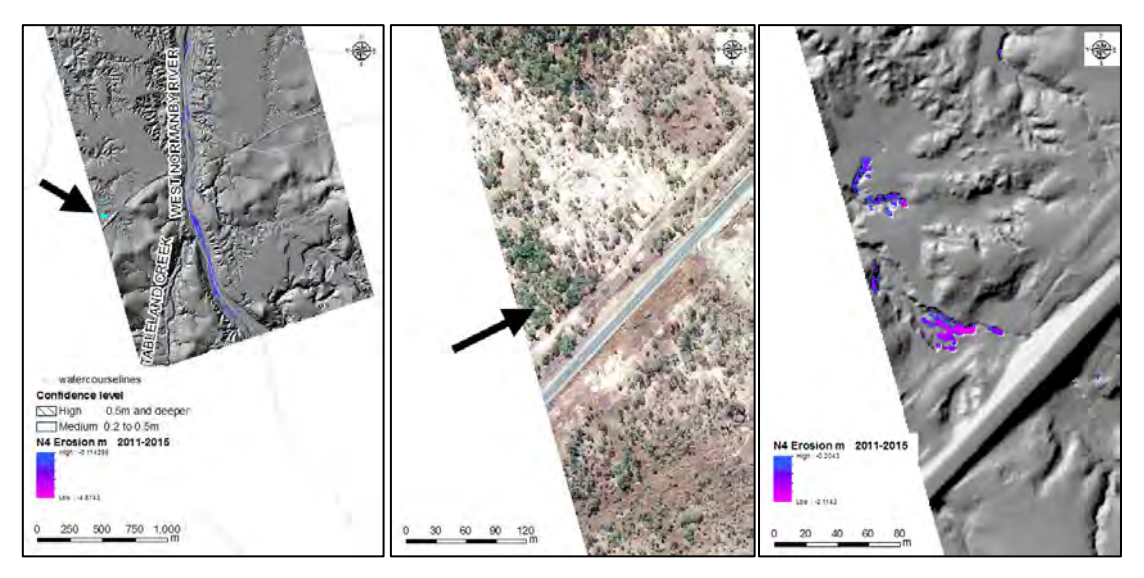


**Figure A43:** The largest erosion patch with-in a gully is seen as an incision into a gully floor here in this gully spanning the main road near the West Normanby. 328m³ of material in total was exported between the Lidar imaging.

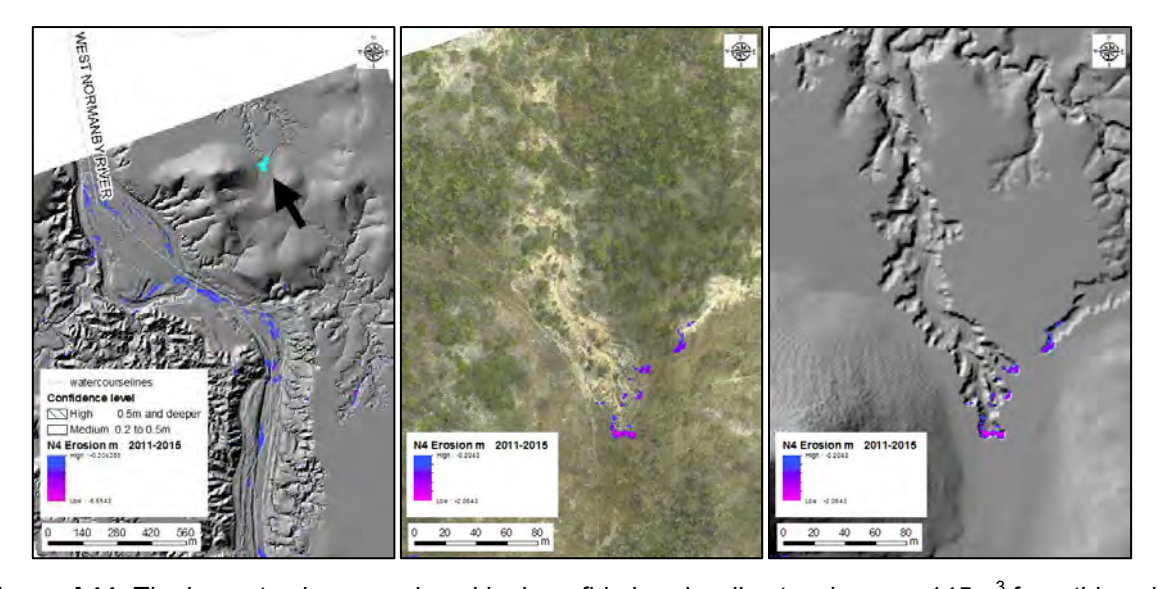
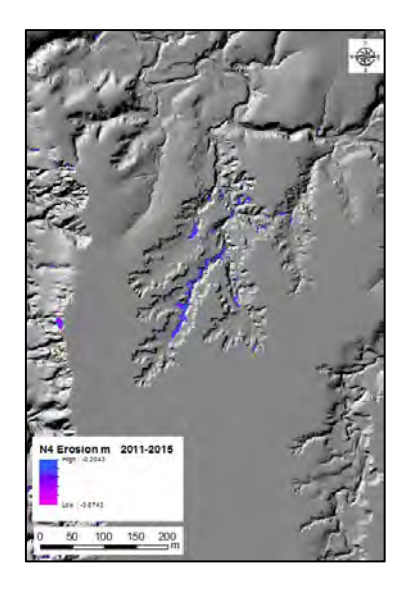


Figure A44: The largest volume produced by bonafide head wall extension was 145m<sup>3</sup> from this gully.



**Figure A45:** Development of this gully was mapped with historical air photo imagery. The main activity has been an advance of the incision in the gully floor. Total erosion from within the gully was 989m<sup>3</sup>.

Of this, 924m<sup>3</sup> was from incisions.

## 3.1.10 Observations from Deposition processing of the 2011 to 2015 timestep

- 82% of real deposition was onto main channel bedload surfaces.
- Areas of "shallow deposition" that with a depth of between 20cm and 50cm, had a total volume that was 76% of the volume of deep deposition.
- The West Normanby main channel had 95% of bedload deposition; the East had 5% of total bedload deposition.

# 3.2 Normanby LiDAR Block 5

Normanby LiDAR block 5 (Norm 5) covered the junction of the East and West Normanby rivers, which was approximately 250 km inland. The alluvial plains were at 80m elevation, surrounding hills rose to 305 m. Surprisingly few really active erosion sites were found in this block despite there being massive gully complexes visible in the orthophoto. Seven gullies were able to be tracked through time with historical air photos.

A very extensive and broad secondary channel occupied the western part of the block. This appeared to have significant amounts of bank erosion.

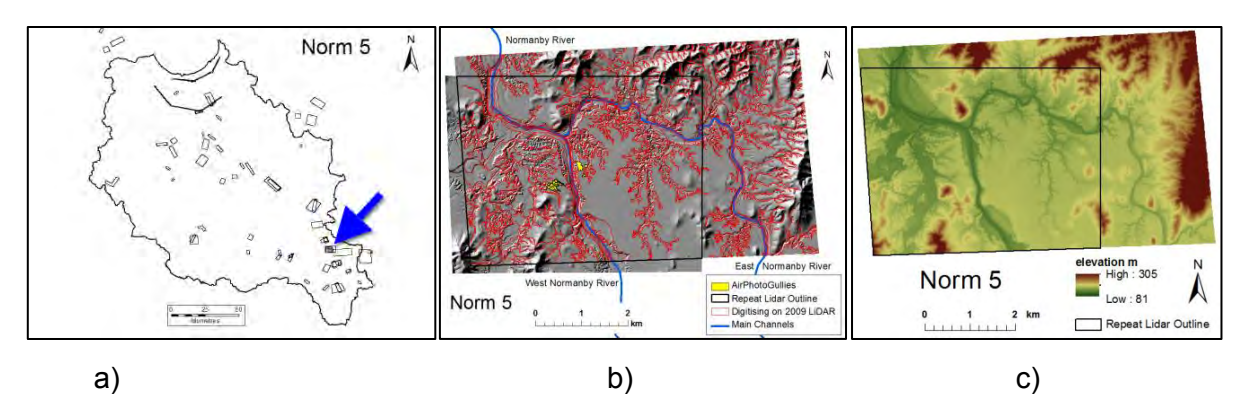


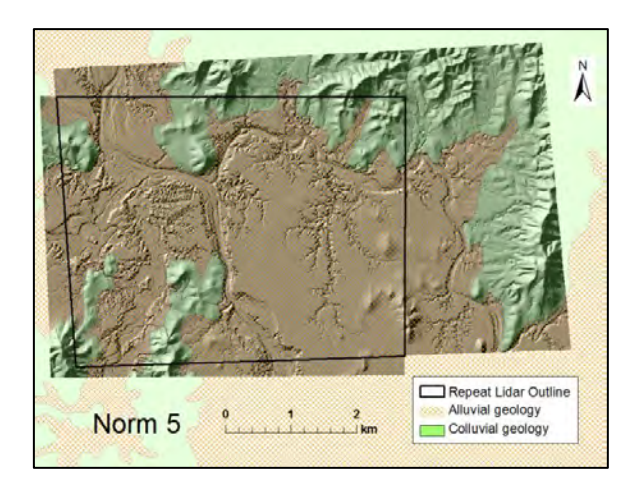
Figure A46: a) N5 location; b) Digitising on 2009 LiDAR; c) 2009 DEM.

Table A20: General statistics for Norm 5.

2009 LiDAR area (ha)	3485
Reprocessed change raster area (ha)	2097
Reprocessed extent elevation range (m)	280 - 270
Number of LiDAR digitised features	703
Number of Google Earth mapped gullies	104

#### Alluvial and Colluvial geology

The alluvial geology within the repeat LiDAR footprint was 75% of the block area. East of the repeat LiDAR footprint, colluvial slopes rose to 170m above the main channel elevation. Accuracy of boundary of alluvial/colluvial zone seemed reasonable in this block.



**Figure A47:** Alluvial and colluvial geology in Norm 5. Note that some low hills near the south east corner of the repeat LiDAR footprint are not mapped as colluvial, but possible should be, but overall the mapped boundary nicely delineates flat alluvial surfaces from slopes of colluvial surfaces.

## 3.2.1 Google Earth mapped gullies

Gullies mapped from Google earth were numerous on alluvial plains, with a total area of 39.6 ha. The area of GE gullies mapped on colluvial geology was 0.4ha.

The area of GE gullies was 11% of that mapped from LiDAR in the alluvial zone.

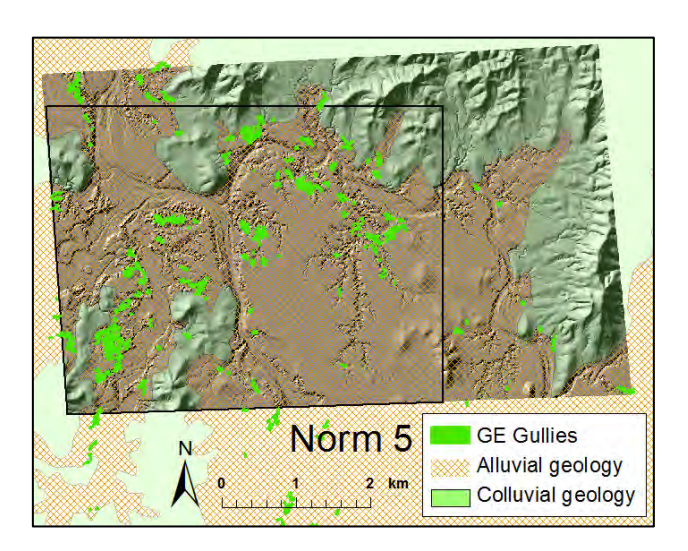


Figure A48: Location of Google Earth gullies in Norm 5.

Normanby 5	Area ha	Area of all features digitised from LiDAR ha	Features as % of zone	Area of gullies digitised from LiDAR ha	Area of gullies as % of zone	Area of Google Earth digitised gullies	GE gullies as % of zone
Alluvial zone	1684	881.4	52.3	344.8	20.5	39.6	2.4
Colluvial zone	412.7	49.6	12.0	40.1	9.7	1.7	0.4

Table A21: Quantifying LiDAR and GE gullies in alluvial and colluvial geology.

Of the alluvial geology in Norm 5, 20% of the area had been affected by gully erosion, and 30% by main or secondary channels. On colluvial slopes gully activity affected approximately 10% of the area.

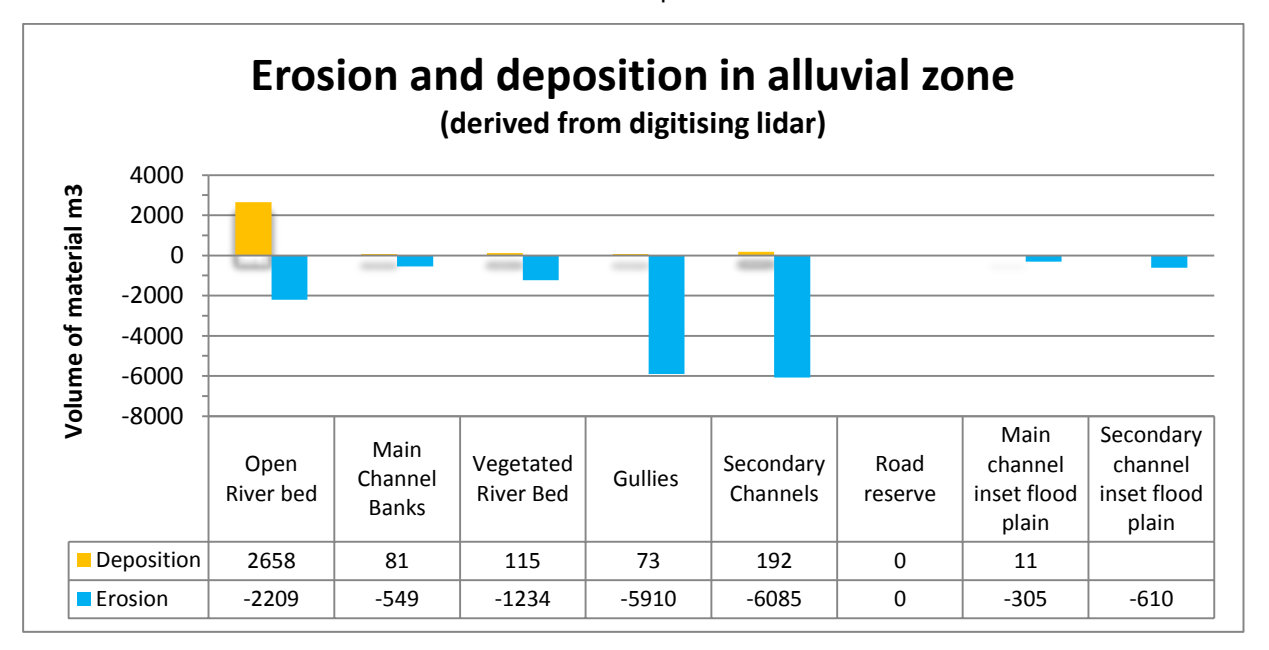


Table A22: Values for erosion and deposition on land units in Norm 5.

- The volume of erosion measured from alluvial gullies, 5910m3, was similar to the volume from secondary channels, 6085.
- The area of alluvial gullies was 345ha, whereas secondary channels were 141 ha.
- Yield from alluvial gullies was 8m3/ha/yr, but yield from secondary channels was significantly higher at 21m3/ha/yr.
- Open riverbed had a nett gain of 9m3/ha/yr, though vegetated channel bed, bank and inset flood plains had nett losses to erosion of 22, 4 and 1 m3/ha/yr respectively.

#### 3.2.2 Comparison of alluvial gullies to colluvial gullies

Table A23: Comparison of erosion and deposition between alluvial and colluvial geology.

Alluvial gullies			Colluvial gullies				
area ha	deposition m3	erosion m3	yield m3/ha/yr	area ha	deposition m3	erosion m3	yield m3/ha/yr
344.79	73	-5910	-8	40	15	-448	-5

Total erosion from alluvial gullies was an order of magnitude larger than erosion from colluvial gullies in Norm 5; 5910 m³ compared to 448 m³. Yield per hectare per year was similar for the two classes of geology; alluvial 8 m³/ha/yr, colluvial 5 m³/ha/yr; but the colluvial zone was 12% of the alluvial area.

#### 3.2.3 Comparison of Google Earth gullies to LiDAR gullies in the alluvial zone

Table A24: Comparison of erosion activity in LiDAR and Google Earth gullies.

	Area ha	Erosion m <sup>3</sup>	Yield m³/ha/yr
LiDAR alluvial gullies	344.8	-5910.3	-8.5
GE alluvial gullies	40	-904	-11

The area of Google Earth gullies was 11% of the area of LiDAR mapped gullies in the alluvial zone, but the volume of erosion coming from the area mapped as GE gullies was 15% of the total volume of erosion from LiDAR mapped gullies. This pattern is consistent with that found in other LiDAR blocks. The similar value of yield per hectare per year is a product of the differences in area of the two data sets.

#### 3.2.4 Gully Expansion 2009 - 2011

Mean area of expansion per site of erosion was reasonable low, at 2.4m2 per location. Overall, 111 m2 of alluvial land was overtaken by gully erosion between 2009 and 2011.

Table A25: Area of expansion of gullies between 2009 and 2011.

Gully Expansion 2009 - 2011	
number of gully expansion locations	47
sum area of gully expansions ha	111
mean area of expansion m2	2.4

## 3.2.5 Landscape Classification

Inset flood plains are present beside main and secondary channels. The 127 ha area of inset flood plain adjacent to secondary channels was approximately the same as the area mapped as secondary channel, 141 ha. The secondary heading to the south east corner of Figure A49 has progressed approximately 3 km from the main channel. It has 8 or more separate gullies radiating from it like octopus arms, dividing the flood plain into smaller units.

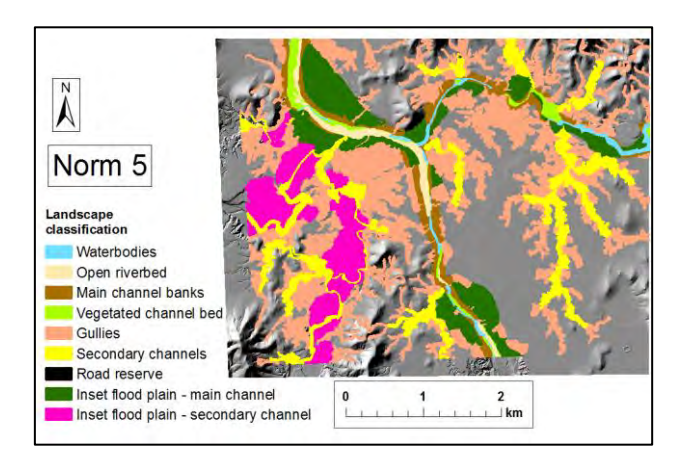


Figure A49: Distribution of landscape classes in Norm 5.

Area of each landscape classification 400 300 200 100 Main Secondary Main channel channel Open Vegetated Secondary Road Channel Gullies inset inset River bed River Bed Channels reserve **Banks** flood flood plain plain ■ Alluvial ha 24 345 141 0 138 127 61 26 ■ Colluvial ha 2 0 40 0 0

Table A26: Area of each landscape classification in block

### 3.2.6 Historical air photos

**Table A27:** Meta data of air photos used to identify gullies in Norm 5.

Image date	Photo ID	Scale	Flying height	RMS error	Air photo relative to 2009 LiDAR block
1/01/1952	QAP0310_030	23900	12750ft	0.86617	
1/01/1957	QAP0711_018	40000	20000ft	1.30106	
1/01/1982	QAP3977_162	25000	4600m	2.96476	
1/01/1987	QAP4112_159_1987	25000	4310m	1.85934	

Three gullies to the east of the main channel and one to the west of the main channel were identified from air photos with sufficient clarity to allow delineation of features in successive air photos. Erosion rates over five decades (1950s to 2009) and two decades (1980s to 2009) were 320% and 430% respectively higher than the rate over the 2 year period from 2009 to 2011 calculated from repeat LiDAR (See table A28). This was different to the average erosion rates over the same time frames for all LiDAR blocks, which showed a 2 year rate of 115 m3/ha/yr, compared to 91 m3/ha/yr (5 decades) and 112 m3/ha/yr (2 decades).

**Table A28:** Erosion rates for 4 gullies over 5 decades, 2 decades (from air photos) and 2 years (from LiDAR).

		Yield: volume material lost divided by area of 2009 gully divided by interval m3/ha/yr					
		Air pho	to data	LiDAR data			
	2009 area ha	1950s to 2009	2009 to 2011				
N05 eg1	0.33	no data	22	28.00			
N05 eg2	0.30	51	91	0.00			
N05 eg3	1.81	47	161	46.00			
N05 wg1	4.08	111	97	13.00			
Mean	1.63	70	93	22			

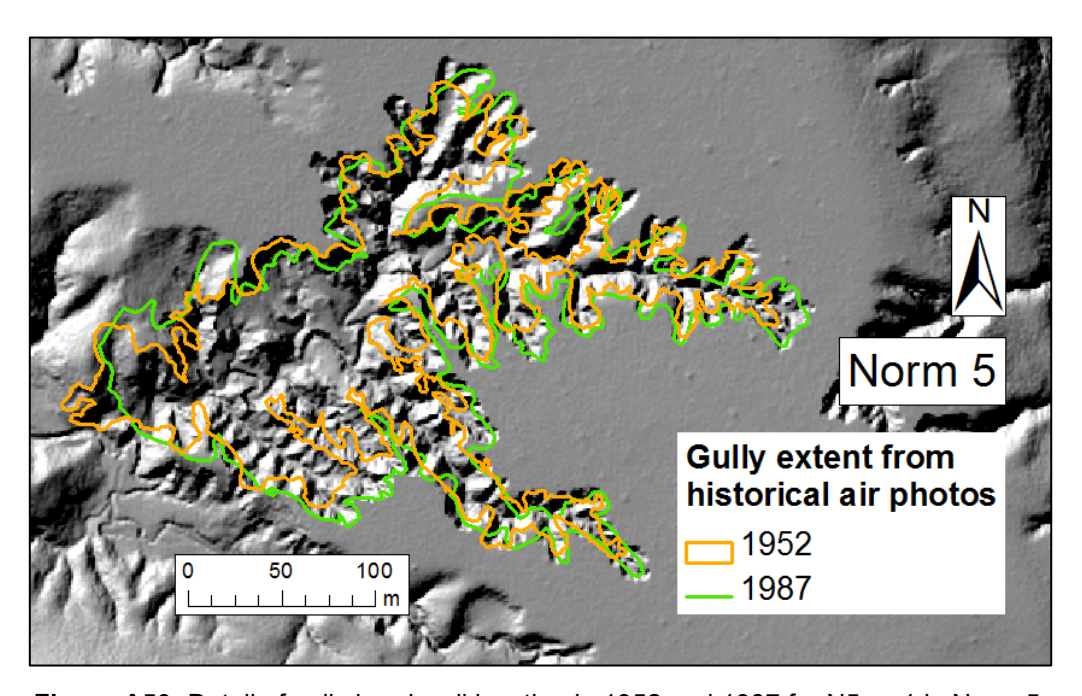
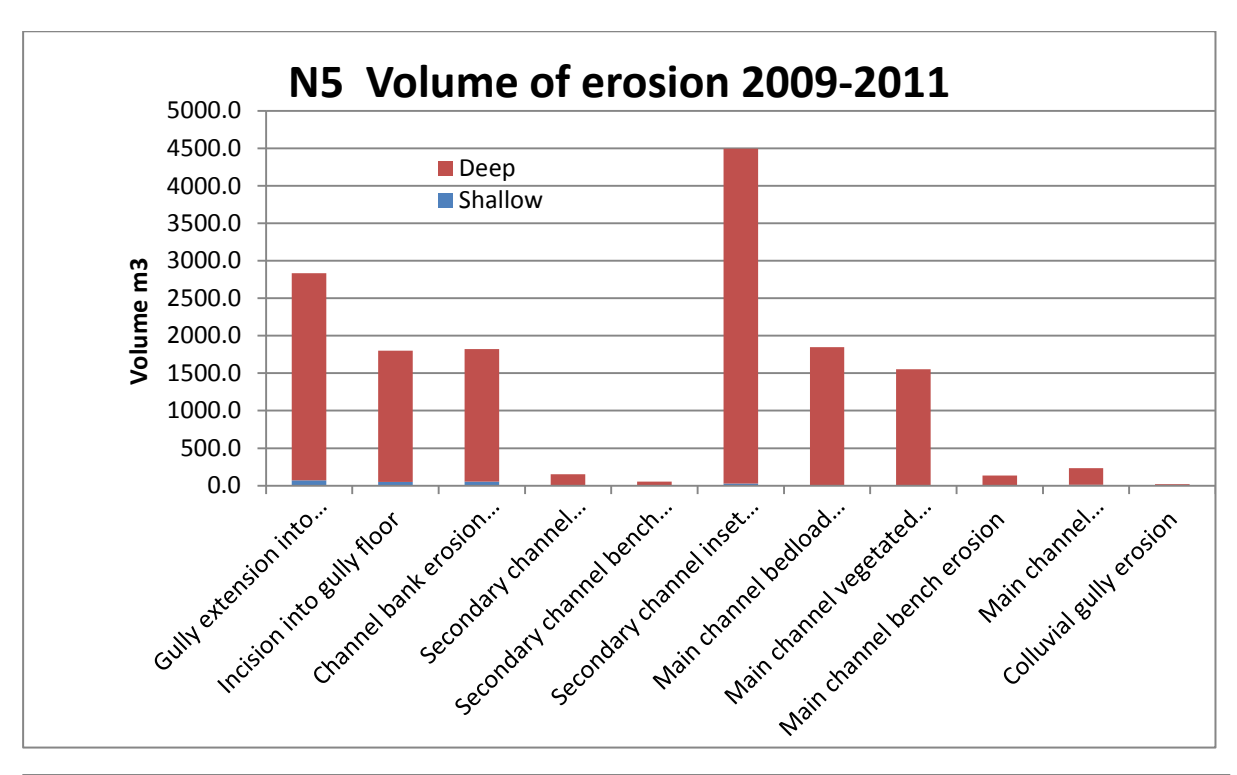


Figure A50: Detail of gully head wall location in 1952 and 1987 for N5 wg1 in Norm 5.

## 3.2.7 Summary results 2011 - 2015 and reprocessed 2009-11 data



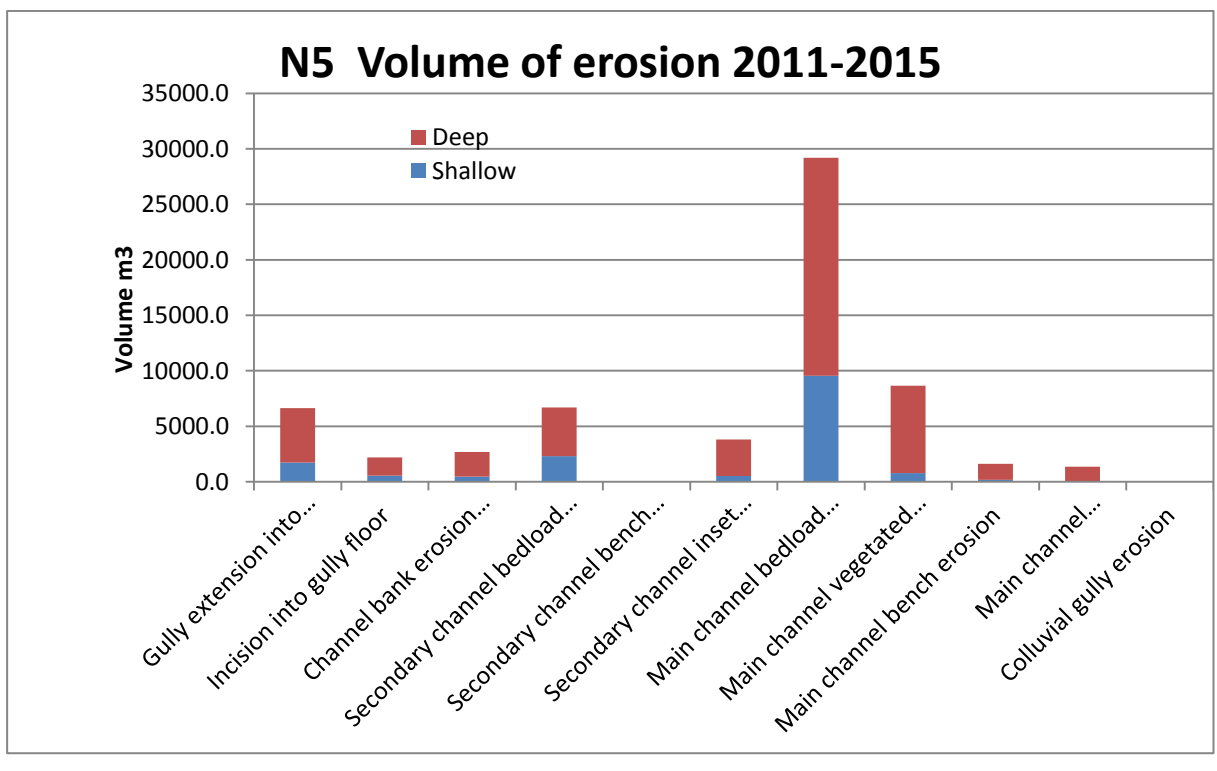
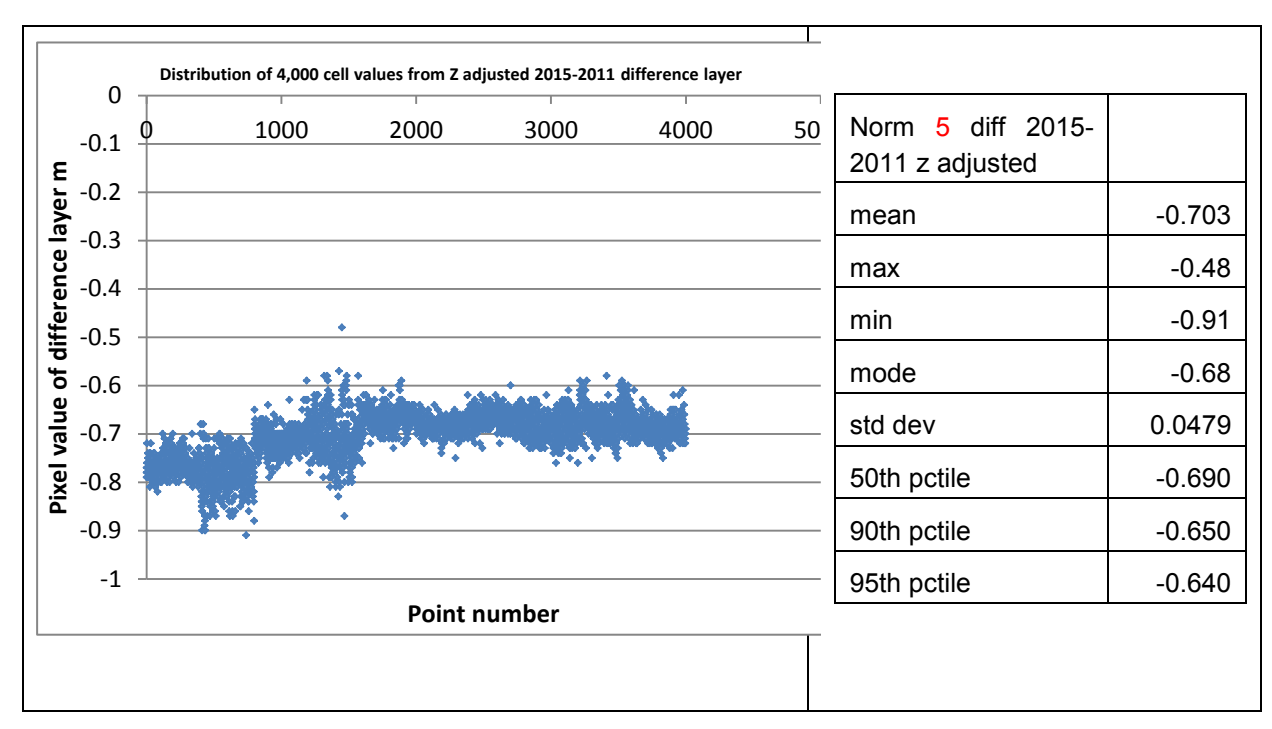


Figure A51: Erosion stats for Block 5 by geomorphic unit; 2009-11 (top); 2011-15 (bottom).

Z correction: 0.70253m was added to the 2015 Lidar.



**Figure A52:** Plot of 4000 points sampled to calculate correction factor. On right is statistics around the noise.

**XY correction:** 2015 DEM was nudged by X = 0, Y = +1m, which was the best of the shifts using 1m increments. But, the difference layer still looked very messy, and the volume of erosion polygons to edit was still overwhelming and likely to miss the real signal!!!

To further improve DEM alignment, the 2015 DEM was shifted by an experimental increment of X=0.5 and Y=0.25, with a subsequent conversion of Raster to TIN, and conversion of TIN back to raster; aligning cells with 2011 DEM, thus effectively sliding the slopes of the hillsides across and north a minor amount and resampling to get a DEM with a sub-metre coordinate shift. The result was to greatly reduce the number of junk polygons to edit from the Deep Erosion polygon layer.

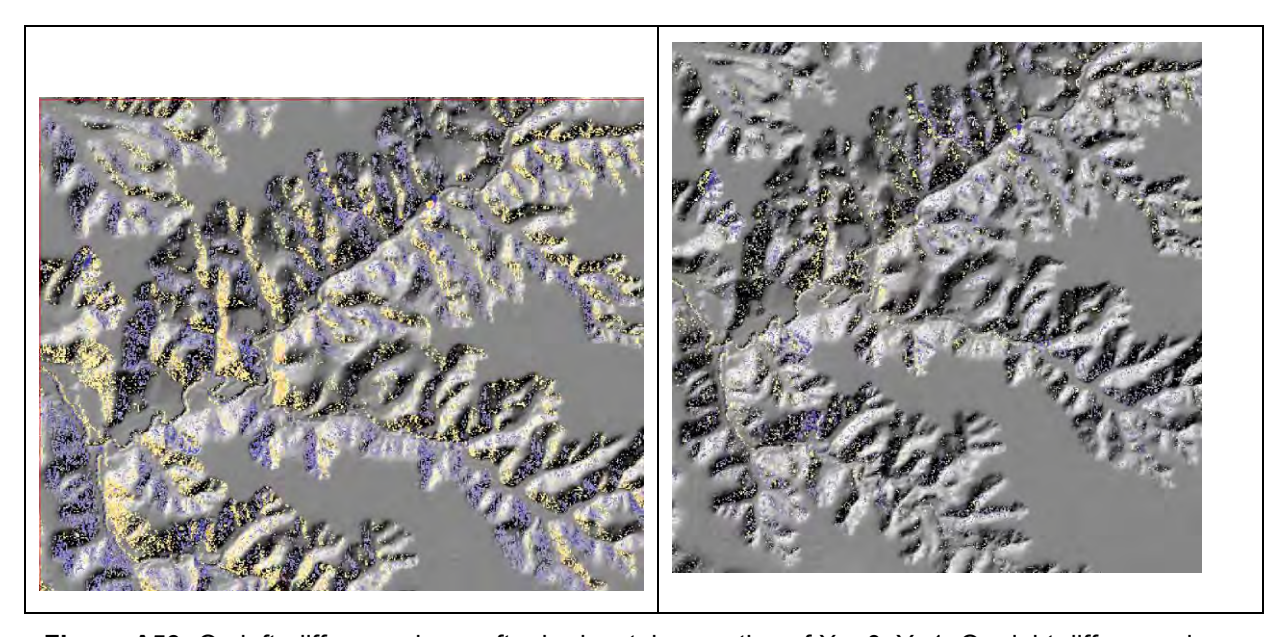
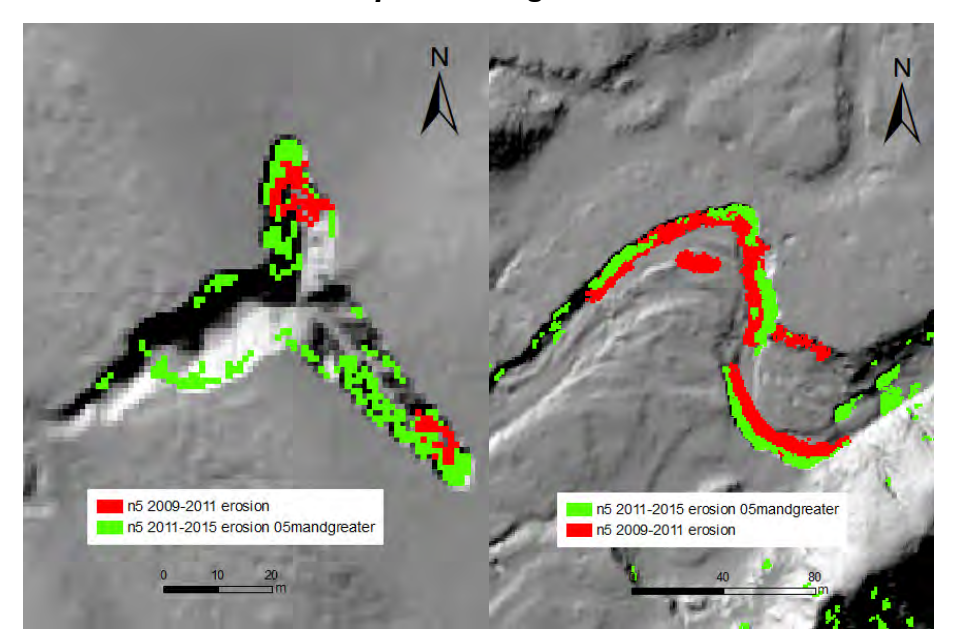


**Figure A53:** On left, difference layer after horizontal correction of X = 0, Y=1. On right difference layer after furthur horisontal correction of X=0.5 and Y=0.25.

Values	Statistic	OptimumCoordShift	Reference X0Y0
0.032438	Lowest mean	2015X_3Y_3	-0.010894528
1.41252	Lowest max	2015X0Y1_m	2.092519999
-1.95747	Smallest min	2015X0Y1_m	-2.737479925
-0.00748	mode	2015X_1Y_1	-0.00747681
0.17443	std dev	2015X0Y1_m	0.358214339
-0.02748	50th pctile	2015X3Y_3_	-0.00747681
0.152519	90th pctile	2015X0Y1_m	0.412521005
0.252525	95th pctile	2015X0Y1_m	0.602523983

Figure A54: Statistics supporting the XY shift to minimise variance in 25,000 points sampled.

## 3.2.8 Observations from Erosion processing



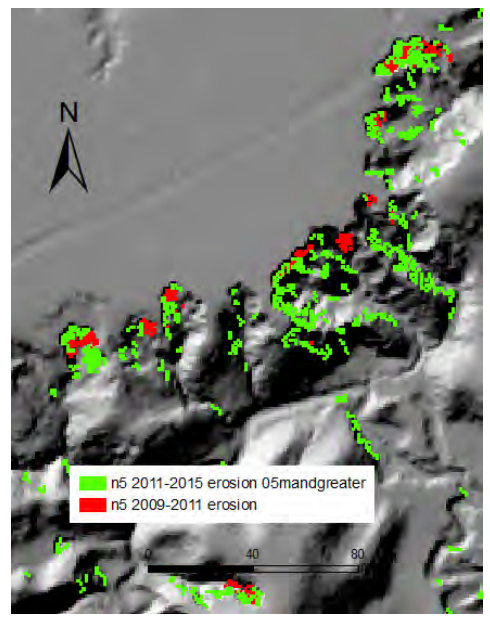


Figure A55: Differences between erosion 2009-11; 2011-15.

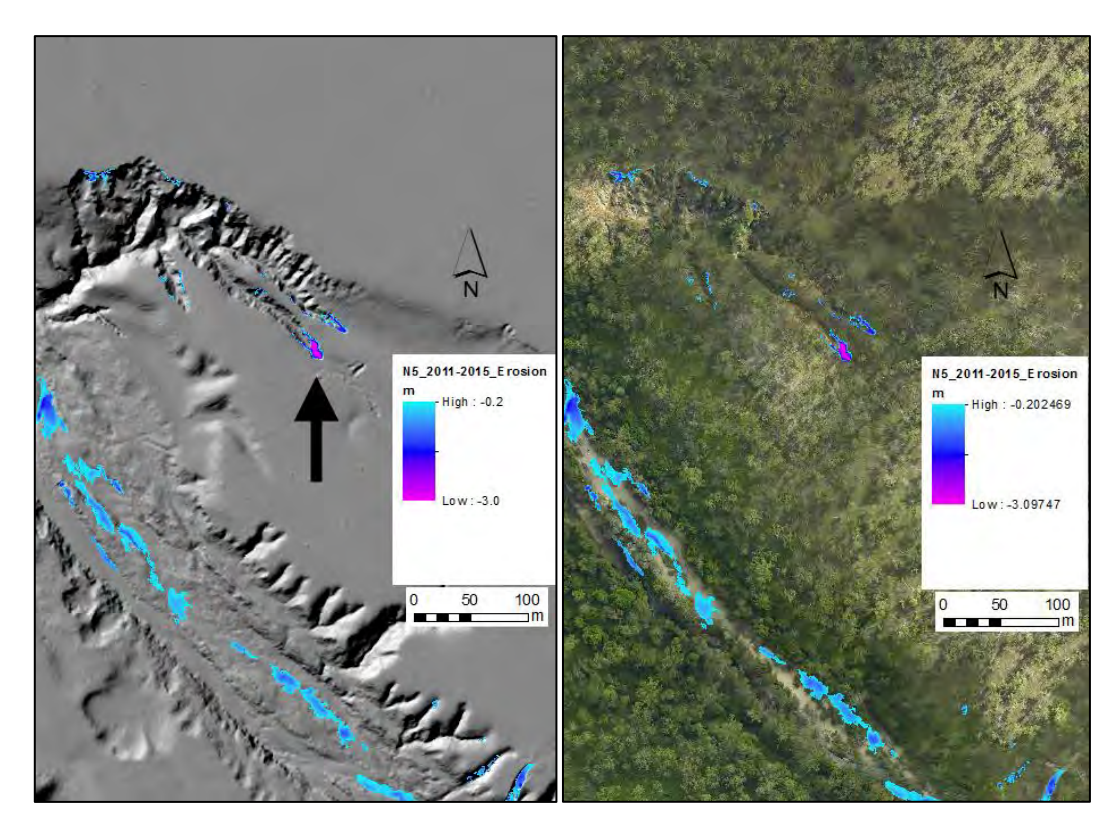
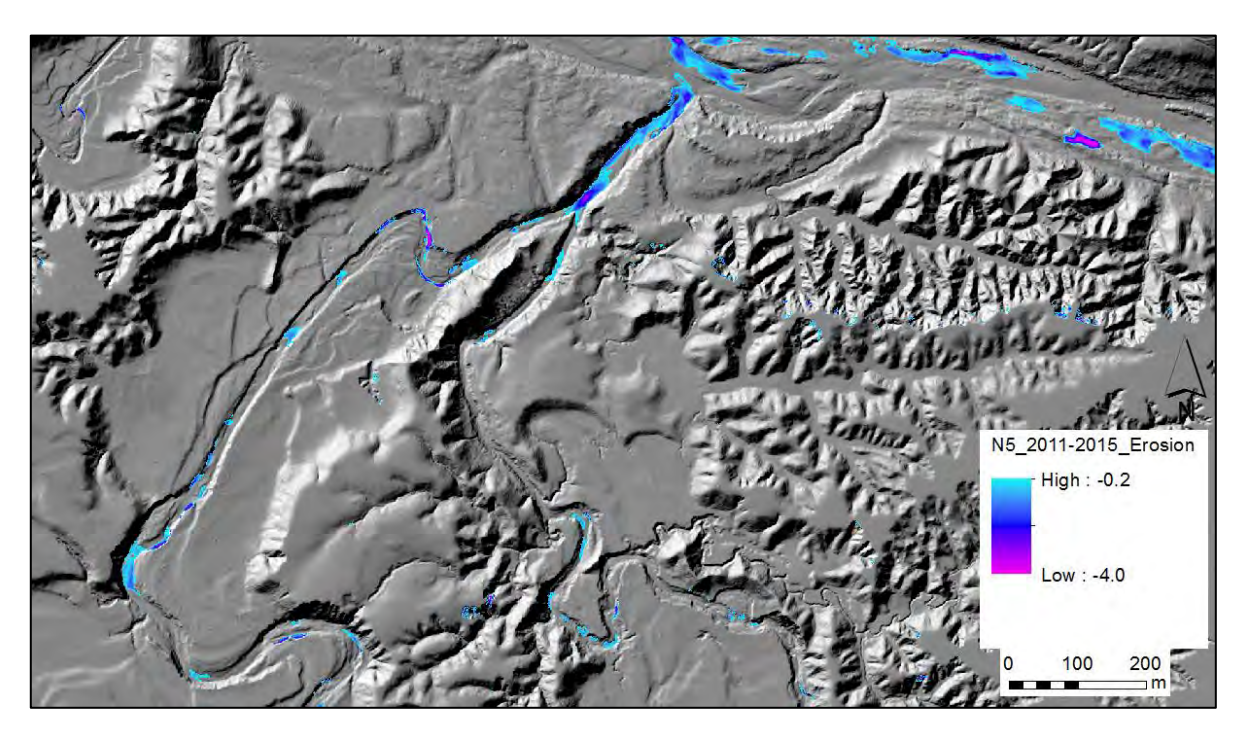


Figure A56: Arrowed gully advanced 20m between 2011 and 2015 Lidar.



**Figure A57:** Detail of secondary channel; note inset flood plain getting eroded at hairpin bend near top left of picture.

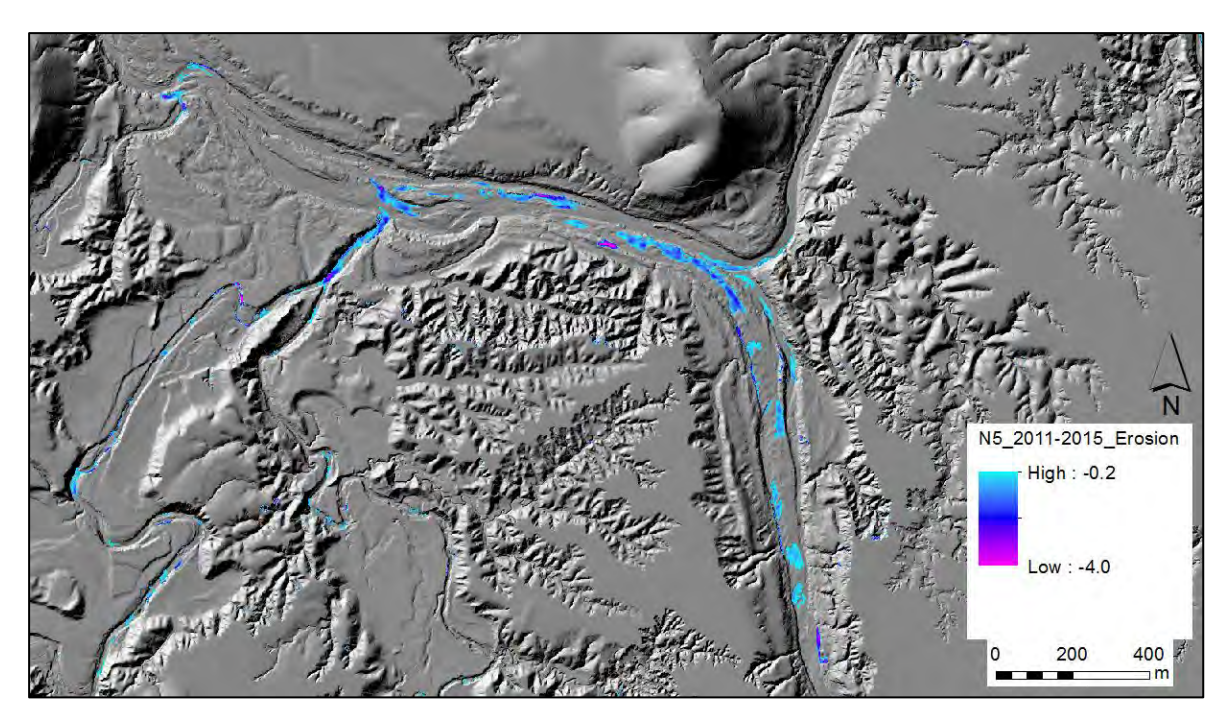


Figure A58: Overview of erosion in main channel and secondary stream.



Figure A59: Erosion in main channel and secondary stream with orthophoto from 2009.

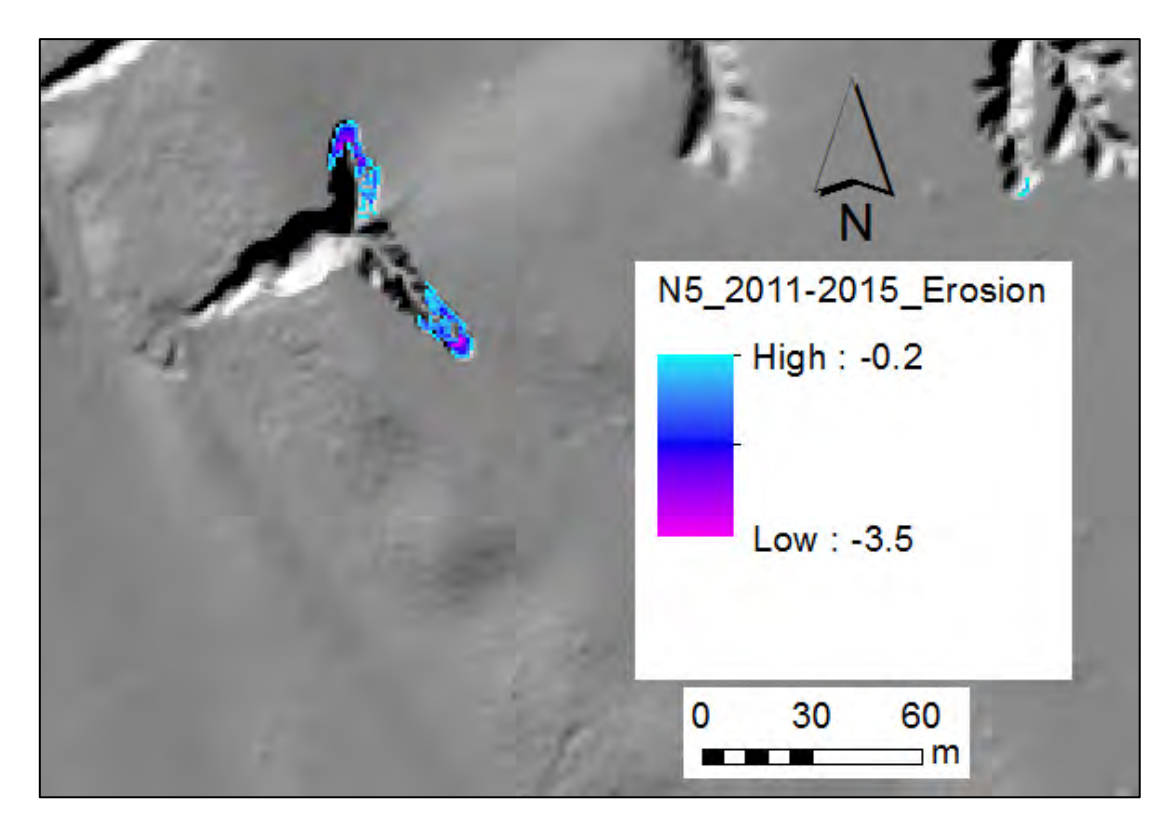


Figure A60: Gully with advance of around 20m.

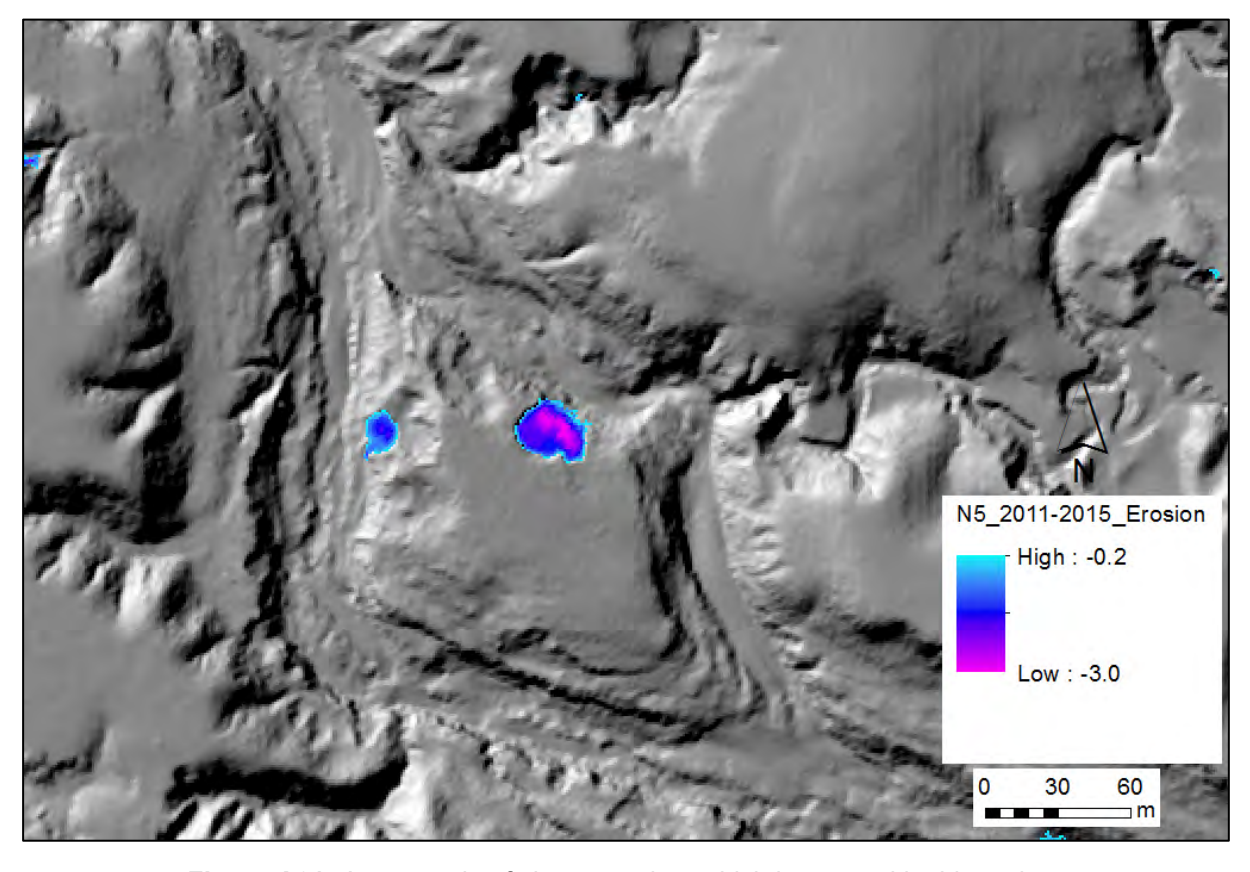


Figure A61: An example of slump erosion, which is unusual in this region.

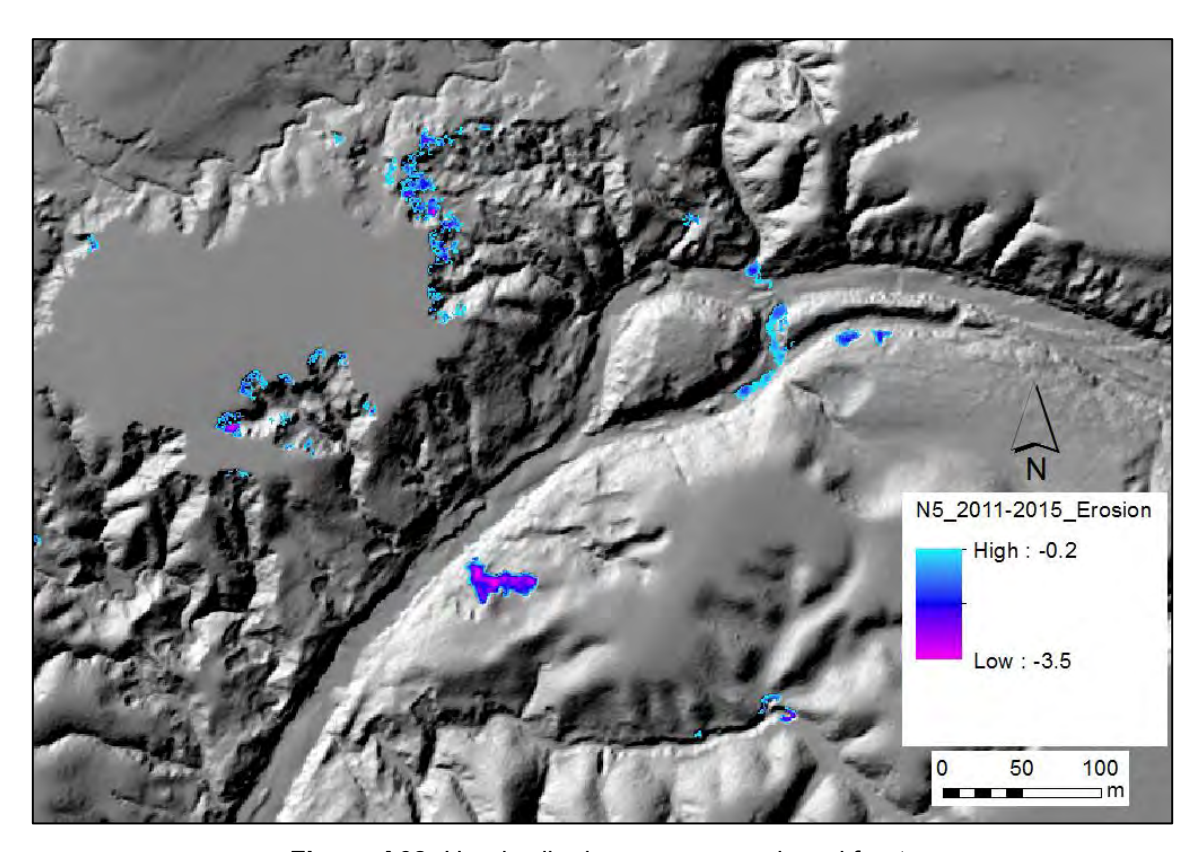


Figure A62: Headwall advance across a broad front.

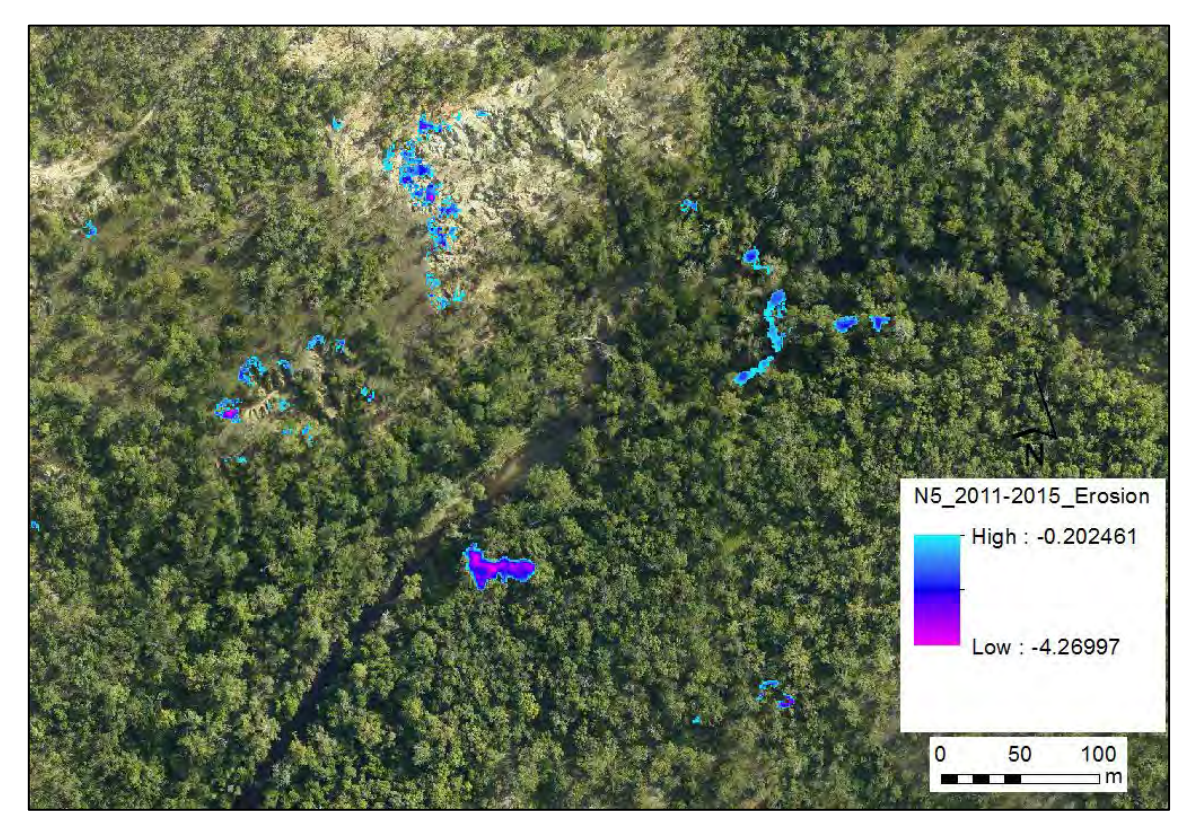


Figure A63: Advancing gully headwalls with orthophoto from 2009 for context.

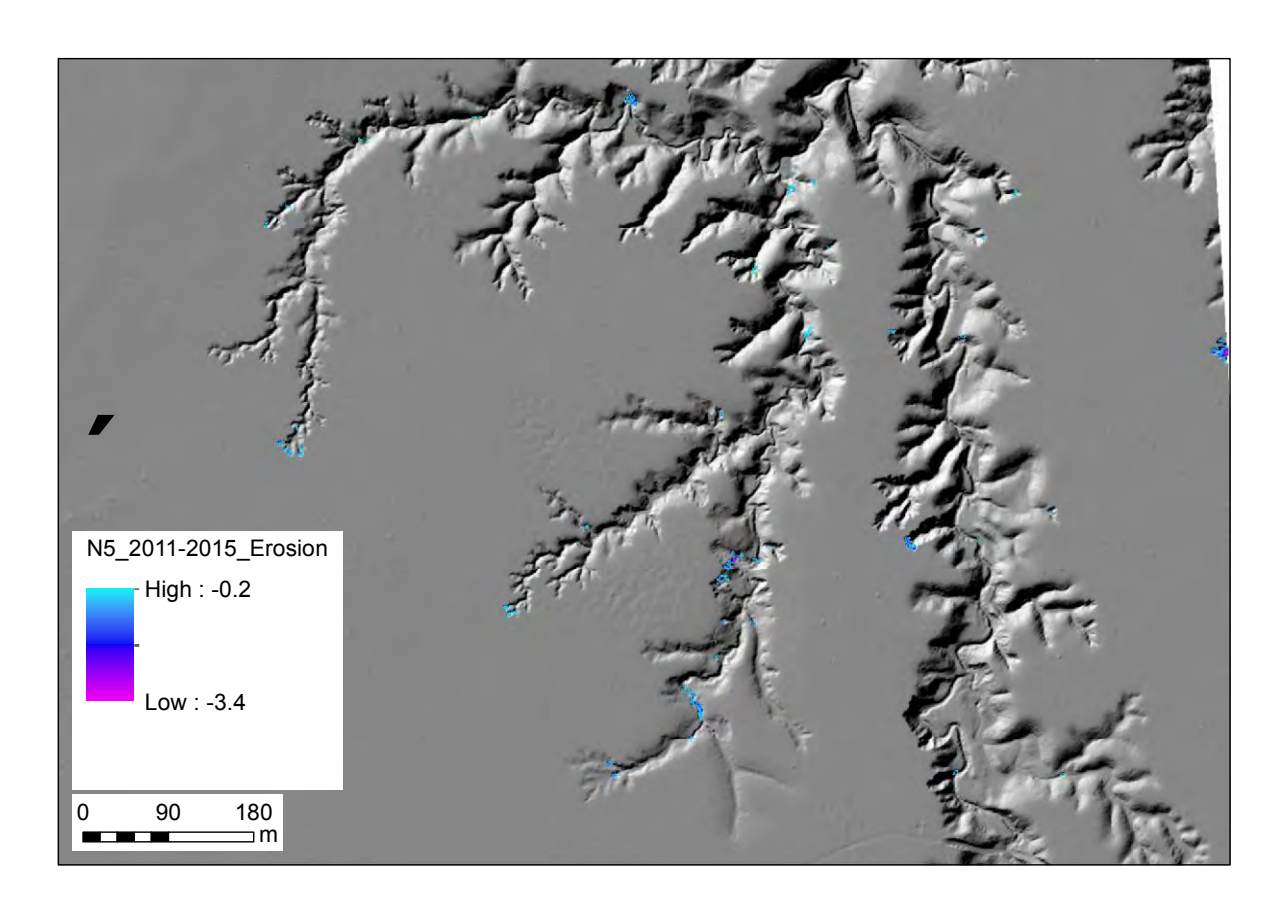


Figure A64: Detail of gully extension and incisions into gully floor. Headwalls have advanced 5-10m.

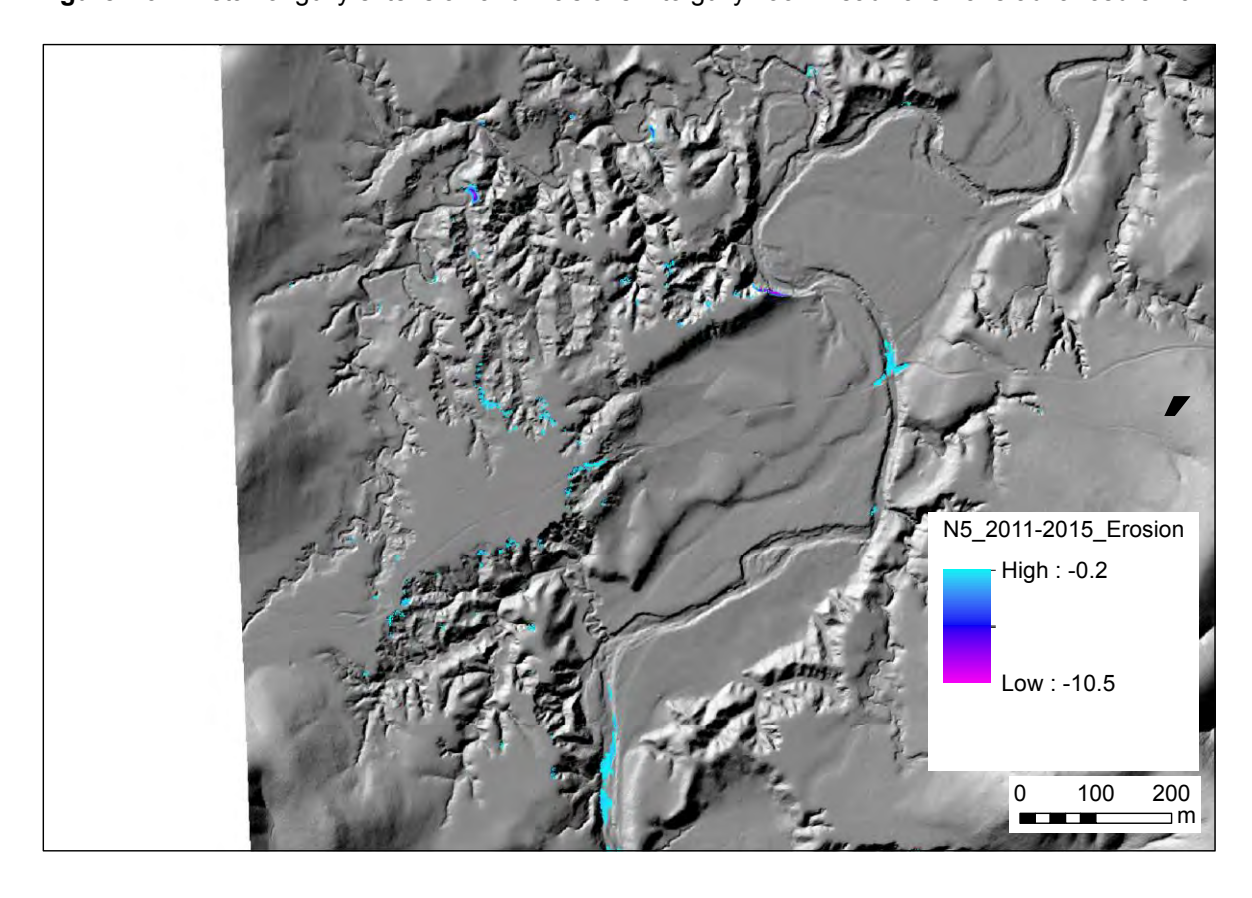


Figure A65: Detail of massive gully head wall advances.

# 3.2.9 Observations from Deposition processing

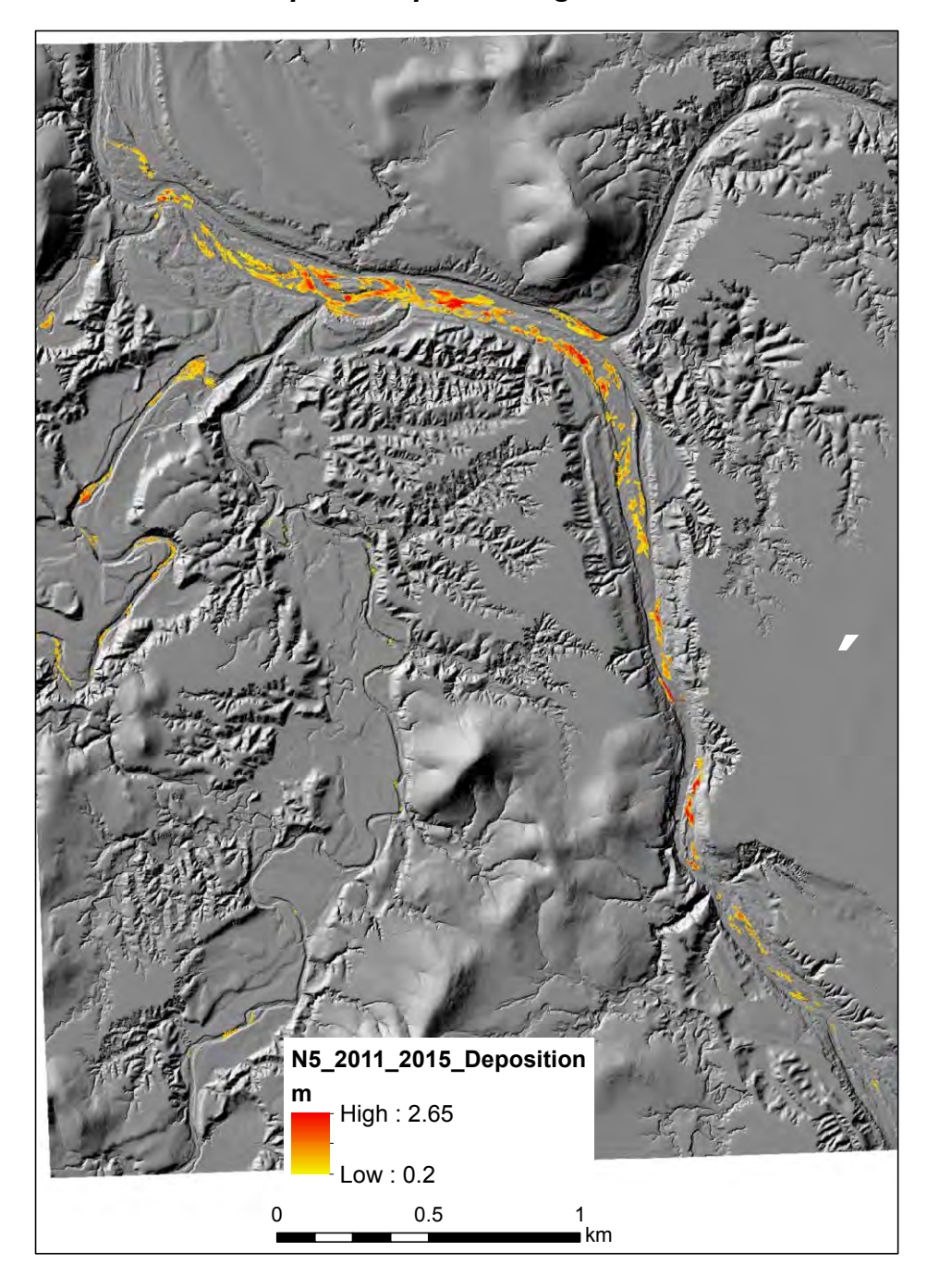


Figure A66: Patterns of deposition in N5 between 2011 and 2015.

## 3.3 Normanby LiDAR Block 7

Normanby 7 LiDAR block was the highest in the catchment, a narrow corridor of alluvial geology between ranges rising to 320m above the alluvial flats. The main stream running through the block was the Granite Normanby River. This block had the second highest volume of alluvial gully erosion measured of the 14 repeat LiDAR blocks, 14,000 m3 between 2009 and 2011. Major erosion was seen along head walls of amphitheatre gullies encroaching virgin flood plain, also from incisions in floors of massive gullies and extension of linear gullies.

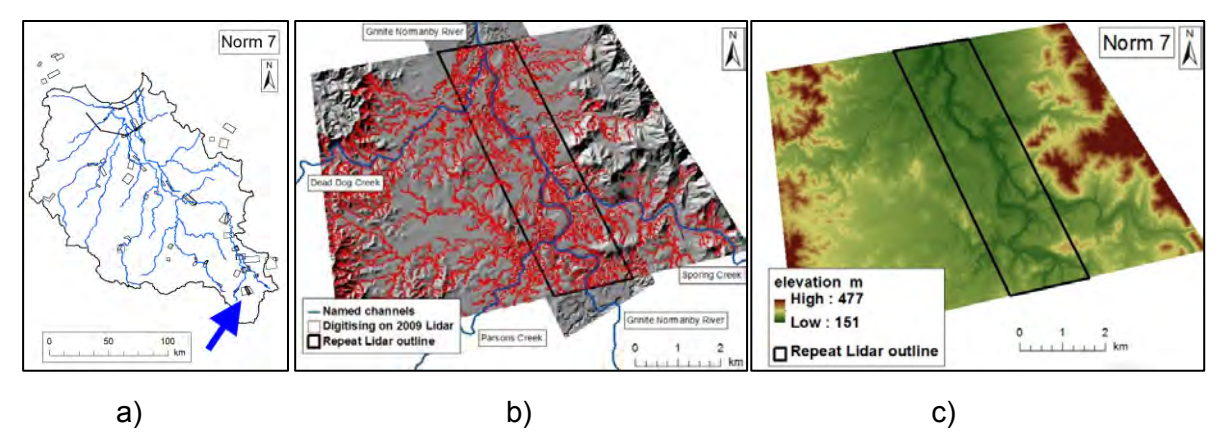


Figure A67: a) Norm 7 location;

b) Digitising on LiDAR; c) DEM from 2009 LiDAR.

**Table A29:** General statistics for Normanby 7 LiDAR block.

2009 LiDAR area (ha)	5200
Reprocessed change raster area (ha)	150 - 240
Reprocessed extent elevation rang (m)	150 - 240
Number of LiDAR digitised features	655
Number of Google Earth mapped gullies	134

## 3.3.1 Alluvial and Colluvial geology

Though surrounded by colluvial geology, the narrow boundary of the repeat LiDAR footprint limited the colluvial zone to 5% of the area used for erosion detection from repeat LiDAR. 50% of the alluvial zone had erosion features that were digitised, whereas the colluvial zone had few erosional features, and only 15% of the foothills extending into the block were digitised as gullies.

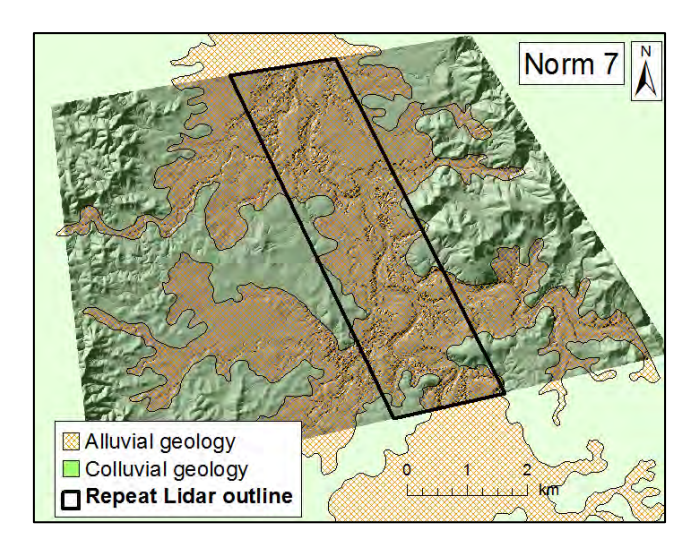


Figure A68: Alluvial and colluvial geology in Norm 7.

## 3.3.2 Google Earth mapped gullies

Gullies mapped from Google earth were very abundant in this highest part of the catchment. But despite looking to dominate the map, just 7.3% of the alluvial zone was mapped as gullies from Google Earth, compared to 24% of the alluvial area mapped as gullies from LiDAR, see table A30. Gullies did extend into the colluvial zone, 7% was mapped as gullies from LiDAR, but these gullies were not so visible in Google Earth imagery, as a bare 1% of the colluvial zone was mapped as being a gully from Google Earth.

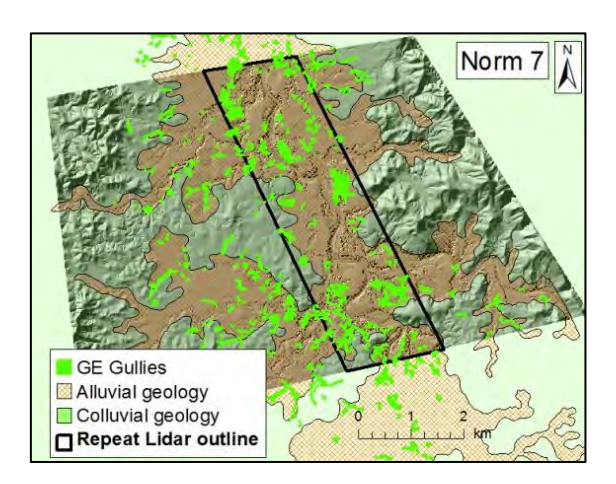


Figure A69: Distribution of gullies mapped from Google Earth.

T 11 400 0 "	11 10		
l able A30: Gully area	i digitised from LiDAR and	l Google Earth in alluvial an	d colluvial geology.

Normanby 7	Area ha	Area of all features digitised from LiDAR ha	Features as % of zone	Area of gullies digitised from LiDAR ha	Area of gullies as % of zone	Area of Google Earth digitised gullies	GE gullies as % of zone
Alluvial zone	966	474.6	49.1	229.1	23.7	70.6	7.3
Colluvial zone	148	21.5	14.6	10.40	7.0	1.5	1.0

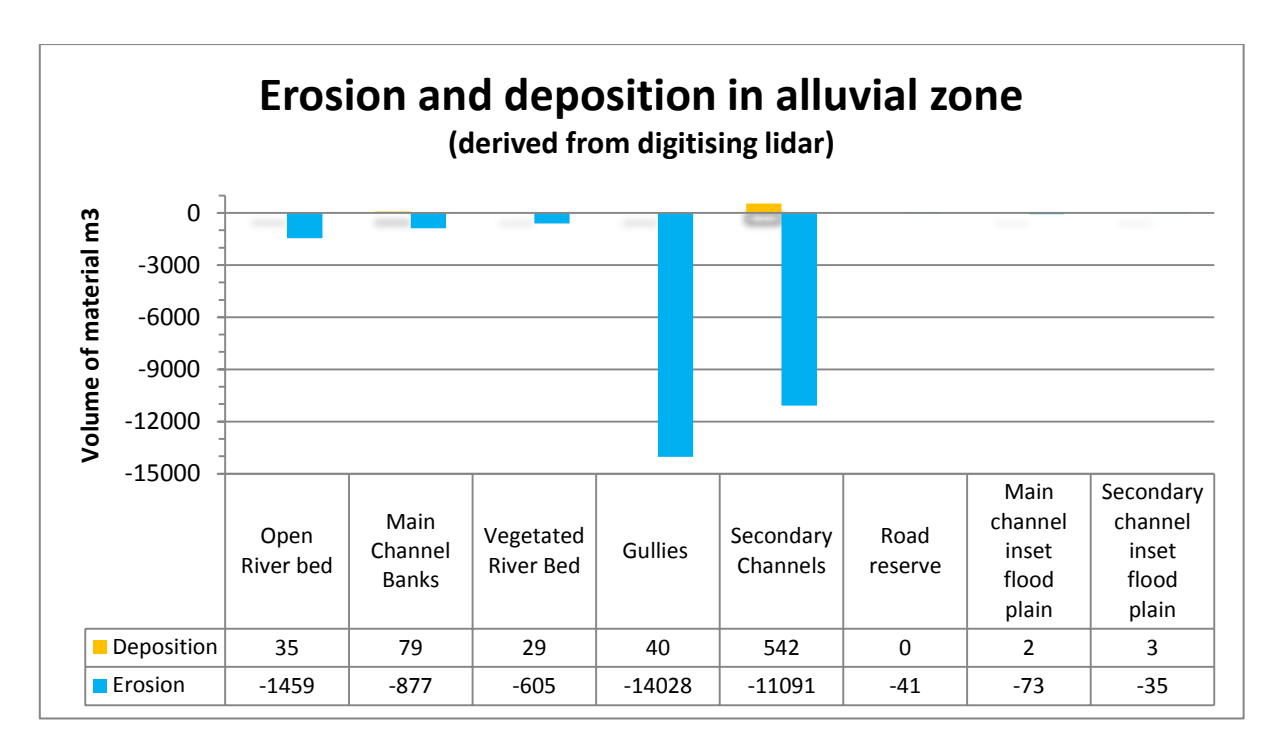


Figure A70: Quantifying erosion and deposition in alluvial and colluvial zones

- Huge amounts of material have eroded from alluvial gullies between 2009 and 2011, 14,000 m3, which was nearly matched by erosion from within secondary channels, 11,091 m3 over two years.
- Erosion from road runoff exceeded the amount of material removed from inset flood plains in secondary channels.
- 74% of deposition in this block occurred in secondary channels, but the volume of deposition was a mere 5% of the volume eroded from within secondary channels. A major export from secondary channels has occurred.
- Main channel landscape units each suffered large amounts of erosion, with little deposition measured in the main channel.

#### 3.3.3 Comparison of alluvial gullies to colluvial gullies

**Table A31:** Comparison of erosion activity in alluvial and colluvial gullies.

Alluvial gullies				Colluvia	l gullies		
area ha	deposition m <sup>3</sup>	erosion m <sup>3</sup>	yield m³/ha/yr	area ha	deposition m <sup>3</sup>	erosion m <sup>3</sup>	yield m³/ha/yr
229.07	40	-14028	-31	10	0	-553	-27

The area of gullies in colluvial geology in the repeat LiDAR footprint was relatively small, 10 ha, but in keeping with the highly active nature of this landscape, the volume of erosion from those 10 ha of gullies, 553 m3, was similar to the volume of erosion from 14ha of vegetated river bed, 605 m3.

## 3.3.4 Comparison of Google Earth gullies to LiDAR gullies in the alluvial zone

Table A32: Comparison of erosion activity in LiDAR and Google Earth gullies.

	Area ha	Erosion m <sup>3</sup>	Yield m³/ha/yr
LiDAR alluvial gullies	229	-14028	-31
GE alluvial gullies	71	-7842	-55

In Norm 7, the area of gullies visible and digitised from Google Earth imagery was 31% of then area of alluvial gullies defined from LiDAR, which was actually quite a high representation compared to other blocks. Google Earth gully foot print captured 56% of erosion that was measured in LiDAR gullies, also a high value compared to some blocks.

#### 3.3.5 Gully Expansion 2009 - 2011

The active rates of erosion in Norm 7 were reflected in the number of locations where erosion was measured at the boundary of gullies between 2009 and 2011. Gully expansion occurred at 172 locations, with an average 7.7 m<sup>2</sup> lost in each instance over two years.

Table A33: Area of expansion of gullies between 2009 and 2011.

Gully Expansion 2009 - 2011	
Number of gully expansion locations	172
Sum area of gully expansions ha	0.13
Mean area of expansion m2	7.4

## 3.3.6 Landscape Classification

Several secondary channels have developed in parallel with the Granite Normanby River, the main drainage in the valley. Gullies on alluvial geology were the dominant landscape feature in the LiDAR block, being 51% of the alluvial area, or 49% of the total area. A proportion of the 117 ha of secondary channels could be reclassified as secondary channel flood plain if time had been available to add detail at that scale.

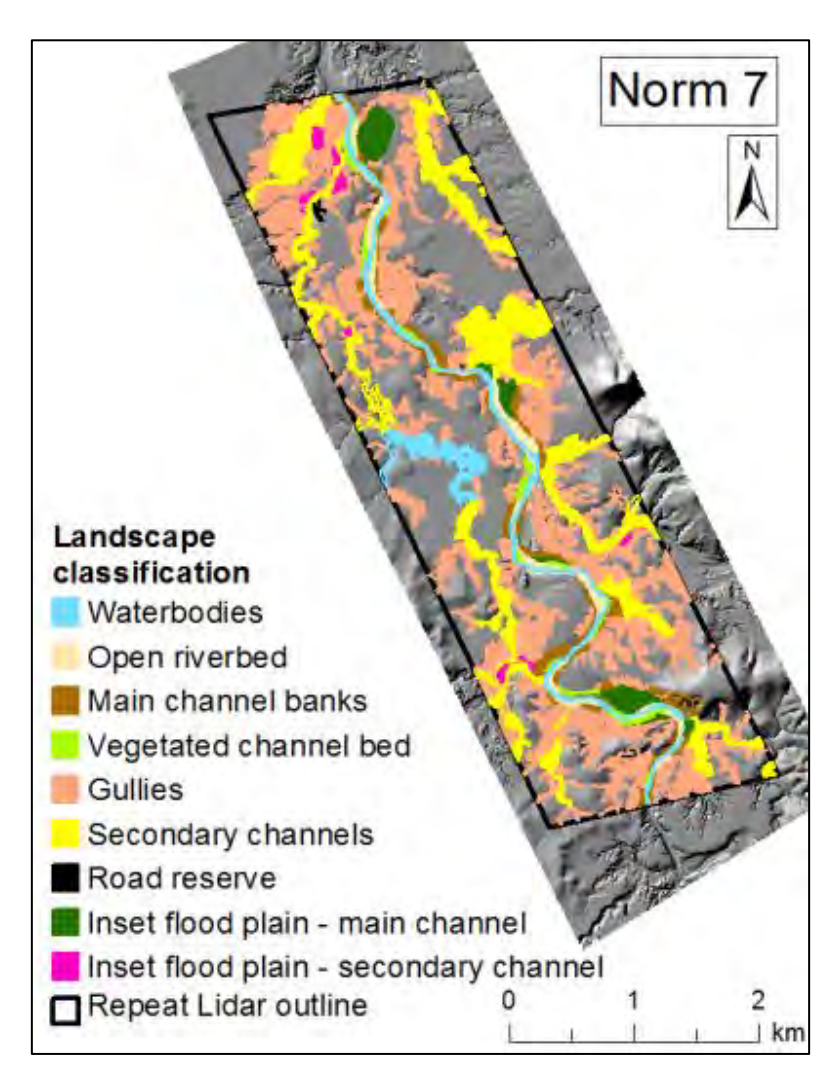


Figure A71: Landscape classification in Norm 7.

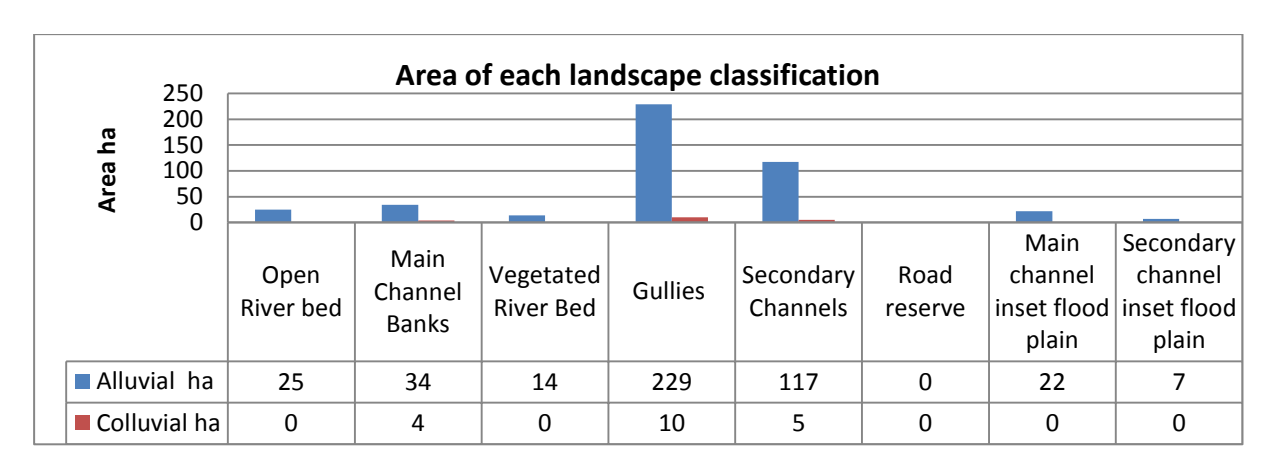
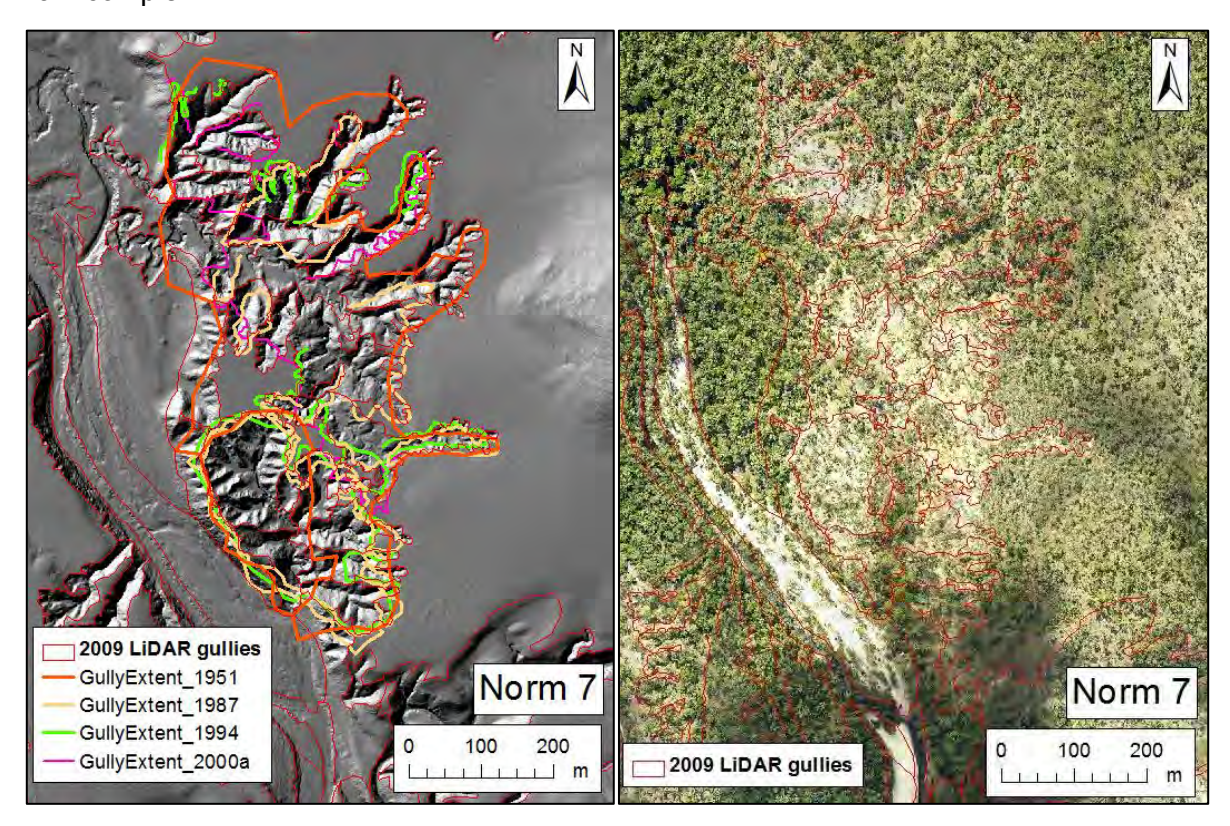


Figure A72: Area of each landscape unit in alluvial and colluvial zones.

### 3.3.7 Historical air photos

Despite many massive and active gullies throughout Norm 7, there was no success defining gully perimeters to acceptable levels of accuracy. Figure A73 shows digitising done at 4 time slices, with various problems such as miss-registration of air photo imagery, incomplete digitisation of gully walls due to poor definition of features, a lack of visible head walls, and vegetation on the walls of linear gullies radiating from the main complex.



**Figure A73:** Example of a gully that looked so clear in LiDAR (left), but was frustratingly difficult to define from visual imagery (right).

### 3.3.8 LiDAR 2015 Erosion Summary Data & Reprocessed 2009-11 data

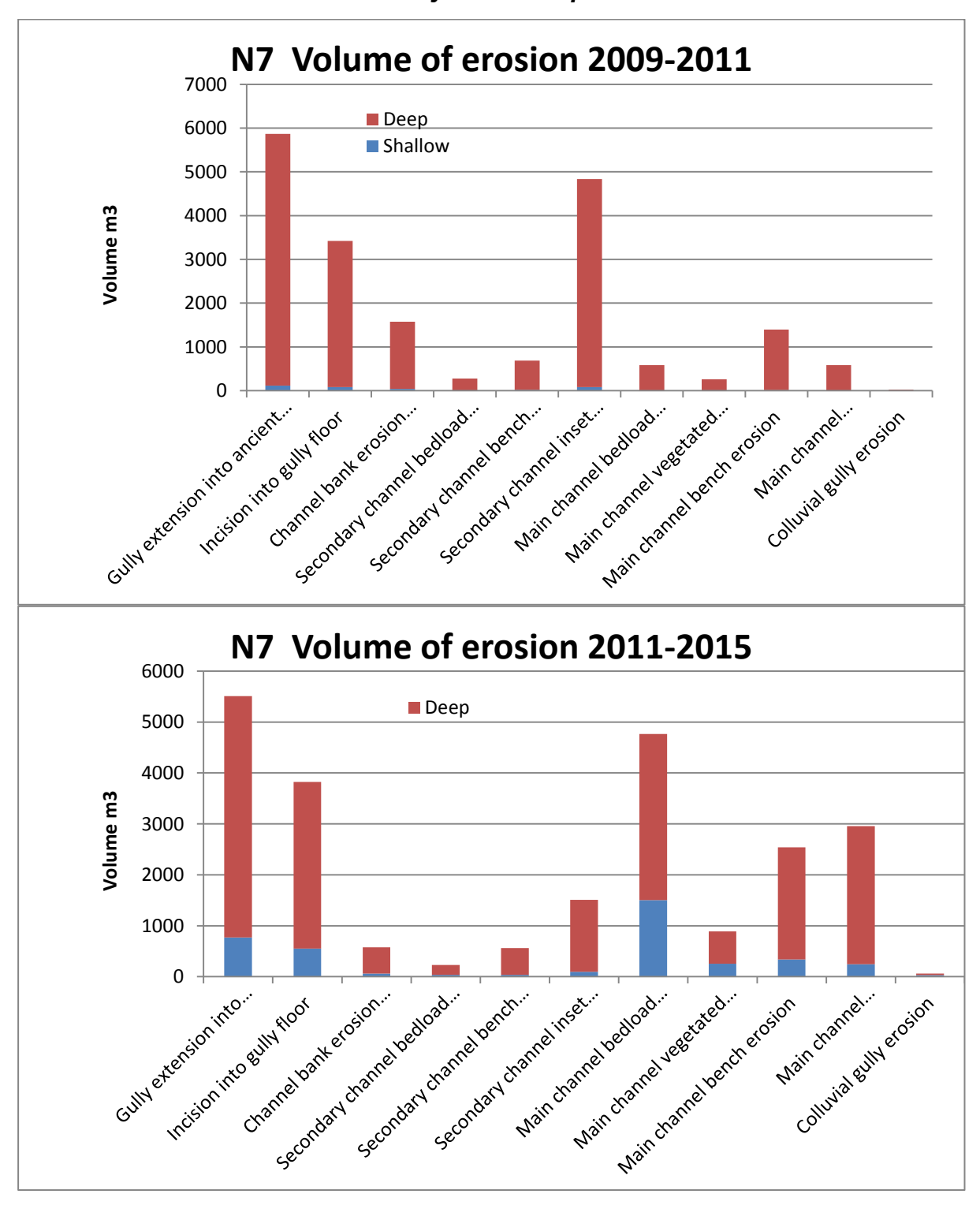


Figure A74: Erosion stats for Block 7 by geomorphic unit 2009-11 (top); 2011-15 (bottom).

## 3.4 Normanby LiDAR Block 9

Normanby LiDAR block 9 (Norm 9) was the furthest upstream block on the East Normanby River, laying 290 km inland, covered 501 ha at the junction of the East Normanby River and

Welch Creek, and had the distinction of having the largest volume of erosion from main channel banks of all LiDAR study blocks. Elevation ranged from 145 m on alluvial flats to 255m peaks to the south east of the repeat LiDAR footprint.

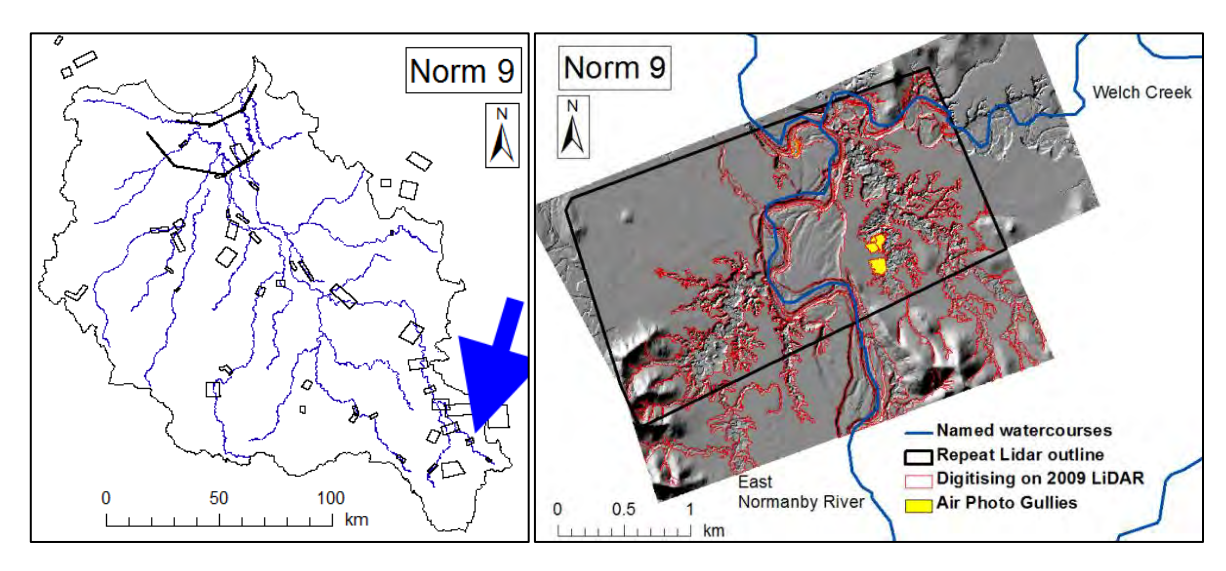


Figure A75: Location of Norm 9 (left); Features in Norm 9 (right).

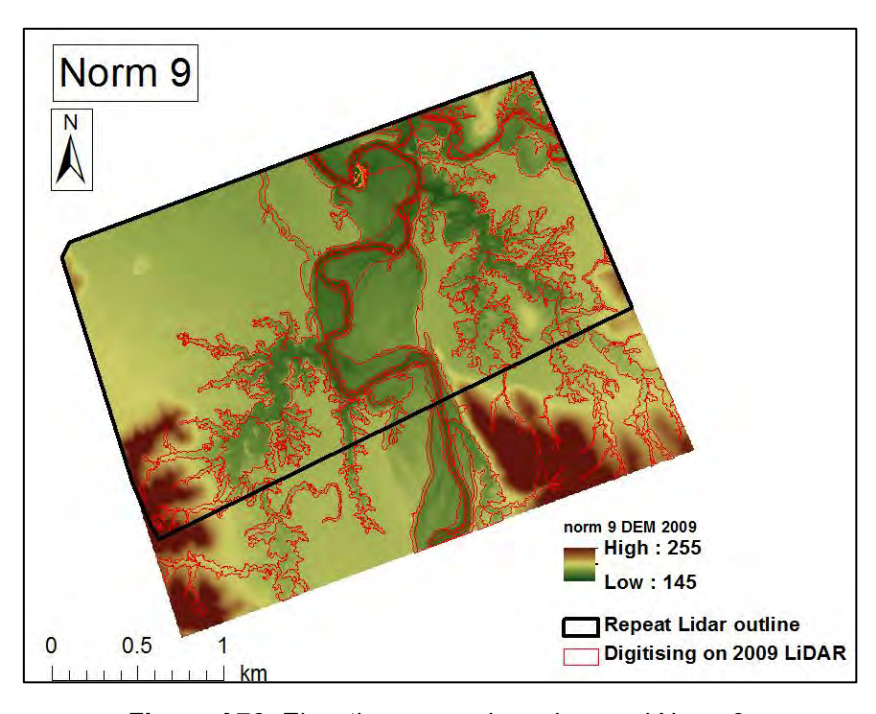
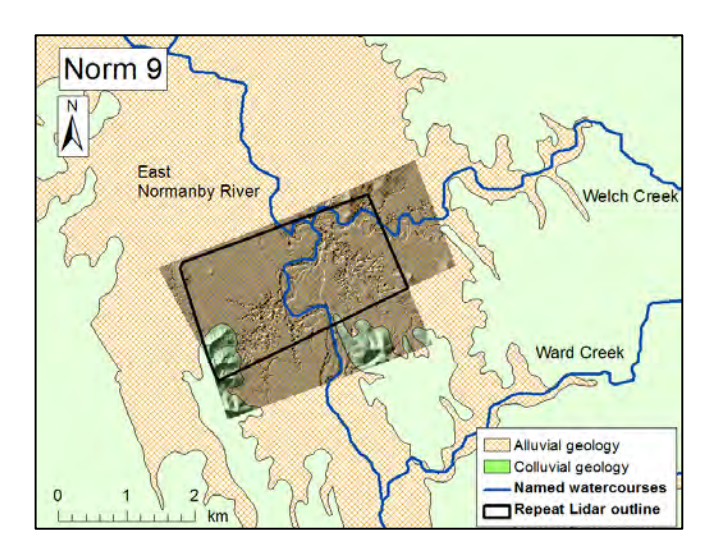


Figure A76: Elevation ranges in and around Norm 9.

Table A34: General statistics for Block 9.

Reprocessed change raster area ha	501.5162
Block elevation range m	134 to 234
Number of LiDAR digitised features	236
Number of Google Earth mapped gullies	54

## 3.4.1 Alluvial and Colluvial geology



**Figure A77:** Norm 9 sits at the head of a broad alluvial plain. Narrower bands of alluvium follow water courses between rising slopes of colluvial geology to the east and south of the block. 93% of the repeat LiDAR footprint was alluvial geology.

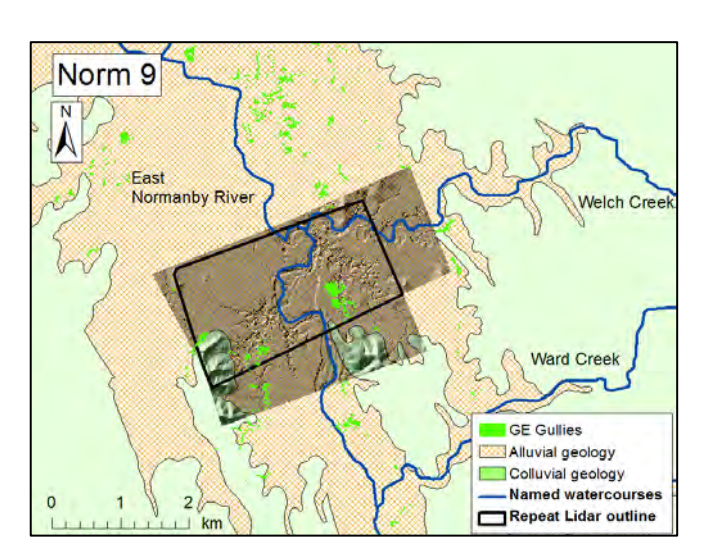


Figure A78: Distribution of Google Earth (GE) mapped gullies in and around Norm 9.

**Table A35:** Just under half the area of alluvial surfaces was eroded by gullies or channels at different stages of development. 15% of alluvial surfaces were eroded by gullies, but GE gullies captured under half of this extent. Few gullies extended into colluvial areas.

Norm 9	Area ha	Area of all features digitised from LiDAR ha	Features as % of zone	Area of gullies digitised from LiDAR ha	Area of gullies as % of zone	Area of Google Earth digitised gullies	GE gullies as % of zone
Alluvial zone	468.74	209.15	44.6	70.17	16.5	5.86	1.3
Colluvial zone	32.77	3.60	11.0	3.39	10.3	0.25	0.8

#### 3.4.2 LiDAR derived data

### **Horizontal adjustments**

Polygons digitised from 2009 LiDAR, CHM and PFC rasters have been nudged to align with reprocessed 2009 LiDAR by:

X,Y nudge (m)	2,-2
---------------	------

### **Vertical adjustments**

Adjustment for vertical offset of 2009 and 2011 DEMs

20 polygons of  $1000 \text{ m}^2$  were put in areas where very little change would be expected to occur; ancient flood plain. Mean value of change raster within the 20 locations was used as a correction to the whole change raster.

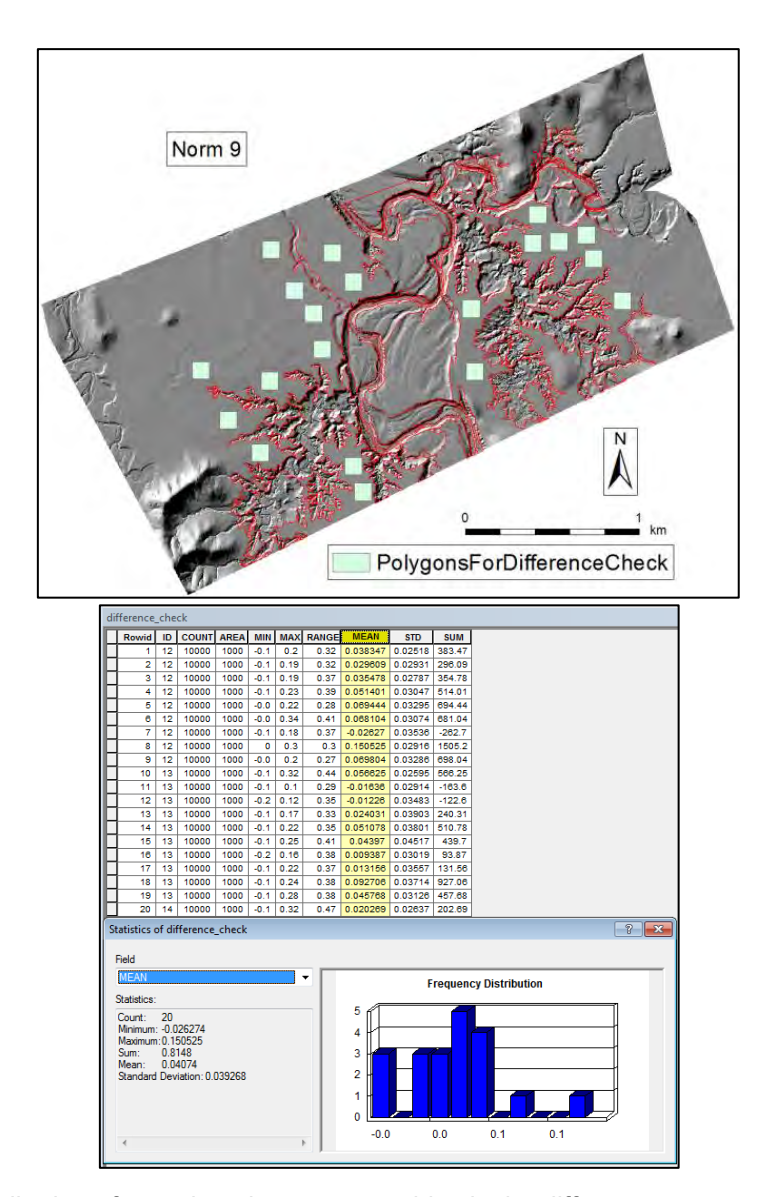


Figure A79: Distribution of sample polygons to test bias in the difference raster; and statistics table.

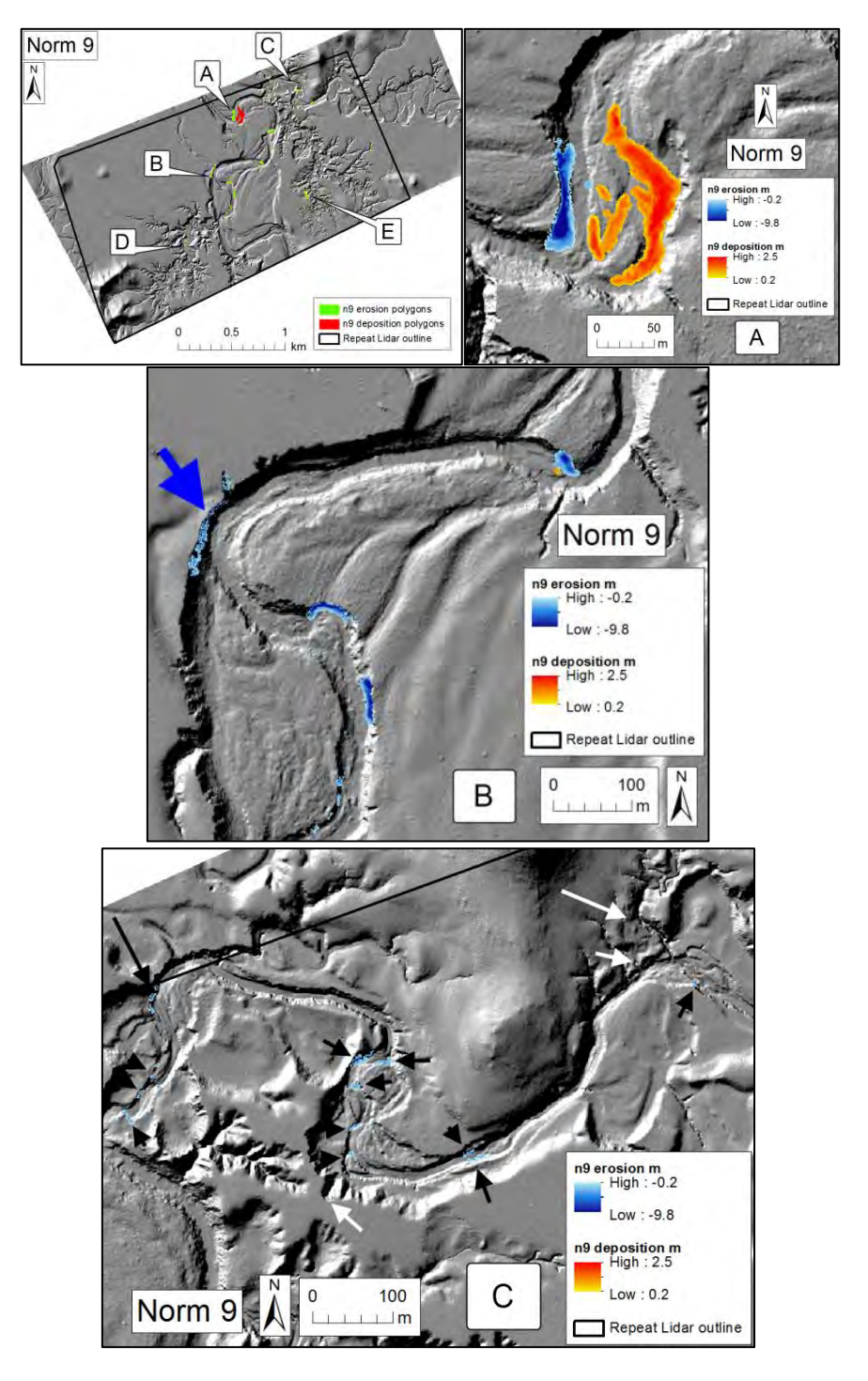
Table A36: Statistics from adjusting difference raster for bias.

Layer	min	max	Mean	s.d.
Norm_9_Difference_2009- 2011_Reprocessed.tif (as supplied by Terranean)	-11.16	9.5	-0.03	0.18
Norm_9 with edge effect removed	-9.76	5.42	-0.016	0.17
Areas of minimal change	-0.026274	0.150525	0.04074	0.039268
N9_Diff_adjusted	-9.80	5.38	-0.057	0.17

**Table A37:** Values of adjusted change raster filtered to remove noise from terraces.

raster	Values filtered
erosion	-0.2 to 0
deposition	0 to 0.2

## 3.4.3 Observations



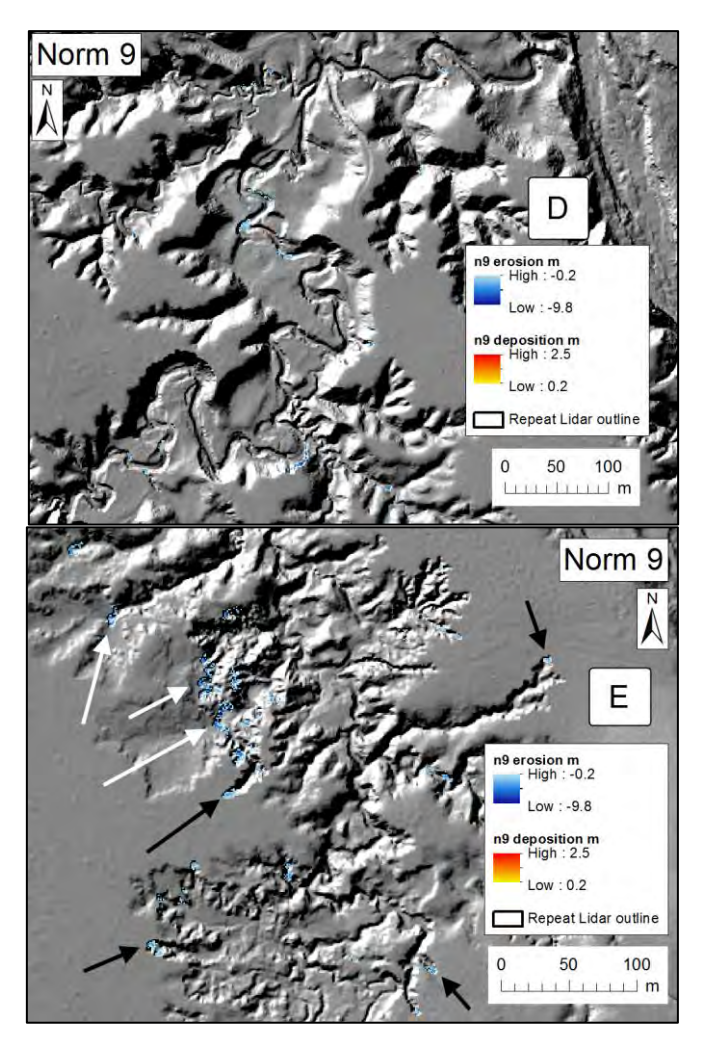


Figure A80: Location diagram and erosion and deposition hot spots in Norm 9.

Location A: The largest single deposition seen anywhere in this study, 4620m<sup>3</sup> material was deposited among trees on an old channel bed of the East Normanby River. Depth of deposit was up to 2.5m. A 100m section of bank opposite the deposition was cut back by up to 15 m, with the full height of the 6m bank losing material.

Location B: Erosion on both banks of the East Normanby River, cutting into inset flood plains at different levels. The blue arrow points to a 13 m high bank that appears to have collapsed along its upper edge, whereas other erosion sites have been eaten away from the waterline upwards. Volume of erosion from the sites in this picture alone was 5700m<sup>3</sup>.

Location C: The tributary Welch Creek had numerous erosion sites along the channel (black arrows), but few sites of erosion in gullies along this reach (white arrows).

Location D: A secondary channel with numerous erosion sites.

Location E: A gully complex 700m by 300m shows 2 distinct phases of gully development; reworking of old gully scars (white arrows) and headwalls advancing into uneroded alluvium (black arrows).

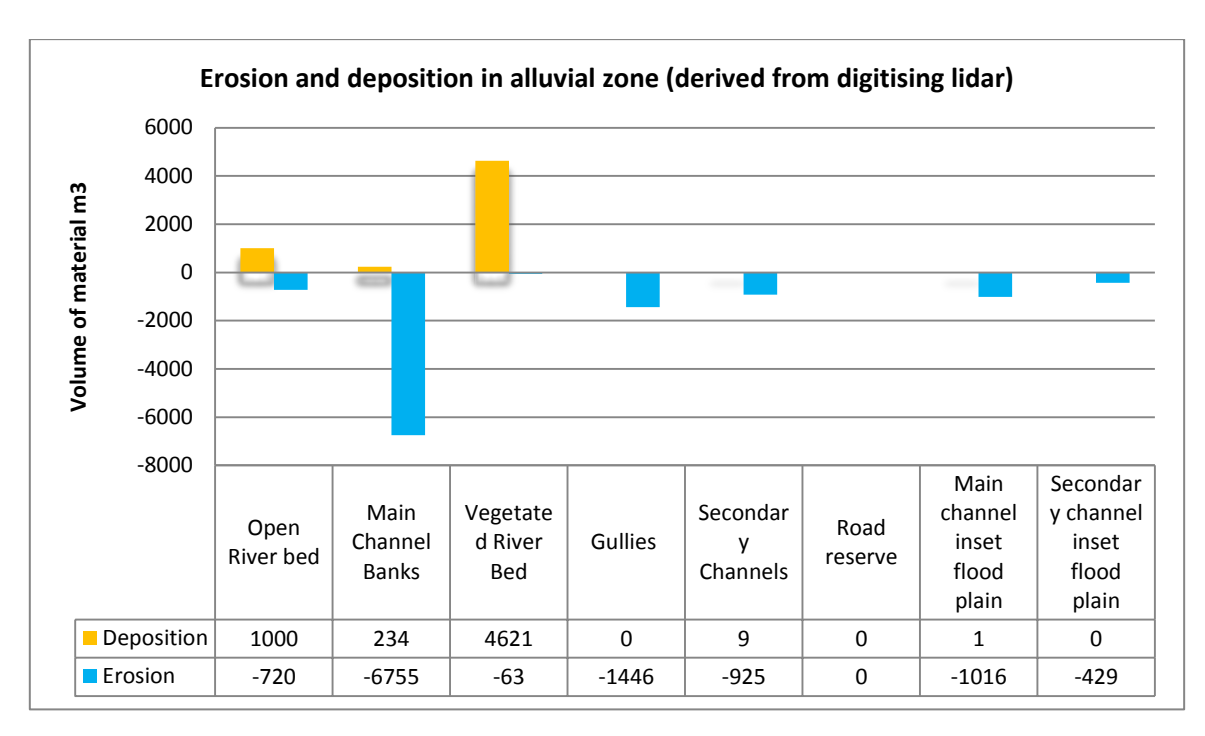


**Figure A81:** Sum of erosion and deposition for landscape classes in the alluvial zone. In a significant deviation from the pattern in other LiDAR blocks, erosion from main channel banks dominated losses from other sources. Deposition on open and vegetated river main channel bed in Norm 9 was the largest volumes measured of all LiDAR blocks except Norm 40, which covered a section of Morehead River that had many anabranching channels with significant movement of sandbanks and bars. These data suggests the upper East Normanby River to be actively reforming main channel dimensions.

#### 3.4.4 Comparison of Google Earth gullies to LiDAR gullies in the alluvial zone

The area of gullies identified from Google Earth was 8% of the area of gullies identified from LiDAR, but erosion captured from Google Earth mapped gullies was 30% of the volume of erosion from alluvial gullies. The average value (excluding outliers) over 11 blocks was 14%. Reworking of unvegetated old gully scars with incisions and down cutting explains this higher than average value.

 Table A38: Comparison of erosion from LiDAR alluvial gullies and Google Earth mapped gullies.

	Area ha	Erosion m <sup>3</sup>	yield m³/ha/yr
LiDAR gullies alluvial	70.17	-1393.41	-9.93
GE gullies alluvial	5.86	-408.34	-34.84

#### 3.4.5 Gully Expansion 2009 - 2011

Very little expansion of alluvial gullies occurred between 2009 and 2011, with no locations standing out as having rapid extension compared to other LiDAR blocks. Gully boundaries were expanded in 17 locations, with a total of 52.2 m<sup>2</sup> increase in gully area.

Large areas of bank erosion do not show up in these statistics. Gully expansion measures the advance of head scarps into ancient flood plain not eroded (or digitised) previously.

Table A39: Gully expansion between 2009 and 2011.

Gully Expansion 2009 - 2011	
Number of gully expansion locations	17
Area of gully expansions m2	52.2
Mean area of expansion m2	3.1

## 3.4.6 Landscape Classification

The main channel has large areas of vegetated channel bed approximately 6m above the main channel, and extensive areas of inset flood plain approximately 2m above the vegetated channel bed. Three secondary channels join the main channel in this block, with the channel in the north east quarter of the block having a broad, vegetated bed.

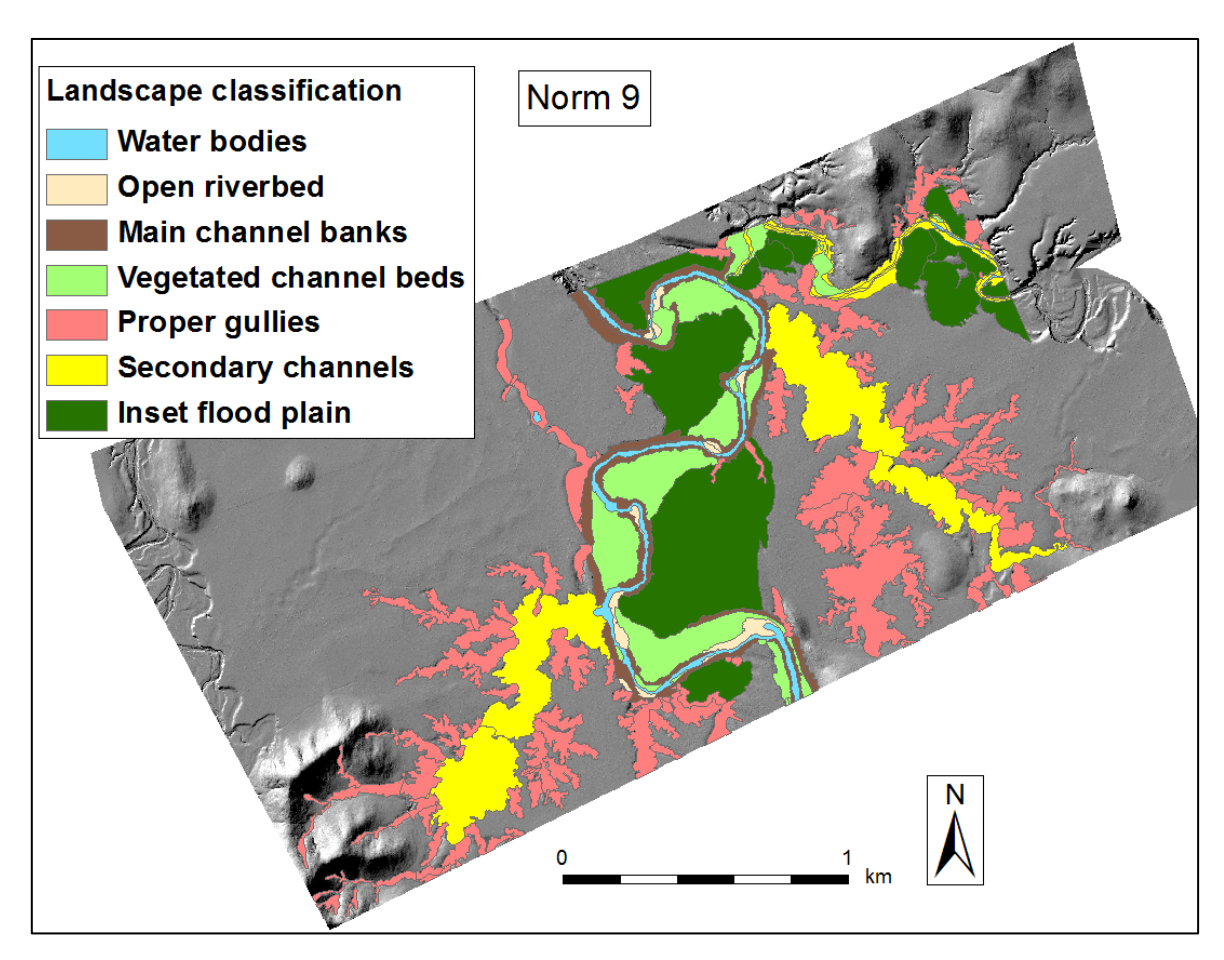
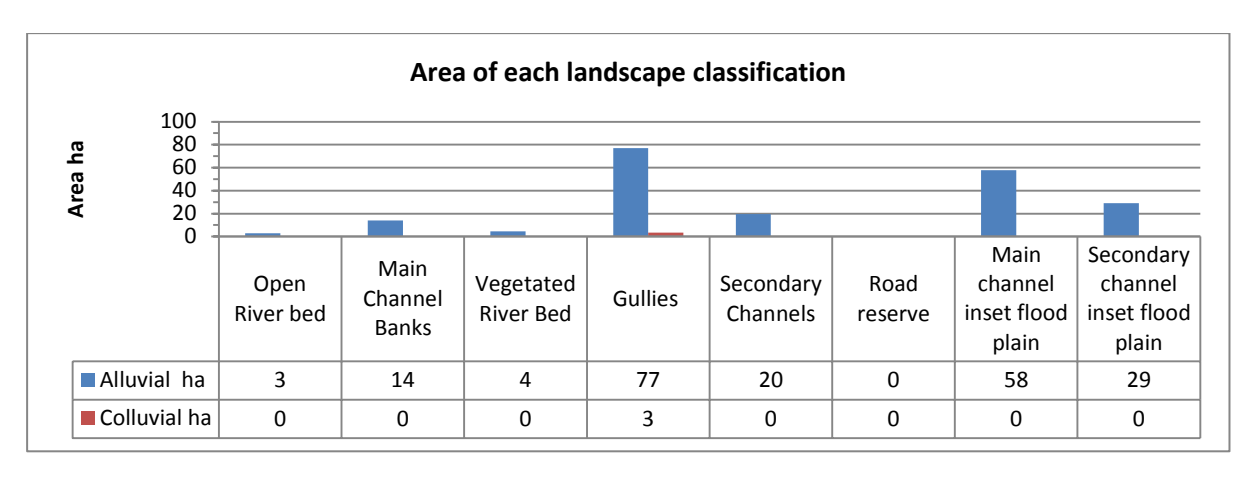


Figure A82: Landscape classification in Norm 9.



**Figure A83:** Gullies were 38% of the block area, combined area of main and secondary channel flood plains was 42%.

## 3.4.7 Historical air photos

**Table A40:** Details of air photos covering a broad expanse of gully to the east of the main channel in Norm 9.

Image date	Photo ID	Scale	Flying height	RMS error  of georeferenced air photo	Air photo position relative to 2009 LiDAR block
1/01/1951	QAP0204_040	24000	12750ft	0.76140	
1/01/1987	QAP4112_093	25000	4310m	2.31157	
19/10/1994	QAP5321_046	25000	4630m	1.77000	

1/06/2000	QAP5818_101	25000	4610m	3.66543	
-----------	-------------	-------	-------	---------	--

### 3.4.8 Historical gully extent

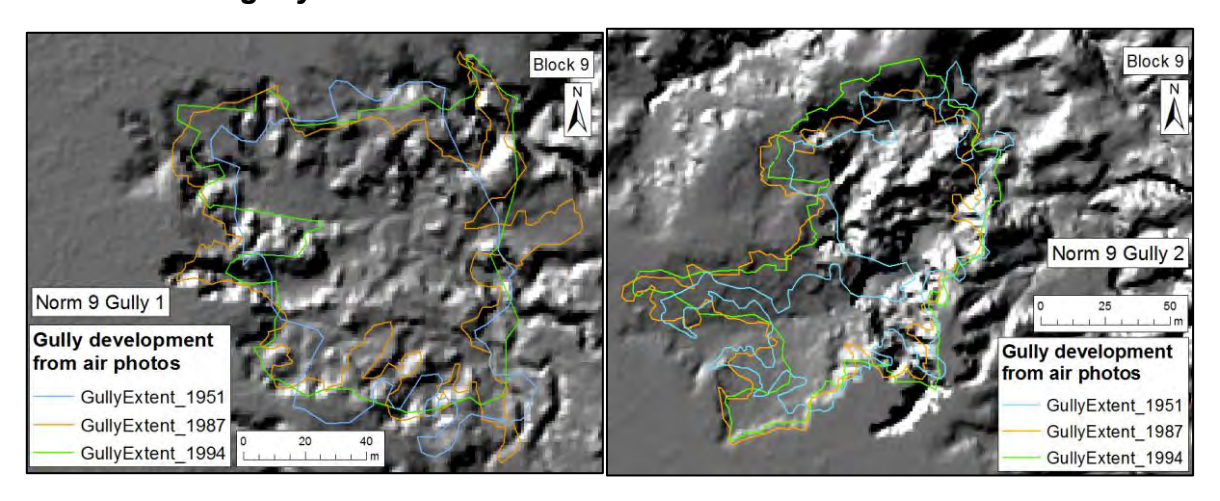


Figure A84: Development of gully one and 2 between 1951 and 2009.

**Table A41:** Variability of erosion rates from different gullies over different time scales is highlighted by comparing N09g1 and N09g2. Yield calculated from gully 1 between 2009 and 2011 was 43% of 5 decade average, but 23% of 2 decade average. Erosion from gully 2 between 2009 and 2011 was 90% of 5 decade average, but 180% of 2 decade average. These values oscillated above and below the average yield of 13 air photo gullies over the same time scales.

		Yield: volume material lost divided by area of 2009 gully divided by interval m3/ha/yr		
		Air photo data	LiDAR data	
	1950s to 2009	1980s to 2009	2009 to 2011	
N09 g1	86	164	37	
N09 g2	177	89	160	
average of 13 air photo gullies	91	112	115	

### 3.4.9 LiDAR 2015 data analysis

			reference X0	
		CoordShift	Y0	2015X0.5Y1
	Lowest			
0.059816	mean	2015X3Y3_m	0.02093033	0.032957
	Lowest			
1.66	max	2015X1Y1_m	2.230010033	1.795
	Smallest			
-1.63	min	2015X0_Y0_	-1.629999995	-1.57999
0.020004	mode	2015X2Y_3_	0.0500031	0.050003
0.181269	std dev	2015X1Y1_m	0.232008932	0.139148
0.020004	50th pctile	2015X0Y_3_	0.0400085	0.050003
0.180008	90th pctile	2015X0Y1_m	0.240005001	0.140015
0.270004	95 pctile	2015X0Y1_m	0.380005002	0.199997
				2015_Xhalf
637	Count <-0.5	2015X1Y1_m	1031	349
408	Count <-0.5	2015X1Y1_m	1049	152

**Figure A85:** Statistics supporting the XY shift to minimise variance in 40,000 points sampled. 4 shifts are presented here; 1) do nothing, 2) X0 Y1 based on values from the 90<sup>th</sup> and 95<sup>th</sup> percentile, 3) X1 Y1 based on analysis of a count of the number of erosion cells with values less than or equal to -0.5 i.e. how many cells exceeded the threshold for real erosion, 4) nudging the 2015 DEM by X0.5m Y1m – which produced best statistics for Std dev, 90<sup>th</sup> and 95<sup>th</sup> percentiles and had by far the lowest count of noisy cells, nearly half the amount of the next best fit.

## 3.4.10 Erosion/Deposition processing

Threshold for masking noise in the 2011 – 2015 difference layer was 0.5m.

**Table A42:** The reduction in data volume to determine real and defensible erosion and deposition.

	Raw data		Edited data	
	Raster SUM	Number of polygons	Raster SUM	Number of polygons
Real erosion <= -0.5m	-60,998	11,627 reduced to 7,280 after half m X shift	-17,584	568
Shallow erosion <=-0.2 and >-0.5m	-46,418	59,886	·	1,893
Real	17,997	4,564	7,384	79

Deposition			
>= 0.5m			
Shallow erosion	40,817	48,705	421
>=0.2 and <0.5m			

Observations from Erosion processing for 2011 to 2015 time step:

## Effect of XY adjustment in metre and sub-metre increments

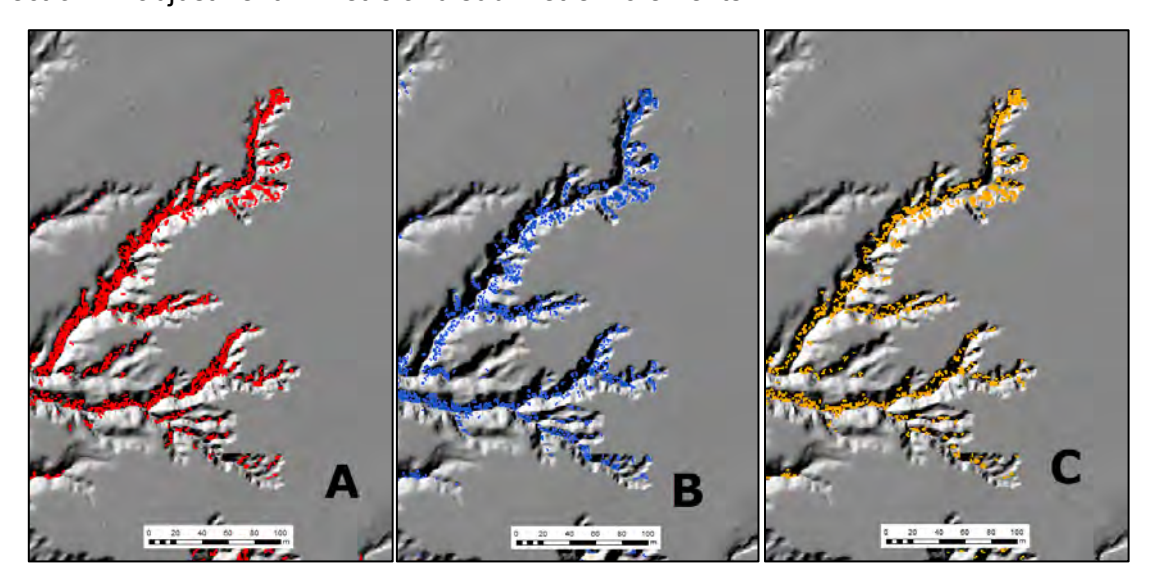


**Figure A86:** Panel A adjustment was X0 Y1, panel B adjustment was X1 Y1, panel C adjustment was X 0.5 Y 1. The area of "deep erosion" in the gully extending towards the top left of the picture, before editing, for A 1944m2; B 1650m2 and C 1300m2. The half metre shift in X direction resulted in 34% less erroneous erosion polygons to sift through to find the real signal, thus proving the worth of pursuing sub metre nudges to correct for mis-alignment in horizontal plane.

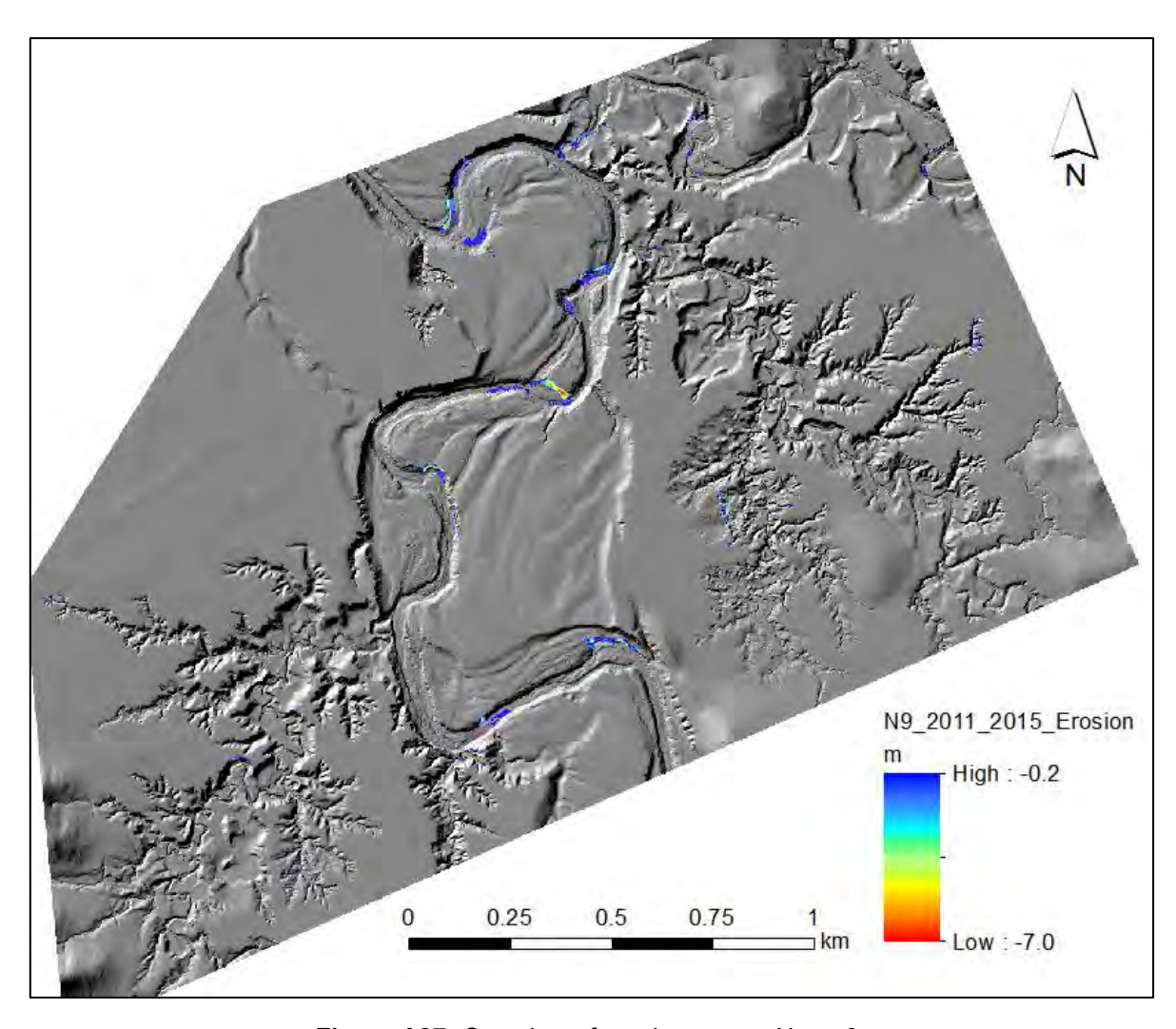


Figure A87: Overview of erosion across Norm 9.

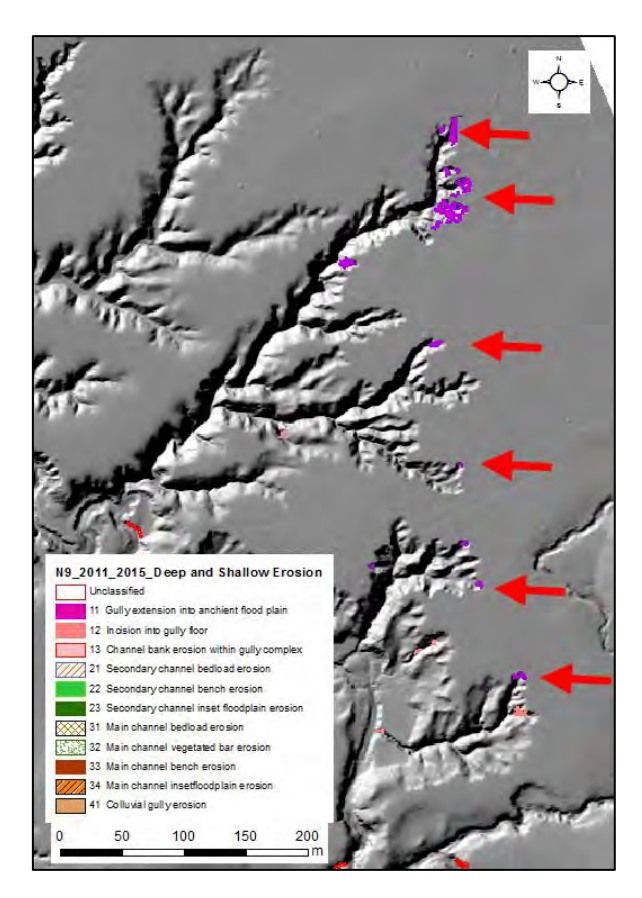


Figure A88: Multiple gully head walls advancing.

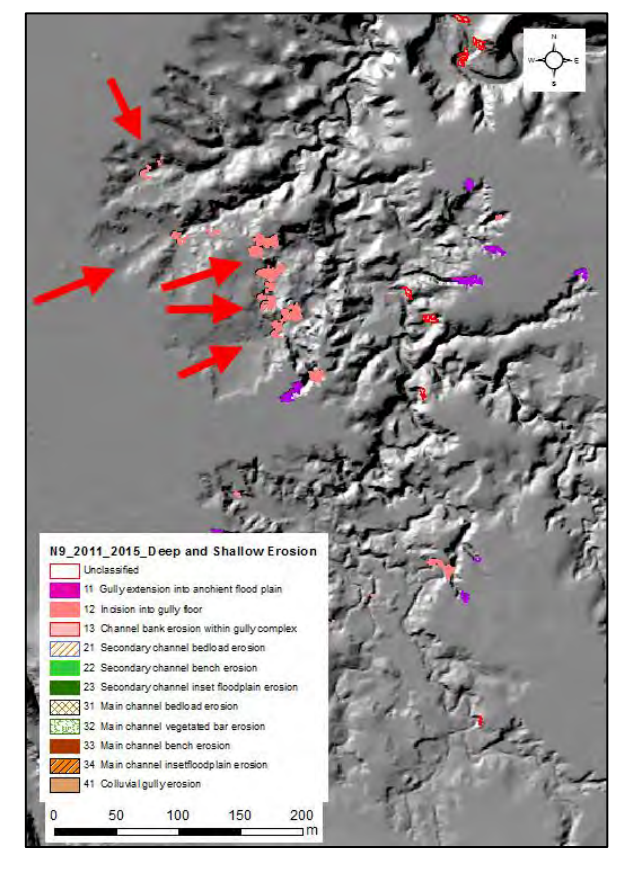
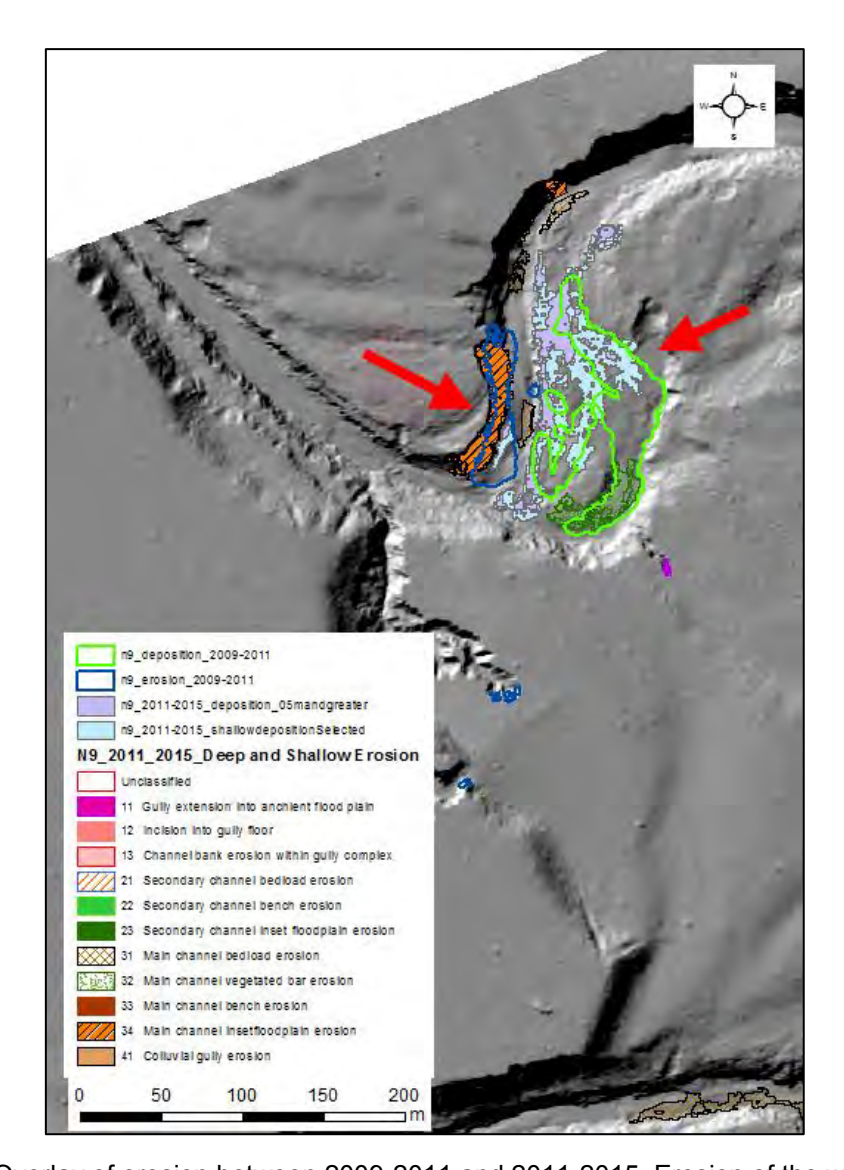
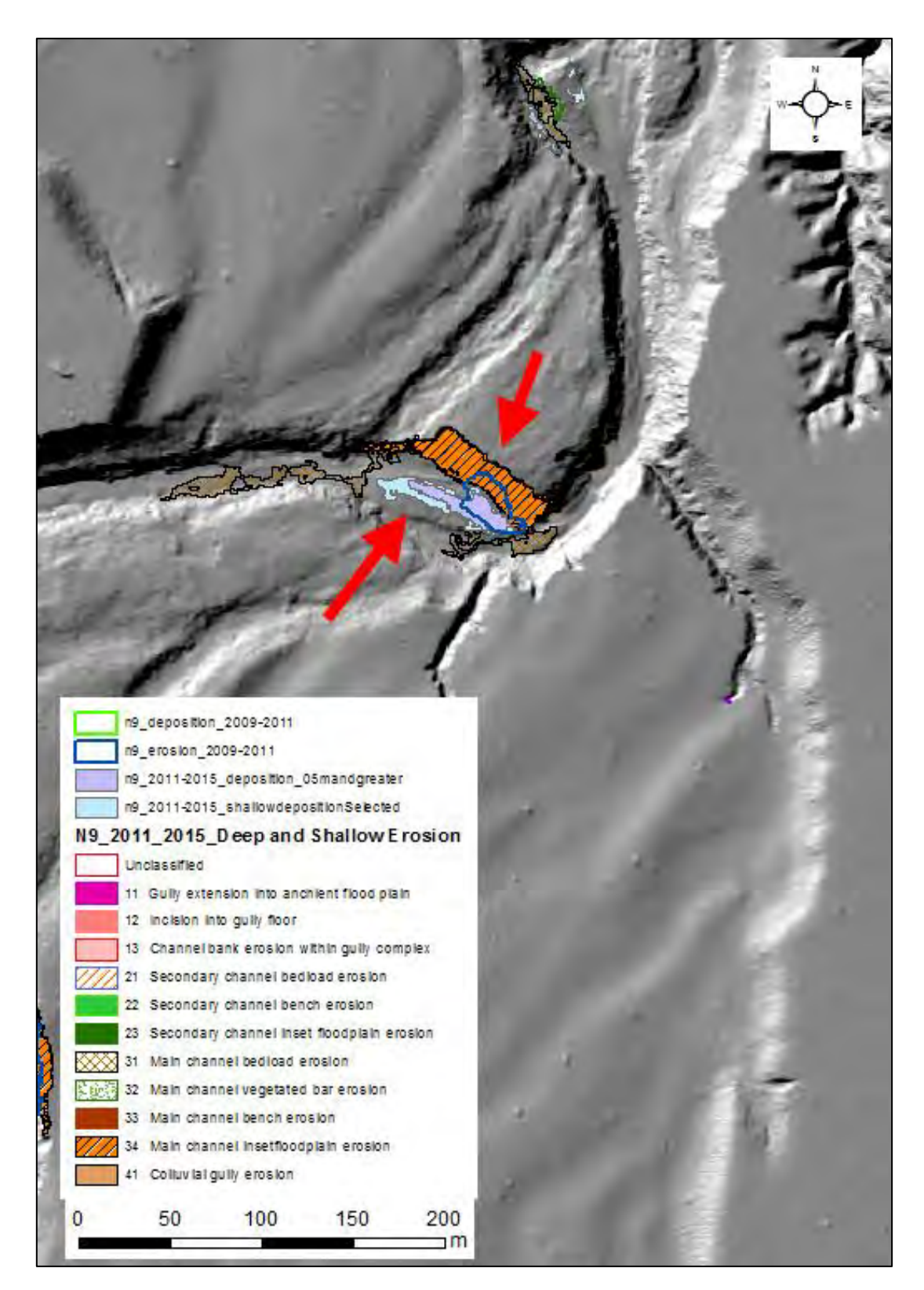


Figure A89: Reworking of the shallow gully floor.



**Figure A90:** Overlay of erosion between 2009-2011 and 2011-2015. Erosion of the west side of the channel between 2009 and 2011, the blue outline, has continued between 2011 and 2015, the orange patch. The large patch of deposition on the east side of the bend between 2009 and 2011 was added to between 2011 and 2015, though not by such a large extent. The lower end of the 09-11 deposition has eroded between 2011 and 2015. It looks as though the channel is migrating towards the inside of the bend.



**Figure A91:** A smallish erosion patch, seen as blue outline, between 09-11 expanded between 11-15. The bar in mid channel has received deposits in both time steps.

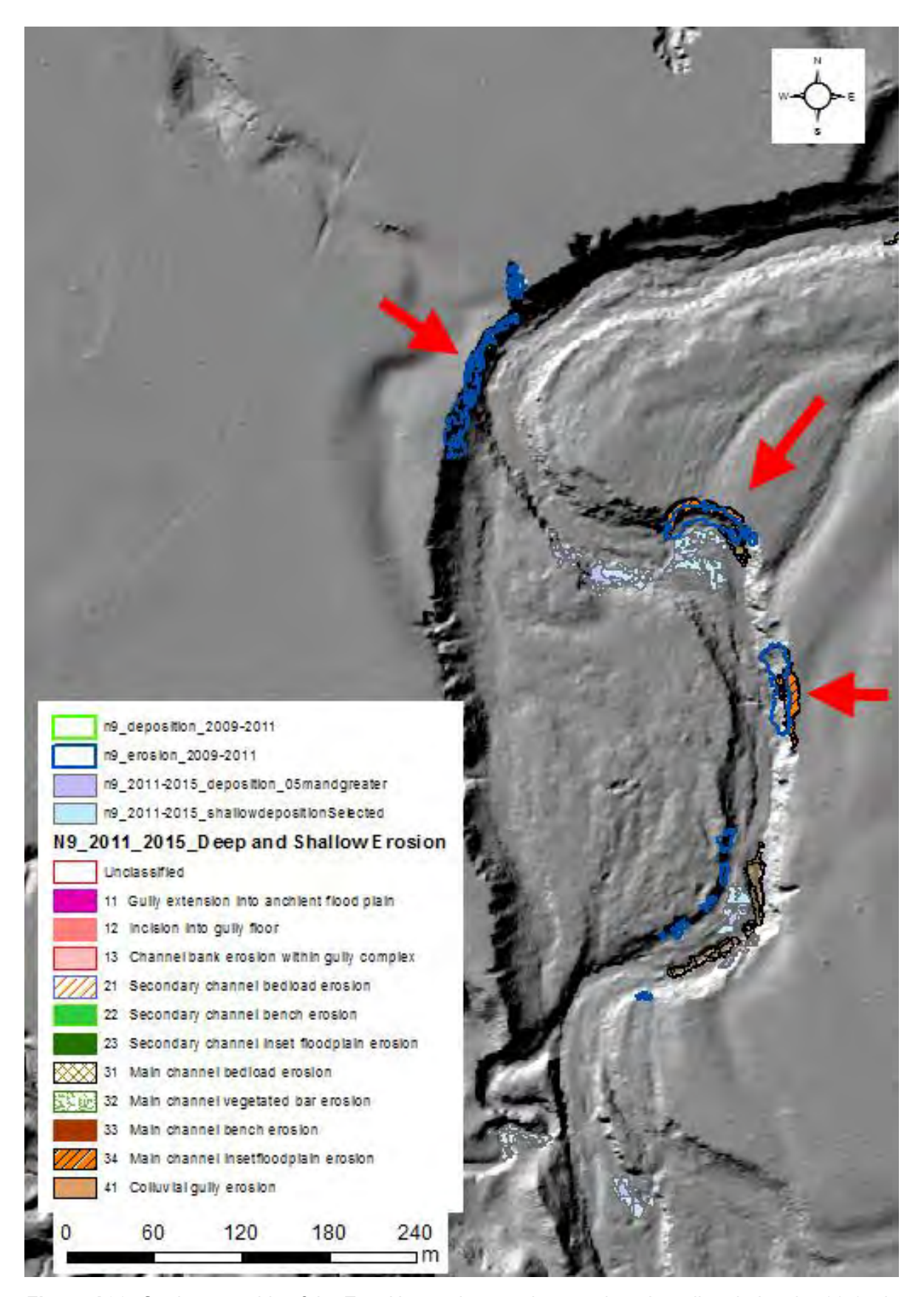


**Figure A92:** On the east side of the East Normanby two sites continued eroding during the 11-15 time step. Erosion on the high bank on the outside of the bend was less between 11-15 than 09-11.

## 3.4.11 Observations from Deposition processing

Deep deposition polygons less than  $10m^2$  were deleted at the start as nearly all small polygons were up banks and in non-deposition places.

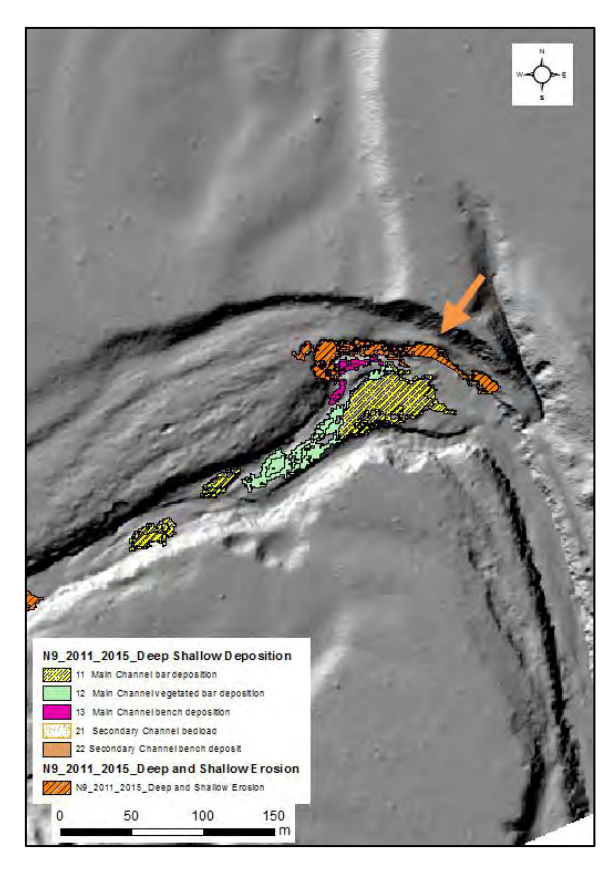


**Figure A93:** Deposition on the bar and bench, erosion on the outside of the bend.

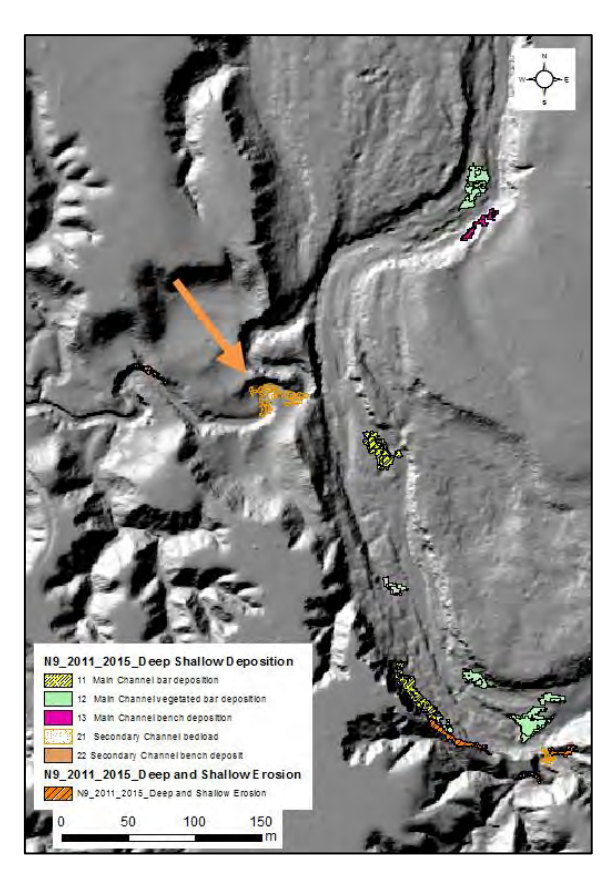
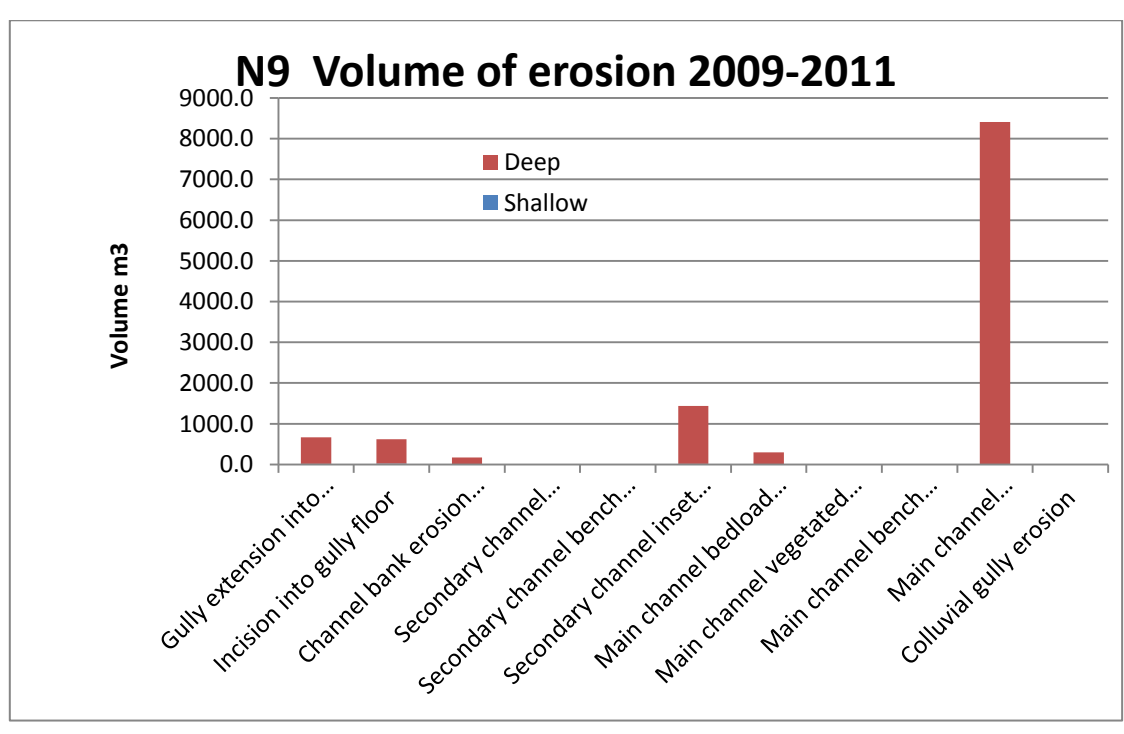


Figure A94: Deposition at junction of secondary channel and main channel.

#### 3.4.12 Summary Erosion 2015 Data & reprocessed 2009-11 data



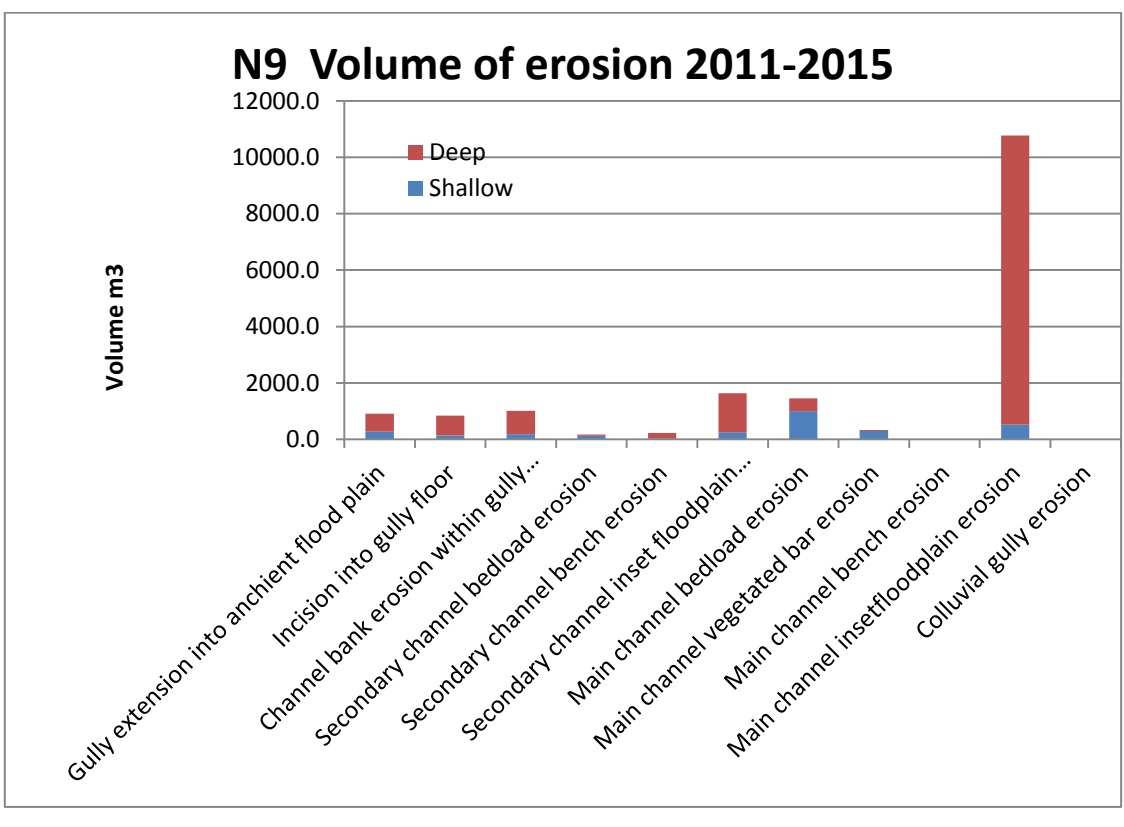


Figure A95: Erosion stats for Block 9 by geomorphic unit; 2009-11 (top); 2011-15 (bottom).

#### 3.5 Normanby LiDAR Block 10

Normanby 10 LiDAR block (Norm 10) straddles the Normanby River approximately 7 km downstream of the junction of the East and West Normanby rivers. The block is centred on alluvial flats around the confluence of Deep Creek with the Normanby River. Elevation of the alluvial flats is approximately 95 m; to the west a significant hill rises to 495 m. Eroded into the flats is a complex arrangement of flood plains at different levels, with dramatic channel systems that tell a story of multiple evolutions in the landscape.

Though total erosion from alluvial gullies was 2700 m<sup>3</sup> between 2009 and 2011, the 8<sup>th</sup> highest of the 14 LiDAR blocks, very little expansion in gully area was measured from repeat LiDAR, a mere 23 m<sup>2</sup> over 2 years. Most of this expansion was measured in one gully, which was also the study gully in air photos.

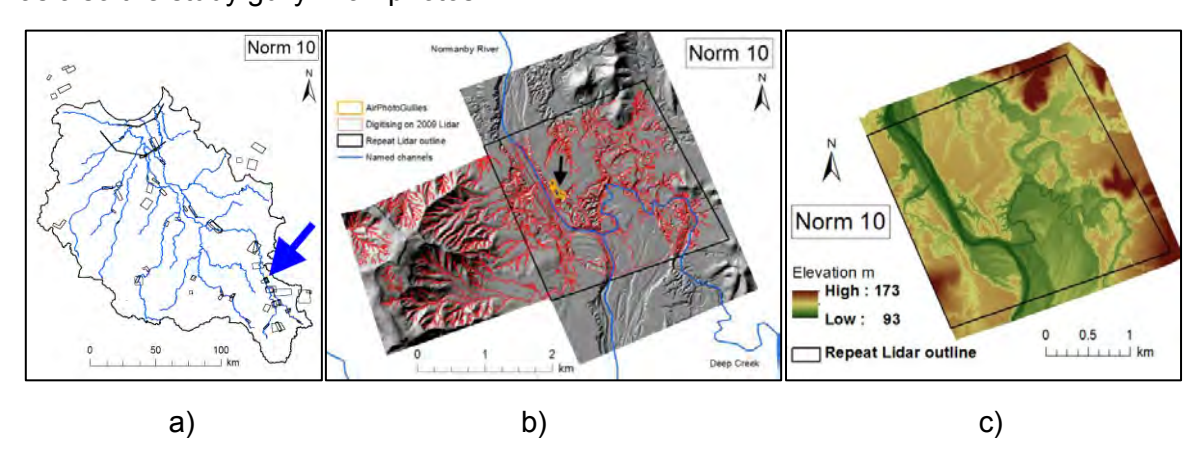


Figure A96: a) Norm 10 location; b) Digitising on LiDAR; c) DEM from 2009 LiDAR.

2009 LiDAR area (ha)	1168
Reprocessed change raster area (ha)	690
Reprocessed extent elevation range (m)	92 - 173
Number of LiDAR digitised features	510
Number of Google Earth mapped gullies	36

**Table A43:** General statistics for Normanby 10 LiDAR block.

#### 3.5.1 Alluvial and Colluvial geology

Small areas of colluvial slopes were included in the repeat LiDAR footprint, 8% of the block area. The original extent of LiDAR in 2009 included large areas of colluvial slopes with many linear gullies running to the ridge top. The opportunity to measure gully erosion on colluvial slopes was here, though owing to technical issues with the repeat LiDAR collection and processing for this project, any changes over 2 years may have been below detectable limits.

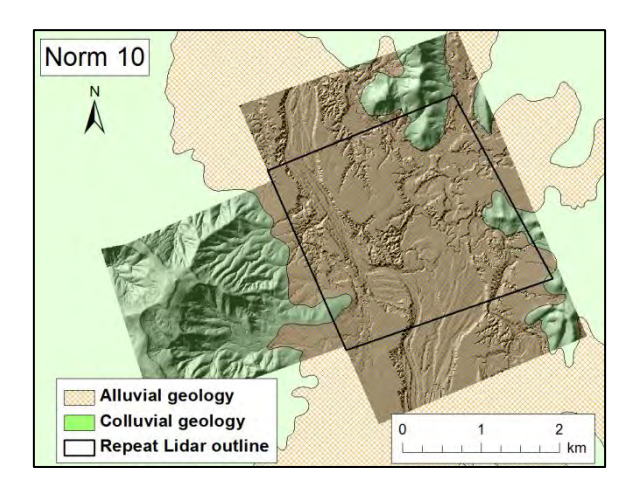


Figure A97: Alluvial and colluvial geology in Norm 10.

#### 3.5.2 Google Earth mapped gullies

Mapping gullies from Google Earth imagery identified 36 bare earth gullies with total area of 7.3 ha within Norm 10. All gullies within the repeat LiDAR footprint were mapped on alluvial geology.

LiDAR imagery identified 346 gully units with a total area of 126 ha. Of these, 3.2 ha or 2.6% of total alluvial gullies were on colluvial geology.

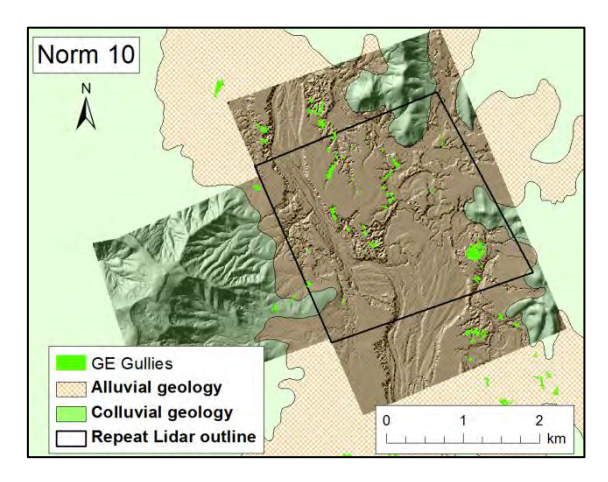


Figure A98: Distribution of gullies mapped from Google Earth.

Table A44: Gully area digitised from LiDAR and Google Earth in alluvial and colluvial geology.

Normanby 10	Area ha	Area of all features digitised from LiDAR ha	Features as % of zone	Area of gullies digitised from LiDAR ha	Area of gullies as % of zone	Area of Google Earth digitised gullies	GE gullies as % of zone
Alluvial zone	639	382.7	59.8	122.8	19.2	7.3	1.14
Colluvial zone	51	3.6	7.1	3.2	6.3	0	0

#### 3.5.3 LiDAR derived data

#### **Horizontal adjustments**

Polygons digitised from 2009 LiDAR, CHM and PFC rasters have been nudged to align with reprocessed 2009 LiDAR by:

X,Y nudge (m)	1,-3		

#### **Vertical adjustments**

#### Adjustment for vertical offset of 2009 and 2011 DEMs

20 polygons of  $1000 \text{ m}^2$  were put in areas where very little change would be expected to occur; ancient flood plain. Mean value of change raster within the 20 locations was used as a correction to the whole change raster.

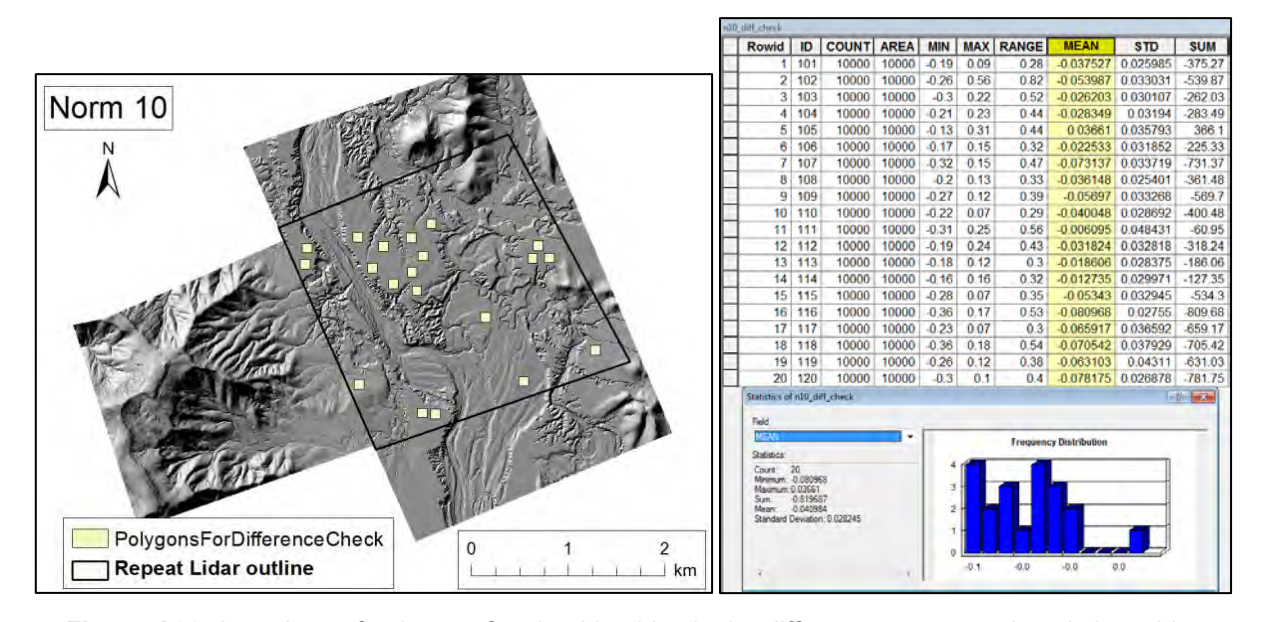


Figure A99: Locations of polygons for checking bias in the difference raster, and statistics table.

**Table A45:** Statistics of raw difference raster, and corrections applied to reduce bias on non-eroding surfaces.

Layer	min	max	Mean	s.d.
Norm_10_Difference_2009- 2001_Reprocessed.tif (as supplied by Terranean)	-9.97	34.18	-0.11	0.66
Extract_tif1 (edges trimmed)	-9.97	10.22	-0.08	0.18
Extract_tif1 (sampled area of minimal change)	-0.08	0.04	-0.04098	0.04
N10_Diff_adjusted	-9.93	10.26	-0.0421	0.16

Table A46: Values of change raster filtered to remove noise.

raster	Values filtered
erosion	-0.2 to 0
deposition	0 to 0.4

Two layers were created from the modified difference data, one layer for erosion, and one layer for deposition.

Aggressive hand editing of erroneous erosion and deposition values from LiDAR interactions with trees and steep slopes removed approximately 11,000 patches of improbable erosion or deposition.

#### 3.5.4 Observations from erosion and deposition analysis

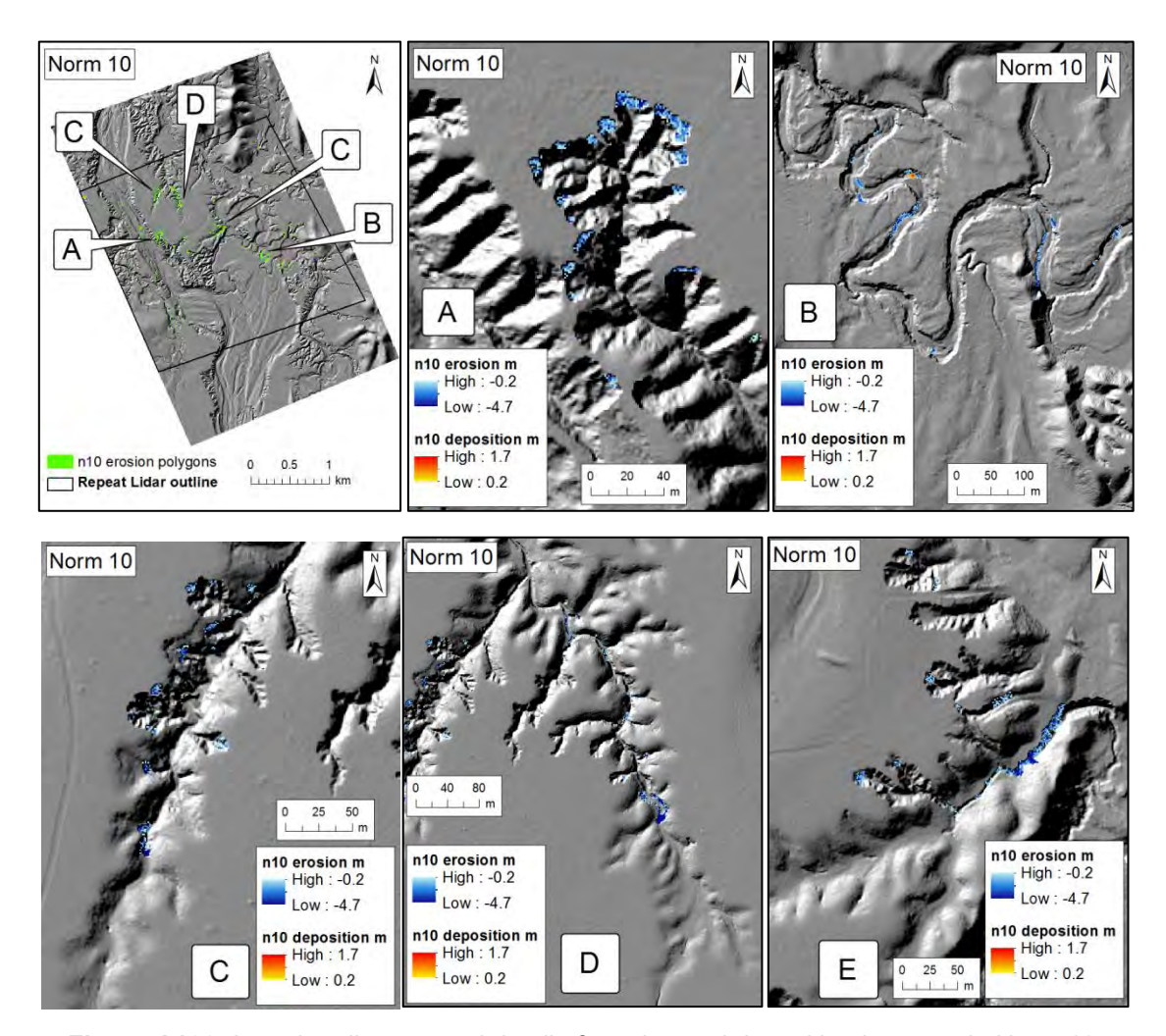


Figure A100: Location diagram and detail of erosion and deposition hotspots in Norm 10.

Location A: This gully accounted for all the measured expansion of gully area in Norm 10 between 2009 and 2012.

Location B: The flow path of Deep Creek has many looping bends, and has migrated significantly from historical paths.

Location C: The shallow rounded shoulders of the head of this gully show phases of greater activity in the past have slowed. Recent erosion activity has been on side walls where lateral amphitheatre gullies have formed.

Location D: This gully, adjacent to Location C, has dwn cutting of the gully floor as the main form of erosion. The head of this gully also shows relative inactivity.

Location E: Multiple roads made up a 10m bank between small amphitheatre gullies.

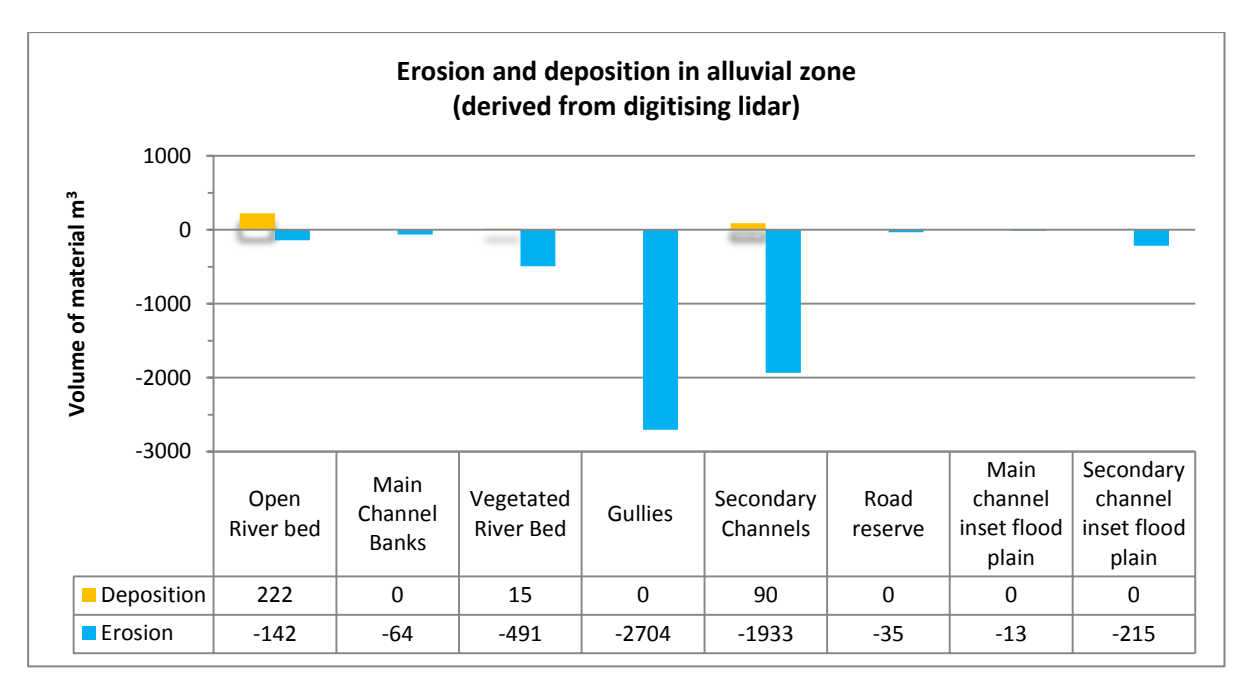


Figure A101: Quantifying erosion and deposition in alluvial and colluvial zones.

- Erosion from alluvial gullies accounted for 48% of erosion measured between 2009 and 2011
- Erosion from secondary channels contributed 35% of the erosion total.
- Vegetated main channel bed erosion was 9% of total erosion.
- Open main channel bed had a nett gain of material of 120 m<sup>3</sup>.
- Erosion from gullies receiving runoff from roads was 35 m<sup>2</sup> between 2009 and 2011.
- Deposition in secondary channels was 90 m<sup>3</sup>, 5% of the 1933 m<sup>3</sup> eroded; again emphasising the role secondary channels play as nett producers of sediment from the landscape.

#### 3.5.5 Comparison of alluvial gullies to colluvial gullies

Though Norm 10 was surrounded by rising colluvial slopes, the placement of the repeat LiDAR footprint essentially missed these slopes. Area of colluvial gullies in Norm 10 was 2% of area of alluvial gullies; 3 ha compared to 122.8 ha. Volume of erosion from colluvial gullies, 36 m³, or 1% of erosion from alluvial gullies.

 Table A47: Comparison of erosion activity in alluvial and colluvial gullies.

	Alluvial	gullies			Colluvial	gullies	
area ha	deposition m <sup>3</sup>	erosion m <sup>3</sup>	yield m³/ha/yr	area ha	deposition m <sup>3</sup>	erosion m3	yield m³/ha/yr
122.8	0	-2704	-11	3	0	-36	-6

#### 3.5.6 Comparison of Google Earth gullies to LiDAR gullies in the alluvial zone

Area of alluvial gullies in Norm 10 was 122 ha but gullies mapped in Google Earth were 6% of this figure; slightly less than the average across 13 LiDAR blocks where Google Earth mapping identified 10% of the area of alluvial gullies mapped from LiDAR.

Table A48: Comparison of erosion activity in LiDAR and Google Earth gullies.

	Area ha	Erosion m <sup>3</sup>	Yield m³/ha/yr
LiDAR alluvial gullies	122.8	-2704	-11
GE alluvial gullies	7.3	-240	-17

Volume of material eroded from Google Earth gullies was 240 m<sup>3</sup> between 2009 and 2011, 9% of the volume eroded from alluvial gullies, a similar order of magnitude.

#### 3.5.7 Gully Expansion 2009 - 2011

Erosion activity was almost entirely within 2009 gully perimeters. Ten lobes of expansion were identified from repeat LiDAR, mostly in one gully, with a total increase in area of 23 m<sup>2</sup> over 2 years; that's 11.5 m<sup>2</sup> per year, which about the size of a small bathroom, and not much at all spread over a 690 ha block. Allowing for shortcomings of repeat LiDAR for this project, the increase in gully area was negligible.

Table A49: Area of expansion of gullies between 2009 and 2011.

Gully Expansion 2009 - 2011	
number of gully expansion locations	10
sum area of gully expansions m <sup>2</sup>	23
mean area of expansion m <sup>2</sup>	2.3

#### 3.5.8 Landscape Classification

A significant feature of Norm 10 was 2 levels of flood plain on either side of a bend in the main channel. Vegetated channel bed, with obvious flow sculptured patterns below a 20 m canopy, was 5 m above main channel bed. Ten metres above main channel height, but 10 m below ancient flood plain height, was an 82 ha surface with channels describing the path of the main channel in times gone by. Secondary channels also had large areas of associated flood plain, 74 ha, on surfaces 8 to 12 m below the level of ancient flood plain.

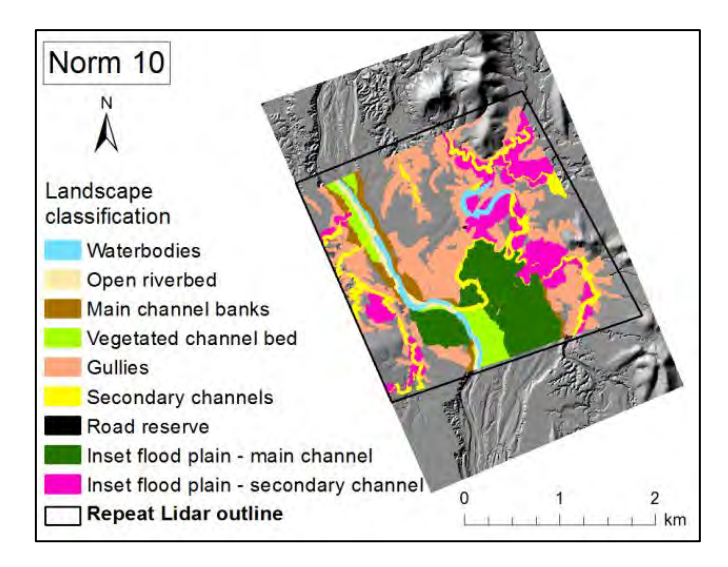


Figure A102: Landscape classification in Norm 10.

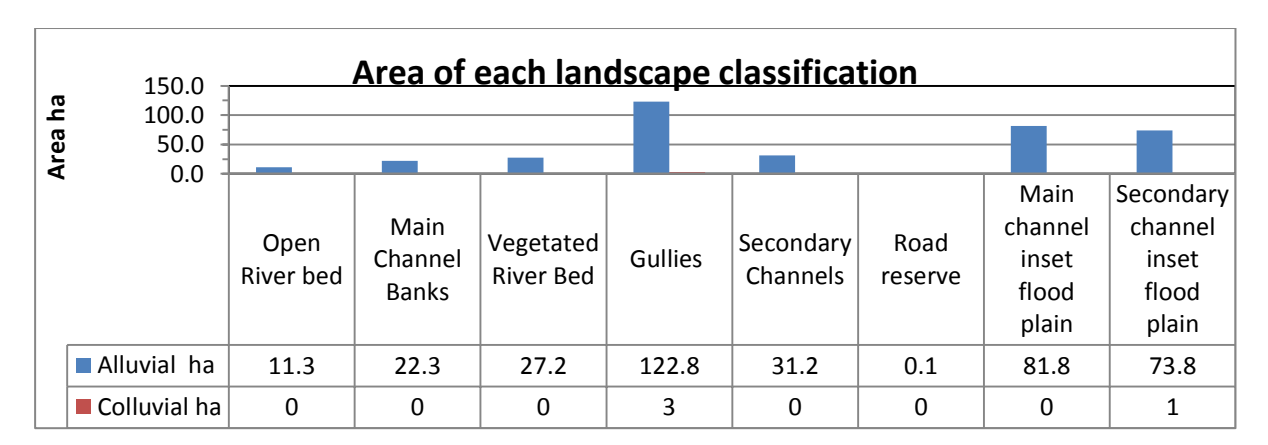


Figure A103: Area of each landscape unit in alluvial and colluvial zones.

#### 3.5.9 Historical air photos

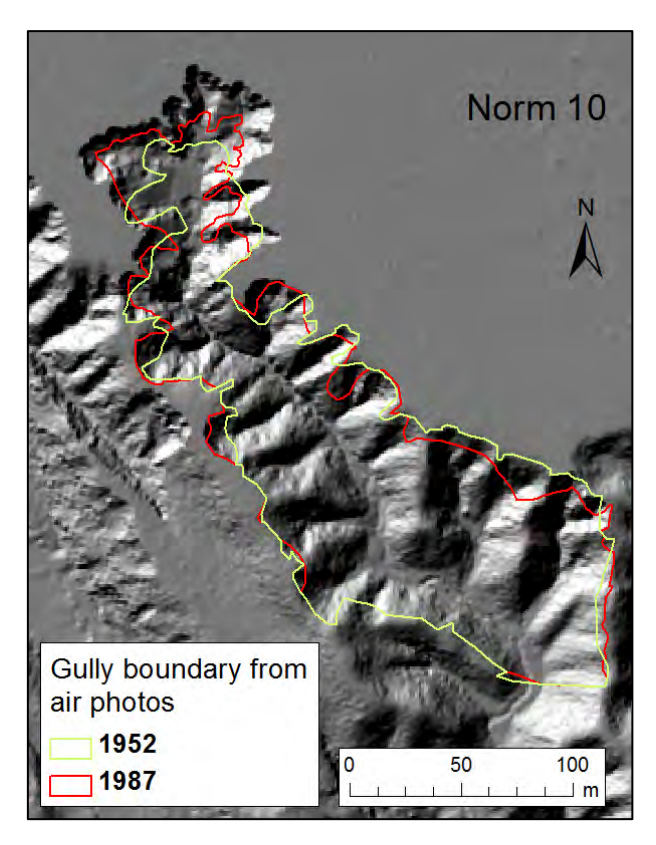
One gully was identified in historical air photos from 1952 and 1987. This gully had active erosion at the head scarp, and was responsible for all of the  $23~\text{m}^2$  of measured gully expansion in Norm 10 between 2009 and 2011.

Table A50: Meta data for air photos in Norm 10.

Image date	Photo ID	Photo ID Scale		RMS error of georeferenced air photo	Air photo position relative to 2009 LiDAR block
01-Jan-52	QAP 311-28	23900	12750ft	1.34	
01-Jan-87	QAP 4111- 173	25000	4310m	3.79	

Gully perimeter defined in 1987 was, in some places, inside the perimeter digitised from 1952 air photo. A good match between gully perimeter in 1952 and 2009 LiDAR was consistent with the appearance of the gully as being relatively inactive on the older surfaces. Misalignment of gully perimeter in 1987 could be due to vegetation obscuring gully edges.

Gully area in 1952 was 20.07 ha, in 1987 2.10 ha.



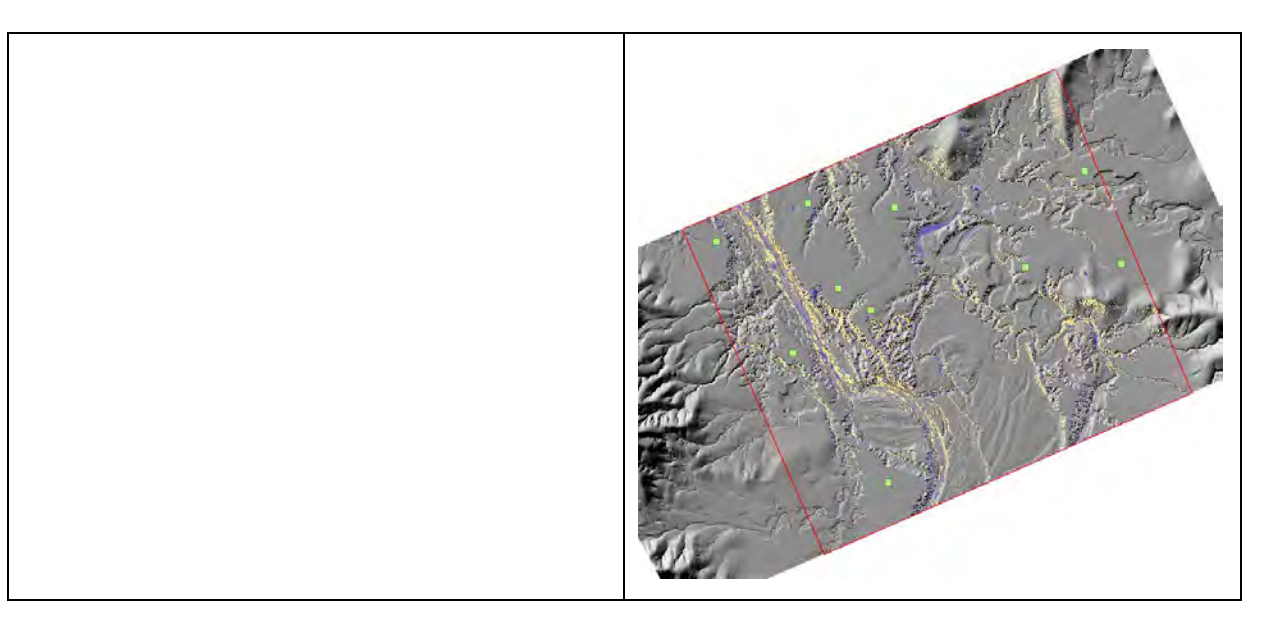
**Figure A104:** Gully perimeter in 1952, 1987 and 2009. Variability in rates of erosion over different time scales was found, with the rate over 5 decades from 1950s to 2009 being 81 m<sup>2</sup>/ha/yr; over 2 decades from 1890's being 170 m<sup>3</sup>/ha/yr, and over 2 years from 2009 to 2011 being 104 m<sup>3</sup>/ha/yr.

**Table A51:** Erosion rates calculated from air photo records and repeat LiDAR analysis for N10 g1. Yield between 2009 and 2011 was 128% of 5 decade rate, but 61% of 2 decade rate. Rate of erosion over 5 decades in N10 g1 was below the average rate of 13 air photo gullies, but rate over 2 decades was greater than average. Yield calculated from Repeat LiDAR was slightly below average rate.

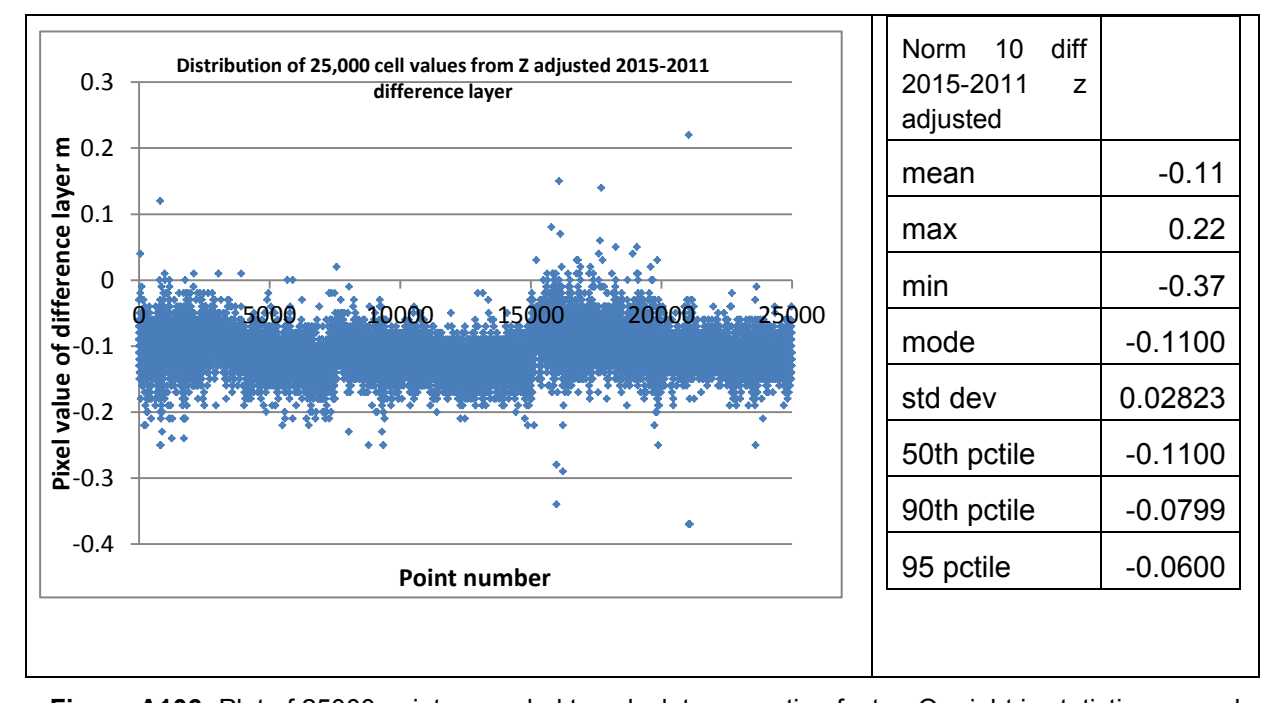
	Yield: volume material lost divided by area of 2009 gully divided by interval m3/ha/yr					
	Air ph	LiDAR data				
	1950s to 2009 1980s to 2009		2009 to 2011			
N10 g1	81	170	104			
average of 13 air photo gullies	91	112	115			

#### 3.5.10 LiDAR 2015 Data Processing

## Z correction: 0.10979m added to 2015 Lidar



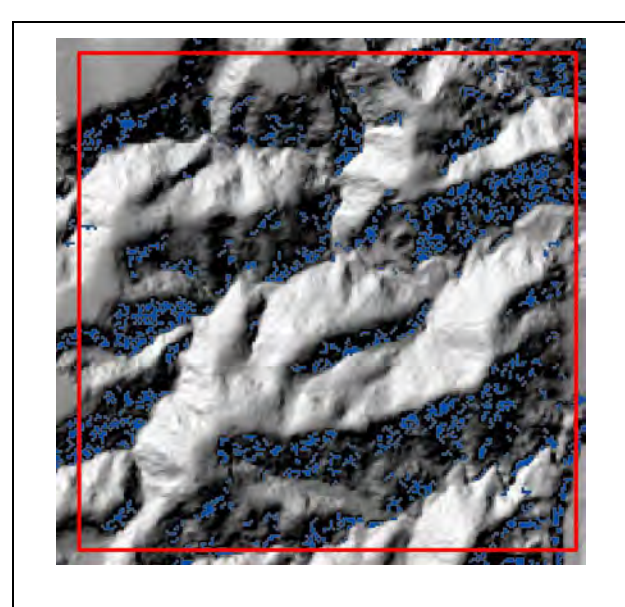
**Figure A105:** On left is un-modified difference layer. On right is difference layer with intervals masked until the flat areas are revealed.



**Figure A106:** Plot of 25000 points sampled to calculate correction factor. On right is statistics around the noise.

XY correction: 2015 DEM was initially nudged by X = 0, Y = +1. Upon seeing the plethora of erroneous "erosion" to be hand edited, an in-depth hunt for sub-metre alignment was done. In a 200m by 200m sampling area, the 2015 DEM was shifted in increments of 25cm

in directions that would reduce the bias of erosion on SW slopes. The GIS steps involved were; Shift Raster > Raster to TIN > TIN to Raster (snapped to align with 2011 DEM). The objective was to recreate the 3D hillslopes and find the new position that had the least variance with the 2011 reference DEM.



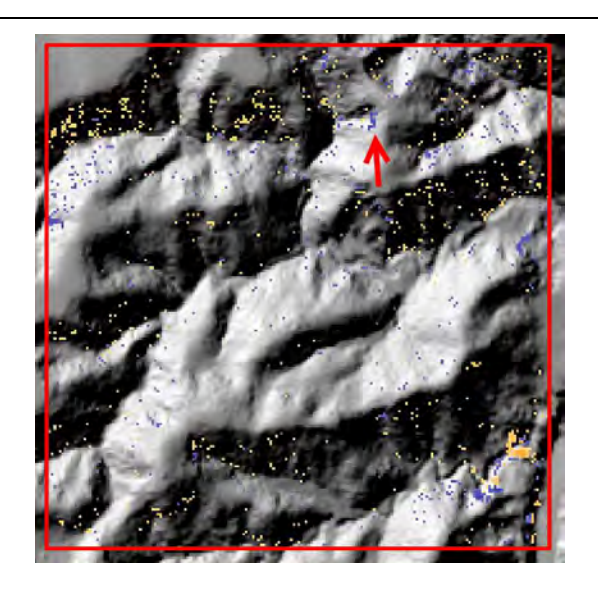


**Figure A107:** On left, difference layer after X0 Y1 correction. On right difference layer after a furthur correction of X 0.5, Y -0.75. The improved alignment of DEM values resulted in about 30,000 polygons for editing being reduced to around 3,300. That is substantial!

Chiff	Coordinata	T	1	1		otd	50th	OOth	95	Coordinata	Court	Coordinata
Shift name	Coordinate shift	mean	max	min	mode	std dev	pctile	90th pctile	pctile	Coordinate shift	Count < - 0.5	Coordinate shift
Harric	Silit	mean	1.40	-	-	ucv	potiic	poliic	petile	Silit	0.5	Silit
18	.5,75	0.022	5	1.880	0.015	0.207	0.017	0.262	0.357	.5,75	613	.5,75
			1.43									
13	.5,5	0.014	5	2.045	0.015	0.197	0.015	0.240	0.325	.5,5	623	.5,5
12	.25,5	0.001	1.39	1.745	0.038	0.203	-0.003	0.235	0.322	.25,5	692	.25,5
	.20, .0	0.001	1.48	-	0.000	0.200	0.000	0.200	0.022	.20, .0	002	.20, .0
14	.75,5	0.029	5	2.213	0.022	0.215	0.030	0.272	0.362	.75,5	694	.75,5
40		0.007	1.46	-	0.007	0.005	0.000	0.040	0.445	75 75	700	75 75
19	.75,75	0.037	0 1.35	2.038	0.007	0.235	0.032	0.312	0.415	.75,75	789	.75,75
17	.25,75	0.007	0	1.878	0.015	0.225	0.000	0.270	0.382	.25,75	872	.25,75
	-,		1.53	-								-, -
08	.5,25	0.006	2	2.088	0.007	0.224	0.007	0.265	0.360	.5,25	927	.5,25
07	05 05	- 0.000	1.48	4 700	-	0.040	0.040	0.000	0.005	05 05	4440	05 05
07	.25,25	0.009	2 1.58	1.788	0.023	0.240	-0.013	0.280	0.385	.25,25	1140	.25,25
09	.75,25	0.021	7	2.388	0.007	0.252	0.022	0.307	0.420	.75,25	1142	.75,25
			1.53	-	-							
23	.5,-1	0.030	0	2.125	0.015	0.270	0.015	0.365	0.480	.5,-1	1152	.5,-1
11	0 5	- 0.016	1.47	1 670	- 0.000	0.050	0.000	0.205	0.440	0 5	1061	0 5
11	0,5	0.016	0 1.54	1.670	0.030	0.252	-0.020	0.295	0.410	0,5	1261	0,5
15	1,5	0.044	0	2.380	0.040	0.272	0.045	0.360	0.470	1,5	1270	1,5
			1.46	-	-							
22	.25,-1	0.015	5	2.123	0.023	0.275	0.000	0.355	0.482	.25,-1	1308	.25,-1
16	0. 75	0.008	1.40	1 070	- 0.000	0.261	-0.018	0.312	0.430	0.75	1353	0.75
10	0,75	0.008	5 1.64	1.870	0.030	0.261	-0.016	0.312	0.430	0,75	1353	0,75
24	.75,-1	0.045	5	2.128	0.007	0.301	0.035	0.412	0.537	.75,-1	1463	.75,-1
			1.51	-								
20	1,75	0.052	5	2.205	0.000	0.297	0.050	0.405	0.525	1,75	1505	1,75
10	1,25	0.036	1.62 0	2.555	0.040	0.293	0.042	0.372	0.497	1,25	1671	1,25
10	1,25	0.030	1.65	2.555	0.040	0.293	0.042	0.372	0.497	1,25	1071	1,25
06	0,25	0.024	0	1.630	0.008	0.292	-0.030	0.340	0.475	0,25	1911	0,25
		-	1.63	-				_	_			
03	.5,0	0.002	0	2.130	0.015	0.296	0.000	0.360	0.480	.5,0	1919	.5,0
21	0,-1	0.000	1.72 0	2.120	0.070	0.314	-0.010	0.390	0.540	0,-1	2001	0,-1
	<b>○</b> ,-1	0.000	1.68		3.070	0.514	-0.010	0.000	0.540	O,-1	2001	J, 1
04	.75,0	0.013	5	2.430	0.040	0.309	0.017	0.377	0.507	.75,0	2061	.75,0
		-	1.77	-	-							
02	.25,0	0.017	0	1.830	0.008	0.317	-0.020	0.377	0.512	.25,0	2305	.25,0
25	1,-1	0.060	1.82 0	2.210	0.000	0.359	0.060	0.500	0.640	1,-1	2430	1,-1
	', '	0.000	1.85		0.000	0.000	3.000	0.000	0.040	4, 1	2400	-, -
05	1,0	0.029	0	2.730	0.000	0.352	0.030	0.440	0.590	1,0	2722	1,0
			2.03									
01	0,0	0.032	0	1.870	0.000	0.365	-0.040	0.430	0.590	0,0	3511	0,0

**Figure A108:** Statistics supporting the sub-metre XY shift to minimise variance in 40,000 points sampled.

# 3.5.11 Erosion/Deposition processing

**Table A52:** The reduction in data volume to determine real and defensible erosion and deposition.

	Raw data		Edited data		Percent reduction in value		
	Raster SUM	Number of polygons	Raster SUM	Number of polygons	Raster SUM	Number of polygons	
Real erosion <= -0.5m		3,314		497			
Shallow erosion <=-0.2 and >-0.5m		109,970		2,585			
Real Deposition >= 0.5m		5,679		293			
Shallow erosion >=0.2 and <0.5m		95,515		2,585			

### Observations from Erosion processing:

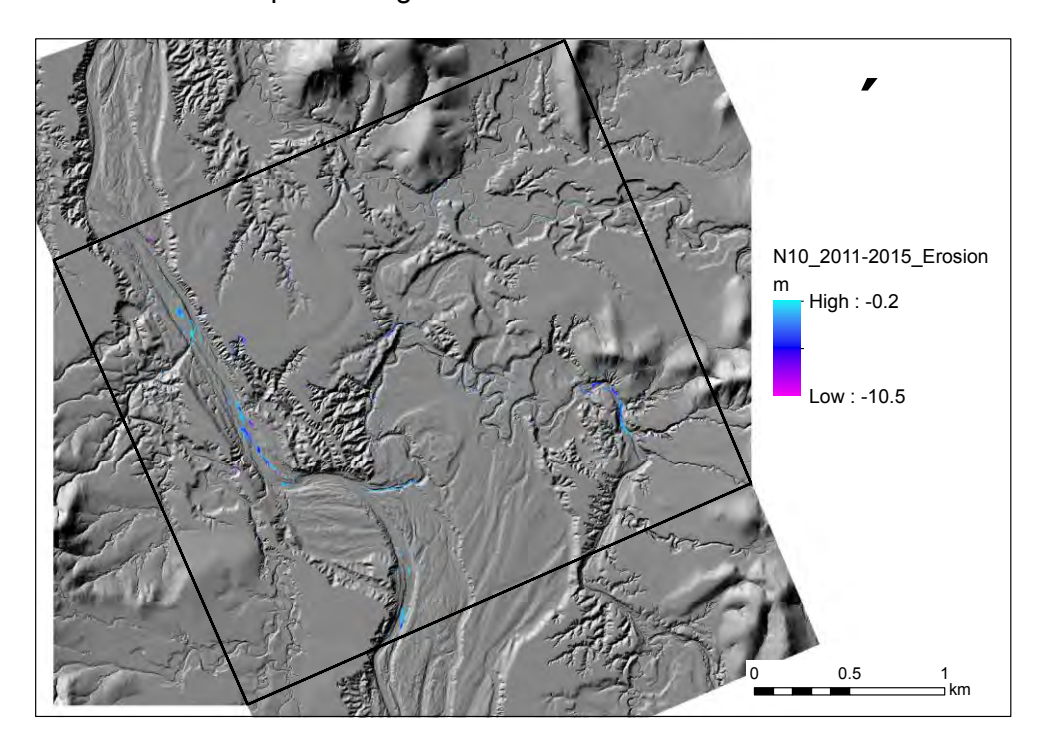
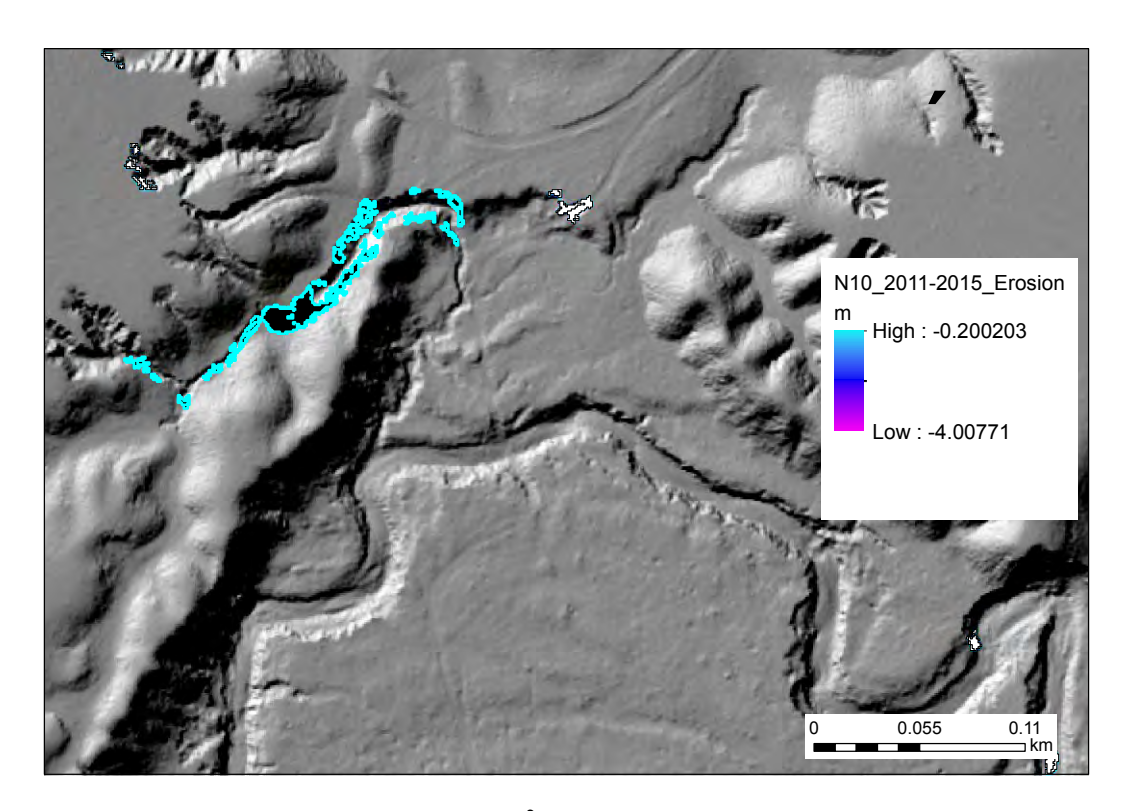
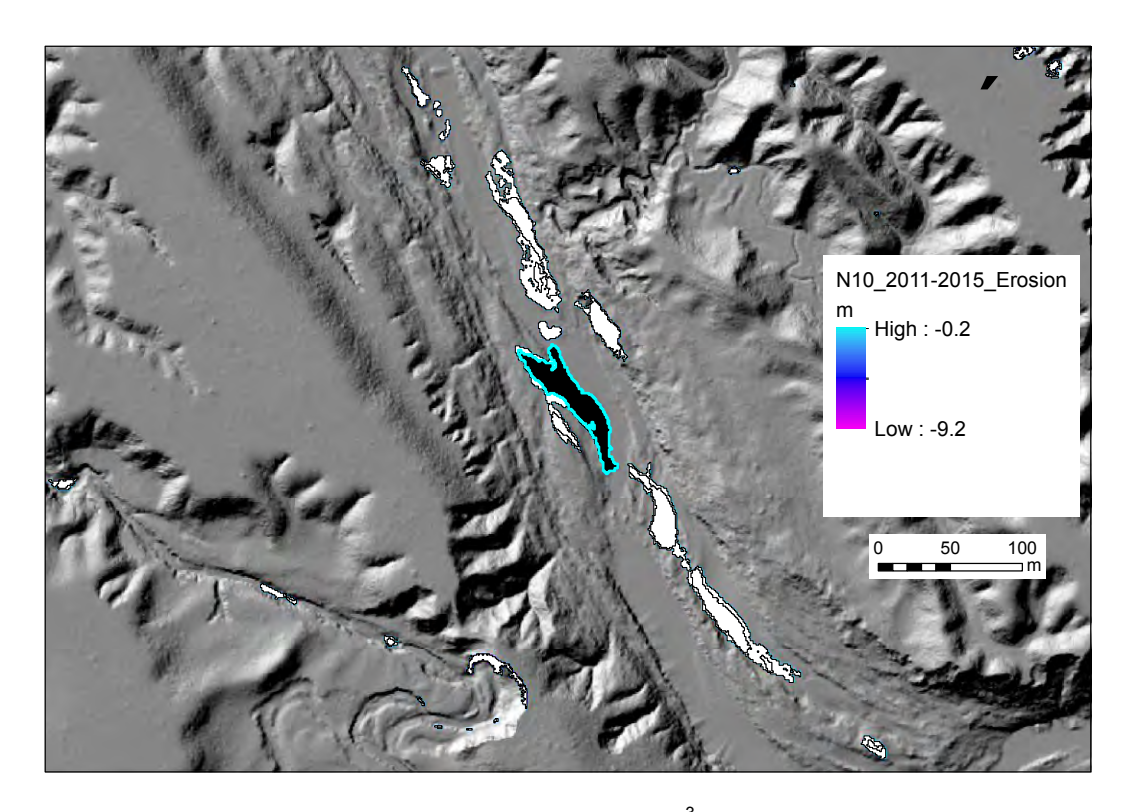


Figure A109: Overview of erosion in N10.



**Figure A110:** The volume of erosion of 1106m<sup>3</sup> from incision into this gully floor and widening of the walls was second only to a patch of erosion bedload erosion in the main channel. See fig 7.



**Figure A111:** The largest patch of erosion by volume; 1190m<sup>3</sup> of bedload erosion in the main channel. Other patches of lesser volume are nearby.

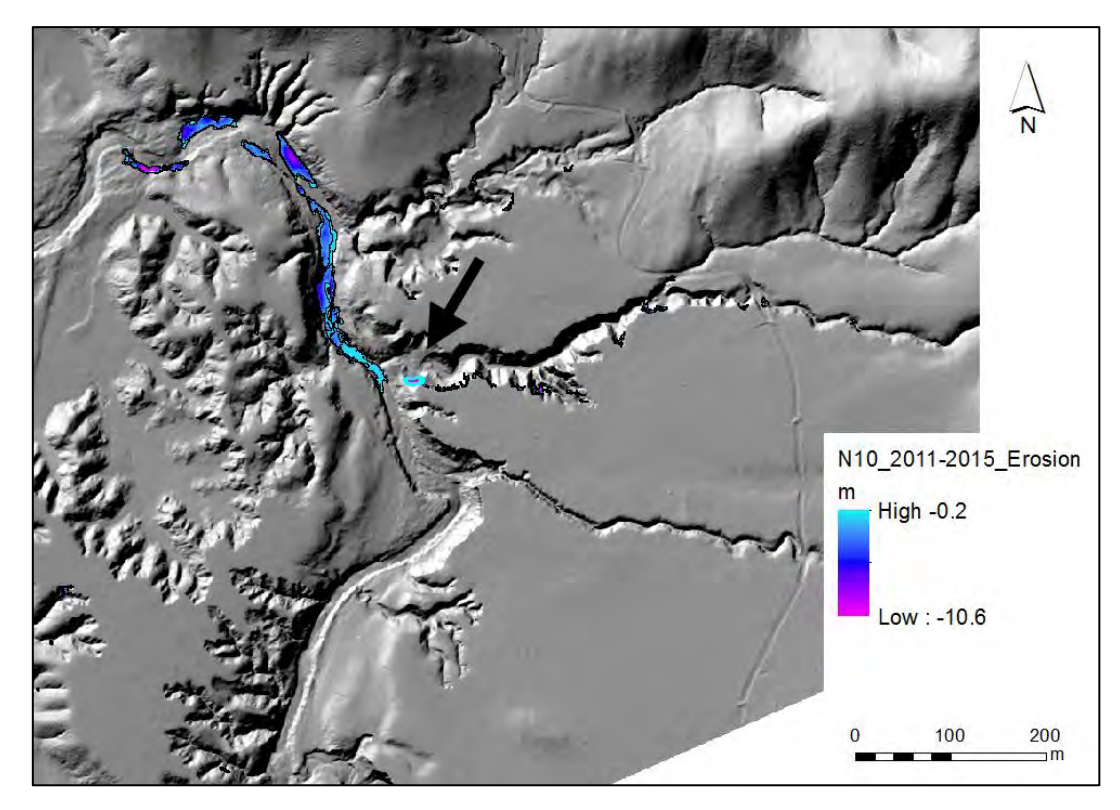


**Figure A112:** The deepest vertical distance of erosion was a collapsed bank at the mouth of a gully – arrowed. There was also plenty of bedload erosion in the secondary channel downstream of the gully outlet.

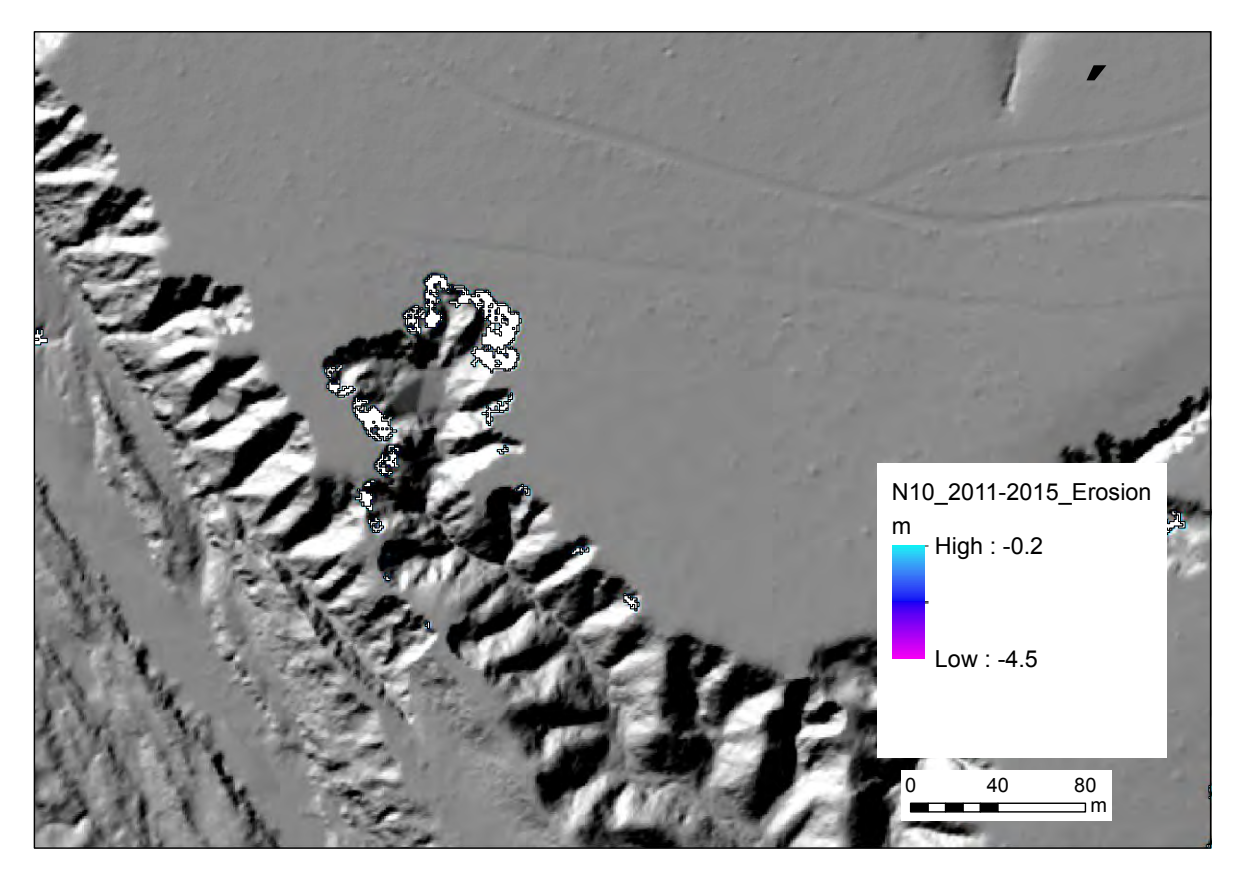
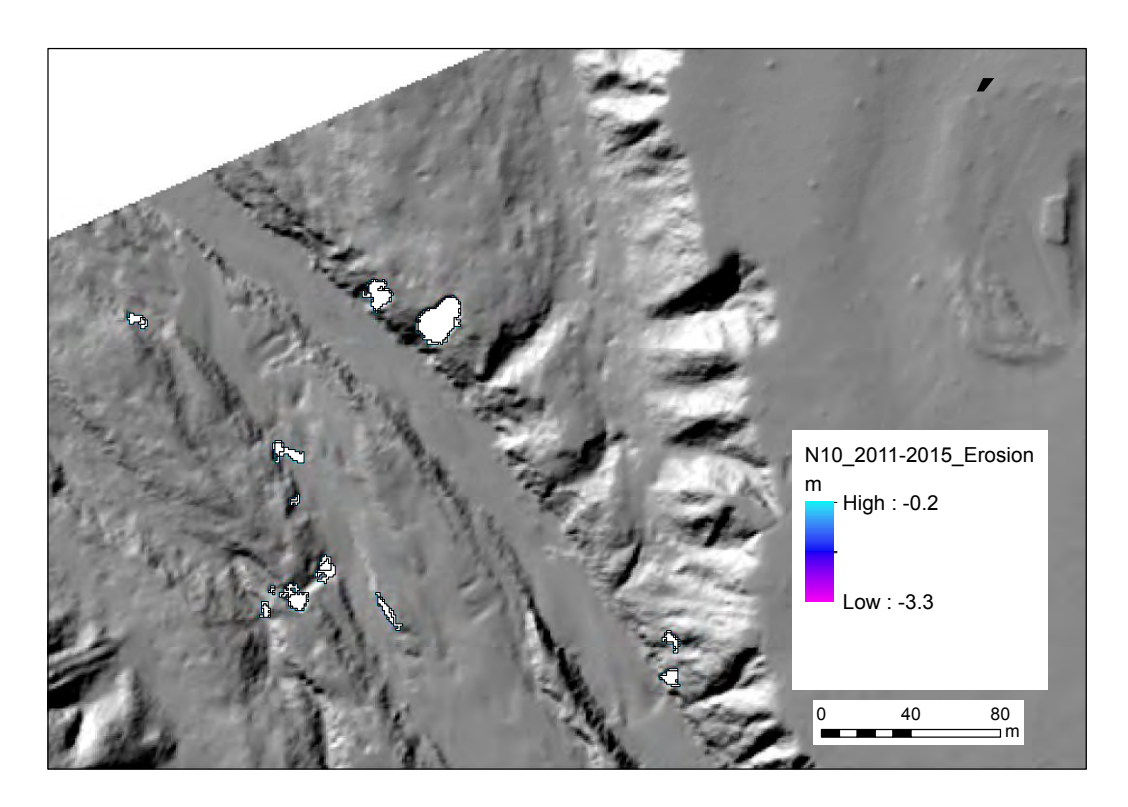


Figure A113: Rapidly expanding gully headscarp migrating into terrace alluvium.



**Figure A114:** Example of a bank mass failure – which are a fairly rare phenomenon in the Normanby.

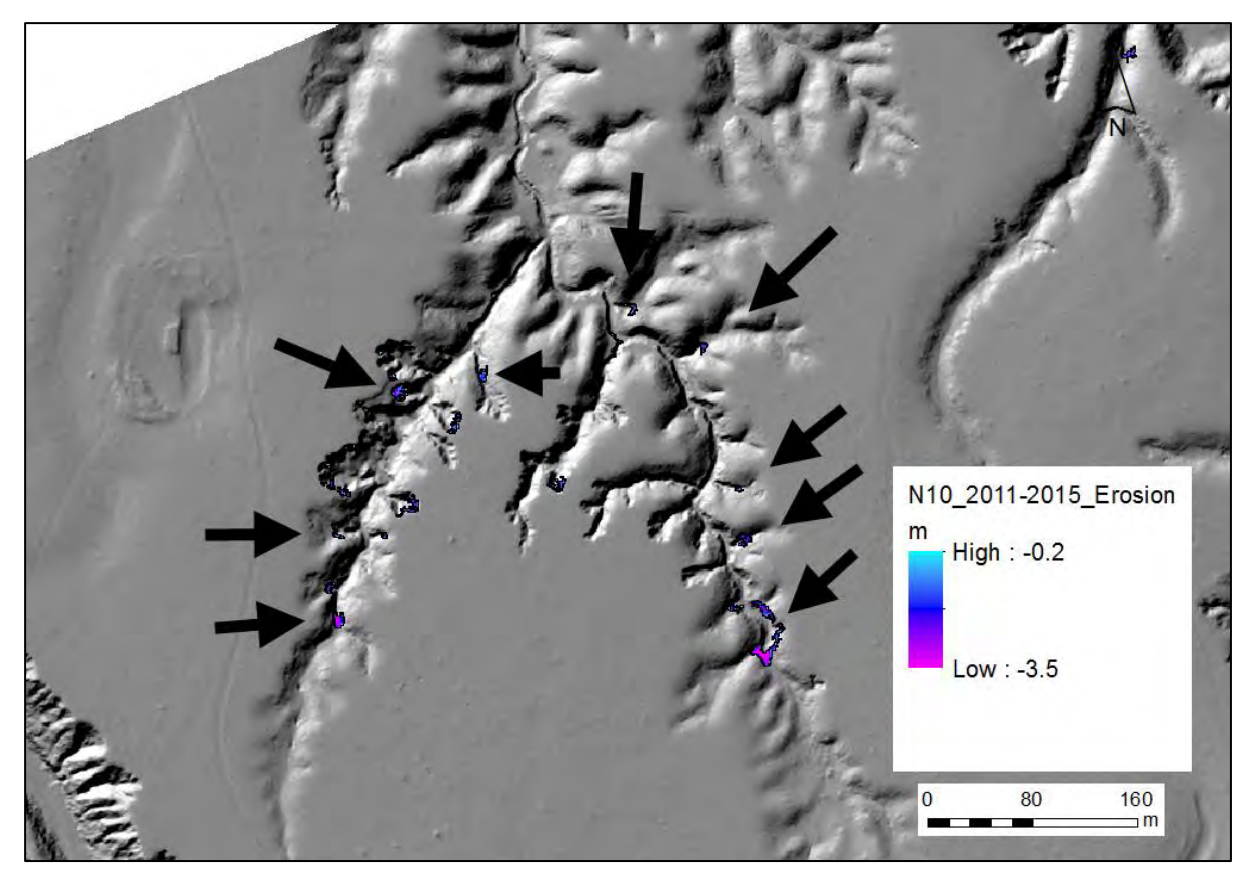


Figure A115: Plenty of examples of reworking of an existing gully floor.

# 3.5.12 Observations from Deposition processing

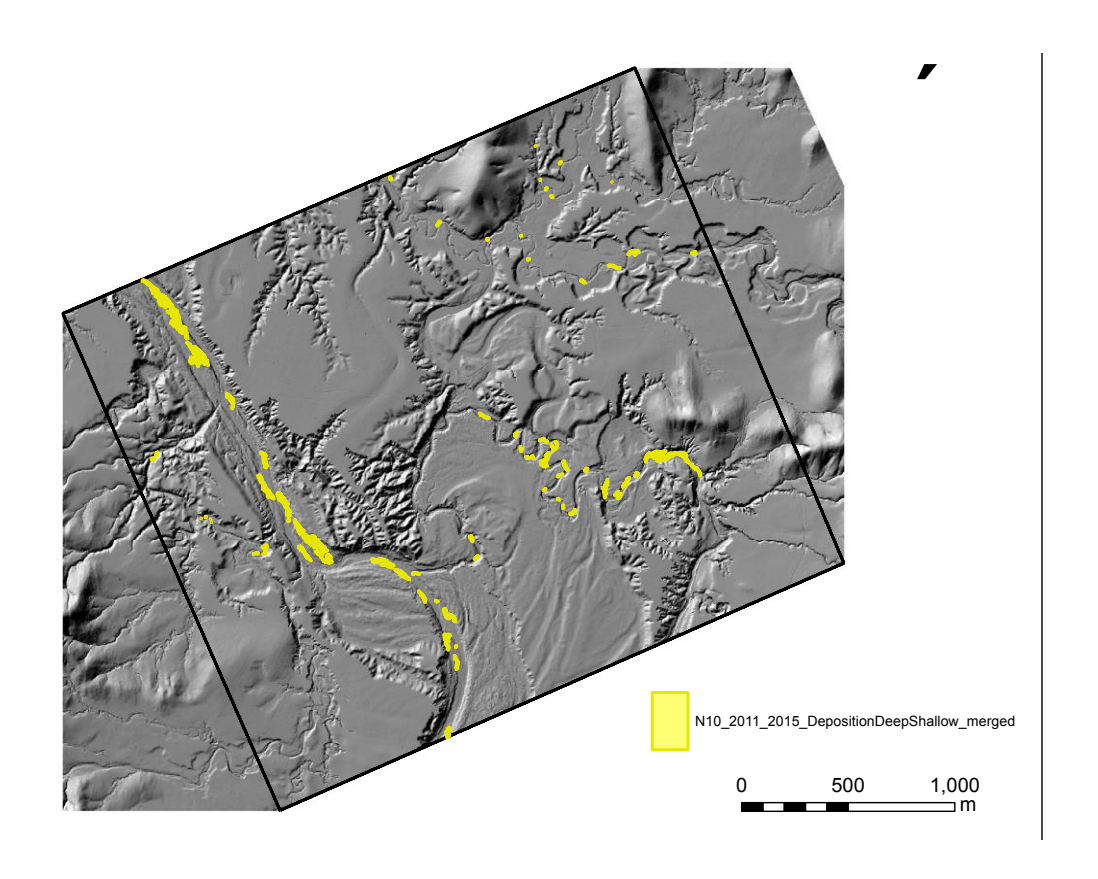
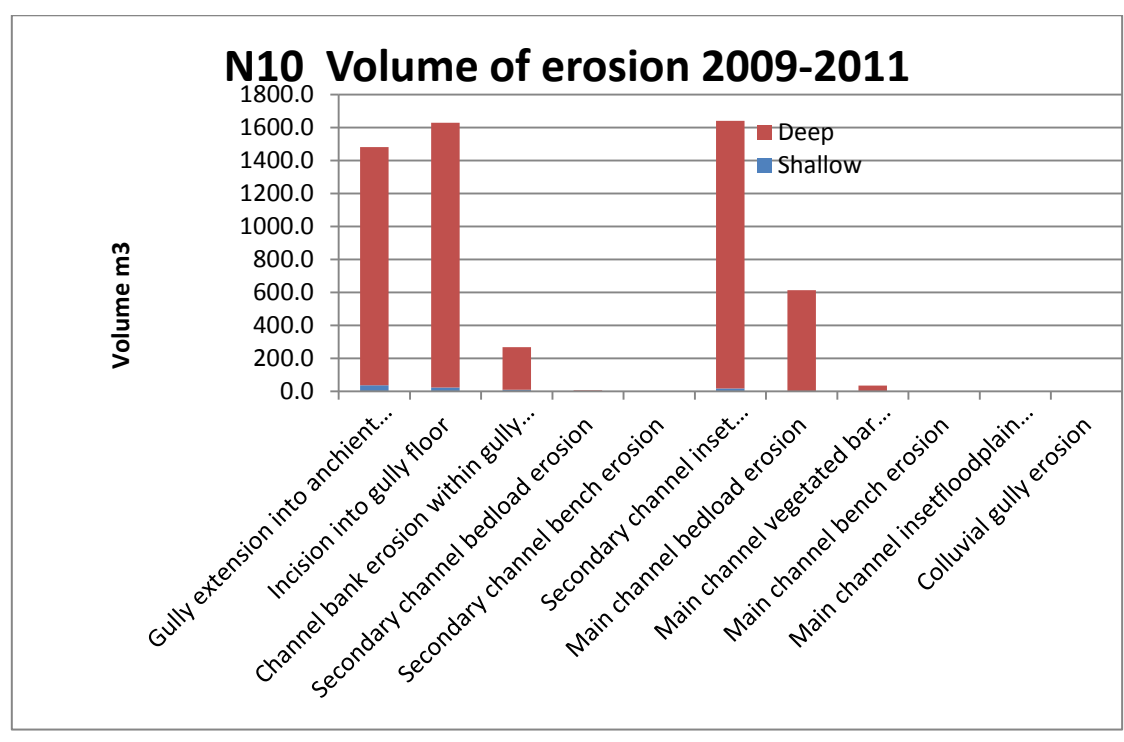


Figure A116: Distribution of deposition in N10, 2011 to 2015.

#### 3.5.13 Summary 2015 Erosion Data + reprocessed 2009-11 data



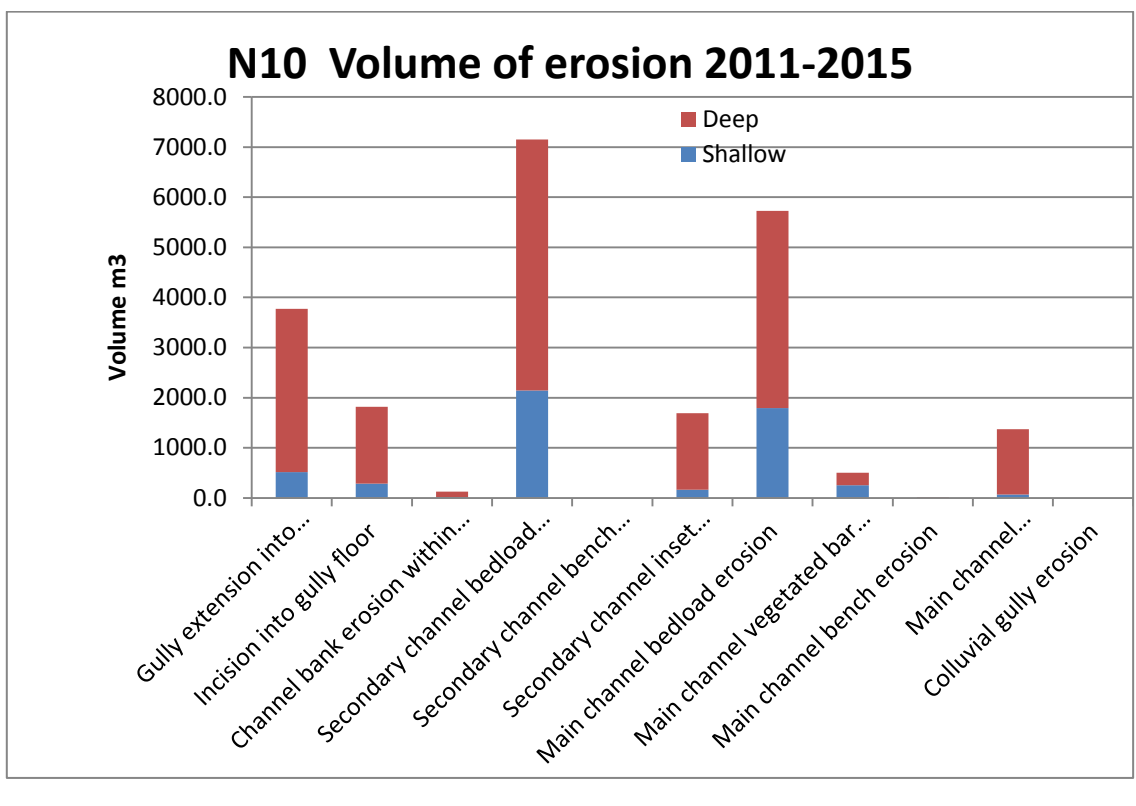
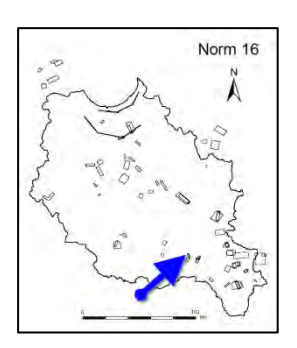


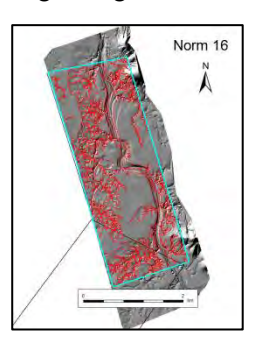
Figure A117: Erosion stats for Block 10 by geomorphic unit 2009-11 (top); 2011-15 (bottom).

# 3.6 Normanby LiDAR Block 16

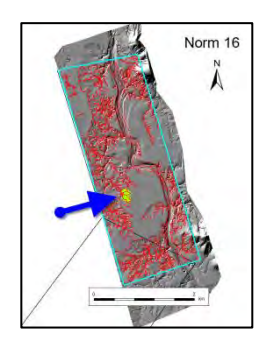
**Block location** 



Digitising on LiDAR



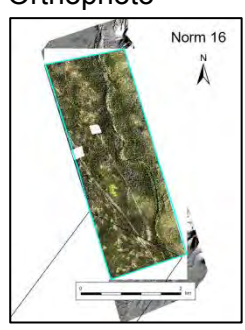
Air photo study gullies



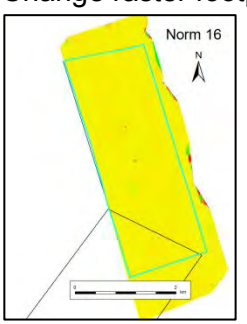
DEM



Orthophoto



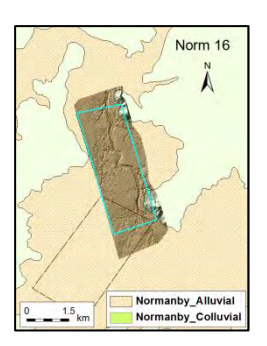
Change raster footprint



Reprocessed change raster area ha	701.7636
Block elevation range m	98 - 221
Number of LiDAR digitised features	443
Number of Google Earth mapped gullies	140

#### 3.6.1 Alluvial and Colluvial zones

#### Alluvial and Colluvial soil



#### Google Earth mapped Gullies



Norm 16	Area ha	Area of all features digitised from LiDAR ha	Features as % of zone	Area of gullies digitised from LiDAR ha	Area of gullies as % of zone	Area of Google Earth digitised gullies	GE gullies as % of zone
Alluvial zone	678.27	262.16	38.7	179.22	26.4	29.57	4.4
Colluvial zone	23.49	13.36	56.9	13.36	56.9	0.00	0.0

#### 3.6.2 LiDAR derived data

#### **Horizontal adjustments**

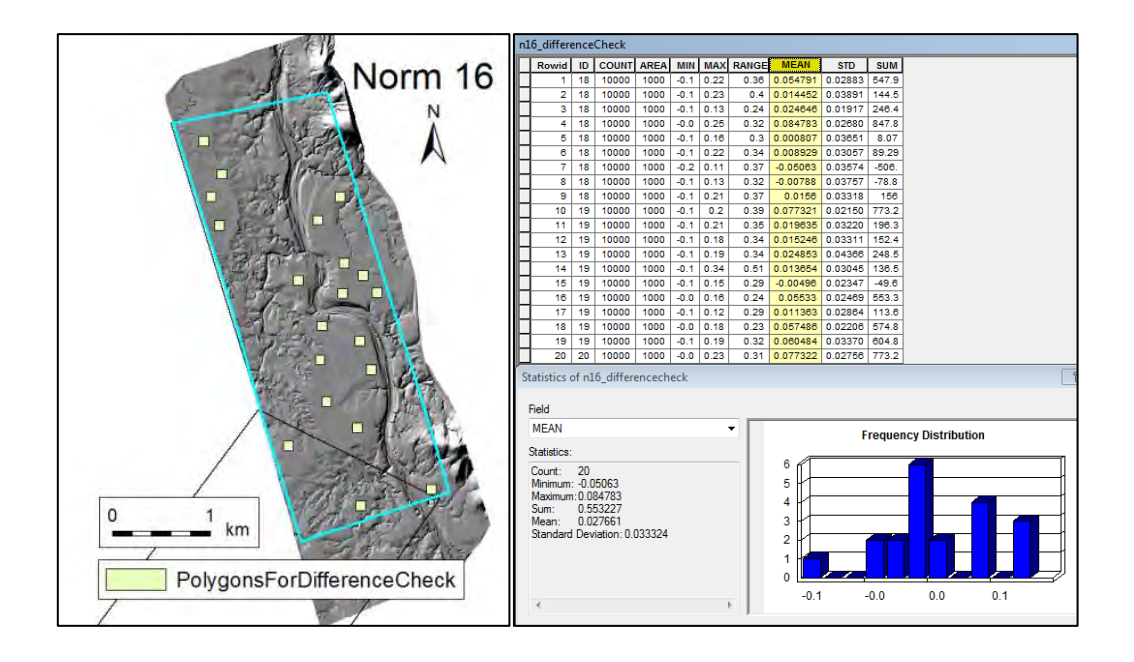
Polygons digitised from 2009 LiDAR, CHM and PFC rasters have been nudged to align with reprocessed 2009 LiDAR by:

X,Y nudge (m)	2 , -1

#### **Vertical adjustments**

Adjustment for vertical offset of 2009 and 2011 DEMs

20 polygons of  $1000 \text{ m}^2$  were put in areas where very little change would be expected to occur; ancient flood plain. Mean value of change raster within the 20 locations was used as a correction to the whole change raster.



#### 3.6.3 Statistics

Layer	min	max	Mean	s.d.
Norm_16_Difference_2009-2011_Reprocessed.tif (as supplied by Terranean)	-16	83	-0.078	0.13
Norm_16 with edge effect removed	-7.12	4.01	0.016	0.12
Areas of minimal change	-0.05	0.08	0.028	0.03
N16_Diff_adjusted	-7.14	3.98	-0.012	0.12

The level of noise on flat flood plain areas has been ascertained, and these values removed from the erosion and deposition layers.

Values of change raster filtered to remove noise on floodplain.

raster	Values filtered
erosion	0 to -0.2
deposition	0 to 0.2

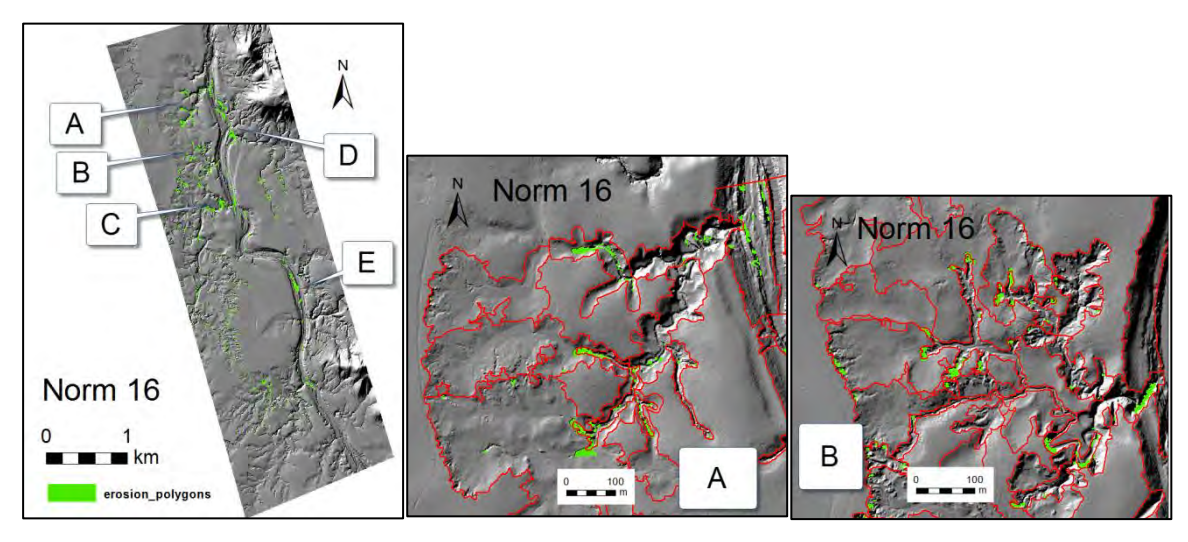
#### 3.6.4 Aggressive filtering of erosion and deposition data

Broad, shallow gullies advancing with wide head scarps Norm 16 were not picked up using a 1m threshold for the change raster, as were many mobile bars in the channel bed. These changes were picked up satisfactorily using a 0.5m threshold.

The table below shows the volume of data removed by hand thinning erroneous erosion and deposition data.

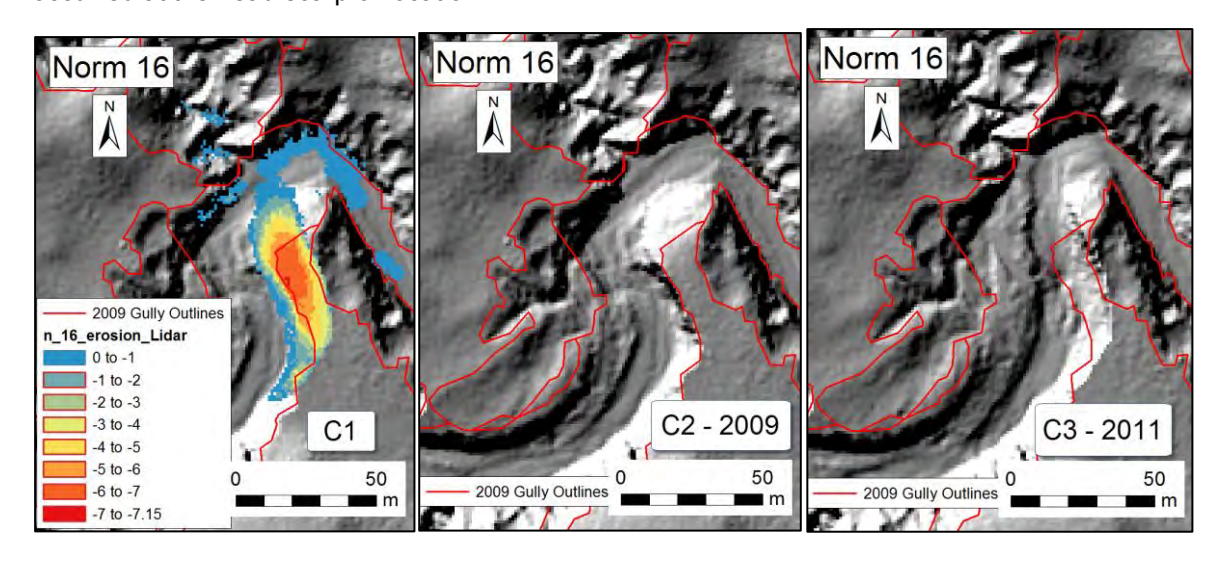
	eı	rosion	dep	osition
	area ha	raster sum	area ha	raster sum
Prior to hand thinning	57823 -38,221		61297	28,097
After hand thinning	23,678	-17,297	4,944	2,167

#### 3.6.5 Observations

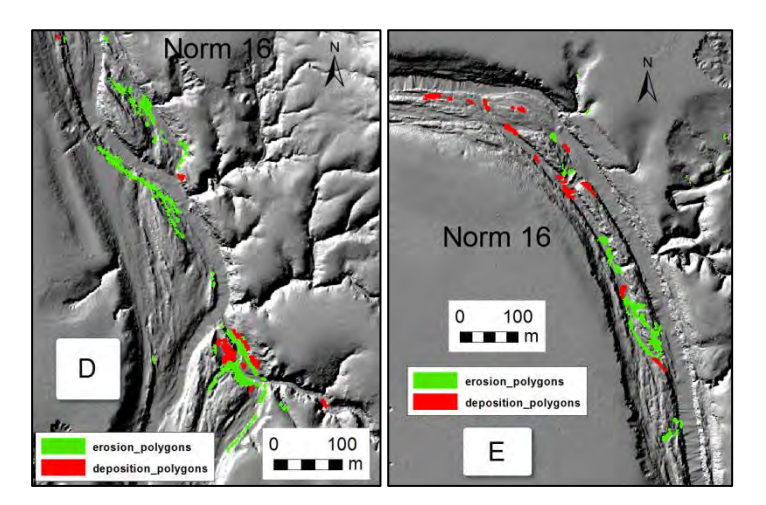


Location A: Recent erosion activity occurred as deepening and extension of incisions into channels that drained aged gully complexes. Each of the main 4 advancing headwalls had erosion activity zones between 40 to 70m.

Location B: A similar pattern to location A, though the areas of erosion activity were in the range of 7 to 20m. Some erosion activity occurred at the ultimate gully head scarp, which was more than occurred at the head scarp of location A.



Location C: A narrow finger of land creating a sharp loop in a secondary channel suffered heavy erosion forces, losing up to 13m of horizontal distance, and over 7m of material vertically. If this continues, a major straightening of the channel will occur.



Location D: High water channels within the meta channel were re-sculptured in the vicinity of a junction with a secondary channel. Stripping occurred along the outside bank of the main flood channel, and possibly a meeting of turbulent flood flows from the secondary channel eroded the confluence zone, kicking up material that was deposited on both banks immediately downstream of the confluence.

Location E: Highwater flows moving from the main channel to a flood channel have stripped material from a vegetated bar. Deposition has occurred within the flood channel, downstream of the erosion, but not within the vegetated bar.

#### 3.6.6 Erosion and deposition

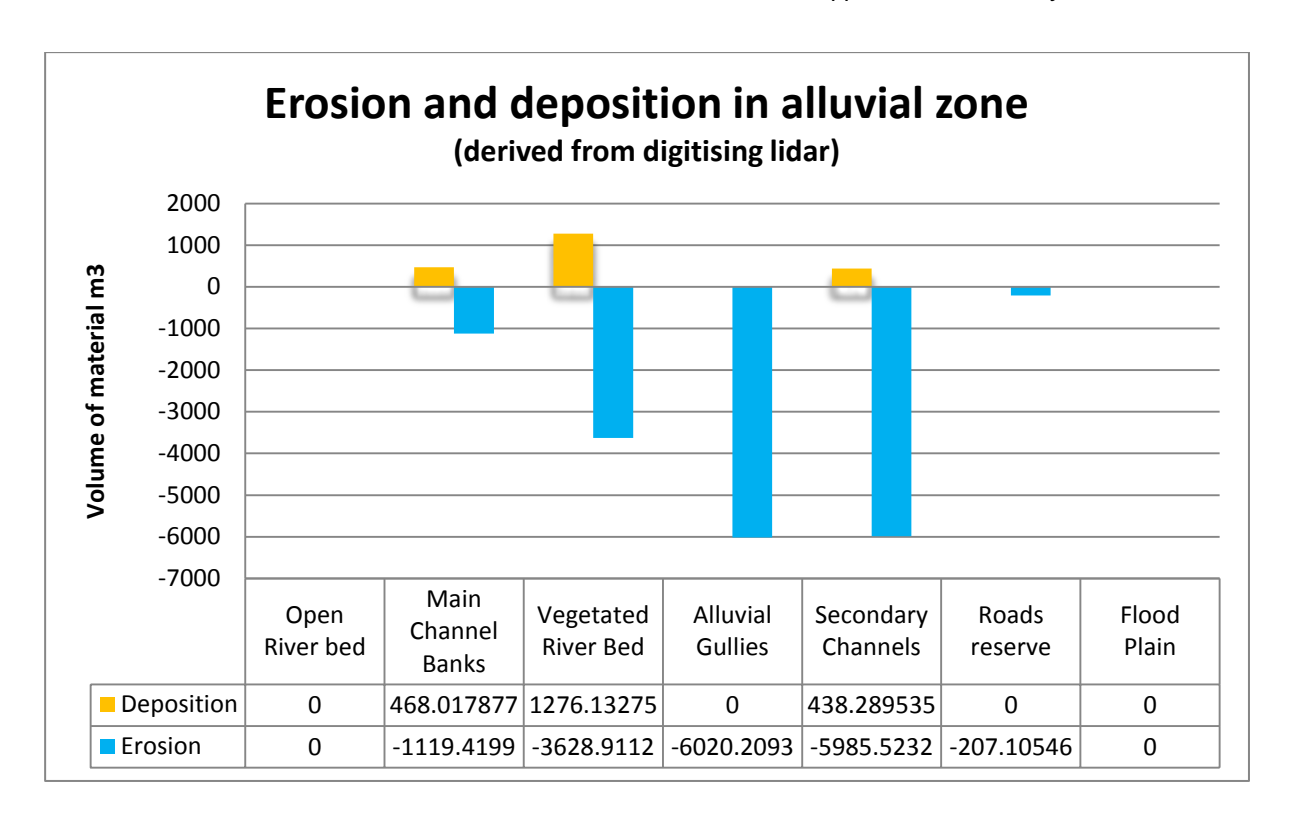
Secondary channels were 10% of the area of alluvial gullies, but similar volumes of erosion at around 6000m<sup>3</sup>.

Values of erosion and deposition for open riverbed were not calculated, as digitising of LiDAR had not been done to isolate these areas. Values for main channel banks include values for open riverbed.

Gullies eating out some vehicle tracks had extended by up to 20m in some places.

Vegetated patches of the main channel gained 1276m3 of materials, but had a net loss of material due to stripping of material as flood waters tore preferential channels through the trees.

Patterns of erosion in alluvial gullies generally followed advancing incisions along the bottom of aged, broad and shallow fan shaped gullies.



#### 3.6.7 Comparison of alluvial gullies to colluvial gullies

Alluvial gullies				Colluvia	l gullies		
	deposition	erosion	yield		deposition	erosion	yield
area ha	m3	m3	m3/ha/yr	area ha	m3	m3	m3/ha/yr
179.22	0	-6020.2	-16.79	22.83	0	-8.2	-0.18

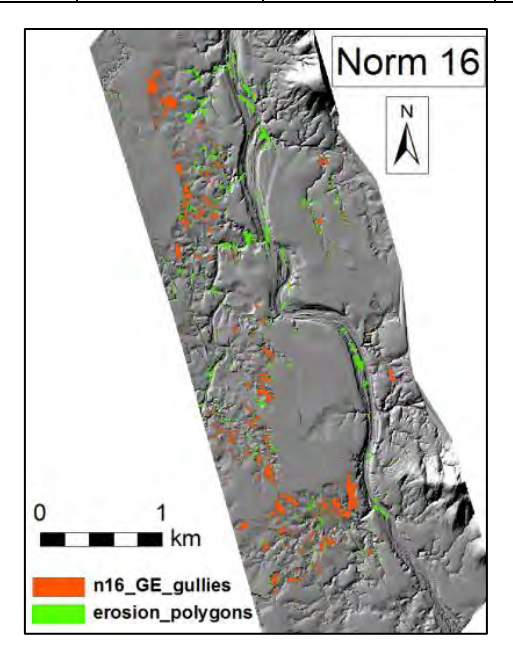
The area of colluvial gullies was 7.5% of the area of alluvial gullies in norm 16, and volume of erosion from colluvial gullies was 0.1% of the volume eroded from alluvial gullies. The contribution of erosion from colluvial sources in the Norm 16 block was very minor.

#### 3.6.8 Comparison of Google Earth gullies to LiDAR gullies in the alluvial zone

The area of Google Earth gullies was 17% of area of alluvial gullies from LiDAR digitising, but erosion from GE gullies was 8% of the volume eroded calculated from alluvial gullies.

Many of the recent active and highly productive incisions were in areas that appeared vegetated in the orthophoto, and so would not have been obvious in Google Earth.

	Area ha	erosion m3	Yield m3/ha/yr
LiDAR alluvial gullies	179.22	-6020.21	-16.80
GE alluvial gullies	30.35	-455.06	-7.50



#### 3.6.9 Gully Expansion 2009 - 2011

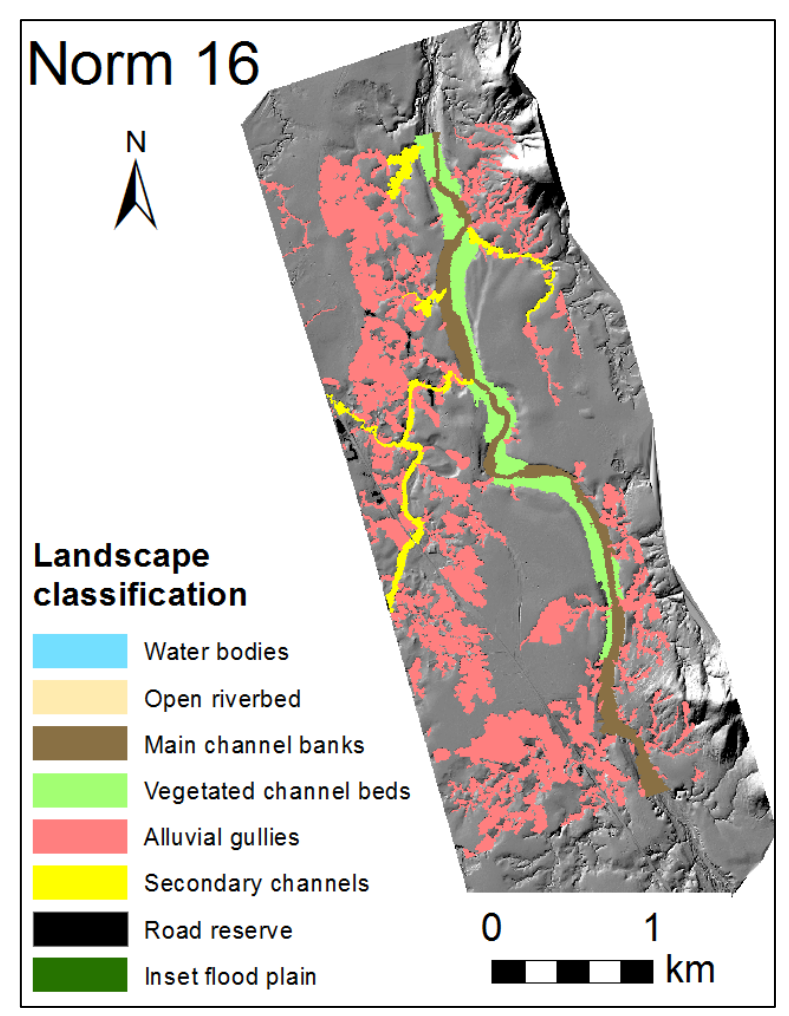
After hand thinning, 2.4ha of erosion surfaces remained across all landscape classes. Over half of the erosion surfaces were within the existing boundaries of alluvial gullies, secondary channels and main channel features. The 2 largest areas of expansion were 452m² where a secondary channel cut deeply into a bank, and 91m² where a sloping vehicle track was becoming a canyon.

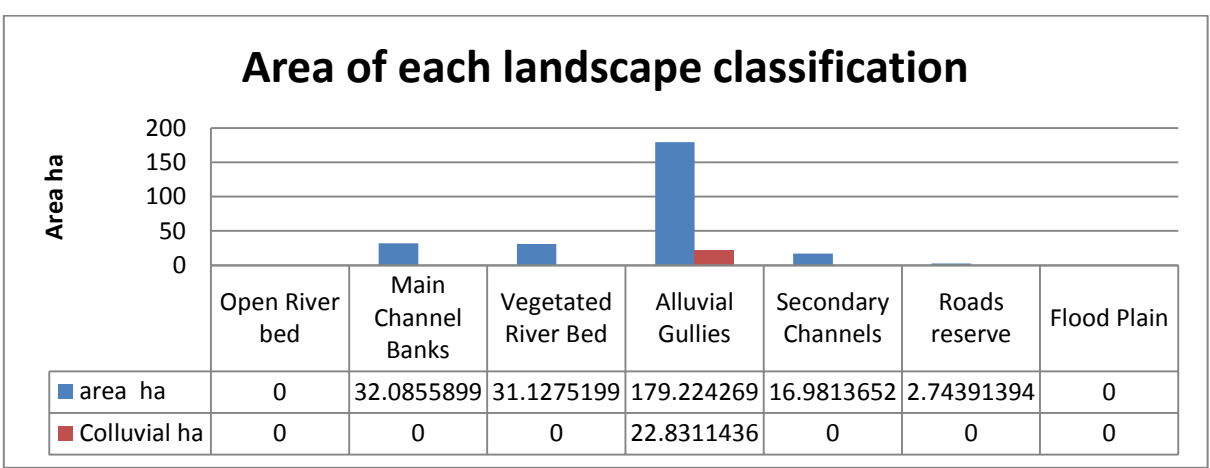
The following table summarises total gully expansion between 2009 and 2011.

Gully Expansion 2009 - 2011	
Number of gully expansion locations	131
Sum area of gully expansions ha	0.1049
Mean area of expansion m2	8

#### 3.6.10 Landscape Classification

This dominant landform in Norm 16 was broad, shallow alluvial gullies that had active incision channels advancing into them. Significant formal and informal roads were visible in the LiDAR, and gullies were classed as road reserve where erosion was following road surfaces and drainage channels.





#### 3.6.11 Historical air photos

One gully in this block has been identified in air historical air photos from 1952 and 1987.

Image date	Photo ID	Scale	Flying height	RMS error of georeferenced air photo	Air photo position relative to 2009 LiDAR block
1/01/1952	QAP 317-10	23900	12750ft	1.89378	
1/01/1987	QAP 4110- 115	25000	4310m	0.80831	

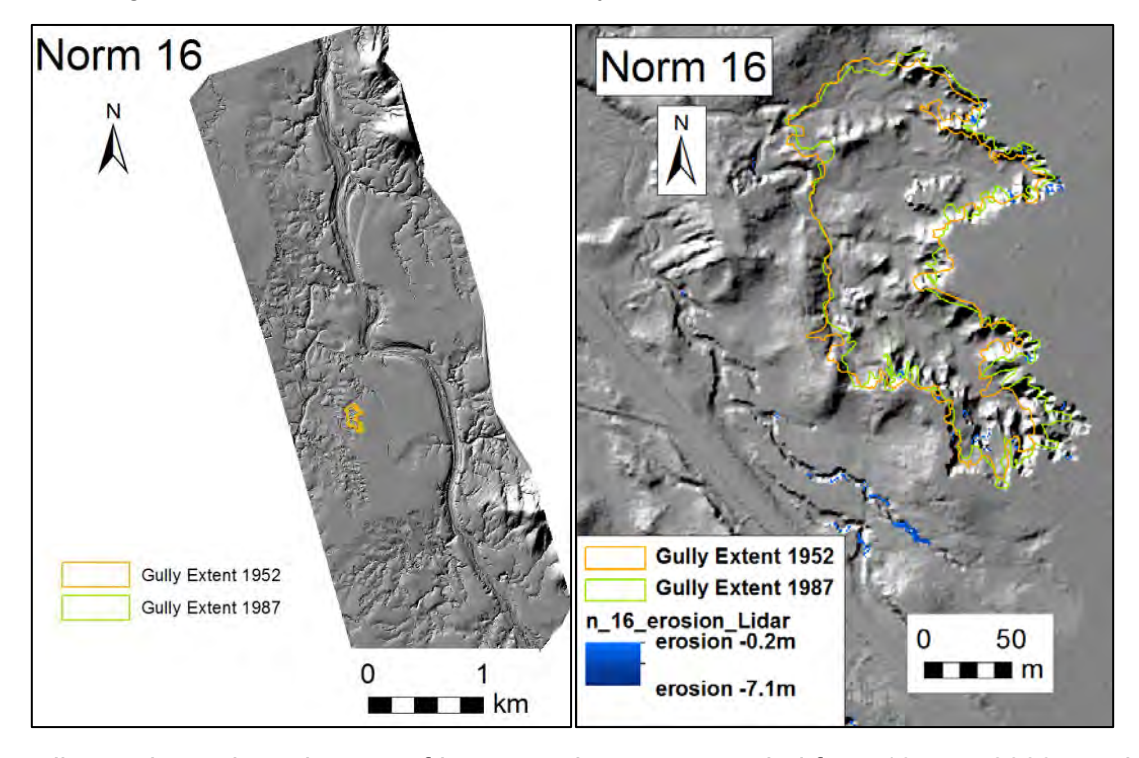
#### 3.6.12 Historical gully extent

**Gully one:** The gully floor was approximately 4m deep across most of its extent, with the remains of a previous floor perched at 2m below the gully rim. Erosion at the north eastern lobe was proceeding at the 3m high headwall, while at the south eastern lobe erosion was occurring at an incision of the floor as well as extension of the headwall in several places.

Between 2009 and 2011 the gully area expanded 4m<sup>2</sup>.

#### Location diagram

#### Gully 1 detail



According to these data, the rate of loss over the 57 year period from 1957 to 2009 was less than half the rate of loss over the 22 year period from 1987 to 2009. There was relatively little increase in gully area between 1952 and 1987, indicating a dry spell with little gully expansion happening, or problems recognising the full extent of the gully from historical air photos.

The rate of erosion between 2009 and 2011 was 10% of the rate between 1987 and 2009.

Interval	Gully area at start Rate of loss of period ha m³/yr		Yield m3/ha/yr Based on 2009 gully area
1952 - 2009	1.7813	207	74
1987 - 2009	1.8636	430	154
2009 - 2011	2.7952	42	15

# 3.6.13 Comparison of gully volume and erosion calculations using reprocessed 2009 LiDAR and original 2009 LiDAR

In this instance, there was very little difference in values of the original 2009 DEM and the reprocessed 2009 DEM, and hence, only small differences in the volume of erosion and yields calculated from both data sets.

This gully was largely spared the foibles of vegetation removal algorithms that also remove terrestrial features, or the human decisions of where and how much to accentuate abrupt edges in LiDAR derived DEMs.

Gully and Interval	Volume of erosion, using reprocesse d 2009 LiDAR, m3	Volume erosion from original 2009 LiDAR m3	% difference in volume 2009repro/ 2009origin al*100	yield using reprocesse d LiDAR m3/ha/yr (using 2009 gully area)	yield using original LiDAR m3/ha/yr (using 2009 gully area)	% difference in yield reprocesse d/original*1 00
Gully 1 1957- 2009	11912.5	11803	101	75	74	101
Gully 1 1987- 2009	9853.5	9465	104	160	154	104

#### 3.6.14 LiDAR 2015 data processing

## Z correction: 0.73965 was added to 2015 Lidar

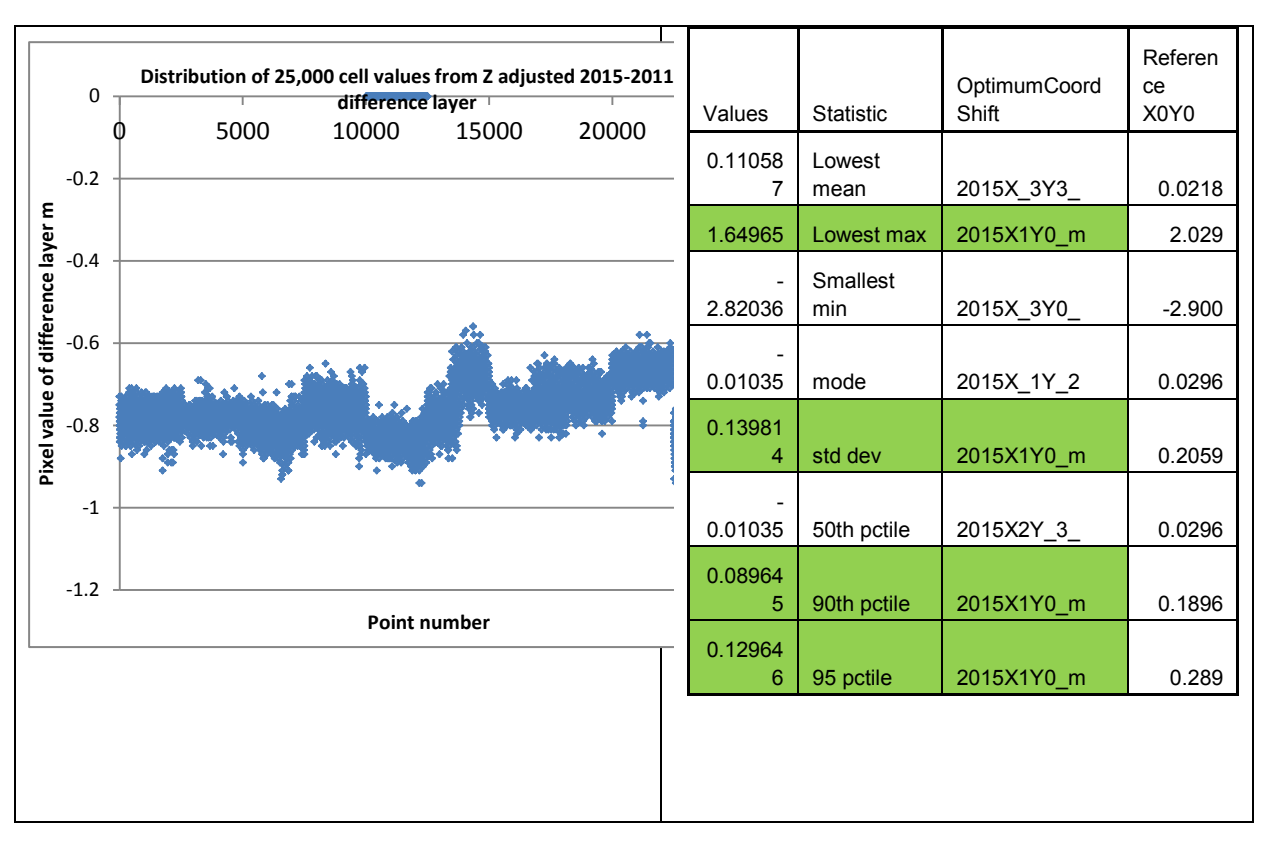


**Figure A118:** Plot of 25,000 points sampled to calculate correction factor. On right is statistics around the noise.

## XY correction: 2015 DEM was nudged by X = +1, Y = +0

And to relieve the mess of false erosion and deposition remaining a lengthy series of trials and errors was done that eventually settled of a further shift of X=0.25 and Y=0.25.

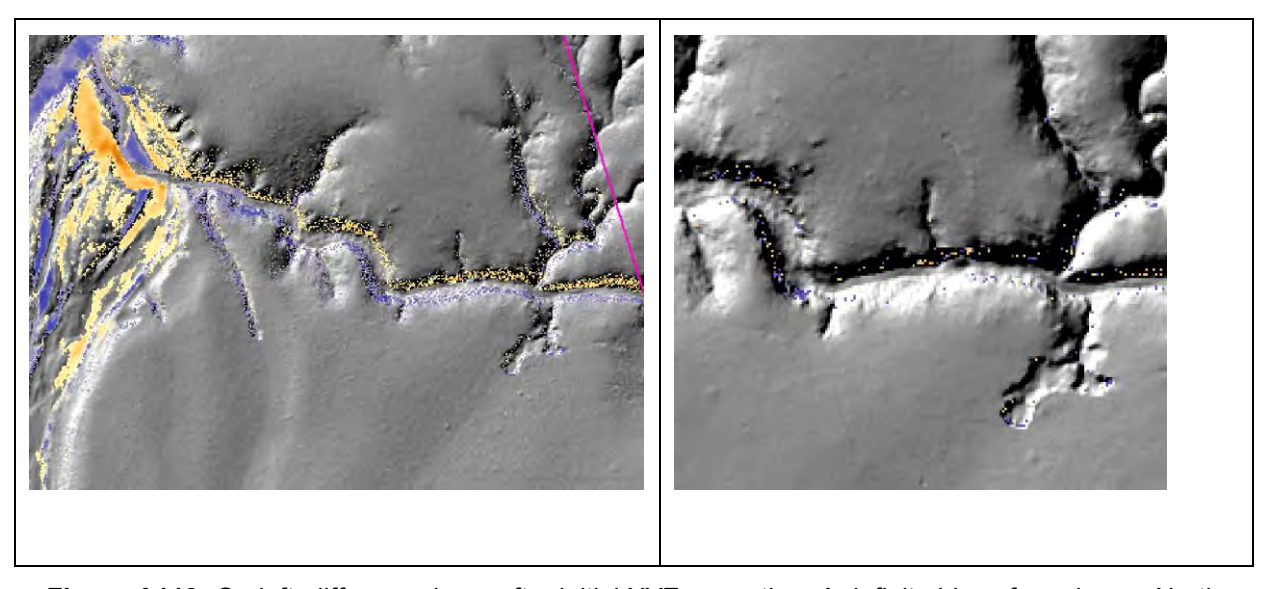


**Figure A119:** On left, difference layer after initial XYZ correction. A definite bias of erosion on North and East facing slopes can be seen. On right difference layer after sub-metre XY correction.

CodeName	01	02	03	04
Coord Shift	X0.25 Y0.25	X0.5 Y0.25	X0.25 Y0.5	X0.5 Y0.5
Min	-2.6579	-2.473	-3.453	-3.505
Max	1.7946	2.000	3.000	4.000
Mean	-0.0548	-0.057	-0.056	-0.059
median	-0.0554	-0.058	-0.058	-0.060
mode	-0.0654	-0.058	-0.065	-0.050
Std dev	0.1011	0.109	0.106	0.124
50th pctile	-0.0554	-0.058	-0.058	-0.060
90th pctile	0.0121	0.017	0.015	0.025
95th pctile	0.0647	0.080	0.070	0.090
Count <= -0.5	192	207	202	294
Count >= 0.5	80	98	69	141

Figure A120: Statistics supporting the XY shift to minimise variance in 40,000 points sampled.

# 3.6.15 Erosion/Deposition processing

**Table A53:** The reduction in data volume to determine real and defensible erosion and deposition.

	Raw data		Edited data		Percent reduction in value	
	Raster SUM	Number of	Raster SUM	Number of	Raster SUM	Number of
		polygons		polygons		polygons
Real erosion		8,339		1,908		
<= -0.5m						
Shallow erosion <=-0.2 and >-0.5m		94,153		5,080		
Real Deposition >= 0.5m		1,530		207		
Shallow erosion >=0.2 and <0.5m		37,605		605		

### 3.6.16 Observations from Erosion processing:

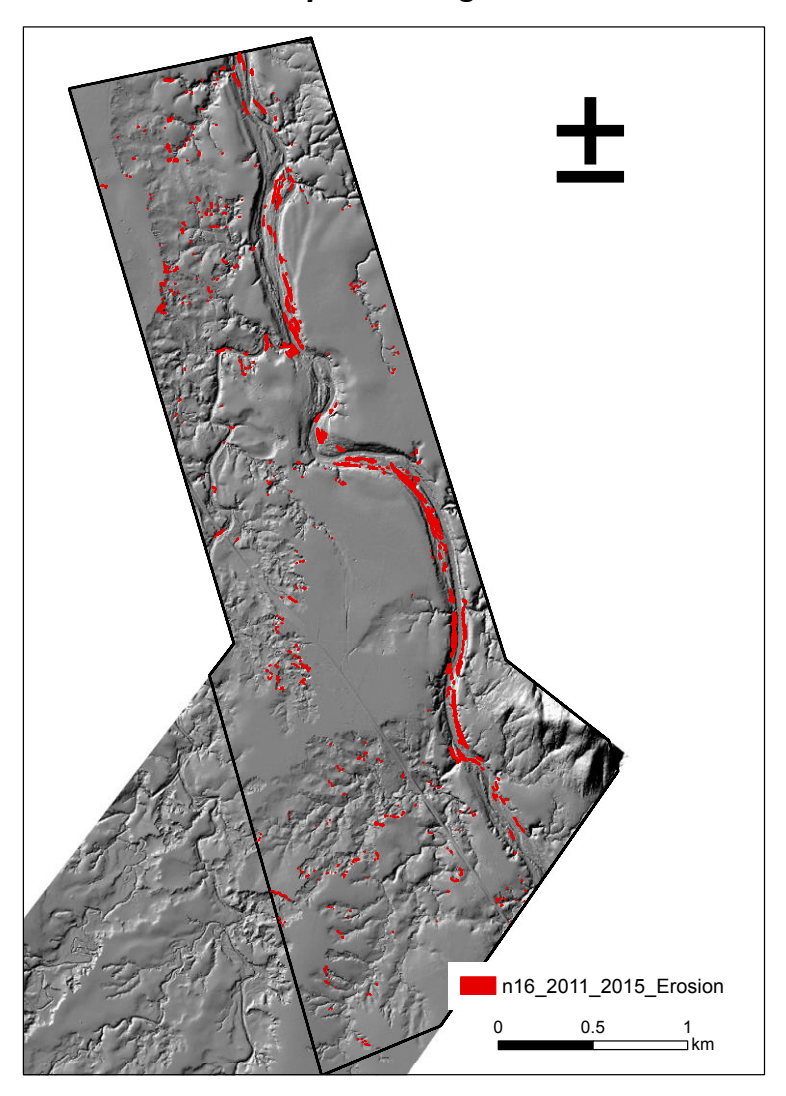
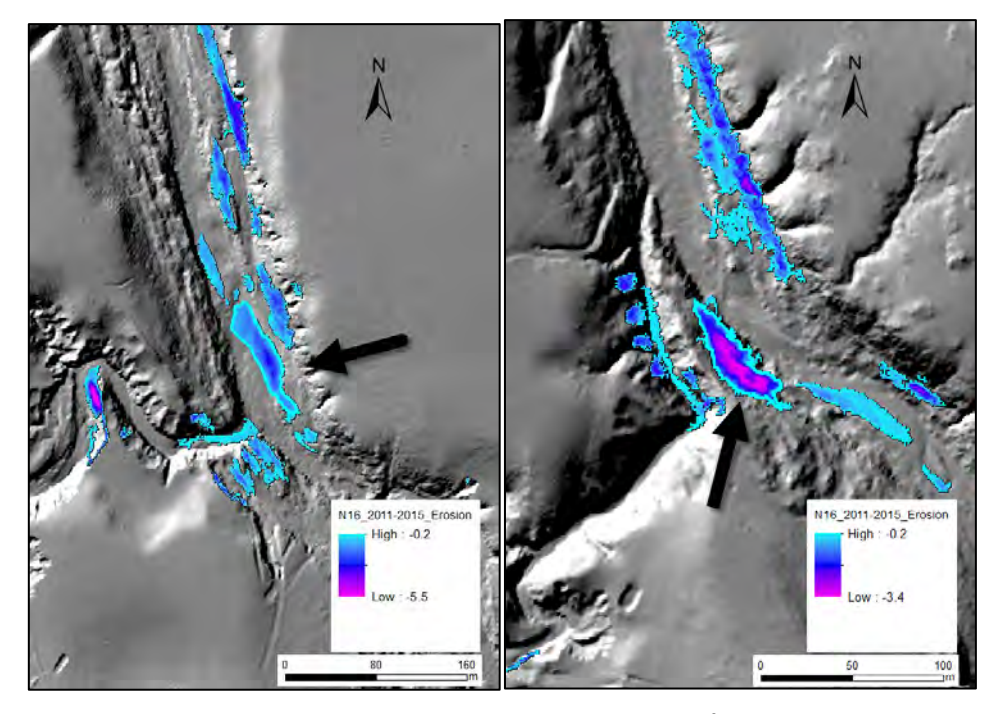


Figure A121: Overview of erosion locations in N16.



**Figure A122:** (L) The largest volume patch of erosion 1613m<sup>3</sup> – main channel bedload. **Figure A123:** (R) Second largest by volume, 1496m<sup>3</sup>, from a bench along the main channel.

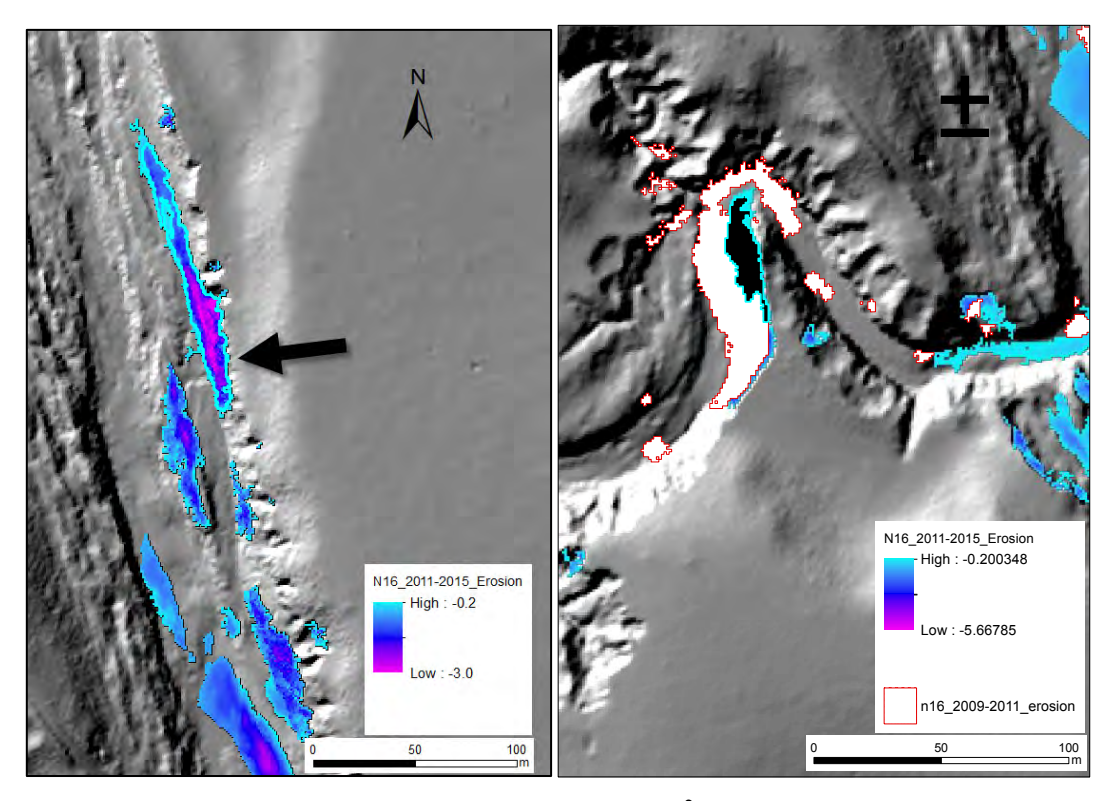
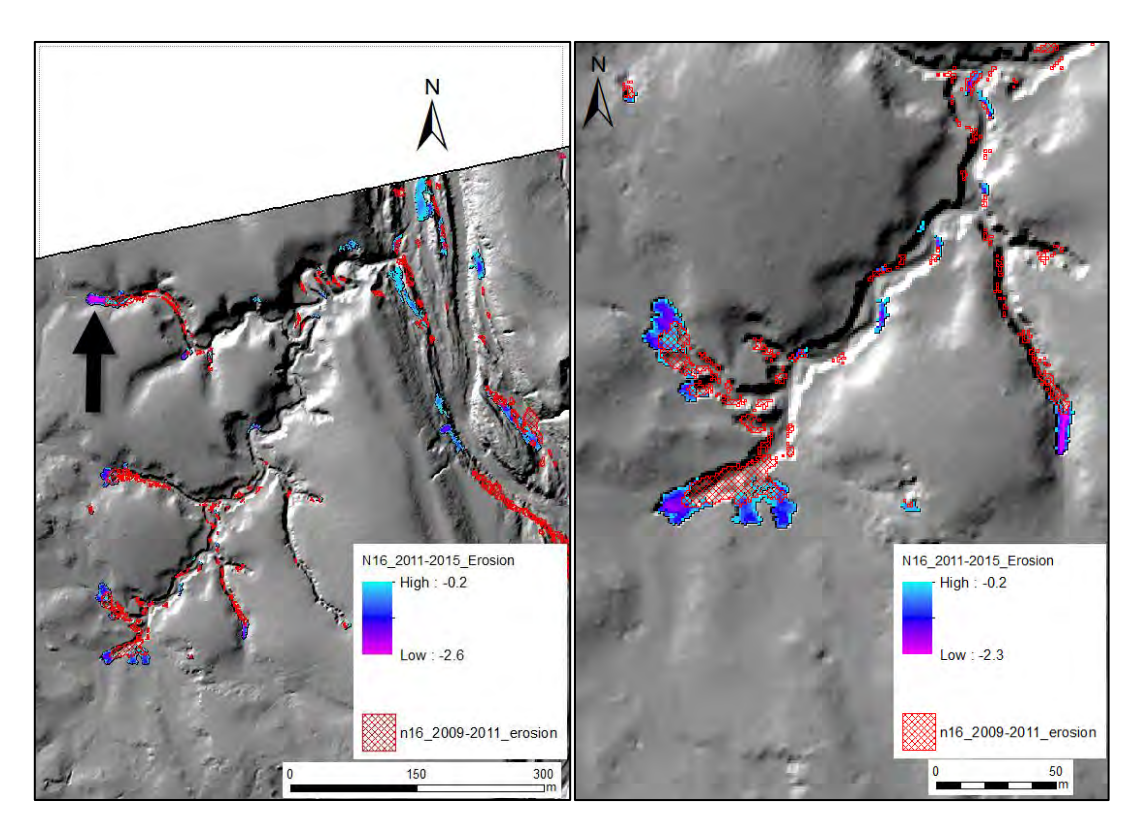


Figure A124: (L) Third largest by volume, 1471m<sup>3</sup>, from main channel bench.

**Figure A125:** (R) This corner of a secondary stream eroded heavily between 2009 and 2011. More recent erosion was less, though we can say a bank face lost material up to 5.6m in depth.



**Figure A126:** (L) Gully arrowed had headwall extension of 32m between 2011 and 2015. Headwall extension between 09 and 11 was 37m.

Figure A127: (R) Extensive gully headwall activity as part of a secondary incision

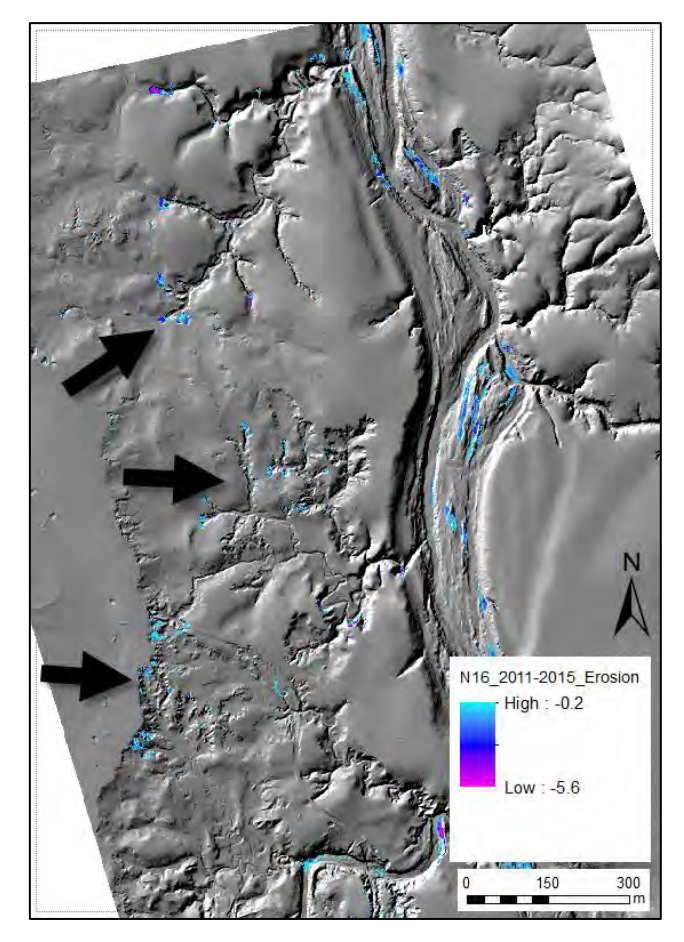


Figure A128: Plenty of reworking of old gully floor, with less activity at headwall zone

### 3.6.17 Observations from Deposition processing

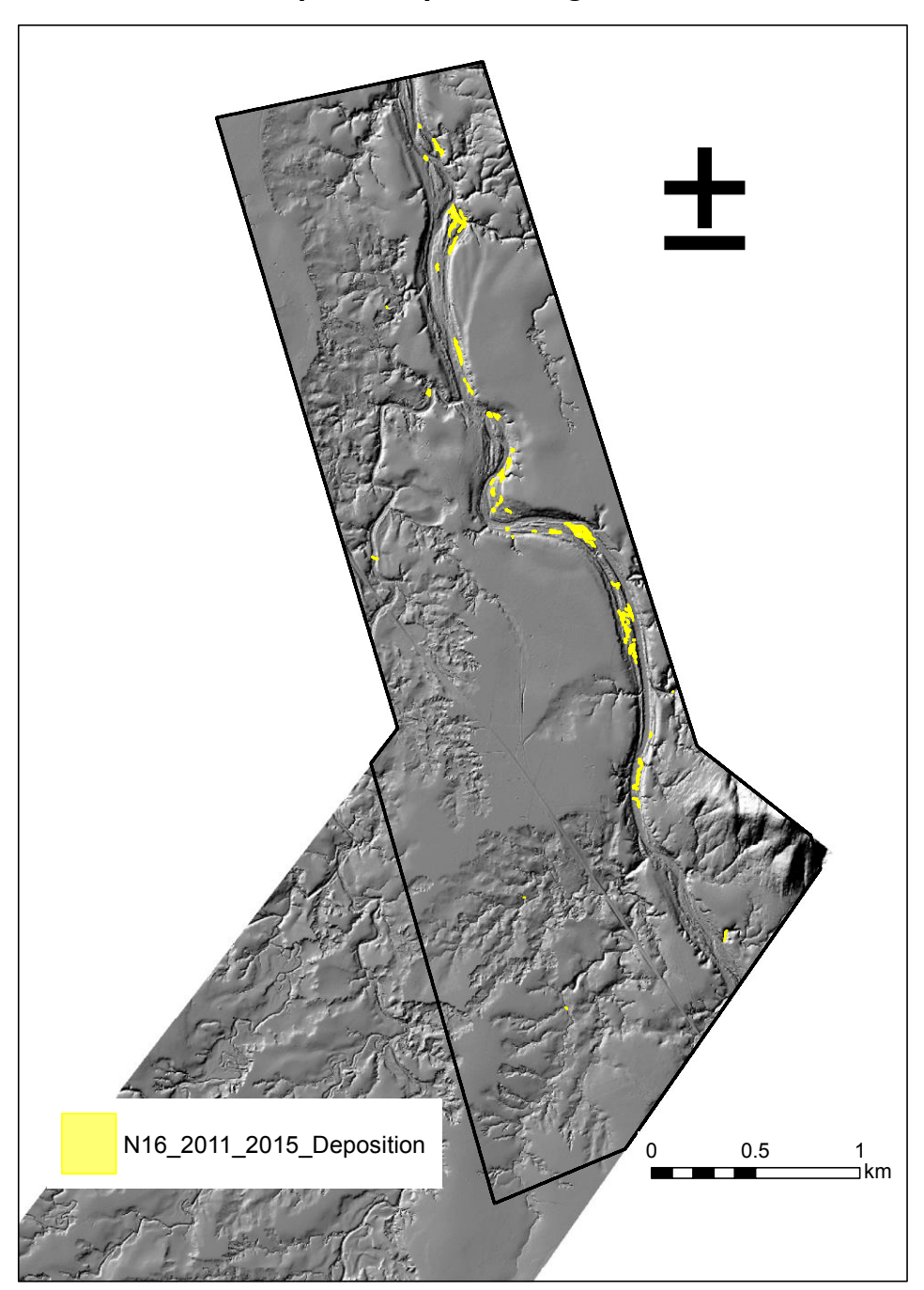
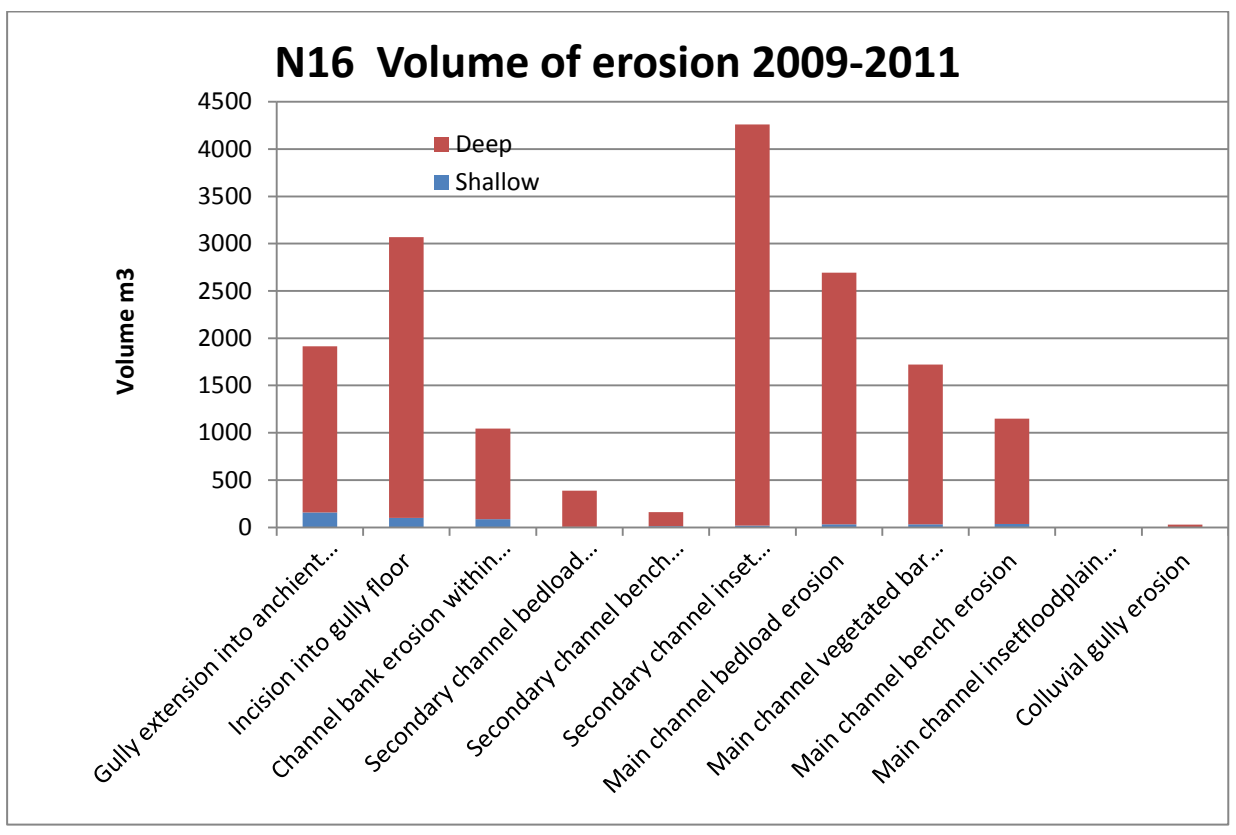


Figure A129: Patterns of deposition in N16.

### 3.6.18 Summary Erosion 2015 data + reprocessed 2009-11 data



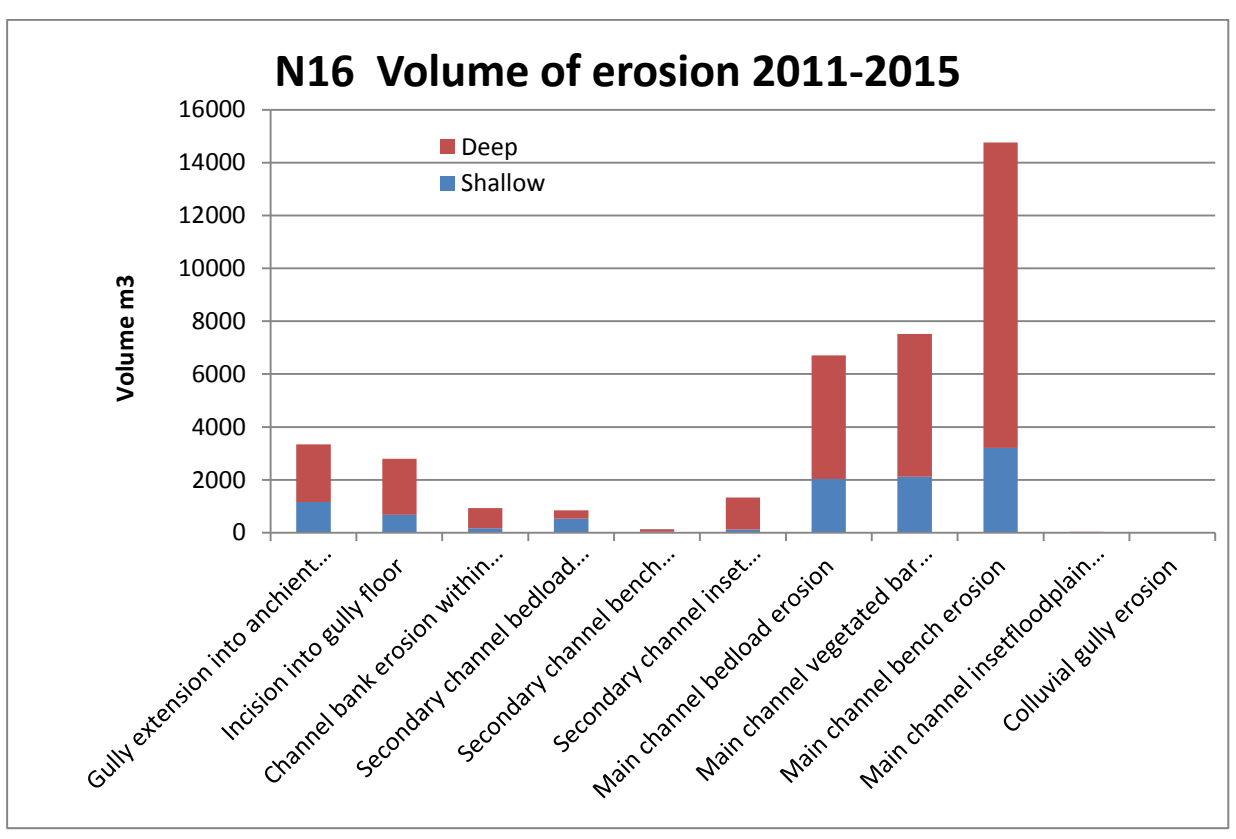
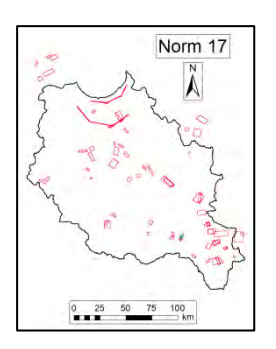


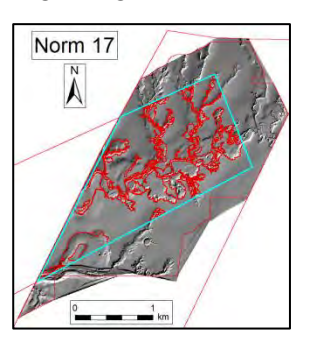
Figure A130: Erosion stats for Block16 by geomorphic unit 2009-11 (top); 2011-15 (bottom).

# 3.7 Normanby LiDAR Block 17

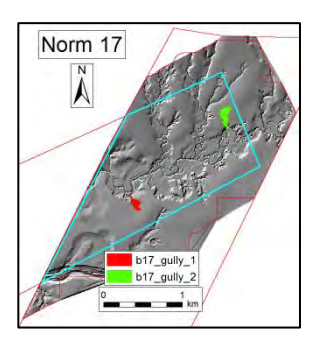
**Block location** 



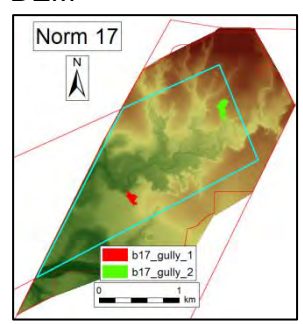
Digitising on LiDAR



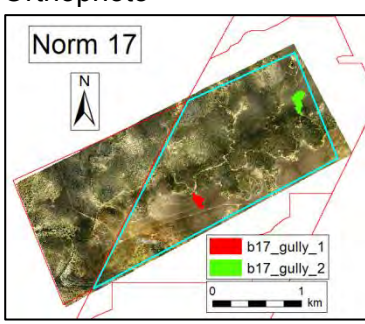
Air photo study gullies



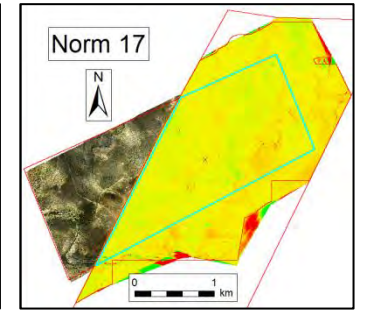
DEM



Orthophoto



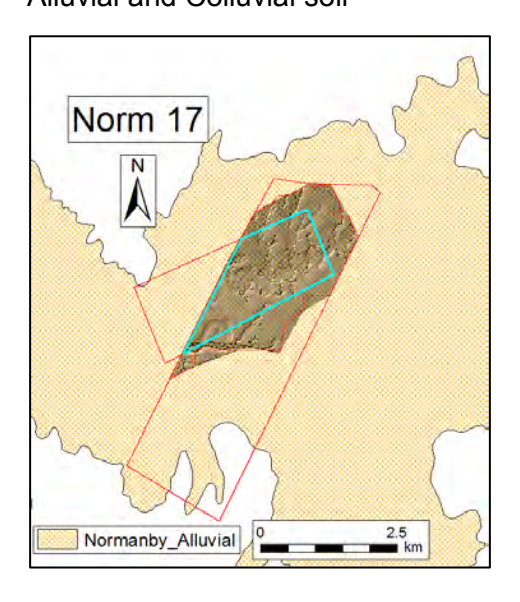
Change raster footprint



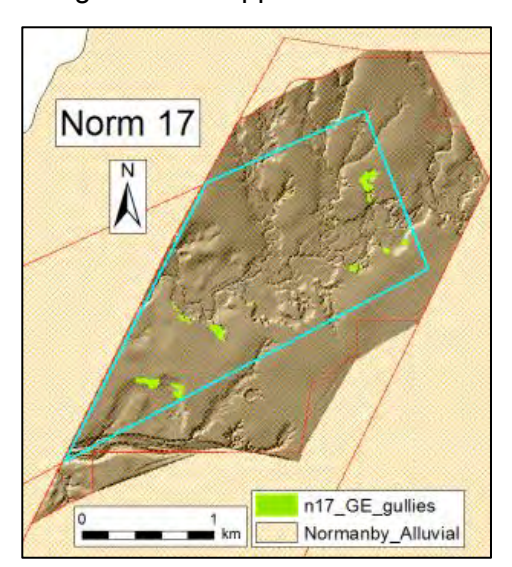
Reprocessed change raster area	ha	297.6646
Block elevation range	m	122 - 162
Number of LiDAR digitised features		185
Number of Google Earth mapped gullie	es	26

### 3.7.1 Alluvial and Colluvial zones

### Alluvial and Colluvial soil



### Google Earth mapped Gullies



Norm 14	Area ha	Area of all features digitised from LiDAR ha	Features as % of zone	Area alluvial gullies digitised from LiDAR ha	Area alluvial gullies as % of zone	Area of Google Earth digitised gullies	GE gullies as % of zone
Alluvial zone	297.6646	99.39	33.4	42.14	14.2	1.76	0.6
Colluvial zone	0.00	0.00	0.0	0.00	0.0	0.00	0.0

### 3.7.2 LiDAR derived data

### **Horizontal adjustments**

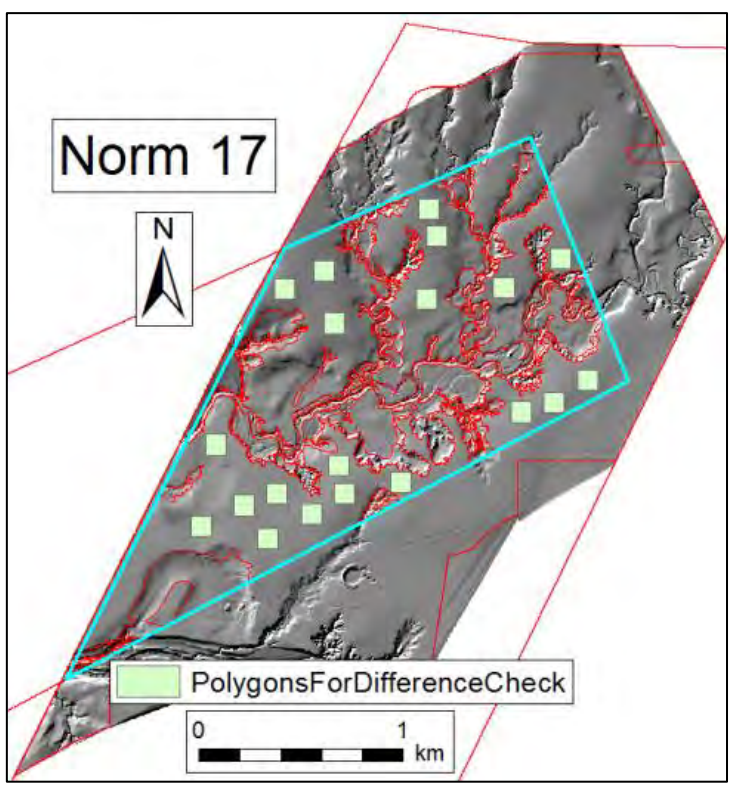
Polygons digitised from 2009 LiDAR, CHM and PFC rasters have been nudged to align with reprocessed 2009 LiDAR by:

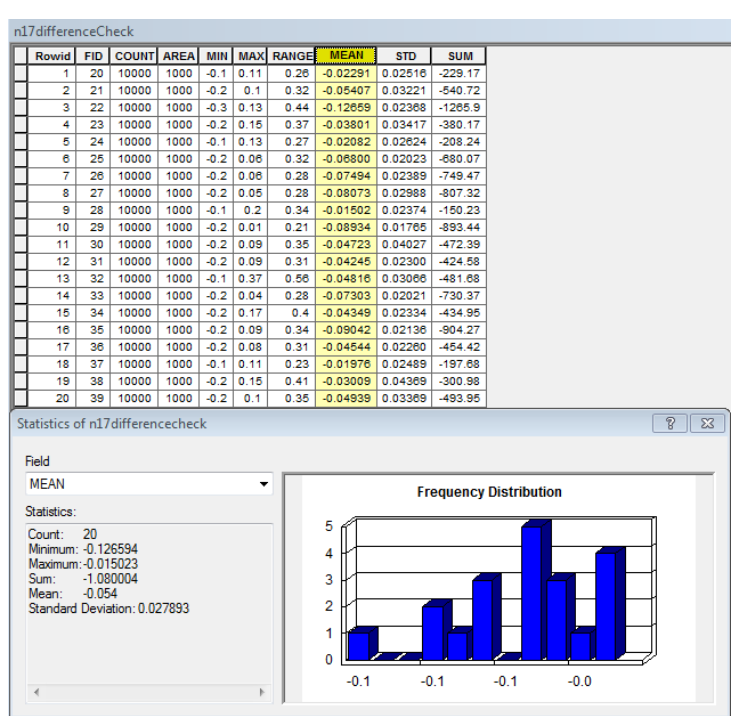
X,Y nudge (m)	1,-1	

### **Vertical adjustments**

Adjustment for vertical offset of 2009 and 2011 DEMs

20 polygons of  $1000 \text{ m}^2$  were put in areas where very little change would be expected to occur; ancient flood plain. Mean value of change raster within the 20 locations was used as a correction to the whole change raster.





### 3.7.3 Statistics

Layer	min	max	Mean	s.d.
Norm_14_Difference_2009-2011_Reprocessed.tif (as supplied by Terranean)	-7.25	5.55	-0.0753	0.25
Norm_14 with edge effect removed	-4.79	3.39	-0.0572	0.08
Areas of minimal change	-0.13	-0.02	-0.054	0.06
N14_Diff_adjusted	-4.74	3.44	-0.003	0.08

The level of noise on flat flood plain areas has been ascertained, and these values removed from the erosion and deposition layers.

Values of change raster filtered to remove noise on floodplain.

raster	Values filtered
erosion	0 to -0.2
deposition	0 to 0.2

### 3.7.4 Aggressive filtering of erosion and deposition data

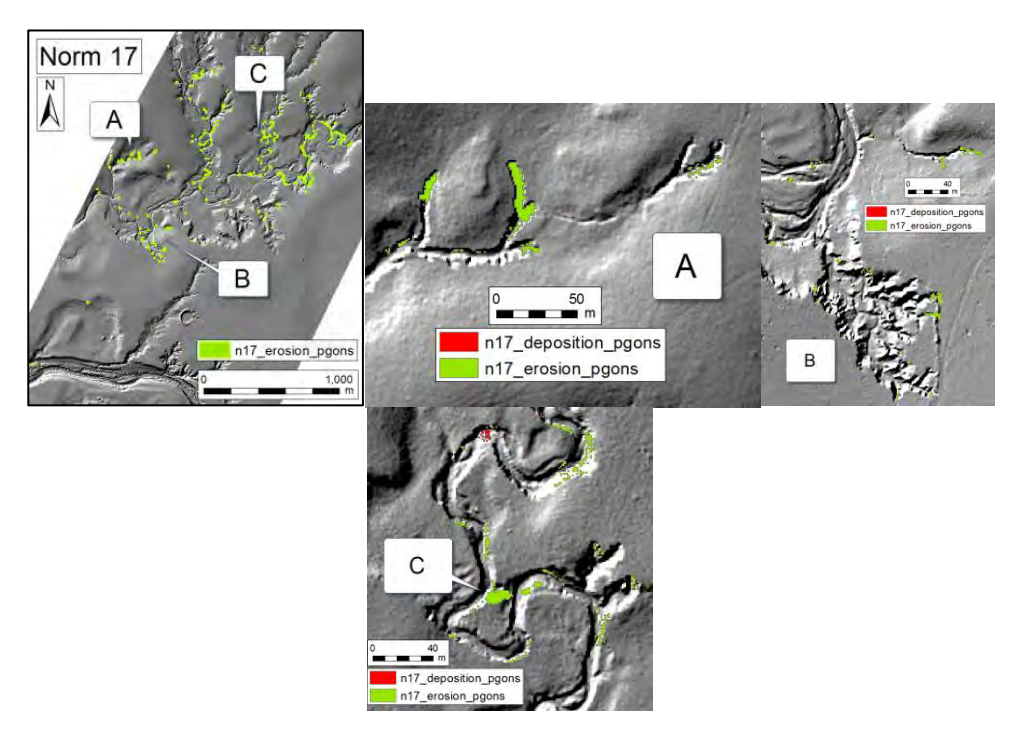
Gully extension in Norm 17 was generally not picked up using a 1m threshold for the change raster, but was picked up satisfactorily using a 0.5m threshold for the difference raster.

Some credible patches of erosion or deposition in the significant secondary channel have not been picked up with the 0.5m threshold, and hand drawn polygons will be used to include these patches in the data set.

The table below shows the volume of data removed by hand thinning erroneous erosion and deposition data.

	eı	rosion	deposition		
	area ha raster sum a		area ha	raster sum	
Prior to hand thinning	1.1072	-12,820	0.1597	6,387	
After hand thinning	0.6164	-3,495	0.0181	148	

#### 3.7.5 Observations



Location A: A narrow gully with elongation at 5 headwalls, longest advance 40m.

Location B: Headwall extension past windrow in the large gully, also 12m extension in the narrow gully above the scale bar

Location C: A breakthrough of a meander, an example of channel straightening.

### 3.7.6 Erosion and deposition

The major location of erosion in Norm 17 was within secondary channels, with some channels having continuous erosion activity along one side or the other, rather than isolated pockets of deep erosion.

Erosion in secondary channels increased with distance from the junction with the main channel.

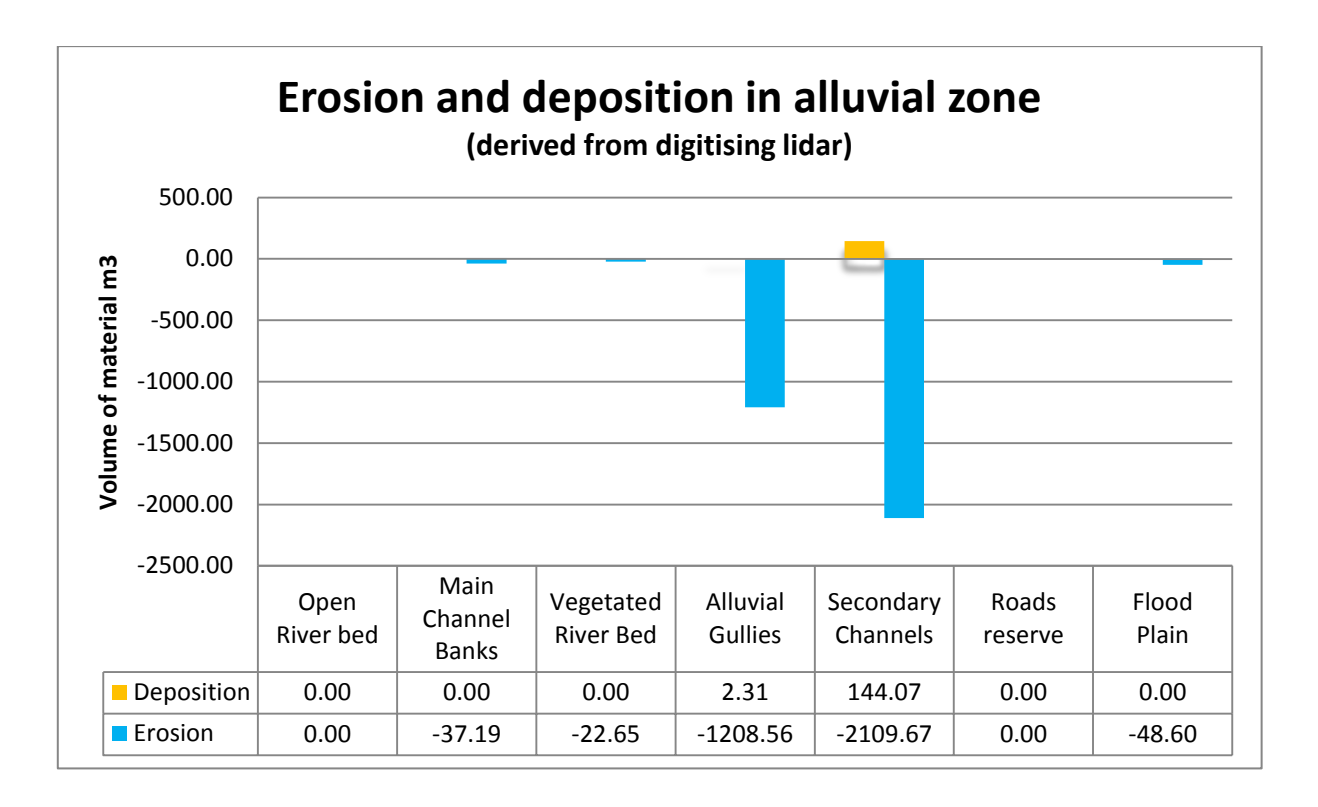
Truncating of meanders occurred in two locations, with looping bends of 150m and 230m being reduced to a direct path of 18m and 80m respectively.

Many gully extensions were along narrow finger like pathways.

Distance of main channel included in the repeat LiDAR was about 200m, limiting the comparisons of erosion/deposition activity with locations removed from the main channel.

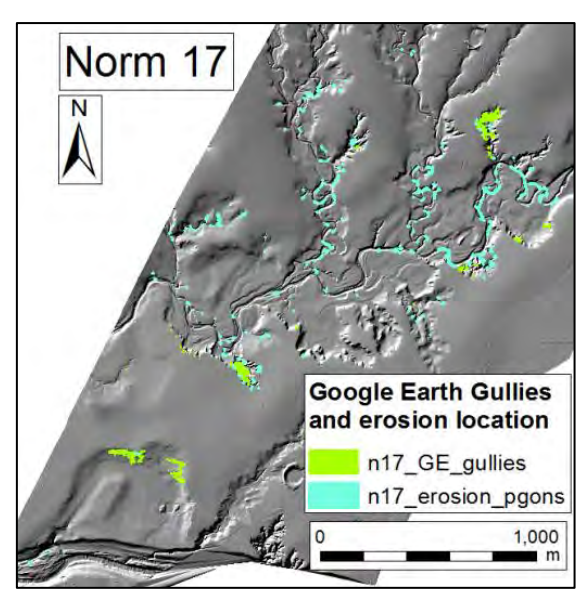
Erosion of flood plains occurred in locations where bank erosion of secondary channels cut into the surface area of the flood plain.

Secondary channels contributed 62% of total erosion, though being only 14% of the area of digitised landscape features.



### 3.7.7 Comparison of Google Earth gullies to LiDAR gullies in the alluvial zone

Erosion activity in Norm 17 was poorly represented by gullies digitised from Google Earth, with only 4% of alluvial gully area represented, and 3% of the erosion volume from alluvial gullies occurring within the GE gullies.



	Area ha	erosion m3	Yield m3/ha/yr
LiDAR alluvial gullies	42.16	-1208.56	-14.31
GE alluvial gullies	1.76	-30.59	-8.67

### 3.7.8 Gully Expansion 2009 - 2011

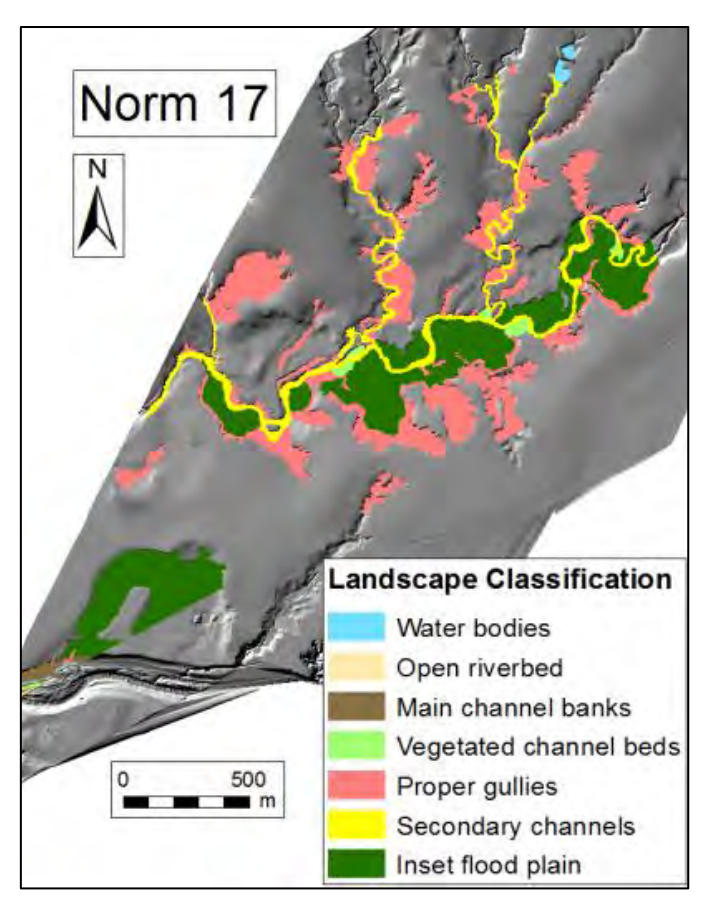
Of the 146 polygons digitised to capture alluvial gullies, gully expansion beyond 2009 boundaries occurred in only 40 locations, with an average expansion area of 7m<sup>2</sup>. Most of the expansion activity was occurred in a few gullies that had multiple head scarps. Erosion activity was measured in 65 out of 146 alluvial gullies and active trench like incisions were advancing in the floor of many old gullies.

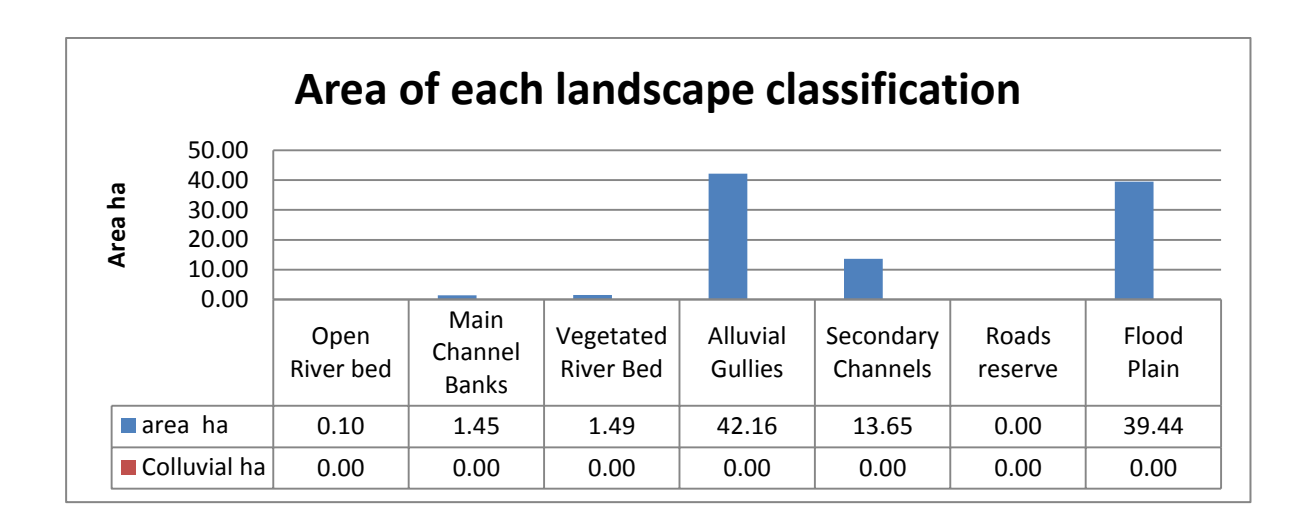
The following table summarises total gully expansion between 2009 and 2011.

Gully Expansion 2009 - 2011	
number of gully expansion locations	40
sum area of gully expansions ha	0.0285
mean area of expansion m2	7

### 3.7.9 Landscape Classification

The area of alluvial gullies and flood plain in Norm 17 was similar, with 42.16ha and 39.44ha respectively. The major secondary channel running diagonally across norm 17 has areas of associated floodplain, mostly to the south side of the channel. Height gain from channel bed to flood plain was 1m near the upstream limit of this block, and 2m for the patch of flood plain closest to where the channel exited this LiDAR block. Of the 1.49ha of vegetated channel bed, 1.3ha was located along the secondary channel, perched between the bed and the flood plain.





### 3.7.10 Historical air photos

Two gullies were identified in historical air photos, gully one having coverage in 1952 and 1987, and gully 2 having coverage in 1987 only.

Image date	Photo ID	Scale	Flying height	RMS error of georeferenced air photo	Air photo position relative to 2009 LiDAR block
1/01/1952	QAP 309-115	23900	12750ft	1.28400	
1/01/1987	QAP 4110- 112	25000	4310m	1.88456	Gully 2

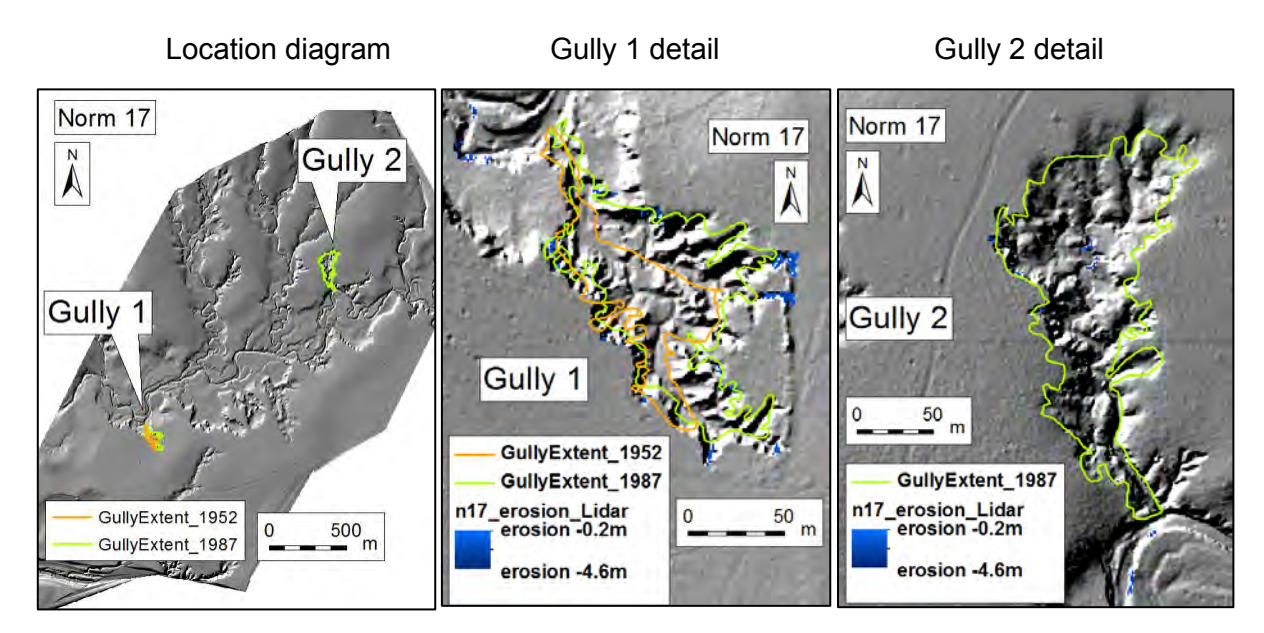
### 3.7.11 Historical gully extent

### **Gully 1**

Gully 1 has been intensively studied by Jeff Shellberg, and has the id code CRGC1, Crocodile Gully Complex 1.

The gully area doubled in the 35 years between 1952 and 1987, from 3655ha to 7235ha, and increased in area by 50% in the 22 year period from 1987 to 2009. Erosion measured by

LiDAR is mainly advancing along 4 narrow headwalls on the east and southern perimeter, with lesser activity along the western edge.



The volume of material loss per year from Gully 1 decreased as the time step became shorter and more recent. This would indicate a slowing of erosion activity. However, the massive increase in yield over the 2009-2011 period runs counter to the rate of loss, and again shows the problems of how to normalise rates of erosion from the same gully at different gully age where the gully has different areas and volumes.

Interval	Gully area at start of period m <sup>2</sup>	Rate of loss m³/yr	Yield m3/ha/yr Based on 2009 gully area
1952 - 2009	3655	205	194
1987 - 2009	7235	153	144
2009 - 2011	10577	67	571

### Gully 2

Gully 2 has significantly reduced erosion loss in recent years as measured by volume per year and yield.

Interval	Gully area at start of period m <sup>2</sup>	Rate of loss m³/yr	Yield m3/ha/yr Based on 2009 gully area	
1987 - 2009	13876	151	85	
2009 - 2011	17834	16	9	

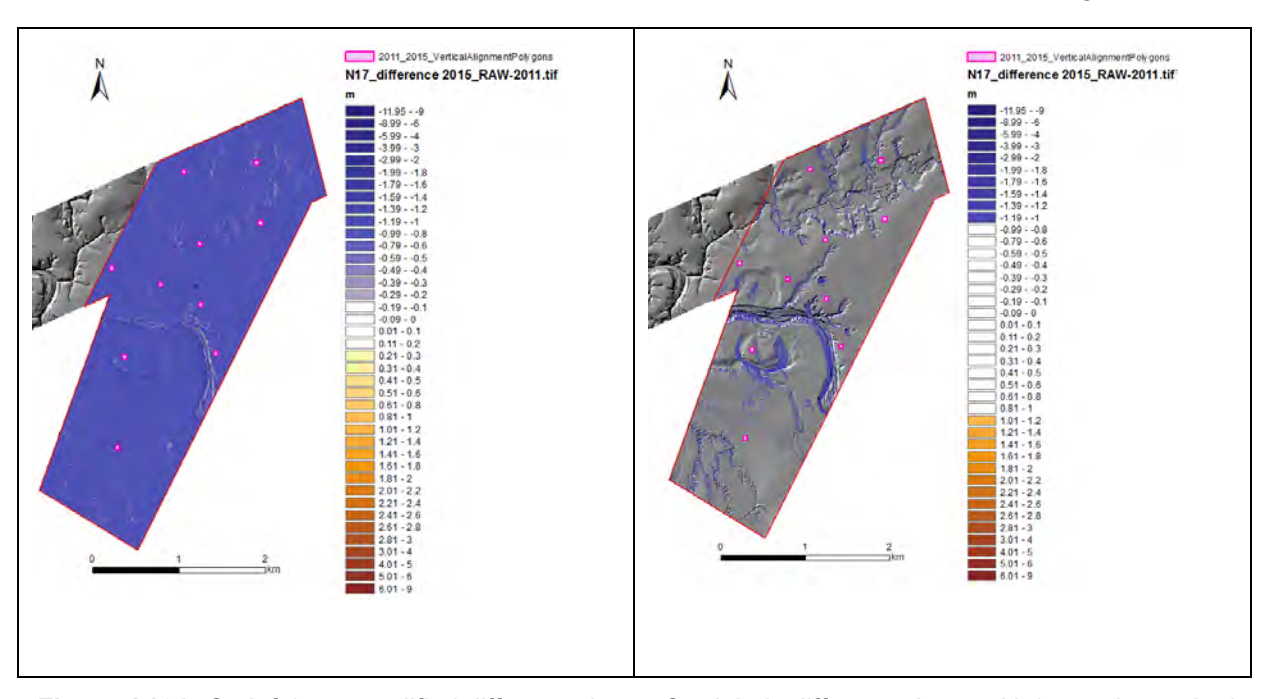
# 3.7.12 Comparison of gully volume and erosion calculations using reprocessed 2009 LiDAR and original 2009 LiDAR.

It appears that the reprocessed 2009 LiDAR consistently has gully volume, and hence yield, as less than at first calculated. Toggling between the 2 HS rasters shows some gully structures such as pedestals and ridges absent in the original data, but present in the reprocessed data.

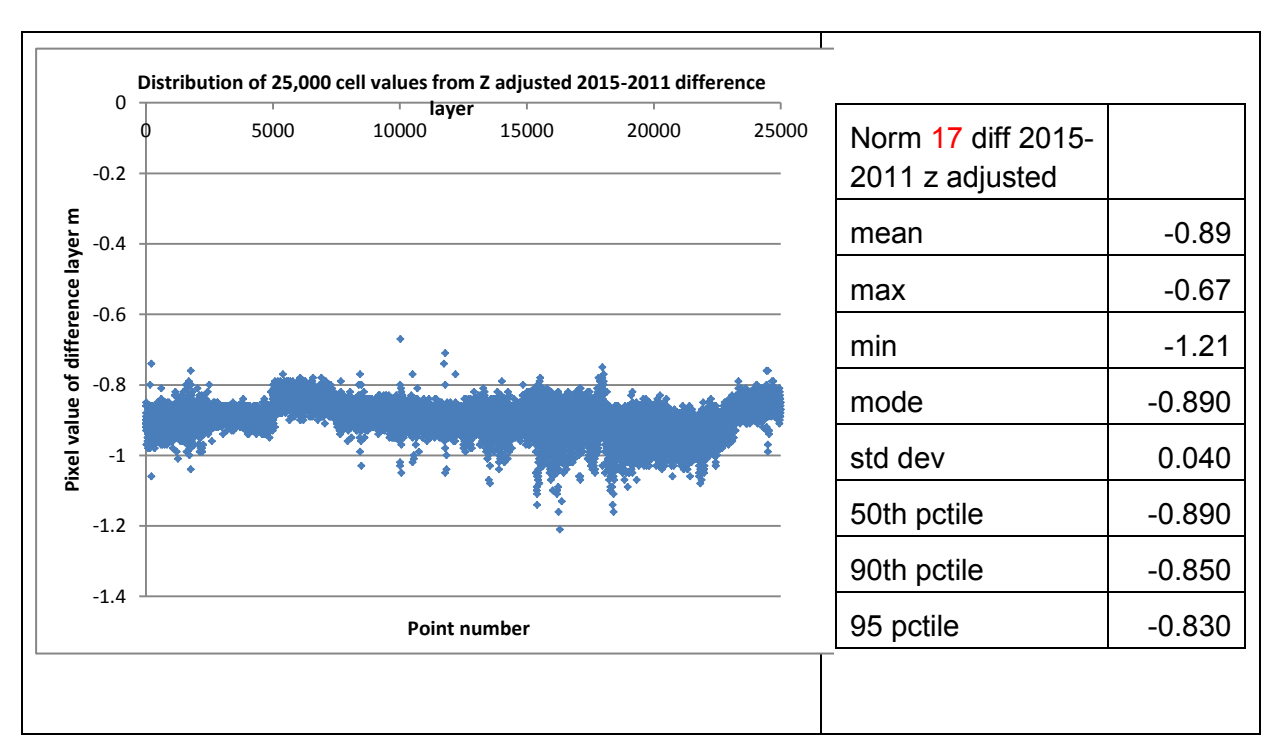
Gully and Interval	Volume of erosion, using reprocesse d 2009 LiDAR, m3	Volume erosion from original 2009 LiDAR m3	% difference in volume 2009repro/ 2009origin al*100	yield using reprocesse d LiDAR m3/ha/yr (using 2009 gully area)	yield using original LiDAR m3/ha/yr (using 2009 gully area)	% difference in yield reprocesse d/original*1 00
Gully 1 1957- 2009	10564	11666	90.5	175	194	91
Gully 1 1987- 2009	2805	3360	83	121	144	83
Gully 2 1987- 2009	2780	3331	83	71	85	83

### 3.7.13 LiDAR 2015 Data Processing

Z correction: 0.8944m was added to the 2015 Lidar to correct for vertical alignment.



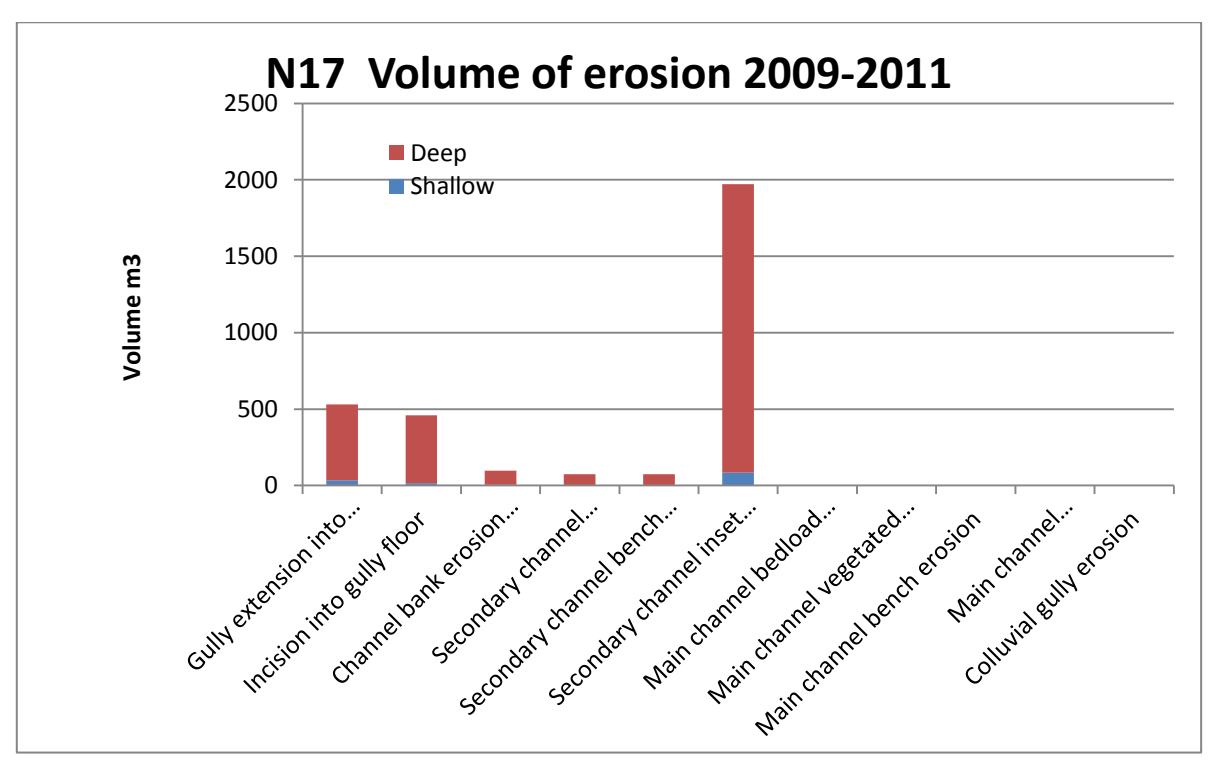
**Figure A131:** On left is un-modified difference layer. On right is difference layer with intervals masked until the flat areas are revealed.



**Figure A132:** Plot of 25000 points sampled to calculate correction factor. On right is statistics around the noise.

XY correction: XXXX DEM was nudged by X = +1.25, Y = +0.25

### 3.7.14 Summary Erosion 2015 data & reprocessed 2009-11 data



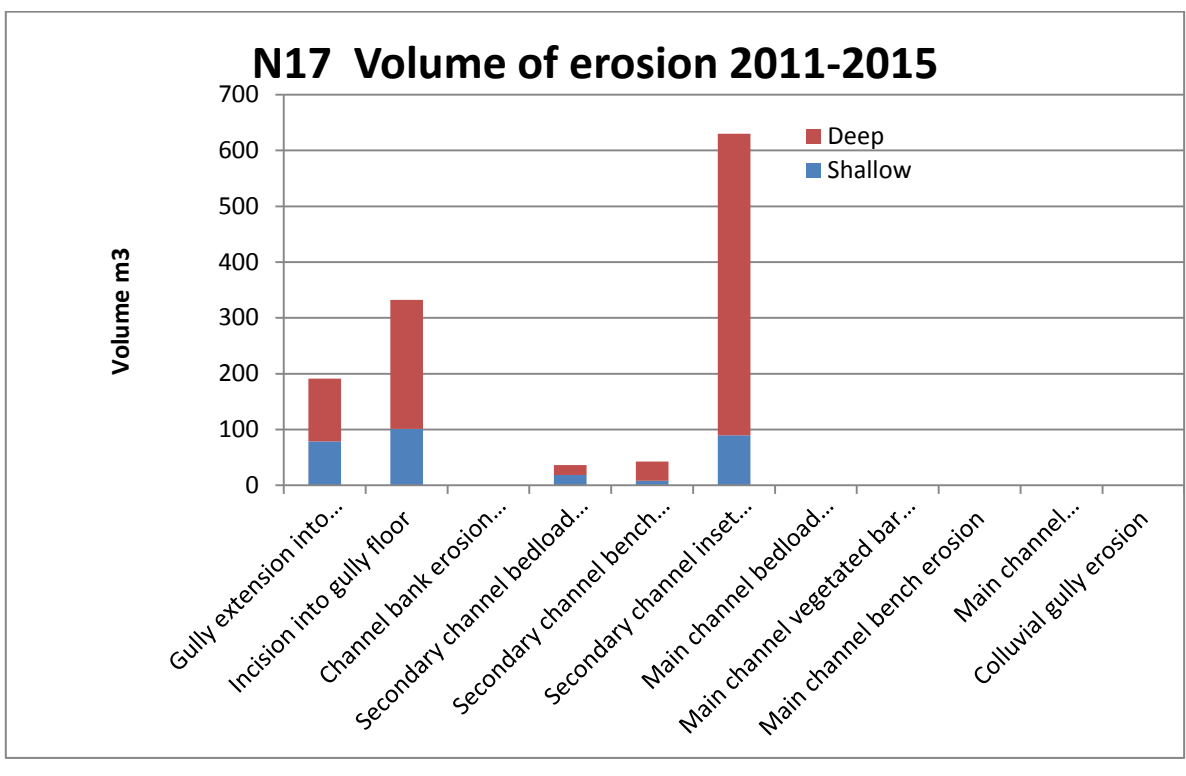


Figure A133: Erosion stats for Block 17 by geomorphic unit (2009-11 (top); 2011-15 (bottom).

### 4. NORMANBY RAINFALL AND FLOW DATA

Prepared by: Andrew Brooks

### 4.1 Rainfall data for study period (2009-2015)

The most complete daily rainfall record in the upper catchment for the period is that from the DNRM Coalseam Ck Gauging station (Figure A9), although it still had gaps. The Coalseam Ck record was gap filled using the BOM Laura Post Office rainfall record, which is 6.5km away (Figure A135) using the monthly correlations rather than the daily ones, which were extremely poor. Monthly data was available at a number of additional sites; Laura PO, the DNRM East Normanby River gauging station and a private record from Kings Plains Station, and because the correlations between the common data were reasonable, gaps were filled in each data set from the closest gauge.

The daily, monthly and annual (water year) rainfall records highlight the fact that rainfall was distinctly different over the latter 4 years of the study period compared to the initial 2 years. Large events were less common in the first two year period, but annual totals were higher and more consistent, particularly across the 2011 water year. Rainfall over the second period (WY 2012 – 2015) was much more erratic with a larger number of extreme events, more periods of low or no rainfall and greater variability more generally. The key characteristics of the two periods are best summarised in Table A54 which shows a similar number of intermediate rainfall events (i.e. >12 or 50mm per day –despite the latter period being twice as long as the earlier period. Furthermore, the latter period is punctuated by three tropical cyclones, which produced varying amounts of rain, compared with no cyclones in the earlier period.

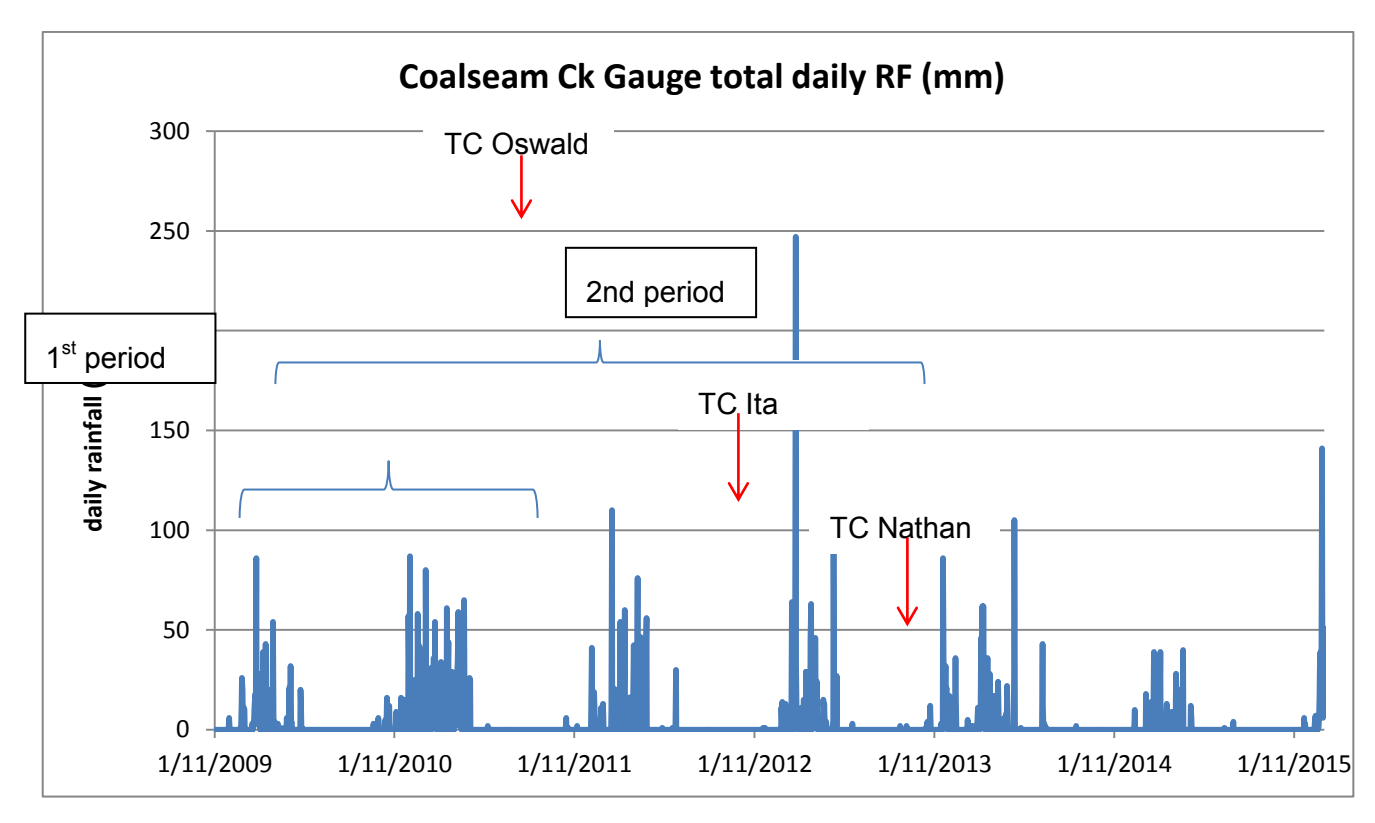


**Figure A134:** Daily rainfall at the DNRM gauging station on the Laura River at Coalseam Ck.

Table A54: Summary of daily rainfall events over threshold for the two observation periods

Daily Summary Stats (Coal Seam Ck)			
	# days >12mm	# days >50mm	# days >100mm
WY 2010-11	64	10	0
WY2012-15	65	9	3



**Figure A135:** Map of the upper Normanby River showing the locations of the 4 sites for which monthly or daily rainfall records are derived.

Table A55: Summary of annual water year rainfall totals over the study period

		Kings Plains Stn.	East Normanby	Laura PO	Coal Seam Ck	all yrs av
period 1	WY2010	1157	1003	598	765	
	WY 2011	1982	1564	1595	1617	1285
	WY 2012	1469	1264	1204	1201	
period 2	WY 2013	1006	922	1057	1156	
	WY 2014	1406	1380	1116	1093	
	WY 2015	987	735	538	391	1058
		ratio period 2	to period 1 =			0.82

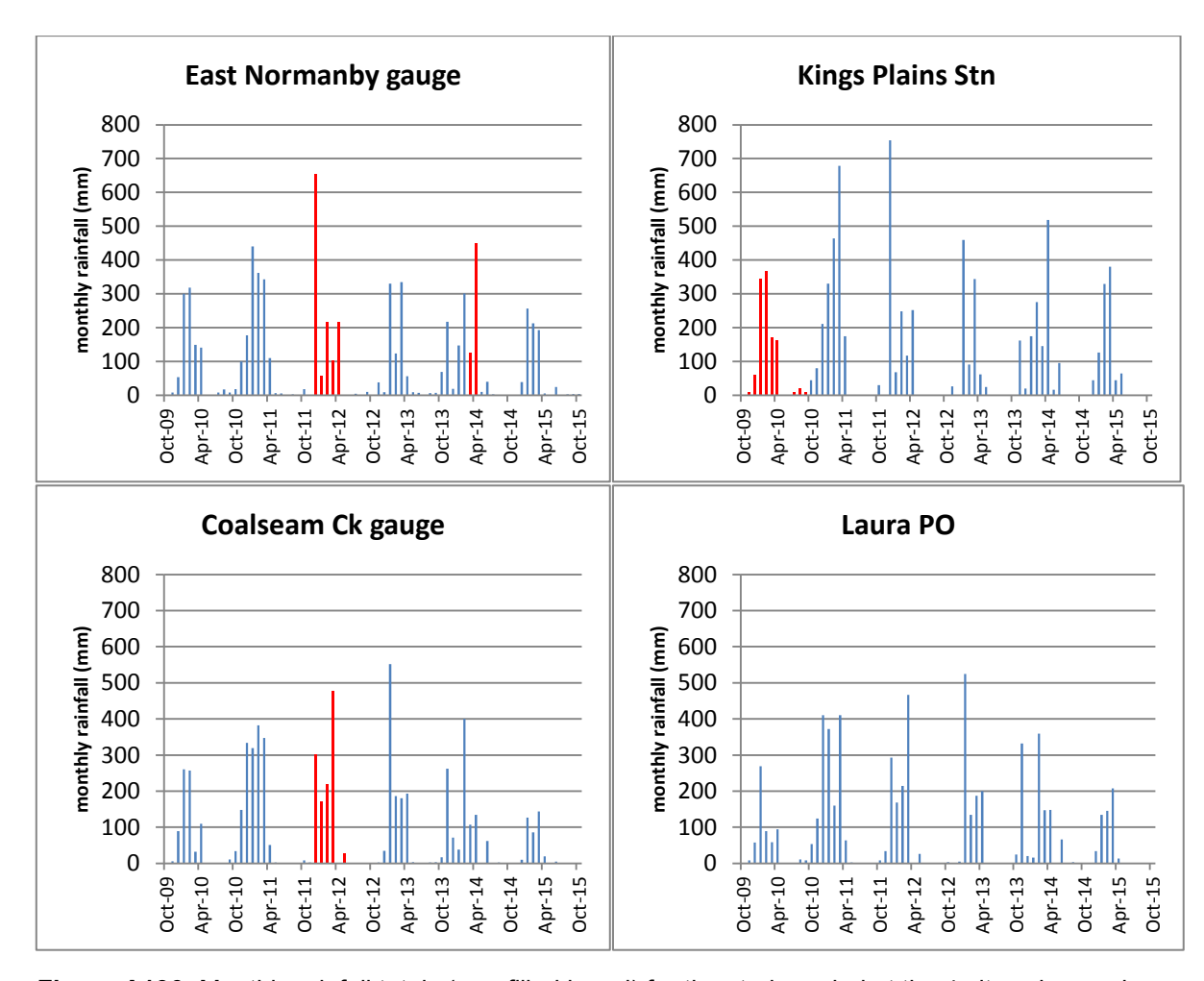
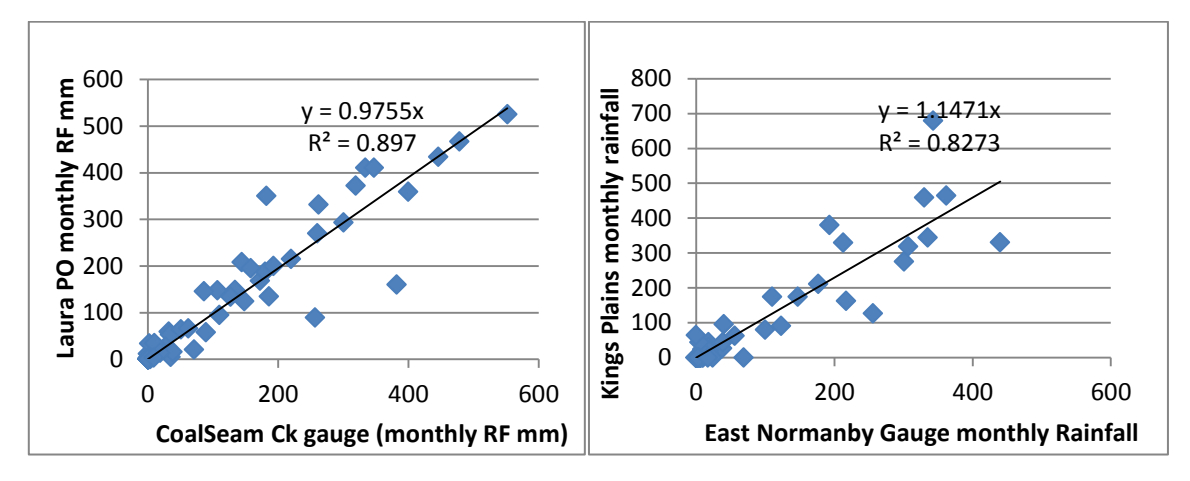
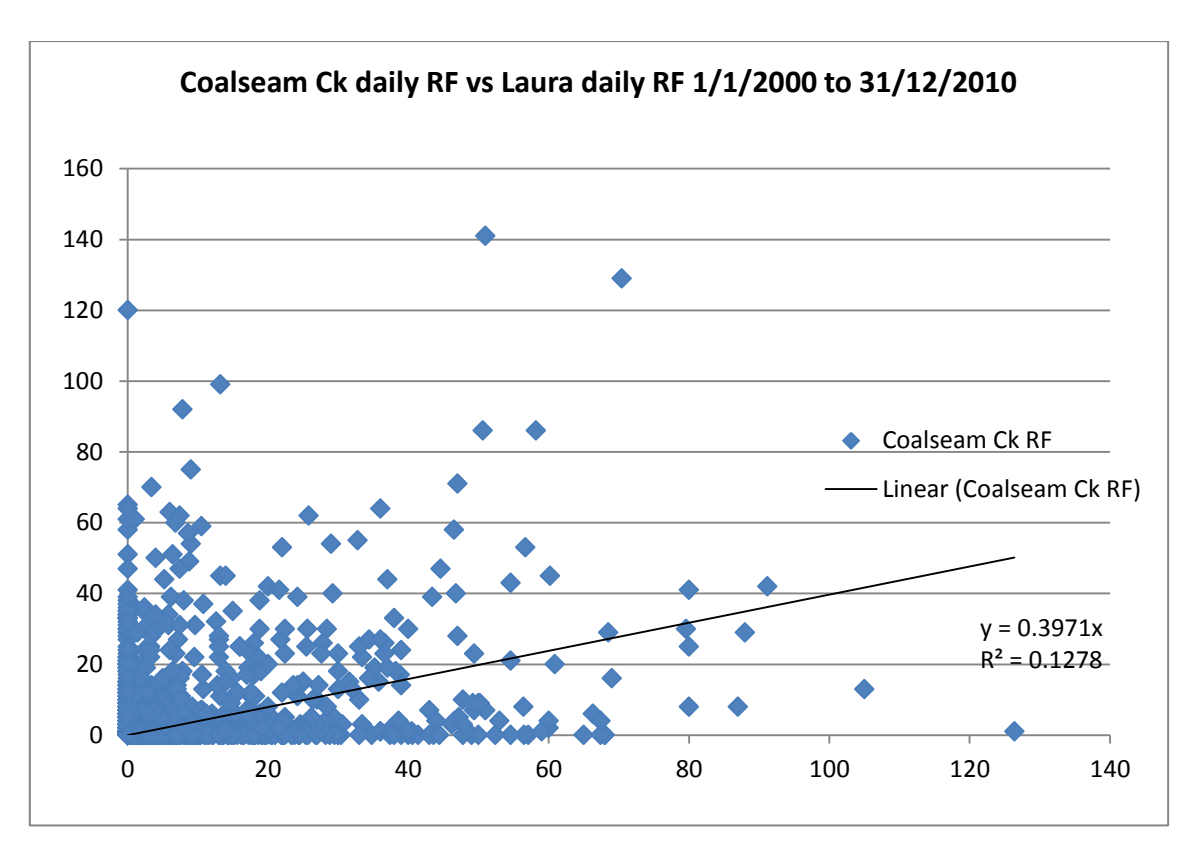


Figure A136: Monthly rainfall totals (gap-filled in red) for the study period at the 4 sites shown above.



**Figure A137:** Correlations between monthly rainfall totals at the Coalseam Ck gauge and the Laura Post Office and the East Normanby gauge site and Kings Plains Station. These relationships were used to fill missing data in the gauge records.



**Figure A138:** Correlation between daily rainfall at Coalseam Ck with Laura Post Office over the last 10 years (missing data days removed).

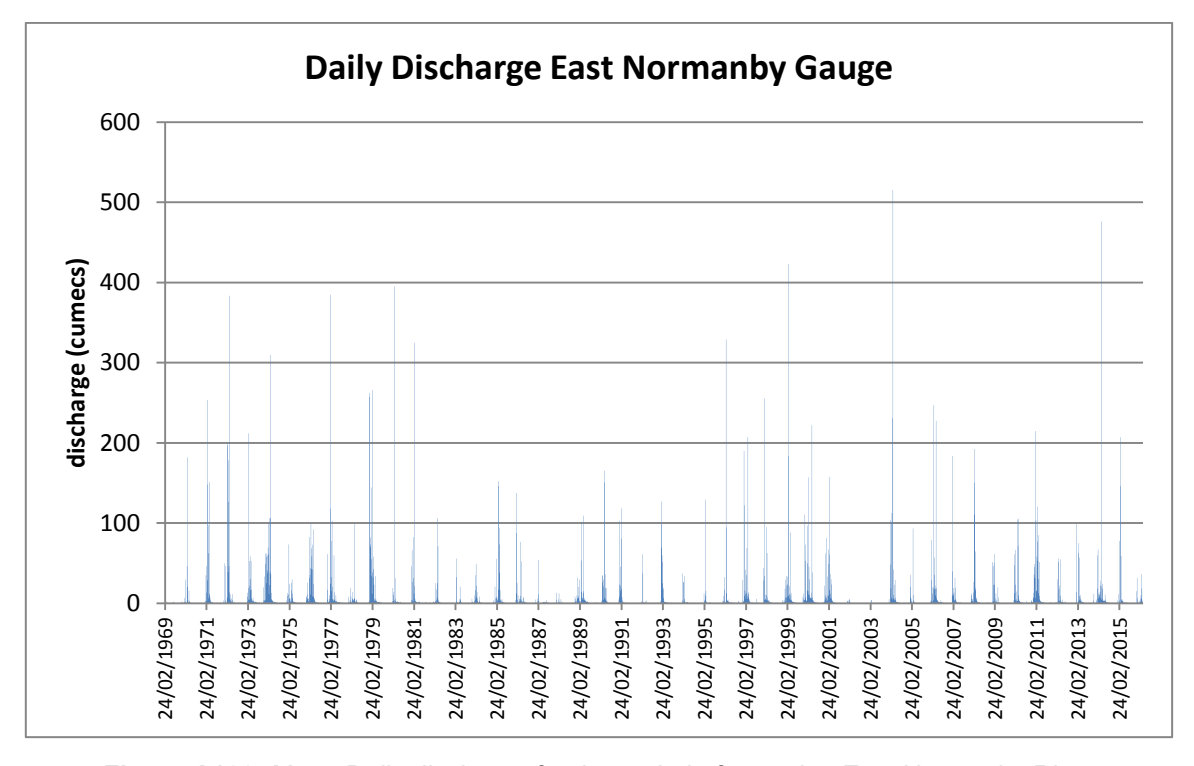


Figure A139: Mean Daily discharge for the period of record at East Normanby River

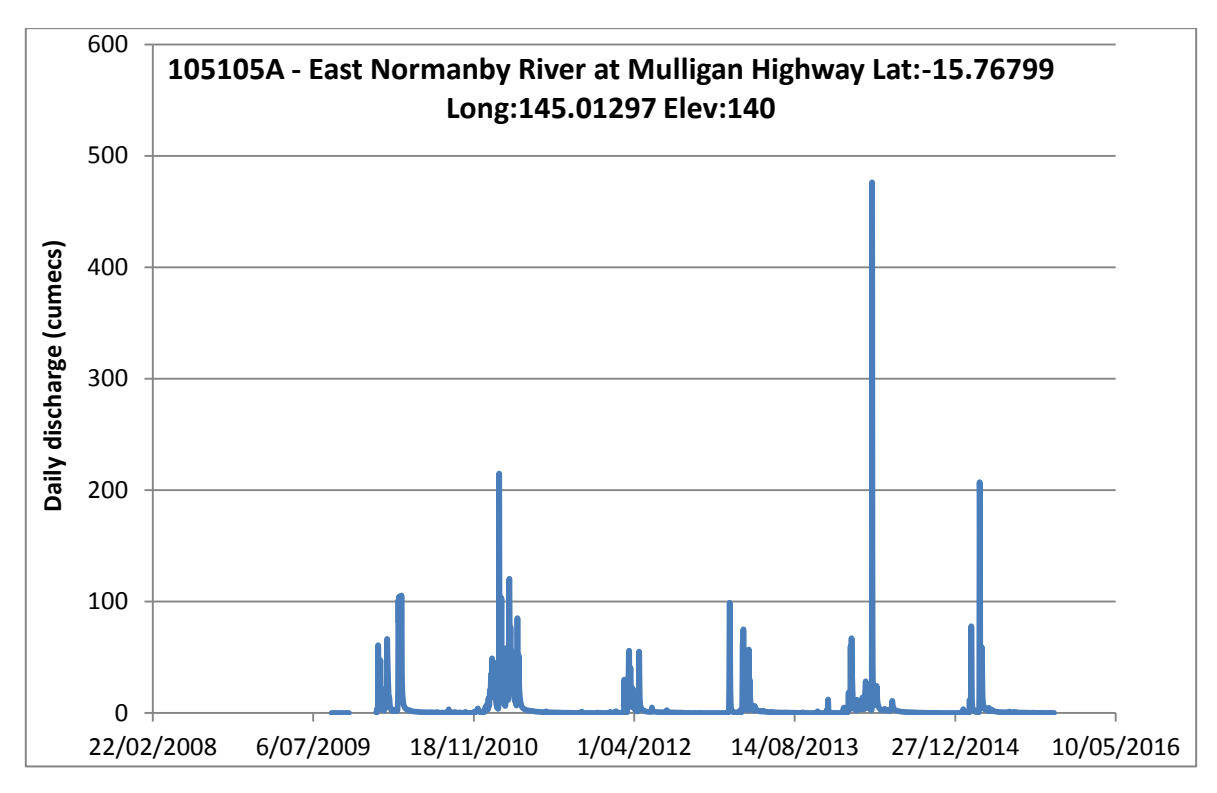
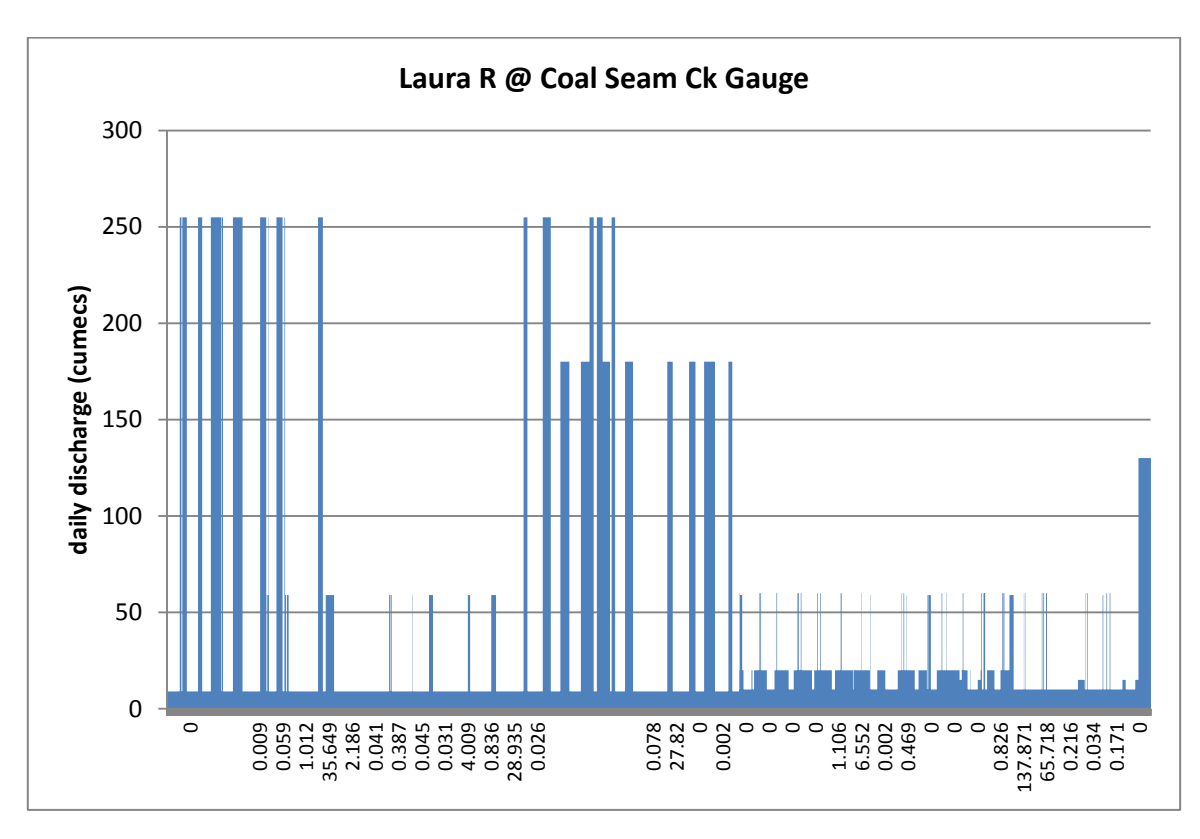
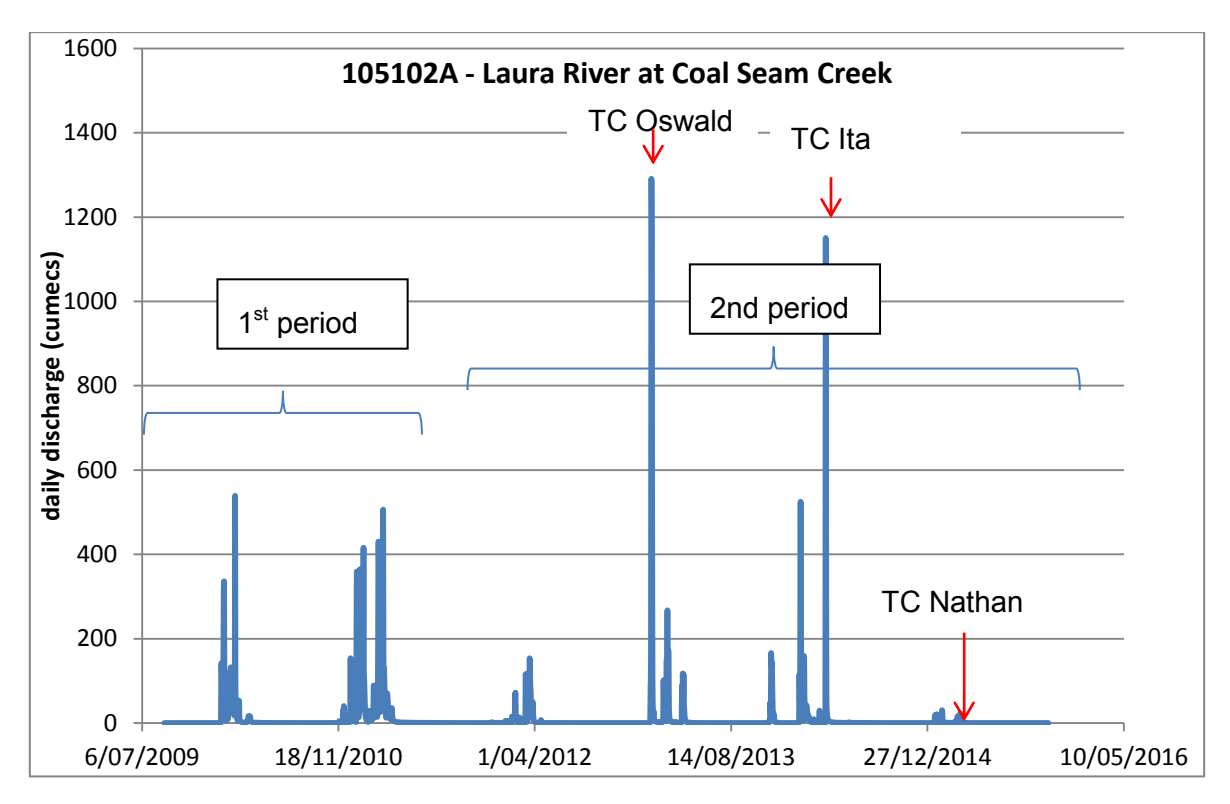


Figure A140: Mean daily discharge for water years 2010 – 2015 at the east Normanby River gauge.



**Figure A141:** Mean daily discharge (cumecs) for the period of record at the Coal seam Ck gauge on the Laura River.



**Figure A142:** Mean daily discharge for water years 2010 – 2015 at the Laura River at Coalseam Ck gauge.

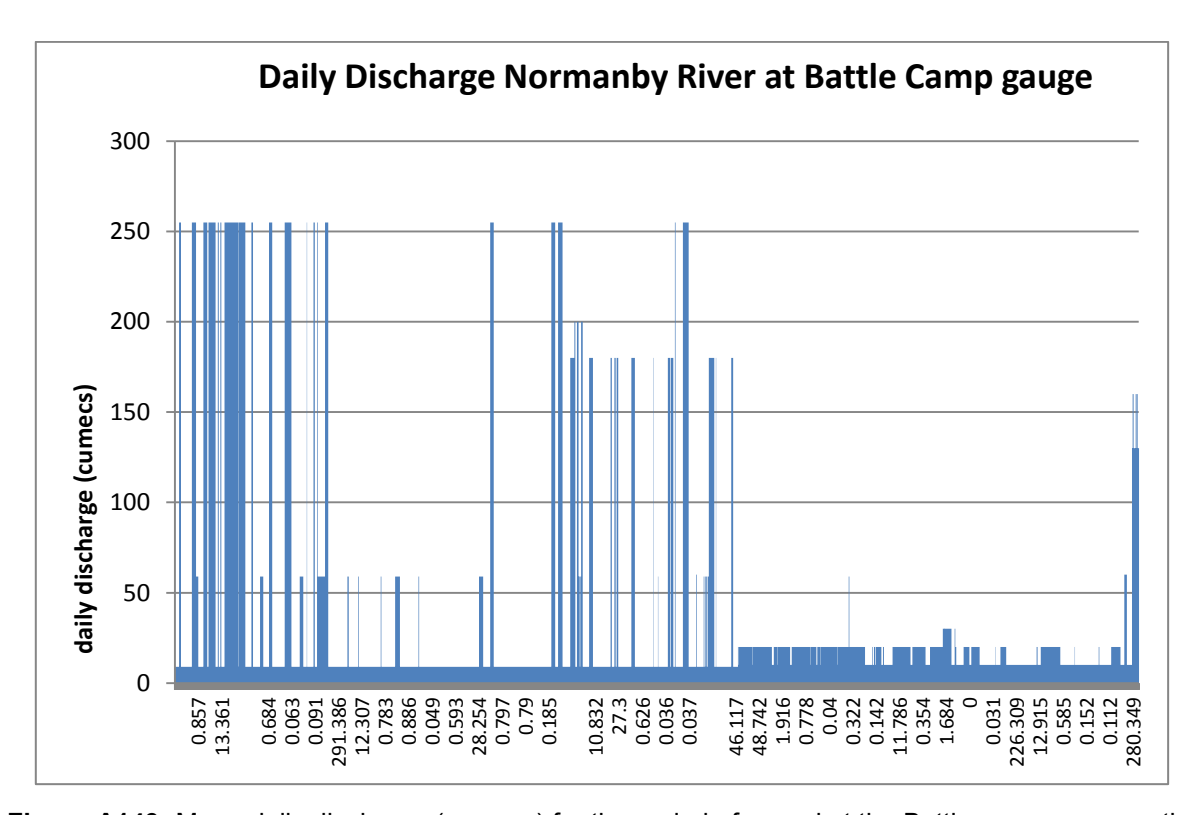


**Figure A143:** Mean daily discharge (cumecs) for the period of record at the Battlecamp gauge on the Normanby River.

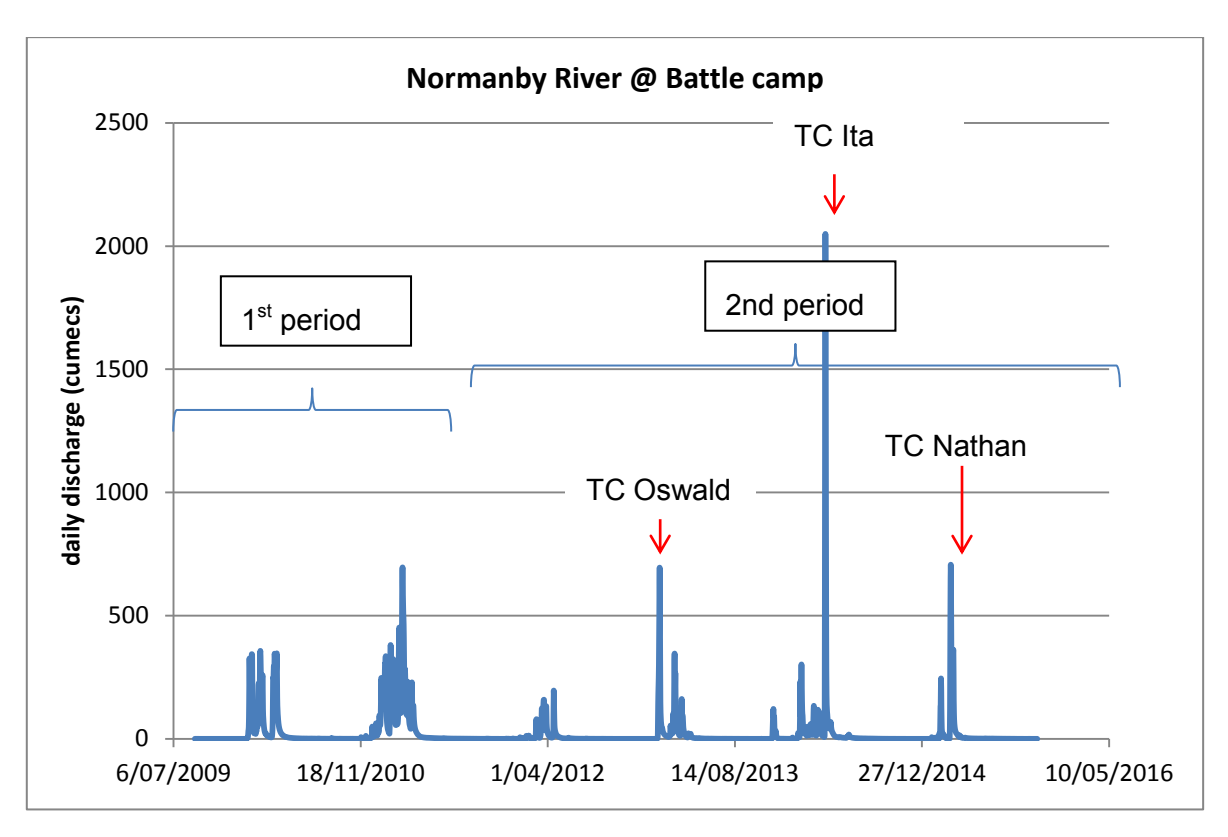


**Figure A144:** Mean daily discharge for water years 2010 – 2015 at the Battlecamp gauge on the Normanby River.

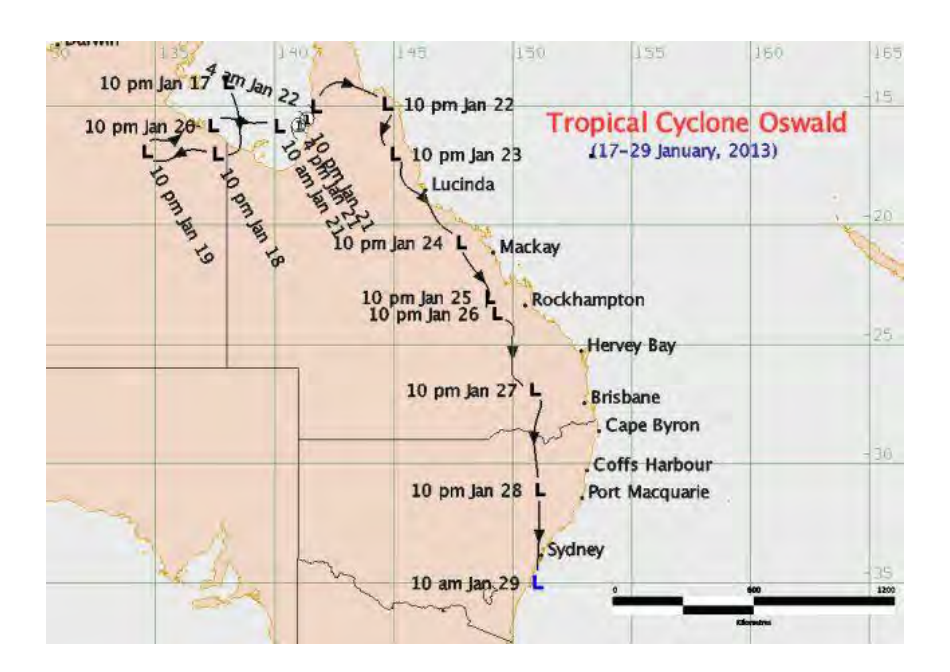
**Table A56:** Summary flow statistics for the Normanby and Laura Rivers over the two survey periods.

	Normanby River at Battlecamp		Laura River at Coalseam Ck	
	2009-11	2011-15	2009-11	2011-15
mean daily Q # days > 100	2.50E+09	2.14E+09	9.96E+08	9.90E+08
cumecs # days > 500	100	49	31	15
cumecs # days > 1000	4	7	2	3
cumecs	0	3	0	2

### 4.2 Cyclones & Tropical lows during the monitoring period

(source: www.bom.gov.au)

### 4.2.1 Cyclone Oswald Jan 22 – 23, 2013 (Tropical Low over Normanby)



A tropical low was first identified in the Gulf of Carpentaria on January 17th. After spending several days over land in the Northern Territory, the low tracked eastward across the Gulf and was named Category 1 Tropical Cyclone Oswald on the afternoon of January 21st, just hours before crossing the western Cape York Peninsula coast near Kowanyama early on January 22nd. Oswald had little impact on its initial landfall, but the remnant low moved southwards and produced severe weather over nearly all of eastern Queensland during the following week. Destructive winds were recorded at Hay Point, near Mackay (a gust of 140 km/h was measured). The low stalled west of Rockhampton for two days on January the 25th and 26th, producing over 1000mm of rainfall in some areas during the 48 hours and major flooding. Over the Wide Bay and Burnett district the system had an even larger impact, with record flooding in the Burnett River, and major flooding in the Mary River. An outbreak of at least five confirmed tornadoes, the numerically largest known in Australia, occurred on the coast near Bundaberg on January 26th, with destruction occurring particularly in the towns of Bargara and Burrum Heads. On Sunday January 27th the system moved further southeastward, and far southeastern Queensland, including Brisbane, the Sunshine Coast, and the Gold Coast was pounded by damaging to destructive winds, torrential rain, dangerous surf, and tidal inundation for up to 24 hours. The Lockyer Creek, Bremer River, and the Brisbane River all flooded, though the flooding in the Brisbane River did not reach the levels seen in the 2011 floods. Torrential rainfall and major flooding also occurred in northeastern New South Wales with the system, which eventually tracked as far south as Sydney before finally moving off the coast.

### **Coastal Crossing Details**

**Crossing time:** 1am EST Tuesday 22nd January 2013

Crossing location: Kowanyama

300km south of Weipa

Category when crossing the coast: 1

### Extreme values during cyclone event (estimated)

Note that these values may be changed on the receipt of later information

Maximum Category: 1

Maximum sustained wind speed: 65 km/h

Maximum wind gust: 140 km/h

Lowest central pressure: 991 hPa



### 4.2.2 Severe Tropical Cyclone Ita - April 11-12, 2014

Tropical cyclone Ita began life as a tropical low southwest of the Solomon Islands in the northeastern Coral Sea on April 2nd, 2014. Over the next few days it drifted westward while slowly intensifying, and was classified as a category 1 cyclone on the afternoon of April 5th.

The cyclone continued to move westward and then stalled south of Sudest Island (Papua New Guinea) for two days while continuing to intensify, reaching category 3 at 11am on April 8th. It then recommenced its westward motion, passing south of the Papua New Guinea mainland while maintaining its intensity as a category 3 cyclone.

On the afternoon of April 10, Ita intensified extremely rapidly, reaching category 4 and then category 5 in the span of 6 hours. At the same time it turned southwest towards the far north Queensland coast, where it made landfall at about 10pm on the evening of Friday April 11th near Cape Flattery. Ita weakened somewhat in the hours leading up to landfall and at this time has been rated as a category 4 cyclone at landfall, although this may be revised later once all the data has been reviewed. Cape Flattery automatic weather station recorded a maximum wind gust of 160 km/h.

Near landfall, the centre of Ita came within 5km of the resort at Lizard Island. Unofficial readings showed the air pressure dropped to approximately 954 hPa and wind gusts reached approximately 155 km/h before the instrument failed. Considerable vegetation damage but only minor structural damage to buildings was recorded there.

Upon landfall, Ita continued to track southward through the inland North Tropical Coast district. It weakened reasonably quickly and passed 20km west of Cooktown (the closest population centre to Ita's initial landfall) as a category 2 cyclone. Wind gusts to approximately 125 km/h were recorded there. 200 buildings there received (mostly minor) damage, with 16 buildings receiving severe damage or total destruction. A storm surge of approximately 1.1 metres occurred at about midnight, though fortunately this arrived coincident with the low astronomical tide and little if any inundation occurred.

Ita weakened further to a category 1 cyclone, but was able to maintain this category through the rest of its two day trek southwards along the north Queensland coast, with much of the time spent over land. Gale force winds and damaging wind gusts were recorded at Lucinda, Townsville, Cape Ferguson, Mackay, and Middle Percy Island. The main impact during this phase of Ita's lifetime, though, was rainfall and flooding. Widespread 24 hour rainfalls of over 300mm, peaking at approximately 400mm, were recorded in the North Tropical Coast and Herbert and Lower Burdekin districts. The Daintree, Mulgrave, Haughton, and Herbert Rivers all recorded major floods. Flash flooding occurred at Bowen where 110mm of rainfall in one hour was recorded.

Ita finally turned southeastward and moved off the Queensland coast for good near Proserpine on the night of April 13th. It maintained category 1 intensity for another 24 hours before transitioning into an extra tropical low and accelerating southeastward further away from the coast.

### **Coastal Crossing Details**

**Crossing time:** 10pm EST Friday 11th April 2014

Crossing location: Cape Flattery

55km N of Cooktown

Category when crossing the coast: 4

### **Extreme values during cyclone event (estimated)**

Note that these values may be changed on the receipt of later information

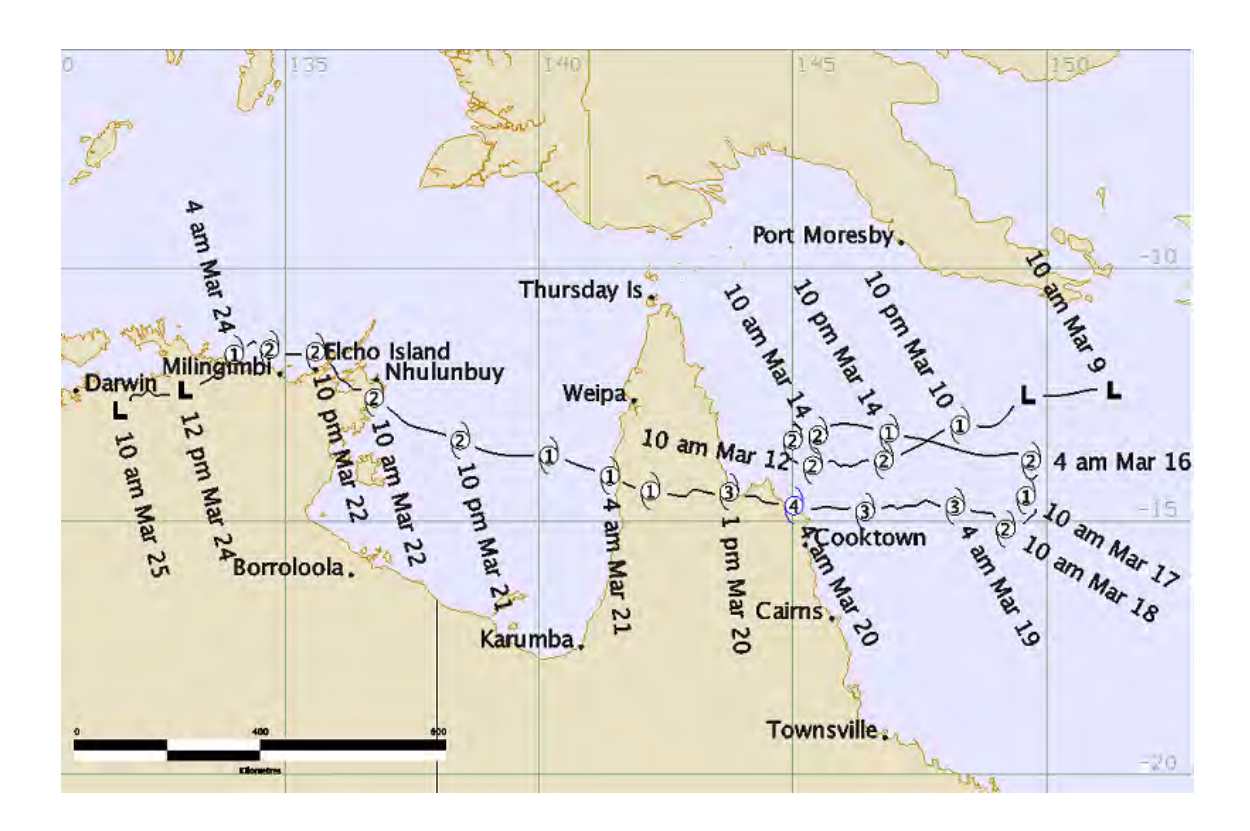
Maximum Category: 5

Maximum sustained wind speed: 215 km/h

Maximum wind gust: 300 km/h

Lowest central pressure: 930 hPa





The tropical low that would become tropical cyclone Nathan was first identified and tracked on the morning of Monday 9 March, 2015 in the northern Coral Sea, to the near south of Papua New Guinea. During the next 36 hours the low drifted towards the west-southwest while slowly intensifying, and was named as category 1 cyclone Nathan on the evening of Tuesday 10 March. The cyclone continued to move west-southwest towards Cape York Peninsula while developing further, reaching category 2 after another 12 hours on the morning of Wednesday 11 March. Following this, Nathan stalled and became slow moving off the Cape York Peninsula coast near Cape Grenville for roughly two days at category 2 strength. During this time, Lizard Island experienced damaging wind gusts but there was little impact on the mainland.

Nathan was then steered to the east away from the coast for the next two days, before becoming slow moving as steering patterns again became confused. Nathan drifted very slowly south for two more days, all this time fluctuating between category 1 and category 2 in intensity. Finally Nathan was again steered westwards towards the Cape York Peninsula coast and intensified, reaching category 3 strength on the morning of Thursday 19 March, and category 4 strength in the last hours before it made landfall at about 4am on Friday 20 March on the east Cape York Peninsula coast near Cape Flattery, not far from where it had stalled a week earlier. The location where Nathan made landfall was unpopulated so impacts were fairly low. Cape Flattery automatic weather station recorded wind gusts to approximately 170 km/h. Some wind damage occurred in Cooktown to the south. Following landfall, Nathan tracked westwards across Cape York, emerging briefly over water again in Princess Charlotte Bay early on Friday afternoon. This contributed to slowing Nathan's weakening, and it was able to maintain marginal category 1 cyclone intensity all the way

across the Cape before it entered the waters of the Gulf of Carpentaria early on the morning of Saturday 21 March.

Tropical cyclone Nathan moved steadily westward across the Gulf of Carpentaria on Saturday 21 March and turned northwest towards the Arnhem coast of the Northern Territory early on Sunday 22 March. Nathan intensified in a favourable environment while over warm Gulf waters and reached high category 2 intensity shortly before crossing the Arnhem coast about 40 kilometres south of Nhulunbuy around 9 am on Sunday. Although wind gusts were estimated to be around 155 km/h near the centre, the town of Nhulunbuy remained outside of the zone of destructive winds and experienced around 3 hours of sustained gales. The highest gust recorded at Gove Airport was 98 km/h at 9:34 am on Sunday. Minor coastal inundation occurred at Nhulunbuy where several yachts were damaged when they broke their moorings.

Nathan maintained category 2 intensity as it emerged from the Gove Peninsula near Arnhem Bay and passed over Elcho Island around 7 pm on Sunday 22 March. Nathan continued westwards over the southern Arafura Sea just north of the Top End coast during Monday, before weakening rapidly as it turned southwest on Monday evening. Nathan made its third and final landfall at category 1 intensity in a remote area between Maningrida and Goulburn Island around 6:30 am Tuesday 24 March. Nathan then weakened below tropical cyclone intensity by 2 pm Tuesday as it tracked inland close to the towns of Gunbalunya and Jabiru. Fortunately the destructive core of the cyclone skirted around the north coast communities of Galiwin'ku, Ramingining and Milingimbi, which were seriously damaged by Severe Tropical Cyclone Lam in February. The strongest gust recorded at Ngayawili AWS near Galiwin'ku was 107 km/h at 7 pm on Sunday 22 March and 3 hours of gale-force winds were observed. Only minor additional damage was reported from the affected communities during Nathan's passage.

Tropical Cyclone Nathan and its remnant tropical depression brought heavy rainfall and flooding to many parts of the Northern Territory's Top End. The highest 24 hour rainfall totals included 208 mm at Alcan Mine on the Gove Peninsula, 261 mm at Fanny Creek and 215 mm at Dorisvale in the Katherine River catchment and 208 mm at Snowdrop Creek in the Waterhouse River catchment. Flood Warnings were issued for both of these rivers.

Nathan was the second cyclone in both the Queensland and Northern Territory areas of responsibility this season, preceded by Marcia in Queensland and Lam in the Northern Territory.

#### **Coastal Crossing Details**

Crossing time: 4am EST Friday 20 March 2015

Crossing location: Cape Flattery

90km NNW of Cooktown

Category when crossing the coast: 4

### Extreme values during cyclone event (estimated)

Note that these values may be changed on the receipt of later information

Maximum Category: 4

Maximum sustained wind speed: 165 km/h

Maximum wind gust: 230 km/h

Lowest central pressure: 963 hPa

# APPENDIX B: CATTLE EXCLUSION PLOT VEGETATION DATA

# Natural Vegetation Recovery Potential of Alluvial Gully Catchments after Cattle Exclusion:

Preliminary Vegetation Change and LiDAR Erosion Results after 4 Years of a Planned Long-Term (20 year) Case Study in the Normanby Catchment

Jeff Shellberg<sup>1</sup>, Andrew Brooks<sup>2</sup>, Graeme Curwen<sup>3</sup>, John Spencer<sup>3</sup>, Fabio Iwashita<sup>1</sup>

<sup>1</sup>Adjunct Research Fellow, Australian Rivers Institute, Griffith University
<sup>2</sup>Senior Research Fellow, Griffith Centre for Coastal Management, Griffith University
<sup>3</sup>Senior Research Assistant, Australian Rivers Institute, Griffith University

# **TABLE OF CONTENTS**

List of Tables	276
List of Figures	277
Executive Summary	280
1. Alluvial Gullies in the Normanby Catchment	282
1.1 Rehabilitation of Alluvial Gullies in the Normanby Catchment	
1.2 Cattle Exclusion and Vegetation Recovery Trials in the Normanby Catchment.	
1.3 Vegetation Plot Assessment	
1.4 Erosion Assessment via Aerial LiDAR	
1.5 Data Limitations and Research Questions	
2. Results	290
2.1 Case Study 1: West Normanby River	290
2.1.1 Methods: West Normanby	
2.1.2 Vegetation Plot Results: West Normanby	
2.1.3 Aerial LiDAR Results: West Normanby	296
2.2 Case Study 2: Crocodile Station Paddock Tributary to the Laura River	297
2.2.1 Methods: Crocodile Paddock	297
2.2.2 Vegetation Plot Results: Crocodile Paddock	298
2.2.3 Aerial LiDAR Results: Crocodile Paddock	301
2.3 Case Study 3: Granite Normanby River	302
2.3.1 Methods: Granite Normanby (2012-2015)	
2.3.2 Results: Granite Normanby (2012-2015)	303
2.3.3 Aerial LiDAR Results: Granite Normanby	
2.4 Case Study 4: Normanby River at Kings Plains	
2.4.1 Methods: Normanby River at Kings Plains (2012-2015)	
2.4.2 Results: Normanby River at Kings Plains (2012-2015)	
2.4.3 Aerial LiDAR Results: Kings Plains	
2.5 Analysis of Pooled Data from Aerial LiDAR	313
3. Discussion	316
3.1 Lessons from Preliminary Cattle Exclusion Trials on Vegetation Recovery	316
3.2 Detecting Short-term Erosion Management Response in Alluvial Gullies usi LiDAR318	ng Aeria
3.3 Supporting Research on Potential Vegetation Recovery in Gullied Areas	319
3.4 Proactive Vegetation Planting and Intensive Gully Rehabilitation	321
Acknowledgements	324
References	325
Pasture Monitoring Template	332
Guidance Sheet to Estimate Percent Cover	
Visual Guides to Estimate Pasture Yield: Yellow Earth	
Visual Guides to Estimate Land Condition: Yellow Earth Example	

# **LIST OF TABLES**

Table B1:	Erosion results from major large-scale LiDAR change at the West Normanby exclusion area
Table B2:	Erosion results from major large-scale LiDAR change at the Granite Normanby exclusion area
Table B3:	Erosion results from major large-scale LiDAR change at the Kings Plains exclusion area at Mosquito Yard
Table B4:	Two tailed t-test results for Normanby grazing exclosure trials314

## **LIST OF FIGURES**

Figure B1:	Examples of alluvial gullies in the Normanby catchment28
Figure B2:	Cross-section drawing of an alluvial gully (bed and scarp) eroding into terrace from a river bank
Figure B3:	Examples of improved cover of native kangaroo grass ( <i>Themeda triandr</i> following 10 years of cattle and fire exclusion on a) rounded gully slopes, arb) a gully scarp with only modest cover improvements compared surrounding uneroded soils (middle Annan River)
Figure B4:	Examples of improved vegetation cover at a) a gully scarp where black spe (Heteropogon contortus) and blady (Imperata cylindrica) grass cover havincreased slightly following 2 years of cattle exclusion and b) a large guscarp where grass cover improvements have been fairly isolated to gustloors, slumped soil blocks, and intact slopes (Normanby River at King Plains).
Figure B5:	Distribution of sub-catchments with significant alluvial gully erosic (tonnes/year/subcatchment) in the Laura-Normanby catchment (from Brook et al. 2013), and locations of fenced cattle exclusion experimental sites, # West Normanby (-15.762320°S, 144.976602°E), #2) Crocodile Paddock 15.710042°S, 144.679232°E), #3) Granite Normanby (-15.896374° 144.994678°E), #4) Normanby River mainstem at Mosquito (-15.598804° 144.916466°E), #5) proposed at Laura River at Crocodile Gap (15.668992° 144.592765°E)
Figure B6:	Aerial view (Nov-2011) of the West Normanby gully complex where cattering exclusion started in September 2012. Note network of pre-existing cattle training on gully ridges and valleys
Figure B7:	West Normanby River below the Cooktown Highway (-15.762320° 144.976602°E) showing a) the location of the fenced cattle exclusion area are vegetation plots with a LiDAR background and b) the location of the fenced area and vegetation plots with an aerial photo background. Note that reareas in Figure B7a are zones of active gully erosion between 2009 and 20° repeat LiDAR.
Figure B8:	Changes in ground cover inside and outside the West Normanby cattering exclusion site from 2011 to 2015 showing a) total % organic cover (grass weeds, leaves, sticks, mulch) and b) % perennial grass cover, c) perenning grass tussock count, and d) pasture biomass yield
Figure B9:	Annual rainfall by water year (Oct-Sept) from 2011 to 2015 at Lakeland ar Kings Plains
Figure B10:	Changes in ground cover at different geomorphic units (terrace, gull hillslope) inside and outside the West Normanby cattle exclusion site fro 2011 to 2015 showing a) total % organic cover (grass, weeds, leaves, stick mulch) and b) % perennial grass cover

Figure B11:	Differences in pasture yield and grass biomass inside (right) and outside (left) the West Normanby cattle exclusion fence on a) the high terrace (left picture) and b) inactive gully slopes (right picture)
Figure B12:	Measurement distributions of scour (negative) or fill (positive) at permanent vegetation plot reference stakes, accurate to 5mm, for fenced and grazed areas of the West Normanby gullies between 2011 and 2015295
Figure B13:	Cattle exclusion area and aerial LiDAR analysis areas (control-impact) along the West Normanby River in block N4 on Springvale Station. Also shown are the locations of the polygons within which erosion was detected by aerial LiDAR in the first period in green (2009-2011, LHS), and the second period in red (2011-2015, RHS).
Figure B14:	Maps of the cattle exclusion fence in the 'Old Hay Paddock' at Crocodile Station (-15.710042° S; 144.679232° E) with a) LiDAR hillshade background and b) aerial photograph background showing locations of vegetation monitoring points inside and outside the exclusion area
Figure B15:	Changes in ground cover in cover inside and outside the Crocodile Station 'Old Hay Paddock' cattle exclusion site from 2011 to 2013 showing a) total % organic cover (grass, weeds, leaves, sticks, mulch) and b) % grass cover (standing perennial or annual grass)
Figure B16:	Changes in vegetation cover and biomass a) before fencing at Plot 508 gully bottom in Nov-2011, b) after fencing at Plot 508 gully bottom in Nov-2012, c) grazed control at Plot 515 hillslope in Nov-2011, d) grazed control Plot 515 hillslope in Nov-2012
Figure B17:	Grass and weed cover inside the cattle exclusion fence (left) and outside (right) in June 2015
Figure B18:	Cattle exclusion area and aerial LiDAR analysis areas (control-impact) at the Crocodile Hay Paddock in block N17 on Crocodile Station. Also shown are the locations of the polygons within which erosion was detected by aerial LiDAR in the first period in green (2009-2011, LHS), and the second period in red (2011-2015, RHS).
Figure B19:	Hillshade LiDAR map of the cattle exclusion fence at GNGC6 (-15.896374°S; 144.994678°E) and neighbouring spelled GNGC9 on the Granite Normanby on Springvale Station. Note that red areas are zones of active gully erosion between 2009 and 2011 repeat LiDAR
Figure B20:	Changes in ground cover inside and outside the Granite Normanby cattle exclusion site from 2012 to 2015 showing a) total % organic cover (grass, weeds, leaves, sticks, mulch) b) % cover of perennial grass, c) perennial tussock count, and d) pasture yield (kg / ha)
Figure B21:	Changes in ground cover at different geomorphic units (terrace, gully, hillslope) inside and outside the Granite Normanby cattle exclusion site from 2012 to 2015 showing a) % cover of perennial grass and b) perennial grass tussock counts

Figure B22:	Differences in grass cover and biomass between the fenced gully (Left, GNGC6) and the grazed area (Right, GNGC9) on the high terrace of the Granite Normanby in a) April 2013 and b) November 2015305
Figure B23:	Measurement distributions of scour (negative) or fill (positive) at permanent vegetation plot reference stakes, accurate to 5mm, for fenced and grazed areas of the Granite Normanby gullies between 2012 and 2015306
Figure B24:	Cattle exclusion area and aerial LiDAR analysis areas (control-impact) along the Granite Normanby River in block N7 on Springvale Station. Also shown are the locations of the polygons within which erosion was detected by aerial LiDAR in the first period in green (2009-2011, LHS), and the second period in red (2011-2015, RHS)
Figure B25:	Hillshade LiDAR map of vegetation plot locations and the cattle holding paddock (Mosquito Yards) at Kings Plains, with modest cattle grazing inside the paddock and cattle spelling outside the paddock. Note that red areas are zones of active gully erosion between 2009 and 2011 repeat LiDAR308
Figure B26:	Changes in ground cover inside and outside the Kings Plains cattle exclusion area from 2012 to 2015 showing a) total % organic cover (grass, weeds, leaves, sticks, mulch) b) % cover of perennial grass, c) perennial tussock count, and d) pasture yield (kg / ha)
Figure B27:	Changes in ground cover at different geomorphic units (terrace, gully, hillslope) inside and outside the Kings Plains cattle exclusion area from 2012 to 2015 showing a) % cover of perennial grass and b) perennial grass tussock counts
Figure B28:	Measurement distributions of scour (negative) or fill (positive) at permanent vegetation plot reference stakes, accurate to 5mm, for fenced and grazed areas of the Kings Plains gullies between 2012 and 2015311
Figure B29:	Cattle exclusion area and aerial LiDAR analysis areas (control-impact) at the Mosquito Yard site on Kings Plains Station in block N10. Also shown are the locations of the polygons within which erosion was detected by aerial LiDAR in the first period in green (2009-2011, LHS), and the second period in red (2011-2015, RHS). Note that the "Fenced" sites in this case are outside of the Mosquito yards.
Figure B30:	Stages of gully channel evolution applicable to valley bottom gullies or arroyos (after Gellis et al. 1995; 2001). This general gully evolution model is only applicable to some alluvial gullies in the Normanby and Mitchell catchments, with many gullies being trapped in the incision, headward retreat, and widening stages for long period of time (Stages B and C), after small initial cycles of incision, aggradation, and re-incision following initial disturbance and gully initiation (Shellberg et al. 2016). Most alluvial gullies will not fill back in with sediment due to permanent degradation
Figure B31:	Alluvial gully management guidelines and a flow chart for potential avenues into rehabilitation, categorized by gully type and stage of gully evolution (following Gellis 1995)

### **EXECUTIVE SUMMARY**

Alluvial gully erosion is widespread across active and inactive floodplains across northern Australia, and has been accelerated by human land use such as cattle grazing, roads and fencelines. Rehabilitation and stabilisation of alluvial gullies are a high priority for reducing sediment loads to the Great Barrier Reef (GBR). Improving vegetation cover in gully catchments above and below gully head cuts is one possible way to reduce water runoff, promote infiltration, and most importantly protect the soil surface from erosion, in addition to other more intensive structural and bioengineering intervention in active erosion zones.

In this study, the natural vegetation recovery potential and erosion reduction were assessed after four years of cattle exclusion from four gully catchments to understand preliminary changes on the trajectory toward potentially unknown long-term recovery (20+ years). Initial results indicated that passive vegetation recovery differed by geomorphic units and size and depth of gully. The un-eroded high terrace surfaces of catchments above alluvial gullies (<25% of gully catchment area) had positive changes to pasture condition (cover, tussock counts, biomass) following grazing exclusion. No vegetation improvements were detected inside deep alluvial gullies with exposed sodic sub-soils, which are likely to be the major contributors of sediment from such gullies. In shallow alluvial gullies, vegetation response was improved on inactive gully slopes and gully bottoms, but was still minimal at the most eroded plots with exposed dispersible sodic sub-soils. Overall, rainfall variability had a greater influence on vegetative conditions than cattle exclusion alone, as seen during below average rainfall years, but with greater vegetation cover and resilience in ungrazed areas during dry years with below average rainfall.

Erosion data measured using aerial LiDAR was only able to detect large-scale erosion processes, like scarp retreat and slumping, but not soil surface erosion or rilling from direct rainfall or overland flow inside or above the gullies. These LiDAR data showed there was a statistical difference in detectable large-scale erosion after cattle exclusion, although the pooled results were heavily influenced by the results from the Kings Plains site, which was the least well constrained trial of the three sites included in the analysis (i.e. relatively low grazing pressure and incomplete exclusion). Plot scale measurements of surface erosion and deposition showed no major trends from grazing exclusion over four years, but did highlight the variability and magnitude of surface erosion and deposition within gullies that are common over large areas and can contribute a significant portion of total sediment yield. More detailed erosion monitoring will be needed at 1) the plot scale using high-resolution terrestrial LiDAR scanning and 2) gully outlets via sediment yield gauging to detect the potential soil surface erosion response, sediment and nutrient yield to improved vegetation cover and grazing management, as well as changes in surface water runoff and soil infiltration.

If major water quality improvements are to be achieved within the next decade in order to reduce sediment loads in the short term, we would need to see significant improvements after four years of cattle exclusion toward this goal, even with coarse-scale aerial LiDAR and several dry years. However, these preliminary data cast doubt that cattle exclusion alone will improve vegetation cover on exposed sodic sub-soils and stop existing large-scale gully erosion. It is likely to take a lot longer than the four years for the effects of grazing exclusion alone to show a measureable change in aerial LiDAR data or surface erosion processes.

Managing cattle on sodic river frontage is an essential prerequisite to address the causes or accelerators of gully erosion, not just the symptoms, such as reducing soil disturbance, cattle pads, and overgrazing. However, more proactive gully rehabilitation measures will be essential beyond only cattle exclusion from deep alluvial gully catchments if major reduction is sediment loads to the GBR are to be achieved. An alluvial gully rehabilitation flow chart is provided to initially help decide if and how to intervene with alluvial gully erosion, following expert advice, design and field oversight of gully rehabilitation measures from trained and experienced geomorphologists, soil conservationists, and bioengineers.

## 1. ALLUVIAL GULLIES IN THE NORMANBY CATCHMENT

Alluvial gully erosion is both a natural and human land use accelerated erosion process. These alluvial gullies or 'breakaways' initiate on steep river and creek banks along river frontages and erode into river terraces and elevated floodplains with highly erodible soils (Figure B1; Figure B2). River incision over geologic time (base level), dispersive or sodic soils (high exchangeable sodium on clay particles), intense monsoon rainfall and flooding are natural factors priming the landscape for gully erosion.

Sediment dating in alluvial gullies on Cape York has shown that gully erosion rates have increased up to 10 times since European settlement in some locations (Shellberg 2011; Brooks et al. 2013; Shellberg et al. 2016). From the same studies, historic aerial photographs also documented increased gully erosion after land use change. Modern gullies have eroded into older floodplain hollows and drainage channels that were earlier phases of gully erosion, as well as into steep river banks. The recent accelerated phase of gullying can be linked to the introduction of cattle that congregate along river frontages, reduction of perennial grass cover, concentration of water along cattle tracks (pads), and an increase in water runoff into gullies, as well as intense late-dry season fires, roads, fence lines, agricultural clearing, and infrastructure development (Shellberg 2011; Brooks et al. 2013; Shellberg and Brooks 2013; Shellberg et al. 2016).

In the Normanby catchment, over 2000 ha of alluvial gullies have been mapped by air photographs, with the potential of up to 10,000 ha of gullies once the masking effect of tree cover has been removed (Brooks et al. 2013). These alluvial gullies are the source of  $\sim$ 24% of the total sediment load input ( $\sim$ 3,000,000 tonnes/yr) in the upper Normanby catchment, compared to  $\sim$ 13% for colluvial gullies,  $\sim$ 54% for small ephemeral creeks,  $\sim$ 8% for river bank erosion, and  $\sim$ 0.5% from hillslopes (Brooks et al. 2013). More recent data presented elsewhere in this report show that there is considerable inter-annual variability in the relative contributions from each of these sources.



**Figure B1:** Examples of alluvial gullies in the Normanby catchment.

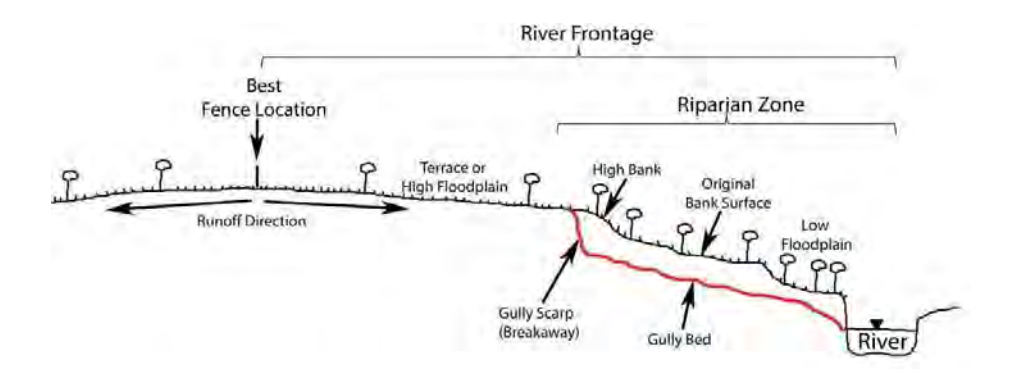


**Figure B2:** Cross-section drawing of an alluvial gully (bed and scarp) eroding into a terrace from a river bank.

### 1.1 Rehabilitation of Alluvial Gullies in the Normanby Catchment

Rehabilitation and stabilization of alluvial gullies in the Normanby Catchment are a high priority for reducing sediment loads to the Great Barrier Reef (GBR) since alluvial gullies are a major source of sediment that has been increased by land use activities (Shellberg and Brooks 2013).

There are three main approaches to prevent gully initiation and reduce gully erosion once started, which generally should be used in combination (Heede 1976; Lal 1992; Haigh 1984; Thorburn and Wilkinson 2013).

- Reduce water runoff into gullies and drainage hollows by increasing vegetation cover (e.g., perennial grass) and infiltration in uplslope catchments (where they exist), as well as other structural elements that divert or retain water before reaching the gully head.
- 2. Stabilise gully headcuts, sidewalls, and drainage hollows with vegetation and/or physical structure.
- 3. Reduce the gully channel slope and increase roughness using grade control structures and/or vegetation, which will trap sediment, reduce channel slope, and promote revegetation.

Over large areas in the Normanby catchment and northern Australia, a long-term (20+ years) land-use management approach to alluvial gully rehabilitation will be needed as a primary prerequisite to addressing broadscale land use impacts that trigger or accelerate gully erosion. The scale of gully erosion and cost limitations likely prevent intensive intervention everywhere, especially in remote locations with older gullies and surrounding catchment slopes at advanced stages of gully evolution, despite these gullies being major sediment and nutrient sources (Shellberg and Brooks 2013; Figure B30). These land-use management actions to reduce the initiation or acceleration of gully erosion include reducing cattle grazing pressure on sensitive soils across large areas of river frontage, changing fire regimes (timing,

frequency, and magnitude) with integrated fire management, and controlling weeds and their expansion. These actions will reduce direct soil disturbance, promote perennial grass health and cover, and potentially improve hydrological functions (e.g., infiltration, retention) that reduce water runoff (McIvor et al. 1995; Roth 2004). By removing chronic stressors as a prerequisite for any gully rehabilitation, the natural resilience and positive feedbacks mechanisms of vegetation recovery within gully evolution cycles (Figure B30; Gellis et al. 1995; 2001) should help promote soil protection, hydrological function, and reduced soil erosion (e.g., Figure B3; Figure B4). At a minimum, the initiation of new alluvial gullies should be reduced by minimizing land management disturbance along fragile river frontage.

Over the short-term (< 10 years) to achieve near-term Reef Protection goals, more intensive efforts of gully rehabilitation also will be essential to more rapidly reduce river sediment loads from alluvial gullies. Targeted investment in intensive gully rehabilitation should focus on young gullies at early stages of gully evolution (Figure B30; Figure B31; Gellis et al. 1995; 2001) and other areas of strategic concern (roads, fencelines and infrastructure) as a preemptive measure to prevent major future erosion (Brooks et al. 2015; Spencer et al. 2016). Intervention in early stages (A or B) of channel evolution is recommended by geomorphic science (Figure B30; Figure B31), as intervention too late in the evolutionary cycle can often lead to engineering failure or ineffective sediment reduction after a majority of soil loss has already occurred (Gellis et al. 1995; Simon and Darby 2002). Intensive rehabilitation efforts could include water runoff diversion, grade control, slope stabilization, soil amendments, and active vegetation planting both above and within gullies (Shellberg and Brooks 2013). Young gullies, roads and fencelines should be prioritized (Brooks et al. 2015; Spencer et al. 2016) with active intervention following guidelines, recommendations and lessons learned in Shellberg and Brooks (2013) and the flow chart in Figure B31. These actions targeting young or priority gullies and roads/fences will need to be conducted in conjunction with the prerequisite of improved land-use management of chronic stressors.



**Figure B3:** Examples of improved cover of native kangaroo grass (*Themeda triandra*) following 10 years of cattle and fire exclusion on a) rounded gully slopes, and b) a gully scarp with only modest cover improvements compared to surrounding uneroded soils (middle Annan River).



**Figure B4:** Examples of improved vegetation cover at a) a gully scarp where black spear (*Heteropogon contortus*) and blady (*Imperata cylindrica*) grass cover have increased slightly following 2 years of cattle exclusion and b) a large gully scarp where grass cover improvements have been fairly isolated to gully floors, slumped soil blocks, and intact slopes (Normanby River at Kings Plains).

Since 2008, the Reef Rescue program in the Normanby catchment has been implementing riparian fencing projects with local landowners to exclude cattle grazing from the erodible banks of rivers and creeks, where many alluvial gullies initiate and propagate. Between 2008 and 2013, 11 riparian fencing projects to exclude cattle were implemented, which excluded cattle from 76 km of riparian zone protecting 8698 ha (RR project data, Isha Segboer personal communication). Project justification was the assumed standard water quality benefits, such as reducing animal nutrients in streams, improving vegetation cover in riparian zones, reducing cattle soil disturbance on banks and cattle pads, and reducing the initiation or expansion of gullies. Most projects had permanent oblique photo points installed to help track changes in vegetation and perhaps erosion over time, but few have been consistently resurveyed to promote learning opportunities. This monitoring was also not quantitative, nor was it focused on areas of active erosion of concern. Any water quality benefits are assumed, especially related to gully erosion. This includes the assumed and modelled reduction in sediment loads in the Normanby catchment from reef rescue investment activities, which are unsubstantiated with field data (Queensland State 2013; McCloskey et al. 2014). In some observed cases for example, riparian fence installation actually increased erosion through improper placement and construction through gully hollows (Shellberg and Brooks 2013).

Due the lack of quantitative field monitoring data, in 2011 the Reef Rescue program invested in a suite of long-term (10+ years) cattle exclusion experiments at fenced riparian zones and alluvial gully sites in the Normanby catchment (Shellberg and Brooks 2013). Before-after control-impacts (BACI) experiments were set up with both vegetation and erosion monitoring at the plot and gully scale. These data are needed to understand the vegetation recovery and erosion reduction potential of different geomorphic units over different time scales, so as to guide future investment. It is currently unknown what recovery pathways are achievable with cattle exclusion or intensive intervention in different types of alluvial gullies. Definitive data results will likely take two decades to collect. Will recovery return conditions towards the pre-existing state fairly quickly (rubber band model), never recover to the pre-existing state (the humpty dumpty model), or return to a pre-existing state after a long recovery period (the

broken leg model) (Sarr 2002)? Preliminary vegetation response to cattle exclusion of individual geomorphic units and gully types are reported on here for the period 2011-2015.

# 1.2 Cattle Exclusion and Vegetation Recovery Trials in the Normanby Catchment

Cattle exclusion trials were implemented in 2011-2012 at four (4) alluvial gully sites in the Normanby catchment. Multiple exclusion sites were established across the catchment so as to capture the spatial and morphological diversity of alluvial gullies (Figure B5). The goal of these trials was to begin to demonstrate and quantify over the long term (20+ years) the potential for vegetation recovery and reduction in sediment erosion and yield in existing alluvial gullies after cattle exclusion and removal of chronic disturbance. Thus, the influence of removing cattle was tested in the absence of any other gully stabilization measures. Short-term results (4 years) can be used as indicative of the future potential for recovery from grazing exclusion, if any, but these short-term results are not intended to be conclusive, and are reported on here as preliminary data.

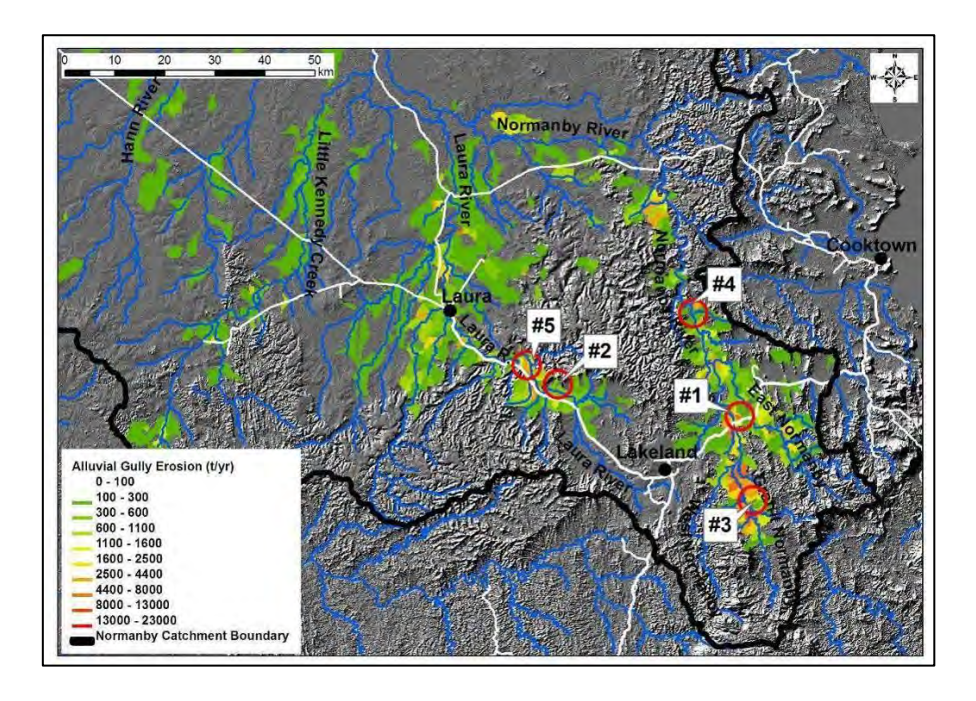


**Figure B5:** Distribution of sub-catchments with significant alluvial gully erosion (tonnes/year/subcatchment) in the Laura-Normanby catchment (from Brooks et al. 2013), and locations of fenced cattle exclusion experimental sites, #1) West Normanby (-15.762320°S, 144.976602°E), #2) Crocodile Paddock (-15.710042°S, 144.679232°E), #3) Granite Normanby (-15.896374°S, 144.994678°E), #4) Normanby River mainstem at Mosquito (-15.598804°S, 144.916466°E), #5) *proposed* at Laura River at Crocodile Gap (15.668992°S, 144.592765°E).

Study designs followed a before-after, control impact (BACI) design (Underwood 1994a; 1994b; Smith 2002) that monitored vegetation, soil conditions, and vertical erosion at the plot scale (4 m²) distributed across gullies (2011, 2012, 2013, 2015), and sediment erosion via repeat aerial LiDAR topographic surveys at the gully-complex scale (2-5 ha) (2009, 2011,

2015). Initial cattle exclusion fencing and "before" vegetation monitoring were installed and conducted in 2011/2012. Repeat aerial LiDAR topographic surveys were flown in 2009 and 2011 for "before" erosion conditions. Initial "after" vegetation monitoring was conducted in 2012/2013 and again in 2015. Repeat aerial LiDAR topographic surveys again were flown in 2015 for "after" erosion monitoring by comparison to 2009 and 2011 data. Rainfall data were collected daily at the following cattle stations: Kings Plain, Springvale, Lakeland, Crocodile.

## 1.3 Vegetation Plot Assessment

Assessment of vegetation and soil conditions at the plot scale followed protocols modified from Wilke (1997), Rolfe et al. (2004) and Karfs et al. (2009) (see data sheets and survey instructions in Appendix). At dozens of plot locations inside and outside the exclosure, a permanent vegetation marker was established at each plot using a star picket. Each plot was 2m x 2m (4m²) and identified by using a PVC grid centred on the star picket. Initial pasture conditions were assessed just before the break-of-season (November), when vegetation conditions are at their annual low before the next wet season. In some years pasture conditions were assessed after the wet season (April) for comparison. Within each plot area (4 m²), a suite of semi-quantitative measurements and photographs were made of the pasture ground vegetation conditions, as well as soil and erosion conditions:

- Aerial projected % cover of all organic material (excluding cow dung)
- Aerial projected % cover of individual cover components (leaves/sticks, dead matted grass, standing vegetation, standing weeds)
- % cover of just perennial grass
- # of species and species identification
- # of perennial tussocks
- Visual pasture yield estimate (standing biomass) from QDPIF picture templates
- Grass and weed species dominance
- Soil condition (erosion, deposition, crust integrity)
- Vertical erosion or deposition at a reference stake (upslope/downslope)(±3mm)
- Overall land condition rating (A,B,C,D)
- Detailed photographs of vegetation plot condition and species from multiple standard angles for future comparisons.

At all plots in March 2012 when the floristic characteristics of grass were best for proper identification, grass and other weed species were collected and pressed at each plot for later identification. The Queensland Herbarium professionally identified the pressed plants. These data will be used for 10-20 year comparisons of vegetation community change.

### 1.4 Erosion Assessment via Aerial LiDAR

The control and treatment areas at each gully site were selected as much as possible to minimise differences in controlling variables. However, with experimental treatment areas it is extremely difficult to find identical gullies. For example soil particle size, geochemistry and sedimentary architecture can vary considerably over short distances, which have not been quantified in this or other studies on equivalent landscapes. Factors such as gully base level elevation can also be important controls on gully activity (Brooks et al., 2009), something which is a factor in opportunistic gully comparisons at the Kings Plains sites. Thus in these situations, the reliance on before-after data is important to define the internal trajectories and behaviour of each gully. Ideally a BACI catchment experiment would be set up with sediment gauges at gully outlets to accurately measure the sediment yield (e.g., Shellberg et al. 2013), along with finer scale erosion data internal to gullies (e.g., terrestrial LiDAR at erosion plots). Unfortunately the funds for detailed monitoring like this were not available for this study. Rather, this study relies on point measurements of erosion/deposition at permanent vegetation plot reference stakes, and most importantly upon two aerial LiDAR surveys that define the "before" conditions over a two year period. A new set of aerial LiDAR was acquired as part of the current project enabling us to assess broad change after 3-4 years of cattle exclusion, as well as 2 years before.

It is essential to note that aerial LiDAR analysis is a fairly crude tool for measuring fine scale erosion detail over relatively short time periods (especially in the vertical dimension < 0.2m). Thus these data can only detect erosion deeper than 0.2m and greater than 2 m² in area, which over this timescale tends to be large-scale scarp retreat and slumping in gullies, as well as secondary incision into the gully floor. Aerial LiDAR cannot detect small-scale soil surface erosion < 0.2m or rilling from direct rainfall or overland flow, which is widespread inside or above the gullies and can represent up to 70% of measured sediment yield outputs at the event to annual scales (e.g., Shellberg et al. 2013). Point measurements of erosion/deposition at permanent vegetation plot reference stakes (average of upslope/downslope) provide some indication of finer-scale processes, but are limited in sample size across these gullies.

To test the statistical significance of the large-scale erosion response (scarp retreat and slumping) to either grazing exclusion and/or rainfall, we have pooled the data for three sites (West Normanby, Granite Normanby, Kings Plains) to increase the sample size for analysis (n=3 plots; incorporating 35 erosion polygons >  $10m^2$  in grazed areas and 29 in fenced areas). The LiDAR change detection undertaken in these plots was the same approach taken in the broader analysis across the 7 common LiDAR blocks (See Appendix 2 & 3). To test the statistical significance of the response, however, we have pooled the data for the three sites to increase the sample size, and filtered any erosion polygons less then  $10m^2$  so that the data is not negatively skewed by a profusion of erosion in single/few cell polygons, given that erosion data at this scale is also less reliable than the larger areas. These data are however, still included in the total erosion data for each of the plots. Erosion polygon data were then normalised for area and then two tailed *t*-test used to test the following hypotheses:

- 1. That there is no difference between the grazed and fenced areas between 2009 and 2011 (i.e. before data)
- 2. That there is no difference between the grazed and fenced areas between 2011 and 2015 (i.e. post treatment data)
- 3. That there was no difference between erosion rates in the fenced area for the two periods (i.e. 2009-2011 vs. 2011-2015)
- 4. That there was no difference between erosion rates in the grazed area for the two periods (i.e. 2009-2011 vs. 2011-2015)

### 1.5 Data Limitations and Research Questions

The experimental monitoring program is intended to continue for at least a 10 to 20 year period for a full assessment of changes over the long-term. Additional LiDAR surveys and vegetation monitoring will be needed. Where data on "before" conditions are limited due to initial 2011/2013 efforts and lack of funding, more detailed data on vegetation, gully erosion, sediment yield, soil heterogeneity, and hydrological conditions should be collected at control and treatment sites to better quantify inherent conditions and potential changes, which will value add to initial efforts (e.g., terrestrial LiDAR, differences in soil infiltration rates, vegetation colonization by species, etc.).

Some key questions this research poses and might be able to answer include:

- How does vegetation cover change over time in existing gullies, surrounding catchments, and specific geomorphic units with and without cattle exclusion?
- Does cattle exclusion and vegetation recovery have any influence on soil erosion?
- How do cattle and animal track density change over time inside/outside exclosures?
- What are the complicating influences of weeds, fire, and wallaby grazing?
- Are experimental methods robust enough for quantification of long-term change?
- What additional information could be collected now or in the future (control/treatment) to value add to these existing data?

## 2. RESULTS

## 2.1 Case Study 1: West Normanby River

### 2.1.1 Methods: West Normanby

On Springvale Station on the West Normanby River, a representative block of alluvial gully erosion through the riparian zone of the east bank of the West Normanby River was selected to monitor changes in erosion and vegetation conditions over time (-15.762320°S, 144.976602°E; Figure B6; Figure B7). A 3 ha riparian area was fenced in October 2012 to exclude cattle. Vegetation conditions were monitored before (Nov 2011, March 2012) and after cattle exclusion fencing (November 2012, 2013, 2015). Two main gully catchments are located inside the exclusion fence, one with overstorey tree vegetation and one without (Figure B6; Figure B7). A control gully without overstorey vegetation is located outside this fenced area, which was selected for monitoring change under status quo conditions with cattle access (Figure B7). Large-scale gully erosion was initially monitored using repeat aerial LiDAR surveys in 2009 and 2011 ('before conditions'), with repeat LiDAR surveys collected again in 2015 ('after conditions') for preliminary results. Point measurements of erosion/deposition at permanent vegetation plot reference stakes also provided an indication of finer-scale erosion.

In November 2011, vegetation monitoring plot locations were randomly selected along five transects parallel to the river from continuous points 10 m apart along each transect to avoid repetition. In a few cases where large trees were encountered at random points, the plot location was adjusted slightly into adjacent more open pasture locations. Each transect was located at different elevations above the river and hence specific ecotones of vegetation. The upper two transects (1 & 2) are located on the high-floodplain (terrace) flats. Transects 3 & 4 are typical of gully channels, slopes, and interfluves, while transect 5 is along the active river bench (bonus data). Overall, 24 plots were located outside the fence, and 26 inside the fence.



**Figure B6:** Aerial view (Nov-2011) of the West Normanby gully complex where cattle exclusion started in September 2012. Note network of pre-existing cattle trails on gully ridges and valleys.

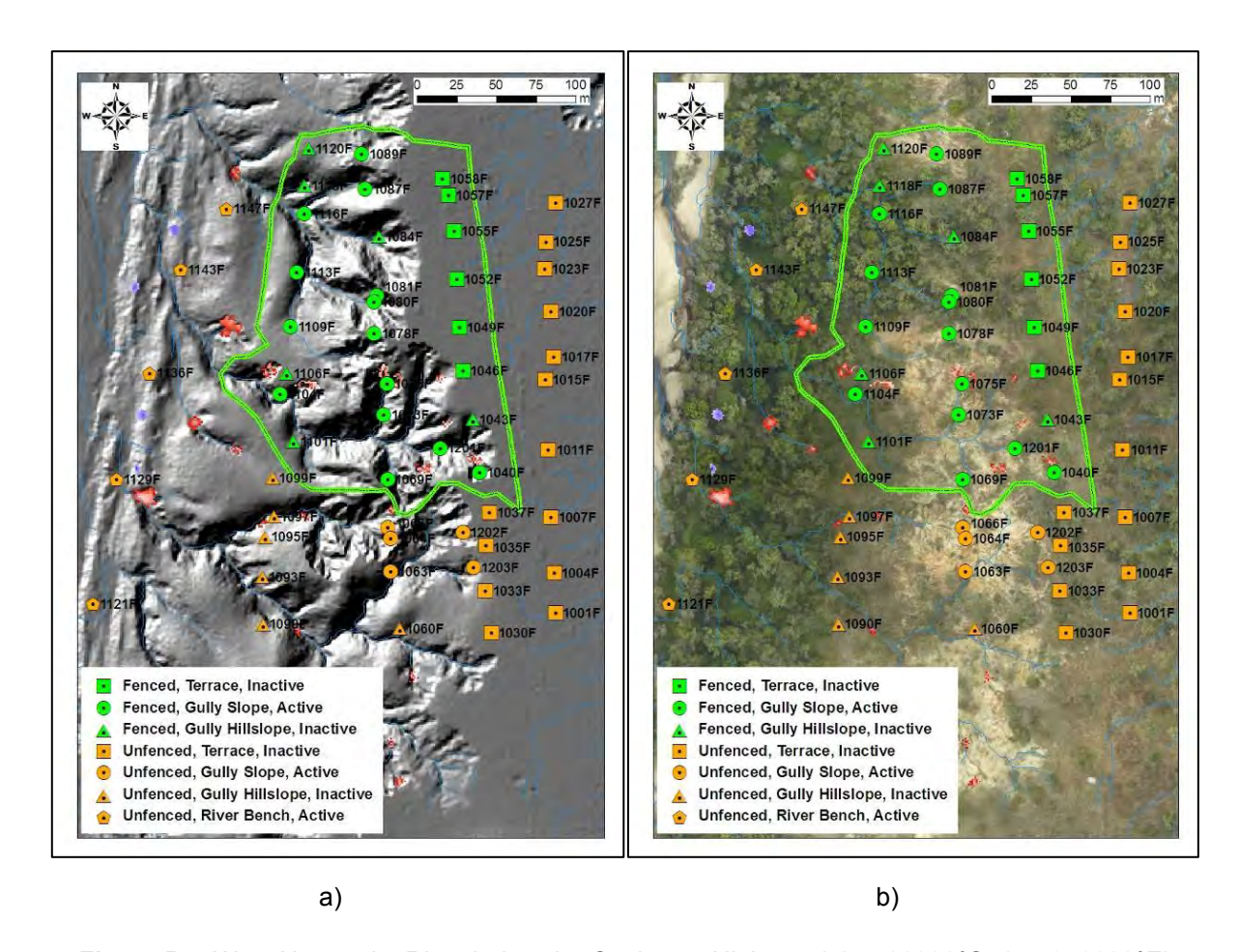


**Figure B7:** West Normanby River below the Cooktown Highway (-15.762320°S, 144.976602°E) showing a) the location of the fenced cattle exclusion area and vegetation plots with a LiDAR background and b) the location of the fenced area and vegetation plots with an aerial photo background. Note that red areas in Figure B7a are zones of active gully erosion between 2009 and 2011 repeat LiDAR.

### 2.1.2 Vegetation Plot Results: West Normanby

Preliminary results between 2011 and 2015 indicated that both % total organic cover and % cover of perennial grass changed seasonally, as expected, with greater cover after the wet season (Figure B8). At both fenced and grazed sites, variability in % total organic cover between Nov-11 and May-13 did not display major trends (Figure B8a). However, total cover was much reduced at both fenced and grazed sites by Nov-15 due to below average rainfall (Figure B9). The % cover of perennial grass increased in both fenced and grazed sites between Nov-11 and May-13 (Figure B8b), but also was reduced by Nov-15 due to below average rainfall (Figure B9). Both tussock counts and pasture yield were also lower by Nov-15 (Figure B8c,d). From these data it appears that rainfall variability and drought can have major influences on ground cover, both inside and outside of cattle exclusion areas.

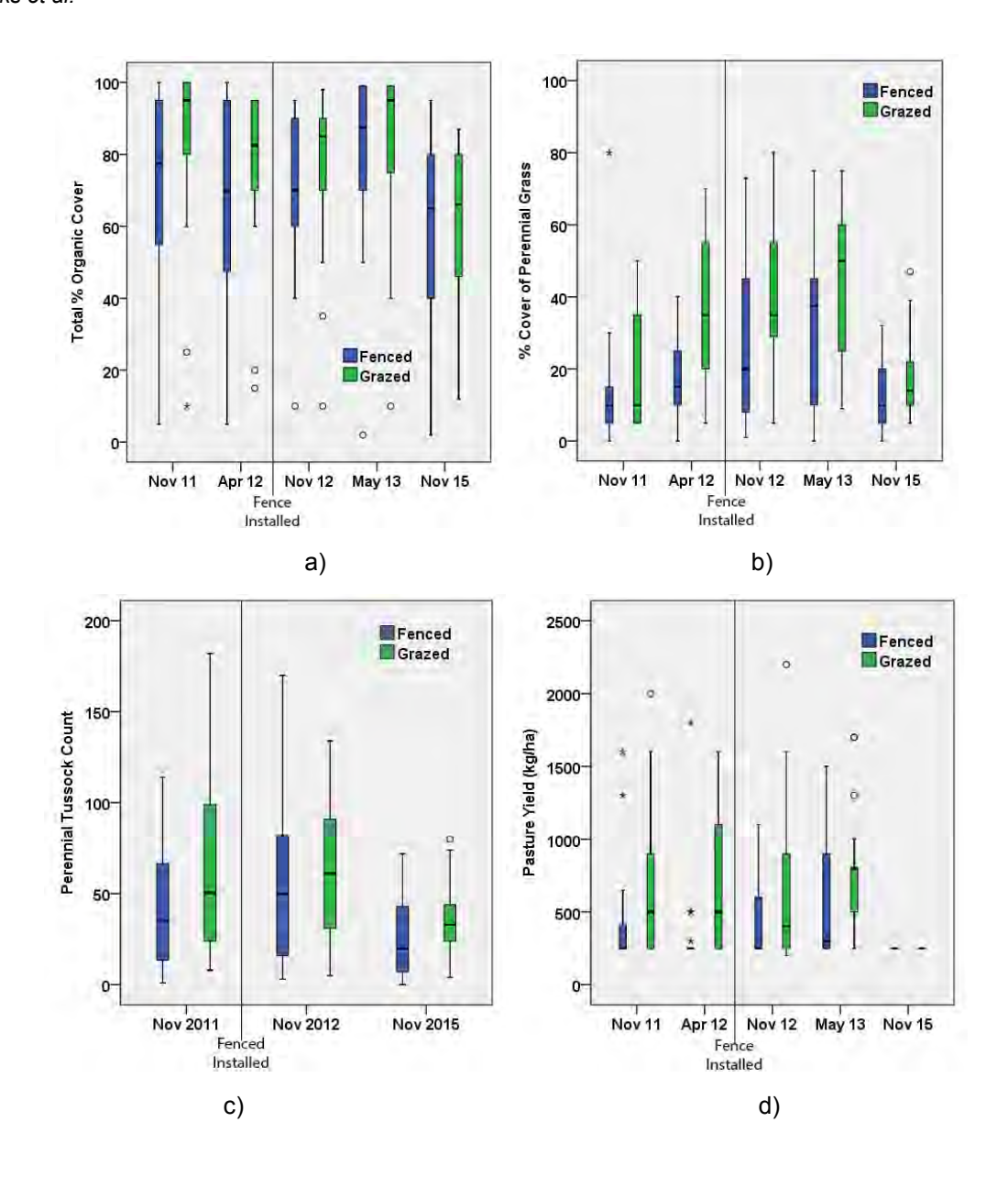


**Figure B8:** Changes in ground cover inside and outside the West Normanby cattle exclusion site from 2011 to 2015 showing a) total % organic cover (grass, weeds, leaves, sticks, mulch) and b) % perennial grass cover, c) perennial grass tussock count, and d) pasture biomass yield.

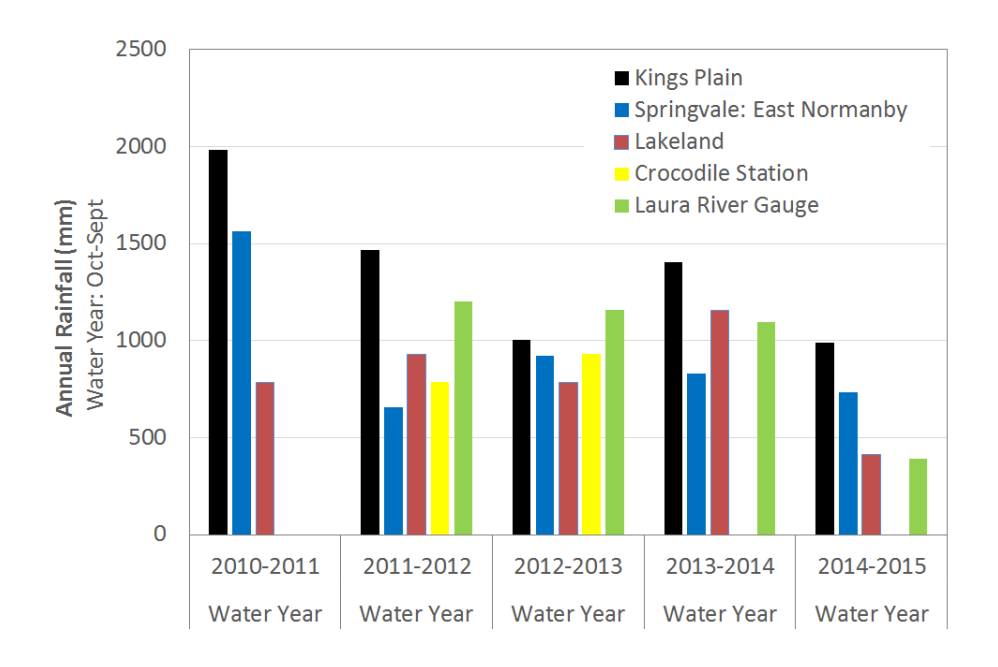
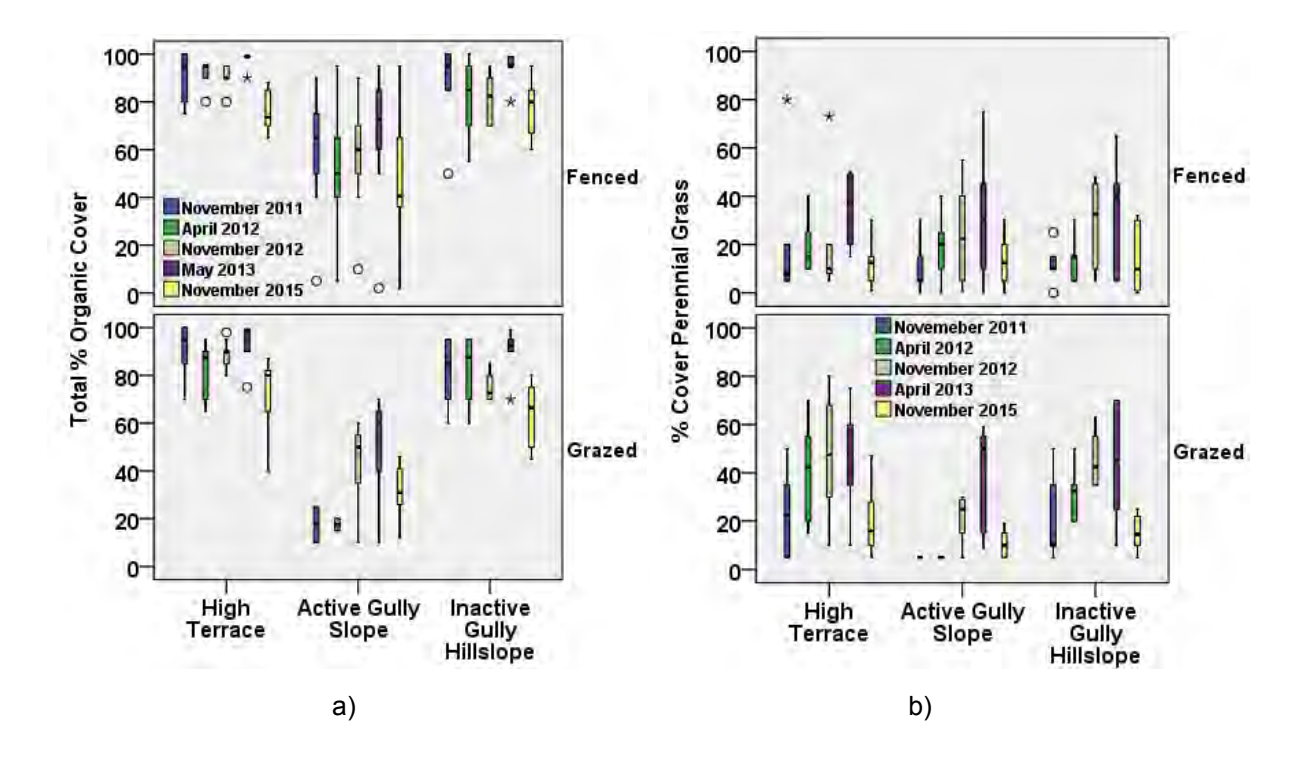


Figure B9: Annual rainfall by water year (Oct-Sept) from 2011 to 2015 at Lakeland and Kings Plains.

When vegetation cover is examined by different geomorphic units (high terrace, active gully slope, inactive gully hillslope) both inside and outside the fence, the general trends were similar. Total % organic cover varied between seasons and years between Nov-11 and Apr-13 with no major trends (Figure B10a). However, Nov-15 total cover was much reduced at all geomorphic units due to below average rainfall (Figure B9). The % cover of perennial grass increased in both fenced and grazed geomorphic units between Nov-11 and May-13 (Figure B10b), but also was reduced by Nov-15 due to below average rainfall (Figure B9).

Cover on intact high terrace flats improved the most for % perennial grass cover in fenced areas, with the largest increase in % grass cover occurring on fenced high terrace flats after fence installation (Figure B10b, Fenced, High Terrace, April 2013). Pasture yield also increased on these terrace flats compared to outside areas, and less so on inactive gully slopes (Figure B11). Removal of cattle grazing on these high terrace flats contributed to this increase. However, % perennial grass cover also increased at grazed (unfenced) high terrace flats, but not as dramatically between Apr-12 and Apr-13. The % perennial grass cover also increased between Nov-11 and Apr-13 at other geomorphic sites, both fenced and unfenced, until the major drop in cover by Nov-15 after below average rainfall.



**Figure B10:** Changes in ground cover at different geomorphic units (terrace, gully, hillslope) inside and outside the West Normanby cattle exclusion site from 2011 to 2015 showing a) total % organic cover (grass, weeds, leaves, sticks, mulch) and b) % perennial grass cover.

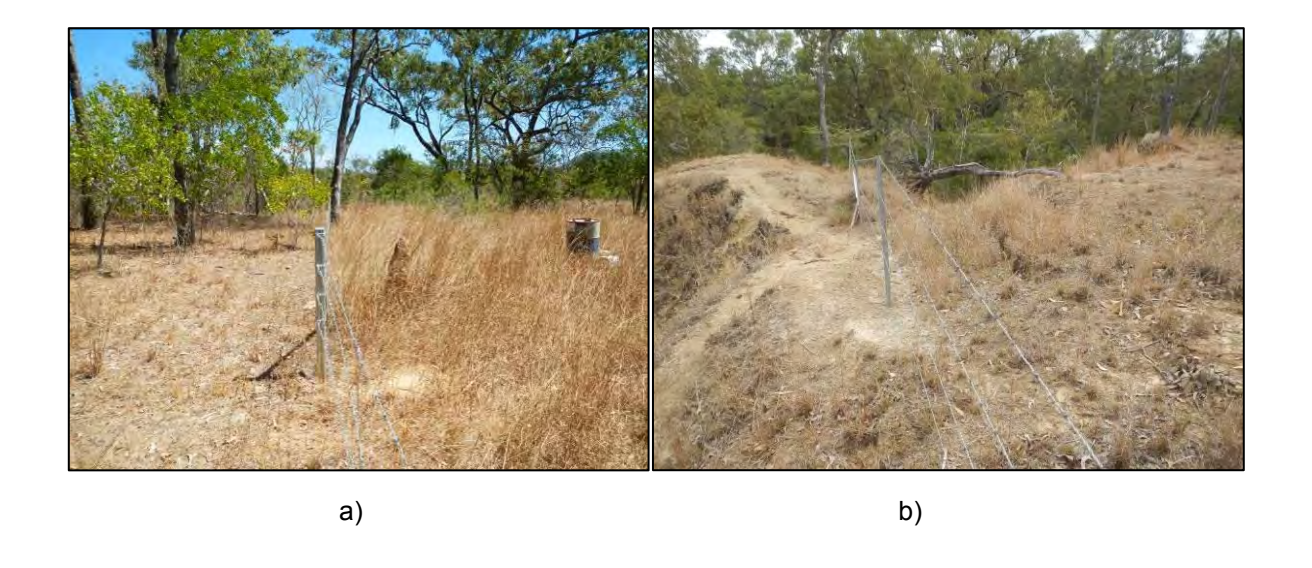


**Figure B11:** Differences in pasture yield and grass biomass inside (right) and outside (left) the West Normanby cattle exclusion fence on a) the high terrace (left picture) and b) inactive gully slopes (right picture).

Point measurements of scour and fill (± 5mm) at permanent vegetation plot reference stakes between 2011 and 2015 indicated much variability, but no clear trends (Figure B12). The spread of the data increased over time due to ongoing erosion and deposition at the most

active gully sites. Longer-term data will be needed to understand trends from rainfall and runoff variability, and gully evolution at the site scale.

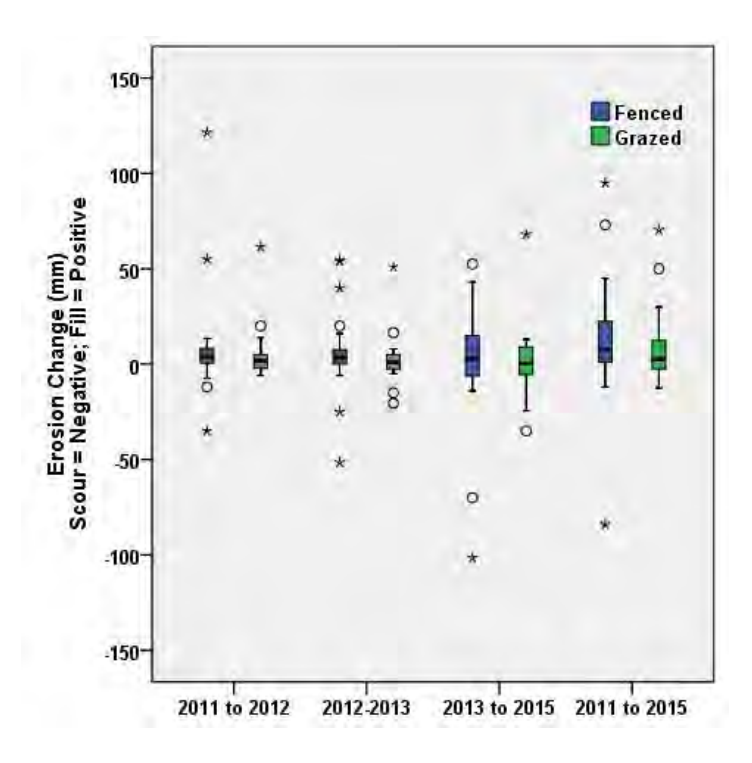


**Figure B12:** Measurement distributions of scour (negative) or fill (positive) at permanent vegetation plot reference stakes, accurate to 5mm, for fenced and grazed areas of the West Normanby gullies between 2011 and 2015.

The preliminary vegetation plot data display the usefulness of a before-after, control-impact (BACI) study design to begin understanding potential changes over time from land management actions (e.g., cattle fencing). The chosen vegetation metrics appear to be picking some positive changes in pasture condition on high terrace catchments above gullies with exclusion of cattle over short-time periods (2011-2015). Improvements in vegetation cover on these specific terraces (<25% of catchment area) is poptentially important in regulating water runoff; but improved vegetation cover inside larger internal gully areas is essential to have any influence on gully erosion impacted by direct rainfall. No vegetation improvements were detected inside the gullies at West Normanby over the short-term, nor were major reductions in plot-scale erosion, casting doubt that cattle exclusion alone will improve vegetation cover on exposed sodic sub-soils and stop existing severe gully erosion.

Overall, the year to year and seasonal variability in rainfall appears to be overriding any influences of grazing, especially during drought years with below normal rainfall (e.g., O'Reagain and Bushell 2011). Longer-term datasets (10-20 years) will allow for more robust statistical analysis of changes and the potential for cattle exclusion, natural resilience and recovery potential to have any influence on vegetation cover above or within gullies and gully erosion yields.

### 2.1.3 Aerial LiDAR Results: West Normanby

The aerial LiDAR change data for before (2009-2011) and after (2011-2015) cattle fencing at West Normanby are displayed in Figure B13 and Table B1. By just comparing the two periods (2009-2011; 2011-2015) at the West Normanby, there has been a reduction in specific sediment yield (t/ha/yr) at both control and treatment sites. This is possibly due to the reduced average annual rainfall during the second period (2011-2015) at Kings Plains and Springvale (Figure B9). When the entire LiDAR block (N4) along the West Normanby was analysed, there was a net increase in erosion rates (block ratio of 1.56) between the two periods (2009-2011; 2011-2015). These data suggest there is large variability site by site, compared to averages across multiple gullies over hundreds of hectares, and that LiDAR data error at locally specific sites could be significant compared to block averages.

Interestingly, the fenced area at West Normanby had a greater reduction in erosion rates than the control areas (Table B1). This could be due to real local reductions in major erosion due to grazing exclusion, or just the error artefacts of the coarse nature of the LiDAR data and inherent differences in chosen control and treatment sites. The lack of major vegetation improvements inside the fenced gully would suggest that significant erosion changes should not be expected. Longer-term monitoring and more detailed datasets of surficial erosion will be needed to better quantify potential changes to grazing exclusion.

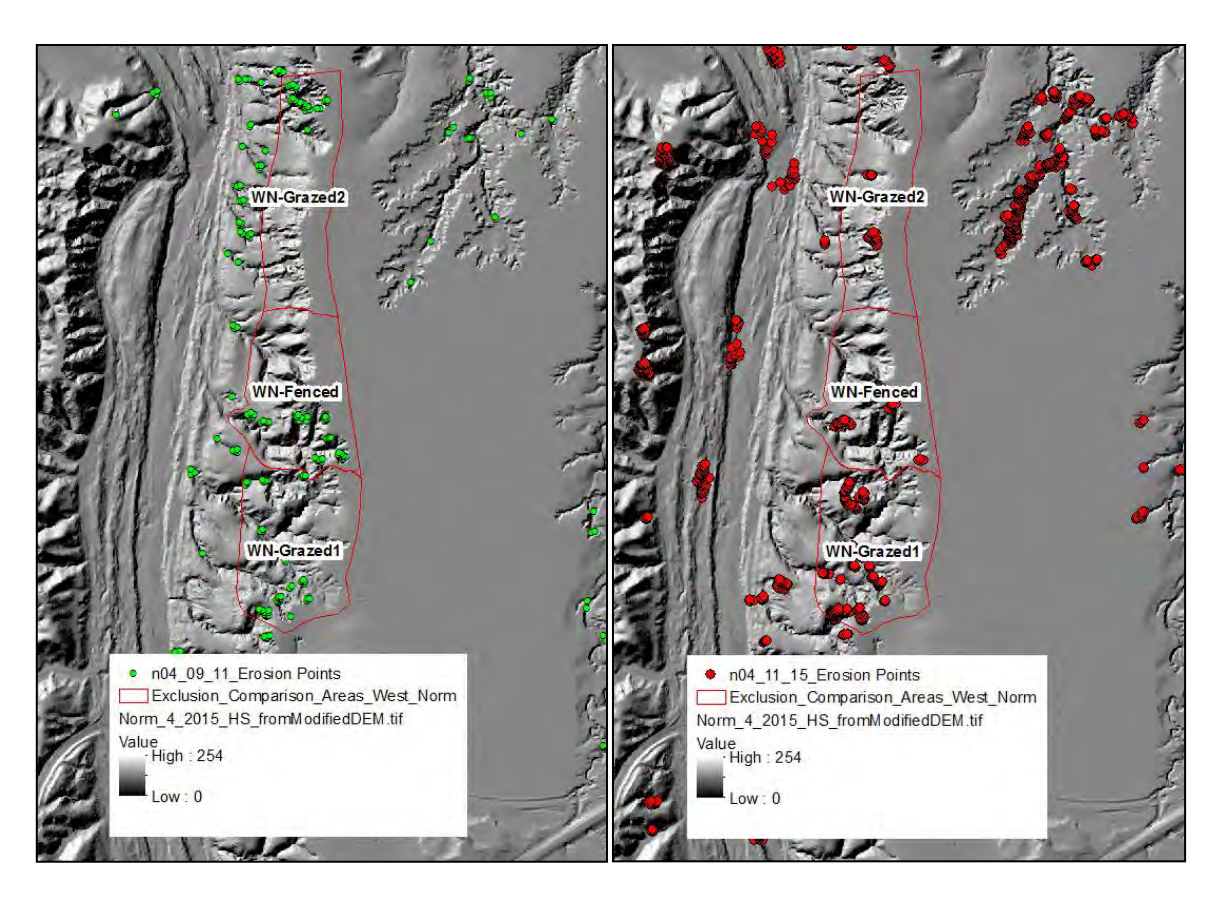


**Figure B13:** Cattle exclusion area and aerial LiDAR analysis areas (control-impact) along the West Normanby River in block N4 on Springvale Station. Also shown are the locations of the polygons within which erosion was detected by aerial LiDAR in the first period in green (2009-2011, LHS), and the second period in red (2011-2015, RHS).

**Table B1:** Erosion results from major large-scale LiDAR change at the West Normanby exclusion area.

		total yield m <sup>3</sup>		specific t/ha/yr	yield		
Area	area m²	2009-11	2011-15	2009-11	2011-15	Area change ratio	Block change ratio
WN4 grazed 1	35127	169.2	264.5	38.5	30.1	0.78	1.56
WN4 grazed 2	30836	135.9	200.5	35.3	26.0	0.74	1.56
WN4 Fenced	32040	238.7	138.2	59.6	17.3	0.29	1.56

## 2.2 Case Study 2: Crocodile Station Paddock Tributary to the Laura River

### 2.2.1 Methods: Crocodile Paddock

At Crocodile Station, a 5 ha area was fenced to exclude cattle in January 2012 in a large cleared paddock (Old Hay Paddock) affected by shallow alluvial gully erosion along a tributary to the Laura River (-15.710042°S; 144.679232°E; Figure B14). Vegetation and LiDAR erosion monitoring followed a similar BACI protocol and monitoring methods reviewed above. Ten (10) 4 m² plots were randomly established inside the fencing exclosure without grazing as a treatment, and six (6) plots were located immediately outside the exclosure with grazing in the open paddock as a control. Vegetation plot data were collected before (Nov 2011) and after fencing (2012, 2013, 2015), while LiDAR data were collected in 2009 and 2011, and then again in 2015.

This cleared paddock is prone to regrowth of *Melaleuca viridiflora* suckers. The landowner conducts biannual tractor 'chaining' of sapling regrowth in the paddock, which knocks the saplings down and rips a few out in extreme cases. This only minimally disturbs the grass understorey community present in open paddocks. This chaining has occurred twice during the study, in 2011 and 2015, both outside the cattle exclusion fence and unfortunately inside. Erosion/deposition data from permanent vegetation plot reference stakes were not available from these sites due to this chaining disturbance.

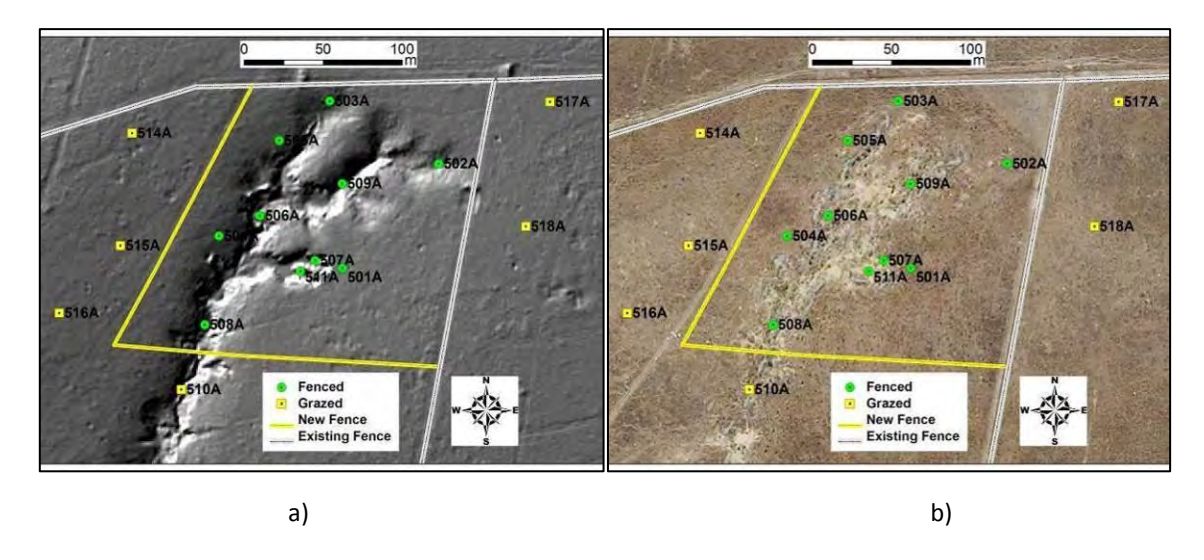


**Figure B14:** Maps of the cattle exclusion fence in the 'Old Hay Paddock' at Crocodile Station (-15.710042° S; 144.679232° E) with a) LiDAR hillshade background and b) aerial photograph background showing locations of vegetation monitoring points inside and outside the exclusion area.

### 2.2.2 Vegetation Plot Results: Crocodile Paddock

Preliminary results indicated that both % total organic cover and % cover of perennial grass changed seasonally, as expected, with greater cover after the wet season (Figure B15). Total % cover at fenced sites within the gully area increased over time between Nov-11 and Apr-13, while % total cover at grazed sites remained relatively constant (Figure B15a). Total cover was reduced at both fenced and grazed sites by Nov-15 due to drought and below average rainfall (Figure B9), but total cover inside the fenced area was generally greater than outside (Figure B15a).

Before the fence was installed, the % perennial grass cover was greater outside the proposed fence area than inside. Over time and after the fence was installed, this pattern shifted, with the median % perennial grass cover greater inside the fence than outside between Apr-12 and Nov-15 (Figure B15b). Increases in both grass and weed cover were quickly observed inside the fenced area between Nov-11 and Nov-12 (Figure B16ab), with less detectable changes outside (Figure B16cd). The drought and below average rainfall in 2015 dramatically reduced the perennial grass cover both inside and outside the fence (Figure B15). However, the grass cover inside the fenced area remained elevated compared to outside even in drought conditions (Figure B15b; Figure B17).

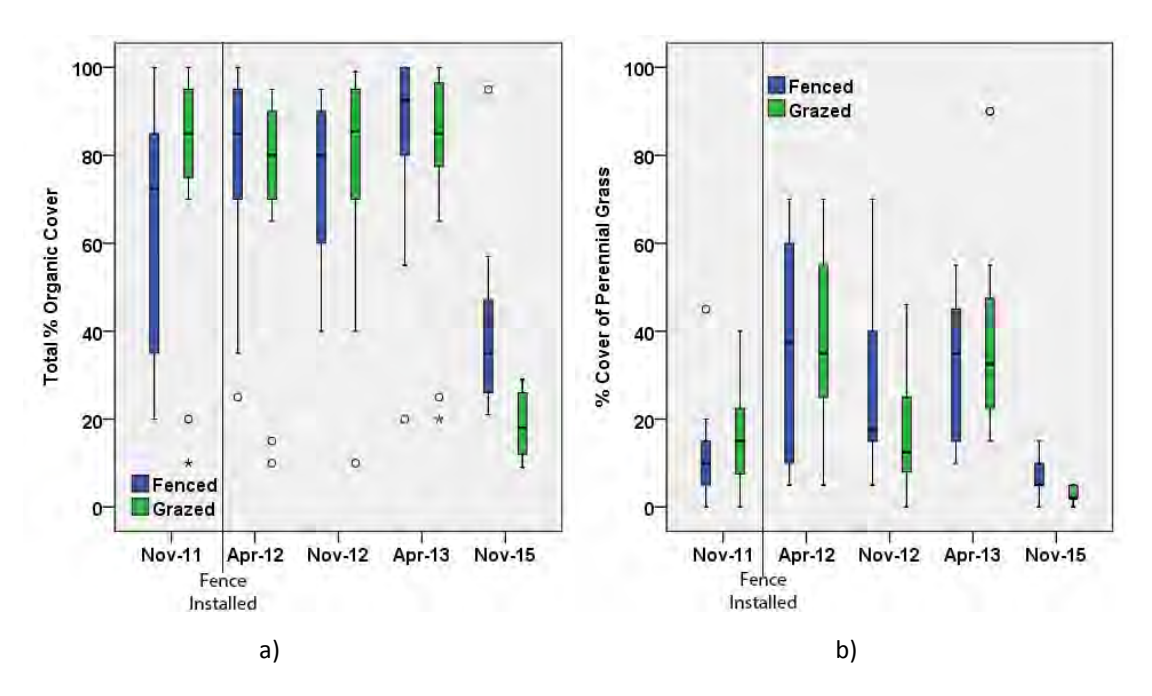


**Figure B15:** Changes in ground cover in cover inside and outside the Crocodile Station 'Old Hay Paddock' cattle exclusion site from 2011 to 2013 showing a) total % organic cover (grass, weeds, leaves, sticks, mulch) and b) % grass cover (standing perennial or annual grass).

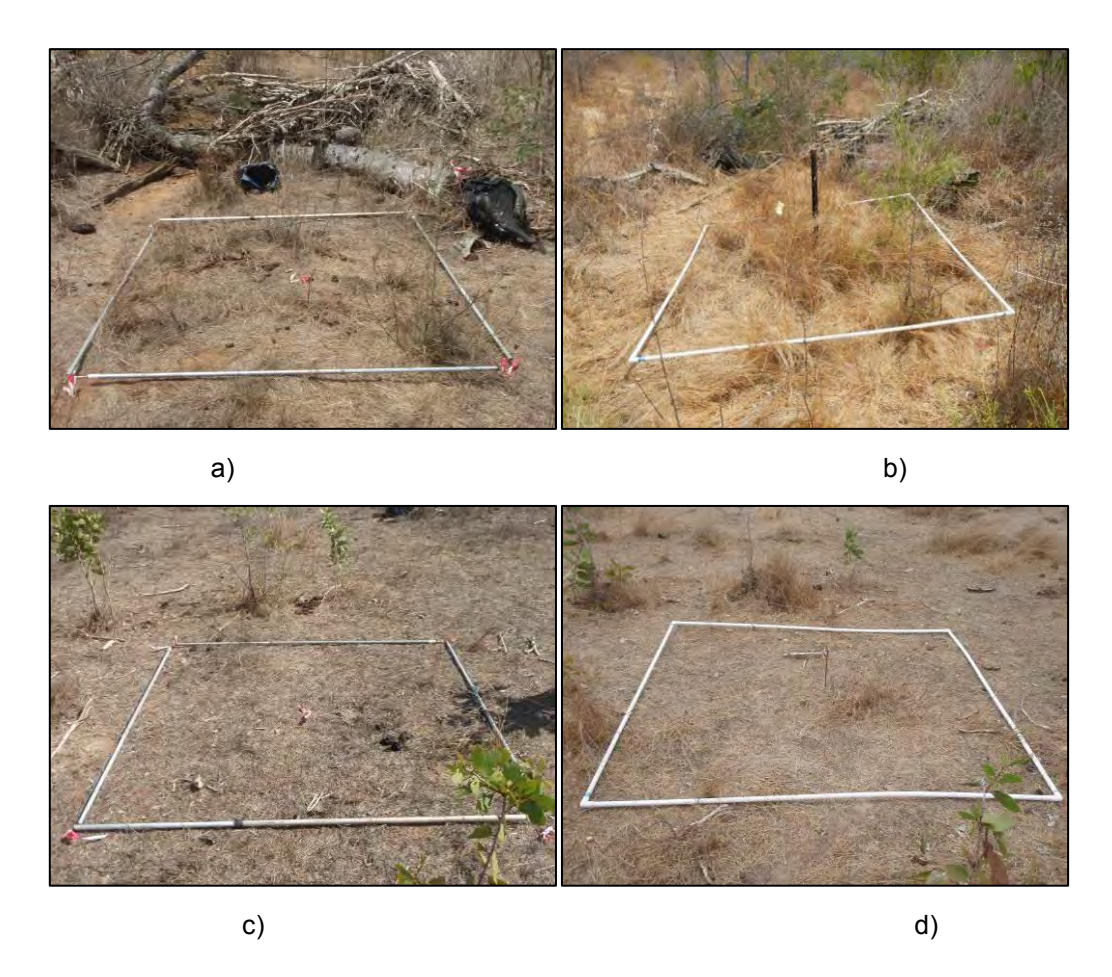


**Figure B16:** Changes in vegetation cover and biomass a) before fencing at Plot 508 gully bottom in Nov-2011, b) after fencing at Plot 508 gully bottom in Nov-2012, c) grazed control at Plot 515 hillslope in Nov-2011, d) grazed control Plot 515 hillslope in Nov-2012.



**Figure B17:** Grass and weed cover inside the cattle exclusion fence (left) and outside (right) in June 2015.

From these data it is evident that both grazing pressure and rainfall variability can have detectable influences on ground cover. However, extreme dry years can lead to a reduction in vegetation cover regardless of grazing pressure, but with greater vegetation cover and resilience during drought in ungrazed areas. Longer term datasets (10-20 years) on pasture condition will allow for the robust statistical analysis of the influence of management treatments (e.g., cattle fencing) on vegetation and erosion, from natural variability due to rainfall or other factors.

### 2.2.3 Aerial LiDAR Results: Crocodile Paddock

The aerial LiDAR data analysis of erosion change at the Old Hay Paddock on Crocodile Station was inconclusive. The erosion rates and scale of these shallower gullies were generally below the detection limit of aerial LiDAR (Figure B18). Thus, no further analysis was conducted. No large-scale erosion was detected in 2009-2011, and a few points of erosion were detected between 2011-2015 (Figure B18). However, field observations indicated that no large-scale erosion (scarp retreat and slumping) occurred between 2011-2015, and that this observed change was a result of vegetation error from tree thinning by the landowner, LiDAR error, or both. Field observations also indicated that surface soil erosion and rilling continued in and around some vegetation monitoring plots, while other plots experienced improved vegetation cover and reduced erosion. Longer-term monitoring and more detailed datasets of surficial erosion (i.e. terrestrial LiDAR) will be needed to better quantify potential changes to grazing exclusion.

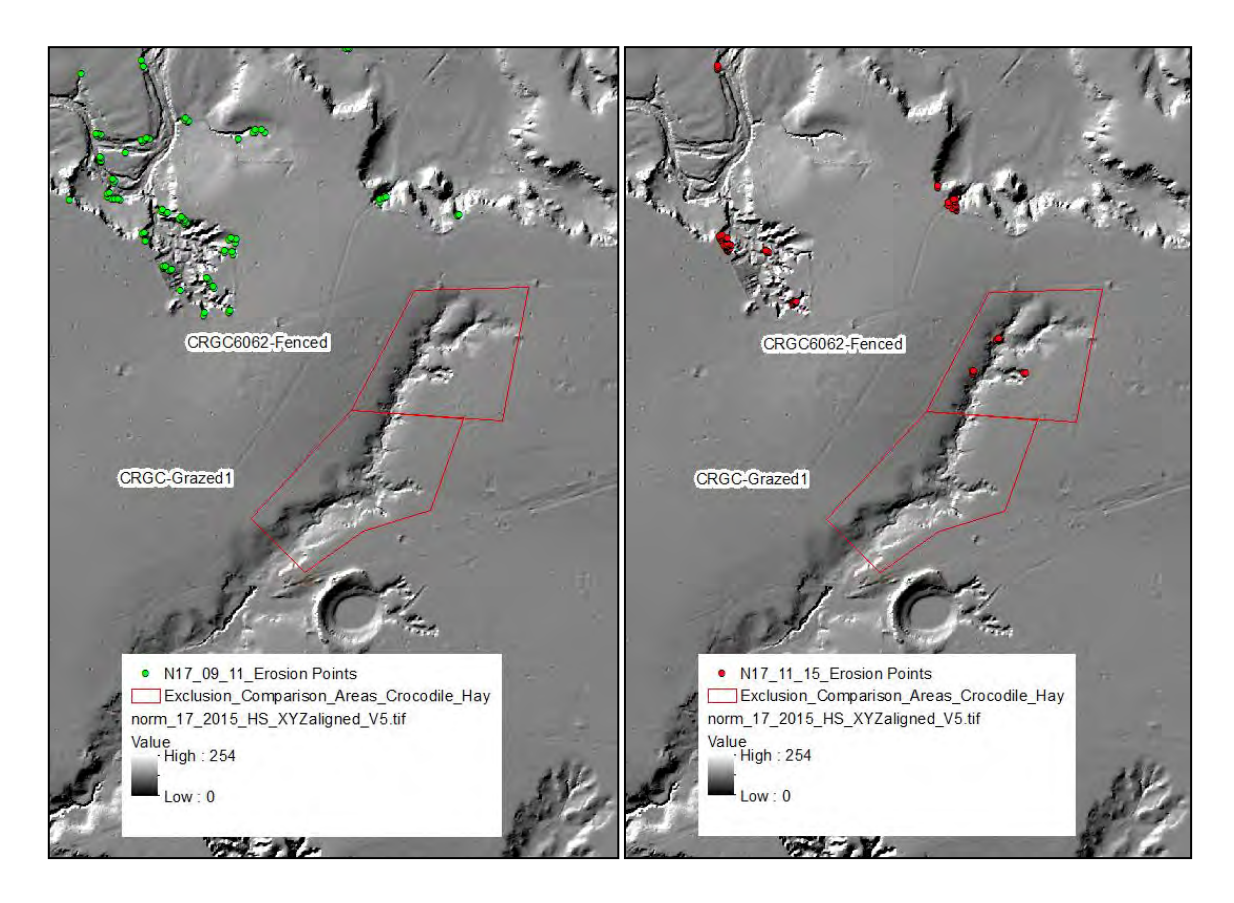


**Figure B18:** Cattle exclusion area and aerial LiDAR analysis areas (control-impact) at the Crocodile Hay Paddock in block N17 on Crocodile Station. Also shown are the locations of the polygons within which erosion was detected by aerial LiDAR in the first period in green (2009-2011, LHS), and the second period in red (2011-2015, RHS).

## 2.3 Case Study 3: Granite Normanby River

### 2.3.1 Methods: Granite Normanby (2012-2015)

On Springvale Station in the Granite Normanby catchment, a 2.3 ha gully complex (GNGC6) was fenced in January 2013 to exclude cattle from a distally draining gully flowing into a tributary of the Granite Normanby River (-15.896374°S; 144.994678°E; Figure B19). Vegetation plots were randomly located at ten (10) locations within the fenced exclusion area, as well as 10 around a control gully (GNGC9) outside the fenced area. Plot locations were stratified by geomorphic unit (uneroded high terrace, active gully slope, inactive gully hillslope) (Figure B19). Vegetation surveys were conducted before (Nov 2012) and after fencing (2013, 2015). Vegetation monitoring followed a similar BACI protocol and monitoring methods as reviewed above. One additional grazed gully (GNGC1) was monitored as a control for vegetation in 2012 and 2013, but was not resurveyed in 2015 due to funding constraints. At all sites, gully erosion was initially monitored ('before conditions') using repeat aerial LiDAR surveys, completed in 2009 and 2011, with repeat LiDAR surveys collected again in 2015 ('after conditions'). Point measurements of erosion/deposition at permanent vegetation plot reference stakes also provided an indication of finer-scale erosion.

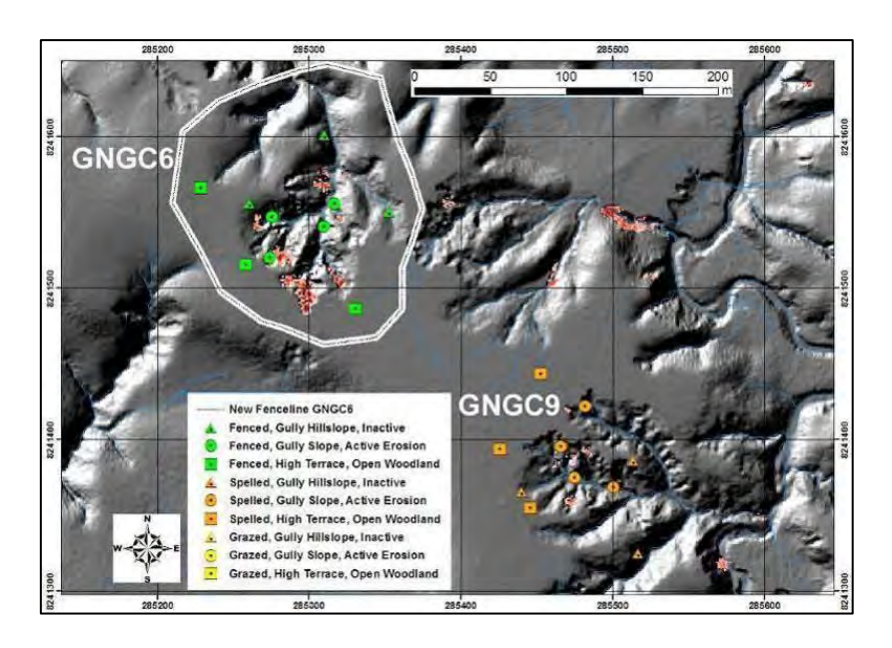


**Figure B19:** Hillshade LiDAR map of the cattle exclusion fence at GNGC6 (-15.896374°S; 144.994678°E) and neighbouring spelled GNGC9 on the Granite Normanby on Springvale Station. Note that red areas are zones of active gully erosion between 2009 and 2011 repeat LiDAR.

### 2.3.2 Results: Granite Normanby (2012-2015)

Preliminary results indicated that both % total organic cover and % cover of perennial grass changed seasonally, as expected, with greater cover after the wet season (Figure B20). Total % cover within the fenced cattle exclusion gully remained relative stable over time between Nov-12 and Nov-15, while % total cover at grazed sites declined over time (Figure B20a). Total cover was reduced at both fenced and grazed sites by Nov-15 due to drought and below average rainfall (Figure B9), but total cover inside the fenced area was generally greater than outside (Figure B15a).

Before the fence was installed, the % perennial grass cover was greater outside the proposed fence area than inside (Figure B20b). Over time and after the fence was installed, this pattern shifted, with the median % perennial grass cover greater inside the fence than outside in Apr-13 and Nov-15 (Figure B20b). Increases in grass cover were quickly observed inside the fenced area on high terrace flats between Nov-12 and Apr-13 (Figure B20b; Figure B22), whereas perennial grass cover actually decreased in the grazed area by Apr-13. By 2015, the drought and below average rainfall reduced the perennial grass cover and tussock counts overall, but the decline was greater in the grazed area than the fenced area (Figure B20b, B164c).

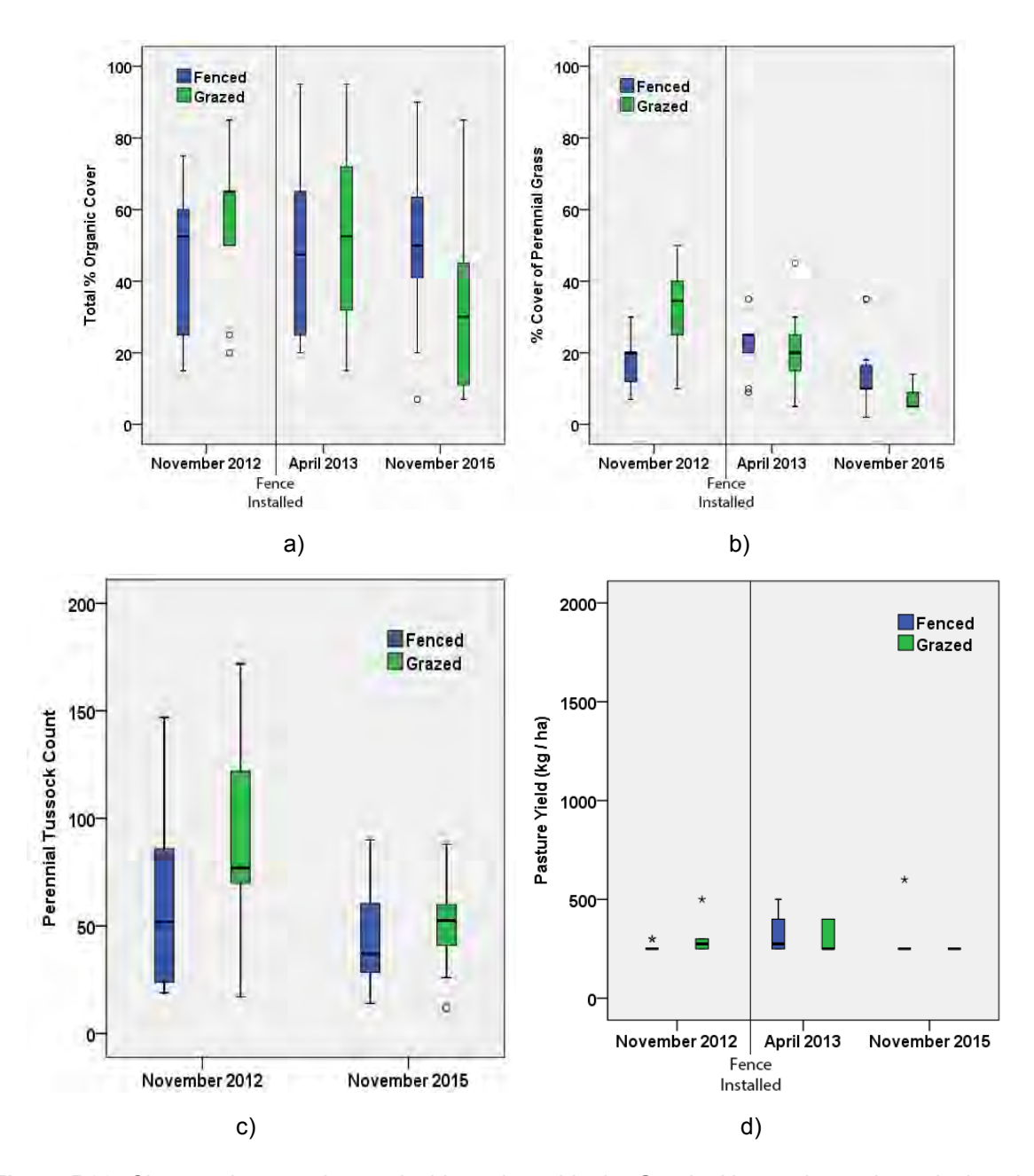


**Figure B20:** Changes in ground cover inside and outside the Granite Normanby cattle exclusion site from 2012 to 2015 showing a) total % organic cover (grass, weeds, leaves, sticks, mulch) b) % cover of perennial grass, c) perennial tussock count, and d) pasture yield (kg / ha).

When % cover of perennial grass is examined by different geomorphic units (high terrace, active gully slope, inactive gully hillslope), perennial grass cover in fenced geomorphic units increased from Nov-12 to Apr-13, and then slightly decreased in Nov-15 after a below average rainfall year (Figure B21a; Figure B9). In comparison, grazed geomorphic units saw more consistent declines in grass cover, especially for active and inactive gully slopes (Figure B21a). Tussock counts decreased for most geomorphic units from Nov-12 to Nov-15, except for fenced active gully slopes that has a slight increase (Figure B21b).

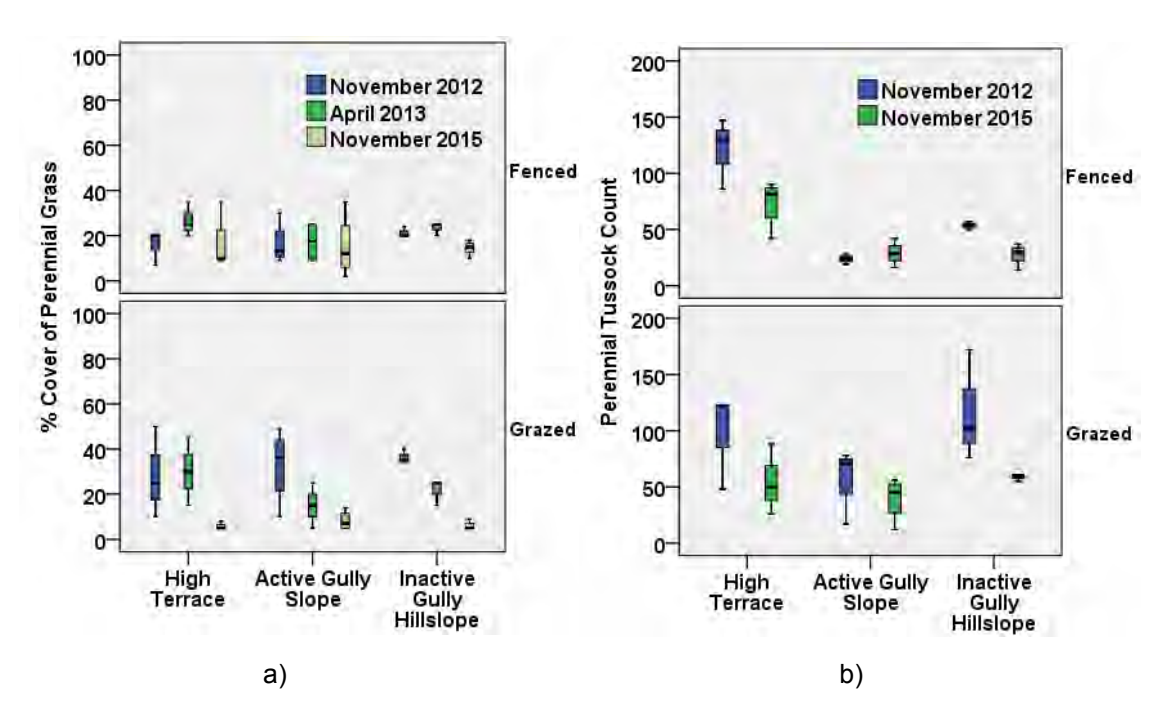


**Figure B21:** Changes in ground cover at different geomorphic units (terrace, gully, hillslope) inside and outside the Granite Normanby cattle exclusion site from 2012 to 2015 showing a) % cover of perennial grass and b) perennial grass tussock counts.



**Figure B22:** Differences in grass cover and biomass between the fenced gully (Left, GNGC6) and the grazed area (Right, GNGC9) on the high terrace of the Granite Normanby in a) April 2013 and b)

November 2015.

Point measurements of scour and fill (± 5mm) at permanent vegetation plot reference stakes between 2012 and 2015 indicated relatively consistent erosion/deposition distributions at fenced sites, and increased erosion at grazed sites (Figure B23). The increased erosion at grazed sites was the result of active surface erosion at two internal gully plots, with questionable influence from ongoing grazing activity on the terrace flat or internal gully.

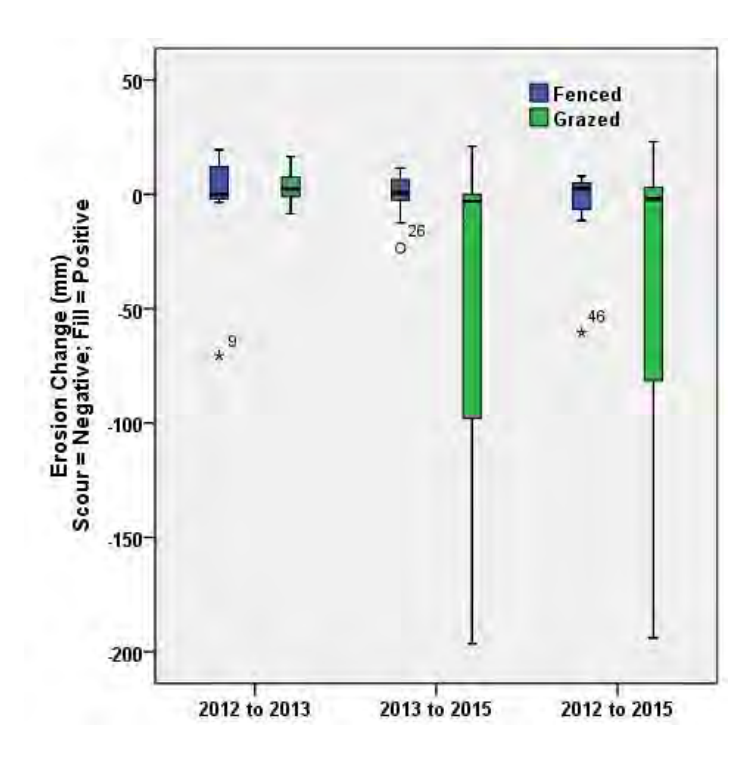


**Figure B23:** Measurement distributions of scour (negative) or fill (positive) at permanent vegetation plot reference stakes, accurate to 5mm, for fenced and grazed areas of the Granite Normanby gullies between 2012 and 2015.

From these vegetation plot data it is evident that both grazing pressure and rainfall variability can have major influences on ground and grass cover. In this case, grazing reduced total and grass cover on most geomorphic units, while cover within the fenced area remained more resilient to climate variability. Longer term datasets (10- 20 years) on pasture condition will allow for the robust statistical analysis of the influence of management treatments (e.g., cattle fencing) on vegetation and erosion, from natural variability due to rainfall or other factors.

### 2.3.3 Aerial LiDAR Results: Granite Normanby

The aerial LiDAR change data for before (2009-2011) and after (2011-2015) cattle fencing at Granite Normanby are displayed in Figure B24 and Table B2. By just comparing the two periods (2009-2011; 2011-2015) at the Granite Normanby, there has been a reduction in specific sediment yield (t/ha/yr) at both control and treatment sites, as well as the entire LiDAR block (N7). This is likely due to the reduced average annual rainfall during the second period (2011-2015) at Springvale (Figure B9).

Both the fenced (GNGC6) and unfenced (GNGC9) gullies on the east side of the Granite Normanby River had reduced erosion compared to the block average and the unfenced (GNGC1) gully on the west side of the river (Table B2). This could be due to real local reductions in large-scale erosion, or just the error artefacts of the coarse nature of the LiDAR data and inherent differences in chosen control and treatment sites. It is also important to note that the landowner was paid by Reef Rescue to spell (reduce) cattle numbers on the east side of the Granite Normanby (Abbey Lea Paddock) in 2013-2015 in and around

GNGC6 and GNGC9. However, this spelling effort was marginal and cattle continued to graze the area as indicated in Figure B22, Figure B22, and field observations. The lack of major vegetation improvements inside the fenced gully at GNGC6, compared to observed improvements on the high terrace of the gully catchment, would suggest that large-scale erosion changes should not be expected. Longer-term monitoring and more detailed datasets of surficial erosion will be needed to better quantify potential changes to grazing exclusion.

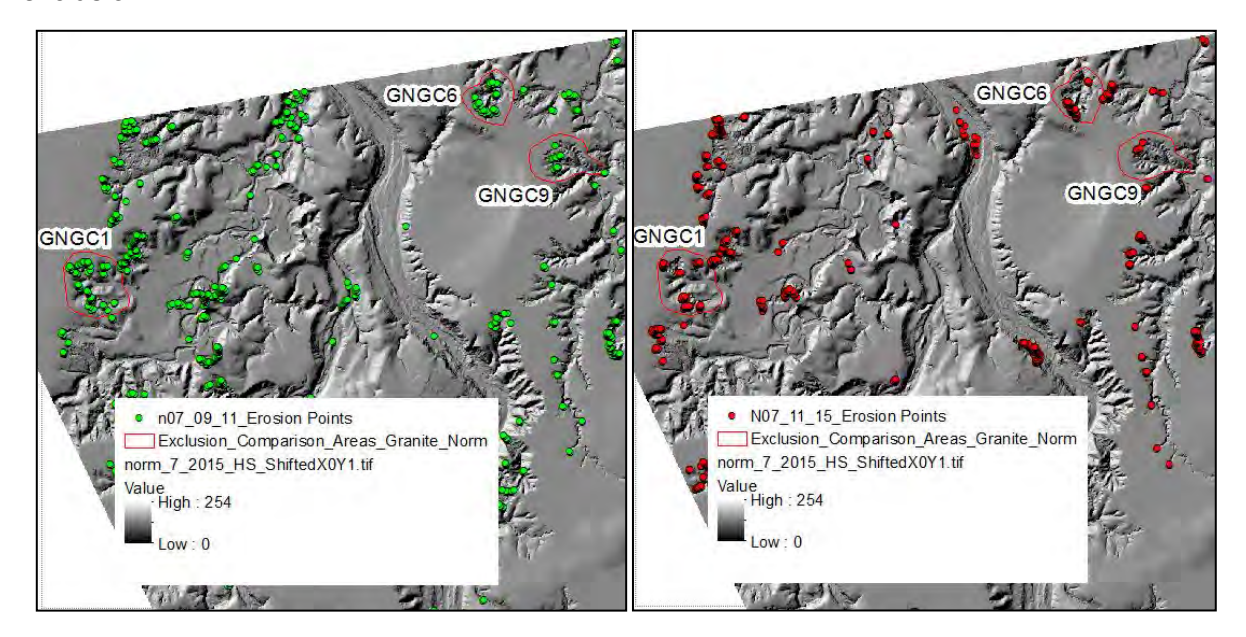


**Figure B24:** Cattle exclusion area and aerial LiDAR analysis areas (control-impact) along the Granite Normanby River in block N7 on Springvale Station. Also shown are the locations of the polygons within which erosion was detected by aerial LiDAR in the first period in green (2009-2011, LHS), and the second period in red (2011-2015, RHS).

**Table B2:** Erosion results from major large-scale LiDAR change at the Granite Normanby exclusion area.

		total yield m <sup>3</sup>			ic yield a/yr		
Summary	area m²	2009-11	2011-15	2009-11	2011-15	plot change ratio	block change ratio
GN7 grazed 1 (GNGC1)	21694	363.9	356.8	134.2	65.8	0.49	0.54
GN7 grazed 2 (GNGC9)	15545	61.5	32.8	31.6	8.4	0.27	0.54
GN7 Fenced (GNGC6)	12487	521.7	345.6	334.2	110.7	0.33	0.54

## 2.4 Case Study 4: Normanby River at Kings Plains

### 2.4.1 Methods: Normanby River at Kings Plains (2012-2015)

On Kings Plains station in 2012, the Reef Rescue cost-share program with a local landowner repaired a riparian fence line and 44ha cattle holding paddock at Mosquito Yards

(-15.598804°S; 144.916466°E; Figure B25). The objective was to reduced cattle grazing along the riparian riverside and the high bank of the Normanby River riddled with alluvial gullies, as well as provide infrastructure for improved cattle mustering and more permanent spelling of the lower river frontage paddocks of Kings Plains. Partial spelling of these paddocks initiated in 2010-2013, and has proceeded with a more serious rigour between 2013-2015, with the new landowner's goal to destock the most rugged and eroded north half of the property. Fencing of Mosquito Yards (Figure B25) has allowed for essentially a 'reverse' cattle exclusion experiment. The land outside the fences is spelled or only lightly grazed by stray cattle, while land inside the fence only occasionally has cattle grazing during active muster times. Overall by 2015, few cattle have been using the yard due to the gradual drawdown of the herd, so overall the experiments should document the improvements over the long-term at both sites as the area is destocked. Unfortunately, "before" conditions were not measured pre-2011, when cattle stocking rates would have been much higher in these areas. However, pre-2011 photos points from the station manager may be useful.

In November 2012, permanent vegetation plots were installed in and around one gully outside the fenced yard (spelled) and one gully inside the grazed Mosquito Yards (Figure B25) to assess any improvements in ground cover from increased cattle spelling between 2012 and 2015. Vegetation plots were randomly located at six (6) vegetation plots inside the fence, and 6 outside, and were stratified by geomorphic unit (uneroded high terrace, active gully slope, inactive gully hillslope) (Figure B25). Vegetation monitoring followed a similar BACI protocol and monitoring methods as reviewed above. Erosion 'before' conditions also were surveyed by repeat aerial LiDAR in 2009 and 2011, with repeat LiDAR surveys collected again in 2015 for comparison. Point measurements of erosion/deposition at permanent vegetation plot reference stakes also provided an indication of finer-scale erosion.

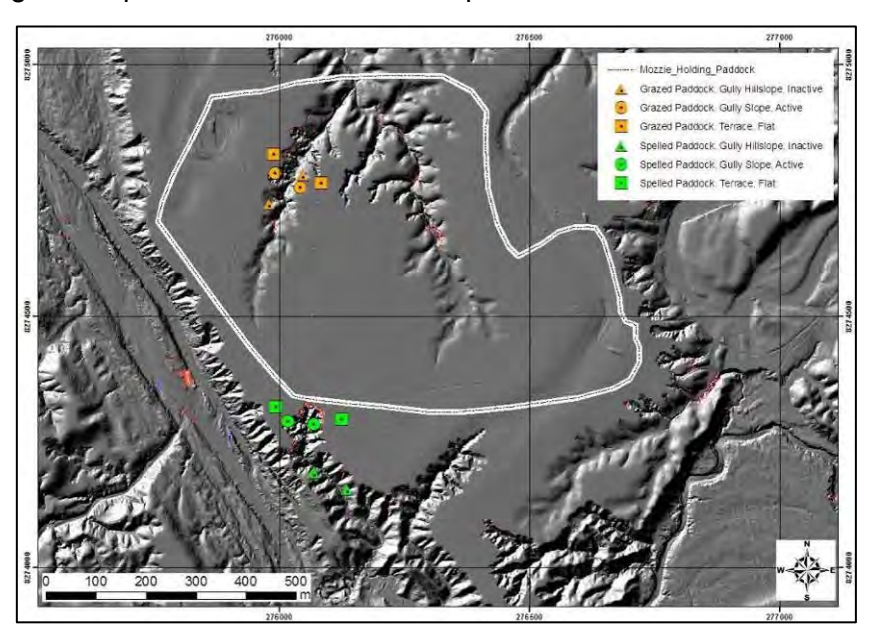


**Figure B25:** Hillshade LiDAR map of vegetation plot locations and the cattle holding paddock (Mosquito Yards) at Kings Plains, with modest cattle grazing inside the paddock and cattle spelling outside the paddock. Note that red areas are zones of active gully erosion between 2009 and 2011 repeat LiDAR.

### 2.4.2 Results: Normanby River at Kings Plains (2012-2015)

Preliminary results indicated that both % total organic cover and % cover of perennial grass changed seasonally, as expected, with greater cover after the wet season (Figure B26ab). Between Nov-12 and Nov-15, the total % cover decreased slightly in the fenced area (outside Mozzie Yard paddock) and remained relatively stable in the grazed area (inside Mozzie Yard paddock) (Figure B26a). The % perennial grass cover also decreased slightly in the fenced area and remained stable or increased in the grazed area (Figure B26b). Perennial grass tussock counts remained stable in the fenced area, and increased the range and declined slightly in the grazed area. Pasture yields declined slightly over time, but especially for grazed areas in Nov-15. Water Year 2012 was much wetter than WY 2013 or WY 2015 (Figure B9), which could have influence the slight reductions in pasture yield by WY 2015.

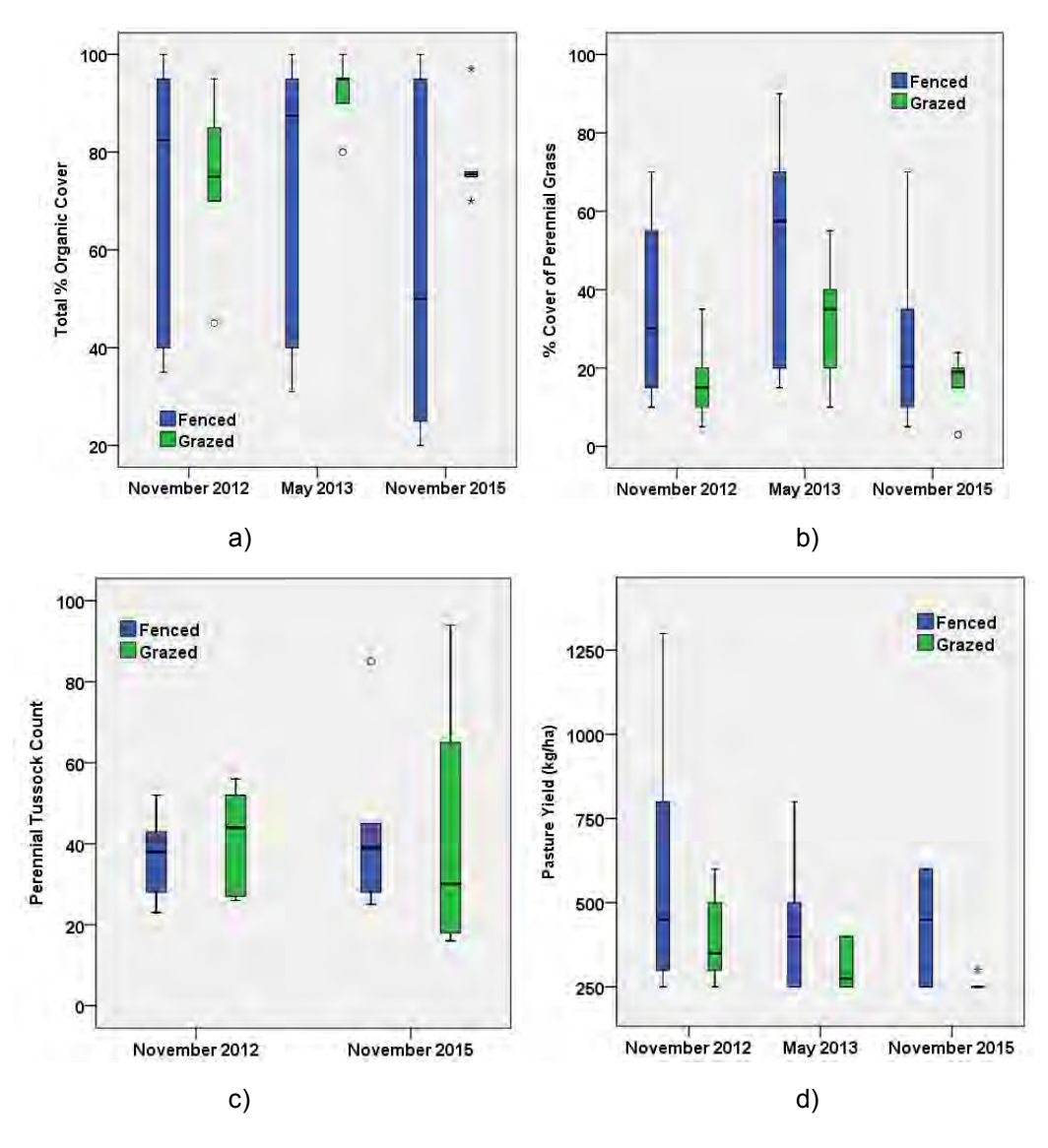


**Figure B26:** Changes in ground cover inside and outside the Kings Plains cattle exclusion area from 2012 to 2015 showing a) total % organic cover (grass, weeds, leaves, sticks, mulch) b) % cover of perennial grass, c) perennial tussock count, and d) pasture yield (kg / ha).

Since both the fenced and grazed gullies at Kings Plains had very low stocking rates toward complete destocking, and low sample sizes of vegetation plots, their data were grouped together to investigate difference in perennial grass cover by geomorphic units (high terrace, active gully slope, inactive gully hillslope). Perennial grass cover did not change much when comparing Nov-12 and Nov-15 data, with only a slight decrease in grass cover on inactive gully hillslopes. Perennial grass tussock counts also did not change much beyond increasing their range.

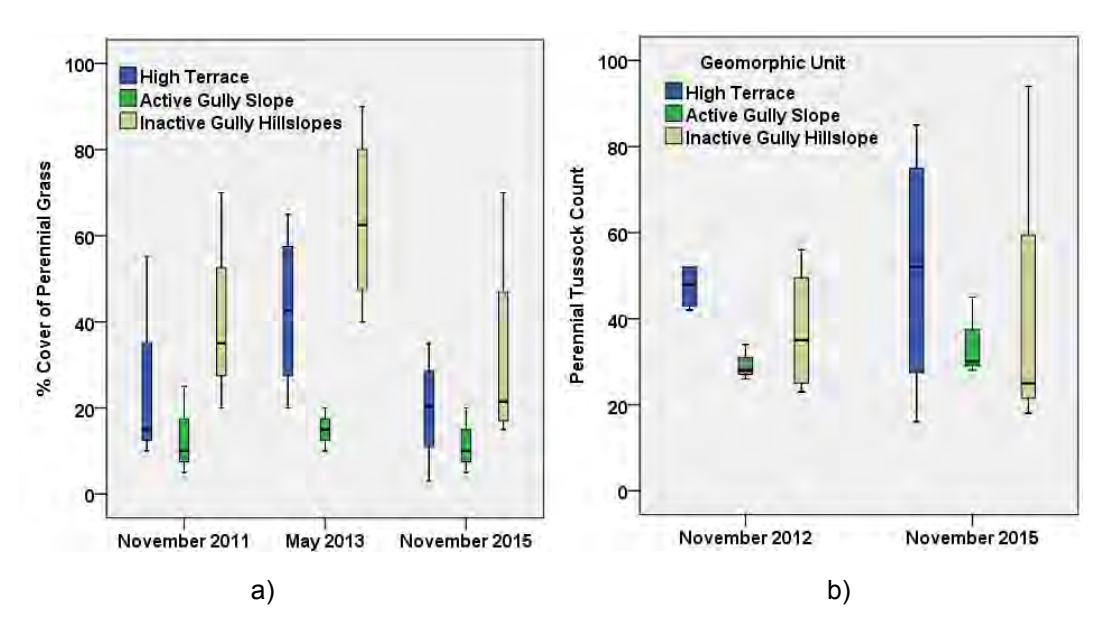


**Figure B27:** Changes in ground cover at different geomorphic units (terrace, gully, hillslope) inside and outside the Kings Plains cattle exclusion area from 2012 to 2015 showing a) % cover of perennial grass and b) perennial grass tussock counts.

Point measurements of scour and fill (± 5mm) at permanent vegetation plot reference stakes between 2012 and 2015 indicated that fill (deposition) dominated at fenced sites, while both depsoiton (scour) and erosion (fill) occurred at the grazed sites (Figure B28). The exact causes of this depsotion are unknown. The measurements are an average of both upslope and downslope sides of the stake (e.g., an average meniscus reading), and thus the stakes are not overly influenced by any minor uplslope deposition. Perennial grass cover and biomass was typically greater at the fenced sites, which could have influence some local deposition. The fenced area also has been spelled of cattle for much longer (since 2010) than the grazed site, and the build-up and recovery of some grass cover inside gullies could be influencing the results as several plot sites (see Figure B4). Longer-term data will be needed to understand future trends and influential factors.

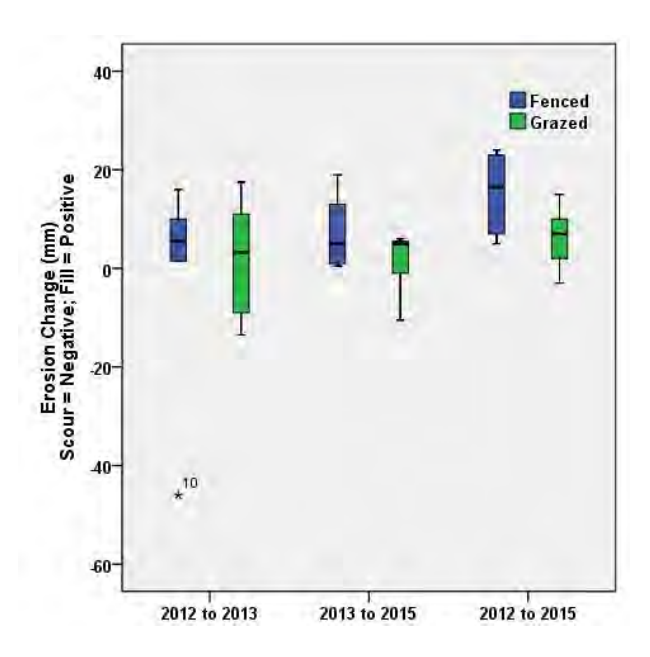


**Figure B28:** Measurement distributions of scour (negative) or fill (positive) at permanent vegetation plot reference stakes, accurate to 5mm, for fenced and grazed areas of the Kings Plains gullies between 2012 and 2015.

From these vegetation plot data at Kings Plains, it is evident that changes in very light grazing pressure and stocking rates did not have major influences on ground cover over the period studied (2012-2015). Under these low grazing situations, rainfall variability is more important than grazing pressure on influencing cover. Additional pre-2011 before data during periods of high stocking rates would have been needed to document the full changes from spelling and destocking, as indicated by anecdotal observations and photos from 2009-2010. Longer term datasets (10-20 years) on pasture condition will be needed to track any additional improvements to ground cover inside and around gullies from total destocking.

### 2.4.3 Aerial LiDAR Results: Kings Plains

The aerial LiDAR change data for before (2009-2011) and after (2011-2015) cattle fencing at Kings Plains Mozzie Yard paddock are displayed in Figure B29 and Table B3. By just comparing the two periods (2009-2011; 2011-2015) at Kings Plains, there has been a reduction in specific sediment yield (t/ha/yr) at treatment sites that are grazed, but mixed results of both increased and decreased erosion at sites with cattle excluded. The entire LiDAR block (N10) has had a slight increase in large-scale erosion (block ratio 1.09) between the two periods. Overall these data are inconclusive. The reduced erosion at some sites could be a result of reduced average annual rainfall during the second period (2011-2015) at Kings Plains (Figure B9), the longer second monitoring period that reduces average erosion rates per year, site-to-site variability in erosion rates and change detection, and/or actual changes due to treatment and cattle exclusion. The lack of major vegetation improvements inside and outside the fenced area, and strong influence of rainfall on vegetation cover, would suggest that large-scale erosion changes should not be expected. Longer-term monitoring and more detailed datasets of surficial erosion will be needed to better quantify potential changes to grazing exclusion.

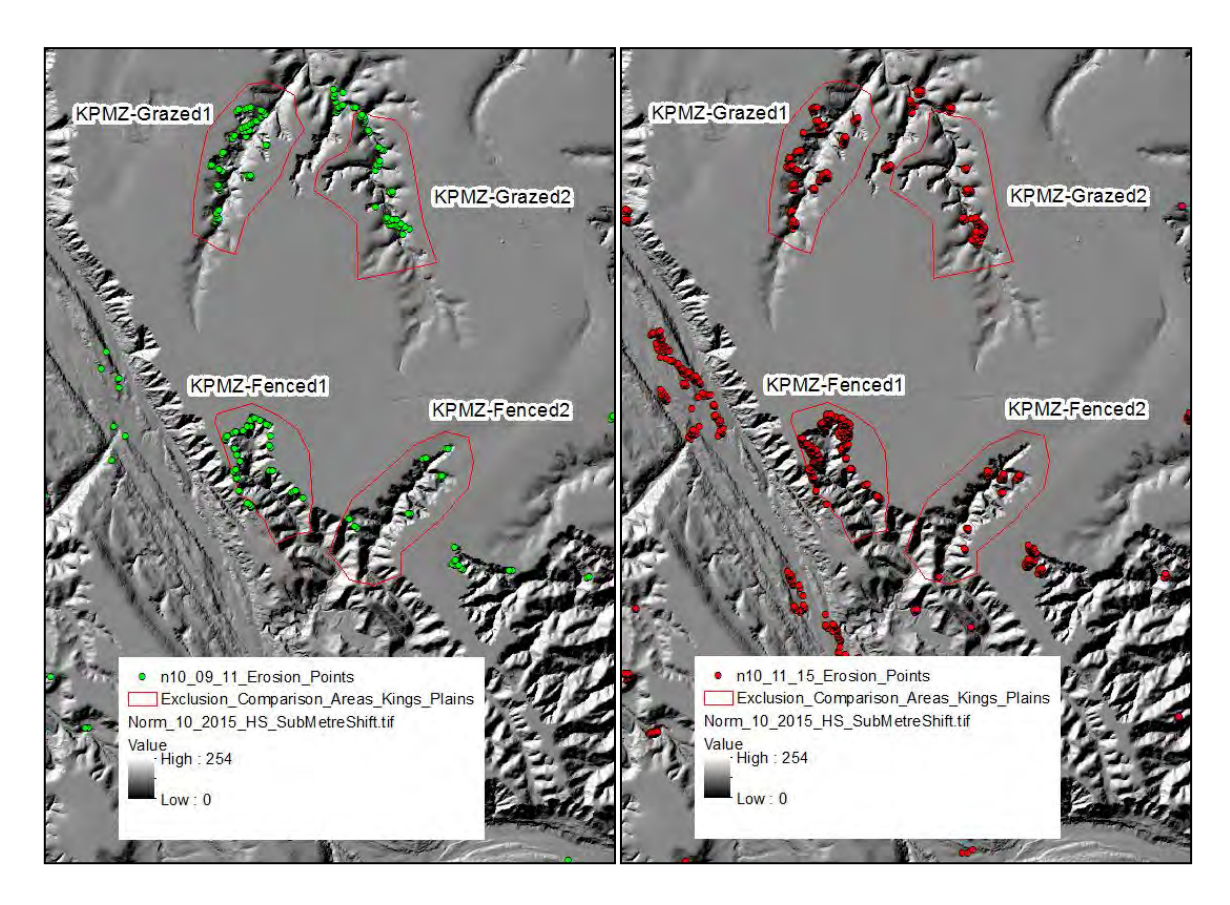


**Figure B29:** Cattle exclusion area and aerial LiDAR analysis areas (control-impact) at the Mosquito Yard site on Kings Plains Station in block N10. Also shown are the locations of the polygons within which erosion was detected by aerial LiDAR in the first period in green (2009-2011, LHS), and the second period in red (2011-2015, RHS). Note that the "Fenced" sites in this case are outside of the Mosquito yards.

**Table B3:** Erosion results from major large-scale LiDAR change at the Kings Plains exclusion area at Mosquito Yard.

		total yiel	d m³	specific t/ha/yr	yield		
Summary	area m²	2009-11	2011-15	2009-11	2011-15	plot change ratio	block change ratio
KPMZ grazed 1	27728	496.9	1265.5	143.4	182.6	1.27	1.09
KPMZ grazed 2	37030	85.6	106.3	18.5	11.5	0.62	1.09
KPMZ Fenced 1	35829	332.2	542.9	74.2	60.6	0.82	1.09
KPMZ Fenced 2	37030	602.4	499.0	130.1	53.9	0.41	1.09

#### 2.5 Analysis of Pooled Data from Aerial LiDAR

The pooled the LiDAR erosion data from three exclusion sites (West, Granite, Kings) were filtered for any erosion polygons less then  $10m^2$ , so that the data are not negatively skewed by a profusion of erosion in single/few cell polygons, given that erosion data at this scale is also less reliable than the larger areas. Thus, these data can only detect erosion deeper than 0.2m and greater than  $10m^2$  in area, which over this timescale tends to be large-scale scarp retreat and slumping in gullies, as well as secondary incision into the gully floor. These data do not include small-scale soil surface erosion or rilling from direct rainfall or overland flow, which is widespread inside or above the gullies and can be substantial sediment sources (e.g., Shellberg et al. 2013a).

To test the statistical significance of the average (mean) erosion response to cattle exclusion, we have pooled the LiDAR erosion data from three exclusion sites (West, Granite, Kings) to increase the sample size (n=3 plots; incorporating 35 erosion polygons > 10m<sup>2</sup> in grazed areas and 29 in fenced areas). This may have the effect of dampening (averaging) the analysis of any individual site response, but is useful to assess the overall regional response, and makes statistical analysis possible. We filtered any erosion polygons less then 10m<sup>2</sup> so that the data is not negatively skewed by a profusion of erosion in single/few cell polygons, given that erosion data at this scale is also less reliable than the larger areas and scale. These data are however, still included in the total erosion data for each of the plots. Thus, these data can only detect erosion deeper than 0.2m and greater than 10m<sup>2</sup> in area, which over this timescale tends to be large-scale scarp retreat and slumping in gullies, as well as secondary incision into the gully floor. These data do not include small-scale soil surface erosion or rilling from direct rainfall or overland flow, which is widespread inside or above the gullies and can be substantial sediment sources (e.g., Shellberg et al. 2013a). Erosion polygon data were then normalised for area and then two tailed t-test and Mann-Whitney test used to test the following hypotheses:

- 1. That there is no difference in large-scale gully erosion between the grazed and fenced areas between 2009 and 2011 (i.e. before data)
- 2. That there is no difference in large-scale gully erosion between the grazed and fenced areas between 2011 and 2015 (i.e. post treatment data)
- 3. That there was no difference in large-scale gully erosion between erosion rates in the fenced area for the two periods (i.e. 2009-2011 vs. 2011-2015)
- 4. That there was no difference in large-scale gully erosion between erosion rates in the grazed area for the two periods (i.e. 2009-2011 vs. 2011-2015)

The results of these tests on pooled data are shown in Table B4 and they indicate the following:

- i) That there was a significant difference in erosion detectable by aerial LiDAR between the fenced and grazed areas prior to the exclosures being established, with there being more erosion in the fenced areas than the unfenced at the start of the study (p=0.0026)
- ii) That there was a significant decline in erosion rates in the second period compared to the first period in both the fenced and grazed plots (p=0.0001)

- iii) That there was a significant difference in gully erosion detectable by aerial LiDAR between the pooled fenced and grazed areas 3-4 years after the establishment of the exclosures (p=0.007)
- iv) Small plot size and the relatively small erosion dataset (n=35 grazed; n=29 fenced erosion cells) and high standard deviations (26 to 36% of mean) affects the statistical power of these tests. More robust statistical analysis following BACI design utilizing higher resolution data from larger exclusion plots will be needed in the future.

**Table B4:** Two tailed t-test results for Normanby grazing exclosure trials

	Mean			Standard Dev			
		Grazed	Fenced	p-value	Grazed	Fenced	F-test p- value
	2011	6,519.88	8,362.05	0.0026	1,490.68	2,895.47	0.0006
	2015	3,815.74	4,257.66	0.1659	1,270.18	1,205.92	0.7975
p-value		0.0001	0.0001		0.08398677	0.0001	

These preliminary LiDAR results indicate there was a detectable response of large-scale deep gully erosion to cattle exclusion over the short-term at three exclusion sites (West, Granite, Kings Plains), although the erosion rates were more influenced by rainfall totals and inherent gully evolution, than the cattle exclusion. The results appear to be particularly influenced by the results from the Kings Plains site, which was the least well constrained of the three sites, in that grazing pressure was intermittent, and the exclusion not complete. The results provide some suggestion that exclusion is an important part of the solution to reducing sediment yields from these gullies, but when combined with other evidence from the broader analysis at the block scale and the finer resolution plot scale data, it suggests that on its own it will not be nearly enough to achieve the ambitious targets of a 50% reduction in sediment yields within a decade. No major changes to vegetation or surface erosion measured in the field at the plot scale were observed in the field inside these mature alluvial gullies after 4 years of cattle exclusion (see section above). However, these results might not be transferable to shallower alluvial gullies, gullies with larger uneroded catchment areas (>25% of total) where grazing is excluded, or gullies earlier in their evolutionary cycle. For example, at the shallow gullies at the Crocodile Old Hay Paddock, vegetation response to cattle exclusion appeared to be more successful, although the erosion response was largely below the LiDAR limit of detection.

Overall, aerial LiDAR is not sufficient in detail to detect soil surface erosion and rilling at the scale of the treatments and vegetation plots measurement points. The soil surface erosion response, currently below the aerial LiDAR detection limit, showed no major trends at the plot scale from grazing exclusion over 4 years, but did highlight the variability and magnitude of surface erosion and deposition within gullies that are common over large areas. Non-

headcut surface erosion in alluvial gullies can represent from 1 to 70% of measured sediment yield outputs at the event to annual scales (e.g., Shellberg et al., 2013a), and hence the sediment yields from these gullies could be significantly higher than reported here. The ratio of sediment load output from gully catchments derived from 1) deep gully erosion vs. 2) surface erosion, stripping, and rilling inside these large gully complexes is unknown.

Longer-term monitoring, sediment yield gauging at gully outlets, and more detailed datasets of surficial erosion (i.e. terrestrial LiDAR) inside alluvial gullies and in catchment areas above scarps, will be needed to better quantify potential sediment yield changes to grazing exclusion or other management intervention. Quantifying the detailed soil surface erosion response at a much finer resolution would require terrestrial LiDAR scanning at 5mm pixel resolution to detect changes over short periods. Furthermore it is likely to take a lot longer than the 4 years of this preliminary trial for the effects of grazing exclusion to show a measureable change in aerial LiDAR data. Hence in this case in the short-term, aerial LiDAR is probably not the right tool to be picking up detailed erosion change.

Recent management strategies proposed by government have placed significant hope in the role of grazing exclusion from gullied areas as a front line strategy for reducing sediment and nutrient yields from gullied areas. Grazing exclusion is a critical first step in any gully management strategy, by removing the chronic disturbance pressure and preventing new gullies from forming as a result of cattle pads, low ground cover, and increased water runoff. However, these initial results would tend to suggest that significant reductions in erosion rates from active alluvial gullies on timescales of 1-2 decades are going to require more intensive stabilization measures if we are to come close to meeting the ambitious 50% sediment yield reduction targets over a decade set by government.

As demonstrated elsewhere in this report (Appendix C), we now know that alluvial gullies are also significant sources of bioavailable nutrients. Hence, any future studies looking at the effect of grazing exclosures on catchment water quality, should also monitor the potential benefits of cattle exclusion on nutrient contributions from gullies. This is especially the case for surface erosion not detected by aerial LiDAR. It may be that the benefits to water quality from fairly subtle increases in vegetation cover and resistance that do not have a measurable impact on large-scale gully sediment production (i.e., scarps and slumps), do have an effect on nutrient retention on soil surfaces and deposits within the gully complex.

#### 3. DISCUSSION

# 3.1 Lessons from Preliminary Cattle Exclusion Trials on Vegetation Recovery

These preliminary data (2011-2015) from cattle exclusion trials in alluvial gullies in the Normanby catchment provide short-term insight into long-term recovery processes. The before-after, control-impact (BACI) study design was useful to begin understanding changes over time from land management actions (e.g., cattle fencing) and rainfall variability on plot-scale vegetation. The chosen vegetation metrics and methods are able to detect basic changes in pasture condition over short-time periods, which evident on high terrace pastures that drain toward gully scarps, and some inactive gully slopes, but very minimal inside deeply eroded gully complexes. On high terrace surfaces, pasture condition and ground cover responded fairly quickly (within one year) to cattle fencing on terrace slopes that drain toward alluvial gully heads.

This was especially evident in areas that had moderate to high cattle stocking rates (Crocodile, Granite Normanby, West Normanby), compared to areas with low stocking rates (Kings Plains). These data are encouraging, as they indicate the potential for partial vegetative recovery of ground cover and perennial grass yield, despite the ongoing issue of weed competition. Overall, vegetation cover on these high terrace pastures can respond fairly quickly to management intervention within a few years ('rubber band model' of Sarr 2002), but are still subject to climate variability.

In theory, the increased ground cover and perennial grass on high terrace surfaces could lead toward hydrological recovery (McIvor et al. 1995; Roth 2004) of these disturbed soils on terrace flats, by promoting water infiltration, increasing roughness and resistance to overland flow, and decreasing water runoff during rainfall events. This is a very important component (#1 above) to gully rehabilitation: managing water runoff from slopes above gullies. Despite their flat appearance, alluvial terraces can pour water runoff into gully heads during tropical rainfall as commonly observed in the field, with vegetation cover acting as a key mitigating factor to erosion resistance and to some degree water yield during moderate events (Shellberg and Brooks 2013). In a 7.8 ha alluvial gully with a 33ha catchment area, Shellberg et al. (2013b) measured reduced water runoff coefficients in the latter half of the wet season after dense grass grew on the un-eroded floodplain, and these runoff differences were correlated to reduced gully scarp retreat rates that were a combined result of floodplain water runoff and direct rainfall. In contrast, research by Bartley et al. (2010a; 2010b; 2014) on colluvial hillslopes catchments indicated that there was minimal hydrological response to increased end-of-dry season cover from 35% to 80% over a 10 year period, with only lower runoff coefficients for the first event in each wet season, but not overall annual runoff coefficients. No reductions in gully erosion rates were detected from improved grazing management, but full cattle exclusion was not trialled which might be needed for major hydrological improvement in some soil types (Roth 2004).

Furthermore, as the age of alluvial gullies increases and headscarps retreat toward the catchment divide of alluvial ridges, the upslope uneroded catchment area decreases and ongoing erosion becomes dominated by direct rainfall in the alluvial gully. In the three mature

alluvial gully catchments studied here, the upslope catchment area was <25% of the total, which indicates that the surrounding uneroded catchment will have diminishing influences on the gully itself. In young gully catchments with a significant catchment area beyond the gully headscarp, the evidence of a significant hydrologic response associated with pasture recovery remains limited (Shellberg et al. 2013b; Bartley 2014). Therefore, more hydrological research will be needed to test any responses to pasture recovery on the hydrological drivers of gully erosion, to see if significant water runoff and erosion reductions can be made in the next 10-20 years.

On active and inactive gully slopes, the pasture condition and ground cover in this study responded not at all, or much more slowly, compared to high terraces between 2011-2015. In the shallowest and least active alluvial gullies (Crocodile), vegetation cover on gully bottoms and inactive slopes responded quickly (within one year) to cattle exclusion and remained elevated compared to control sites even during drought periods ('rubber band model' of Sarr 2002). In contrast on severely scalded sub-soils in shallow gullies, or deeply eroded gully scarps in well-developed active gullies, vegetation cover response was minimal or negligible in both grazed and ungrazed areas. This is to be expected from both the harsh nature of these exposed sodic sub-soils to vegetation colonization, their unstable erosion potential, and the lack of safe access to some of these areas by grazing cattle. Some of these actively eroding sub-soils might slowly respond to cattle exclusion and vegetation recovery over the long-term (10-20 years) as seen at a few plots ('the broken leg model' of Sarr 2002). While many other extremely eroded gully scarps might not ever respond to cattle exclusion and vegetation recovery ('the humpty dumpty model' of Sarr 2002). Unfortunately, it is these exposed bare sodic soils that are likely to be disproportionately contributing to the surface erosion contributions from these alluvial gullies.

In these extremely eroded situations in well-developed gullies, the full process of gully channel evolution and headcut retreat to a stable equilibrium slope and longitudinal profile will be needed for vegetation to be able to progressively colonize lower slopes and channel deposits as headcuts retreat upslope. Shellberg et al. (2016) estimated that this slope evolution process could take 100 to 1000 years once gullies have initiated, depending on the stage of evolution and rate of erosion. In some cases, there may be ways to accelerate this vegetative recovery process by working with the natural tendencies of channel evolution (Figure B30; Brookes and Shields 1996; Ebersole et al. 1997; Thexton 1999; Callahan 2001; Simon et al. 2007), as indicated by space-for-time comparison of channel evolution and vegetation colonization in alluvial gullies in the adjacent Mitchell catchment (Shellberg 2011; Shellberg et al. 2016).

Climatic variability, annual rainfall, and seasonal rainfall had a strong influence on ground cover and pasture yield data between 2011 and 2015. This was especially true during 2015 which had below average rainfall across most study sites (Figure B9). During these very dry years, rainfall appears to override any influence of grazing pressure, with reduced ground cover in both fenced and grazed areas. These influences of climatic variability have been recorded elsewhere in the savannah and arid rangelands of Queensland (O'Reagain and Bushell 2011), and can exacerbate the erosional impacts of cattle that were not destocked from sensitive areas during long dry years (McKeon et al. 2004; Stafford Smith et al. 2007). In this study, vegetation cover inside fenced areas was more resilient to climate variability than outside grazed areas, especially at the Granite Normanby and Crocodile sites. Both grazing management and gully rehabilitation projects need to take into account this climate

variability, and the resilience and ability to maintain vegetative cover on harsh soils in dry years.

A final complicating factor on the results presented here is the potential impact of marsupial grazing (wallabies) on perennial grass recovery inside gullies. While not monitored quantitatively, it was observed that wallabies tended to concentrate feeding and sleeping activities inside large gully complexes, especially at the West Normanby site. These fenced gully areas have remnant native perennial grasses (e.g., Kangaroo grass) on many inactive gully slopes, which are preferentially grazed by wallabies. These alluvial gully complexes have plenty of shady hiding areas in their lower reaches, and have river water nearby. Dingos and pigs are actively poisoned on these properties with 1080 bait, which could increase wallaby populations. Therefore some of the vegetation results of minimal vegetation improvement inside fenced gully areas could be influenced by wallabies, which deserves future research attention. Reduced 1080 baiting of dingos one some conservation minded properties could help keep wallabies on the move and under control.

Overall, longer term datasets (10-20 years) will be needed to understand the dynamics of vegetation recovery, resilience, and erosion response in alluvial gully catchments. Additional data following these metrics and new additional ones will allow for more robust statistical analysis of trends through time. This will be essential to tease apart the influences of cattle exclusion, climate variability, weed competition, fire, and marsupial grazing on natural resilience, vegetative recovery potential, and soil and gully erosion within alluvial gully catchments.

# 3.2 Detecting Short-term Erosion Management Response in Alluvial Gullies using Aerial LiDAR

The chosen erosion metrics and methods using aerial LiDAR were only able to detect largescale changes in gully scarp failure, which were not related to cattle exclusion in the shortterm and more influenced by rainfall totals and inherent gully evolution (i.e. the primary drivers of gully erosion on this landscape). This is to be expected for three well-developed deep alluvial gullies with fully exposed sodic sub-soils, where direct rainfall is the major driving force, in addition to overland flow feeding the gullies from <25% of the total catchment area. Short-term passive management intervention (cattle exclusion alone over 4 years) would not be expected to make a huge difference to vegetation resistance in these deep old gullies. This might not be the case for less active shallower alluvial gullies, gullies with larger uneroded catchment areas (>25% of total) where grazing is excluded, or gullies earlier in their evolutionary cycle in riparian zones. For example, at the shallow gullies at the Crocodile Old Hay Paddock, vegetation response to cattle exclusion appeared to be more successful on inactive gully slopes, gully bottoms (inset floodplains), and slightly scalded soil surfaces, but not on deeply exposed sodic sub-soils. Overall, since alluvial gullies are major sources of sediment and nutrients, and government policy is directing much rehabilitation efforts into riparian fencing programs, expectations for what is likely to be achieved in terms of water quality improvements to the GBR over the next 10 - 20 years may need to be significantly tempered and validated with improved empirical field data from a variety of riparian zones with and without major gullies.

Aerial LiDAR is not sufficient in detail to detect soil surface erosion and rilling at the scale of the treatments and vegetation plots measurement points. Non-headcut surface erosion in alluvial gullies can represent up to 70% of measured sediment yield outputs at the event to annual scales (e.g., Shellberg et al. 2013a). Plot measurements of scour and fill highlight the variability and magnitude of surface erosion and deposition within gullies that are common over large areas. Hence, the data presented here are likely to significantly underestimate the actual sediment yields from the gullies in the study area. Longer-term monitoring, sediment yield gauging at gully outlets, and more detailed datasets of surficial erosion (i.e. terrestrial LiDAR) inside alluvial gullies and in catchment areas above scarps, will be needed to better quantify potential sediment yield changes to grazing exclusion or other management intervention. Quantifying the detailed soil surface erosion response at a much finer resolution would require terrestrial LiDAR scanning at 5mm pixel resolution to detect changes over short periods. Furthermore it is likely to take a lot longer than the 4 years of this preliminary trial for the effects of grazing exclusion to show a measureable change in aerial LiDAR data. Hence in this case in the short-term, aerial LiDAR is probably not the right tool to be picking up detailed erosion change.

If grazing exclusion from river frontage and riparian areas alone was to be a strategy that could significantly reduce existing alluvial gully erosion and improve GBR water quality within practical management timeframes to meet load reduction goals (10-20 years or the Reef 2050 plan), we would hope to be detecting significant changes to vegetation and erosion even after a few years. Reducing sediment and nutrient pollutants sourced from these alluvial gullies is essential to build resilience in order to adapt to climate change induced impacts on the northern GBR. However, we are not detecting short-term changes in major erosion from passive cattle exclusion, notwithstanding several below average rainfall years and measurement scale detection issues. Therefore, a holistic catchment-scale approach will be needed towards rehabilitation and erosion reduction that combines intensive gully rehabilitation measures, proactive vegetation planting, passive vegetation recovery potential, and prevention of new gully erosion initiation or chronic land use disturbance (Shellberg and Brooks 2013).

# 3.3 Supporting Research on Potential Vegetation Recovery in Gullied Areas

Once gully erosion has initiated, gullies typically erode along an evolutionary cycle until an equilibrium slope and form is reached (Figure B30; Schumm and Hadley 1957; Schumm 1973; Graf 1977; 1979; Rutherfurd et al. 1997; Brooks et al. 2009; Shellberg 2011; Shellberg et al. 2016). Vegetation can play an important mitigating role in reducing erosion, trapping transported sediment, and stabilizing gully slopes in a negative feedback cycle. Vegetation is an integral part of most channel evolution processes (Simon and Hupp 1992; Hupp 1992), including gully evolution (e.g., Figure B30; Gellis et al. 1995; 2001). Increasing vegetation with gully channels and networks can occur through removing or changing chronic disturbances inhibiting recovery (e.g., grazing, fire or clearing) and thus promoting natural recovery, or by direct planting of vegetation within or around gully networks (Shellberg and Brooks 2013).

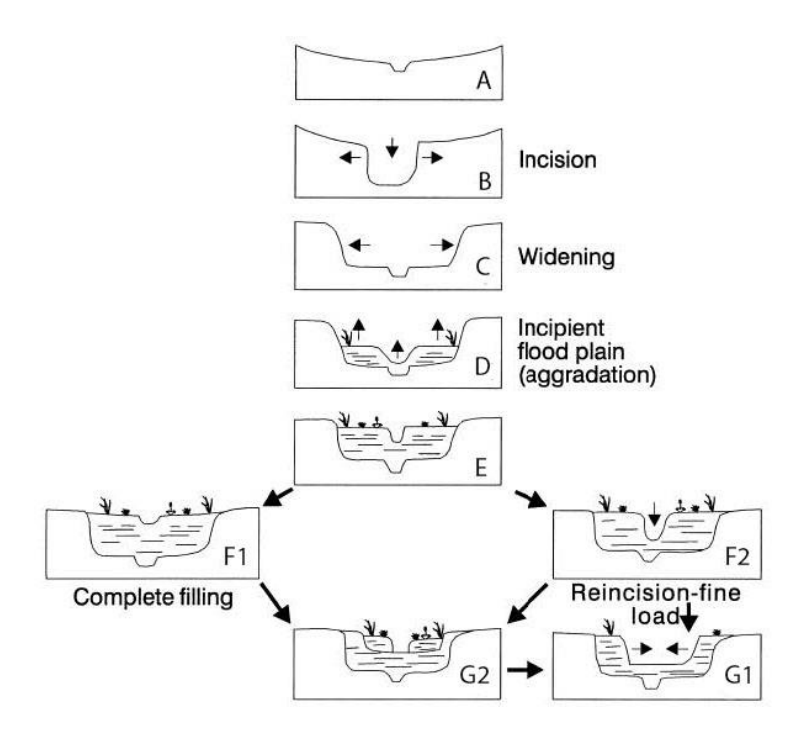


**Figure B30:** Stages of gully channel evolution applicable to valley bottom gullies or arroyos (after Gellis et al. 1995; 2001). This general gully evolution model is only applicable to some alluvial gullies in the Normanby and Mitchell catchments, with many gullies being trapped in the incision, headward retreat, and widening stages for long period of time (Stages B and C), after small initial cycles of incision, aggradation, and re-incision following initial disturbance and gully initiation (Shellberg et al. 2016). Most alluvial gullies will not fill back in with sediment due to permanent degradation.

Recent gully erosion studies have documented the dominant role of recolonizing or planting vegetation (grass, shrubs, trees) in stabilizing gully floors and channels, increasing sediment deposition and promoting channel aggradation, reducing downstream sediment yields, and driving positive feedback loops that promote landscape recovery (Vanacker et al. 2007; Molina et al. 2009; Reubens et al. 2008; Reubens et al. 2009; Sandercock and Hooke 2011). Colonizing plants with specific anchoring traits on badland slopes can be effective at increasing soil cohesion and resistance to erosion (Burylo et al. 2009). The destocking of cattle has been shown to result in the dramatic recovery of savanna vegetation within several seasons in India rangelands (Hudson 1987), including directly within gullies or ravines where stock have been excluded (Haigh 1984; 1998; Raizada et al. 2005).

In Queensland's tropical rangelands, vegetation cover will most typically improve if cattle are excluded or dramatically reduced from a hillslope area or paddock (McIvor et al. 1995; Scanlan et al. 1996; Roth 2004; O'Reagain et al. 2005; Bartley et al. 2010a; 2010b; O'Reagain and Bushell 2011; Silburn et al. 2011). However, the full exclusion of stock from gullied and scalded areas may or may not by itself result in vegetative or hydrological recovery over the short or long-term (Silcock and Beale 1986 cited in Bartley et al. 2010b, Bartley et al. 2014), unless accompanied by other rehabilitation measures. This is especially true for gully erosion areas and scalded soils were topsoils have been lost and sodic subsoils have been exposed (Pressland et al. 1988).

In northern Queensland, Bartley (2010a; 2010b) documented that scalded soil areas immediately above gullies and on gully slopes did not respond to short-term improved Grazing Land Management (GLM), despite modest reductions to runoff from hillslopes above. However, long-term full cattle exclusion from hillslopes and gullies was not trialled in these studies. Long-term cattle exclusion experiments have significantly reduced soil and gully erosion on the extremely degraded "Springvale Station" in the Fitzroy River catchment (e.g., Ciesiolka 1987; Silburn et al. 2011) suggesting that long time periods may be needed for soil and vegetation recovery. For alluvial gullies in the Mitchell catchment, Shellberg (2011) documented both grass and Eucalyptus tree colonization onto gully inset-floodplains following gully scarp retreat, indicating the natural recovery potential over 10-50 years.

#### 3.4 Proactive Vegetation Planting and Intensive Gully Rehabilitation

Proactive vegetation planting and intensive bioengineering intervention inside gullies will be needed for gully rehabilitation in appropriate locations and stages of channel evolution (Shellberg and Brooks 2013). The most appropriate locations for major intervention are young gullies at early stages of gully evolution (Figure B30; Figure B31; Gellis et al. 1995; 2001) and other areas of strategic concern (roads, fencelines and infrastructure) as a preemptive measure to prevent major future erosion. For hillslope gullies, Bartley (2010b) recommended full cattle exclusion, proactive vegetation planting and more intensive mechanical intervention to rehabilitate scalded foot slopes and gullies. However, it was noted that any intervention in these areas needed a cautious approach, since they were major sources of sediment and erosion could be exacerbated by some interventions.

Shellberg and Brooks (2013) trialled a full range of alluvial gully rehabilitation measures, including diversion of hillslope water, grade control structures, active grass seeding and hydromulching, full gully re-shaping and intensive slope stabilisation. Many successes were achieved, along with many pitfalls, outright failures, and cautionary principles learned from locally accelerated erosion from construction works. Generally it was extremely difficult to plant and establish grass or any vegetation in sodic soils of alluvial gullies (Shellberg and Brooks 2013), similar to findings of Coventry (2004). Revegetation success increased with the application of compost or fertilizer and gypsum. However, more trials are needed for appropriate species (e.g., blady grass) and amendments, if any, and in what situations. For example, aerial sowing of grass seeds over large areas of gully slopes in the wet season, when soils are loose and saturated is worth investigating for large scale revegetation efforts (e.g., Campbell 1982; 1992).

Rehabilitation of shallow scalded hillslopes has been successful in semi-arid Australia using deep ripping and contour furrows, gypsum addition, and water ponding (e.g., Jones 1969; Cunningham 1974; Muirhead et al. 1974; Alchin 1983; Thompson 2008). However, these techniques are inappropriate for scalded patches fringing and within gullies, or deep gully erosion. For these gully slopes, other slope stabilization, revegetation and soil amendment techniques are needed (Shellberg and Brooks 2013). They may also be in appropriate in areas subject to active tunnel erosion, as it may increase the sub-surface flow pathways, accelerating tunnelling. For example, the application of compost blankets, mixed with grass seed and other soil amendments like gypsum, can be applied with pneumatic blowers over a variety of gully slopes. Compost blankets are highly effective at erosion control, typically

exceeding the performance of other standard techniques (Faucette et al. 2005; 2007; 2009a). They can be applied either with or without mechanical re-shaping of the soil surface, depending on gully size, depth and age, as trialled by Shellberg and Brooks (2013) in alluvial gullies. Extreme caution is needed for intensive gully rehabilitation, especially bulldozing and reshaping gullies. These types of interventions have had mixed results of application, cost-effectiveness and physical success in sediment erosion reduction in northern Queensland (Shellberg and Brooks 2013) and elsewhere in Australia despite promotion by some funding bodies (Crothers et al. 1990; Bartlett 1991; Hadden 1993; Franklin et al. 2004; Carey 2006; Lovett and Price 2006; Caitcheon 2007; Jenkins and McCaffrey 2008; Miller 2008; Alt et al. 2009; Jolley 2009; Shellberg 2011). Improper intervention in gully stabilization could actually increase sediment yields over the short- and long-term (Shellberg and Brooks 2013, this study).

The following flow chart should be used to initially as a guide to help decide if and how to intervene with alluvial gully erosion (Figure B31). Recommendations and pitfalls outlined in Shellberg and Brooks (2013) should be used as detailed guidance. Only trained geomorphologists, soil conservationists, and bioengineers should plan and design major gully intervention works. These professionals must work closely with implementation crews with detailed oversight on the ground to avoid increasing gully erosion from rehabilitation works and structural failures.

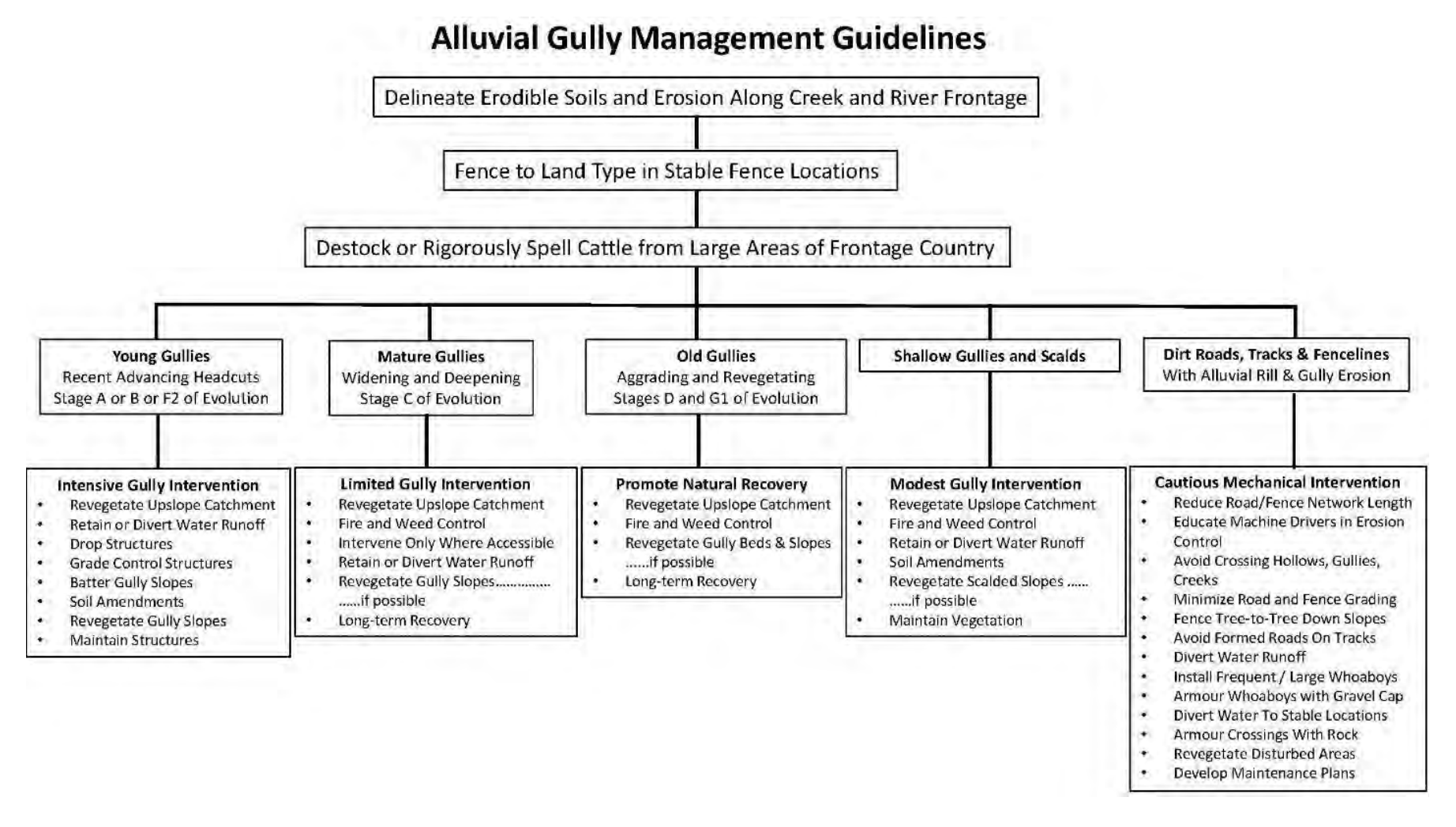


**Figure B31:** Alluvial gully management guidelines and a flow chart for potential avenues into rehabilitation, categorized by gully type and stage of gully evolution (following Gellis 1995).

#### **ACKNOWLEDGEMENTS**

This work would not have been possible without the extremely hard and detailed field work of Lucas Armstrong, Brad Guy, Emma-Lee Harper, and Georgina Friend. Exclusion fencing work following traditional techniques (tree-to-tree) was provided by expert crews lead by Tom Bezant and John Ross. Special thanks go to the managers of Crocodile and Springvale Stations for allowing this research to be conducted on your properties to inform future management decisions.

#### **REFERENCES**

- Alt, S., Jenkins, A., Lines-Kelly, R., 2009. Saving Soil: A Landholder's Guide to Preventing and Repairing Soil Erosion. Northern Rivers Catchment Management Authority and the NSW Department of Primary Industries.
- Alchin, B.M., 1983. Runoff and soil loss on a duplex soil in semi-arid New South Wales. *Journal of Soil Conservation Service, New South Wales*, 39: 176-187.
- Bartley, R., Corfield, J.P., Abbott, B.N., Hawdon, A.A., Wilkinson, S.N. and Nelson, B., 2010a. Impacts of improved grazing land management on sediment yields Part 1: *Hillslope processes. Journal of Hydrology*, 389: 237–248.
- Bartley, R., Wilkinson, S.N., Hawdon, A.A., Abbott, B.N. and Post, D.A., 2010b. Impacts of improved grazing land management on sediment yields Part 2: Catchment response. *Journal of Hydrology*, 389: 249-259.
- Bartley, R., Corfield, J.P., Hawdon, A.A., Kinsey-Henderson, A.E., Abbott, B.N., Wilkinson, S.N., Keen, R.J., 2014. Can changes to pasture management reduce runoff and sediment loss to the Great Barrier Reef? The results of a 10-year study in the Burdekin catchment, Australia. *The Rangeland Journal*, 36(1), 67-84.
- Bartlett, G., 1991 (ed). *Earthmovers Training Course* (20 units). Soil Conservation Service of New South Wales, Chatswood, N.S.W.
- Brookes, A. and Shields, F.D., Jr., 1996. *River Channel Restoration: Guiding Principles for Sustainable Projects*. John Wiley and Sons, Chichester, UK.
- Brooks, A.P., Shellberg, J.G., Spencer, J. and Knight, J., 2009. Alluvial gully erosion: an example from the Mitchell fluvial megafan, Queensland, Australia. Earth Surface Processes and Landforms, 34: 1951-1969, + 2010. Erratum. Earth Surface Processes and Landforms, 35: 242–245.
- Brooks, A., Spencer, J., Olley, J., Pietsch, T., Borombovits, D., Curwen, G., Shellberg, J., Howley, C., Gleeson, A., Simon, A., Bankhead, N., Klimetz, D., Eslami-Endargoli, L., Bourgeault, A., 2013. *An Empirically-Based Sediment Budget for the Normanby Basin: Sediment Sources, Sinks, and Drivers on the Cape York Savannah*. Griffith University, Australian Rivers Institute, Final Report for the Australian Government's Caring for Our Country Reef Rescue Program, April 2013, 506pp. <a href="http://www.capeyorkwaterquality.info/references/cywq-229">http://www.capeyorkwaterquality.info/references/cywq-229</a>.
- Brooks, A., Curwen, G., Spencer, J., 2015. *A Framework for Prioritising Gully Management in the Normanby Basin Cape York*. A report to South Cape York Catchments for the Cape York Water Quality Improvement Plan by the Australian Rivers Institute, Griffith University, 28 pp.
- Burylo, M., Rey, F., Roumet, C., Buisson, E. and Dutoit, T., 2009. Linking plant morphological traits to uprooting resistance in eroded marly lands (Southern Alps, France). *Plant and Soil*, 324(1-2): 31–42.
- Caitcheon, G., 2007. Managing Gully Erosion in the NSW Tablelands to Improve Water Quality and Maintain Productive Wool Pastures. Land and Water Australia, Publication No. PK071411 Canberra, ACT.

- Callahan, P., 2001. Root-rap or restoration: is Rosgen-ism helping or hurting our stream and rivers? In: D.F. Hayes (Editor), *Designing Successful Stream and Wetland Restoration Projects: Proceedings of the 2001 Wetlands Engineering and River Restoration Conference*. American Society of Civil Engineers, Reno, NV.
- Campbell, M.H., 1982. Restricting losses of aerially sown seed due to seed-harvesting ants. *Geobotany*, 4: 25-30.
- Campbell, M.H., 1992. Extending the frontiers of aerially sown pastures in temperate Australia: a review. *Australian Journal of Experimental Agriculture*, 32(1): 137-148.
- Carey, B. 2006. *Gully Erosion*. Queensland Department of Natural Resources and Water, Fact Sheet QNRM05374, Brisbane, QLD.
- Ciesiolka, C., 1987. Catchment Management in the Nogoa Watershed. AWRC Research Project 80/128, Department of Resources and Energy, Australian Water Resources Council, 204 pp.
- Coventry, R.J., 2004. Constraints of highly weathered soils, especially soil sodicity, to plant production in the dry tropics, In: *Prospects for high-value hardwood timber plantations in the 'dry' tropics of northern Australia*, Mareeba, 19th 21st October, 2004 Conference.
- Crothers, R.B., Wilkinson, W.F., Gray, H.J., McLatchey, J.F., 1990. *Gully stabilisation techniques used by the Soil Conservation Service of New South Wales 18 to 21 May 1987.* Queensland Department of Primary Industries, Soil Conservation Services Branch, Study Tour Report QS90002, Brisbane, Qld.
- Cunningham, G.M., 1974. Regeneration of scalded duplex soils in the Coolabah District, New South Wales. *Journal of the Soil Conservation Service of New South Wales*, 30: 157-169.
- Ebersole, J.L., Liss, W.J., and Frissell, C.A. 1997. Restoration of stream habitats in the western United States: restoration as reexpression of habitat complexity. *Environmental Management*, 21: 1-14.
- Faucette, L.B., Jordan, C.F., Risse, L.M., Cabrera, M., Coleman, D.C. and West, L.T., 2005. Evaluation of stormwater from compost and conventional erosion control practices in construction activities. *Journal of Soil and Water Conservation*, 60(6): 288-297.
- Faucette, L.B., Governo, J., Jordan, C.F., Lockaby, B.G., Carino, H.F. and Governo, R., 2007. Erosion control and storm water quality from straw with PAM, mulch, and compost blankets of varying particle sizes. *Journal of Soil and Water Conservation*, 62(6): 404-413.
- Faucette, L.B., Scholl, B., Beighley, R.E. and Governo, J., 2009a. Large-scale performance and design for construction activity erosion control best management practices. *Journal of Environmental Quality*, 38(3): 1248-1254.
- Franklin, J., Glover, S. and Parker, B., 2004. *Gully Erosion Assessment and Control Guide*. N.S.W. Department of Infrastructure, Planning and Natural Resources, Sydney, N.S.W., 28 pp.

- Gellis, A.C., Cheama, A., Laahty, V. and Lalio, S., 1995. Assessment of gully-control structures in the Rio Nutria Watershed, Zuni Reservation, New Mexico. *Water Resources Bulletin*, 31(4): 633-645.
- Gellis, A.C., Cheama, A. and Lalio, S., 2001. Developing an approach for ranking watersheds for rehabilitation, Zuni Indian Reservation, New Mexico. *Geomorphology*, 37: 105-134.
- Graf, W.L., 1977. The rate law in fluvial geomorphology. *American Journal of Science*, 277: 178-91.
- Graf, W.L., 1979. The development of montane arroyos and gullies. *Earth Surface Processes*, 4: 1-14.
- Hadden, K., 1993. Soil Conservation Handbook for Parks and Reserves in the Northern Territory. Conservation Commission of the Northern Territory, Technical Report Number 54, Darwin, N.T.
- Haigh, M.J., 1984. Ravine erosion and reclamation in India. *Geoforum*, 15(4): 543-561.
- Haigh, M.J., 1998. Ravine erosion and reclamation in India. In: D.C. Pandey (Editor), Managing Agriculture for a Better Tomorrow: The Indian Experience. MD Publications PVT LTD, New Delhi, pp. 161-193.
- Heede, B.H., 1976. *Gully Development and Control: The Status of Our Knowledge*. U.S. Department of Agriculture, Forest Service, Rocky Mountain Forest and Range Experimental Station, RM-169, Fort Collins, CO, 42 pp.
- Hudson, N.W., 1987. *Soil and Water Conservation in Semi-Arid Areas*, FAO Soils Bulletin 57. Food and Agriculture Organization (FAO) of the United Nations, Land and Water Development Division, Soil Resources, Management and Conservation Service, Rome, 172 pp.
- Hupp, C.R., 1992. Riparian vegetation recovery patterns following stream channelization: a geomorphic perspective. *Ecology*, 73 (4): 1209-1226.
- Jenkins, C. and McCaffrey, S., 2008. Gully erosion. In: C. Jenkins and S. McCaffrey (Editors), *Management and Rehabilitation of Riparian Lands: A Best Management Practice Guide for the Central West Catchment*. Central West Catchment Management Authority, Wellington, NSW, pp. 191-213.
- Jolley, K., 2009. *Soil Conservation Manual: A Managers Guide 2009*. Savanna Solutions Pty Ltd, Katherine, N.T.
- Jones, R.M., 1969. Scald reclamation studies in the Hay District Part IV-Scald Soils: Their properties and changes with reclamation. *Journal of the Soil Conservation Service of New South Wales*, 25(1): 104-120.
- Karfs, R., Holloway, C., Pritchard, K. and Resing, J., 2009. Land Condition Photo Standards for the Burdekin Dry Tropics Rangelands: A Guide for Practitioners. Burdekin Solutions Ltd and Queensland Department of Primary Industries and Fisheries, Townsville, 76 pp.
- Lal, R., 1992. Restoring land degraded by gully erosion in the tropics. *Advances in Soil Science*, 17: 123-151.

- Lovett, S. and Price, P., 2006. *Managing Gullies on Wool-Producing Farms*. Land and Water Australia, Land Water and Wool Fact Sheet PF061166, Canberra ACT
- McCloskey, G.L., Waters, D.K., Ellis, R., Carroll, C., 2014. Modelling reductions of pollutant loads due to improved management practices in the Great Barrier Reef catchments Cape York NRM region. Technical Report, Volume 2, Department of Natural Resources and Mines, Cairns, Queensland.
- McIvor, J.G., Williams, J. and Gardener, C.J., 1995. Pasture management influences runoff and soil movement in the semi-arid tropics. *Australian Journal of Experimental Agriculture*, 35: 55-65.
- McKeon, G., Hall, W., Henry, B., Stone, G. and Watson, I., 2004. *Pasture Degradation and Recovery in Australia's Rangelands: Learning From History*. Queensland Dept. of Natural Resources, Mines and Energy, Indooroopilly, Qld., 256 pp.
- Miller, W., 2008. *Practical Guide to Soil Erosion: A Guide to Preventing, Assessing, and Treating Soil Erosion*. Border Rivers Gwydir Catchment Management Authority, pp. 56.
- Molina, A., Govers, G., Cisneros, F. and Vanacker, V., 2009. Vegetation and topographic controls on sediment deposition and storage on gully beds in a degraded mountain area. *Earth Surface Processes and Landforms*, 34 (6): 755–767.
- Muirhead, W.A., Jones, R.M. and Williamson, D.R., 1974. Response by scalds to gypsum on the riverine plain New South Wales. *Journal of the Soil Conservation Service of New South Wales*, 30: 112-144.
- O'Reagain, P.J., Brodie, J., Fraser, G., Bushell, J.J., Holloway, C.H., Faithful, J.W. and Haynes, D., 2005. Nutrient loss and water quality under extensive grazing in the upper Burdekin River catchment, North Queensland. *Marine Pollution Bulletin*, 51: 37-50.
- O'Reagain, P.J. and Bushell, J.J., 2011. *The Wambiana Grazing Trial: Key Learnings for Sustainable and Profitable Management in a Variable Environment.* The State of Queensland, Department of Employment, Economic Development and Innovation with funding from Meat and Livestock Australia, 51 pp.
- Pressland, A.J., Mills, J.R., Cummins, V.G., 1988. Landscape degradation in native pastures. In: W.H. Burrows, J.C. Scanlan, M.T. Rutherford (Eds.), *Native Pastures in Queensland: the Resources and Their Management*. Queensland Department of Primary Industries, Information Series QI87023, Brisbane pp. 174-197.
- Queensland State, 2013. Cape York Region, Second Report Card 2010, Reef Water Quality Protection Plan. Reef Water Quality Protection Plan Secretariat, State of Queensland, April 2013.
- Raizada, A., Samra, J.S., Prajapati, M.C. and Bhushan, L.S., 2005 Chronosequence of grass species succession under continued protection in ravines of sub-tropical India. *International Journal of Ecology and Environmental Sciences*, 31(2): 119-131.
- Reubens, B., Nyssen, J., Poesen, J., Woldekidan, H., Zenebe, A., Girmay, G., Deckers, J., Taha, N., Tewoldeberhan, S., Gebrehiwot, K., Bauer, H., Haile, M. and Muys, B., 2008. *Establishment and Management of Woody Vegetation to Control Gully*

- *Erosion*. Tigray Livelihood Papers No. 8, VLIR Mekelle University IUC Programme, 35pp.
- Reubens, B., Poesen, J., Nyssen, J., Leduc, Y., Abraha, A.Z., Tewoldeberhan, S., Bauer, H., Gebrehiwot, K., Deckers, J. and Muys, B., 2009. Establishment and management of woody seedlings in gullies in a semi-arid environment (Tigray, Ethiopia). *Plant and Soil*, 324(1-2): 131-156.
- Rolfe, J., Shaw, K., English, B. and Kernot, J., 2004. *Regional Land Condition Assessment:* Grazing Management to Improve Regional Ecosystems, Land Condition and Optimise Beef Production in the Northern Gulf. Queensland Department of Primary Industries and Fisheries, pp. 26.
- Roth, C.H., 2004. A framework relating soil surface condition to infiltration and sediment and nutrient mobilization in grazed rangelands of northeastern Queensland, Australia. *Earth Surface Processes and Landforms*, 29(9): 1093-1104.
- Rutherfurd, I.D., Prosser, I.P. and Davis, J., 1997. Simple approaches to predicting rates and extent of gully development. In: S.S.Y. Wang, E.J. Langendoen and F.D.J. Shields (Editors), *Proceedings of the Conference on Management of Landscapes Disturbed by Channel Incision*. The Centre for Computational Hydroscience and engineering. The University of Mississippi, pp. 1124-1130.
- Sarr, D.A., 2002. Riparian livestock exclosure research in the western United States: a critique and some recommendations. *Environmental Management*, 30(4): 516-526.
- Sandercock, P.J. and Hooke, J.M., 2011. Vegetation effects on sediment connectivity and processes in an ephemeral channel in SE Spain. *Journal of Arid Environments*, 75: 239-254.
- Scanlan, J.C., Pressland, A.J. and Myles, D.J., 1996. Run-off and soil movement on midslopes in North-east Queensland grazed woodlands. *Rangelands Journal*, 18: 33-46
- Schumm, S.A. and Hadley, R.F., 1957. Arroyos and the semiarid cycle of erosion. *American Journal of Science*, 255: 161-74.
- Schumm, S.A., 1973. Geomorphic thresholds and complex response of drainage systems. In: M. Morisawa (Editor), *Fluvial Geomorphology*. Allen and Unwin, London, pp. 299-310.
- Shellberg, J.G. 2011. Alluvial Gully Erosion Rates and Processes Across the Mitchell River Fluvial Megafan in *Northern Queensland, Australia*. Griffith University, PhD Thesis, Brisbane, Australia, November 2011, 283pp.
- Shellberg, J.G., Brooks, A.P., Rose, C.W., 2013a. Sediment production and yield from an alluvial gully in northern Queensland, Australia. *Earth Surface Processes and Landforms*, 38, 1765-1778.
- Shellberg, J.G., Brooks, A.P., Spencer, J. and Ward, D., 2013b. The hydrogeomorphic influences on alluvial gully erosion along the Mitchell River fluvial megafan, northern Australia. *Hydrological Processes*. DOI: 10.1002/hyp.9240.
- Shellberg, J.G., Brooks, A.P., 2013. Alluvial Gully Prevention and Rehabilitation Options for Reducing Sediment *Loads in the Normanby Catchment and Northern Australia*.

- Griffith University, Australian Rivers Institute, Final Report for the Australian Government's Caring for our Country Reef Rescue Initiative, 312pp. http://www.capeyorkwaterguality.info/references/cywg-223.
- Shellberg, J.G., Spencer, J., Brooks, A.P., Pietsch, T., 2016. Degradation of the Mitchell River Fluvial Megafan by Alluvial Gully Erosion Increased by Post-European Land Use Change, Queensland, Australia. *Geomorphology*, http://dx.doi.org/10.1016/j.geomorph.2016.04.021.
- Silcock, R.G. and Beale, I.F., 1986. Complete de-stocking will not reclaim some Australian rangelands. *Water papers of the 4th Biennial Conference of the Australian Rangeland Society*, Armidale: 150-153.
- Silburn, D.M., Carroll, C., Ciesiolka, C.A.A., deVoil, R.C. and Burger, P., 2011 Hillslope runoff and erosion on duplex soils in grazing lands in semi-arid central Queensland. I. Influences of cover, slope, and soil. *Soil Research*, 49(2): 105-117.
- Simon, A. and Hupp, C.R., 1992. *Geomorphic and Vegetative Recovery Processes Along Modified Stream Channels of West Tennessee*. USGS; Open-File Report 91-502, Denver, CO.
- Simon, A. and Darby, S.E., 2002. Effectiveness of grade-control structures in reducing erosion along incised river channels: the case of Hotophia Creek, Mississippi. *Geomorphology*, 42 229- 254.
- Simon, A., Doyle, M., Kondolf, M., Shields, F.D.J., Rhoads, B. and McPhillips, M., 2007. Critical evaluation of how the Rosgen classification and associated "natural channel design" methods fail to integrate and quantify fluvial processes and channel response. *Journal of the American Water Resources Association*, 43(5): 1117-1131.
- Smith, E.P., 2002. BACI design. In: A.H. El-Shaarawi and W.W. Piegorsch (Editors), *Encyclopaedia of Environmetrics*. Wiley, New York, pp. 1-8.
- Spencer, J., Brooks, A., Curwen, G., Tews, K., 2016. *A Disturbance Index Approach for Assessing Water Quality Threats in Eastern Cape York*. A report to South Cape York Catchments and Cape York NRM for the Cape York Water Quality Improvement Plan, by the Australian Rivers Institute, Griffith University, 42 pp.
- Stafford-Smith, D.M., McKeon, G.M., Watson, I.W., Henry, B.K., Stone, G.S., Hall, W.B. and Howden, S.M., 2007. Learning from episodes of degradation and recovery in variable Australian rangelands. *Proceedings of the National Academy of Sciences of the United States of America*, 104(52): 20691.
- Thexton, E. 1999. Rehabilitation of the lower Genoa River, far east Gippsland, Victoria with assisted regeneration. In: *Second Australian Stream Management Conference*. Edited by I. Rutherfurd and R. Bartley. Cooperative Research Centre for Catchment Hydrology, Monash University, Adelaide, SA pp. 623-628.
- Thompson, R., 2008. Waterponding: Reclamation technique for scalded duplex soils in western New South Wales rangelands. *Ecological Management & Restoration*, 9(3): 170-181.

- Thorburn, P.J., Wilkinson, S.N., 2013. Conceptual frameworks for estimating the water quality benefits of improved agricultural management practices in large catchments. *Agriculture, Ecosystems and Environment*, 180(1): 192-209.
- Underwood, A.J., 1994a. Spatial and temporal problems with monitoring. In: P. Calow and G.E. Petts (Editors), *The Rivers Handbook: Hydrological and Ecological Principles*; Volume Two. Blackwell Scientific Publications, Oxford, United Kingdom, pp. 101-123.
- Underwood, A.J., 1994b. On beyond BACI: sampling designs that might reliably detect environmental disturbances. *Ecological Applications*, 4(1): 3-15.
- Vanacker, V., von Blanckenburg, F., Govers, G., Molina, A., Poesen, J. and Deckers, J., 2007. Restoring dense vegetation can slow mountain erosion to near natural benchmark levels. *Geology*, 35: 303-306.
- Wilkie, A., 1997. A Manual for the Production of Photographic Standards for Use in Herbage Yield and Cover *Estimates*. Technical Bulletin 264, Northern Territory Department of Primary Industry and Fisheries, 19 pp.

# **Pasture Monitoring Template**

Site Name	Plot ID			
Date Time	Plot Area (m²)			
GPS Tracklog Running? Yes   No				
Photo of GPS Time Stamp? <b>Yes</b> D <b>No</b> D				
GPS Position Waypoint of Marker Stake? ( <i>Time Averaged</i> ) <b>Yes</b> No				
<u>Plot Photos</u>				
Plot edge oriented North-South? (Use comp	ass) Yes 🗌 No 🗌			
2.5 m from Stake, Cantered on Stake, (North	n Looking South) Photo #			
2.5 m from Stake, Cantered on Stake, (Sout	h Looking North) Photo #			
6.0 m from Stake, Cantered on Stake, (North	n Looking South) Photo #			
6.0 m from Stake, Cantered on Stake, (Sout	h Looking North) Photo #			
Vertical Plot Photo (NE Quad) Photo #				
Vertical Plot Photo (NW Quad) Photo #				
Vertical Plot Photo (SW Quad) Photo #				
Vertical Plot Photo (SE Quad) Photo #				
Additional Site Area Photos (with Stake Ref.	) Photo #s			
Additional Plant Part Close-up Photos #s				
Ground Cover (aerial projection downward)				
Total % Organic Ground Cover				
(Nearest 5 %, standing grass/weeds, dead r	matted grass, roots, leaves, sticks, wood)			
% of total = leaves/sticks	<u></u>			
% of total = dead matted grass				
% of total = standing vegetation (all)_				
% of total = standing weeds				
Perennial Pasture Grass Cover (rooted, star	nding, not herbaceous weeds)			
(Aerial Projection downward, not just	basal area)			
# of Species				
Total Count (#) of Perennial Tussock	s			

NE Quad, NVV Quad, SVV Quad, SE Quad			
Species Names (if Known)			
Pasture Yield Estimate (kg/ha) (use plot area and immediate surroundings)			
Pasture Grass Yield (kg/ha)			
(exotic or native grass w/out herbaceous weeds, shrubs, trees)			
250, 300, 400, 500, 600, 800, 900,1100,			
1300 🗌 1600 🔲, 1700 🔲, 2000 🔲, 2200 🔲, 2400 🔲			
Yield Guide Used (Frontage, Yellow Earth, Granite)			
Pasture Grass Yield (with herbaceous or woody weeds kg/ha)			
250, 300, 400, 500, 600, 800, 900,1100,			
1300 🗌 1600 🔲, 1700 🔲, 2000 🔲, 2200 🔲, 2400 🔲			
<u>Land Condition</u>			
Total % Organic Ground Cover (see above)			
Perennial Pasture Grass Cover (see above)			
Dominant Pasture Plants (list top 4 and total #)			
Dominant Weed Plants (list top 4 and total #)			
Weed Dominance (% of individual plants)			
Abundant > 50% ☐, Mod 20-50% ☐, Low 5-20% ☐, Slight <5% ☐, None ☐			
Soil Crust Condition (broken-ness)			
Intact < 5% ☐, Slight 5-20% ☐, Moderate 21-50% ☐, Extensive >50% ☐			
Erosion Features (gullies, rills, tracks/pads, sheeting, scalds, hummocks, terracettes)			
Insignificant < 5% ☐, Slight 5-20% ☐, Moderate 21-50% ☐, Extensive >50% ☐			
Deposited Material (silt, sand, gravel, rock, not organic)			

Insignificant < 5% \_\_, Slight 5-20% \_\_, Moderate 21-50% \_\_, Extensive >50% \_\_

Vertical Distance from Stake Top to Soil Surface (use tape measure)

Upslope (mm) \_\_\_\_\_

Downslope (mm) \_\_\_\_\_

Overall Land Condition Class

A \_\_ Good (dense perennial grass, no signif. weeds, no signif. erosion)

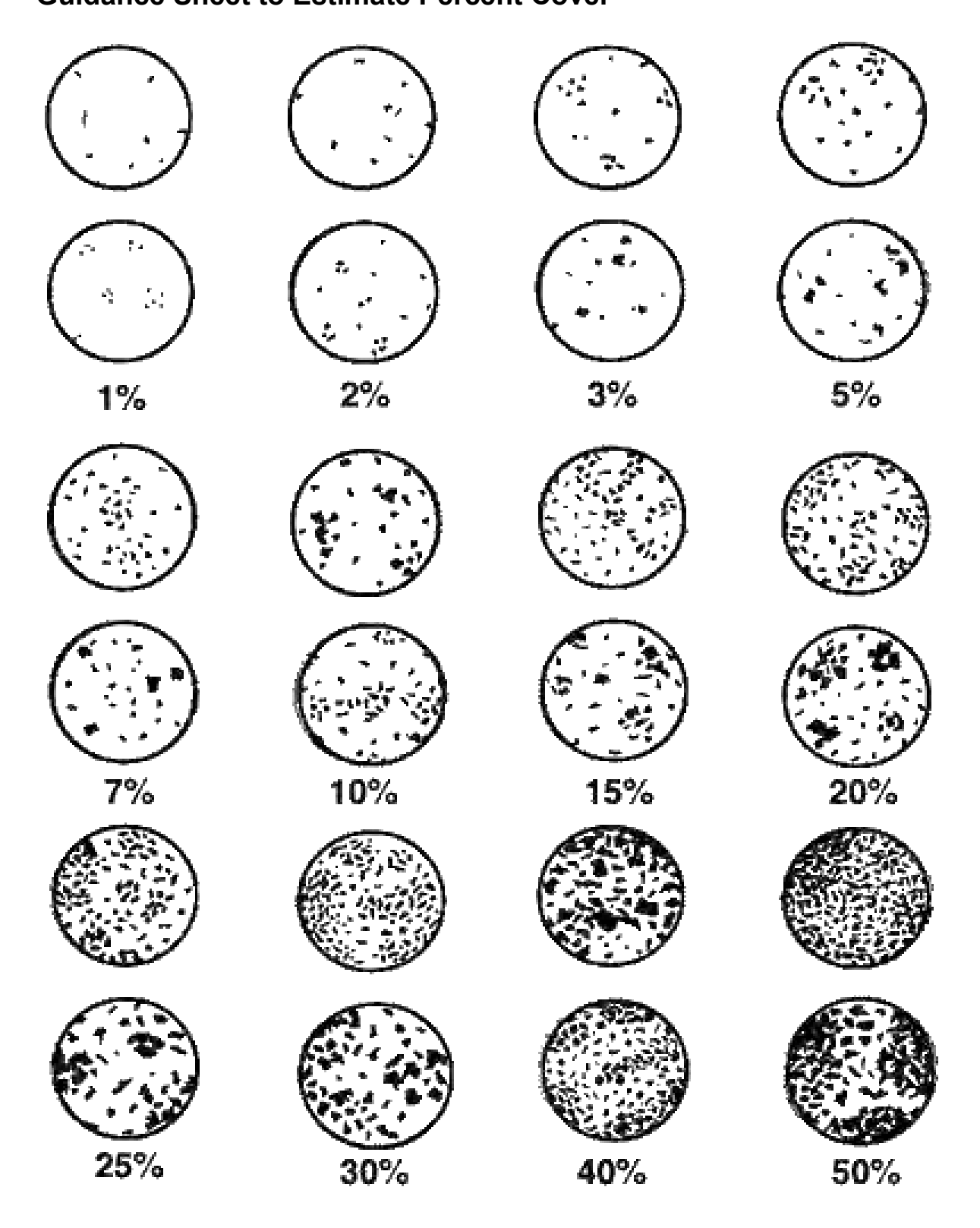
B \_\_ Fair (mod. perennial grass, a few weeds, minor erosion)

C \_\_ Poor (low perennial grass, weeds common, obvious erosion/scalds)

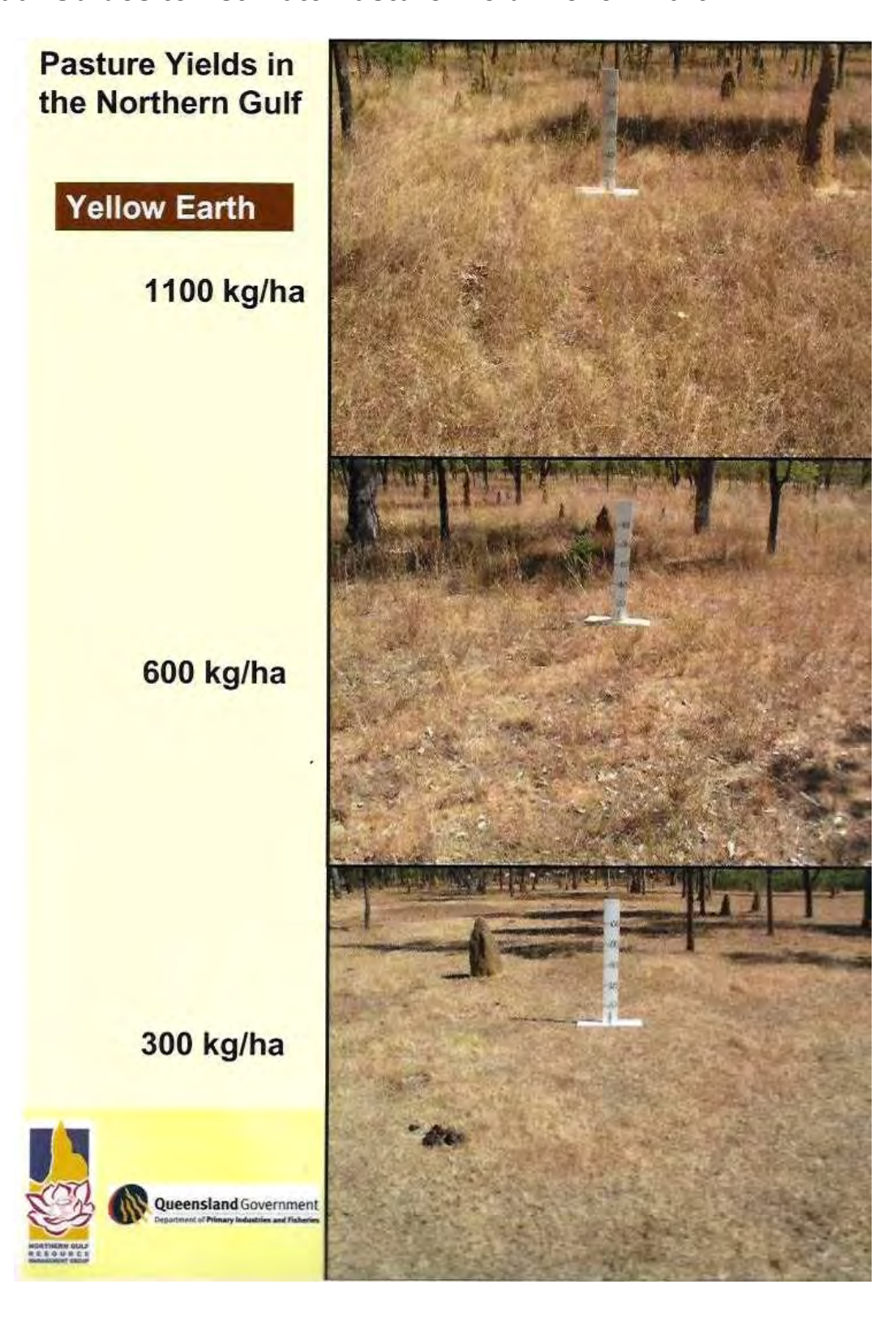
D \_\_ Very Poor (few perennial grass, weeds infestation, severe erosion/scalds)

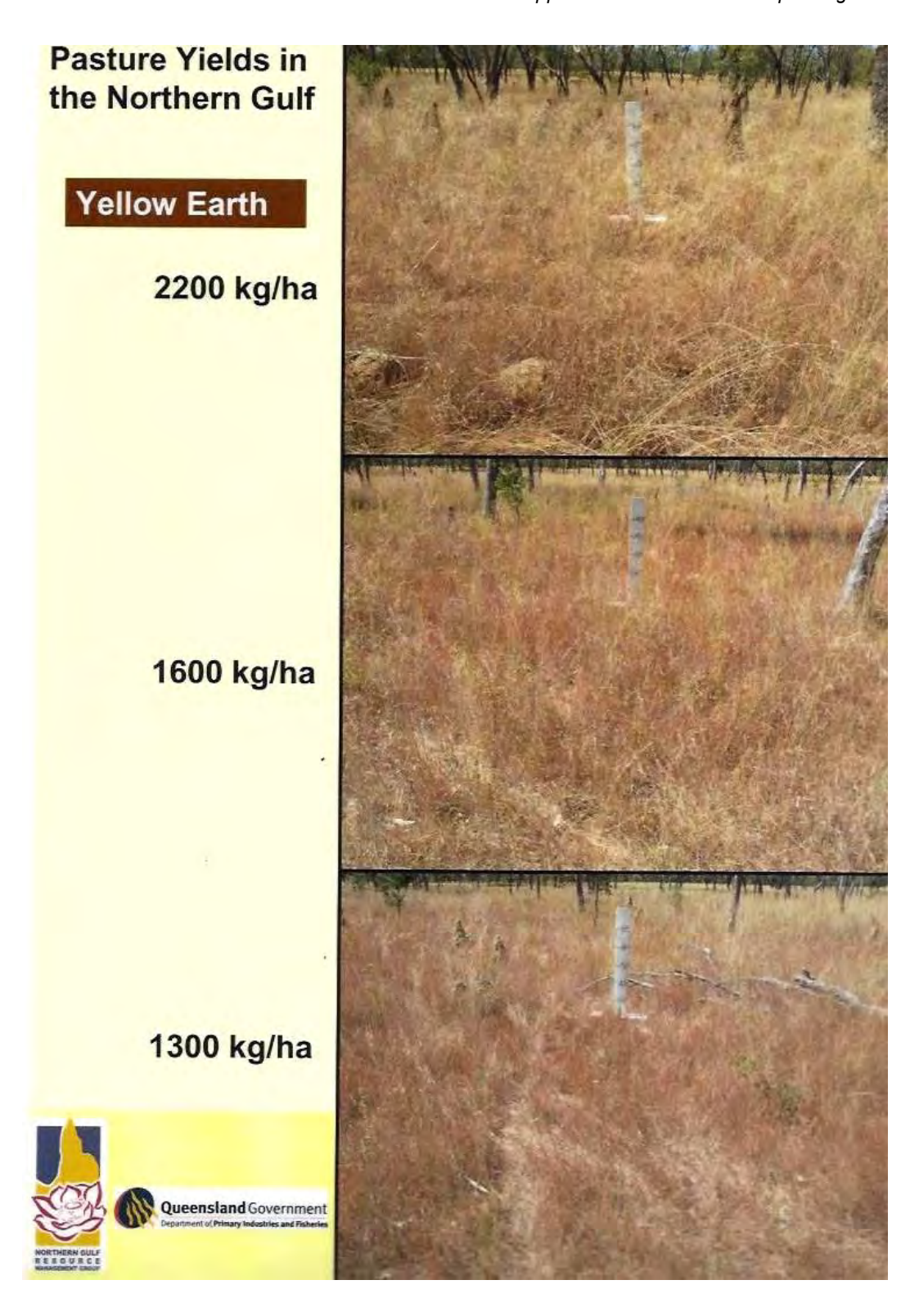
COMMENTS

### **Guidance Sheet to Estimate Percent Cover**

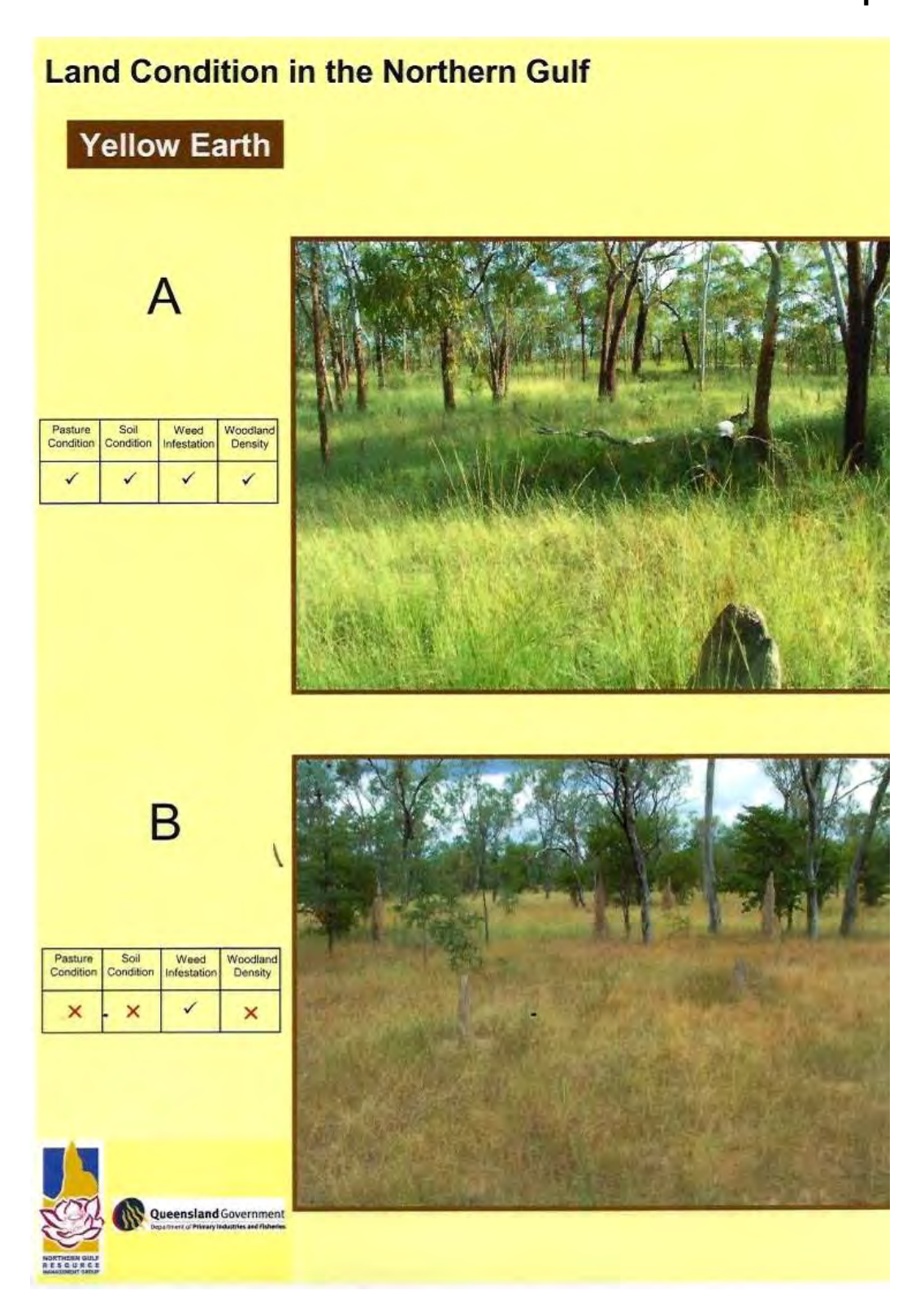


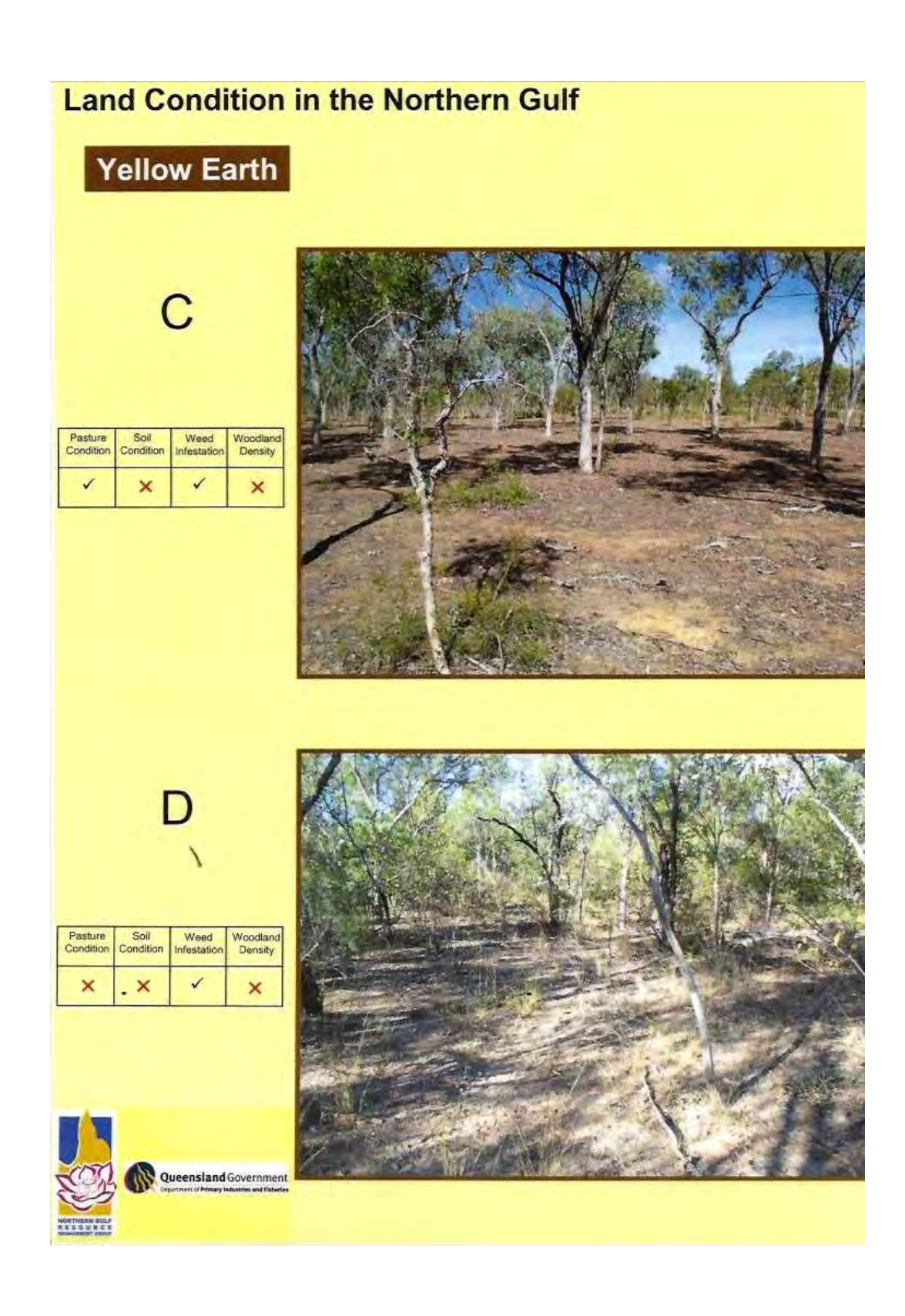
### Visual Guides to Estimate Pasture Yield: Yellow Earth





# Visual Guides to Estimate Land Condition: Yellow Earth Example





# APPENDIX C: BIOAVAILABLE NUTRIENTS AND ORGANICS IN ALLUVIAL GULLY SEDIMENT

Alexandra Garzon-Garcia<sup>1, 2</sup>, Joanne Burton<sup>1, 2</sup>, Andrew P Brooks<sup>2</sup>

<sup>1</sup>Australian Rivers Institute, Griffith University, Brisbane, Australia <sup>2</sup>Department of Science, Information Technology and Innovation (DSITI), Brisbane, Australia

# **TABLE OF CONTENTS**

List of Tables	342
List of Figures	343
Executive Summary	346
1. Introduction	351
2. Methods	352 357
3. Results and Discussion	363
3.1 Bioavailable nutrients and organics in alluvial gullies 3.2 Bioavailable nutrients and organics in different geomorphic units of alluvial gullies 3.2.1 The role of particle size 3.3 Bioavailable nutrients and organics export from alluvial gullies 3.3.1 Case study 1: Granite Normanby alluvial gully 3.3.2 Case study 2: Laura Crocodile Station alluvial gully 3.3.3 Case study 3: Laura Crocodile Gap alluvial gully 3.3.4 Sensitivity analysis	.367 368 373 373 378
4. Main Conclusions and Implications for management	391
Acknowledgements	393
References	394
Appendix C1: Sample analyses	397
Appendix C2: Bioavailable nutrient and organics indicators for all sampled gugeomorphic units and particle size fractions (ND: Non-detectable, NA: Not available)	
Appendix C3: Summary statistics for bioavailable nutrient and organics indicators by geomorphic unit and particle size fraction (ND: Non-detectable, NA: Not available)	
Appendix C4: Fine sediment content (<63 um, <10 um) for all sampled gullies by geomounit	•

# **LIST OF TABLES**

Table C1:	List of sampled gullies and gully geomorphic units353
Table C2:	Nitrogen, phosphorus, carbon and other physical and chemical parameters measured in total soil/sediment, <63um and <10um soil/sediment fractions
Table C3:	Summary statistics for bioavailable nutrient and organics indicators by gully type and particle size fraction (ND: Non-detectable, NA: Not available)364
Table C4:	Observed erosion rate from gully 2011-2015 and estimated contributions from each source component
Table C5:	Observed erosion rate from gully 2011-2015 and estimated contributions from each source component
Table C6:	Observed erosion rate from gully 2011-2015 and estimated contributions from each source component
Table C7:	Annual exports per unit area of sediment, nitrogen (TN) and phosphorus (TP) from alluvial gullies (this study) and various modelled land uses in the Wet Tropics*

# **LIST OF FIGURES**

Figure C1:	Example of primary gully erosion into an alluvial terrace on Springvale Station Normanby catchment
Figure C2:	Example of secondary incision into a >50 yr old primary gully floor – Springvale Station – Normanby catchment
Figure C3:	Map of the Normanby catchment showing the locations of the sampled gullies in the upper Laura and Normanby Rivers
Figure C4:	Bank subsurface geomorphic unit in the Granite Normanby alluvial gully and Laura Crocodile gap alluvial gully
Figure C5:	Bank surface geomorphic unit in the Granite Normanby alluvial gully (clearly differentiated by colour from the bank subsurface unit)355
Figure C6:	Buried A horizon geomorphic unit in the Laura Crocodile Gap alluvial gully. 355
Figure C7:	Terrace surface soil geomorphic unit in the Granite Normanby and Laura Crocodile station alluvial gullies
Figure C8:	Hillslope geomorphic unit in the Parsons Creek hillslope gully356
Figure C9:	Gully floor geomorphic unit in the Granite Normanby alluvial gully357
Figure C10:	Key pools and processes of the nitrogen cycle. The trend of bioavailable nitrogen over time is indicated in the figure (Adapted from Burton et al. 2015).
	359
Figure C11:	Key pools and processes of the phosphorus cycle. The trend of bioavailable phosphorus over time is indicated in the figure (Burton et al., 2015)360
Figure C12:	Key pools, processes and attributes of the carbon cycle (Burton et al., 2015)
Figure C13:	Percent total organic carbon (TOC), total nitrogen (TN), mineral N and total phosphorus (TP) in alluvial and hillslope gully soil/sediment for the total (green), <63 um (yellow) and <10 um (blue) particle size fractions. Boxes are intersected by median values and enclose data between the first and third quartiles, with lines extending to maximum and minimum values excluding outliers (values above and below 1.5 times the inner quartile range from the first and third quartiles, respectively). Box width is proportional to the square root of n for each group. Absence values indicate the parameter was non-detectable in any of the samples
Figure C14:	Ammonium (NH <sub>4</sub> -N), nitrate (NO <sub>3</sub> -N), sorbed phosphorus (P) and dissolved reactive phosphorus (DRP) in alluvial and hillslope gully soil/sediment for the total (green), <63 um (yellow) and <10 um (blue) particle size fractions. Boxes are intersected by median values and enclose data between the first and third quartiles, with lines extending to maximum and minimum values excluding outliers (values above and below 1.5 times the inner quartile range from the first and third quartiles, respectively). Box width is proportional to the square root of n for each group. Absence values indicate the parameter was non-detectable in any of the samples

Figure C15:	Percent total organic carbon (TOC), total nitrogen (TN), total phosphorus (TP), mineral N (mg/kg),TOC:TN ratio and TN:TP ratio by gully geomorphology component for the total (green), <63 um (yellow) and <10 um (blue) particle size fractions. Boxes are intersected by median values and enclose data between the first and third quartiles, with lines extending to maximum and minimum values excluding outliers (values above and below 1.5 times the inner quartile range from the first and third quartiles, respectively). Box width is proportional to the square root of n for each group. Absence values indicate the parameter was non-detectable in any of the samples
Figure C16:	Ammonium (NH4-N), nitrate (NO3-N), sorbed P, phosphorus buffer index (PBI) and dissolved reactive P (DRP) by gully geomorphology component for the total (green), <63 um (yellow) and <10 um (blue) particle size fractions. Boxes are intersected by median values and enclose data between the first and third quartiles, with lines extending to maximum and minimum values excluding outliers (values above and below 1.5 times the inner quartile range from the first and third quartiles, respectively). Box width is proportional to the square root of n for each group. Absence values indicate the parameter was non-detectable in any of the samples
Figure C17:	Enrichment ratios between (a) terrace surface soil and bank subsurface soil and (b) gully floor sediment and bank subsurface soil, for various nutrient and organics parameters in the total soil, and fine fractions (<63 um and <10 um) of alluvial gullies sampled in the Normanby catchment
Figure C18:	Enrichment ratio of various nutrient and organics bioavailability indicators in the fine fractions (<63 um and <10 um) of gullies sampled in the Normanby catchment
Figure C19:	Granite Normanby Gully showing the headscarp erosion in red between 2011 & 2015. Also shown (purple dots) are the sample locations for the gully. Note that the erosion detected by the aerial LiDAR in this gully is an absolute minimum amount of erosion due to the conservative limit of detection applied (0.5m change)
Figure C20:	Estimated annual mass contributions of sediment, organics and nutrient export from different geomorphic units in the Granite Normanby alluvial gully376
Figure C21:	Percent contributions of exported organics and nutrient fractions from different gully geomorphic units in the Granite Normanby alluvial gully377
Figure C22:	Crocodile Station gully showing the headscarp erosion in red between 2011 & 2015. Also shown (purple dots) are the sample locations. Note that the erosion detected by the aerial LiDAR in this gully is an absolute minimum amount of erosion due to the conservative limit of detection applied (0.5m change)
Figure C23:	Estimated annual mass contributions of sediment, organics and nutrient export from different geomorphic units in the Laura Crocodile Station alluvial gully.
Figure C24:	Percent contributions of exported organics and nutrient fractions from different gully geomorphic units in the Laura Crocodile Station alluvial gully381

Figure C25:	Laura Crocodile Gap alluvial gully complex showing the headscarp & secondary incision erosion in red between 2011 & 2015. Also shown (purple dots) are the sample locations. Note that the erosion detected by the aerial LiDAR in this gully is an absolute minimum amount of erosion due to the conservative limit of detection applied (0.5m change)
Figure C26:	Estimated annual mass contributions of sediment, organics and nutrient export from different geomorphic units in the Laura Crocodile Gap alluvial gully385
Figure C27:	Percent contributions of exported organics and nutrient fractions from different gully geomorphic units in the Laura Crocodile gap alluvial gully386
Figure C28:	Observed erosion in Granite Normanby distal gully over the period 2009-11 in orange and 2011-15 in red. Modelled scenarios have then been derived to show relative nutrient contributions with gully deepening387
Figure C29:	Estimated annual mass contributions of sediment, organics and nutrient export from different geomorphic units in a hypothetical developing alluvial gully388
Figure C30:	Percent contributions of all exported organics and nutrient fractions from different gully geomorphic units in a 0.5 m deep hypothetical gully (60% subsurface soil contribution to sediment yield and 40% terrace surface soil contribution to sediment yield)

#### **EXECUTIVE SUMMARY**

Gully erosion is a major source of fine sediment pollution to the Great Barrier Reef (GBR)). This can be inferred from the knowledge that the large, dry, grazing-dominated catchments in the Tropics (e.g. Fitzroy, Burdekin) deliver the largest sediment loads to the GBR (Garzon-Garcia et al., 2015; Joo et al., 2012; Kroon et al., 2012) and from sediment source tracing studies that have indicated that subsurface soil is the predominant sediment source in these catchments, particularly in areas with active gully erosion (Hughes et al., 2009; Olley et al., 2013; Wilkinson et al., 2015). Alluvial gully erosion has been shown to be the dominant form of gully erosion in the Normanby Catchment (Brooks et al., 2013), and while data doesn't exist as to the relative contribution of the different gully forms for other catchments, it is likely that in catchments such as the Bowen River, alluvial gullies are a significant, if not the dominant source. Fine sediment and nutrient delivery to the GBR has detrimental chemical/biological effects on the reef (Bainbridge et al., 2012; Brodie et al., 2010; Brodie et al., 2012; Wolanski et al., 2008). Recent work undertaken in the Burdekin and Johnstone River catchments has demonstrated that there are significant quantities of bioavailable nutrients (nitrogen and phosphorus) associated with fine sediments derived from eroded soils (Burton et al., 2015). This work also indicated that sediments have the ability to produce dissolved inorganic nitrogen (DIN) from their organic N sources as they move through the waterways, thereby contributing to the DIN pool. Hence, given that we know alluvial gully erosion constitutes a significant component of the anthropogenically accelerated sediment load in the Normanby and Mitchell catchments where it has been studied in detail (Brooks et al., 2013; Shellberg et al., 2010; Shellberg et al., in press), by extension they are also contributing substantially to the anthropogenic DIN pool. Consequently, effective management practices should aim at reducing not only sediment yields from alluvial gullies, but also organic and nutrient yields. Research has been carried out in a number of key catchments within the GBR to identify the key sources of fine sediment (Bainbridge et al., 2016; Bainbridge et al., 2014; Hughes et al., 2009; Olley et al., 2013; Wilkinson et al., 2015), however very little is currently known about sources of organics and nutrients, particularly within the catchments of the dry tropics dominated by grazing. An understanding of the key sources of organics and nutrients and their bioavailability and quantity associated with alluvial gully erosion is fundamental to inform management decisions.

In this report, results for various key indicators of bioavailable nutrients and organics (the term carbon is used interchangeably with organics in this report) are presented and analysed for three alluvial and one hillslope gully in the Normanby River catchment. The key indicators were selected based on previous and ongoing research conducted by Burton et al. (2015). The nutrient fractions and organic pools associated with different particle size fractions (total soil, <63 um, and 10 um) were determined for different gully geomorphic units including terrace surface soil, bank surface soil, bank subsurface soil and gully floor deposits. The total sediment, organic and nutrient export from the three alluvial gullies and their geomorphic units, was estimated using detailed annual sediment budgets coupled with nutrient and organic composition data from this study. A sensitivity analysis was also carried out to understand the effect of changes in gully depth, sediment yield and geomorphic unit on relative contributions to organics and nutrient export from alluvial gullies.

Note that this report presents nutrient export budget results and interpretation of data from a limited number of gullies. Considering the low level of replication, results are to be

considered as an indication only of the nutrient and organic pools within different components of gully complexes and of the range of organic and nutrient yields from gullies in the Normanby catchment, and should not be extrapolated.

#### Main findings include the following:

- Alluvial gullies are important sources of organics and potentially bioavailable nutrients to the aquatic environment.
- The data indicate little difference between bioavailable nutrient indicators in sampled hillslope (n=1) and alluvial gullies (n=3) for all particle size fractions sampled.
- There are significant differences in C, N, and P content among soils/sediments in the geomorphological units measured with the general pattern being terrace > bank surface > gully floor > bank subsurface. This result indicates that accurate estimation of nutrient and organic losses from gullies must rely on sampling and measurement of the different units.
- The upper 10-20cm of alluvial terrace soil profiles appear to be an important long term store of bioavailable nutrients and organics, whilst gully floors may act as a temporary store depending on gully evolution stage.
- TOC soil content in the terrace surface soils was from 54 to 77 times larger (depending on particle size fraction) and TN from 5 to 10 times larger than in bank subsurface soil in alluvial gullies.
- Primary gully erosion into terrace alluvium is ubiquitous in catchments like the Normanby and Burdekin (Figure C1).
- Particle size significantly influences nutrient and organic content and would influence bioavailability - hence particle size fractionation should be a major consideration in future study designs.
- The <10um fraction is generally enriched in bioavailable nutrients compared to the <63um fraction (1.4 to 3.3 times on average for carbon and nitrogen fractions), which is generally enriched compared to whole soil irrespective of gully geomorphic unit (with some exceptions e.g., DRP) (1.4 to 9.5 times on average for carbon and nitrogen fractions). These results from gullies in the Normanby catchment are consistent with results from key soil types in the Burdekin and Johnstone catchments (Burton et al., 2015).</li>
- Although terrace soil had the highest concentration of most nutrients and organics, bank subsoil was generally the main source of sediment in these alluvial gullies, due to the sheer volume of sub-soil delivered from active gully erosion.
- The sources of organics and nutrient export from alluvial gullies would vary depending on the type of erosional process occurring in the alluvial gully (i.e. headscarp retreat versus secondary incision) and their stage of evolution (e.g., gully depth and sediment yields) – however these findings should be confirmed with larger sample replication.
- In general, terrace soil was found to be the main source of total organic carbon export when headscarp retreat contributes the majority of sediment.
- The contribution of terrace soil to nutrient export varied with the stage of gully evolution. In the initial stages of gully evolution [very shallow gullies (<1.0 m) growing fast into the terrace deposits], terrace soil is the main source of nutrient export. As a

- result it should be a priority to protect terrace deposits from fast headscarp retreat as these deposits contain large pools of carbon and nutrients that, when lost, would be very difficult to restore. These terrace soil organic and nutrient pools may also be the most bioavailable and have a larger relative impact once in the aquatic environment.
- As gully incision occurs, the main source of most nutrient fractions was clearly bank subsurface sediment. Although this sediment has lower nutrient concentration than terrace surface soil or gully floors, the sheer quantity of exported sediment from this source makes it the largest contributor to export. Therefore, despite the nutrient enrichment of the surface soils (which are a component of both gully headscarp and sidewall retreat) gully subsoils would tend to be the main source of nutrients. Hence, there is no one component of a gully system that can be prioritised over another; the whole gully should be stabilised as all components are significant nutrient sources.
- When secondary incision erodes organic and nutrient rich sediment deposited on gully floors, this sediment may become a very important source of organics and nutrient export; even more so than bank subsurface soil. The protection of gully floor organics and nutrient deposits should be part of gully rehabilitation designs and should be prioritized when these deposits are rich in organics and nutrients.
- The majority of the nitrogen in alluvial gully soils/sediments is in organic form (more than 96% in all particle sizes and geomorphic units). The exported organic N from alluvial gullies is potentially bioavailable and thus may be mineralized into dissolved inorganic nitrogen during stream transport, once it gets to the estuarine or marine environment, or be used directly by algae in dissolved organic form.
- While it has long been recognised that gullies are an important source of fine sediment to the GBR, it is also apparent the gully sources are a much underappreciated source of nutrients as well. When compared to typical values of anthropogenic nitrogen and phosphorous from other major land uses in GBR catchment, it is apparent that gullies could be even more significant sources than intensive agricultural land per unit area.

Gully/land use	sediment (t/ha/y) TN (kg/ha/y)		TP (kg/ha/y)
Granite Normanby	114.0	54.0	23.7
Laura - Crocodile station	29.2	10.5	0.3
Laura - Crocodile Gap	28.8	12.6	1.6
Sugar cane	1.2	22.2	2.7
Banana	1.8	25.3	3.1
Nature conservation	0.2	3.6	0.3

(See Table 7 in report)

One of the most important implications of our findings is that alluvial gully erosion cannot continue to be overlooked as an important source of nutrients and potentially bioavailable nutrients to the aquatic environment. It is fundamental to increase our understanding of the links between organics and nutrient sources, alluvial gully erosional processes and instream processing. For example, it is crucial to understand differences in the bioavailability of exported sediment from different geomorphic unit sources once in the aquatic environment.

Although various indicators of the bioavailability of these sediments were quantified in this study, research is still necessary and on-going to define which of these indicators would be the best to predict the impact of organics and nutrients on primary production in the freshwater and marine environment (Burton et al., 2015) and what controls this bioavailability (Garzon-Garcia et al. in prep). The role of vegetation and litter has been proposed as crucial, not only to the rehabilitation of carbon and nitrogen pools in gullied landscapes, but to reduce the impacts of eroded sediment during its transport in the aquatic environment by promoting mineral nitrogen use by microbes during mineralization of vegetation litter carbon (Garzon-Garcia, 2014). Further research is necessary to better understand the role of vegetation in mediating these relationships.

This study gives some indication of management priorities to reduce organics and nutrient export from alluvial gullies and identifies the importance of (i) sampling and analysing key gully features separately, and (ii) understanding the stage of evolution of the gully / combination of erosion processes occurring (i.e. head scarp retreat versus secondary incision - Figure C2). The findings of this study should be further tested by sampling a larger number of alluvial gullies (replicated by gully type), including sampling of exported sediment, examining the effects of changes in sediment particle size, determining the relative bioavailability of nutrient derived from different sources, and using sediment source tracing to determine the relative contribution of each geomorphic unit. It is recommended that sampling design targets main geomorphic units from gully categories based on erosional process (e.g., fast headscarp retreat, primary incision, secondary incision, widening, gully depth, etc.)



**Figure C1:** Example of primary gully erosion into an alluvial terrace on Springvale Station Normanby catchment.



**Figure C2:** Example of secondary incision into a >50 yr old primary gully floor – Springvale Station – Normanby catchment.

.

## 1. INTRODUCTION

Gully erosion is a major source of fine sediment pollution to the Great Barrier Reef (GBR). This can be inferred from the knowledge that the large, dry, grazing-dominated catchments in the Tropics (e.g. Fitzroy, Burdekin) deliver the largest sediment loads to the GBR (Garzon-Garcia et al., 2015; Joo et al., 2012; Kroon et al., 2012) and from sediment source tracing studies that have indicated that subsurface soil is the predominant sediment source in these catchments, particularly in areas with active gully erosion (Hughes et al., 2009; Olley et al., 2013; Wilkinson et al., 2015). Alluvial gully erosion has been shown to be the dominant form of gully erosion in the Normanby Catchment (Brooks et al., 2013), and while data doesn't exist in any of the other catchments as to the relative contribution of the different gully forms. it is likely that in catchments such as the Bowen River, alluvial gullies are a significant, if not dominant, source. The effects of fine sediment delivery to the GBR go beyond physical impacts (e.g., increased turbidity, reduced light attenuation and smothering of seagrass meadows and corals) and include chemical and biological effects related to the nutrients and organics associated with sediment particles, which are key to the formation of marine snow and the generation of dissolved inorganic nitrogen (DIN), an important driver of crown of thorns starfish outbreaks (Bainbridge et al., 2012; Brodie et al., 2010; Brodie et al., 2012; Wolanski et al., 2008). Consequently, effective management practices should aim at reducing not only sediment yields from alluvial gullies, but also organic and nutrient yields. Understanding key sources of organics and nutrients associated with alluvial gully erosion and their bioavailability is fundamental to inform mitigation management.

In this report, results for various indicators of bioavailable nutrients and organics for three alluvial and one hillslope gully in the Normanby River catchment are presented and analysed. The key indicators were selected based on previous and on-going research conducted by Burton et al., (2015). The differences in various nutrient fractions and organic pools for different gully geomorphic units (e.g., gully bank subsurface soil, terrace soil) and different particle size fractions were examined. Using detailed annual sediment budgets for the three alluvial gullies, the organics and nutrient composition of their geomorphic units and potential contributions from each of these units to sediment export were used to estimate annual export of organics and nutrients from these alluvial gullies. A sensitivity analysis was also carried out to understand the effect of changes in gully depth, sediment yield and geomorphic unit on the relative contributions to organics and nutrient export from alluvial gullies.

# 2. METHODS

# 2.1 Sample collection

Samples have been collected from the gullies and gully geomorphic units listed in **Table C1** and shown in **Figure C3**.

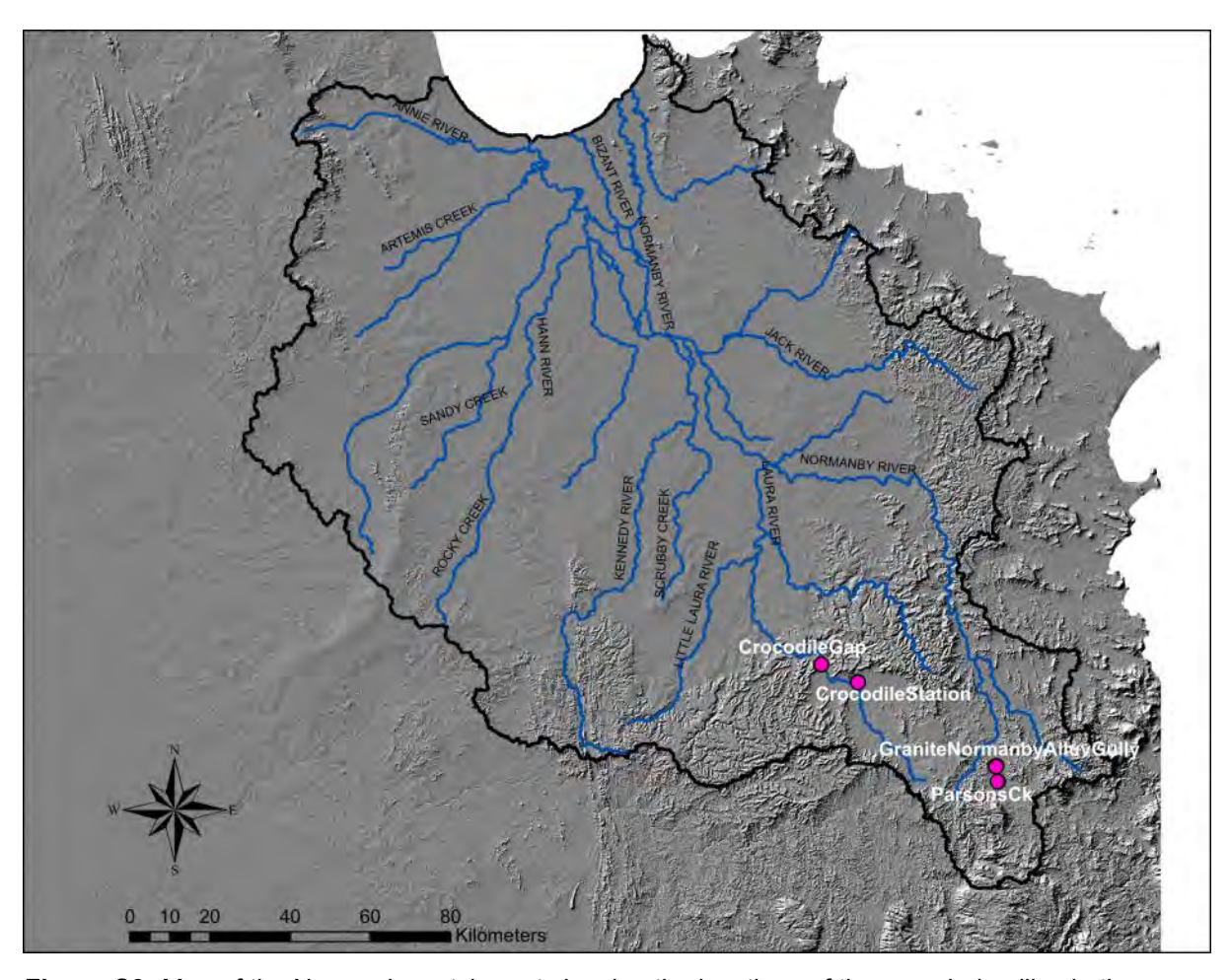


**Figure C3:** Map of the Normanby catchment showing the locations of the sampled gullies in the upper Laura and Normanby Rivers.

Table C1: List of sampled gullies and gully geomorphic units

Gully name	Gully type	Stream	Sampled Geomorphic Unit	Sampling date	Longitude	Latitude	Elevation (m)	Comments			
Granite Alluvial	Granite	Bank subsurface	20/07/2015	144.98599	-15.89717	184	Springvale				
Normanby		Normanby	Bank surface	20/07/2015	144.98624	-15.89703	182	Station.			
			Terrace surface soil	20/07/2015	144.98527	-15.89859	189				
			Gully floor	20/07/2015	144.98658	-15.89730	177				
Parsons Ck	Hillslope	Parsons	Bank subsurface	20/07/2015	144.98962	-15.93184	201	Gully on			
		Creek	Bank surface	20/07/2015	144.98964	-15.93198	203	unnamed tributary of			
			Gully floor	20/07/2015	144.98972	-15.93180	202	Parsons Creek;			
			Hillslope surface soil	20/07/2015	144.98903	-15.93226	202 208 146	which is tributary of Granite Normanby; Springvale Station.			
Laura	Alluvial	Laura	Bank subsurface	21/07/2015	144.67646	-15.70928	146	Alluvial gully on			
Crocodile Station		River	Bank surface	21/07/2015	144.67648	-15.70931	147	Laura River; Crocodile			
Cidion			Terrace surface soil	21/07/2015	144.67619	-15.70949	149	Station. Gully			
			Gully floor	21/07/2015	144.67643	-15.70923	146	rehabilitation trial site.			
Laura	Alluvial	Laura	Bank subsurface	22/07/2015	144.59428	-15.66981	115	Alluvial gully on			
Crocodile gap		River	Bank surface	22/07/2015	144.59409	-15.66965	114	Laura River; Crocodile Gap			
3~4			Buried A horizon	22/07/2015	144.59428	-15.66985	115	area.			
			Terrace surface soil	22/07/2015	144.59420	-15.66954	116				
			Gully Floor	22/07/2015	144.59445	-15.66995	116				



**Figure C4:** Bank subsurface geomorphic unit in the Granite Normanby alluvial gully and Laura Crocodile gap alluvial gully.

Different gully geomorphic units and corresponding sampling methods are described as follows:

- Bank subsurface: Subsurface soil (excluding the organic A horizon), which was visually differentiated on exposed gully banks was sampled. First the gully wall was cleaned and then a sample was collected using a shovel or trowel.
- Bank (or gully wall) surface: The organic A horizon, which was visually differentiated on exposed gully banks was sampled. First the gully wall was cleaned and then a sample was collected from the gully bank surface (0-10 cm) using a trowel and spade.



**Figure C5:** Bank surface geomorphic unit in the Granite Normanby alluvial gully (clearly differentiated by colour from the bank subsurface unit).

 Buried A horizon: In the Crocodile Gap gully a distinct buried A horizon was sampled from the gully bank. First the sampling wall was cleaned and then a sample was collected from the buried A horizon using a trowel and spade.



Figure C6: Buried A horizon geomorphic unit in the Laura Crocodile Gap alluvial gully.

• Terrace: Alluvial gullies are developed by the erosion of previously deposited material in river terraces. Terrace surface soil samples were taken from deposits not affected by gully erosion by removing any vegetation from the surface of the soil and then collecting the surface soil (0-10 cm) using a trowel and spade. Material at these sites is assumed to represent bank surface material prior to any influence from gullying. Hence it is assumed bank/gully wall surface material will have similar characteristics as the terrace surface soil when an active gully scarp migrates through a terrace. The reason for sampling both is that the gully wall surface material is

leached and altered due to its proximity to the gully incision, and so the terrace surface material is assumed to better represent the organic and nutrient status of these soils at the time the soil is first delivered to the gully.



**Figure C7:** Terrace surface soil geomorphic unit in the Granite Normanby and Laura Crocodile station alluvial gullies.

 Hillslope: Hillslope gullies are distinct from alluvial gullies in that they are eroding into colluvial hillslope material. The hillslope sample was taken from intact hillslope material (not affected by gully erosion) by removing any vegetation and litter from the surface of the soil and then collecting the surface soil (0-10 cm) using a trowel and spade.



Figure C8: Hillslope geomorphic unit in the Parsons Creek hillslope gully

 Gully floor: Deposited sediment in the bottom of gullies was sampled by removing any vegetation from the surface of the soil and then collecting the surface soil (0-10 cm) using trowel and spade.



Figure C9: Gully floor geomorphic unit in the Granite Normanby alluvial gully.

At all sites a composite sample of approximately 5-10kg was collected from various representative locations for each feature.

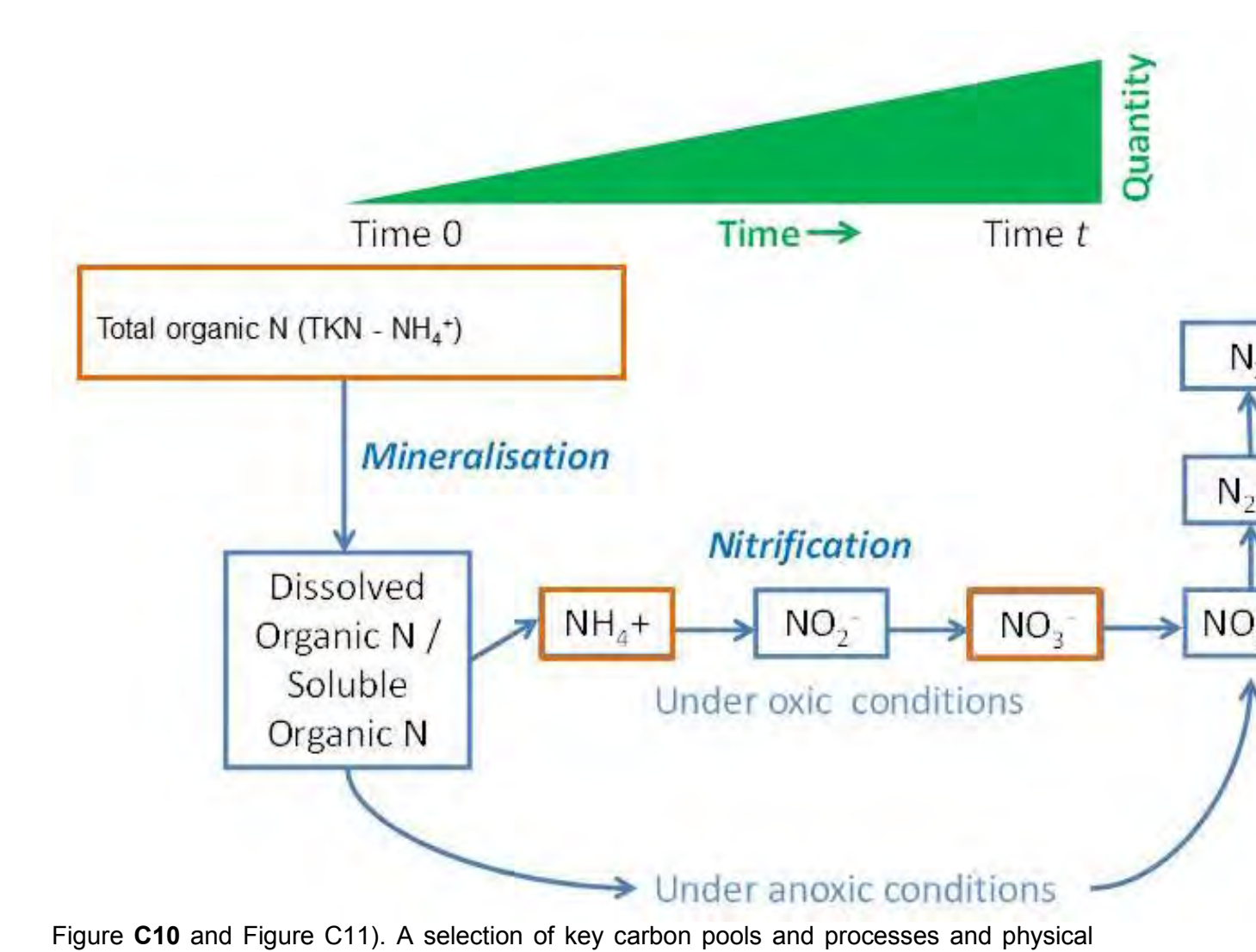
# 2.2 Sampling preparation

The following steps were taken to prepare the samples:

- Organic matter (including litter, roots and charcoal) was removed from whole soil samples. Soil lumps were broken down by hand to as small as possible and samples were then air dried at 40°C. Once air-dried, samples were checked a second time to remove any remaining organic matter and then mixed well.
- The sample was then processed through a jaw crusher set to 2 mm. Any organic matter found was removed. The sample was then mixed well.
- Once mixed, this sample was split into three sub-samples
- Sub-sample 1 was processed through a 2mm sieve and used for whole soil/sediment lab analysis in the Chemistry Centre DSITI and the analyses described in Table 2 were conducted.
- Sub-samples 2 and 3 were further processed to separate the <63 um and <10um fraction respectively, using the standard laboratory method for water-dispersible clay and the appropriate settling time based on Stoke's Law. Following separation, the <63 um and <10um fractions were each dried at 40°C and then gently mixed and homogenised using a mortar and pestle. Following this, the samples were submitted to the DSITI Chemistry Centre and the analyses listed in Table 2 were conducted on each particle size fraction.</li>

# 2.3 Sample analysis

Nitrogen (N) and phosphorus (P) analyses conducted in this project cover key pools and processes in the nitrogen and phosphorus cycles (



also

measured

parameters

were

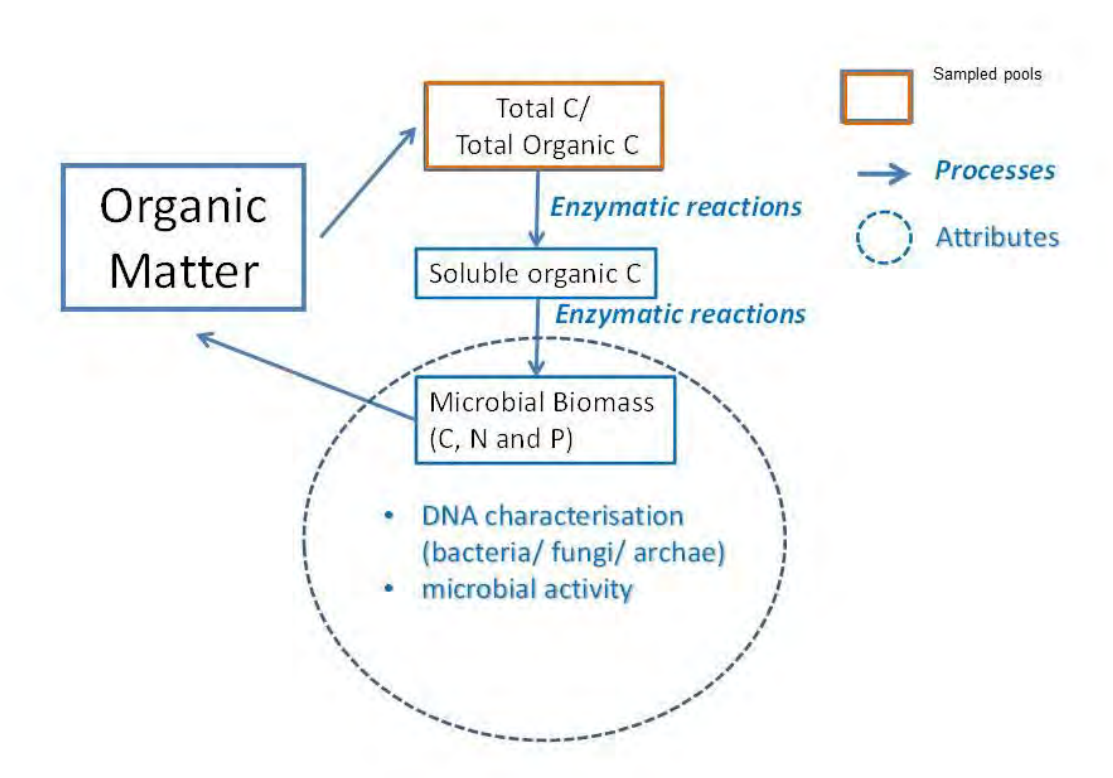
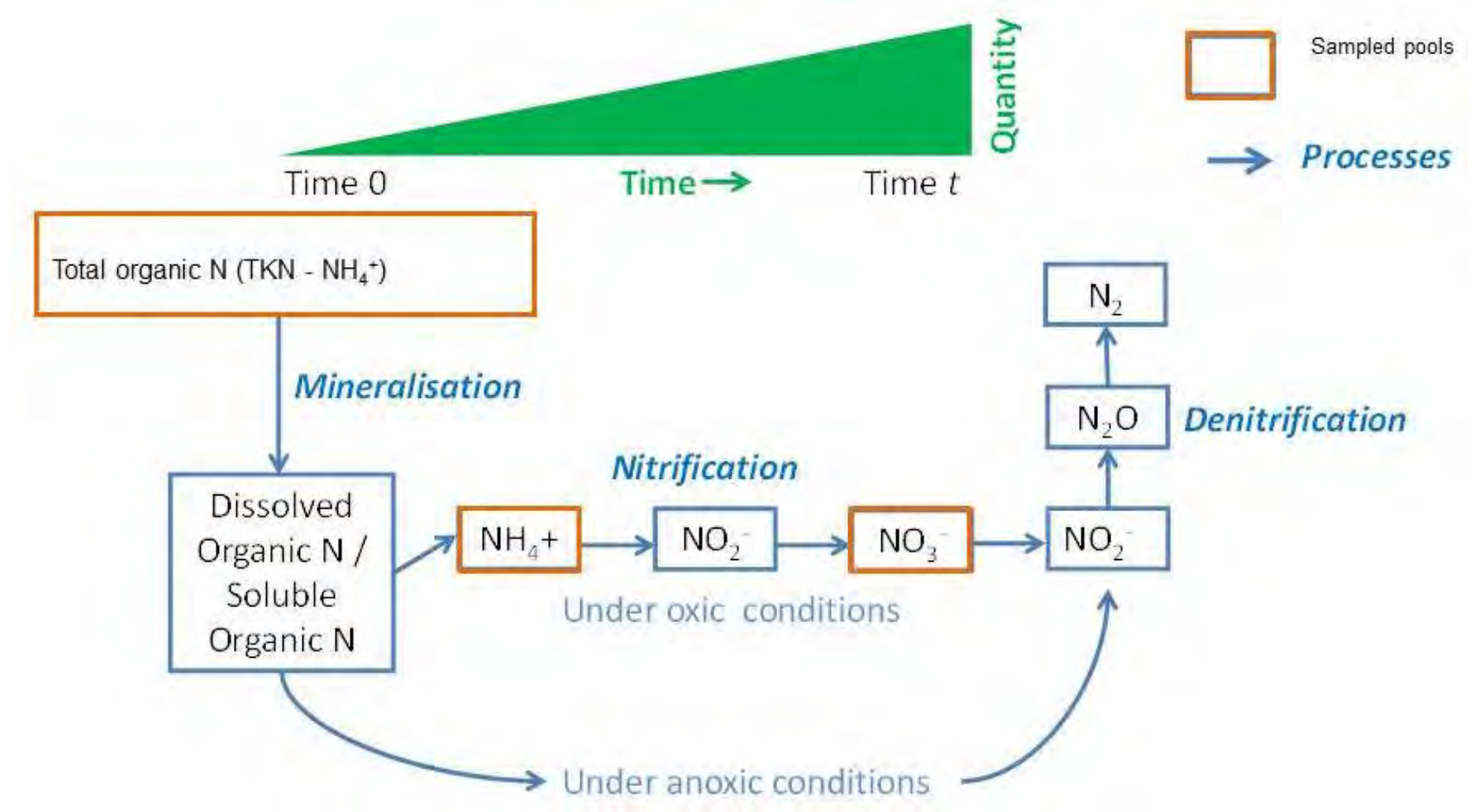


Figure **C12**). These parameters will be used to explain N and P pools and their bioavailability in the studied gullies and gully geomorphic units. The parameters analysed are summarised in Table C2 with full methods and references provided in Appendix A. Equivalencies to water quality metrics are presented in Box 1.



**Figure C10:** Key pools and processes of the nitrogen cycle. The trend of bioavailable nitrogen over time is indicated in the figure (Adapted from Burton et al. 2015).

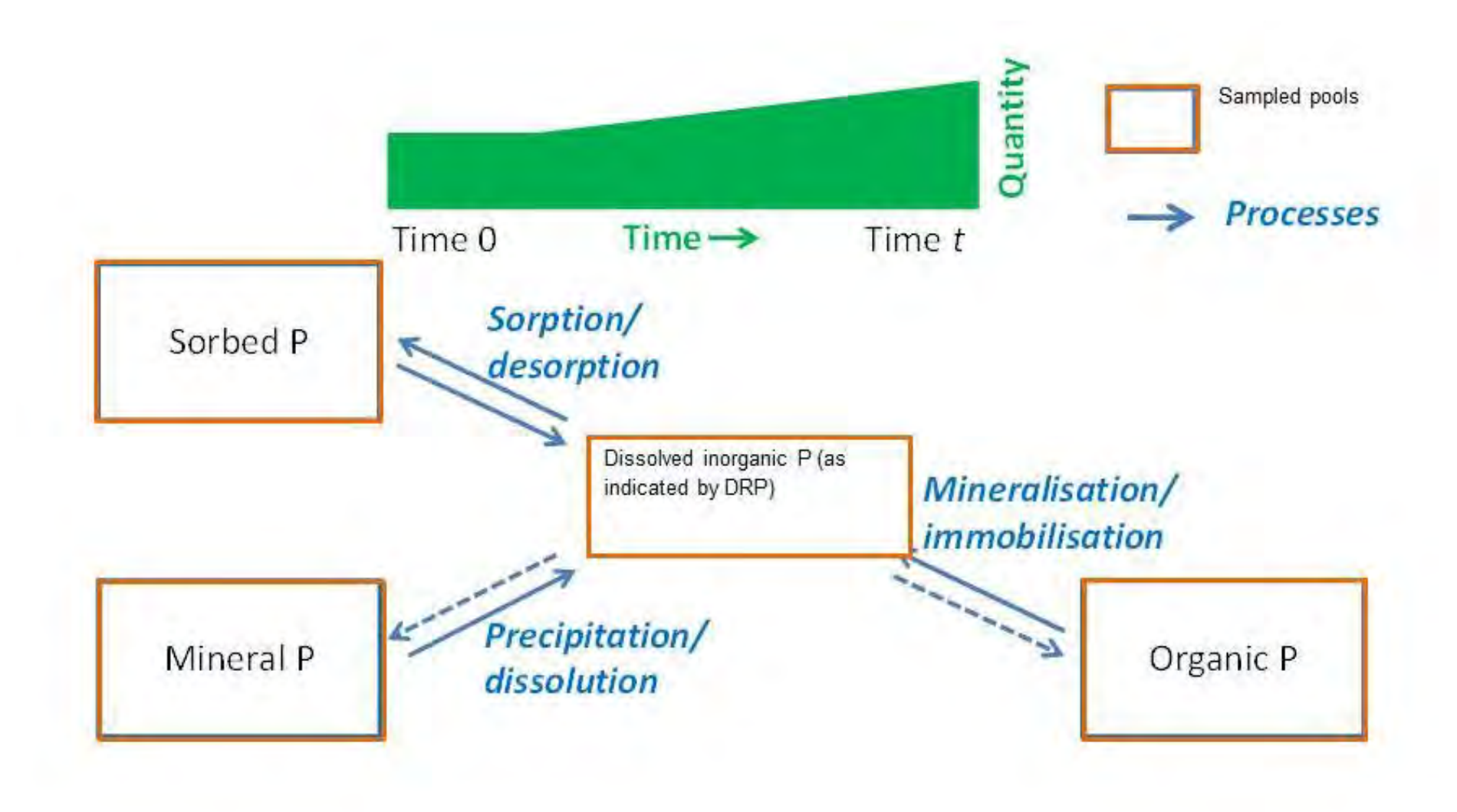


Figure C11: Key pools and processes of the phosphorus cycle. The trend of bioavailable phosphorus over time is indicated in the figure (Burton et al., 2015).

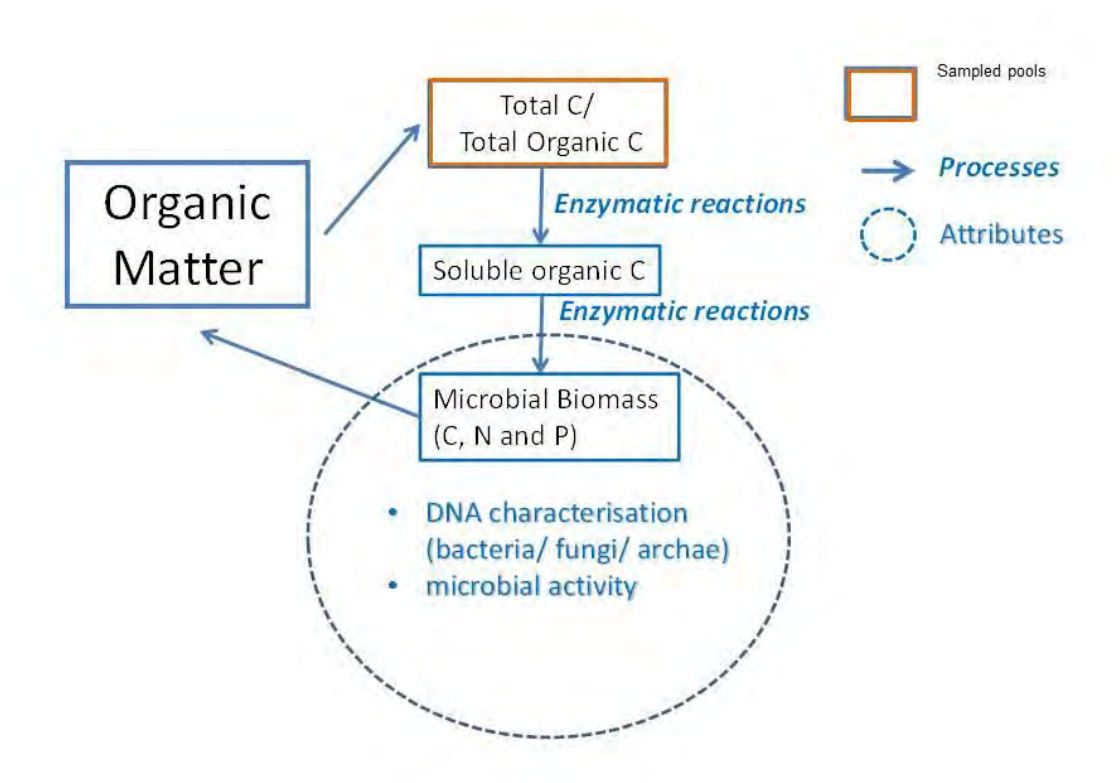


Figure C12: Key pools, processes and attributes of the carbon cycle (Burton et al., 2015).

Box 1. Approximate equivalencies betwe water quality metrics	en soil/sediment chemical parameters and
Soil/sediment parameter	Water quality metric
Total N (TN)	Total nitrogen
Mineral N	No equivalency – Although it quantifies the same fractions as Dissolved inorganic N (DIN) (NO $_3$ <sup>-</sup> N + NH $_4$ <sup>+</sup> -N), mineral N is a KCI extraction on the soil/sediment, which would not equal the potential production of DIN as the sediment/soil mineralizes, it is just an indicator of this
Total P (TP)	Total phosphorus
Sorbed P	No equivalency
Mineral P	No equivalency
DRP	No equivalency

**Table C2:** Nitrogen, phosphorus, carbon and other physical and chemical parameters measured in total soil/sediment, <63um and <10um soil/sediment fractions.

Nitrogen (N)	Phosphorus (P)	Carbon (C)/ organics	Other possible explanatory measures
<ul> <li>Total N (TN)         (refers to the total N pool) –         Measured by the Dumas method</li> <li>Mineral N (directly bioavailable pool)         (refers to NH<sub>4</sub><sup>+</sup>-N plus NO<sub>3</sub><sup>-</sup>-N)</li> <li>NO<sub>3</sub><sup>-</sup>-N (directly bioavailable pool that is extracted by the KCI method)</li> <li>NH<sub>4</sub><sup>+</sup>-N (directly bioavailable pool – that is extracted by the KCI method)</li> </ul>	Total P (TP) (refers to the total P pool) – Measured by the total Kjeldahl P method Sorbed P (refers to the P sorbed to the soil/sediment surface that is extracted by the Colwell-P method) Mineral P (refers to P that is part of the soil/sediment mineral matrix. It is calculated as BSES-P minus Colwell-P) Phosphorus Buffer Index (PBI) (an indicator of how tightly sorbed P is bound to the soil/sediment surface) Dissolved reactive P calculated (DRP) (calculated as Colwell-P/PBI)	Total C (includes both the organic and inorganic C) Total organic carbon (TOC)  Total organic carbon (TOC)	Particle size (laser diffraction)     Oven dry moisture (105)

## 3. RESULTS AND DISCUSSION

This report presents the results and interpretation of key carbon (C), nitrogen (N) and phosphorus (P) parameters measured in soils and sediments from a limited number of alluvial gullies (3) and one hillslope gully in the Normanby River catchment. Considering the low level of replication, results are to be considered only as an indication of the range of values that might comprise the nutrient and organic carbon pool in these gullies as well as the range of organics and nutrients exported from these types of gullies in the Normanby catchment. Consequently they should not be extrapolated.

To increase confidence in the range of bioavailable nutrient and organics present and exported from different gully types, further sampling would need to be undertaken to increase the number of replicates.

# 3.1 Bioavailable nutrients and organics in alluvial gullies

There were no large differences in most of the total nutrient and organic soil pools (TOC and TN) between gullies and gully types (alluvial versus hillslope). Most of the gullies had very low or undetectable TP. The statistics for all bioavailable nutrient and organics indicators by gully type (alluvial versus hillslope) are summarised in Table **C3**, Figure C13 and Figure C14. Data for all sampled gullies and geomorphic units are presented in Appendix 2.

Some of the differences found in bioavailable nutrient indicators between gullies follow:

- The alluvial Laura Crocodile station gully had larger bioavailable N fractions including NH<sub>4</sub><sup>+</sup>-N (5-8 times larger), NO<sub>3</sub><sup>-</sup>-N (2-3 times larger) and mineral N (3-4 times larger) in the finer fractions than the other gullies. Factors known to affect bioavailable N in soils/sediment include biomass input, wet and dry cycles, vegetation type, and external inputs (e.g. manure, urine), among others (Austin et al., 2004; Evans et al., 2006; Garten and Ashwood, 2002; Gomez et al., 2012; Manzoni et al., 2010). Larger bioavailable N fractions in the Laura Crocodile station gully compared to other gullies could be driven by a larger contribution of organic material and nutrients from the surrounding terrace unit at this site compared to others (Appendix 2). The terrace unit in this gully had higher NH<sub>4</sub><sup>+</sup>-N values than other gully terrace units. Further investigation of the factors listed above is required to improve our understanding of differences in bioavailable N among different gullies/gully types.
- The alluvial Granite Normanby gully had higher TP and sorbed P values in the <10 um fraction, and higher DRP values in all fractions compared to the other gullies (in all gully components). Mineral P was only present in this gully. Such differences could be caused by differences in the parent material of soils/sediments present in this gully. However, there are no differences in the underlying or headwater geology, therefore further investigation is required.</li>

#### **Key summary points of information:**

 The data indicate little difference between bioavailable nutrient indicators in different hillslope and alluvial gullies for all studied size fractions— however it must be remembered that we have limited replication of alluvial gullies and no replication of hillslope gullies, therefore further investigation is necessary to confirm this result.

Table C3: Summary statistics for bioavailable nutrient and organics indicators by gully type and particle size fraction (ND: Non-detectable, NA: Not available)

		TOC (%)			TN(%)			NH4-N air.dry (mg/kg)			NO3-N air dry (mg/kg)				Mineral N (mg/kg)						
<b>Gully type</b>	<b>Size Fraction</b>	Mean	SD	Rar	nge	Mean	SD	Rar	nge	Mean	SD	R	ange	Mean	SD	Ra	nge	Mean	SD	Ra	nge
Alluvial	<10 um	1.71	1.98	0.06	5.44	0.20	0.19	0.04	0.62	20.38	43.09	2.00	161.00	53.92	68.42	6.00	226.00	74.31	105.37	8.00	387.00
Alluvial	<63 um	0.94	1.13	0.04	3.24	0.11	0.10	0.03	0.31	18.78	31.47	3.00	100.00	19.80	20.39	2.00	69.00	36.40	43.52	5.00	139.00
Alluvial	Total	0.78	0.94	0.01	3.14	0.09	0.06	0.04	0.20	4.33	2.88	2.00	10.00	3.43	0.98	2.00	5.00	5.00	3.20	2.00	13.00
Hillslope	<10 um	1.69	1.64	0.14	3.82	0.16	0.12	0.04	0.32	11.33	10.41	3.00	23.00	17.00	9.49	8.00	29.00	27.33	21.73	11.00	52.00
Hillslope	<63 um	0.74	0.97	0.06	2.16	0.12	0.09	0.05	0.18	13.00	0.00	13.00	13.00	7.33	3.79	3.00	10.00	16.00	6.00	10.00	22.00
Hillslope	Total	0.44	0.50	0.04	1.15	0.05	0.03	0.03	0.07	ND	ND	ND	ND	12.00	NA	12.00	12.00	12.00	NA	12.00	12.00

			TKP (%)			Colwell P (mg/kg)					DRP (mg/kg)						
<b>Gully type</b>	<b>Size Fraction</b>	Mean	SD	R	ange	Mean	SD	Ra	nge	Mean	SD	Ra	nge	Mean	SD	Rai	nge
Alluvial	<10 um	0.04	0.02	0.02	0.09	12.38	15.14	2.00	57.00	137.62	75.96	46.00	291.00	0.12	0.14	0.01	0.41
Alluvial	<63 um	0.02	0.01	0.02	0.04	6.54	4.96	1.00	18.00	66.00	37.39	24.00	161.00	0.14	0.13	0.02	0.43
Alluvial	Total	0.02	0.01	0.02	0.04	5.46	6.05	1.00	24.00	31.15	19.55	8.00	83.00	0.24	0.17	0.04	0.63
Hillslope	<10 um	0.02	NA	0.02	0.02	3.00	1.41	1.00	4.00	96.00	27.24	56.00	117.00	0.05	0.02	0.03	0.07
Hillslope	<63 um	ND	ND	ND	ND	2.25	0.50	2.00	3.00	31.25	22.49	7.00	57.00	0.12	0.11	0.04	0.29
Hillslope	Total	ND	ND	ND	ND	1.50	1.00	1.00	3.00	16.00	11.60	5.00	31.00	0.16	NA	0.16	0.16

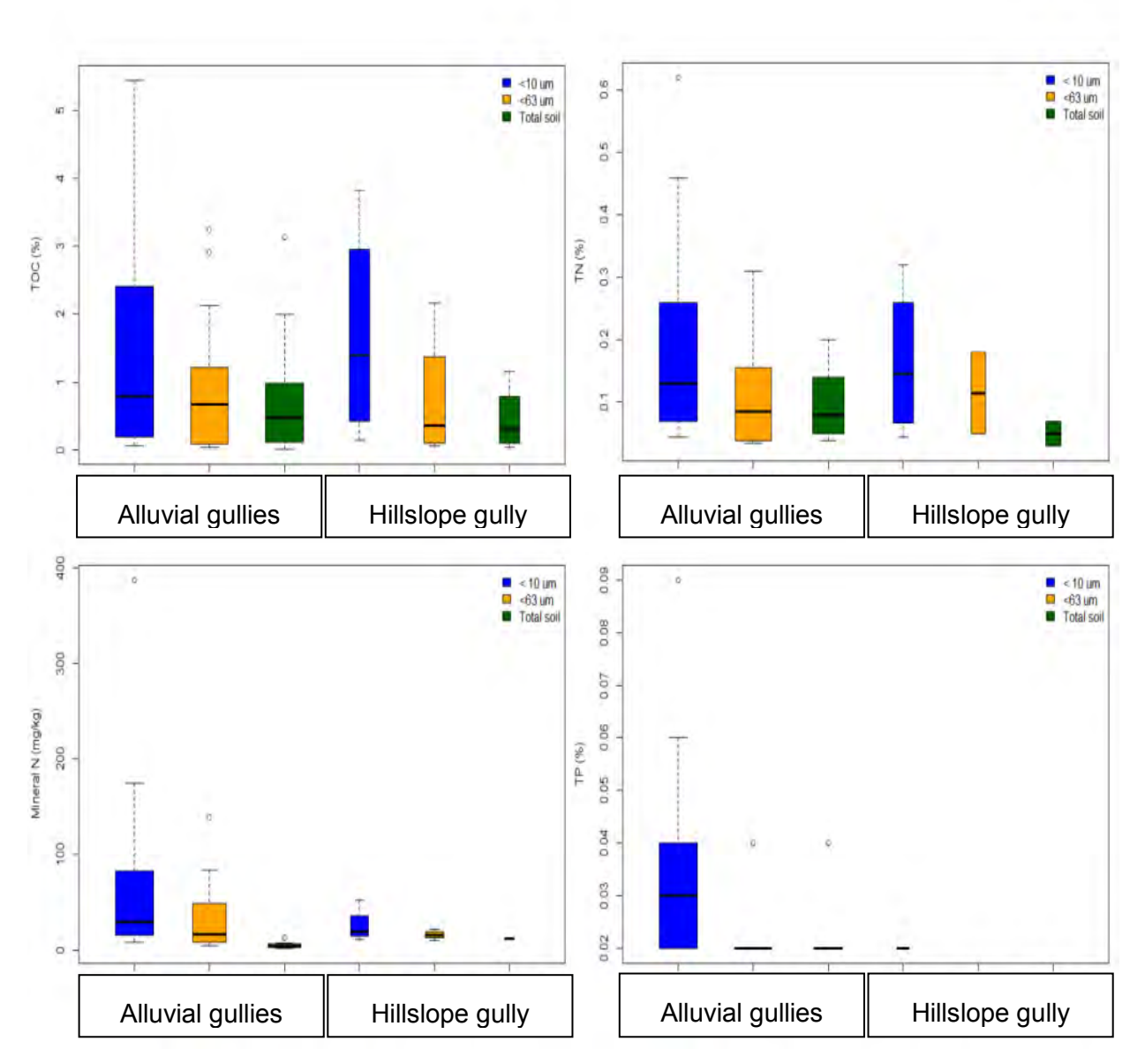


**Figure C13:** Percent total organic carbon (TOC), total nitrogen (TN), mineral N and total phosphorus (TP) in alluvial and hillslope gully soil/sediment for the total (green), <63 um (yellow) and <10 um (blue) particle size fractions. Boxes are intersected by median values and enclose data between the first and third quartiles, with lines extending to maximum and minimum values excluding outliers (values above and below 1.5 times the inner quartile range from the first and third quartiles, respectively). Box width is proportional to the square root of n for each group. Absence values indicate the parameter was non-detectable in any of the samples.

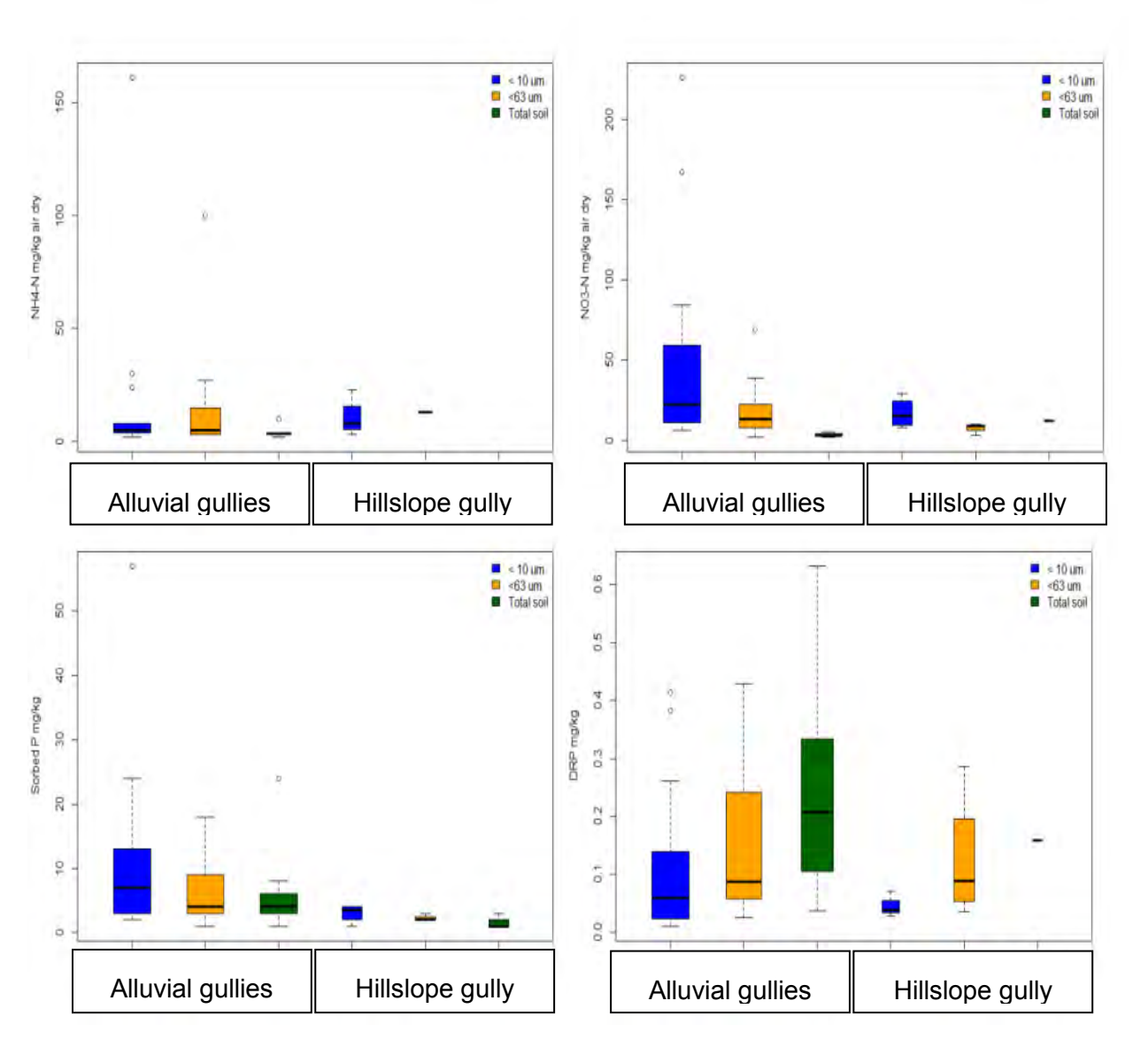


**Figure C14:** Ammonium (NH<sub>4</sub>-N), nitrate (NO<sub>3</sub>-N), sorbed phosphorus (P) and dissolved reactive phosphorus (DRP) in alluvial and hillslope gully soil/sediment for the total (green), <63 um (yellow) and <10 um (blue) particle size fractions. Boxes are intersected by median values and enclose data between the first and third quartiles, with lines extending to maximum and minimum values excluding outliers (values above and below 1.5 times the inner quartile range from the first and third quartiles, respectively). Box width is proportional to the square root of n for each group. Absence values indicate the parameter was non-detectable in any of the samples.

# 3.2 Bioavailable nutrients and organics in different geomorphic units of alluvial gullies

There are clearer differences between different gully components than between gully types (alluvial versus hillslope) for most parameters (TOC, TN, TOC:TN ratios, mineral N, DRP and TN:TP ratios) (Figure C15 and Figure C16 versus Figure C13 and Figure C14). Summary statistics for bioavailable nutrients and organics indicators by geomorphic unit and particle size fraction are presented in Appendix 3.

Irrespective of particle size the terrace geomorphic unit had significantly higher TOC and TN values followed by hillslope and bank surface geomorphic units (Figure C15). TOC soil content in the terrace unit was from 54 to 77 times larger (depending on particle size fraction) and TN from 5 to 10 times larger than in bank subsurface soil in alluvial gullies (

Figure **C17**a). The presence of trees in terraces and the hillslope, which would contribute organic matter inputs to the soil, and the fact that there is a thin A soil horizon layer that has not been completely eroded in these units, would explain the larger presence of C and N pools in this unit as compared to the others. Interestingly, TN values in the terrace soils were similar to average TN values found in fertilized cane and banana soils in the Wet Tropics (Burton et al., 2015). Mineral N values, though 1.7 to 2.0 times lower in the total soil fraction, were 1.5 times higher in the <10um fraction in the terrace soils compared to cane and banana soils in the Wet Tropics (Burton et al., 2015).

The gully floor and bank subsurface had the lowest values for most parameters (TOC, TN, TP and TOC:TN values), which was expected (Figure C15). Previous research indicates that organic C in subsurface soil, the main likely source of gully floor sediment, is highly stabilized with most labile carbon already processed by microorganisms (Fontaine and Barot, 2005; Fontaine et al., 2007). It is likely that the very low presence of fresh organic matter in subsoils is driving the low TOC:TN ratio in the subsoils compared with surface or terrace soils. The gully floor sediment tended to be enriched in TOC compared to the bank subsurface (from 2 to 6 times higher content depending on particle size fraction in alluvial gullies) (

Figure **C17**b), and to have higher TOC:TN ratios. It is likely this is caused by the enrichment of gully floor sediment with vegetation litter while it sits in the gully floor (Garzon-Garcia et al., 2014). Gully floor sediment also had higher DRP (Figure C16,

Figure C17b). A larger proportion of fine sediment in the gully floor does not seem to be the main factor controlling these higher values, as the proportion of fine fraction was only slightly higher for the <10 um fraction in the alluvial Granite Normanby gully. All other gullies have lower amounts of fines than the bank subsurface (See fine content for different geomorphic units and gullies sampled in Appendix 4). The higher TOC and DRP values are likely to be the result of accumulation of organics and their associated nutrients that have moved from the landscape and accumulated in the gully floor. Similar results have been found in hillslope gullies of subtropical Queensland (Garzon-Garcia et al., 2014).

The buried A horizon in the alluvial Laura Crocodile gap gully and the bank surfaces in all gullies were very similar in all parameters, except for PBI, extractable nitrate and ammonium, which were higher in the former, and DRP, which was lower (Figure C16). This gully feature is different in its most bioavailable nutrient fractions most likely because of more frequent contact with water. These results indicate that when present, the buried A horizon should be considered as a separate geomorphic unit for sampling of bioavailable nutrients until there is enough replication to verify these findings.

The concentration of the most available forms of nitrogen ( $NO_3$ -N and  $NH_4$ <sup>+</sup>-N – i.e. mineral N) were higher in the finer fractions of the terrace geomorphic unit compared to other unit fine fractions (Figure C16). The lowest extractable nitrate concentrations from the finer fractions occurred for the bank subsurface and the lowest extractable ammonium concentrations for the gully floor and bank subsurface units. Nitrate in the terrace fine soil was on average 5 to 17 times higher and ammonium was 24 times higher in the <10 um fraction, when compared with bank subsurface soil fine fractions in alluvial gullies (

Figure **C17**a). These findings indicate that the terrace geomorphic unit in the sampled alluvial gullies is an important store of bioavailable forms of nitrogen in its fine soil fractions.

The fine sediment fractions of the gully floor were slightly more enriched with extractable  $NO_3$ -N (from 2 to 4 times higher content depending on particle size fraction), sorbed P (2 times higher) and DRP (2 times higher) compared to the bank subsoil fine fractions. The <10 um fraction of the gully floor was more enriched with TN (1.3 times higher) and had higher PBI values and TN:TP ratios compared to the bank subsurface soil <10 um fraction (

#### Figure C17b).

Sorbed P and DRP concentrations were higher in the terrace geomorphic unit followed by the gully floor (Figure C16). The TP was more enriched in the finer fraction of the terrace geomorphic unit compared to the other units (Figure C15). These findings indicate that the terrace is also an important store of phosphorus in the sampled alluvial gullies, which have low contents of this element overall.

It is important to note here that the parameters that are being measured, though considered indicators of nutrient bioavailability, are not direct measurements of the quantities of bioavailable nutrients from different sources that would be contributed in the aquatic environment (Burton et al. 2015). For example, as can be inferred from mass balances (subtraction of the inorganic nitrogen fraction from the total nitrogen fraction), the majority of the nitrogen in these soils/sediments is in organic form (more than 96% for all geomorphic units and particle sizes). The relative bioavailability of this organic fraction from different geomorphic unit sources and particle size fractions, combined with their selectivity for erosion and transport, would determine the relative geomorphic unit source impact in the streams receiving this sediment and ultimately, their relative impact in the Great Barrier Reef.

#### 3.2.1 The role of particle size

Most bioavailable nutrients and organics indicators including TOC, TN,  $NH_4^+$ -N,  $NO_3^-$ -N, mineral N, sorbed P and PBI generally increased their concentration as the particle size reduced. Average enrichment ratios (nutrient parameter in the fine fraction / nutrient parameter in the total soil) for all gullies sampled, between the total soil and the <63 um and <10um particle size fractions and for all nutrient and organics bioavailability indicators are presented in Figure C18. Values greater than 1 indicate enrichment in the finer fractions.

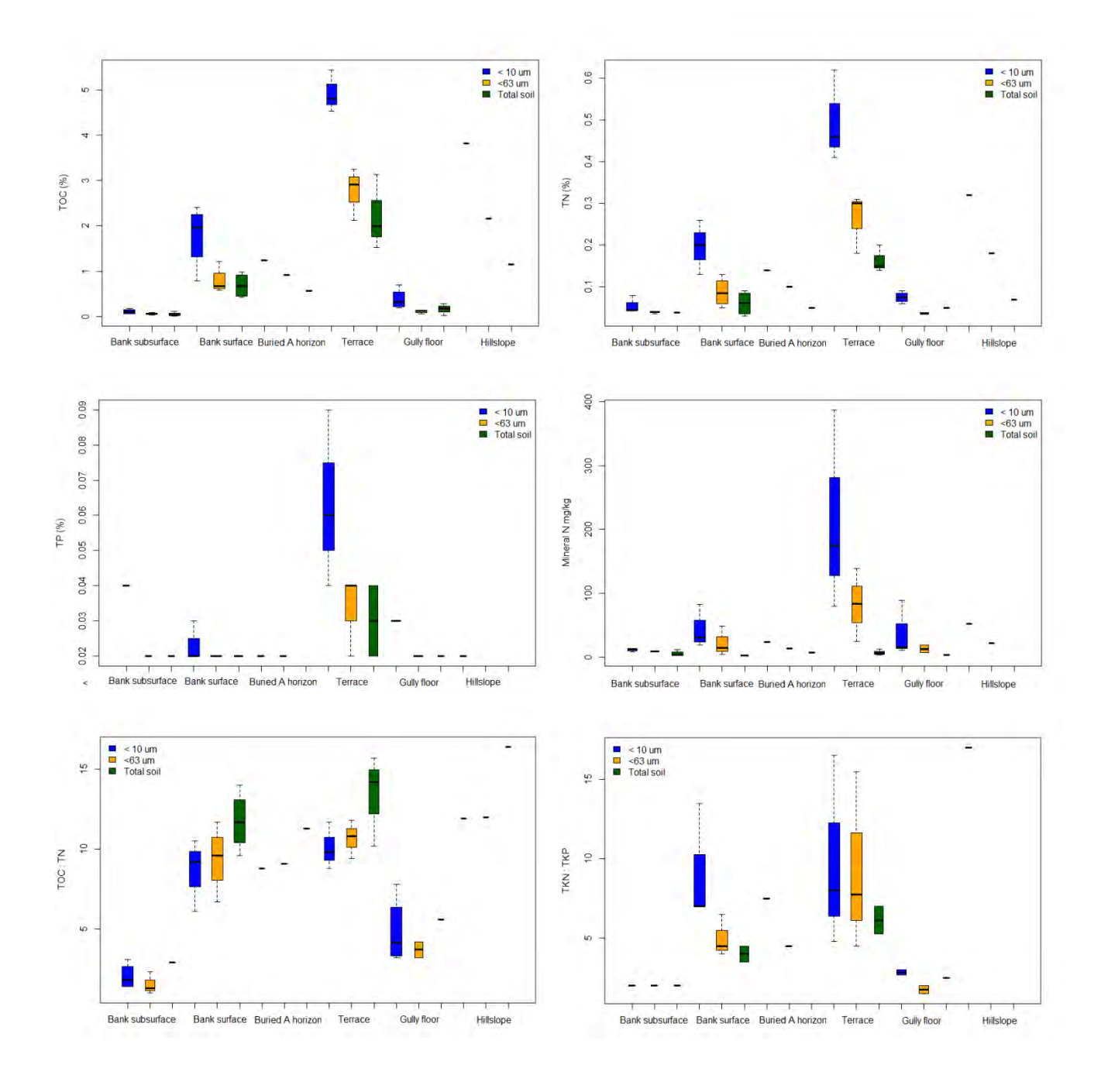
A larger enrichment in nitrogen with fraction size reduction compared to carbon or phosphorus was found, evident in a lower TOC:TN ratio in both fine fractions and a larger TN:TP ratio in the <10 um fraction (Figure C18).

The largest enrichments with particle size reduction occurred for the most bioavailable fractions of nitrogen, with enrichments of 10 to 24 times on average for  $NO_3^--N$  and 6 to 7 times on average for  $NH_4^+-N$  (Figure C18). Average mineral N enrichment in the <10 um fraction in these soils/sediments was larger than the enrichment found in some banana, cane and dairy soils for the same fraction in the Wet Tropics (2.0 to 2.6 times larger enrichment ratios) (Burton et al., 2015).

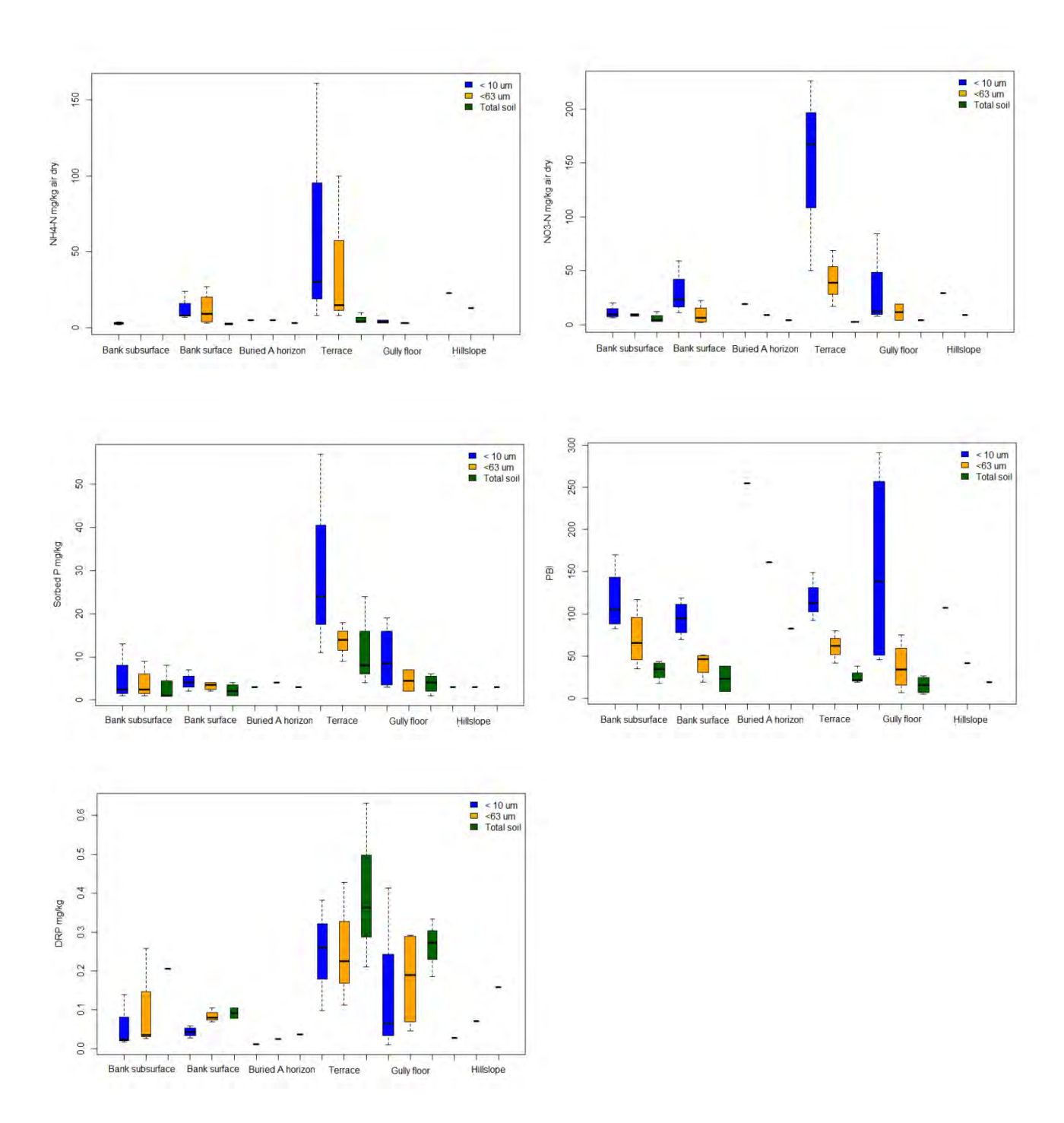
Although sorbed P increased in the <10 um fraction by 2 times on average, the PBI, which is an indicator of how tightly P is bound to the sediment surface, increased by 7 times. This is the reason why the DRP is the only measure of bioavailable nutrients that reduced for smaller particle sizes (Figure C18).

#### **Key summary points of information:**

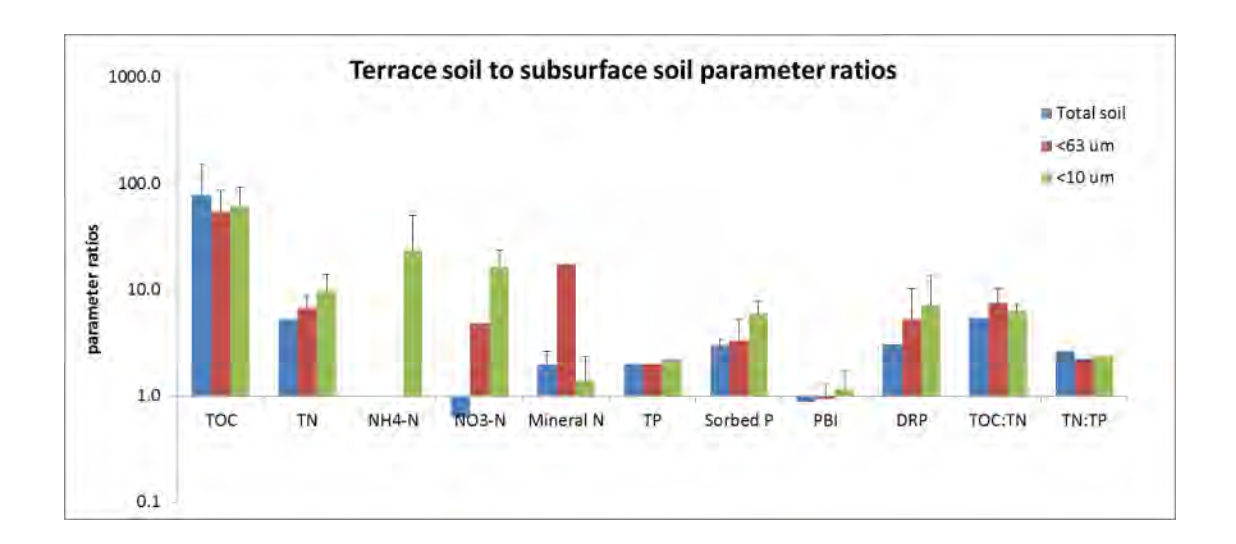
- There are significant differences in C, N, and P content between the geomorphic units
  measured with the general pattern being terrace>surface>gully floor>subsurface. This
  result indicates that accurate estimation of nutrient and organic losses from gullies
  will rely on sampling and analysing all the different units.
- Terraces appear to be an important long term store of bioavailable nutrients and organics, whilst gully floors may act as a temporary store depending on gully evolution.
- Particle size also significantly influences nutrient and organic content and would influence bioavailability; it must therefore be included in design and analysis of future studies.
- The <10um fraction is generally enriched in bioavailable nutrients compared to the <63um fraction, which is generally enriched compared to whole soil irrespective of gully geomorphic unit (with some exceptions e.g., DRP). These results from gullies in the Normanby catchment are consistent with results from key soil types in the Burdekin and Johnstone catchments (Burton et al., 2015).</p>



**Figure C15:** Percent total organic carbon (TOC), total nitrogen (TN), total phosphorus (TP), mineral N (mg/kg),TOC:TN ratio and TN:TP ratio by gully geomorphology component for the total (green), <63 um (yellow) and <10 um (blue) particle size fractions. Boxes are intersected by median values and enclose data between the first and third quartiles, with lines extending to maximum and minimum values excluding outliers (values above and below 1.5 times the inner quartile range from the first and third quartiles, respectively). Box width is proportional to the square root of n for each group. Absence values indicate the parameter was non-detectable in any of the samples.



**Figure C16:** Ammonium (NH4-N), nitrate (NO3-N), sorbed P, phosphorus buffer index (PBI) and dissolved reactive P (DRP) by gully geomorphology component for the total (green), <63 um (yellow) and <10 um (blue) particle size fractions. Boxes are intersected by median values and enclose data between the first and third quartiles, with lines extending to maximum and minimum values excluding outliers (values above and below 1.5 times the inner quartile range from the first and third quartiles, respectively). Box width is proportional to the square root of n for each group. Absence values indicate the parameter was non-detectable in any of the samples.



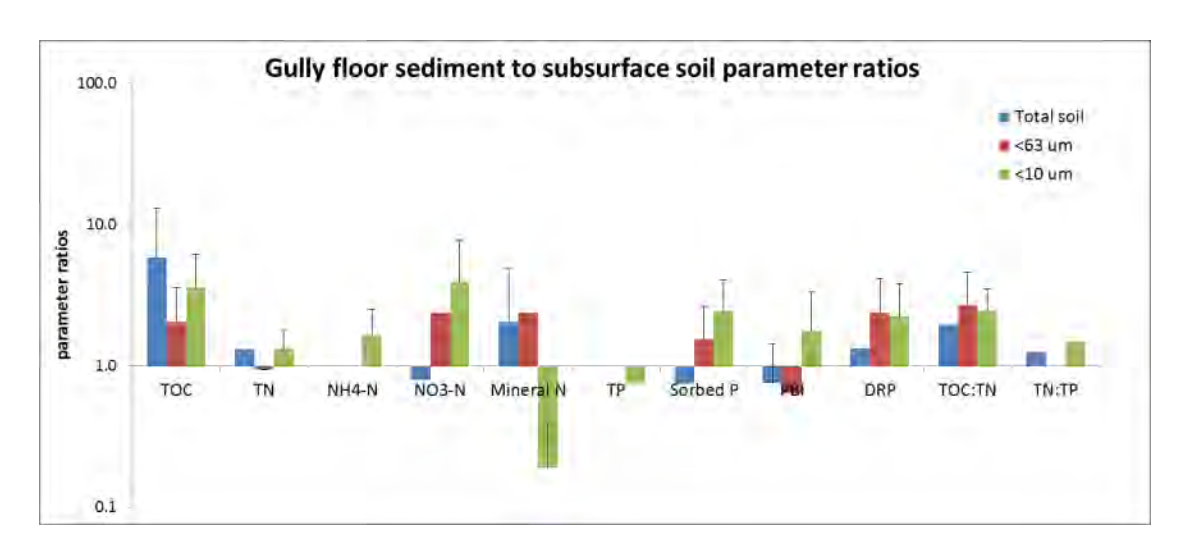


**Figure C17:** Enrichment ratios between (a) terrace surface soil and bank subsurface soil and (b) gully floor sediment and bank subsurface soil, for various nutrient and organics parameters in the total soil, and fine fractions (<63 um and <10 um) of alluvial gullies sampled in the Normanby catchment.

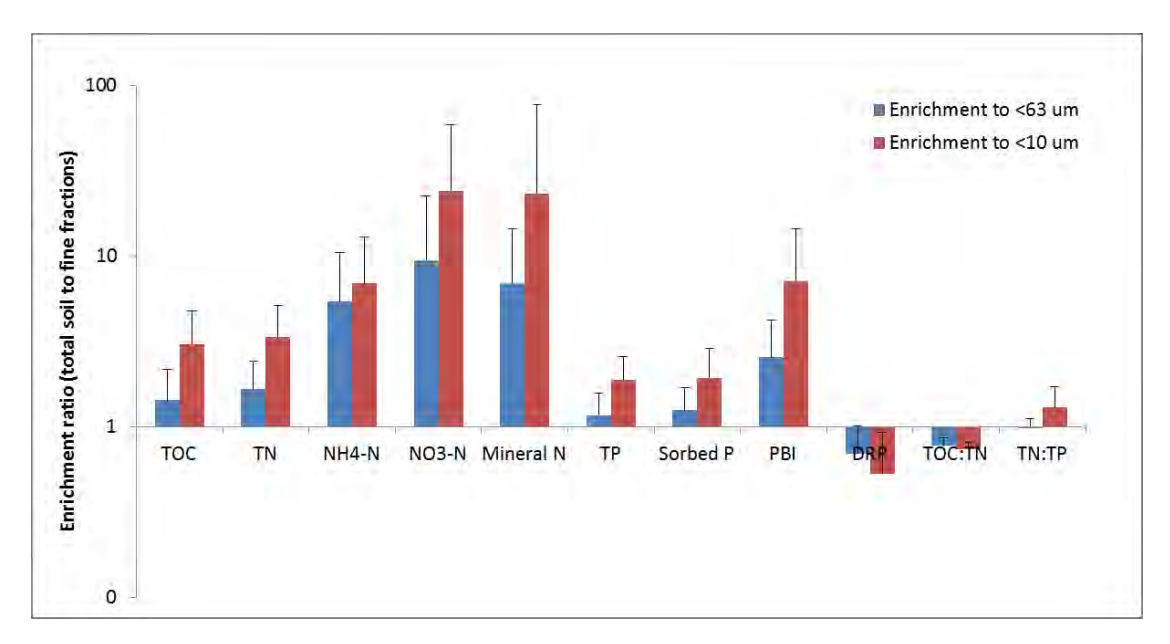


**Figure C18:** Enrichment ratio of various nutrient and organics bioavailability indicators in the fine fractions (<63 um and <10 um) of gullies sampled in the Normanby catchment.

## 3.3 Bioavailable nutrients and organics export from alluvial gullies

The key sources of organics and nutrients exported from alluvial gullies at any point in time would depend on geomorphic unit contents at source and their relative contributions to exported sediment. To understand how the key sources may change between different alluvial gullies we have developed mass balances of organics and nutrient export using detailed knowledge of sediment yields and hypothetical source contributions based on experience, for the three alluvial gullies sampled in this study.

To understand how the key sources may change during different stages of gully evolution, we have also developed a sensitivity analysis to source contribution for a hypothetical alluvial gully using the average of geomorphic unit contents for the three sampled alluvial gullies (Table 3).

Considering that there is not enough information at this time on particle size fraction export from these gullies, it was assumed that there was no selectivity in particle size fraction transport and thus the total soil organics and nutrient fraction values were used for the budgets. Considering finer sediment fractions were found to be enriched in organics and nutrients, results presented here are likely an underestimation of export from these gullies.

#### 3.3.1 Case study 1: Granite Normanby alluvial gully

Here we present annual sediment yields for the Granite Normanby alluvial gully as well as hypothetical breakdown of key source contributions to sediment export. In this gully, a secondary incision has eroded the rich gully floor material of the primary gully incision. This type material, considered to be similar to the bank surface soil, was not sampled as part of the gully floor geomorphic unit. Only the secondary incision floor was sampled. Considering

this, for the organics and nutrient export budgets it was assumed that the primary incision gully floor had similar characteristics to the bank surface geomorphic unit.

**Table C4:** Observed erosion rate from gully 2011-2015 and estimated contributions from each source component.

	m <sup>3</sup>	t	t/yr	gully area (ha)	sediment yield (t/ha/yr)
Headscarp retreat	255.5	408.8	102.2		
Gully Floor Incision	69.3	110.9	27.7		
Total	324.8	519.7	129.9	1.14	114.0
	typical dept	h (m)			
headscarp	3.5				
2ndry incision	2				
Estimated breakdown of component contribution	Headscarp retreat	2ndry Incision			
terrace surface	0.05	0			
bank surface	0.05	0			
sub-surface	0.85	0.9			
gully floor (secondary)	0.05	0			
gully floor (primary)	0	0.1			

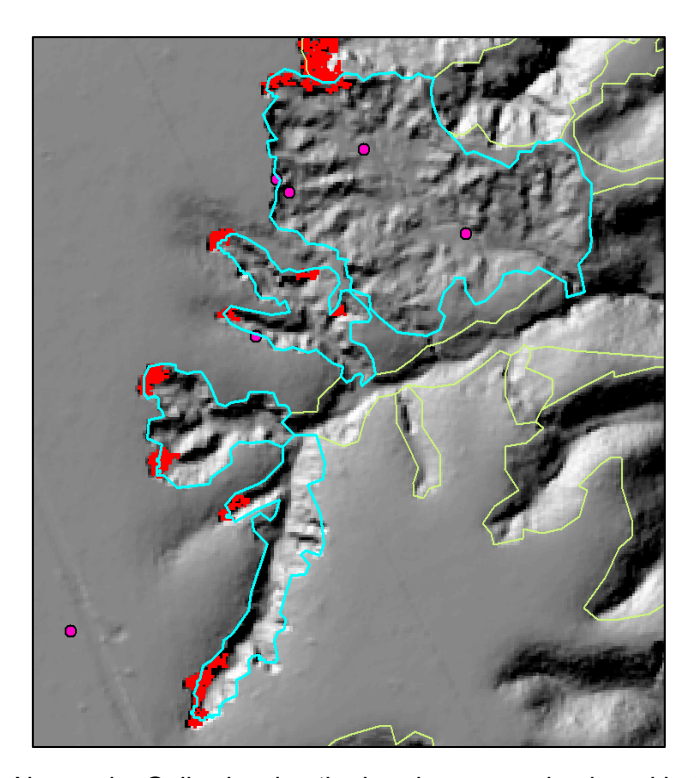


**Figure C19:** Granite Normanby Gully showing the headscarp erosion in red between 2011 & 2015. Also shown (purple dots) are the sample locations for the gully. Note that the erosion detected by the aerial LiDAR in this gully is an absolute minimum amount of erosion due to the conservative limit of detection applied (0.5m change).

Estimated annual mass contributions to sediment, organics and nutrient export from different geomorphic units in the Granite Normanby alluvial gully are presented in Figure C20. Percent contributions of exported fractions from geomorphic units are summarized in Figure C21.

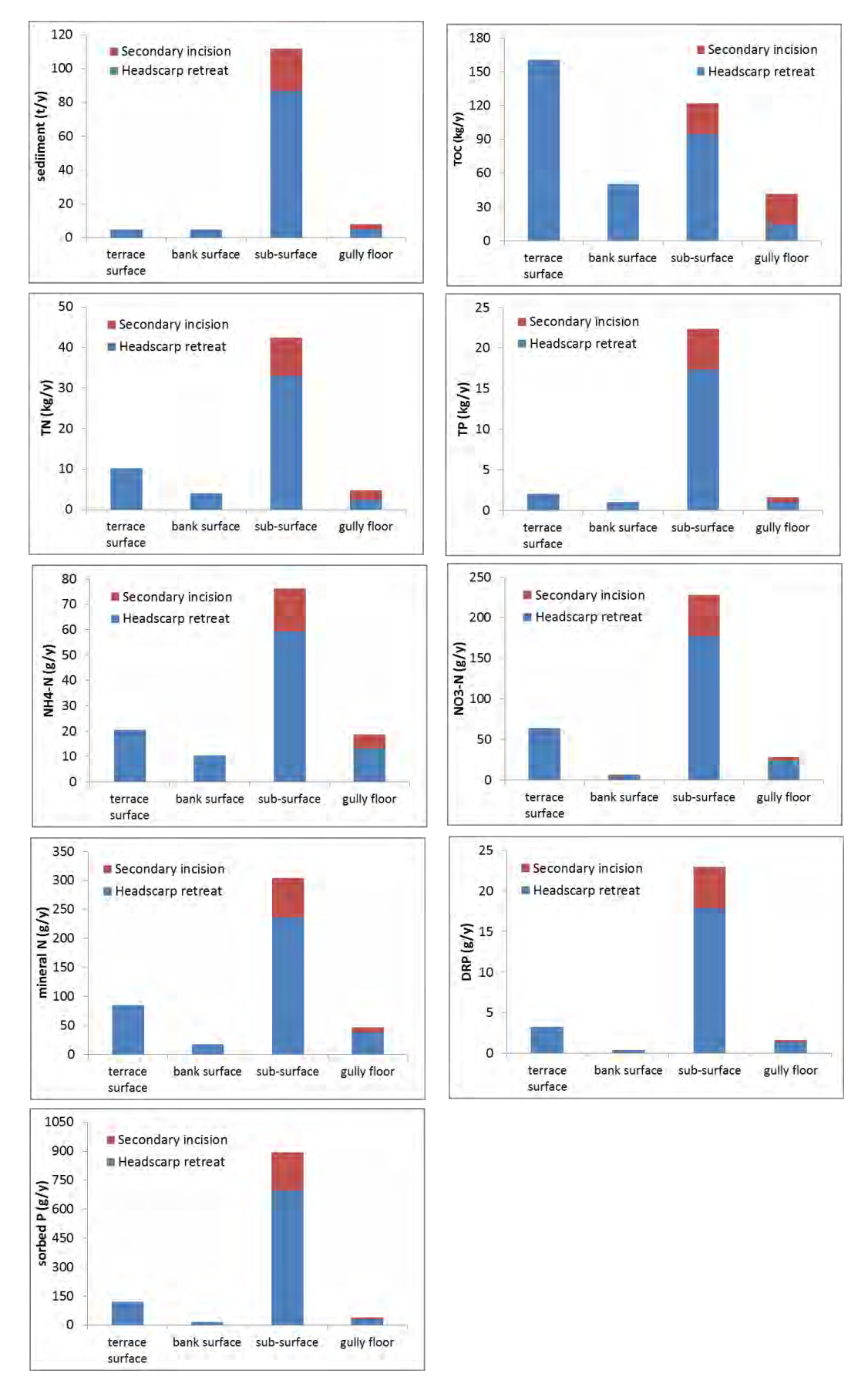


**Figure C20:** Estimated annual mass contributions of sediment, organics and nutrient export from different geomorphic units in the Granite Normanby alluvial gully.

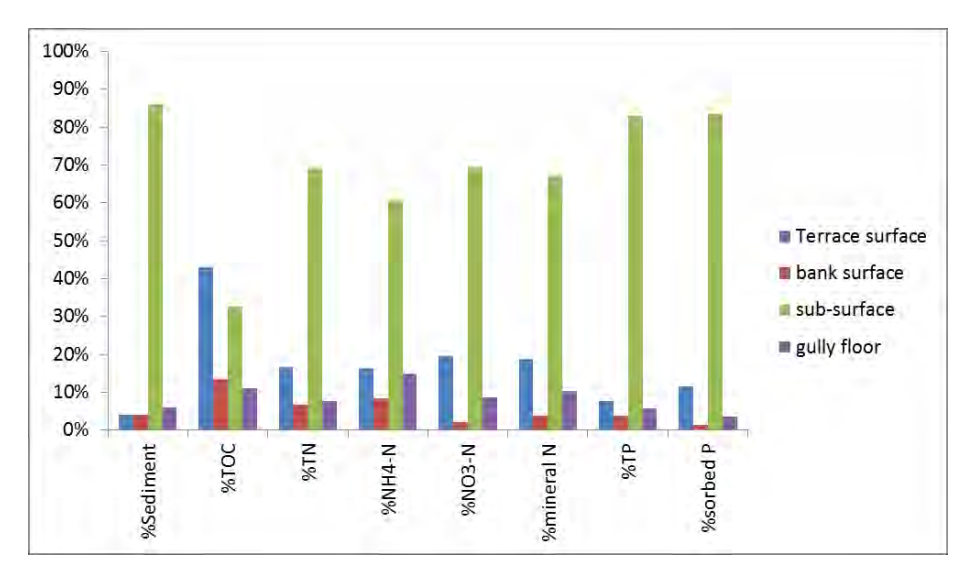


**Figure C21:** Percent contributions of exported organics and nutrient fractions from different gully geomorphic units in the Granite Normanby alluvial gully.

#### **Key conclusions from Granite Normanby alluvial gully budgets:**

- Headscarp retreat would be contributing most of the export of organics and nutrient pools; this is driven by headscarp retreat contributing 79% of the sediment export in this gully.
- The relative contribution to export from different geomorphic units is not homogenous between organics and nutrient fractions.
- Subsurface soil was the main source of export for all nutrient fractions, contributing from 61% to 84% of the TN and sorbed P exported, respectively. This is caused by the large contribution of subsurface soil to sediment export in this gully (86%).
- Terrace surface soil was the main source of TOC export contributing 43% of the exported TOC, followed by subsurface soil which contributed 33%.
- Although terrace surface soil is richer in all organics and nutrient fractions than subsurface bank soil, the larger amount of sediment sourced from subsurface soil in this gully compared to the amount sourced from terrace soil (86% versus 4%) makes subsurface bank soil the main source of all nutrients. However, terrace soil is the main source of TOC due to the terrace soil in this gully having 29 times more TOC than bank subsurface soil, and the latter source only contributing 22 times more sediment than the former.
- Given that more than 96% of the TN for all geomorphic units is organic N, the relative bioavailability of the exported organic nutrient fraction would determine which source would cause a larger impact in the aquatic environment (both freshwater and marine).

# 3.3.2 Case study 2: Laura Crocodile Station alluvial gully

Here we present annual sediment yields for the Laura Crocodile Station alluvial gully as well as hypothetical breakdown of key source contributions to sediment export.

**Table C5:** Observed erosion rate from gully 2011-2015 and estimated contributions from each source component.

	m³	t	t/yr	gully area (ha)	sediment yield (t/ha/yr)
Headscarp retreat	71.2	114.0	28.5		
Gully Floor Incision	11.9	19.0	4.8		
Total	83.1	133.0	33.2	1.14	29.2
	typical de	pth (m)			
headscarp	4				
2ndry incision	1				
Estimated breakdown of components	Headscarp retreat	2ndry Incision			
floodplain surface	0.05	0			
bank surface	0.05	0			
sub-surface	0.85	0.9			
gully floo (secondary)	r 0.05	0.1			

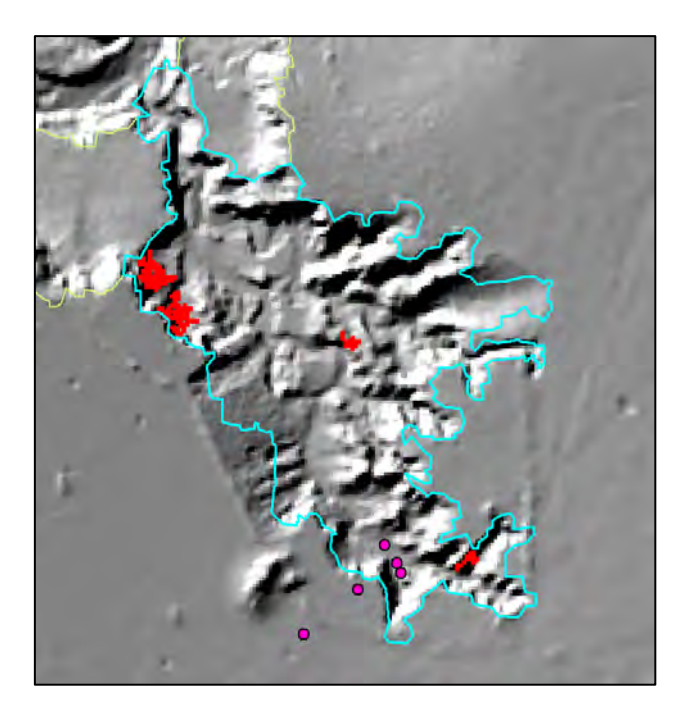


**Figure C22:** Crocodile Station gully showing the headscarp erosion in red between 2011 & 2015. Also shown (purple dots) are the sample locations. Note that the erosion detected by the aerial LiDAR in this gully is an absolute minimum amount of erosion due to the conservative limit of detection applied (0.5m change).

Estimated annual mass contributions to sediment, organics and nutrient export from different geomorphic units in the Laura Crocodile Station alluvial gully are presented in Figure C23. Percent contributions of exported fractions from geomorphic units are summarized in Figure C24.

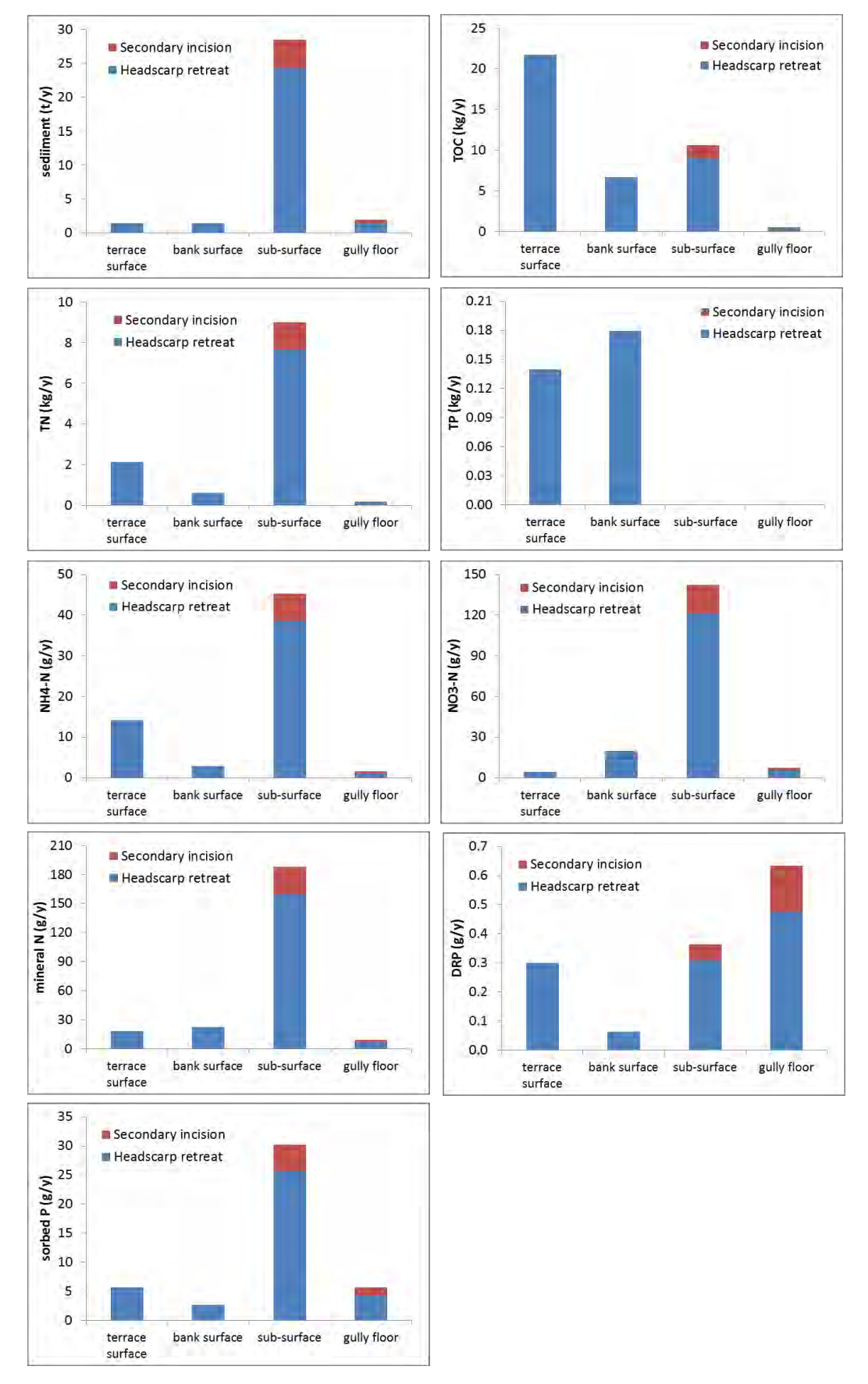


**Figure C23:** Estimated annual mass contributions of sediment, organics and nutrient export from different geomorphic units in the Laura Crocodile Station alluvial gully.

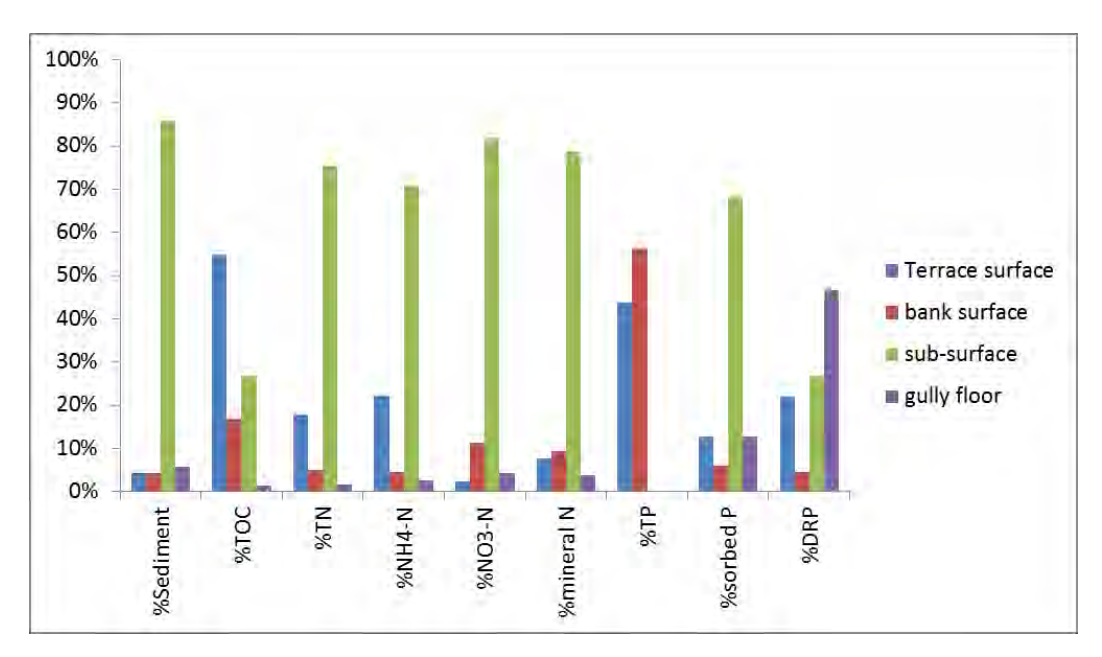


**Figure C24:** Percent contributions of exported organics and nutrient fractions from different gully geomorphic units in the Laura Crocodile Station alluvial gully.

#### **Key conclusions from Laura Crocodile Station alluvial gully budgets:**

- This gully had very similar results to the Normanby Granite alluvial gully in terms of geomorphic unit contributions to pollutant export. This was expected considering headscarp retreat is also the main sediment source in this gully and relative contributions from geomorphic units were assumed to be the same, except for gully floor contributions from the secondary incision, which were assumed to come from the secondary incision gully floor in this gully. The annual sediment yield was 4 times lower in this gully.
- Lower sediment yields in this gully compared to the Normanby Granite alluvial gully caused from 2 (NH<sub>4</sub><sup>+</sup>-N) to 85 (TP) times higher yields of organics and nutrients from the Normanby Granite alluvial gully.
- Headscarp retreat would be contributing most of the export of organics and nutrient pools; this is driven by headscarp retreat contributing 86% of the sediment export in this gully.
- The relative contribution to export from different geomorphic units is not homogenous between organics and nutrient fractions
- Subsurface soil was the main source of nutrient export for most fractions, contributing
  from 71% to 82% of the exported nitrogen fractions. This is due to the large
  contribution from subsurface soil (86%) to sediment export. Exceptions to subsurface
  soil being the main nutrient source included TP, which was undetectable in gully
  bank subsoil; and DRP, which was higher in the gully floor sediment in this gully
  compared to other sources.
- Terrace surface soil was the main source of TOC export contributing 55% of the exported TOC, followed by subsurface soil which contributed 27%.
- Although terrace surface soil is richer in all organics and nutrient fractions than subsurface bank soil, the larger amount of sediment sourced from subsurface soil in this gully compared to the amount sourced from terrace soil (86% versus 4%) makes

subsurface bank soil the main source of most nutrients. However, terrace soil is the main source of TOC due to its higher concentration. Terrace soil in this gully had 41 times more TOC than bank subsurface soil, and the latter source is only contributing 22 more times sediment than the former.

 Given that more than 96% of the TN for all geomorphic units is organic N, the relative bioavailability of the exported organic nutrient fraction would determine which source will cause the larger impact in the aquatic environment (both freshwater and marine).

## 3.3.3 Case study 3: Laura Crocodile Gap alluvial gully

Here we present annual sediment yields for Laura Crocodile Gap alluvial gully as well as a hypothetical breakdown of key source contributions to sediment export. In this gully, a secondary incision has eroded the rich gully floor material of the primary gully incision. This type material, considered to be similar to the bank surface soil, was not sampled as part of the gully floor geomorphic unit. Only the secondary incision floor was sampled. Considering this, for the organics and nutrient export budgets it was assumed that the primary incision gully floor had similar characteristics to the bank surface geomorphic unit.

**Table C6:** Observed erosion rate from gully 2011-2015 and estimated contributions from each source component.

	m <sup>3</sup>	t	t/yr	gully area (ha)	sediment yield (t/ha/yr)
Headscarp retreat	64.3	103.0	25.7		
Gully Floor Incision	1071.7	1714.8	428.7		
	1136.1	1817.7	454.4	15.8	28.8
	typical depth	(m)			
Headscarp	1.8				
2ndry incision	2.4				
Estimated breakdown of components	Headscarp retreat	2ndry Incision			
floodplain surface	0.2	0	1		
bank surface	0	0	1		
sub-surface	0.8	0.7	1		
gully floor (secondary)	0	0.1			
gully floor (primary)		0.2			

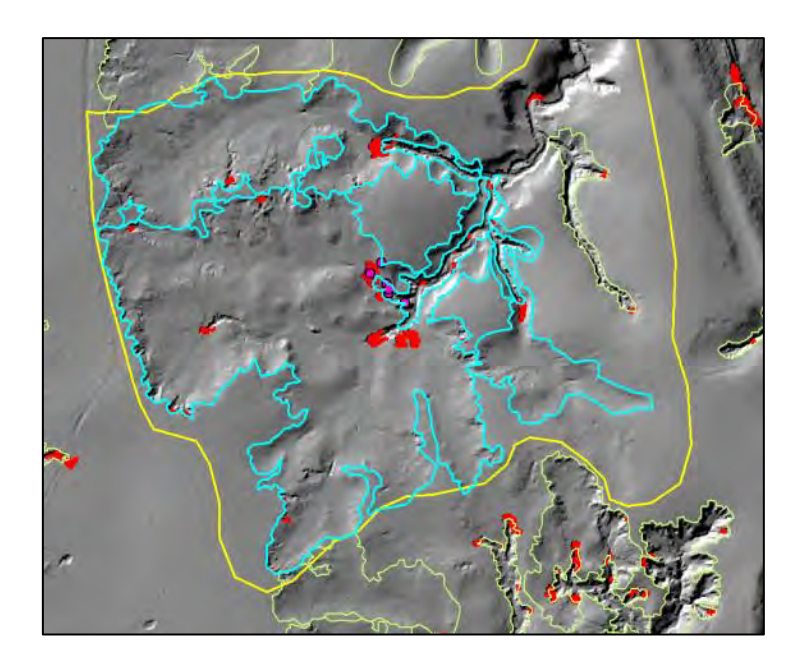


**Figure C25:** Laura Crocodile Gap alluvial gully complex showing the headscarp & secondary incision erosion in red between 2011 & 2015. Also shown (purple dots) are the sample locations. Note that the erosion detected by the aerial LiDAR in this gully is an absolute minimum amount of erosion due to the conservative limit of detection applied (0.5m change).

Estimated annual mass contributions of sediment, organics and nutrient export from different geomorphic units in the Laura Crocodile Gap alluvial gully are presented in Figure C26. Percent contributions from geomorphic units for exported fractions are summarised in Figure C27.

## Key conclusions from Laura Crocodile Gap alluvial gully budgets:

- This gully had very different results to the Normanby Granite and Laura Crocodile Station alluvial gullies in terms of geomorphic unit contributions to export. This was expected considering the gully floor secondary incision is the main sediment source in this gully and not headscarp retreat. The secondary incision mainly sourced sediment from the gully bank subsurface and from the primary gully floor and secondary gully floor incisions; the former was assumed to be much richer in organics and nutrient content than the latter and similar to the surface bank soil. The annual sediment yield was 3.5 to 14 times higher in this gully.
- The secondary gully floor incision is mostly contributing to the export of organics and nutrients; this is driven by the secondary incision contributing 94% of the sediment export in this gully.
- The relative contribution to export from different geomorphic units is not homogenous between organics and nutrient fractions
- Subsurface soil was the main source of nutrient export for most fractions, contributing
  from 52% to 66% of the exported nitrogen fractions. This is caused by the large
  contribution of the subsurface soil to sediment export in this gully (71%). Exceptions
  to subsurface soil being the main nutrient source included TP, which was
  undetectable in gully bank subsoil; and DRP, which was higher in the gully floor

- sediment in this gully compared to other sources. In these two cases, the gully floor was the main source to export.
- Gully floor sediment can be the main source of TOC and some nutrient fractions
  when gully incision and not headscarp retreat, dominates sediment export. This was
  the case in this gully where it was the main source of TOC export, contributing 85%
  of the exported TOC, followed by terrace soil which contributed 11%.
- Although terrace surface soil is richer in all organics and nutrient fractions than all other sources, the larger amount of sediment sourced from subsurface soil in this gully compared to the amount sourced from terrace soil (71% versus 1%) makes subsurface bank soil the main source of most nutrients.

Given that more than 96% of the TN for all geomorphic units is organic N, the relative bioavailability of the exported organic nutrient fraction would determine which source would cause the larger impact in the aquatic environment (both freshwater and marine).

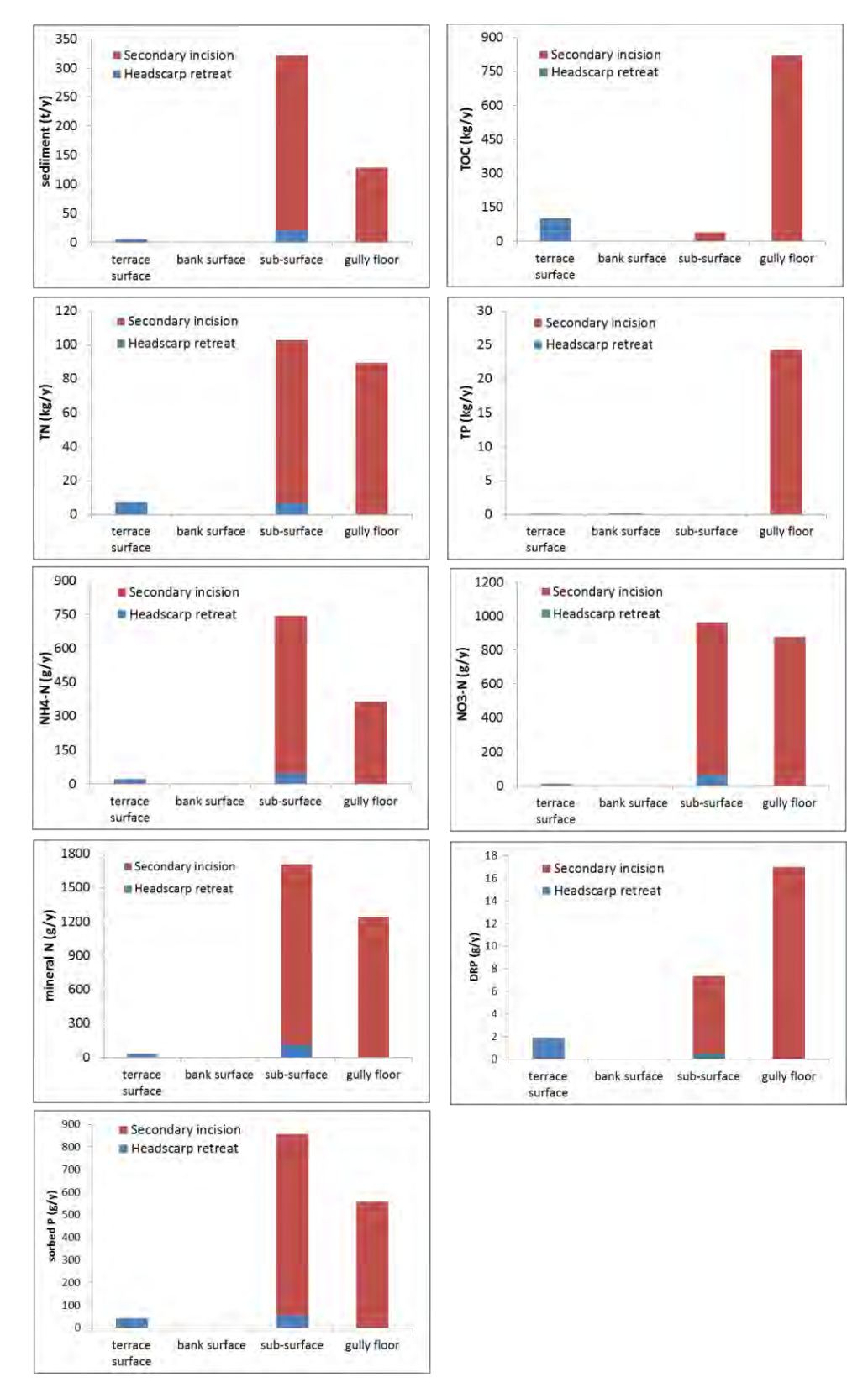


**Figure C26:** Estimated annual mass contributions of sediment, organics and nutrient export from different geomorphic units in the Laura Crocodile Gap alluvial gully

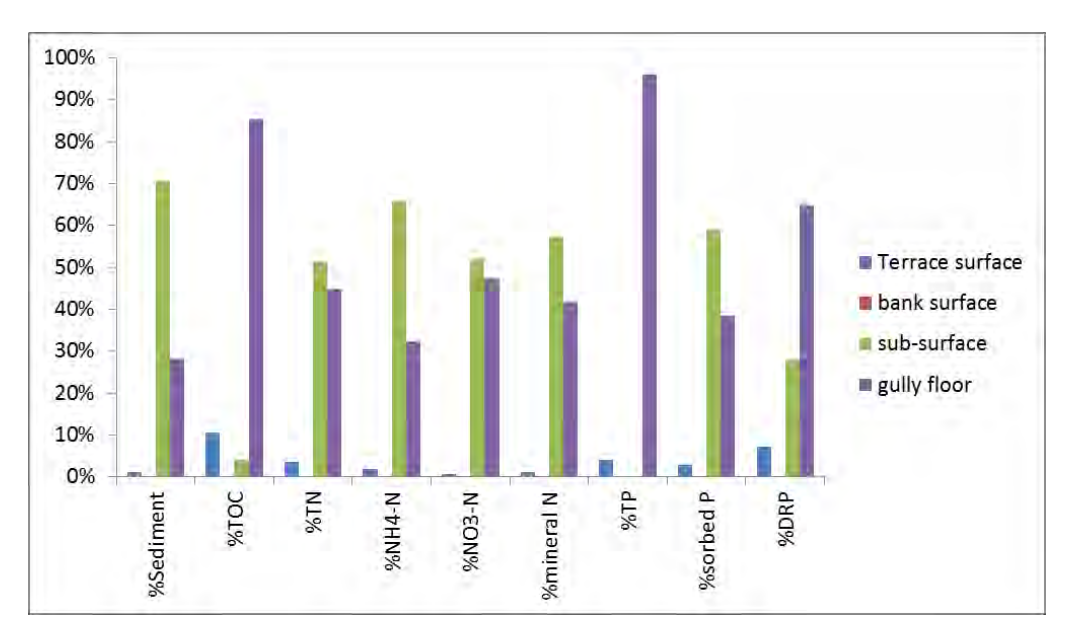


**Figure C27:** Percent contributions of exported organics and nutrient fractions from different gully geomorphic units in the Laura Crocodile gap alluvial gully.

#### 3.3.4 Sensitivity analysis

Here we present a sensitivity analysis for source contribution on organics and nutrient export outcomes when there are changes in sediment yields and relative source contributions to sediment export. This analysis has been carried out for a hypothetical alluvial gully that is retreating and deepening. We explore how sediment source contributes to sediment, organics and nutrient export as the gully develops for 5 gully stages as follows:

		m³	t	t/yr	gully area (ha)	sediment yield (t/ha/yr)
Headscarp retreat Obs		267.1	427.4	106.8		51.6
Headscarp retreat Obs +0.	5m	487.6	780.2	195.0		94.2
Headscarp retreat Obs + 1	.0m	708.1	1133.0	283.2		136.8
Headscarp retreat Obs + 1	.5m	928.6	1485.8	371.4		179.4
Headscarp retreat Obs + 2	.0m	1149.1	1838.6	459.6		222.0
	typical depth	ı (m)				
main gully	1.5					
Estimated breakdown of components	Headscarp retreat (obs)	obs + 0.5m	obs + 1.0m	obs + 1.5m	obs + 2.0m	
floodplain surface	0.1	0.055	0.038	0.029	0.023	
bank surface	0.05	0.050	0.050	0.050	0.050	
sub-surface	0.8	0.845	0.862	0.871	0.877	
gully floor	0.05	0.05	0.05	0.05	0.05	

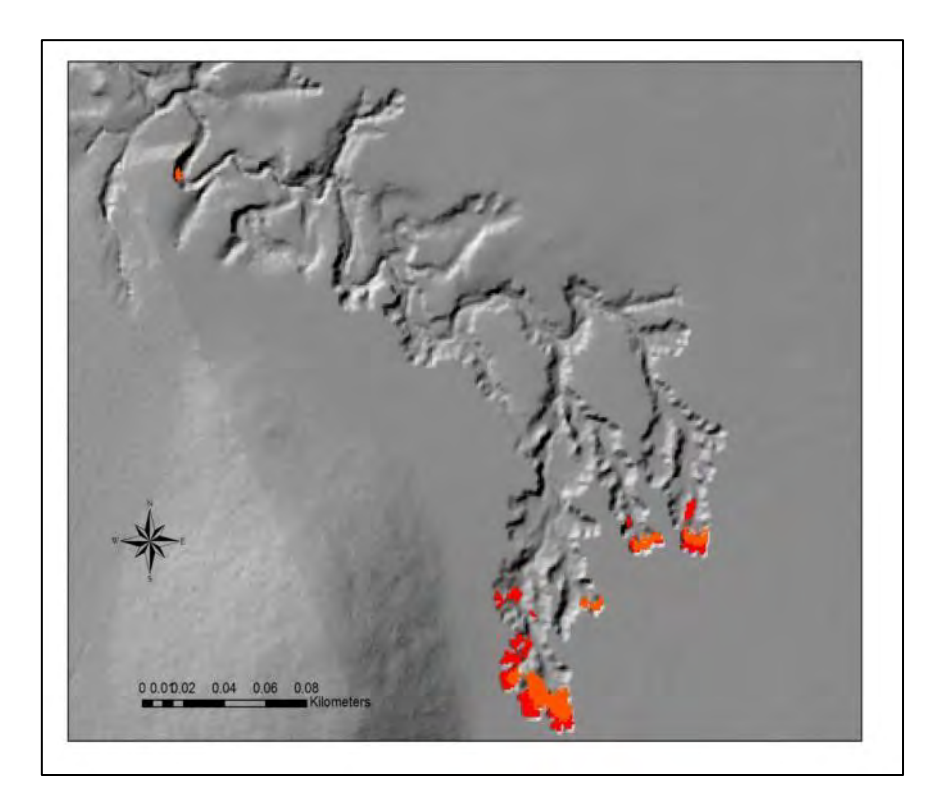


**Figure C28:** Observed erosion in Granite Normanby distal gully over the period 2009-11 in orange and 2011-15 in red. Modelled scenarios have then been derived to show relative nutrient contributions with gully deepening.

Estimated annual mass contributions of sediment, organics and nutrient export from different geomorphic units in the hypothetical developing alluvial gully are presented in Figure C29.

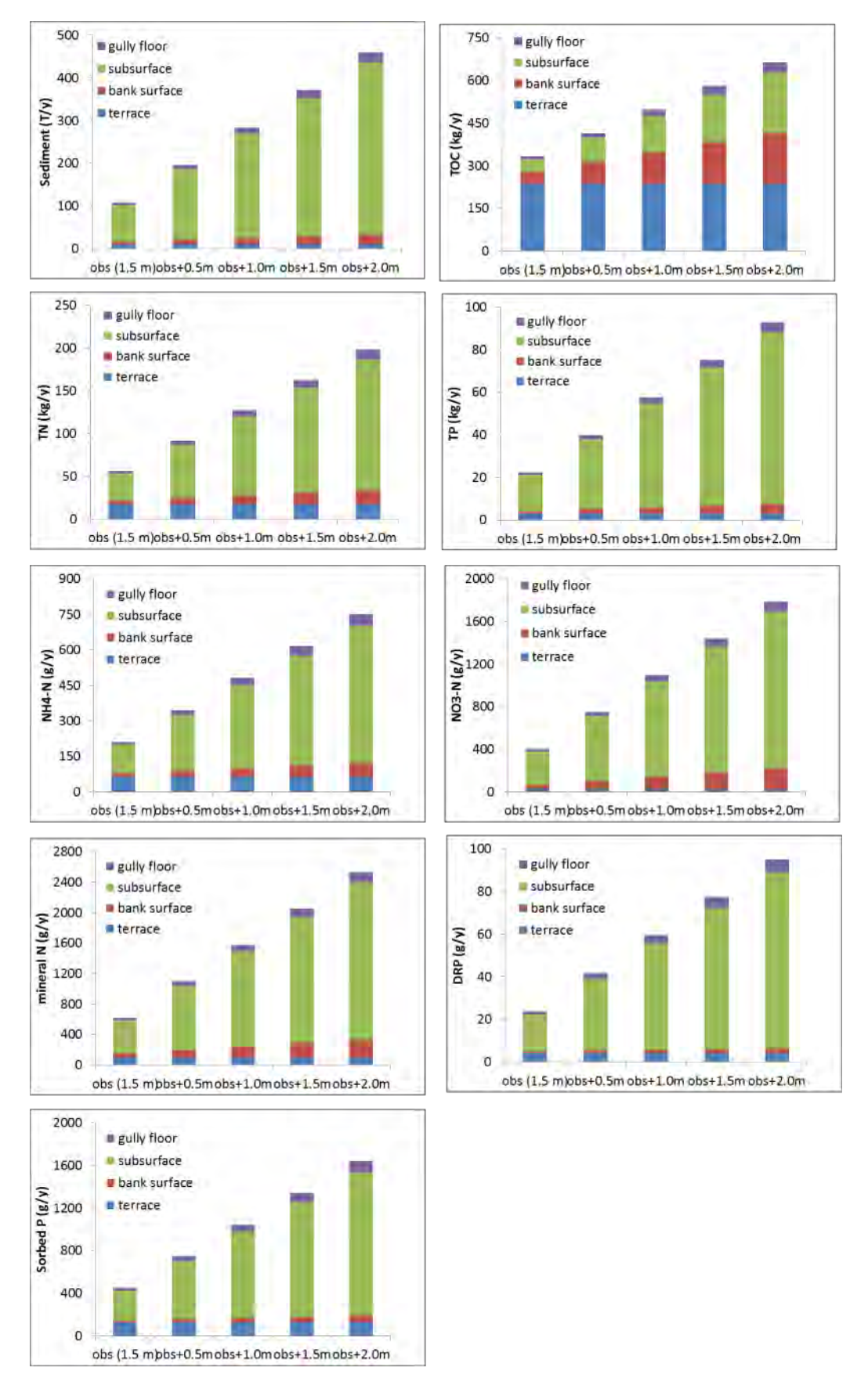


**Figure C29:** Estimated annual mass contributions of sediment, organics and nutrient export from different geomorphic units in a hypothetical developing alluvial gully.

#### Key conclusions from the empirical modelling of gully sediment and nutrient budgets:

- Sediment, organics and nutrient yields increase as the gully grows. In this case, it
  was assumed sediment loads increased linearly as for organics and nutrient fraction
  export.
- The relative contribution to export from different geomorphic units is not homogenous as the gully develops.
- As the gully develops, the contribution of subsurface bank soil to sediment and nutrient export increases more rapidly than the contribution of other geomorphic units, making it the more dominant source as the gully becomes larger.
- Subsurface bank soil was the main source of nutrient export for all gully stages, contributing from 58% of TN export in the first stage to 87% of DRP export in the last stage. This is caused by the large contribution of subsurface soil to sediment export for all stages (from 80% to 88%).
- Terrace surface soil was the main source of TOC export for all gully stages, contributing from 71% of the exported TOC in the first stage to 36% of the exported TOC in the last stage. The secondary source of TOC export was subsurface bank soil which contributed from 14% of the exported TOC in the first stage to 32% of the exported TOC in the last stage.
- Although terrace surface soil is richer in organics and nutrient fractions subsurface bank soil, the larger amount of sediment sourced from this hypothetical gully compared to the amount sourced from terrace soil times more in the first stage to 38 times more in the last stage) makes bank soil the main source of nutrients. Nonetheless, terrace soil is the TOC due to the much higher concentrations of this parameter compared sources (see

•

- Figure C17a). Terrace soil has on average 77 times more TOC than bank subsurface soil.
- For even earlier stages of gully evolution (gullies <1.5 m deep), terrace surface contributions to nutrient export would be larger and may be the main source. In Figure C30, simulated contributions for a hypothetical 0.5 m deep gully with a 0.2 m deep A horizon can be seen. For this case, it is assumed that subsurface soil would contribute 60% of the sediment yield and terrace surface soil 40%. It is shown that terrace surface soil may be the main source to organics and nutrient fraction export in early stages of gully evolution.</p>
- The relative bioavailability of the exported organic nutrient fraction (e.g. more than 96% of the TN for all geomorphic units) will determine which source would cause the larger impact in the aquatic environment (both freshwater and marine).

To be able to frame these results, they were compared with modelled annual average exports per unit area for different landuses in the Wet Tropic catchments (Hateley et al., 2014) (see Table C7). It can be seen that annual TN and TP export per unit area from alluvial gullies can be larger than that from sugarcane and banana crops. On average 46% of sugarcane and 59% of banana crops TN would be exported as dissolved inorganic N (mineral N) in the Wet Tropics (Hateley et al., 2014), compared with only 2% for alluvial gullies (measured as KCI extractable mineral N). However, the exported organic N from

alluvial gullies (98% of TN) is potentially bioavailable and thus may be mineralized into dissolved inorganic N during stream transport, once it gets to the estuarine or marine environment, or be used directly by algae in dissolved organic form. As a consequence, mineral N yields estimated here from alluvial gully soil/sediments, do not reflect the contribution of alluvial gullies to dissolved inorganic N downstream. This result shows the importance of understanding not only sources of organics and nutrients from alluvial gullies, but also their in-stream processing.

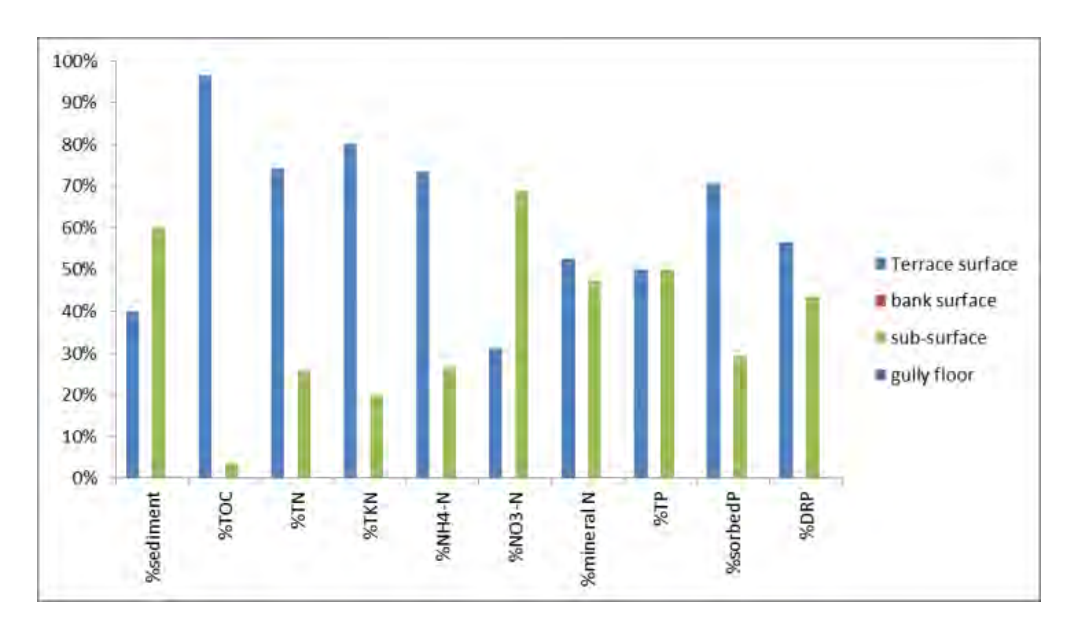


**Figure C30:** Percent contributions of all exported organics and nutrient fractions from different gully geomorphic units in a 0.5 m deep hypothetical gully (60% subsurface soil contribution to sediment yield and 40% terrace surface soil contribution to sediment yield).

**Table C7:** Annual exports per unit area of sediment, nitrogen (TN) and phosphorus (TP) from alluvial gullies (this study) and various modelled land uses in the Wet Tropics\*

Gully/land use	sediment (t/ha/y)	TN (kg/ha/y)	TP (kg/ha/y)
Granite Normanby	114.0	54.0	23.7
Laura - Crocodile station	29.2	10.5	0.3
Laura - Crocodile Gap	28.8	12.6	1.6
Sugar cane	1.2	22.2	2.7
Banana	1.8	25.3	3.1
Nature conservation	0.2	3.6	0.3

<sup>\*</sup>Modelled values from Hateley et al. (2014)

# 4. MAIN CONCLUSIONS AND IMPLICATIONS FOR MANAGEMENT

In summary, research findings indicate that nutrient and organics soil/sediment pools are not distributed equally in alluvial or hillslope gullied landscapes or across their soil/sediment particle sizes. Although there were not very large differences between the sampled gullies overall, there were differences between the gully geomorphic units. The most eroded areas in a gully complex tend to have the least amount of nutrients and organics, and in their least readily bioavailable forms. This is likely caused by the sediment present in eroded areas being predominantly sourced from the subsurface soil horizons, which tend to be particularly poor in organics and nutrients when compared with bank surface soils or terrace soils (Garzon-Garcia et al., 2014). The finer fractions of soil/sediment also tended to be richer in nutrients and organics and in their most bioavailable forms (Burton et al., 2015), and in the richer geomorphic units like terrace soils and surface gully bank soils also have larger nutrient enrichment ratios.

Although terrace soil had the largest pools of most nutrients and organics, bank subsoil was generally the main source of sediment in these alluvial gullies and has been shown to be the main source of sediment in the wet tropics and dry tropics catchments of the GBR (Bainbridge et al., 2016; Bainbridge et al., 2014; Hughes et al., 2009; Olley et al., 2013; Wilkinson et al., 2015). In this study it is shown that the sources of organics and nutrient export from alluvial gullies would vary depending on the type of erosional process occurring in the alluvial gully (i.e. headscarp retreat versus secondary incision) and their stage of evolution (gully depth and sediment yields). These aspects will ultimately determine the relative contribution of different geomorphic units to sediment yields and consequently to organics and nutrient export. These findings should be confirmed with larger sampling replication.

In general, terrace soil was found to be the main source to TOC export when headscarp retreat contributes the majority of sediment. The contribution of terrace soil to nutrient fraction export varied with the stage of gully evolution. In the initial stages of gully evolution [very shallow gullies (<1.0 m) growing fast into the terrace deposits], terrace soil would be the main source of nutrient export. This implies that it should be a priority to protect terrace deposits from fast headscarp retreat as these deposits contain large pools of carbon and nutrients that, when lost, would be very difficult to restore. As gully incision occurs, the main source of most nutrient fractions export clearly becomes bank subsurface sediment. Although bank subsurface sediment has much smaller nutrient pools than terrace surface soil, the sheer quantity of exported bank subsurface sediment over compensates for its lower nutrient content making it the main source. In the longer term, gully bank subsoils would tend to be the main source of nutrients. As a consequence, the long term aim should be the stabilization of gully banks and reduction of incision, which would have a larger effect on reducing nutrient export due to gully erosion.

When secondary incision occurs and there is organic and nutrient rich sediment deposited on the gully floor, this sediment may become a very important source of organics and nutrient export, even more so than bank subsurface soil. The deeper and older the deposits, the more important this source would be. The protection of gully floor organics and nutrient deposits should be part of gully rehabilitation designs and should be prioritized when these deposits are of importance.

These findings point to the importance of increasing our understanding of the links between organics and nutrient sources, alluvial gully erosional processes and instream processing. For example, it is crucial to understand differences in the bioavailability of exported sediment from different geomorphic unit sources once in the aquatic environment. Although various indicators of the bioavailability of these sediments were quantified in this study, research is still necessary to define which of these indicators would be the best to predict the impact of organics and nutrients to primary production in the freshwater and marine environment (Burton et al., 2015) and what controls this bioavailability (Garzon-Garcia et al. in prep). The role of vegetation and litter has been proposed as fundamental, not only to the rehabilitation of carbon and nitrogen stores in gullied landscapes, but to reduce the impacts of the mineralization of eroded sediment in the aquatic environment by promoting nitrogen retention (Garzon-Garcia, 2014). Further research is necessary to better understand the role of vegetation in mediating these relationships.

This study gives some indication of how to establish management priorities to reduce organics and nutrient export, which would depend on key alluvial gully erosional processes. Findings should be validated by sampling a larger number of alluvial gullies, including sediment export sampling, the role of particle size in export, relative bioavailability of different sources, and ideally source tracing. It is recommended that sampling design targets key geomorphic units from gully categories based on the erosional process (e.g. fast headscarp retreat, primary incision, secondary incision, widening, gully depth, etc).

## **ACKNOWLEDGEMENTS**

This document has been prepared by the Department of Science, Information Technology and Innovation. The project was funded by NESP, led by Griffith University and with in-kind contributions from the Chemistry Centre, Department of Science, Information Technology and Innovation (DSITI). Sample processing and analysis was conducted by the Chemistry Centre and Soil Processes (DSITI). In particular, we thank Rob De Hayr, Benjamin Hall, Kate Dolan, Siok Yo, Dan Yousaf and Angus Mcelnea. We also specially thank Dr. Phil Moody, Prof Jon Olley and Rob Dehayr for reviewing the manuscript.

## **REFERENCES**

- Austin AT, Yahdjian L, Stark JM, Belnap J, Porporato A, Norton U, et al. Water pulses and biogeochemical cycles in arid and semiarid ecosystems. Oecologia 2004; 141: 221-235.
- Bainbridge Z, Lewis S, Smithers S, Wilkinson S, Douglas G, Hillier S, et al. Clay mineral source tracing and characterisation of Burdekin River (NE Australia) and flood plume fine sediment. Journal of Soils and Sediments 2016; 16: 687-706.
- Bainbridge ZT, Lewis SE, Smithers SG, Kuhnert PM, Henderson BL, Brodie JE. Fine-suspended sediment and water budgets for a large, seasonally dry tropical catchment: Burdekin River catchment, Queensland, Australia. Water Resources Research 2014; 50: 9067-9087.
- Bainbridge ZT, Wolanski E, Alvarez-Romero JG, Lewis SE, Brodie JE. Fine sediment and nutrient dynamics related to particle size and floc formation in a Burdekin River flood plume, Australia. Marine Pollution Bulletin 2012; 65: 236-248.
- Brodie J, Schroeder T, Rohde K, Faithful J, Masters B, Dekker A, et al. Dispersal of suspended sediments and nutrients in the Great Barrier Reef lagoon during river-discharge events: conclusions from satellite remote sensing and concurrent flood-plume sampling. Marine and Freshwater Research 2010; 61: 651-664.
- Brodie JE, Kroon FJ, Schaffelke B, Wolanski EC, Lewis SE, Devlin MJ, et al. Terrestrial pollutant runoff to the Great Barrier Reef: An update of issues, priorities and management responses. Marine Pollution Bulletin 2012; 65: 81-100.
- Brooks AP, Spencer JR, Olley JM, Pietsch T, Borombovits D, Curven G, et al. An empirically-based sediment budget for the Normanby Basin: sediment sources, sinks, and drivers on the Cape York Savannah. Brisbane: Australian Rivers Institute, Griffith University on behalf of the Australian Government's Caring for our Country Reef Rescue Inititative, 2013.
- Burton J, Moody P, DeHayr R, Chen C, Lewis S, Olley J. Sources of bioavailable particulate nutrients: Phase 1 (RP128G). Department of Science, Information Technology and Innovation, Brisbane, Australia, 2015.
- Evans CD, Reynolds B, Jenkins A, Helliwell RC, Curtis CJ, Goodale CL, et al. Evidence that soil carbon pool determines susceptibility of semi-natural ecosystems to elevated nitrogen leaching. Ecosystems 2006; 9: 453-462.
- Fontaine S, Barot S. Size and functional diversity of microbe populations control plant persistence and long-term soil carbon accumulation. Ecology Letters 2005; 8: 1075-1087.
- Fontaine S, Barrot S, Barre P, Bdioui N, Mary B, Rumpel C. Stability of organic carbon in deep soil layers controlled by fresh carbon supply. Nature Letters 2007; 450: 277-281.
- Garten CT, Ashwood TL. Landscape level differences in soil carbon and nitrogen: Implications for soil carbon sequestration. Global Biogeochemical Cycles 2002; 16: 61-1-61-14.

- Garzon-Garcia A. Effects of gully and channel erosion on carbon and nitrogen storage, mineralization and export in a subtropical catchment. Science, Environment, Engineering and Technology. PhD. Griffith University, Brisbane, 2014, pp. 124.
- Garzon-Garcia A, Olley J, Bunn S, Moody P. Gully erosion reduces carbon and nitrogen storage and mineralization fluxes in a headwater catchment of southeastern Queensland, Australia. Hydrological Processes 2014; 28: 4669-4681.
- Garzon-Garcia A, Wallace R, Huggins R, Turner RDR, Smith RA, Orr D, et al. Total suspended solids, nutrient and pesticide loads (2013–2014) for rivers that discharge to the Great Barrier Reef. Great Barrier Reef Catchment Loads Monitoring Program Department of Science, Information Technology and Innovation, Brisbane, Australia, 2015.
- Gomez R, Arce MI, Sánchez JJ, Sánchez-Montoya MdM. The effects of drying on sediment nitrogen content in a Mediterranean intermittent stream: a microcosms study. Hydrobiologia 2012; 679: 43-59.
- Hateley LR, Ellis R, Shaw M, Waters D, Carroll C. Modelling reductions of pollutant loads due to improved management practices in the Great Barrier Reef catchments Wet Tropics NRM region. Volume 3. Queensland Department of Natural Resources and Mines, Cairns, 2014.
- Hughes AO, Olley JM, Croke JC, McKergow LA. Sediment source changes over the last 250 years in a dry-tropical catchment, central Queensland, Australia. Geomorphology 2009; 104: 262-275.
- Joo M, Raymond MAA, McNeil VH, Huggins R, Turner RDR, Choy S. Estimates of sediment and nutrient loads in 10 major catchments draining to the Great Barrier Reef during 2006-2009. Marine Pollution Bulletin 2012; 65: 150-166.
- Kroon FJ, Kuhnert PM, Henderson BL, Wilkinson SN, Kinsey-Henderson A, Abbott B, et al. River loads of suspended solids, nitrogen, phosphorus and herbicides delivered to the Great Barrier Reef lagoon. Marine Pollution Bulletin 2012; 65: 167-181.
- Manzoni S, Trofymow JA, Jackson RB, Porporato A. Stoichiometric controls on carbon, nitrogen, and phosphorus dynamics in decomposing litter. Ecological Monographs 2010; 80: 89-106.
- Olley JM, Brooks A, Spencer JS, Pietsch T, Borombovits DK. Subsoil erosion dominates the supply of fine sediment to rivers draining into Princess Charlotte Bay, Australia. Journal of Environmental Radioactivity 2013; 124: 121-129.
- Shellberg JG, Brooks AP, Spencer J. Land-use change from indigenous management to cattle grazing initiates the gullying of alluvial soils in northern Australia. Soil Solutions for a Changing World, 19th World Congress of Soil Science, Brisbane, 2010, pp. 59-62.
- Shellberg JG, Spencer J, Brooks AP, Pietsch T. Alluvial gully erosion rates across the Mitchell River fluvial megafan, northern Australia. Geomorphology In review.
- Waterhouse J, Brodie J, Lewis S, Mitchell A. Quantifying the sources of pollutants in the Great Barrier Reef catchments and the relative risk to reef ecosystems. Marine Pollution Bulletin 2012; 65: 394-406.

- Wilkinson SN, Olley JM, Furuichi T, Burton J, Kinsey-Henderson AE. Sediment source tracing with stratified sampling and weightings based on spatial gradients in soil erosion. Journal of Soils and Sediments 2015; 15: 2038-2051.
- Wolanski E, Fabricius KE, Cooper TF, Humphrey C. Wet season fine sediment dynamics on the inner shelf of the Great Barrier Reef. Estuarine Coastal and Shelf Science 2008; 77: 755-762.

### APPENDIX C1: SAMPLE ANALYSES

Methods used by the DSITI Chemistry Centre generally follow the Australian Laboratory Handbook Method codes as per Rayment, G.E. and Lyons, D.J. (2011). "Soil Chemical Methods – Australasia". This is the principal reference manual for soil analytical methods in Australia/New Zealand. Where methods follow the procedures specified in Rayment and Lyons (2011), they are referred to by manual's method code in parentheses. Additional (original) references are provided for further information, or where the analytical method is not described in Rayment and Lyons (2011).

#### Air Dry moisture (2A1)

The Air Dried Moisture Content (ADMC) was determined gravimetrically. This determination (ADMC) expresses moisture content of air dried soils (dried at 40°C) as a percentage on an oven-dried basis, i.e. soils which have been further dried to 105°C for at least 16 h. It is necessary to determine ADMC where it is required to correct soil chemical results performed on air-dry samples to an oven-dry basis for consistency.

#### Total Kjeldahl Nitrogen (7A2) and Phosphorus (9A3a)

Total Kjeldahl Nitrogen (TKN) and Total Kjeldahl Phosphorus (TKP) were determined on soil samples subjected to Kjeldahl digestion with sodium sulfate and selenium as catalyst. Following dilution with water, ammonium-nitrogen was determined by an automated segmented-flow colorimetric procedure based principally on the indophenol reaction with salicylate and sodium hypochlorite. Similarly, after conversion of all, or almost all, P to orthophosphate, orthophosphate was determined colorimetrically, based on the reaction of ammonium molybdate and potassium antimony tartrate. This method covers procedures for the quantitative determination of total nitrogen, (excluding nitrates) and of phosphorus as orthophosphate in soils.

#### Mineral Nitrogen (7C2a)

Samples were extracted with 2 M KCl (1:10 soil to solution ratio for 1 h at 25°C) to determine their mineral-nitrogen concentrations automated colorimetric procedures to determine ammonium-nitrogen (NH<sub>4</sub>-N) and nitrate-nitrogen (NO<sub>3</sub>-N).

#### Bicarbonate Extractable (Colwell) P (9B2) and Organic P

Colwell P (Colwell 1963) (referred to in this report as Sorbed P) was determined by extracting air dried sample with  $0.5M\ NaHCO_3$  buffered to pH 8.5 with NaOH at a 1:100 soil/solution ratio for 16 h at  $25^{\circ}C$ . The sample extract phosphorus concentration is determined by an automated modification of the Murphy and Riley (1962) colorimetric method.

#### Acid Extractable (BSES)-P (9G2)

Air dried samples were extracted at the rate 1:200, with  $0.005M H_2SO_4$  on an end over end tumbler for 16 h. The orthophosphate level determined by an automated colorimetric by segmented flow analysis. This method is based on the extraction method developed by Kerr and von Stieglitz (1938) and Murphy and Riley (1962).

#### Adjusted Phosphorus Buffer Index (PBI) (9I2b)

Sample is equilibrated in an end-over-end shaker for 16 h in a 0.01M CaCl<sub>2</sub>.2H<sub>2</sub>O solution containing 100 mgP/L with a soil/solution ratio of 1:10.

PBI is derived from the Freundlich equation for describing the relationship between total P sorbed and final solution P concentration (i.e. the P sorption curve). The total amount of P sorbed by the soil is calculated as the amount of previously sorbed P, plus the amount of freshly sorbed P. The previously sorbed P is estimated as the Colwell–P (Colwell 1963) status of the soil. Therefore, the 'total P sorbed' for use in calculating PBI is the addition of Colwell P to the amount of freshly sorbed P. The amount of freshly sorbed P in the soil (mg P/kg) is calculated as the difference between the initial amount of P added (=1000 mg P/kg at the specified soil/solution ratio of 1:10) and the amount of P left in the equilibrating solution, expressed as mg P/kg air dry soil. Sample solution freshly sorbed P concentration is quantified by ICP-OES.

$$PBIadj = \frac{total\ P\ sorbed\ (mg/kg)}{residual\ P\ (mg/L)^{0.41}}$$

total sorbed  $P = Colwell \ P(mg/kg) + P \ added \ (mg/kg) - (residual \ P \ mg/L \times 10)$ 

To simulate marine conditions, PBI was also carried out using the above procedure but with 0.5M NaCl replacing 0.01M CaCl<sub>2</sub>.2H<sub>2</sub>O as the background solution.

#### **Total Organic Carbon (6B3)**

Following acid pre-treatment to remove carbonates, samples (<0.5mm) are analysed by Dumas high temperature combustion and infrared/thermal conductivity detection on a C-N Analyzer.

#### Particle size -

#### By laser diffraction

Samples were re-suspended in water without chemical dispersant into the Malvern Mastersizer 2000 and the particle size distribution determined after mechanical dispersion following AS 4863.1-2000 (ISO 13320-1:1999).

# APPENDIX C2: BIOAVAILABLE NUTRIENT AND ORGANICS INDICATORS FOR ALL SAMPLED GULLIES, GEOMORPHIC UNITS AND PARTICLE SIZE FRACTIONS (ND: NON-DETECTABLE, NA: NOT AVAILABLE)

Gully name	Gully type	Gemorphology Unit	Fraction	TOC (%)	TN(%)	TOC:TN ratio	NH4-N air dry (mg/kg)	NO3-N air dry (mg/kg)	Mineral N (mg/kg)	TP (%)	Sorbed P (mg/kg)	PBI	DRP (mg/kg)	Mineral P (mg/kg)
		Gully floor	total	0.28	0.05	5.6	<2	<2	ND	0.02	6	22	0.27	65
Granite Normanby	Alluvial	Bank surface	total	0.98	0.08	12.2	<2	<2	ND	0.02	3	38	0.08	ND
Granite Normanby	Alluviai	Bank subsurface	total	0.11	0.04	2.9	<2	3	3	0.02	8	39	0.21	ND
		Terrace	total	3.14	0.2	15.7	4	<2	4	0.04	24	38	0.63	ND
		Bank surface	total	0.42	0.03	14.0	<2	<2	ND	<0.01	<2	9	ND	ND
Parsons Creek	Hillslope	Bank subsurface	total	0.04	<0.03	NA	<2	12	12	<0.01	<2	31	ND	ND
Parsons Creek	пінзіоре	Gully floor	total	0.17	<0.03	NA	<2	<2	ND	<0.01	<2	5	ND	ND
		Hillslope	total	1.15	0.07	16.4	<2	<2	ND	<0.01	3	19	0.16	ND
		Gully floor	total	0.03	<0.03	NA	<2	4	4	<0.01	3	9	0.33	ND
Laura Croc Station	Alluvial	Bank subsurface	total	0.04	<0.03	NA	<2	5	5	<0.01	<2	44	ND	ND
Laura Croc Station	Alluviai	Bank surface	total	0.47	0.04	11.2	2	<2	2	<0.01	<2	8	ND	ND
		Terrace	total	1.52	0.15	10.2	10	3	13	<0.01	4	19	0.21	ND
		Terrace	total	1.99	0.14	14.2	4	2	6	0.02	8	22	0.36	ND
		Bank surface	total	0.87	0.09	9.6	3	<2	3	0.02	4	38	0.11	ND
Laura Croc gap	Alluvial	Buried A	total	0.57	0.05	11.3	3	4	7	<0.01	3	83	0.04	ND
		Bank subsurface	total	0.01	<0.03	NA	<2	3	3	<0.01	<2	18	ND	ND
		Gully floor	total	0.17	<0.03	NA	<2	<2	ND	<0.01	5	27	0.19	ND

Appendix C: Bioavailable nutrients and organics in alluvial gully sediment

Gully name	Gully type	Gemorphology Unit	Fraction	TOC (%)	TN(%)	TOC:TN ratio	NH4-N air dry (mg/kg)	NO3-N air dry (mg/kg)	Mineral N (mg/kg)	TP (%)	Sorbed P (mg/kg)	РВІ	DRP (mg/kg)	Mineral P (mg/kg)
		Gully floor	<10 um	0.24	0.07	3.4	5	11	16	0.03	19	46	0.41	91
Granite Normanby	Alluvial	Bank surface	<10 um	1.84	0.2	9.2	8	25	33	0.03	7	119	0.06	ND
Graffite Normanby	Alluviai	Bank subsurface	<10 um	0.18	0.08	2.2	2	6	8	0.04	13	93	0.14	47
		Terrace	<10 um	4.81	0.41	11.7	30	50	80	0.09	57	149	0.38	ND
		Bank surface	<10 um	2.09	0.2	10.5	8	11	19	<0.01	4	104	0.04	ND
Parsons Creek	Hillslope	Bank subsurface	<10 um	0.14	0.04	3.1	<2	20	20	<0.01	<2	117	ND	ND
raisons creek	пінзіоре	Gully floor	<10 um	0.70	0.09	7.8	3	8	11	<0.01	4	56	0.07	ND
		Hillslope	<10 um	3.82	0.32	11.9	23	29	52	0.02	3	107	0.03	ND
		Gully floor	<10 um	0.19	0.06	3.2	5	84	89	<0.01	3	291	0.01	ND
Laura Croc Station	Alluvial	Bank subsurface	<10 um	0.06	0.05	1.4	3	10	13	<0.01	2	83	0.02	ND
Laura Croc Station	Alluviai	Bank surface	<10 um	2.40	0.26	9.2	24	59	83	0.02	4	86	0.05	ND
		Terrace	<10 um	5.44	0.62	8.8	161	226	387	0.04	11	113	0.10	ND
		Terrace	<10 um	4.53	0.46	9.8	8	167	175	0.06	24	92	0.26	ND
		Bank surface	<10 um	0.79	0.13	6.1	7	22	29	0.02	2	70	0.03	ND
Laura Croc gap	Alluvial	Buried A	<10 um	1.24	0.14	8.8	5	19	24	0.02	3	255	0.01	ND
		Bank subsurface	<10 um	0.06	0.05	1.4	4	9	13	<0.01	3	170	0.02	ND
		Gully floor	<10 um	0.39	0.08	4.9	3	13	16	0.03	13	222	0.06	ND

#### Brooks et al.

Gully name	Gully type	Gemorphology Unit	Fraction	TOC (%)	TN(%)	TOC:TN ratio	NH4-N air dry (mg/kg)	NO3-N air dry (mg/kg)	Mineral N (mg/kg)	TP (%)	Sorbed P (mg/kg)	PBI	DRP (mg/kg)	Mineral P (mg/kg)
		Gully floor	<63 um	0.12	0.04	3.2	3	<2	3	0.02	7	24	0.29	70
Granite Normanby	Alluvial	Bank surface	<63 um	0.69	0.07	9.8	3	2	5	0.02	4	51	0.08	ND
Granite Normanby	Alluviai	Bank subsurface	<63 um	0.09	0.04	2.3	<2	<2	ND	0.02	9	35	0.26	ND
		Terrace	<63 um	2.13	0.18	11.8	8	17	25	0.04	18	42	0.43	ND
		Bank surface	<63 um	0.58	0.05	11.7	13	3	16	<0.01	2	19	0.11	ND
Parsons Creek	Hillslope	Bank subsurface	<63 um	0.06	<0.03	NA	<2	10	10	<0.01	2	57	0.04	ND
raisons creek	пінзіоре	Gully floor	<63 um	0.14	<0.03	NA	<2	<2	ND	<0.01	2	7	0.29	ND
		Hillslope	<63 um	2.16	0.18	12.0	13	9	22	<0.01	3	42	0.07	ND
		Gully floor	<63 um	0.06	<0.03	NA	<2	19	19	<0.01	2	44	0.05	ND
Laura Croc Station	Alluvial	Bank subsurface	<63 um	0.05	0.04	1.3	<2	8	8	<0.01	<2	74	ND	ND
Laura Croc Station	Alluviai	Bank surface	<63 um	1.22	0.13	9.4	27	22	49	0.02	3	43	0.07	ND
		Terrace	<63 um	2.91	0.31	9.4	100	39	139	0.02	9	80	0.11	ND
		Terrace	<63 um	3.24	0.3	10.8	15	69	84	0.04	14	62	0.23	ND
		Bank surface	<63 um	0.67	0.10	6.7	5	9	14	0.02	4	50	0.08	ND
Laura Croc gap	Alluvial	Buried A	<63 um	0.91	0.10	9.1	5	9	14	0.02	4	161	0.02	ND
		Bank subsurface	<63 um	0.04	0.04	1.0	<2	<2	ND	<0.01	3	117	0.03	ND
		Gully floor	<63 um	0.14	0.03	4.2	3	4	7	0.02	7	75	0.09	ND

# APPENDIX C3: SUMMARY STATISTICS FOR BIOAVAILABLE NUTRIENT AND ORGANICS INDICATORS BY GULLY GEOMORPHIC UNIT AND PARTICLE SIZE FRACTION (ND: NON-DETECTABLE, NA: NOT AVAILABLE)

			TOC	(%)				7	N(%)				TOC:T	N ra	tio			NH4-N a	ir dry (ı	mg/kg)		NO3-N air dry (mg/kg)				
Geomorphology Unit	Fraction	Mean	Median	SD	Rai	nge	Mean	Median	SD	Ran	ige	Mean	Median	SD	Rai	nge	Mean	Median	SD	Ra	nge	Mean	Median	SD	Ra	nge
Bank subsurface	<10	0.11	0.10	0.06	0.06	0.18	0.05	0.04	0.02	0.04	0.08	2.0	1.8	0.8	1.4	3.1	3.0	3.0	1.0	2.0	4.0	11.3	9.5	6.1	6.0	20.0
Bank subsurface	<63	0.06	0.06	0.02	0.04	0.09	0.04	0.04	0.00	0.04	0.04	1.5	1.3	0.7	1.0	2.3	ND	ND	ND	ND	ND	9.0	9.0	1.4	8.0	10.0
Bank subsurface	Total	0.05	0.04	0.04	0.01	0.11	0.04	0.04	NA	0.04	0.04	2.9	2.9	NA	2.9	2.9	ND	ND	ND	ND	ND	5.8	4.0	4.3	3.0	12.0
Bank surface	<10	1.78	1.97	0.70	0.79	2.40	0.20	0.20	0.05	0.13	0.26	8.8	9.2	1.9	6.1	10.5	11.8	8.0	8.2	7.0	24.0	29.3	23.5	20.7	11.0	59.0
Bank surface	<63	0.79	0.68	0.29	0.58	1.22	0.09	0.09	0.04	0.05	0.13	9.4	9.6	2.1	6.7	11.7	12.0	9.0	10.9	3.0	27.0	9.0	6.0	9.2	2.0	22.0
Bank surface	Total	0.69	0.67	0.28	0.42	0.98	0.06	0.06	0.03	0.03	0.09	11.8	11.7	1.8	9.6	14.0	2.5	2.5	0.7	2.0	3.0	ND	ND	ND	ND	ND
Buried A	<10	1.24	1.24	NA	1.24	1.24	0.14	0.14	NA	0.14	0.14	8.8	8.8	NA	8.8	8.8	5.0	5.0	NA	5.0	5.0	19.0	19.0	NA	19.0	19.0
Buried A	<63	0.91	0.91	NA	0.91	0.91	0.10	0.10	NA	0.10	0.10	9.1	9.1	NA	9.1	9.1	5.0	5.0	NA	5.0	5.0	9.0	9.0	NA	9.0	9.0
Buried A	Total	0.57	0.57	NA	0.57	0.57	0.05	0.05	NA	0.05	0.05	11.3	11.3	NA	11.3	11.3	3.0	3.0	NA	3.0	3.0	4.0	4.0	NA	4.0	4.0
Terrace	<10	4.93	4.81	0.47	4.53	5.44	0.50	0.46	0.11	0.41	0.62	10.1	9.8	1.5	8.8	11.7	66.3	30.0	82.7	8.0	161.0	147.7	167.0	89.6	50.0	226.0
Terrace	<63	2.76	2.91	0.57	2.13	3.24	0.26	0.30	0.07	0.18	0.31	10.7	10.8	1.2	9.4	11.8	41.0	15.0	51.2	8.0	100.0	41.7	39.0	26.1	17.0	69.0
Terrace	Total	2.22	1.99	0.83	1.52	3.14	0.16	0.15	0.03	0.14	0.20	13.4	14.2	2.8	10.2	15.7	6.0	4.0	3.5	4.0	10.0	2.5	2.5	0.7	2.0	3.0
Gully floor	<10	0.38	0.32	0.23	0.19	0.70	0.08	0.08	0.01	0.06	0.09	4.8	4.2	2.1	3.2	7.8	4.0	4.0	1.2	3.0	5.0	29.0	12.0	36.7	8.0	84.0
Gully floor	<63	0.12	0.13	0.04	0.06	0.14	0.04	0.04	0.00	0.03	0.04	3.7	3.7	0.7	3.2	4.2	3.0	3.0	0.0	3.0	3.0	11.5	11.5	10.6	4.0	19.0
Gully floor	Total	0.16	0.17	0.10	0.03	0.28	0.05	0.05	NA	0.05	0.05	5.6	5.6	NA	5.6	5.6	ND	ND	ND	ND	ND	4.0	4.0	NA	4.0	4.0
Hillslope	<10	3.82	3.82	NA	3.82	3.82	0.32	0.32	NA	0.32	0.32	11.9	11.9	NA	11.9	11.9	23.0	23.0	NA	23.0	23.0	29.0	29.0	NA	29.0	29.0
Hillslope	<63	2.16	2.16	NA	2.16	2.16	0.18	0.18	NA	0.18	0.18	12.0	12.0	NA	12.0	12.0	13.0	13.0	NA	13.0	13.0	9.0	9.0	NA	9.0	9.0
Hillslope	Total	1.15	1.15	NA	1.15	1.15	0.07	0.07	NA	0.07	0.07	16.4	16.4	NA	16.4	16.4	ND	ND	ND	ND	ND	ND	ND	ND	ND	ND

#### Brooks et al.

Mineral N (mg/kg)				TP (%)						Sorbed P (mg/kg)						PBI			DRP (mg/kg)							
Geomorphology Unit	Fraction	Mean	Median	SD	Ra	inge	Mean	Median	SD	Ra	nge	Mean	Median	SD	Ra	ange	Mean	Median	SD	Ra	nge	Mean	Median	SD	Ra	nge
Bank subsurface	<10	11.3	13.0	2.9	8.0	13.0	0.04	0.04	NA	0.04	0.04	4.8	2.5	5.6	1.0	13.0	115.8	105.0	38.9	83.0	170.0	0.06	0.02	0.07	0.02	0.14
Bank subsurface	<63	9.0	9.0	1.4	8.0	10.0	0.02	0.02	NA	0.02	0.02	3.8	2.5	3.6	1.0	9.0	70.8	65.5	34.7	35.0	117.0	0.11	0.04	0.13	0.03	0.26
Bank subsurface	Total	5.8	4.0	4.3	3.0	12.0	0.02	0.02	NA	0.02	0.02	2.8	1.0	3.5	1.0	8.0	33.0	35.0	11.3	18.0	44.0	0.21	0.21	NA	0.21	0.21
Bank surface	<10	41.0	31.0	28.6	19.0	83.0	0.02	0.02	0.01	0.02	0.03	4.3	4.0	2.1	2.0	7.0	94.8	95.0	21.3	70.0	119.0	0.04	0.04	0.01	0.03	0.06
Bank surface	<63	21.0	15.0	19.3	5.0	49.0	0.02	0.02	0.00	0.02	0.02	3.3	3.5	1.0	2.0	4.0	40.8	46.5	14.9	19.0	51.0	0.08	0.08	0.02	0.07	0.11
Bank surface	Total	2.5	2.5	0.7	2.0	3.0	0.02	0.02	0.00	0.02	0.02	2.3	2.0	1.5	1.0	4.0	23.3	23.5	17.0	8.0	38.0	0.09	0.09	0.02	0.08	0.11
Buried A	<10	24.0	24.0	NA	24.0	24.0	0.02	0.02	NA	0.02	0.02	3.0	3.0	NA	3.0	3.0	255.0	255.0	NA	255.0	255.0	0.01	0.01	NA	0.01	0.01
Buried A	<63	14.0	14.0	NA	14.0	14.0	0.02	0.02	NA	0.02	0.02	4.0	4.0	NA	4.0	4.0	161.0	161.0	NA	161.0	161.0	0.02	0.02	NA	0.02	0.02
Buried A	Total	7.0	7.0	NA	7.0	7.0	ND	ND	ND	ND	ND	3.0	3.0	NA	3.0	3.0	83.0	83.0	NA	83.0	83.0	0.04	0.04	NA	0.04	0.04
Terrace	<10	214.0	175.0	157.2	80.0	387.0	0.06	0.06	0.03	0.04	0.09	30.7	24.0	23.7	11.0	57.0	118.0	113.0	28.8	92.0	149.0	0.25	0.26	0.14	0.10	0.38
Terrace	<63	82.7	84.0	57.0	25.0	139.0	0.03	0.04	0.01	0.02	0.04	13.7	14.0	4.5	9.0	18.0	61.3	62.0	19.0	42.0	80.0	0.26	0.23	0.16	0.11	0.43
Terrace	Total	7.7	6.0	4.7	4.0	13.0	0.03	0.03	0.01	0.02	0.04	12.0	8.0	10.6	4.0	24.0	26.3	22.0	10.2	19.0	38.0	0.40	0.36	0.21	0.21	0.63
Gully floor	<10	33.0	16.0	37.4	11.0	89.0	0.03	0.03	0.00	0.03	0.03	9.8	8.5	7.6	3.0	19.0	153.8	139.0	122.0	46.0	291.0	0.14	0.06	0.19	0.01	0.41
Gully floor	<63	13.0	13.0	8.5	7.0	19.0	0.02	0.02	0.00	0.02	0.02	4.5	4.5	2.9	2.0	7.0	37.5	34.0	29.2	7.0	75.0	0.18	0.19	0.13	0.05	0.29
Gully floor	Total	4.0	4.0	NA	4.0	4.0	0.02	0.02	NA	0.02	0.02	3.8	4.0	2.2	1.0	6.0	15.8	15.5	10.4	5.0	27.0	0.26	0.27	0.07	0.19	0.33
Hillslope	<10	52.0	52.0	NA	52.0	52.0	0.02	0.02	NA	0.02	0.02	3.0	3.0	NA	3.0	3.0	107.0	107.0	NA	107.0	107.0	0.03	0.03	NA	0.03	0.03
Hillslope	<63	22.0	22.0	NA	22.0	22.0	ND	ND	ND	ND	ND	3.0	3.0	NA	3.0	3.0	42.0	42.0	NA	42.0	42.0	0.07	0.07	NA	0.07	0.07
Hillslope	Total	ND	ND	ND	ND	ND	ND	ND	ND	ND	ND	3.0	3.0	NA	3.0	3.0	19.0	19.0	NA	19.0	19.0	0.16	0.16	NA	0.16	0.16

# APPENDIX C4: FINE SEDIMENT CONTENT (<63 UM, <10 UM) FOR ALL SAMPLED GULLIES BY GEOMORPHIC UNIT

